Pathology of the Pancreas

A Practical Approach

Fiona Campbell
Caroline S. Verbeke

Second Edition

Springer

Pathology of the Pancreas

Fiona Campbell • Caroline S. Verbeke

Pathology of the Pancreas

A Practical Approach

Second Edition

Springer

Fiona Campbell
Department of Pathology
Royal Liverpool University Hospital
Liverpool
UK

Caroline S. Verbeke
Department of Pathology
Oslo University Hospital
University of Oslo
Oslo
Norway

ISBN 978-3-030-49847-4 ISBN 978-3-030-49848-1 (eBook)
https://doi.org/10.1007/978-3-030-49848-1

© Springer Nature Switzerland AG 2021
This work is subject to copyright. All rights are reserved by the Publisher, whether the whole or part of the material is concerned, specifically the rights of translation, reprinting, reuse of illustrations, recitation, broadcasting, reproduction on microfilms or in any other physical way, and transmission or information storage and retrieval, electronic adaptation, computer software, or by similar or dissimilar methodology now known or hereafter developed.
The use of general descriptive names, registered names, trademarks, service marks, etc. in this publication does not imply, even in the absence of a specific statement, that such names are exempt from the relevant protective laws and regulations and therefore free for general use.
The publisher, the authors and the editors are safe to assume that the advice and information in this book are believed to be true and accurate at the date of publication. Neither the publisher nor the authors or the editors give a warranty, expressed or implied, with respect to the material contained herein or for any errors or omissions that may have been made. The publisher remains neutral with regard to jurisdictional claims in published maps and institutional affiliations.

This Springer imprint is published by the registered company Springer Nature Switzerland AG
The registered company address is: Gewerbestrasse 11, 6330 Cham, Switzerland

Preface

There have been many advances in pancreatic pathology since we wrote the first edition of this book. Emerging endoscopy and tissue sampling procedures, such as pancreatoscopy, micro-forceps biopsies, and fine-needle biopsies, are now being incorporated into routine diagnostic practice, and neoadjuvant therapy has become part of standard treatment. New diagnostic entities have been described, classifications and international guidelines have been updated, and molecular pathology is beginning to play a role in diagnostics and patient management. All of these advances have been incorporated into this new edition of the book.

The book covers the spectrum of pancreatic pathology from congenital abnormalities and hereditary disorders to inflammatory disease and neoplasia, and it now also includes an entirely new chapter on pancreas transplant pathology (kindly provided by René Michel). There is also limited information on the small super-specialized area of pediatric pancreatic pathology, and the cytology chapter has been kindly revised by M. Priyanthi Kumarasinghe and Ian Yusoff. The book incorporates the recent WHO 2019 classification and TNM8, and brief summaries of the main molecular alterations found in the most common pancreatic neoplasms have also been added.

This is a practical bench book, intended for trainees in histopathology and consultants, who deal with pancreatic specimens. It aims to provide both practical information for all aspects of the diagnostic process and in-depth, up-to-date knowledge that is required for the pathologist's participation in the multidisciplinary team meetings and discussions.

There are more than 200 new macroscopic and microscopic images, enabling us to illustrate the wide range of appearances that the same tumor or disease entity can exhibit. The numerous illustrations are also used to provide a detailed, practical, step-by-step guide to macroscopic examination and specimen handling, as well as to explain the embryology and anatomy of the pancreas. There are more quick-reference tables, and the potential mimics and diagnostic pitfalls are included in differential diagnoses. There is extensive cross-referencing to allow the reader easy access to relevant information.

Reporting checklists are provided for the main diagnostic entities with a summary of key data items to include in the pathology report.

We do hope that the reader will enjoy reading this new edition of the book and that it will continue to serve as a comprehensive resource in daily diagnostic practice and multidisciplinary team discussion.

Liverpool, UK — Fiona Campbell
Oslo, Norway — Caroline S. Verbeke

Acknowledgements

We are grateful to Øystein Horgmo, University of Oslo, for his professional help with the photography. We thank Paul Brown, Specialist Medical Illustrator, The Leeds Teaching Hospitals NHS Trust, Leeds, UK for Medical Drawings. We would also like to thank all of our pathology and clinical colleagues in Liverpool, Oslo, and Stockholm who, knowingly or unknowingly, have contributed to our knowledge and understanding of pancreatic pathology.

Permission to use copyrighted illustrations has kindly been granted by

- Elsevier (Cancer Treatment Reviews 2015;41:17–26) for Fig. 1.27
- Elsevier (Surgical Pathology 2016;19:523–38) for Figs. 3.19 and 3.34
- Springer Nature (Springer eBook—Operative specimen handling and evaluation of resection margins) for Fig. 3.31
- Blackwell Publishing Limited (Histopathology 2010;56:669–82) for Figs. 20.11 and 20.12
- John Wiley and Sons (American Journal of Transplantation 2003;3:599–605) for Fig. 22.12

Chapter 22 on Pathology of Pancreas Transplantation is an updated version of the chapter 'Pancreas Transplantation' in: Michel RP, Berry GJ, editors. Pathology of Transplantation A Practical Diagnostic Approach. Switzerland: Springer; 2016. p. 265–98.

Contents

Part VII Cytology

Part I

General Principles

Check for updates

1 Embryology, Anatomy, and Histology

1.1 Introduction

The pancreas is located deeply in the retroperitoneum, in close association with several vital structures, which complicates access to the organ for diagnostic and therapeutic procedures. Equally complex is the histology of the pancreas, which is characterized by the unusual combination of exocrine and endocrine tissue within the same organ. This chapter focuses on the description of anatomical, histological, and embryological features that are of diagnostic relevance. Where appropriate, reference will be made to the various book chapters in which a particular anatomical or histological feature is part of diagnostic considerations.

1.2 Embryology

The embryogenesis of the pancreas encompasses broadly three processes:

1. The development of the ventral and dorsal pancreatic anlage from the foregut endoderm
2. The morphogenesis of the pancreas as an organ by growth and branching
3. The differentiation of multipotential progenitor cells into committed endocrine and exocrine cells.

As explained in more detail below, the latter two processes are tightly interconnected.

1.2.1 Development of the Ventral and Dorsal Pancreatic Primordia

The pancreas develops during the fourth to seventh gestational week. It takes its origin from ventral and dorsal evaginations of the foregut endoderm. These evaginations consist of cuboidal epithelium, which develops into a complex branching epithelial tree. The larger, dorsal bud appears first, and is followed by the smaller ventral anlage, which develops from the base of the hepatic diverticulum (Fig. 1.1). By the fifth week, both buds have a duct system that opens into the developing gut. In the seventh gestational week, following coiling of the primitive gut to the right, the ventral pancreatic anlage rotates clockwise while the hepatic diverticulum elongates. As a result, the duodenum acquires its characteristic 'C' shape, and the two pancreatic primordia fuse to form a single organ. The dorsal anlage gives rise to the pancreatic body and tail and the cranial portion of the head, whereas the ventral bud constitutes the caudal part of the pancreatic head and uncinate process. The duct systems of both primordia also fuse, such that the main pancreatic duct (also known as Wirsung's duct) is derived from the dorsal anlage in the pancreatic body and tail, as well as from the ventral bud in the pancreatic head. The resulting unified duct drains through the ampulla of Vater and the major duodenal papilla. The part of the

© Springer Nature Switzerland AG 2021
F. Campbell, C. S. Verbeke, *Pathology of the Pancreas*,
https://doi.org/10.1007/978-3-030-49848-1_1

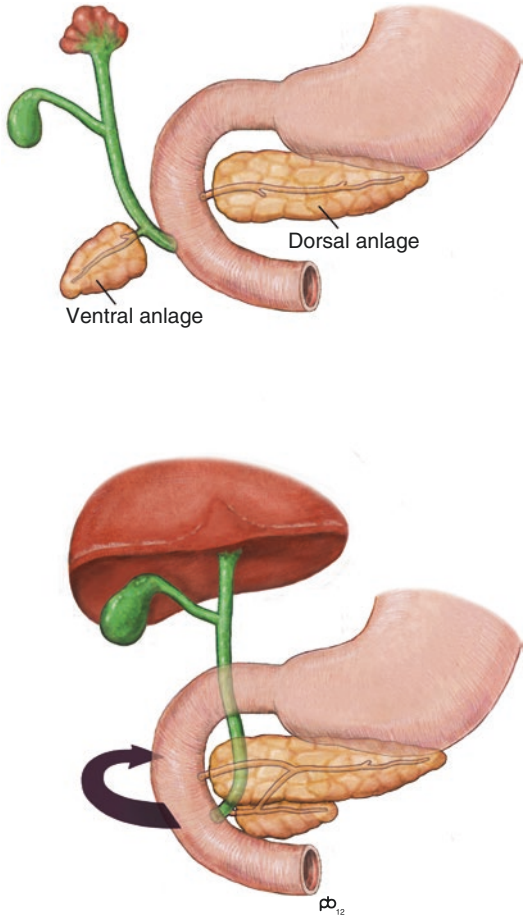

Fig. 1.1 Embryogenesis: the pancreas develops from a ventral and a dorsal evagination of the foregut endoderm. In the seventh gestational week, the ventral anlage rotates, and aligns and fuses with the dorsal anlage. The latter forms the body, tail, and cranial part of the head of pancreas, whereas the ventral bud constitutes the caudal moiety of the pancreatic head and the uncinate process (Image courtesy and copyright of Paul Brown, The Leeds Teaching Hospitals NHS Trust, Leeds, UK)

duct that is derived from the posterior anlage and drains the cranial moiety of the pancreatic head may persist as Santorini's duct, which empties through the minor ampulla and papilla (Fig. 1.2). Aberrant union or regression of the duct systems or pancreatic primordia may lead to rare developmental anomalies of the pancreas, which are described in Chap. 13.

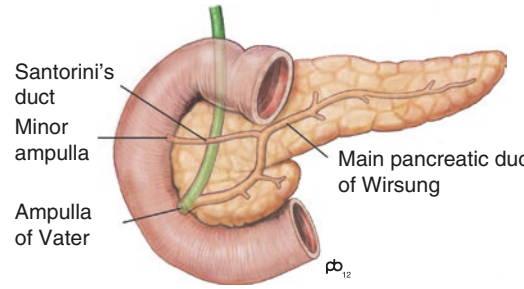

Fig. 1.2 Formation of the pancreaticobiliary duct system: the distal part of the dorsal pancreatic duct remains patent and forms Santorini's duct, which drains through the minor ampulla. The remainder of the dorsal pancreatic duct and the ventral duct fuse to form the main pancreatic duct (Wirsung's duct) (Image courtesy and copyright of Paul Brown, The Leeds Teaching Hospitals NHS Trust, Leeds, UK)

1.2.2 Pancreatic Organogenesis

At the end of the seventh gestational week the pancreas appears as a single fused organ, and in the following months the structural organisation of both the parenchyma and duct system continues to develop. Traditionally, this has been regarded as a process of simple branching morphogenesis. However, the current concept is more complex and includes phases of epithelial plexus formation, proliferation, remodelling, and further expansion.

According to the current views, the branches extending from the growing primitive epithelial tree are segregated in tip and trunk domains. The former contain multipotential pancreatic cells, which will transform into acinar-fated progenitors, whereas the trunk epithelial regions consist of an endocrine-duct bipotential progenitor cell pool. Subsequently, endocrine-committed progenitors present in the trunk region leave the epithelial cord to assemble in clustered endocrine islets. During the fourth month, lobulation of the pancreatic parenchyma becomes clearly apparent, and in the following weeks, the lobules continue to develop, while the surrounding connective tissue decreases, such that at term the pancreas consists of the typical densely packed, angulated lobules.

1.2.3 Lineage Commitment

Differentiation into endocrine and exocrine cells occurs by weeks 12–14. It is the end result of a complex spatiotemporally regulated process in which multiple signalling pathways are involved. At an early stage, the *PDX1* gene plays a central role, as *PDX1*-expressing progenitors produce acini, ducts, and endocrine cells of the pancreas. During a subsequent phase, endocrine subtype lineage allocation takes place, for which a large number of controlling factors, including PDX1 and Notch signaling, have been identified. Fewer transcription factors involved in acinar development are known, but Wnt/β-catenin signalling appears to play a key role. Current knowledge is very limited regarding the development of the pancreatic duct system with its functionally and structurally distinct cell populations lining the main, interlobular, intralobular, and intercalated ducts.

1.3 Anatomy

Knowledge of the anatomy of the pancreas and its neighboring structures is important to allow accurate correlation of observations made in surgical resection specimens with findings identified intraoperatively or on preoperative imaging. Detailed understanding of the anatomy of the pancreatic head is key to correct identification of the origin of adenocarcinomas in this area—pancreatic, ampullary, or bile duct cancer—as these are usually histologically indistinguishable (see Chap. 9, Sect. 9.12.3). This section provides a description of the local anatomy, with the aim to facilitate accurate diagnostic reporting and clinicopathological correlation.

1.3.1 Pancreas

1.3.1.1 General Considerations

The pancreas is a roughly hammer-shaped organ, which in the adult measures 14–20 cm in length and has an average weight of 100 g. It consists of pale-tan to ochre-colored tissue, which is composed of closely packed angulated lobules. The prominent lobulation of the pancreas is similar to that of the major salivary glands. It is a characteristic feature that may be lost in certain pathological conditions, particularly in the context of pancreatitis (see Chap. 7, Sect. 7.2.4).

The pancreas is traditionally divided into three main anatomical areas. The *pancreatic head* (caput pancreatis) lies to the right of the left border of the confluence of the superior mesenteric and portal veins. The *pancreatic body* (corpus pancreatis) is located between the left border of the superior mesenteric vein and the left border of the aorta. The *pancreatic tail* (cauda pancreatis) extends from the latter site to the hilum of the spleen. The term *pancreatic neck* (collum pancreatis) refers to the narrower part of the pancreas, which measures 1–2 cm in anteroposterior dimension and connects the pancreatic head and body. The pancreatic neck crosses the mesenteric blood vessels anteriorly and represents the site where surgical transection for pancreatoduodenectomy is usually performed (see Chap. 2, Sect. 2.1) (Fig. 1.3). The pancreatic head is the thickest part of the pancreas, with an anteroposterior dimension measuring 3.5–5.5 cm. It represents 60–70% of the total pancreatic volume. The body and tail of the pancreas, which together measure up to 13 cm in length, are flatter than the head region and measure usually no more than 3 cm in maximum anteroposterior dimension.

The *uncinate process* is a blunt extension of the pancreatic head that projects from its left-lateral aspect and hooks behind the mesenteric vessels (uncus is the Latin word for ‘hook’). The uncinate process is of varying prominence, and in some specimens it may be hardly present as such (Fig. 1.4).

1.3.1.2 Anatomical Relationship to Neighboring Structures

The pancreas is located deeply in the retroperitoneum, where the body of the gland crosses the vertebral column at the level of the second

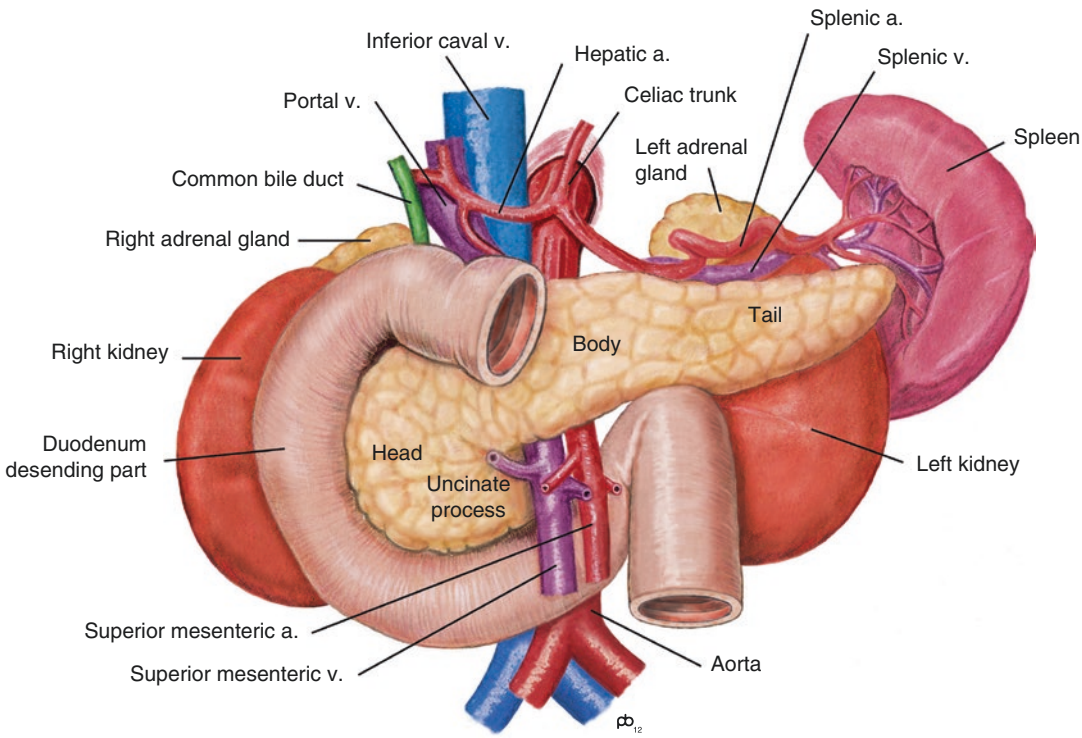

Fig. 1.3 Anatomy: the anatomical relationship between the pancreas and the surrounding structures is complex (a.: artery, v.: vein) (Image courtesy and copyright of Paul Brown, The Leeds Teaching Hospitals NHS Trust, Leeds, UK)

and third lumbar vertebra. It lies behind the left lobe of the liver and the stomach, and its anterior surface faces the lesser sac (bursa omentalis). Although in principle the anterior pancreatic surface is covered with peritoneum, this is almost always absent in the pancreatic head region but seen more frequently on the anterior surface of the body and tail. The lack of peritoneal lining may be explained at least in part by the natural presence of bare areas, where the mesenteries of the colon and small bowel overly the anterior surface. As illustrated in Fig. 1.5, the root of the transverse mesocolon runs over almost the entire length of the caudal part of the anterior pancreatic surface. It is not uncommon for pancreatic resection specimens to include adipose tissue from the mesocolon, which is attached to the anteroinferior aspect of the pancreas.

The pancreas is intimately associated with various anatomical structures, which has obvious surgical implications and explains the potential risk of extension of pancreatic disease—inflammatory or neoplastic—into the surrounding organs and tissues.

The pancreatic head is adherent to the duodenal 'C' (the second and third portions of the duodenum) by a narrow soft tissue plane, which is sometimes referred to as the pancreatoduodenal interface or groove. This small anatomical compartment is of particular importance in paraduodenal pancreatitis (also known as groove pancreatitis), an inflammatory process, which occurs in this area (see Chapt. 7, Sect. 7.2.8).

On its left-lateral side, the pancreatic head is flanked by the superior mesenteric artery (SMA) and vein (SMV), which run anterior to the uncinate process but behind the pancreatic neck (Fig. 1.3). The SMV lies in a slightly curved, shallow indentation of the pancreatic surface, the so-called SMV groove, which has a smooth surface (see Chap. 3, Sect. 3.3.2, Fig. 3.7). The superior mesenteric artery lies to the left and posterior of the vein and is connected to the pancreatic head by a fibroadipose tissue plane

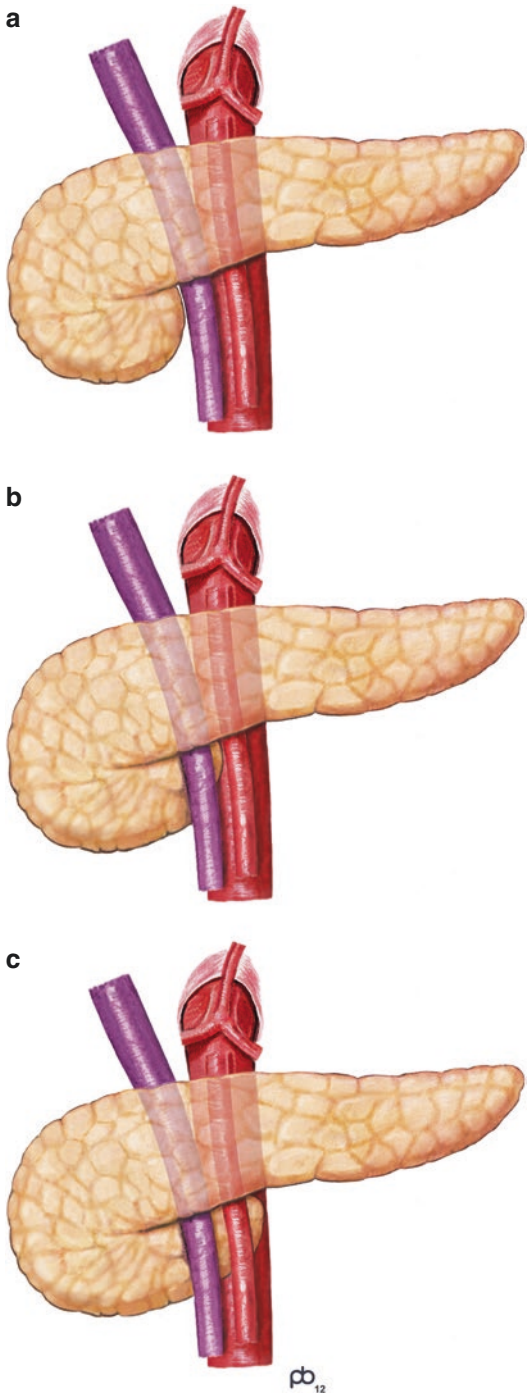

Fig. 1.4 Uncinate process: the prominence of the uncinate process varies. It may just flank the lateral aspect of the superior mesenteric vein (**a**) or may reach behind it (**b**). In some patients, it can extend behind both the superior mesenteric artery and vein (**c**) (Image courtesy and copyright of Paul Brown, The Leeds Teaching Hospitals NHS Trust, Leeds, UK)

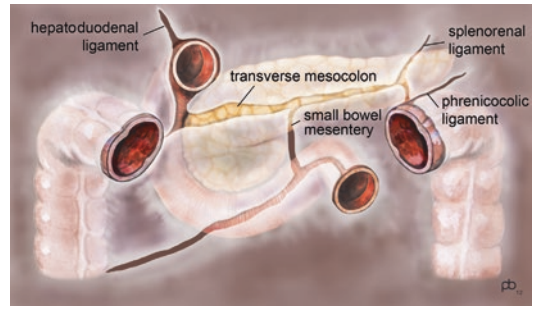

Fig. 1.5 Peritoneal lining: the entire pancreas is located retroperitoneally. Peritoneal lining of the anterior surface is lacking at the root of the transverse mesocolon and the small bowel mesentery. The bare area of the former is contiguous with the splenorenal and phrenicocolic ligaments (adapted from [1]) (Image courtesy and copyright of Paul Brown, The Leeds Teaching Hospitals NHS Trust, Leeds, UK)

that requires sharp dissection during pancreatoduodenectomy. The splenic artery and vein run along the superior-posterior aspect of the pancreatic body and tail. The confluence of the splenic and superior mesenteric vein forming the portal vein is located posterior to the pancreatic neck. Therefore, if a part of the superior mesenteric vein is resected during pancreatoduodenectomy (or total pancreatectomy), the venous segment will be found attached to the caudal two thirds of the SMV groove (see Figs. 3.23 and 3.24). In contrast, a resected segment of the portal vein can be identified at the top end of the SMV groove (see Fig. 9.7). The extrapancreatic common bile duct lies to the right of the portal vein. It enters the pancreatic head slightly to the right of the pancreatic neck, that is, to the right of the transection line of the pancreas during pancreatoduodenectomy.

The pancreas is closely related to the left kidney and adrenal gland, from which it is separated by a soft tissue plain that consists of adipose tissue in the anterior pararenal space and Gerota's fascia. The latter wraps around the kidney, adrenal gland, and surrounding perirenal fat. The pancreatic body rests on the aorta, whereas the head of the pancreas overlies the inferior caval vein and the right renal vessels. The tip of the pancreatic tail tapers and extends close to the splenic hilum. Adherent to the cranial aspect of the pan-

creatic head there may be adipose tissue, which blends with the infrapyloric fat.

1.3.1.3 The Pancreatic Duct System

The pancreatic ducts form a hierarchical system of collecting ducts of gradually increasing caliber, which drain into the main pancreatic duct. The latter runs centrally through the pancreas and drains the gland over its entire length. In the pancreatic head, the main duct makes a sharp turn towards the caudal aspect, following which it courses slightly obliquely towards the duodenum (Fig. 1.6). The distal end of the main pancreatic duct joins the ampulla, which is the terminal conduit that spans the duodenal wall and drains the pancreatic juice into the duodenal lumen. If patent, the accessory pancreatic or Santorini's duct drains the superior part of the pancreatic head through the minor ampulla and lesser duodenal papilla (Fig. 1.7). In over 30% of individuals, Santorini's duct is not patent and has lost its connection to the minor ampulla and/or main pancreatic duct. Only the main pancreatic duct and occasionally Santorini's duct are sufficiently large to be identified by naked-eye inspection, while under normal conditions branch ducts remain macroscopically invisible. Although the main pancreatic duct becomes slightly wider with age (see Chap. 5, Sect. 5.6), its diameter does not usually exceed 3 mm and may be as small as 1.5 mm. The duct wall is membranous and of a pale white color. Santorini's duct is usually less than 1 mm wide. Developmental anomalies of the pancreatic duct system are discussed in Chap. 13.

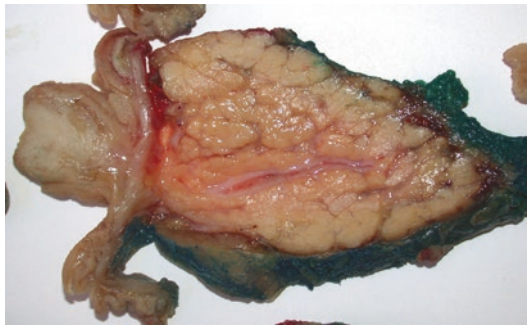

Fig. 1.6 Main pancreatic duct: the distal part of the main pancreatic duct runs in an almost axial plane towards the ampulla of Vater. The duct wall is thin and of a pale white color. In this case, the duct lumen is mildly dilated due to obstruction by an ampullary tumor. Note the compact lobulation of the pancreatic parenchyma

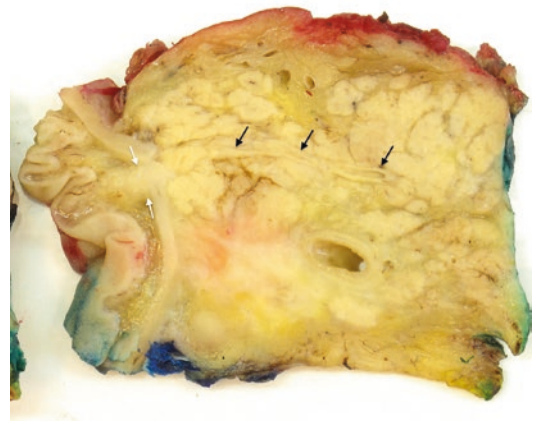

Fig. 1.7 Santorini's duct and minor ampulla: Santorini's duct (*black arrows*) is slightly dilated in this case. The minor ampulla is identifiable as a small nodular structure that traverses the duodenal muscle layer (*white arrows*)

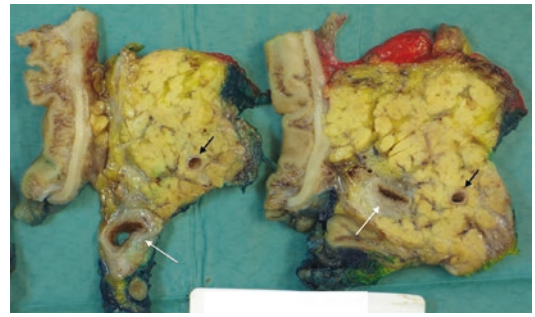

Fig. 1.8 Common bile duct: the extrapancreatic portion of the common bile duct (*white arrow*) is surrounded by a thin cuff of soft tissue (*left*). The intrapancreatic part of the bile duct (*white arrow*) lies in the posterior aspect of the pancreatic head and is surrounded by pancreatic parenchyma (*right*). Note the mild dilatation of the pancreatic duct (*black arrows*) and bile duct in both specimen slices

1.3.2 Common Bile Duct

From a pancreatologist's perspective, the common bile duct consists of an extra- and an intrapancreatic part (Fig. 1.8). In surgical specimens, the extrapancreatic common bile duct is

usually represented by a 1–2 cm long stump, as the bile duct is transected just proximal to the junction of the common hepatic duct with the cystic duct. The extrapancreatic portion of the common bile duct is surrounded by a thin sheath of soft tissue, which usually contains one or more lymph nodes. It also contains a prominent plexus of nerves, which run parallel to the bile duct and portal vein and may occasionally be so large as to be visible macroscopically (see Sect. 1.4.6, Fig. 1.28). The common bile duct enters the pancreas close to the pancreatic neck and descends in a slightly curved fashion through the posterior part of the pancreatic head to finally join the ampulla of Vater (Fig. 1.2). Under normal conditions, the common bile duct has an average outer diameter of 0.7 cm. However, in resection specimens for pancreatic head tumors, the bile duct is often dilated and its wall may be thickened (normal width: 1 mm). The larger size, thicker wall, and location in the posterior aspect of the pancreatic head distinguish the common bile duct from the main pancreatic duct, which is smaller, thin-walled, and located more centrally.

1.3.3 Ampulla and Papilla of Vater

The ampulla of Vater (or major ampulla) is a relatively firm, nodular structure that traverses the duodenal wall and forms the terminal conduit of the main pancreatic duct and the intrapancreatic common bile duct before the pancreatic juice and bile are drained into the duodenal lumen (Fig. 1.9; see also Fig. 3.19). Both ducts may join the ampulla together or separately. While this can be well observed on imaging and during endoscopy, these anatomical features are usually only visible microscopically and will therefore be discussed in more detail in the histology section of this chapter (see Sect. 1.4.7).

The slightly elevated, nipple-like surface of the duodenal mucosa at and around the orifice of the central channel of the ampulla is referred to as the papilla of Vater (or major duodenal papilla). It measures approximately 1 cm in length and 0.5 cm in breadth, but there is much variation. In a significant proportion of individuals, the cranial part of the papilla of Vater is partially or completely covered by a triangular duodenal mucosal fold (so-called hooding fold), while a frenulum-like longitudinal mucosal fold may extend from the caudal end of the papilla (Fig. 1.10). The ampulla and papilla of Vater are usually located in the descending duodenum at approximately 8 cm from the pylorus. In a small proportion of individuals, the papilla may be located between the descending and horizontal part (12%) or in the horizontal part of the duodenum (6%) [2].

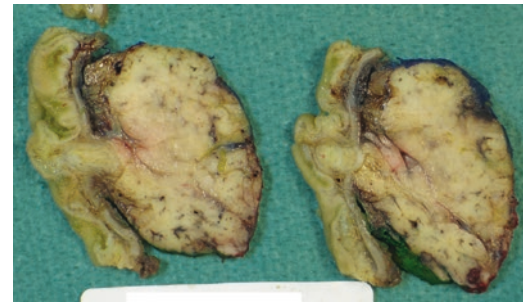

Fig. 1.9 Ampulla of Vater: this oblong nodular structure traverses the duodenal muscularis propria (*left*) and extends into the lamina propria (*right*) to join the overlying duodenal mucosa, that is, the papilla of Vater

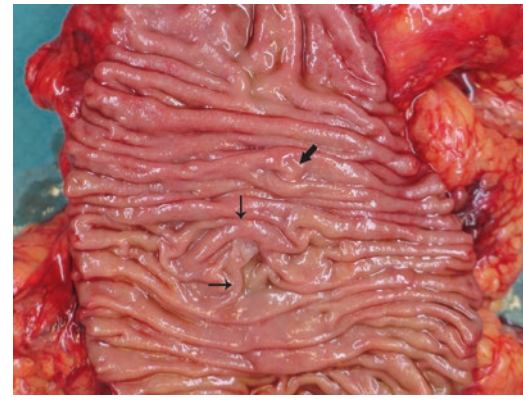

Fig. 1.10 Major and minor duodenal papilla: the major duodenal papilla is partially covered by a so-called hooding fold, while a frenulum-like fold extends longitudinally from the distal end of the papilla (*arrows*). The minor papilla is present approximately 2 cm proximal to the major papilla (*block arrow*)

1.3.4 Minor Ampulla

This is a smaller and usually more rudimentary ampullary structure, which connects Santorini's duct with the duodenal lumen (Fig. 1.7). The minor ampulla and associated minor (or lesser duodenal) papilla are located approximately 2 cm cranial to the ampulla and papilla of Vater. While both structures are virtually always present, they may be very small, that is, macroscopically invisible, and of limited functionality. However, in certain pathological conditions (e.g., intraductal papillary mucinous neoplasia), both Santorini's duct and the minor ampulla may become dilated, macroscopically prominent structures (see Chap. 17, Fig. 17.1).

1.3.5 Vasculature

The arterial supply to the pancreas is derived from branches of the celiac trunk and superior mesenteric artery. It can be divided into two main regions, the head and the body/tail of the pancreas. However, numerous anastomoses between both regions exist, and there is significant anatomical variation (Fig. 1.11).

The gastroduodenal artery provides the main arterial supply to the pancreatic head. It is located and macroscopically identifiable in the adipose tissue that overlies the anterior-superior surface of the pancreatic head (see Chap. 3, Figs. 3.22 and 9.40). The tributaries of the gastroduodenal artery, the anterior and posterior pancreatoduodenal arteries, supply the respective aspects of the pancreatic head. They branch and form arcades with tributaries of the superior mesenteric artery (the anterior and posterior inferior pancreatoduodenal arteries). These arterial arcades are located in the soft tissue of the pancreatoduodenal groove, at the bottom of the natural crevice between the duodenal wall and the anterior or posterior pancreatic surface, respectively. The inferior pancreatoduodenal artery is often visible as a small artery or plexus of arterial vessels in the mediocaudal aspect of the pancreatic head (Fig. 1.12).

The splenic artery provides the blood supply to the body and tail of the pancreas. It has several main branches (dorsal, inferior and greater pancreatic arteries), which form an anastomosing network around the pancreatic body and tail up to the neck of the pancreas. At the latter location, communicating anastomoses between the splenic and pancreatoduodenal arterial systems commonly occur.

The greater pancreatic artery, a large tributary of the splenic artery, penetrates the pancreas and provides branches that run parallel to the main pancreatic duct and form anastomoses with the other tributaries of the splenic artery. The inter-

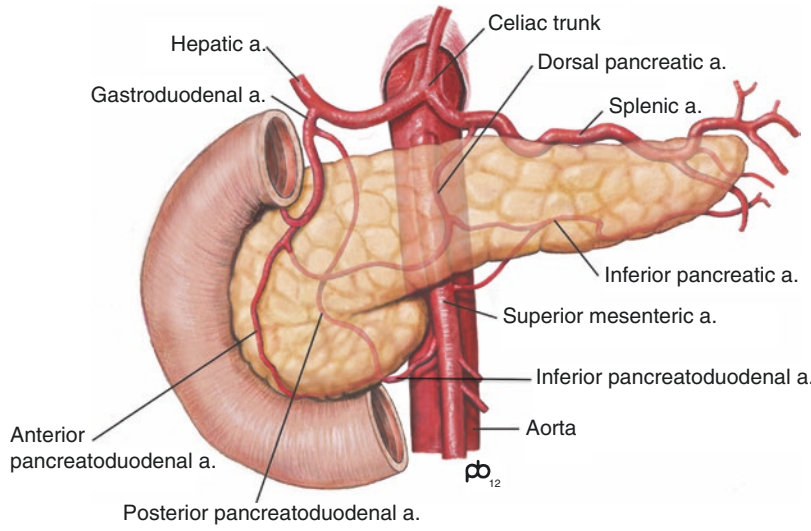

Fig. 1.11 Arterial blood supply: branches from the celiac trunk and superior mesenteric artery (SMA) supply the pancreas with arterial blood. The pancreatic head is supplied by the gastroduodenal artery and the inferior pancreatoduodenal artery, the body/tail by the splenic artery and branches from the SMA. Anastomoses connect both areas (Image courtesy and copyright of Paul Brown, The Leeds Teaching Hospitals NHS Trust, Leeds, UK)

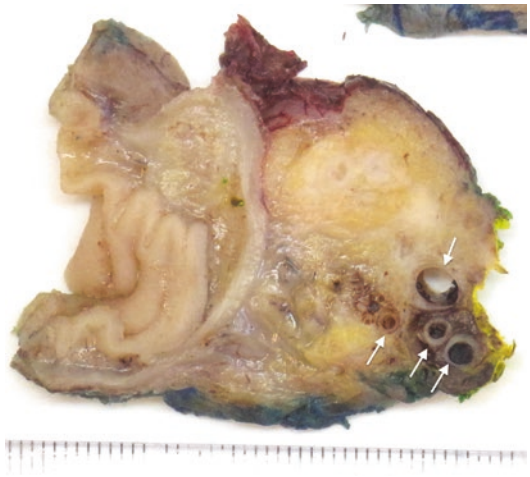

Fig. 1.12 Inferior pancreatoduodenal artery: this tributary of the superior mesenteric artery is present in the medio-caudal aspect of the pancreatic head and surrounding adipose tissue, where it often forms a small plexus (*arrows*)

lobular and intralobular arteries represent ramifications of the greater pancreatic artery.

A network of small veins (vv. pancreaticae) drains from the pancreatic head into the superior mesenteric vein (SMV), while venous blood from the body and tail of the pancreas collects in the splenic vein. The confluence of the splenic vein and SMV to form the portal vein is located immediately posterior to the pancreatic neck, that is, the line of surgical transection for pancreatoduodenectomy. The SMV and lower end of the portal vein run through the SMV groove, that is, the shallow indentation of the flanking pancreatic parenchyma (see Figs. 3.23, 3.24, and 3.25).

1.3.6 Lymph Nodes

Lymph nodes are present in the soft tissue around the pancreas and extrapancreatic common bile duct, and in the adipose tissue at the splenic hilum. The various positions of the lymph nodes have been classified for diagnostic purposes (see Chap. 3, Table 3.2, Fig. 3.27). Lymph nodes adjacent to the extrapancreatic common bile duct are often sizeable, attaining a diameter of 1–2 cm or more, due to reactive changes, which may be particularly prominent in patients with biliary obstruction. In a Whipple's or total pancreatectomy specimen, lymph nodes may also be found in the infrapyloric and perigastric adipose tissue.

1.4 Histology

In this chapter, the description of the histology of the pancreas and surrounding structures will be limited to those features that can be appreciated on routine histological staining and that are of diagnostic relevance. An overview of the immunoprofile of the three main cell populations that constitute the pancreas is given in Table 1.1.

1.4.1 Pancreatic Lobules

The pancreas has a lobulated architecture, which is also visible macroscopically. The lobules vary in size (1–10 mm) and shape, from angulated to rounded (Fig. 1.13). They are densely packed and separated from each other only by a very thin layer of loose paucicellular stroma, which contains vessels and nerves. The pancreas has no capsule, and occasionally, especially if the gland is affected by a degree of atrophy or fatty replacement, the delineation of the pancreas from the surrounding soft tissue may not be entirely sharp. Isolated lobules may be found at a short distance 'off-shore' from the main parenchymal mass, and a cluster of such lobules may occasionally be confounded with a small peripancreatic lymph node during macroscopic examination.

1.4.2 Acinar Cells

Approximately 85% of the pancreas consists of acinar cells. They are arranged in characteristic acini or rounded nests with a central lumen that is barely discernable and usually becomes more apparent when it is pathologically dilated (see Chap. 5, Sect. 5.2, Fig. 5.2). Acinar cells are approximately pyramidal in shape and have a basal round and uniform nucleus, which often contains an inconspicuous central nucleolus. Due

Table 1.1 Immunohistochemical profile of acinar, ductal, and endocrine cells

	AE1/AE3	CK7	CK8	CK18	CK19	CK20	CEA[a]	CA19-9	Pancreatic enzymes Trypsin Chymotrypsin Lipase Amylase	Endocrine markers Chromogranin Synaptophysin Specific hormones (insulin, glucagon, somatostatin, PP)	PR	PDX1
Acinar	(+)	–	+	+	–	–	–	–	+	–	–	–
Ductal	+	+	+	+	+	–	–	+	–	–	–	–
Endocrine	–	–	(+)	(+)	–	–	–	–	–	+	+	+

(+) Weak immunostaining possible
[a]Monoclonal CEA antibody

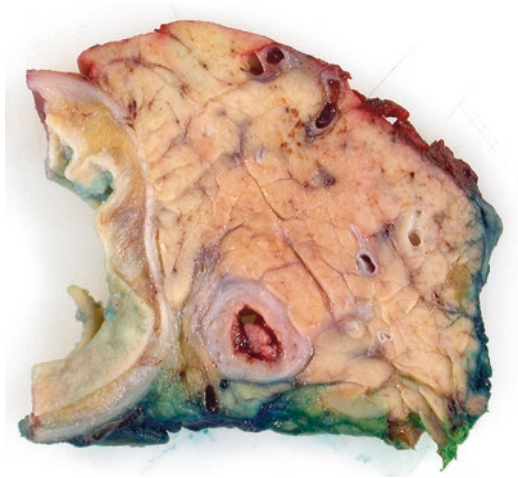

Fig. 1.13 Pancreatic parenchymal lobulation: the pancreatic parenchyma is composed of densely packed, slightly angulated, pale ochre-colored lobules. There is no organ capsule. Note the normal-sized main pancreatic duct and dilated bile duct containing polypoid tumor tissue

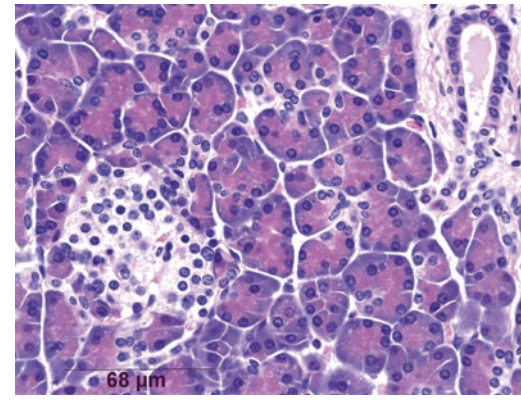

Fig. 1.14 Normal acini, duct, and Langerhans islet: acinar cells have cytoplasm that is characteristically basophilic at the basal pole and eosinophilic at the apical pole. The lumen is hardly visible. Note the islet, which is composed of loosely packed pale-staining cells, and the small intralobular duct

to the high content of rough endoplasmic reticulum with a high concentration of ribonucleoproteins, the cytoplasm is basophilic at the basal aspect of the acinar cell. In contrast, the apical part is eosinophilic and granular due to the accumulation of zymogen granules (Fig. 1.14). The latter are positive on periodic acid-Schiff (PAS) staining, with a variable resistance to diastase digestion. Acinar cells synthesize and secrete the digestive (pro-)enzymes and as such they stain positively with antibodies against the pancreatic enzymes lipase, amylase, trypsin, chymotrypsin, and elastase. Acinar cells also label for certain but not all epithelial markers (positive: CAM5.2/cytokeratin 8 and 18; negative: cytokeratin 7, 19, 20; AE1/AE3) (Table 1.1).

1.4.3 Pancreatic Duct System

The pancreatic duct system encompasses the small peripheral ramifications, that is, the intercalated and intralobular ducts, up to the interlobular ducts and the main pancreatic duct (Wirsung's and Santorini's). Not only the caliber, but also the epi-

thelial lining of the various parts of the duct system differ, and divisions are not always simply dichotomous, but ramifications into three or more branches may be seen at any level of the duct system. Besides its obvious draining function, the duct system has also a secretory function. The duct cells secrete water, chloride, and bicarbonate, which buffer the pancreatic juice at a pH of approximately 6.5. The buffering function of the duct-epithelial secretion is key to the stabilisation of the proenzymes that are released by the acinar cells.

The *centroacinar cells* represent the most peripheral ramifications of the duct system. They are small, have a clear cytoplasm, and are found in or near the lumen of the acini, where they partially cover the apical surface of the acinar cells. The *intercalated ducts* represent the next component of the duct system downstream from the centroacinar cells, that is, outside the acini. They are lined by a low cuboidal epithelium, which is similar to the centroacinar cells (Fig. 1.15). The *intralobular duct* system comprises ducts of varying caliber. The small-order ducts are only slightly larger than the intercalated ducts, whereas higher-order intralobular ducts are not only larger but also surrounded by a thin sheath of fibrous tissue (Fig. 1.16). Intralobular ducts join and form tributaries of *interlobular ducts*, which in turn eventually drain into the main pancreatic duct. With increasing duct caliber, the height of the lining epithelium increases, but it always remains flat (i.e., without folding or tufting). A sheath of fibrous tissue including a collar of elastin fibers envelops the ducts once they leave the lobules (Figs. 1.17 and 1.18). Pancreatic ducts of any caliber lack a smooth muscle layer. The microscopic anatomy of the periductal cuff can be a useful criterion to distinguish native pancreatic ducts or intraductal neoplastic processes (pancreatic intraepithelial neoplasia, intraductal papillary mucinous neoplasia, or duct canceri-

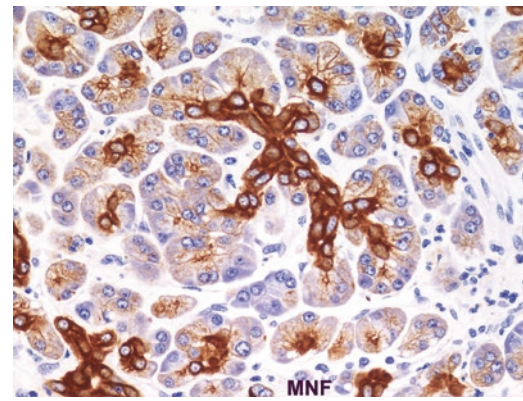

Fig. 1.15 Intercalated ducts and centroacinar cells: immunostaining highlights the presence of the centroacinar cells, which are located within the acini, and the delicate intercalated ducts, which consist of a single row of similar, low cuboidal epithelial cells (immunostaining for MNF116)

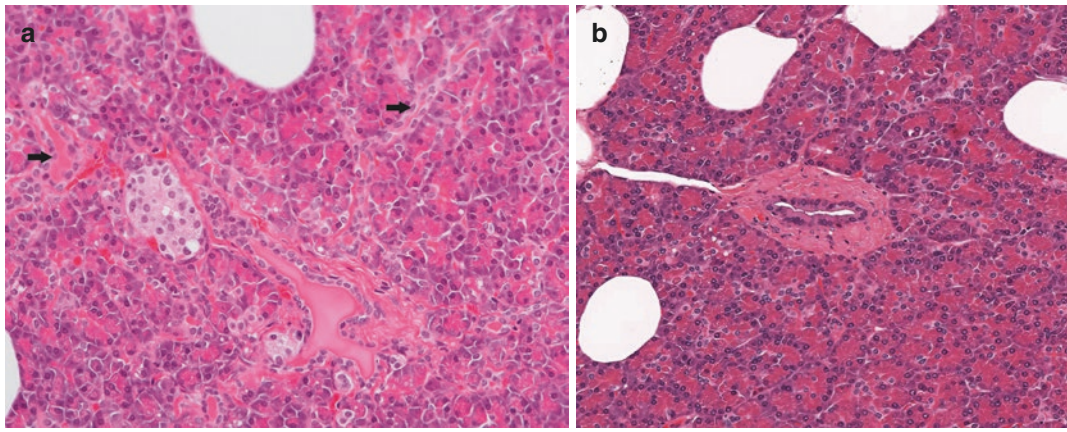

Fig. 1.16 Intralobular ducts: an intralobular duct lies between densely packed acini. Its lumen is lined with low-columnar non-mucinous epithelium. Note the presence of small intralobular duct ramifications and intercalated ducts (*arrows*) (**a**). A thin cuff of fibrous tissue surrounds this larger intralobular duct (**b**)

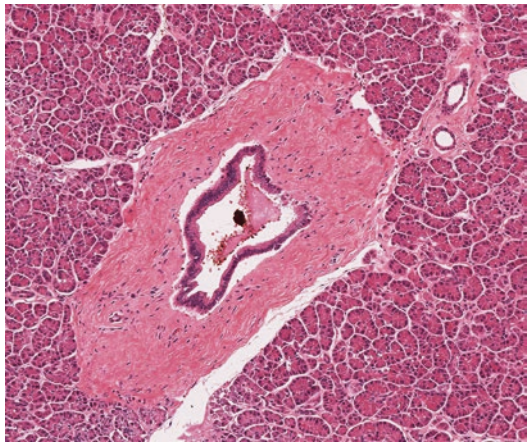

Fig. 1.17 Interlobular duct: this duct of larger caliber is surrounded by a broad sheath of fibrous tissue and lined by higher columnar epithelium. The duct lies within the thin fibrous septum that separates two neighboring lobules

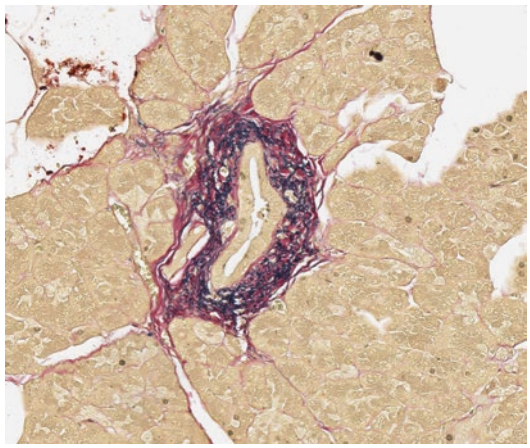

Fig. 1.18 Elastin fibers around interlobular ducts: elastica staining demonstrates the presence of loosely packed elastin fibers within the fibrous tissue cuff that surrounds this interlobular duct

sation) from intravascular cancer propagation and stroma-invasive ductal adenocarcinoma (see Chaps. 8 and 9, Sect. 8.6.3 and 9.10, Fig. 9.36). Mucin is absent in the centroacinar cells and intercalated duct epithelium but can be detected with the help of mucin stains in the cytoplasm of epithelium lining intra- and interlobular ducts as well as the main pancreatic duct. The duct epithelium stains positively for cytokeratins (CK7, 8, 18, 19) and EMA. Under normal circumstances it does not label for CEA (monoclonal antibody) (Table 1.1). Expression of members of the MUC family varies throughout the pancreatic duct system. Labeling for MUC6 is seen in centroacinar cells and intercalated ducts, while MUC1 stains positively in small intralobular and intercalated ducts. MUC2 and MUC5AC are not normally expressed. In contrast to the salivary glands, the pancreatic ducts do not contain basal or myoepithelial cells. Based on ductal corrosion cast studies, so-called periductal glands were described as small, blind-ending outpouches of the main pancreatic duct and large branch ducts, which are lined with mucin-producing columnar epithelial cells [3]. While inconspicuous under normal conditions, the periductal glands may become hyperplastic in response to injury (see Chap. 5, Sect. 5.4, Fig. 5.5).

Histologically, the main pancreatic duct can be distinguished from the common bile duct by the absence of a muscle coat in its wall. However, the layer of smooth muscle fibers in the common bile duct may be incomplete and thin, and it usually becomes more prominent only at the junction with the ampulla of Vater and sphincter of Oddi. A further distinguishing histological feature between both ducts is the absence of ducts that drain into the common bile duct. The sacculi of Beale should not be mistaken for draining side branch ducts (see Sect. 1.4.9).

1.4.4 Endocrine Compartment: Islets of Langerhans and Extrainsular Endocrine Cells

The endocrine compartment of the pancreas represents approximately 2% of the overall mass of the gland. There are an estimated 10^5–10^6 islets, with islets being somewhat more concentrated in the tail of the pancreas. The islets are scattered individually throughout the pancreatic lobules. Two types of islets are distinguished. The vast majority (90%) are so-called *compact islets*. They have smooth and well-circumscribed contours and a roundish shape but lack any capsular structure (Fig. 1.14). The size varies, with an

average of approximately 150 μm and an upper limit of 300 μm (see Chaps. 20 and 21, Sects. 20.15 and 21.1). The islet cells are arranged in a loose complex of anastomosing loops, and they are medium-sized and ovoid in shape. They contain a moderate amount of pale eosinophilic to amphophilic cytoplasm and an ovoid nucleus with coarse chromatin and possibly a small dot-like nucleolus. Some variation in nuclear size is normal, and the occasional presence of an enlarged nucleus is not uncommon. Pancreatic islets contain numerous capillary-type blood vessels, but these may be difficult to identify on routine histology.

At least four different endocrine cell types are recognized: glucagon-producing α-cells, insulin-producing β-cells, δ-cells producing somatostatin and the PP-cells, which secrete pancreatic polypeptide. These cell populations have a characteristic distribution in terms of relative numbers and localization within the islet. By far most numerous are the β-cells, which make up 60–80% of the islet cell population. The α-cells represent 15–20%, while δ-cells comprise only 5–10%, and PP-cells are sparse (less than 2%), except in islets derived from the ventral pancreatic anlage (see below). Whereas α-cells and to a lesser extent δ-cells occur in the periphery of the islets, the β-cells are located more centrally (Figs. 1.19 and 1.20). These features are important criteria to distinguish enlarged islets from endocrine (micro-) adenomas. Recently, a fifth cell population of ghrelin-secreting ε-cells has been described, which is also present in the stomach. Ghrelin is a key regulator of appetite and energy balance and plays an important role in glucose homeostasis. It has a complex effect, both directly and indirectly, on β-cells [4].

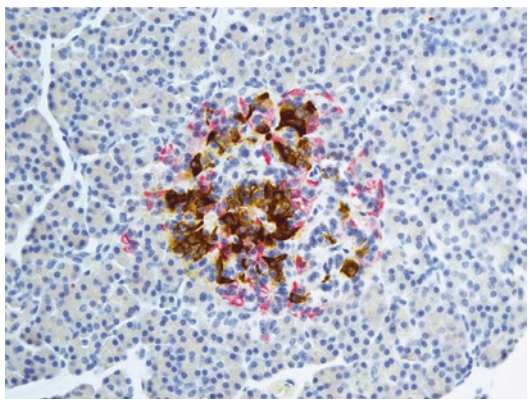

Fig. 1.19 Compact islet: this round and well-defined islet contains numerous insulin-producing cells (*brown*), which are located in the center of the islet. Glucagon-positive cells (*red*) are less numerous and take up a more peripheral location (immunohistochemical double staining for insulin and glucagon)

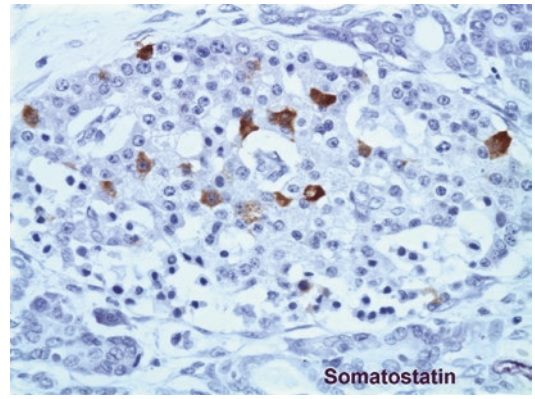

Fig. 1.20 Compact islet: immunostaining highlights the presence of a small number of randomly placed somatostatin-producing cells

The composition and morphology of islets derived from the ventral pancreatic anlage, (i.e., in the uncinate process and the inferior part of the pancreatic head) differ substantially from that in the remainder of the pancreas. These so-called *diffuse islets* are more irregular in shape and less well demarcated from the surrounding acini. They have a more trabecular cell arrangement and are often of a larger size (up to 450 μm) (Fig. 1.21). Some of the endocrine cells may acquire a columnar shape. Diffuse islets are rich in PP-cells, and the PP−/β-cell ratio in diffuse islets is the reverse of that in compact islets (70–80% and less than 2%, respectively).

Islet cells immunostain for neuroendocrine markers (synaptophysin, chromogranin, CD56), PDX1, progesterone receptor, and CD99. Cytokeratins are usually not expressed, although weak immunolabeling for CAM5.2 may be seen.

In the adult pancreas, less than 10% of all endocrine pancreatic cells are found outside the islets. They are scattered throughout the acinar parenchyma and located within or

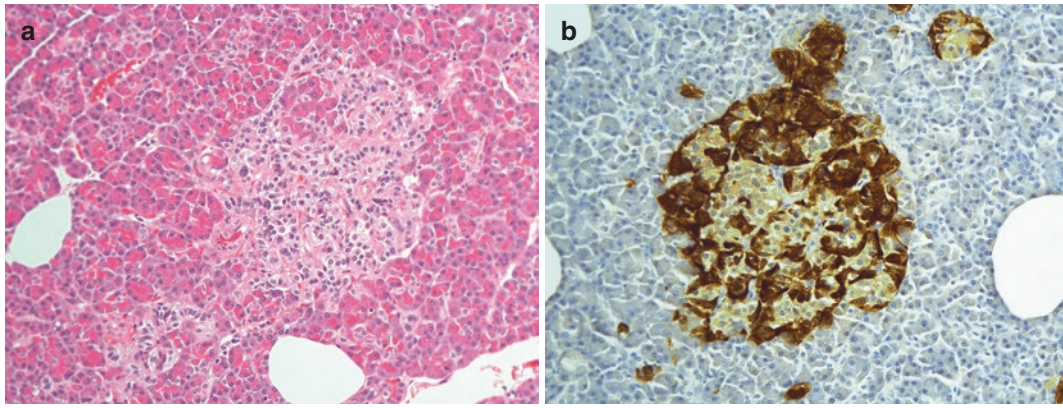

Fig. 1.21 Diffuse islet: in the inferior part of the pancreatic head, islets are larger, show a more trabecular cell arrangement, and are less well defined. Note the apparent extension of islet cells in between adjacent acini (**a**). Immunostaining highlights the presence of numerous PP-cells (**b**)

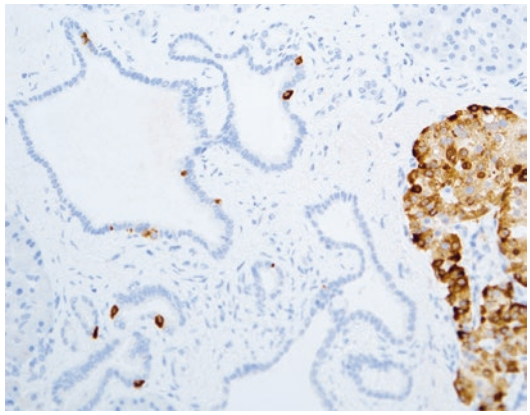

Fig. 1.22 Extrainsular endocrine cells: immunostaining for synaptophysin reveals the presence of scattered single endocrine cells within the epithelial lining of some pancreatic ducts

close to pancreatic ducts (Fig. 1.22). These extrainsular cells are mainly PP-cells, only rarely α-, β-, or δ-cells. Some of the extrainsular endocrine cells that are present in large pancreatic ducts may also produce serotonin, implying that these cells may be the origin of the very rare true carcinoid tumors of the pancreas (see Chap. 20, Sect. 20.3). In contrast to the paucity of extrainsular endocrine cells in postnatal life, numerous endocrine cells occur in close contact with the duct epithelium during intrauterine development. Reoccurrence of periductal endocrine cells, often denoted as the formation of ductulo-insular complexes, has been described in a variety of reactive changes, including chronic pancreatitis (see Chap. 5 and 7, Sects. 5.8 and 7.2.4, Fig. 7.31).

The histology of the endocrine compartment of the pancreas changes rapidly during early postnatal life. In fetal and neonatal pancreas, it is normally more prominent (10% of the neonatal pancreatic volume) than later in life, because of the relative underdevelopment of the acinar tissue. Overall, during the first year, there is a rapid decrease in volume of the endocrine compartment relative to the exocrine compartment, and the proportion of β-cells increases (from 50% in neonates to 70% in adults), while that of δ-cells decreases (from 30% to 10%).

1.4.5 Interstitium

Within the pancreatic lobules, the interstitium consists of a barely visible, delicate network of capillaries. The interlobular septa are thin and composed of a small amount of loose fibrous stroma, which supports interlobular pancreatic ducts, peripheral nerves, lymphatic channels, and blood vessels. The latter usually appear as paired venous and arterial branches, whose course is separate from that of the interlobular ducts (Fig. 1.23). This observation may be useful in the distinction between well-differentiated ductal

adenocarcinoma and native ducts. However, it has to be noticed that this applies only to muscularised, thick-walled medium-sized blood vessels, whereas small-caliber thin-walled blood (or lymphatic) vessels may be found close to interlobular ducts or within lobules. Autonomic ganglia are present in the interlobular septa, and may occasionally also be found in between acini. Small peripheral nerves are sometimes present within the periphery of acinar lobules and on rare occasion they surround a cluster of acini (Fig. 1.24).

Pancreatic stellate cells are biologically and morphologically similar to the hepatic stellate (or Ito) cells. In a quiescent state they store vitamin A, while upon activation they lose their vitamin A stores and produce extracellular matrix components. Therefore, pancreatic stellate cells play a central role in the development of fibrosis in chronic pancreatitis and are the main source of the desmoplastic stroma in pancreatic ductal adenocarcinoma. Under normal conditions, these cells are not identifiable on routine microscopy, but if activated, they can be identified by immunolabeling for α-smooth muscle actin. Despite their important role in pancreatic fibrogenesis and their complex interactions with ductal adenocarcinoma cells, pancreatic stellate cells are usually not considered in diagnostic pancreatic pathology.

A further cellular component of the pancreatic interstitium are the recently described interstitial cells of Cajal, which share morphological and immunohistochemical properties with their namesakes in the tubular digestive tract.

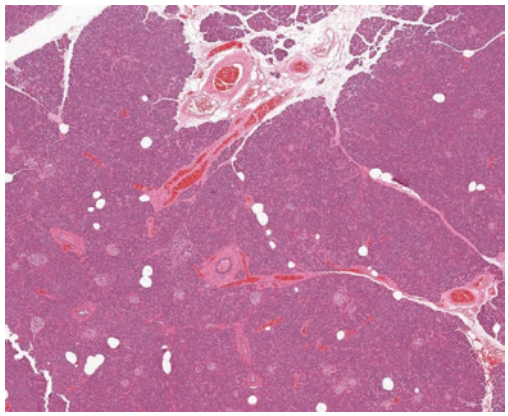

Fig. 1.23 Separation of blood vessels and ducts: pancreatic ducts and muscular blood vessels follow a different course and are separated by acinar parenchyma

1.4.6 Peripancreatic Soft Tissue

The soft tissue that surrounds the pancreas consists mainly of adipose tissue and includes blood vessels, lymphatic channels, peripheral nerves, and occasional small paraganglia. The number and size of the peripheral nerves varies significantly depending on the localization. Peripheral nerves are particularly numerous

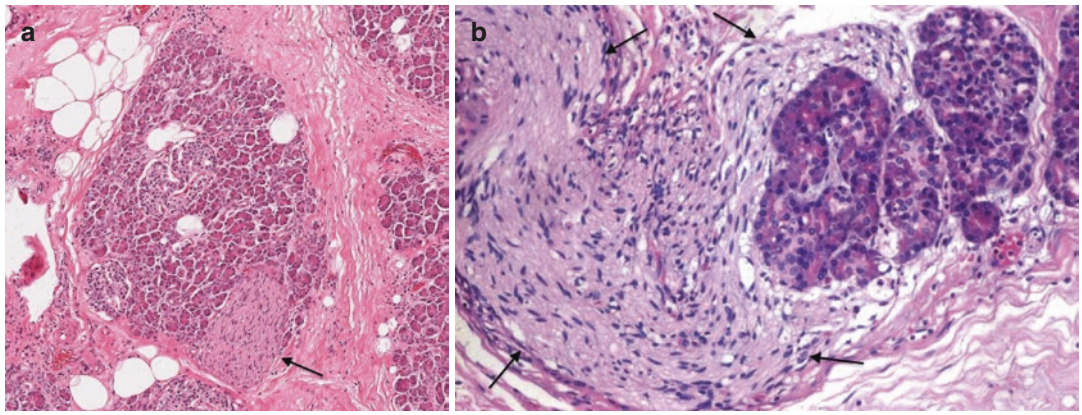

Fig. 1.24 Intrapancreatic nerve: peripheral nerves are usually located within interlobular septa, but may also be found at the edge of or within a pancreatic lobule (**a**, *arrow*). On rare occasion, clusters of acini appear to be surrounded by peripheral nerves (**b**, *arrows*)

in the soft tissue facing the superior mesenteric artery (Fig. 1.25). A moderate number of peripheral nerves is seen in the posterior peripancreatic soft tissue, while the adipose tissue overlying the anterior surface of the pancreas contains relatively few peripheral nerves, except for the small plexus that surrounds the gastroduodenal artery. Similarly, a small nerve plexus exists around the splenic artery, while the superior mesenteric artery and celiac trunk are associated with a prominent nerve plexus (Figs. 1.26 and 1.27). Numerous, often large, nerve bundles are also normally present along the extrapancreatic common bile duct (Fig. 1.28). Benign glandular inclusions in peripheral nerves have been described, but this is an extremely rare finding (Fig. 1.29).

Pacinian corpuscles may be present in the peripancreatic soft tissue, mainly posteriorly and around the portal and splenic veins (Fig. 1.30). On occasion, these corpuscles can be present even within the peripheral parts of the pancreatic parenchyma. As they can reach a size of up to 3 mm, they may be macroscopically visible as small translucent vesicular structures.

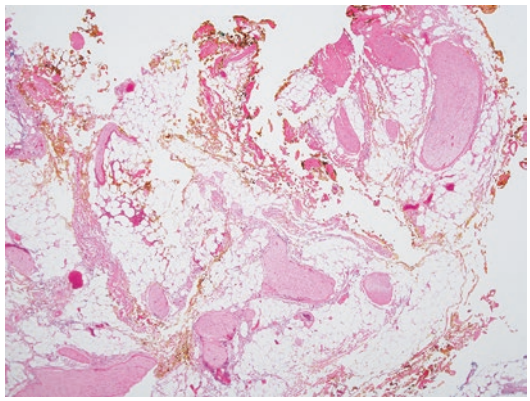

Fig. 1.25 Peripancreatic nerves: numerous peripheral nerves of varying caliber are present in the peripancreatic fat flanking the superior mesenteric artery

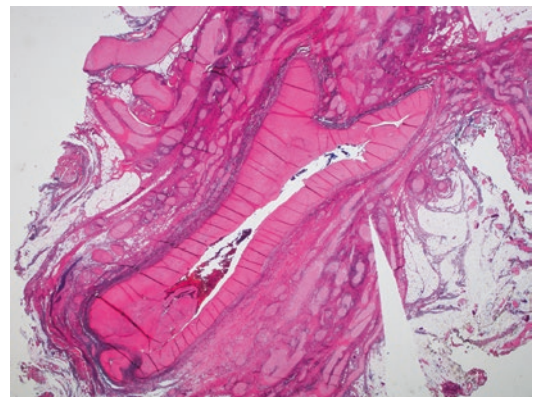

Fig. 1.27 Periarterial nerve plexus: the superior mesenteric artery is surrounded by a prominent nerve plexus (Reproduced with permission from Verbeke [5], Elsevier)

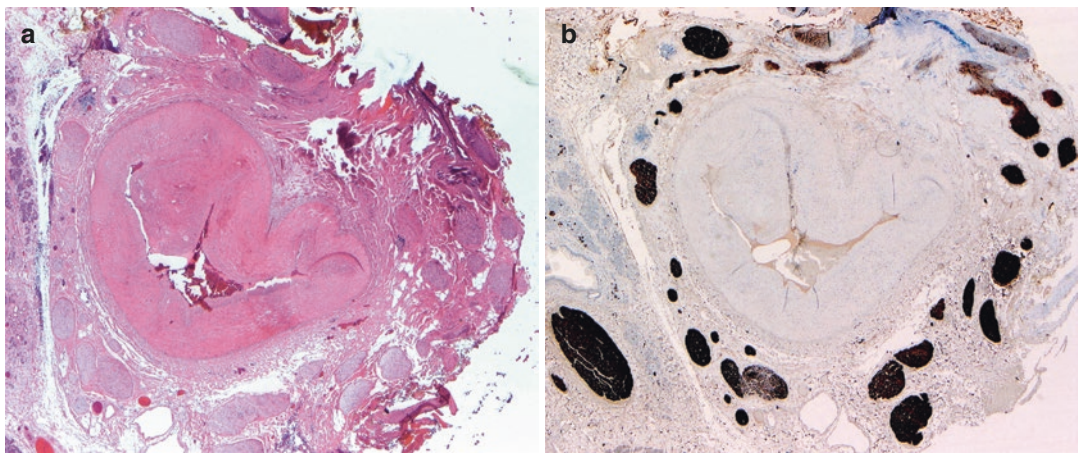

Fig. 1.26 Periarterial nerve plexus: like the other main arteries that supply the pancreas, the splenic artery is surrounded by a nerve plexus (**a**) that is highlighted with immunostaining for S100 (**b**)

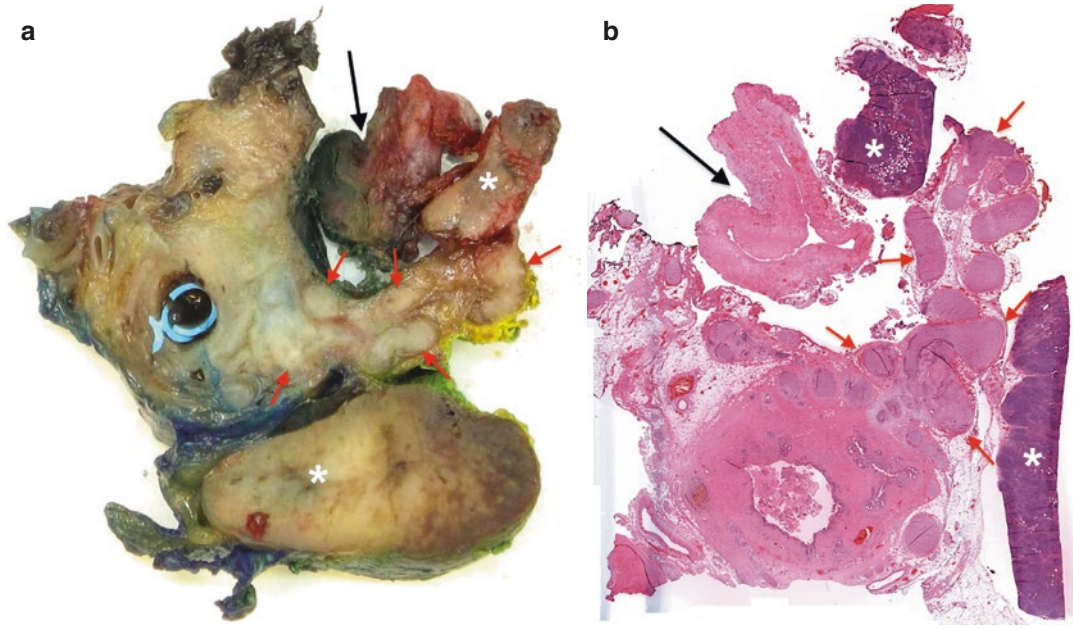

Fig. 1.28 Nerve plexus along extrapancreatic common bile duct: prominent, macroscopically visible nerve bundles (*red arrows*) run in parallel with the common bile duct (with stent) and portal vein (*black arrow*) within the hepatoduodenal ligament (**a**, **b**). Note the large flanking lymph nodes (*asterisks*)

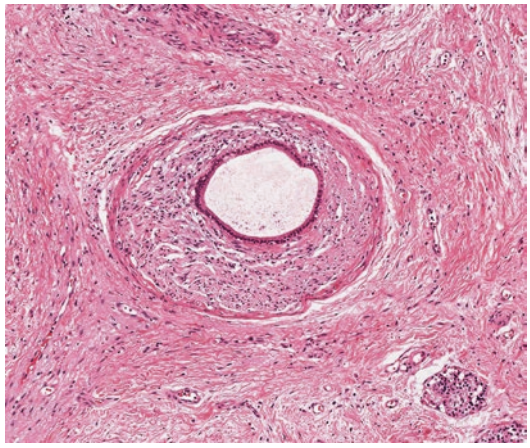

Fig. 1.29 Benign neural glandular inclusion: inclusion of a benign simple gland within a peripheral nerve is an exceptionally rare finding

Arterial and venous branches can be seen in all areas of the peripancreatic soft tissue. Blood vessels are particularly numerous in the adipose tissue facing the superior mesenteric artery, in the anterior adipose tissue surrounding the gastroduodenal artery, and in the anterior and posterior pancreatoduodenal crevices, where the arcades of the pancreatoduodenal arteries are located (see Sect. 1.3.5). Venous branches draining into the superior mesenteric vein (SMV) may be seen near the SMV groove.

Lymph nodes are present in the peripancreatic soft tissue, along the bile duct and the large blood vessels. The clinical grouping system of the lymph nodes in their various locations is described in Chap. 3 (see Fig. 3.27).

1.4.7 Major Ampulla and Papilla

The ampulla is the olive-shaped structure at the distal end of the pancreatic and common bile ducts, where the latter traverse the duodenal wall to empty their content into the duodenal lumen. The main pancreatic duct reaches the ampulla just caudal to the common bile duct (Fig. 1.2) (see Fig. 3.19). Both ducts are enveloped by the sphincter of Oddi, a circular muscle, which anchors in the duodenal muscularis propria and mucosae but functions independently of these. The sphincter muscle controls the flow of bile and pancreatic juice. It also prevents reflux of

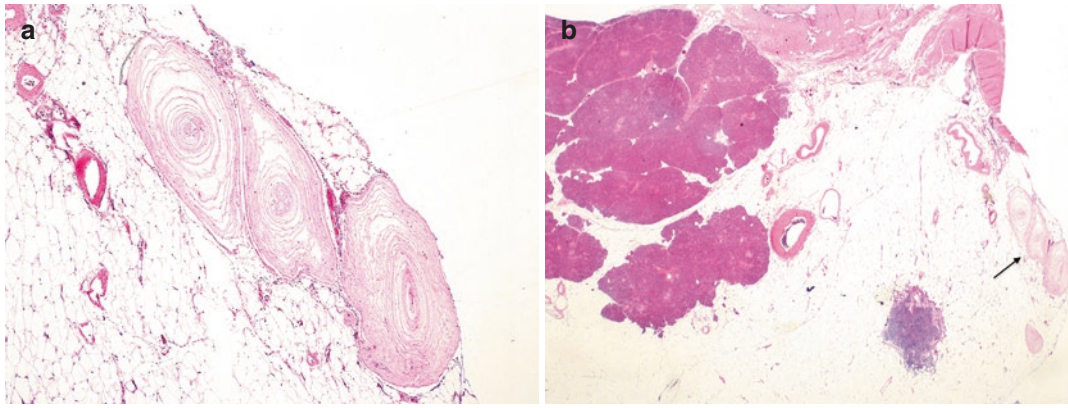

Fig. 1.30 Pacinian corpuscles: these specialized mechanoreceptors with a characteristic lamellar structure (**a**) are present in the adipose tissue surrounding the pancreas (**b**, *arrow*). They may be visible macroscopically, and on occasion they may be submitted for frozen section examination because of the intraoperative suspicion of micronodular cancer spread

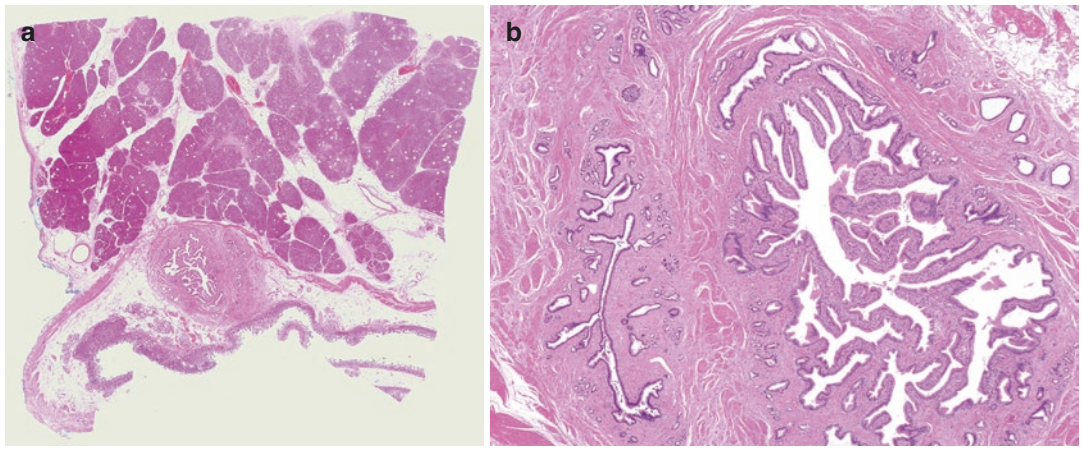

Fig. 1.31 Ampulla of Vater with separate lumina: the sphincter of Oddi envelops the main pancreatic and common bile duct together (**a**), but the lumina of both ducts are separated by a fibromuscular septum (**b**)

duodenal content, bile, and pancreatic juice into the pancreatic and bile duct.

The relationship between the pancreatic and common bile duct at the ampulla is complex. In the prototypical ampulla, both ducts join to form a single common channel. Alternatively, the lumina from both ducts can remain separated by a septum, while they drain through a single shared orifice at the mucosal surface of the papilla of Vater (Fig. 1.31). In a third variant, both ducts have separate lumina and they open separately into the duodenum, the ostia being located 1 mm to up to 1 cm or more apart (Fig. 1.32). The relative frequency of these three configurations varies between studies. Overall, over two thirds of individuals have a common channel, while an interposed septum is found in less than 10%. The length of the common channel varies from 1 mm to 12 mm, with an average of 4.4 mm. A 'long common channel', is defined as measuring over 6 mm in length such that the junction of both ducts is located outside the duodenal wall and the sphincter of Oddi cannot functionally affect the junction. This can lead to regurgitation and is associated with an increased risk of pancreatitis and biliary cancer (see Chap. 13).

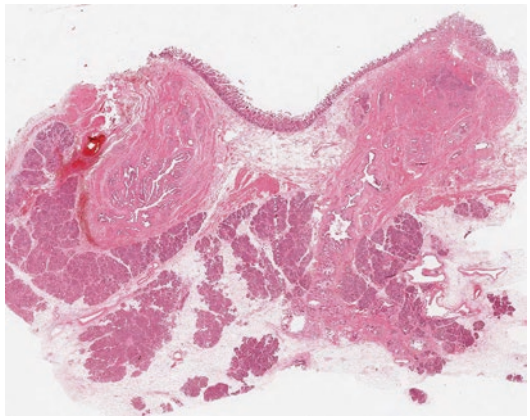

Fig. 1.32 Ampulla of Vater with separate channels: the common bile duct (*left*) and main pancreatic duct (*right*) open separately into the duodenum and are surrounded by their own sphincter muscle

Despite the fact that the word ampulla refers to a flask-like structure, the lumen of the ampullary channel is usually narrower than that of the joining ducts. Consequently, the mucosal lining of the ampulla is excessively folded, resulting in the characteristically star-shaped outlines of the mucosal surface. The long mucosal fronds of the ampullary mucosa, which are sometimes referred to as the vallecula, are covered with pancreatobiliary type epithelium (Fig. 1.33). The transition between the pancreatobiliary epithelium of the ampulla and the intestinal type epithelium lining the papilla of Vater is abrupt, although a small number of scattered goblet cells may be present within the ampullary mucosa. A considerable number of ducts and clustered glands are usually present around the ampulla and papilla. They drain into the recesses between the papillary mucosal fronds and are lined by simple mucinous columnar epithelium. Papillary folding of the mucosa lining the ampulla of Vater is believed to contribute to the prevention of reflux of duodenal content.

The point of junction of the ampulla with the common bile duct is characterized by the sudden transition of the sphincter of Oddi into the much thinner and lacunar muscle layer of the bile duct, and the abrupt flattening of the furrowed structure of the ampullary mucosa to the small irregular pleats of the bile duct mucosa (Fig. 1.34).

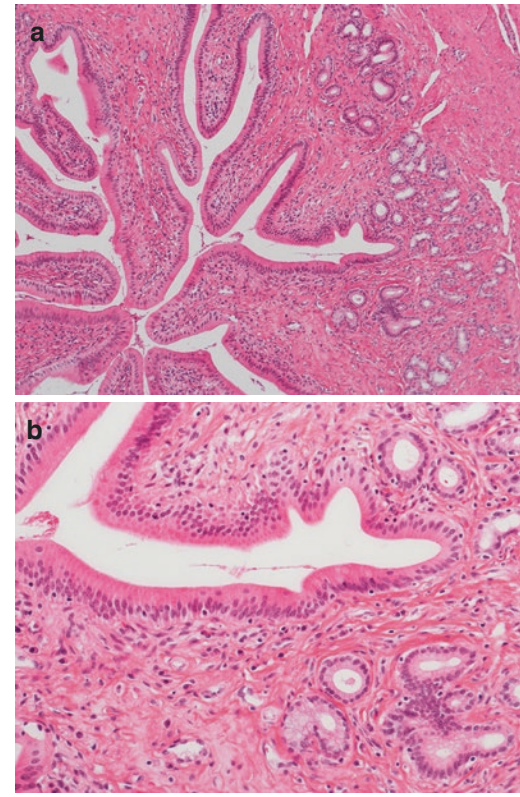

Fig. 1.33 Epithelial lining of ampulla of Vater: the ampulla has a star-shaped lumen and a highly folded mucosa (**a**). A single row of pancreatobiliary type epithelium lines the mucosa, and small mucinous glands empty into the recesses between the mucosal folds (**b**)

The mucosa of the ampulla and the surrounding duodenal submucosa contain numerous small blood vessels and lymphatic channels. Peripheral nerves are usually inconspicuous.

1.4.8 Minor Ampulla and Papilla

The terminal portion of the accessory pancreatic duct is the main component of the minor ampulla/papilla. It is always present but often regresses to a varying degree. A patent Santorini's duct is present in over 50% of individuals. The mucosal lining of Santorini's duct at the minor ampulla shows mild folding and is lined with simple pancreatobiliary type columnar epithelium. There is a circular coat of smooth muscle fibers, but it is controversial whether this has a sphincter func-

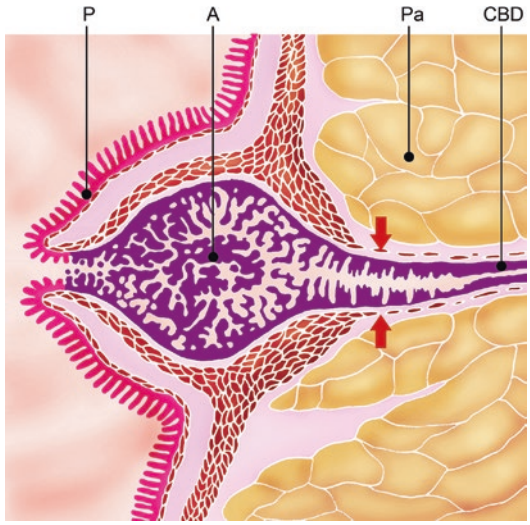

Fig. 1.34 Junction of ampulla of Vater and common bile duct: at the junction of both structures (*arrows*), the thin and lacunar muscle coat and the flatly pleated epithelium of the bile duct abruptly change into the deeply furrowed epithelium of the ampulla and the thick sphincter muscle (*A* ampulla, *CBD* common bile duct, *Pa* pancreatic parenchyma, *P* papilla of Vater) (Image courtesy and copyright of Paul Brown, The Leeds Teaching Hospitals NHS Trust, Leeds, UK)

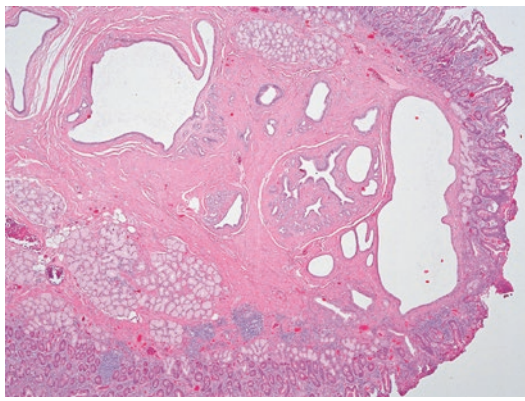

Fig. 1.35 Minor ampulla: in this case, Santorini's duct is dilated in some parts, but has retained its slightly folded mucosa in others. There is a thin smooth muscle coat

tion (Fig. 1.35). In 80% of individuals, pancreatic tissue is found in the minor ampulla, which may or may not show a connection with the pancreas proper (see Chap. 13, (Fig. 1.35). Tiny clusters of endocrine cells containing somatostatin- and PP-producing cells are frequently found within the minor ampulla [6].

1.4.9 Common Bile Duct

The bile duct mucosa usually forms flat pleats and is lined by epithelium that is identical to the epithelium of the main pancreatic duct. The sacculi of Beale are small pits of the bile duct epithelium, which dip into the bile duct wall. Towards their deep end, they are usually surrounded by a cluster of small, branched or simple glands. The latter drain into the sacculus, are lined by a cuboidal or low-columnar mucin-containing epithelium and may be encircled by condensed stroma (Fig. 1.36). The clustered arrangement of the small glandular lumina of the peribiliary glands aids in distinguishing the bile duct from the main pancreatic duct, as pancreatic branch ducts draining into the main duct are usually not surrounded by such glandular clusters.

The bile duct epithelium is supported by a layer of dense collagenous tissue, which in its turn is surrounded by a looser connective tissue layer that contains a varying number of discontinuous smooth muscle fibers. The latter become more prominent at the distal end of the common bile duct, proximal to the junction with the ampulla of Vater.

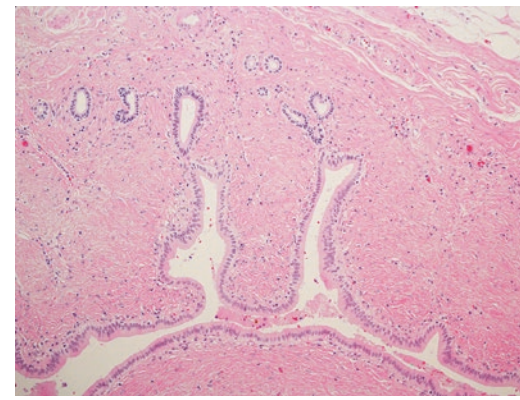

Fig. 1.36 Common bile duct: bile duct mucosa is lined by a single row of pancreatobiliary type epithelium. Sacculi of Beale extend from the lumen and communicate at their deep end with a small cluster of simple mucinous glands. The bile duct is surrounded by condensed fibrous stroma and a fragmented smooth muscle coat

References

1. Vikram R, Balachandran A, Bhosale PR, Tamm EP, Marcal LP, Chamsangavej C. Pancreas: peritoneal reflections, ligamentous connections, and pathways of disease spread. Radiographics. 2009;29:e34.
2. Horiguchi S-I, Kamisawa T. Major duodenal papilla and its normal anatomy. Dig Surg. 2010;27:90–3.
3. Strobel O, Rosow DE, Rakhlin EY, Lauwers GY, Trainor AG, Alsina J, Fernandez-Del Castillo C, Warschaw AL, Thayer SP. Pancreatic duct glands are distinct ductal compartments that react to chronic injury and mediate Shh-induced metaplasia. Gastroenterology. 2010;138:1166–77.
4. Sakata N, Yoshimatsu G, Kodama S. Development and characteristics of pancreatic epsilon cells. Int J Mol Sci. 2019;20:1867.
5. Verbeke C, Löhr M, Severin Karlsson J, Del Chiaro M. Pathology reporting of pancreatic cancer following neoadjuvant therapy: Challenges and uncertainties. Cancer Treat Rev. 2015;41:17–26.
6. Suda K. Histopathology of the minor duodenal papilla. Dig Surg. 2010;27:137–9.

Further Reading

Pan FC, Wright C. Pancreas organogenesis: from bud to plexus to gland. Dev Dyn. 2011;240:530–65.
Reichert M, Rustgi AK. Pancreatic ductal cells in development, regeneration, and neoplasia. J Clin Invest. 2011;121:4572–8.
Klimstra DS, Hruban RH, Pitman MB. Pancreas. In: Mills SE, editor. Histology for pathologists, 3rd edn, Chapt 30. Philadelphia: Lippincott Williams & Wilkins; 2007. p. 723–56.

Pancreatic Specimen Types

2

While the majority of surgical pancreatic specimens result from pancreatoduodenectomy and distal pancreatectomy procedures, a range of other specimen types may be received for pathology examination. This chapter provides a brief description of the various specimen types and the main indications for the corresponding surgical procedures. The handling of pancreatic specimens and biopsies is discussed in Chap. 3.

2.1 Pancreatoduodenectomy Specimens

Pancreatoduodenectomy is the standard surgical procedure for any tumor in the head of the pancreas, and the corresponding resection specimens are the most frequent in the pancreatic field. They can be divided into pancreatoduodenectomy specimens following the classical Whipple's resection, and those following the pylorus-preserving variant procedure (Fig. 2.1). Both specimen types are identical, except for the fact that the former includes the distal stomach, whereas the latter does not. Both specimen types comprise the duodenum from the pylorus to the ligament of Treitz, the pancreatic head, the extrapancreatic common bile duct up to the junction with the cystic duct, and the gallbladder (Fig. 2.2).

The surgical reconstruction following pancreatoduodenectomy involves a pancreatic anastomosis (pancreaticogastrostomy, pancreaticojejunostomy, or numerous variations), a hepaticojejunostomy, and a duodeno- or gastrojejunostomy (Fig. 2.3). If required, the surgical procedure can also include resection of a tangential or segmental part of the superior mesenteric or portal vein (see Figs. 3.23 and 3.24). In some pancreatic cancer centers, part of the hepatic artery or superior mesenteric artery may occasionally be resected in highly selected patients (see Fig. 9.83). If the remainder of the pancreas is healthy, resection of the pancreatic head, which

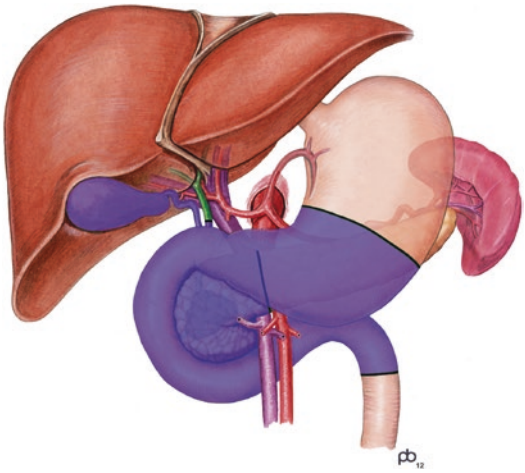

Fig. 2.1 Pancreatoduodenectomy: in the classical Whipple's operation, the pancreatic head is resected along with the duodenum, the common bile duct, cystic duct and gallbladder, and the distal stomach (areas shaded *blue*) (Image courtesy and copyright of Paul Brown, The Leeds Teaching Hospitals NHS Trust, Leeds, UK)

© Springer Nature Switzerland AG 2021
F. Campbell, C. S. Verbeke, *Pathology of the Pancreas*,
https://doi.org/10.1007/978-3-030-49848-1_2

Fig. 2.2 Whipple's resection specimen: pancreatoduodenectomy specimen including the distal stomach (classical Whipple's operation). Note the attached gallbladder

represents 60–70% of the bulk of the pancreas (see Chap. 1, Sect. 1.3.1.1), leaves sufficient pancreatic parenchyma behind for the exocrine (and to a lesser extent endocrine) function to be safeguarded. It is generally regarded that up to 80% of the (healthy) pancreas can be resected without causing exocrine or endocrine insufficiency.

The term *pancreaticoduodenectomy* specimen is commonly used synonymously. The radix pancreatico- refers to the pancreatic duct, whereas pancreato- refers to the pancreas. The term pancreatoduodenectomy is therefore more appropriate.

2.2 Distal Pancreatectomy Specimens

Distal pancreatectomy is the standard procedure for tumors in the body or tail of the pancreas, that is, any tumor located above or to the left of the superior mesenteric vein. The procedure consists of the resection of the pancreatic tail with vary-

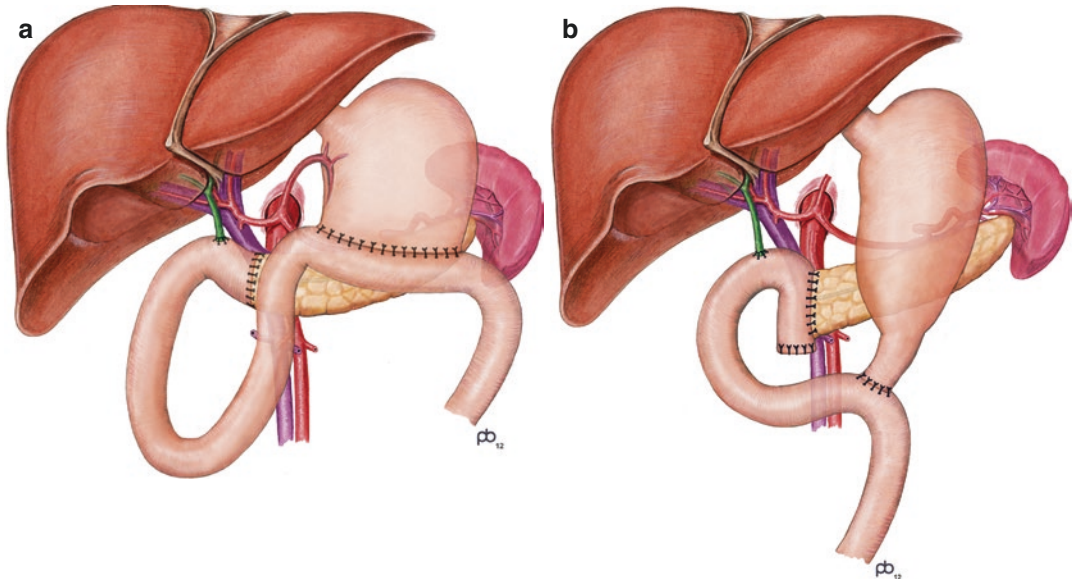

Fig. 2.3 Reconstruction following pancreatoduodenectomy: after a classical Whipple's operation, the pancreatic body, proximal stomach, and common bile duct are anastomosed onto a jejunal loop (**a**). Following a pylorus-preserving pancreatoduodenectomy, a similar procedure is followed, with exception of the anastomosis of the preserved short proximal duodenal stump onto the jejunum (**b**). (Image courtesy and copyright of Paul Brown, The Leeds Teaching Hospitals NHS Trust, Leeds, UK)

Fig. 2.4 Distal pancreatectomy specimen: the pancreatic body and tail have been resected for a pancreatic tumor causing fusiform swelling of the pancreas. Included in the resection is the unremarkable spleen

ing portions of the pancreatic body (Fig. 2.4). The dorsal resection plane is defined at the level of either the anterior pararenal space or Gerota's fascia. Resection of Gerota's fascia is useful in cases of suspected tumor growth towards the left adrenal gland, which is not uncommon in tumors of the pancreatic tail. Distal pancreatectomy specimens usually include the spleen, due to the close anatomical association of the tip of the pancreatic tail to the splenic hilum and of the splenic vessels to the dorsum of the body and tail of the pancreas. In accordance with oncological principles, the spleen is always included in distal pancreatectomy procedures for malignancy.

Distal pancreatectomy specimens are usually outnumbered by pancreatoduodenectomy specimens, firstly because of the overall later presentation of pancreatic cancer of the pancreatic body and tail, and secondly because cancer of the ampulla, distal common bile duct, and proximal duodenum is also resected by pancreatoduodenectomy.

In particular in the surgical community, the term *left-sided pancreatectomy* specimen is interchangeably used with distal pancreatectomy.

2.3 Total Pancreatectomy Specimens

The indications for this procedure are extensive main-duct intraductal papillary mucinous neoplasia (IPMN), IPMN with progression to carcinoma, familial or multifocal pancreatic cancer, pancreatic endocrine tumors in patients with multiple endocrine neoplasia type 1 (MEN1), or multiple metastases. This procedure may also be necessary to achieve complete resection of a centrally localized tumor of the pancreatic body. Resection of the portal vein, superior mesenteric vein and/or artery, or the celiac trunk can be part of the procedure, especially following neoadjuvant therapy in patients with tumor regression or stable disease (see Fig. 9.84).

In the context of pancreas transplantation, the native pancreas may be explanted and become available for pathology examination (see Chap. 22, Sect. 22.2).

2.4 Duodenum-Preserving Pancreatic Resection Specimens

The indications for duodenum-sparing procedures—pancreatic head resections or (sub-)total pancreatectomies—include chronic pancreatitis, benign or low-grade malignant neoplasms, slow-growing metastasis to the pancreas, MEN1, and patients with a high risk for pancreatic cancer (hereditary or familial pancreatic cancer) and early suspicious lesions on imaging. It can also be performed for persistent neonatal and infantile or adult hyperinsulinemic hypoglycemia. This is a more conservative procedure, with which a pancreatic head remnant of varying size can be left in situ (Fig. 2.5). It is a complex and more

Fig. 2.5 Duodenum-preserving subtotal pancreatectomy: a large proportion of the pancreatic head has been removed together with the entire body and tail of the pancreas in a patient with MEN1. Only a thin crescent of pancreatic tissue flanking the duodenum was left in situ

demanding procedure, which is performed only in specialist centers.

2.5 Complex Multivisceral En Bloc Resection Specimens

Pancreatoduodenectomy, distal pancreatectomy, or total pancreatectomy procedures may be extended by inclusion of one or several of the following organs: left adrenal gland, left kidney, stomach, omentum, colon, transverse mesocolon, small bowel, or a part of the liver (Figs. 2.6, 2.7, and 2.8) (see Chaps. 3 and 9, Sects. 3.6 and 9.17.3, Figs. 3.32, 3.33, 3.34, and 3.35). Resection of venous or arterial blood vessels may also be part of these complex surgical procedures.

2.6 Central Pancreatectomy Specimens

Pancreatic tumors located in the neck of the gland are a challenging surgical problem. The usual surgical options are pancreatoduodenectomy, distal pancreatectomy, or occasionally total pancreatectomy. Especially for small, well-circumscribed benign or non-invasive neoplastic tumors, central pancreatectomy is sometimes performed in selected patients as a function-preserving minimally invasive surgical proce-

Fig. 2.6 Complex multivisceral en bloc resection specimen: this resection specimen consists of the pancreatic body and tail, spleen, stomach, and colon. Resection was performed for a large, centrally located ductal adenocarcinoma (invisible on this picture), which had infiltrated all resected structures. Note the large tumor-induced ulcers of the gastric mucosa. A slice of this specimen is illustrated in Fig. 9.3

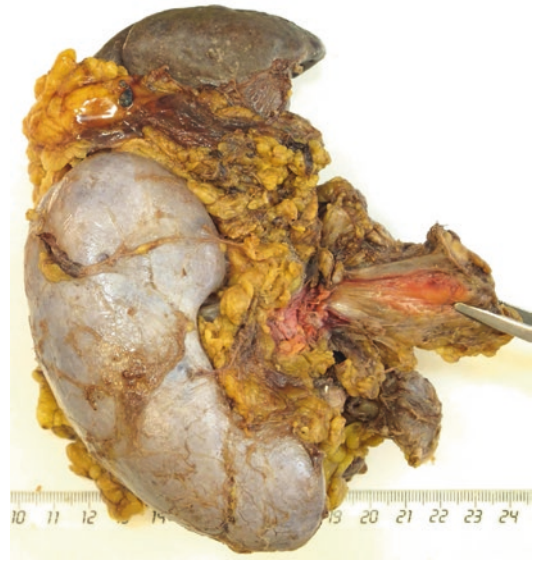

Fig. 2.7 Extended distal pancreatectomy specimen: view onto the posterior aspect of a distal pancreatectomy specimen with splenectomy and resection of the left kidney. Also included, but invisible on the photograph, are the left adrenal gland and a segment of colon (same specimen as in Fig. 3.33)

Fig. 2.8 Extended distal pancreatectomy specimen: view onto the anterior aspect of a distal pancreatectomy specimen with splenectomy and resection of a segment of colon that was adherent to a ductal adenocarcinoma arising from the pancreatic tail

dure. As the procedure requires the establishment of two pancreatic anastomoses, the postoperative risk of anastomatic leakage is of concern.

2.7 Enucleation Specimens

Pancreatic tumor enucleation is a further tissue- and function-preserving procedure, which is occasionally performed in highly specialized centers. The indications for this procedure are in principle small, well-circumscribed benign or low-grade lesions that are located away from the main pancreatic duct and common bile duct, including small pancreatic endocrine tumors, benign or low-grade cystic lesions, or side-branch intraductal papillary mucinous neoplasms (IPMNs). As indicated by the name of the procedure, the lesion is removed with (at most) a minimal amount of surrounding pancreatic tissue. The orientation of these specimens can be difficult, and marker sutures to facilitate identification of the anterior/posterior and proximal/distal aspect of the specimen may be helpful. In case of a side-branch IPMN, the surgeon may wish to mark the transection margin of the branch duct, with which the lesion was connected to the pancreatic duct system. An example of an enucleated side-branch IPMN is shown in Fig. 2.9.

Fig. 2.9 Enucleation specimen: a unilocular side-branch intraductal papillary mucinous neoplasm has been enucleated from the pancreatic tail. Note the absence of adherent pancreatic parenchyma on the surface of the collapsed cystic lesion

2.8 Specimens Following Frey, Beger, or Puestow Procedures

These surgical procedures are performed for chronic pancreatitis, with severe pain as the main indication. The procedures aim at decompressing the pancreatic duct system, which is deemed to be a major (but not exclusive) cause of pain in chronic pancreatitis.

The Frey procedure consists of a local resection of the pancreatic head combined with a pancreaticojejunostomy via a Roux loop (Fig. 2.10). The parenchymal resection consists of the coring out of 4–12 g of diseased tissue from the pancreatic head, leaving a 'tissue crater' in the pancreatic head. The latter is drained by the same Roux loop that is anastomosed onto the longitudinally opened main pancreatic duct. The tissue specimen received for pathology examination consists usually of multiple irregular fragments of firm, pale, often calcified tissue, which cannot be further orientated and which require com-

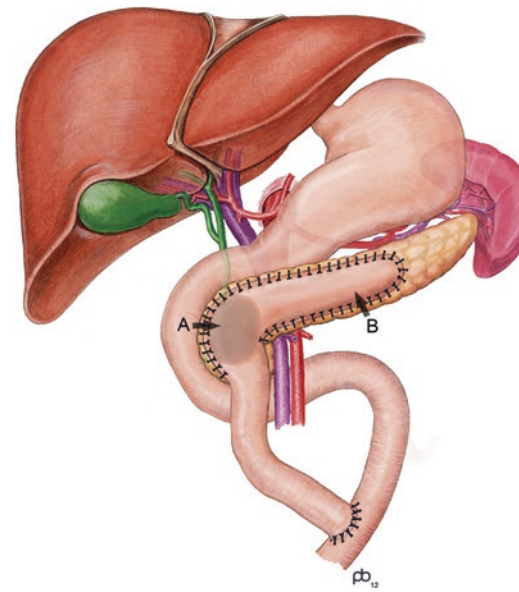

Fig. 2.10 Frey procedure: tissue is cored out of the pancreatic head while preserving the bile duct. A jejunal loop is anastomosed over the tissue crater (**a**) and the longitudinally opened pancreatic duct (**b**) (Image courtesy and copyright of Paul Brown, The Leeds Teaching Hospitals NHS Trust, Leeds, UK)

plete embedding and histological examination to exclude malignant transformation in the context of chronic pancreatitis.

According to the Beger procedure, a part of the pancreatic body and most of the pancreatic head are resected, preserving a sleeve of pancreatic tissue adjacent to the duodenum such that the blood supply to the latter is ensured. The intrapancreatic common bile duct is also preserved. Reconstruction is performed through a Roux loop with an anastomosis to the pancreatic remnants of the head and body of the gland (Fig. 2.11). The specimen resulting from this procedure consists of a fragment of pancreatic head and body, which may be received en bloc or as separate parts or fragments. For the same reason as outlined for the handling of Frey specimens, the sample should be embedded in it is entirety.

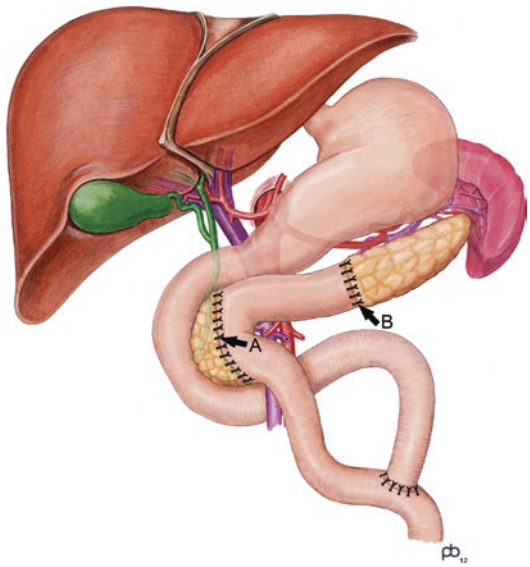

Fig. 2.11 Beger procedure: a part of the pancreatic body and most of the pancreatic head are resected, leaving a thin crescent of the latter and the intrapancreatic common bile duct in situ. A jejunal loop is anastomosed on the transection margins of the remnant head (**a**) and body (**b**) of the pancreas (Image courtesy and copyright of Paul Brown, The Leeds Teaching Hospitals NHS Trust, Leeds, UK)

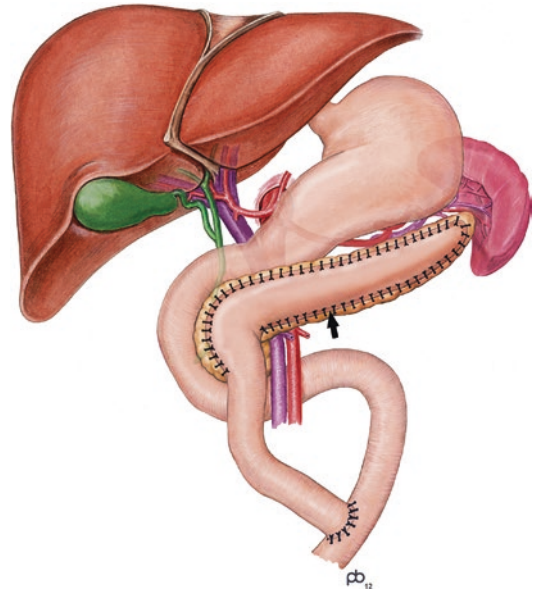

Fig. 2.12 Puestow procedure: the main pancreatic duct is opened longitudinally over 8–10 cm. Drainage of pancreatic secretion is ensured by anastomosis with a jejunal loop (*arrow*) (Image courtesy and copyright of Paul Brown, The Leeds Teaching Hospitals NHS Trust, Leeds, UK)

The Puestow procedure consists of exposure of the main pancreatic duct from the neck to the tail of the gland, whereby a Roux loop is anastomosed to the anterior pancreatic surface to allow direct drainage of the main and secondary pancreatic ducts over a length of 8–10 cm (Fig. 2.12). During the procedure, calculi may be removed from the ducts, and on occasion, small fragments of tissue may also be resected and submitted for pathology examination.

2.9 Laparoscopic and Robot-Assisted Resection Specimens

Some of the above surgical resection procedures, in particular distal pancreatectomy and enucleation, may be performed laparoscopically or

using a robot-assisted approach. The mode of surgery—open, laparoscopic, or robot-assisted—should not affect any aspect of the surgical specimen, except for the fact that transection margins, in particular the resection margin of the pancreas, are usually closed with a staple line.

2.10 Pancreas Allograft

A failed pancreas allograft may be removed at the time of re-transplantion. The components of this surgical specimen type are described in detail in Chap. 22, Sect. 22.3.1, Table 22.2.

Further Reading

Aimoto T, Uchida E, Nakamura Y, Yamahatsu K, Matsushita A, Katsuno A, Cho K, Kawamoto M. Current surgical treatment for chronic pancreatitis. J Nippon Med Scheme. 2011;78:352–9.

Matsuoka L, Parekh D. The minimally invasive approach to surgical management of pancreatic diseases. Gastroenterol Clin N Am. 2012;41:77–101.

Matsuoka L, Selby R, Genyk Y. The surgical management of pancreatic cancer. Gastroenterol Clin N Am. 2012;41:211–21.

Check for updates

3 Specimen Dissection and Sampling

Macroscopic examination is a key step in the process of reporting on pancreatic resection specimens. The complexity of the local anatomy, the large number of inflammatory and neoplastic diseases that can occur in the pancreas, and the existence of anatomical variation and developmental anomalies require an accurate and 'fail-proof' approach to the dissection and sampling of pancreatic specimens. This chapter provides detailed practical guidance on the various aspects of specimen handling and macroscopic examination. Where appropriate, alternative techniques will be discussed.

3.1 Handling of Fresh Specimens

While dissection of surgical pancreatic resection specimens is best and easiest performed after fixation of the tissue, it is desirable to receive specimens fresh within a controlled, short time interval following surgical removal. The prime motivation is obviously the procurement of fresh tissue samples for biobanking or dedicated research purposes. In addition, reception of the fresh specimen allows preliminary preparation of the tissues to ensure optimal fixation. On occasion, it may be desirable to take photographs of particular lesions prior to fixation.

Most pathology departments will have established a standardized operating protocol describing the locally agreed procedures for fresh tissue sampling and subsequent (cryo-)preservation, storage, and registration. Sampling should be accomplished in the shortest possible time, and recording of the time from specimen reception to tissue sampling is recommended. Which tissues are to be sampled depends on local agreement, but usually, tissue fragments from the tumor and the tumor-free pancreas are collected.

As an important general rule, fresh tissue sampling for biobanking or other purposes should never jeopardize correct and detailed diagnostic reporting. It is therefore of key importance to limit incisions and sampling volumes to a minimum and to refrain from sampling in case the tumor is small or cannot be identified with certainty. The latter is not an uncommon problem, as the tumor is often invisible on external specimen inspection and may not be identifiable on palpation due to concomitant fibrosis of the surrounding pancreatic tissue. The following findings may be helpful in locating the tumor:

- Irregularity of the specimen surface: bulging of the pancreatic surface, retraction of the groove of the superior mesenteric vein (SMV groove), adherence to the pancreas of a segment of SMV or other structures or organs.
- Ulceration or irregularity of the duodenal mucosa or papilla of Vater.
- A palpable mass.
- Dilatation of the main pancreatic duct or common bile duct: if absent, the tumor is likely to

© Springer Nature Switzerland AG 2021
F. Campbell, C. S. Verbeke, *Pathology of the Pancreas*,
https://doi.org/10.1007/978-3-030-49848-1_3

be located in the uncinate process or in the caudal half of the pancreatic head, inferior to the level of the ampulla.

The incision(s) to be made for fresh tissue sampling should be in line with the dissection technique that is used. As explained below, serial specimen slicing in the axial plane offers several advantages and is therefore the recommended technique. If this technique is used, incision of the fresh specimen should be in the axial plane, at the level where the tumor has been located, and, if possible, avoiding transection of an overlying segment of resected vein.

When sampling the tumor, care should be taken to avoid areas of involvement of anatomical structures that are important for correct reporting and staging, that is, for the assessment of the TNM descriptors, in particular T, N, and R. In practice, this means that samples are best taken from central tumor areas to avoid interference with the tumor periphery, which is relevant for tumor measurement (pT-stage) and assessment of the surfaces and margins of the specimen (R-status) (Fig. 3.1). For small tumors, it may be impossible to avoid sampling of these critical areas, which on occasion may preclude fresh tissue procurement.

The use of disposable biopsy corers is recommended, because they allow sampling of tissue pieces that are uniform in size and shape. As the corers are available in different sizes, they facilitate precise sampling. Tumor-free pancreatic tissue may be easily sampled at the transection margin of the pancreatic neck, provided this is well away from the tumor. Alternatively, tumor-free tissue can be taken from the incision that has been made for sampling of the tumor, if the latter is sharply delineated from the surrounding pancreatic parenchyma. Using a separate knife, scalpel, and forceps for sampling of tumor and tumor-free tissue may be helpful in avoiding cross-contamination.

To allow optimal formalin-fixation, it is important that all hollow organs are opened and rinsed. This can be done after fresh tissue sampling to minimize bacterial contamination, unless the tumor is present at the duodenal mucosal surface and opening of the duodenum is required to allow sampling. In the case of a Whipple's specimen (see Chap. 2, Sect. 2.1), the distal part of the stomach is opened along the greater curvature. At the pylorus, the longitudinal incision is continued along the duodenal wall opposite to the papilla of Vater. To avoid inadvertent cutting through lesions in the duodenum, the latter should be carefully probed with the finger to identify possible lesions prior to longitudinal incision. If included in the specimen, the gallbladder should also be opened longitudinally. Subsequently, all opened structures are rinsed with cold water.

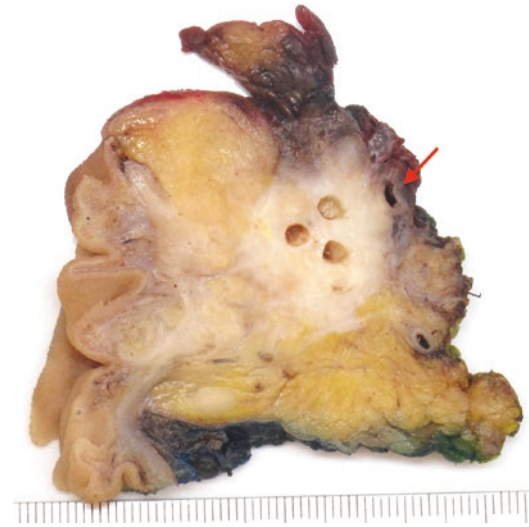

Fig. 3.1 Biobanking of tumor tissue from a pancreatoduodenectomy specimen: using a tissue corer, fresh tumor tissue can be sampled easily from an axial incision through the pancreatic head. Samples are taken from the center of the tumor, leaving untouched the tumor periphery and its relationship to the adjacent venous resection (*arrow*) and specimen surface. On microscopic examination, the punched-out holes allow unequivocal identification of the site of biobanking

In the case of large cystic tumors, if these are not already opened for the purpose of biobanking, it may be advisable to make a controlled linear incision of the wall (where the latter exhibits no specific features, that is, no adherence to other structures or palpable solid mass) to allow drainage of content and filling of the cyst cavity with formalin. A similar approach may be considered for bulky solid tumors, should these not have been incised for fresh tissue sampling.

Color-coded inking of the various specimen surfaces is usually done after formalin fixation, as the ink tends to adhere better to fixed tissue (see Sect. 3.3.2). Alternatively, inking can be performed on the fresh specimen, and if staining is required prior to fresh tissue sampling, the use of dry ground pigment rather than the usual liquid specimen stains may be considered. Immediately before application, the ground pigment is dissolved in acetone, which allows almost instantaneous drying of the ink. This avoids smearing of the various colors, which is not uncommonly a problem with liquid inks.

3.2 Specimen Fixation

Pancreatic specimens should be fixed in a large volume of 10% buffered formalin. The specimen can float freely in the fixative, as the risk of fixation-induced tissue shrinkage is low in this solid organ. However, in some pathology departments, the specimen is pinned onto a corkboard to limit fixation-induced distortion of the area that was incised for fresh tissue sampling. Fixation for 48 hours is usually adequate, but shorter fixation times may be appropriate for smaller specimens such as those resulting from central pancreatectomy or surgical enucleation (see Chap. 2, Sects. 2.6 and 2.7). On occasion, additional fixation of the cassetted tissue samples may be required prior to tissue processing.

3.3 Macroscopic Examination of Pancreatoduodenectomy Specimens

Because pancreatoduodenectomy specimens differ from other surgical pancreatic resection specimens in the anatomy of their constituting tissues, they require a different dissection technique, which is the focus of this section. The approach to other parts of the macroscopic examination process, for example, tissue sampling, macroscopic description, and photodocumentation, is not particular to pancreatic head resection specimens and can be applied to any surgical resection specimen of the pancreas. A summary of the various steps to be undertaken during specimen dissection and sampling is provided in Table 3.1.

Table 3.1 Summary of handling of pancreatoduodenectomy specimens

Before fixation
• Open longitudinally and rinse the stomach, duodenum, gallbladder
• Make one or two axial incisions for biobanking, if required
Fixation (approximately 48 hrs)
After fixation
• Take measurements: stomach, duodenum, head of pancreas (in 3 dimensions), gallbladder, cystic duct, extrapancreatic common bile duct, and any other structures or organs included in specimen (e.g., venous resection)
• Carefully remove surgical sutures and clips
• Sample the transection margins: proximal (gastric or duodenal), distal (duodenal), pancreatic neck, common bile duct
• Inspect and sample the gallbladder and cystic duct
• Ink the pancreatic surfaces according to an agreed color code: anterior, SMV groove, surface facing SMA, posterior, around extrapancreatic common bile duct. Ink in different colors any other important structures (e.g., venous resection)
• Remove the distal duodenal 'tail' and clip the duodenal 'wings' (if normal)
• Serially slice the specimen in the axial plane, slice thickness 3 mm
• Lay out the specimen slices in sequential order
• Take photographs: overview and close-ups
• Describe the tumor: shape, texture, solid/cystic, color, size and localization (in 3 dimensions), relationship to key anatomical structures (ampulla, duodenum, common bile duct, peripancreatic soft tissue, vein), and distance to the nearest margins
• Describe any other lesions, including their size and localization
• Take tissue samples following the sequential order of the specimen slices; record in the block key the number of the slice from which the samples stem
• Take at least one whole mount sample, if possible, from the slice where the tumor is at its largest
• Take standard-size samples from other specimen slices by dividing them in a geometrical way and including anatomical 'landmarks'
• Ensure that all lymph nodes are sampled 'en bloc' with the inked specimen surface and/or other anatomical 'landmarks'

Abbreviations: *SMA* superior mesenteric artery, *SMV* superior mesenteric vein

3.3.1 Dissection Techniques

Worldwide, a variety of dissection techniques for pancreatoduodenectomy specimens are currently being used. The three main approaches differ in the plane of dissection, and whether or not the pancreatic and bile duct are opened longitudinally.

3.3.1.1 Bivalving or Multivalving Technique

According to this technique, the main pancreatic duct and common bile duct are probed, and the specimen is sliced once (bivalving) or several times (multivalving) along the plane defined by both probes (Fig. 3.2). In this way, both ducts are exposed longitudinally in only two specimen slices facing the same dissection plane. This technique is challenging, not only when it comes to the insertion of the probes into the narrow ducts that are often distorted or obstructed by tumor. Equally difficult is the subsequent slicing of the specimen along the probes. The resulting slices are large and require further dissection, which is usually done by slicing in an additional, perpendicular plane. The use of different planes, one of which varies between specimens depending on the configuration of the pancreatic and bile duct, hinders the pathologist's mental 3-dimensional reconstruction of the tumor and its exact localization within the pancreatic head.

3.3.1.2 Bread Loaf Slicing Technique

Following this technique, the main pancreatic duct and common bile duct are left untouched. Instead, the pancreatic head is serially sliced along a plane perpendicular to the longitudinal axis of the pancreatic neck (Fig. 3.3). The main disadvantage of this technique is of a practical nature. The rubbery texture of the duodenum renders it difficult to slice the latter and the flanking pancreas in a longitudinal fashion, with the result that the specmen slices through the ampulla and the junction with the pancreatic and common bile duct may be suboptimal, for example incomplete, fragmented, or thicker than desired.

Serial slicing perpendicular to an axis that follows the curvature of the pancreatic head is advocated by the Japan Pancreas Society (JPS) [1]. It solves the above-mentioned practical problem but has the disadvantage that sectioning is

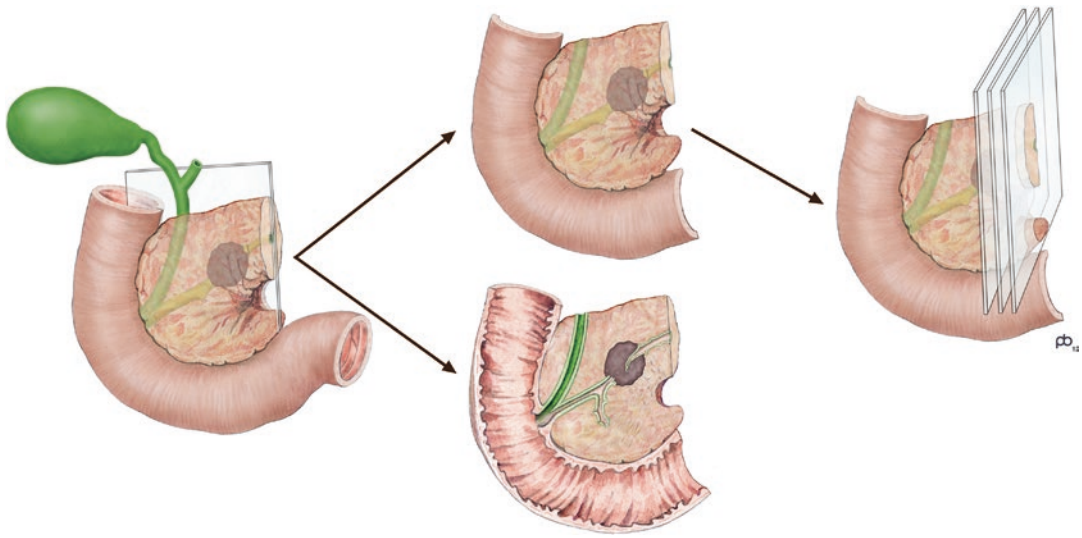

Fig. 3.2 Bivalving or multivalving dissection technique: the pancreatoduodenectomy specimen is sliced in a plane defined by probes in the main pancreatic duct and common bile duct. As the resulting slices are large, further dissection is usually performed in a plane perpendicular to the pancreatic neck (Image courtesy and copyright of Paul Brown, The Leeds Teaching Hospitals NHS Trust, Leeds, UK)

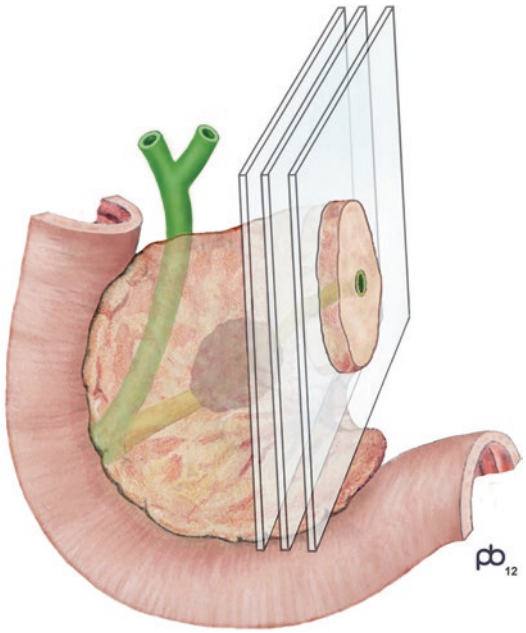

Fig. 3.3 Bread loaf slicing technique: the pancreatoduodenectomy specimen is serially sliced in a plane perpendicular to the pancreatic neck (Image courtesy and copyright of Paul Brown, The Leeds Teaching Hospitals NHS Trust, Leeds, UK)

not parallel but fan-like and the resulting specimen slices are wedge-shaped rather than square.

3.3.1.3 Axial Slicing Technique

According to this technique, the specimen is sliced in an axial plane, that is, perpendicular to the longitudinal axis of the descending duodenum (Fig. 3.4). Slicing is easy to perform, as the duodenum is sliced in a cross-sectional fashion, and it results in a large number of thin slices (on average 12 or more), which allow good views and from which it is easy to take tissue samples for microscopic examination. As the axial dissection plane is identical to that of CT- or MRI-imaging, correlation between pathology and imaging is straightforward and usually much appreciated by the radiologists and surgeons. The dissection plane is fixed, that is, independent of duct configuration as is the case for the bivalving or multivalving technique, with the result that key anatomical structures such as the ampulla, common bile duct, and main pancreatic duct, always occur at the same position in the specimen slices and are therefore easily identified.

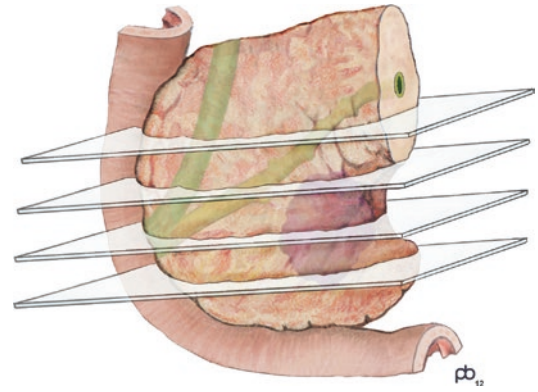

Fig. 3.4 Axial slicing technique: the pancreatoduodenectomy specimen is serially sliced in a plane perpendicular to the longitudinal axis of the descending duodenum (Image courtesy and copyright of Paul Brown, The Leeds Teaching Hospitals NHS Trust, Leeds, UK)

Consequently, any deviation from normal, either as an anatomical variant or a pathological lesion, is easy to identify and to locate in relationship with the surrounding anatomical structures. The latter is particularly important for the correct identification of the origin of the cancer, that is, whether adenocarcinoma in the pancreatic head is derived from the pancreas, ampulla, or distal common bile duct. Regarding the assessment of the margin status, it is important to note that the entire surface of the pancreatic head can be inspected in every specimen slice (Fig. 3.5).

The combination of these advantages allows not only exact identification of the 3-dimensional localization and extent of the tumor in the specimen, it also facilitates accurate margin assessment [2–5]. The proximity of the tumor to the various resection margins can be examined in detail in every specimen slice (see also Fig. 3.29). In some countries and pancreatic cancer centers, the axial specimen slicing technique has been accepted as an integral part of the national recommendations for the handling of pancreatoduodenectomy specimens [6, 7].

3.3.2 Inking of Surfaces

Inking of resection margins and specimen surfaces can be done before or after fixation. Prior

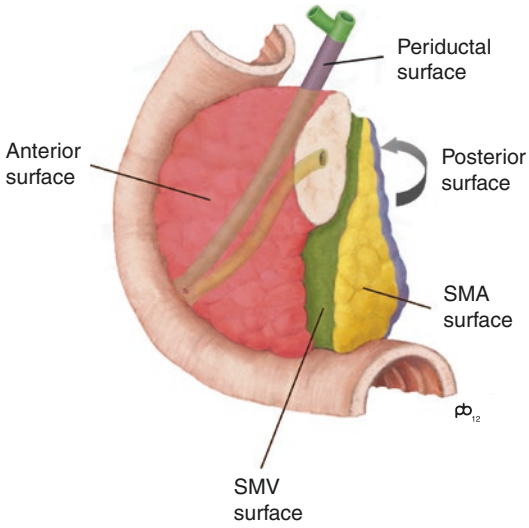

Fig. 3.5 Circumferential resection margins in a pancreatoduodenectomy specimen: color-coded inking facilitates identification of the circumferential margins: anterior (*red*), facing the SMV (*green*), facing the SMA (*yellow*), posterior (*blue*), and periductal (*purple*) (Image courtesy and copyright of Paul Brown, The Leeds Teaching Hospitals NHS Trust, Leeds, UK)

Fig. 3.6 Fixation of inks on the specimen surface: acetic acid is sprayed onto the inked surfaces through a thin paper towel to avoid running of colors due to the jet of the spray

to application of the ink, all surgical sutures and metal clips should be carefully removed to allow unhampered specimen slicing. Removal of the clips and sutures should be done without tissue disruption, as the tissue at the specimen surface represents the circumferential resection margin. If conventional liquid inks are used, it is important to pad dry the specimen surface before applying the ink and to spray with acetic acid (10%) to improve adhesion of the ink to the specimen surface. The acid is best sprayed through a paper towel that is wrapped around the specimen, such that the jet of the spray does not make the ink run over the tissue surface (Fig. 3.6). The use of different colors of ink for the various parts of the specimen surface according to an agreed color-code allows unequivocal identification of these surfaces both during macroscopic and microscopic examination. The following section lists the structures that require color-coded inking and describes how these can be identified (Fig. 3.5).

The *transection margin of the pancreatic neck* is readily identifiable, and it is therefore a good starting point when identifying the various pancreatic surfaces. The transection margin shows bare pancreatic parenchyma and contains the main pancreatic duct, which in many cases is dilated. The length of the neck can vary slightly, but in most cases it is less than 1 cm long and protrudes somewhat from the superior left-lateral aspect of the pancreatic head (Fig. 3.7). Inking of this margin is best done after en face sampling of the transection margin (see Sect. 3.3.8), because this allows assessment of completeness of excision at this margin. If unequivocal identification of the main pancreatic duct may be of particular importance (e.g., in case of intraductal papillary mucinous neoplasia), introducing a small amount of ink into the main duct at the transection margin may be helpful.

The surface of the groove of the superior mesenteric and portal vein ('*SMV margin*' or '*SMV groove*') is located immediately posterior to the pancreatic transection margin (see Chap. 1, Sect. 1.3.1.2). It runs in a slightly curved fashion along the left-lateral aspect of the pancreatic head. Its surface is normally smooth and slightly shiny, and it may sometimes be flanked on either side by multiple clips or sutures on small veins that drain from the pancreatic head into the superior mesenteric vein (Fig. 3.7). If a venous resection was undertaken, the segment of vein

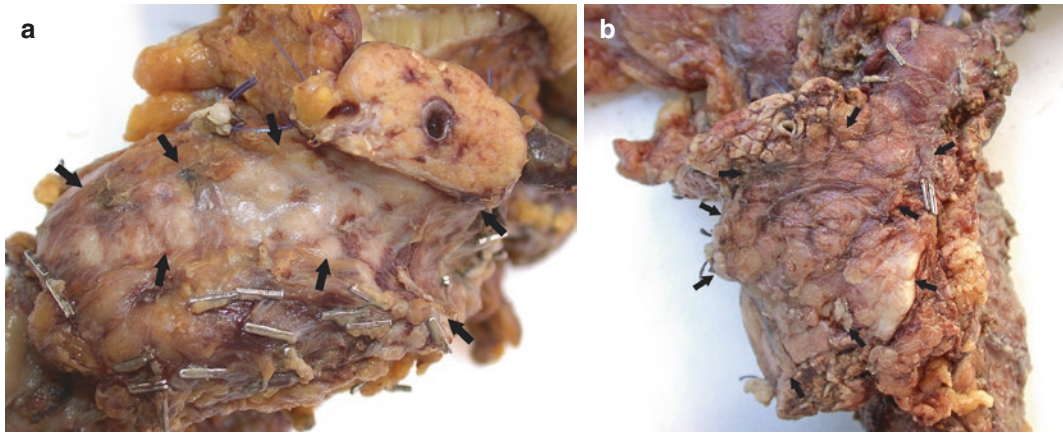

Fig. 3.7 SMV groove and pancreatic neck: the transection margin of the pancreatic neck is easily identified by the presence of lobulated parenchyma and the cross-sectioned main pancreatic duct. The SMV groove (*arrows*) runs posterior to the pancreatic neck, is slightly curved, and can be fairly narrow and deep (**a**) or wide and shallow (**b**). Note the rows of metal clips on small veins draining into the SMV

will be found adherent to the SMV groove. It is recommended to ink the resected piece of vein with a different color to facilitate identification following specimen slicing and during microscopic examination (Fig. 3.8).

The resection margin facing the superior mesenteric artery ('*SMA margin*') lies posterior and to the left of the SMV groove. In contrast to the latter, the surface of the SMA margin is rough, fibrous, and often irregular. It is usually wedge-shaped, that is, narrower towards the cranial aspect of the pancreatic head and broader towards the inferior pole (Fig. 3.5).

The *posterior margin* is the fibrous but relatively smooth, flat surface at the back of the pancreatic head. It extends from the left-lateral side of the SMA margin to the posterior duodenal wall. The angle between the SMA and posterior margin is usually acute and well-defined.

The *anterior surface* of the pancreas is not a true margin, but rather a free anatomical surface, which faces the lesser sac. It extends from the SMV groove to the anterior duodenal wall. It is usually smooth but can on occasion be overlaid with adipose tissue. As breaching of this surface by a cancer bears the risk of local tumor spread or recurrence, the anterior surface should be part of the macroscopic and microscopic assessment (see Chap. 9, Sect. 9.11.4, Fig. 9.44).

Finally, the surface of the soft tissue sheath surrounding the extrapancreatic common bile duct stump also represents a circumferential resection margin, which is sometimes referred to as the '*periductal margin*' or '*radial bile duct margin*'. The extrapancreatic stump of the common bile duct can be easily found by following the SMV groove in a cranial direction, as the bile duct stump lies immediately adjacent to the cranial end of the SMV groove.

3.3.3 Stents, Coils, and Glues

Because obstructive jaundice is the most common presenting symptom of pancreatic head tumors, many pancreatoduodenectomy specimens contain a stent. The latter lies within the common bile duct and protrudes over a short distance from the papilla of Vater. The presence and material (plastic or metal) of a stent should be recorded in the macroscopic description. Plastic stents are usually inserted with a view to short-term jaundice relief, whereas metal stents are indicated if biliary drainage should be ensured for a longer period of time. For this reason, pancreatic resection specimens following neoadjuvant treatment often contain a metal stent to allow biliary drainage during the entire preoperative treatment period.

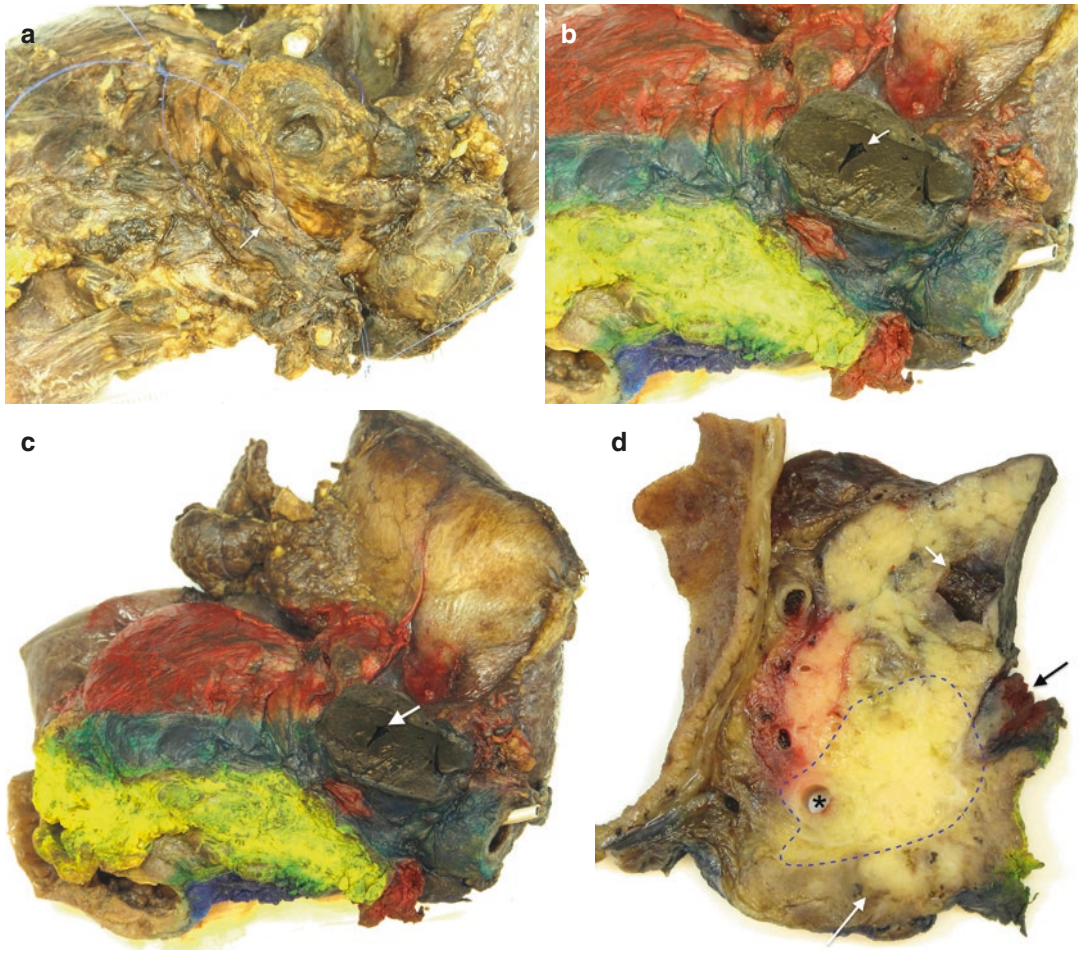

Fig. 3.8 Inking of a Whipple's specimen with venous resection: a small venous resection (*arrow*) consisting of a sleeve of the superior mesenteric vein (SMV) is attached to the SMV groove at the level of the pancreatic head. Note the surgical marker suture (**a**). The vascular sleeve is labeled with red ink, while the other surfaces are inked according to an agreed color code (pancreatic transection margin: *black*, SMV groove: *green*, SMA margin: *yellow*, anterior surface: *red*). Note the dilated main pancreatic duct (*arrow*) and a plastic stent in the common bile duct (**b**, **c**). An axial specimen slice through the venous resection (*black arrow*) shows it close relationship to the poorly circumscribed tumor (*dotted line*). Note the punched-out lumen of the tumor-obstructed common bile duct (*asterisk*), a lymph node metastasis in the posterior peripancreatic fat (*long white arrow*), and the dilated main pancreatic duct (*short white arrow*) (**d**)

Plastic stents are difficult to remove as they are barbed, but since they can be sliced easily, they are best left in place and removed from the slices prior to tissue sampling (Fig. 3.9).

Metal stents obviously require removal before slicing. Because tumor tissue may have grown into the meshwork of the stent, removal of it by simple pulling bears the risk of marked tissue disruption. A more gentle removal is achieved by extracting the metal wires one by one with forceps, which may be facilitated by cutting as many as possible of the wires that protrude from the papilla of Vater, such that the metal mesh is partially broken up. After removal of the stent, the common bile duct will typically be widely open, often with a visible imprint of the metal mesh onto the bile duct mucosa (Fig. 3.10). A plastic stent of a smaller caliber than a plastic

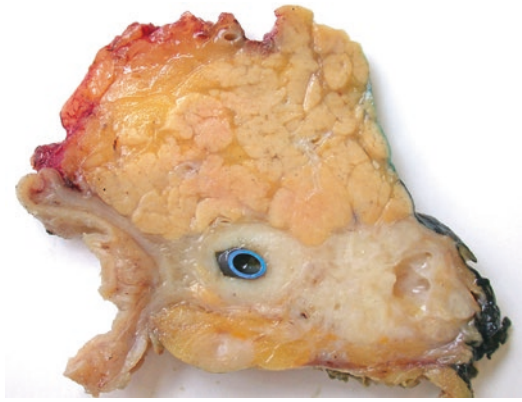

Fig. 3.9 Plastic biliary stent: a blue plastic tube secures biliary drainage through the common bile duct, which is infiltrated and narrowed by carcinoma

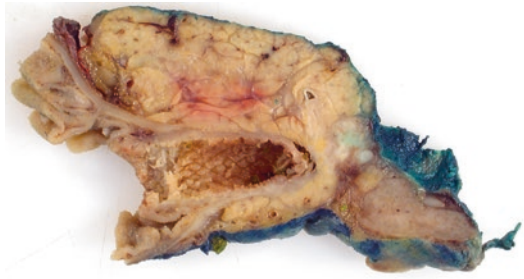

Fig. 3.10 Biliary dilatation due to metal stent insertion: after removal of a metal stent, the common bile duct remains widely open and a reticular imprint of the metal mesh can be seen on the bile duct mucosa

biliary stent may be found in the main pancreatic duct in patients with chronic obstruction (Fig. 3.11).

Fibrin glue or sealant is a surgical formulation used to create a fibrin clot for hemostasis or wound healing and may be used, for example, following enucleation of a small lesion (Fig. 3.12). Duct occlusion in the remnant pancreas by injection of a non-biodegradable "glue" of varying chemical composition, is a procedure that mainly belongs to the past (Fig. 3.13). It was used to prevent postoperative anastomotic leakage following pancreatoduodenectomy and induced atrophy of the pancreatic remnant with ensuing exocrine and endocrine insufficiency.

On rare occasion, coil embolization for massive hemorrhage may have preceded resection of

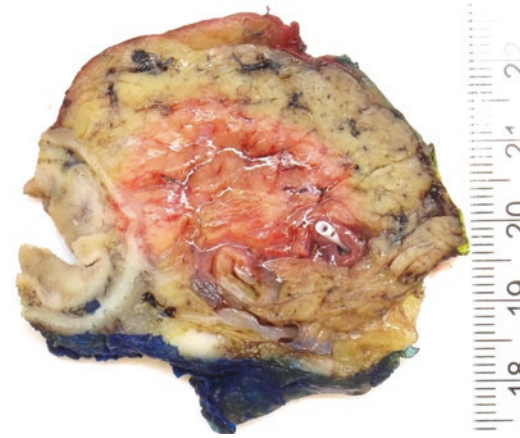

Fig. 3.11 Pancreatic duct stent: a plastic stent with a small caliber is inserted in the main pancreatic duct because of chronic duct obstruction

usually large pancreatic cancers, and the small metal coil may be identified during specimen dissection (Fig. 3.14). Other, non-metallic embolization particles may be seen only microscopically in blood vessels adjacent to areas of tumor necrosis (Fig. 3.15).

3.3.4 Axial Specimen Slicing

As outlined above, according to the axial dissection technique, pancreatoduodenectomy specimens are sliced along the axial plane, that is, perpendicular to the descending part of the duodenum. The specimen slices should be thin—approximately 3 mm in thickness—which is important in view of the small dimensions of the native anatomical structures in the pancreatic head. For example, if slices are considerably thicker than 3 mm, then the main pancreatic duct, which is normally no more than 3 mm wide, may be concealed from macroscopic inspection.

Axial slicing of the specimen may be easier if the 'tail' of distal duodenum that is not adherent to the pancreatic head is removed. Similarly, clipping of the 'wings' of the opened duodenal wall that extend on either side of the pancreatic head may facilitate slicing. Wiping the blade of the dissection knife blade during serial slicing may help to prevent smearing of ink. The use of a long

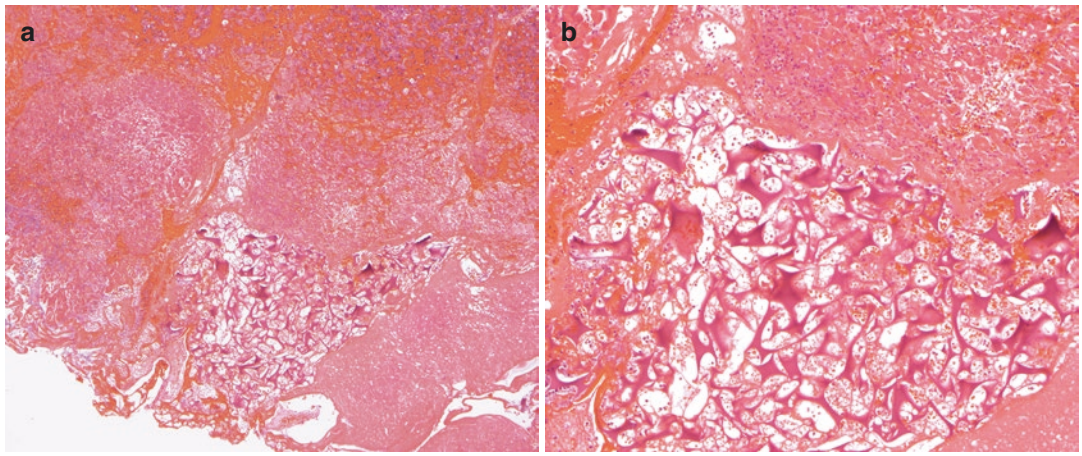

Fig. 3.12 Fibrin sealant: fibrin glue is applied to the pancreatic surface of the surgical bed following enucleation of a small neuroendocrine tumor (**a**). The fibrin glue forms a biodegradable hemostatic mesh (**b**)

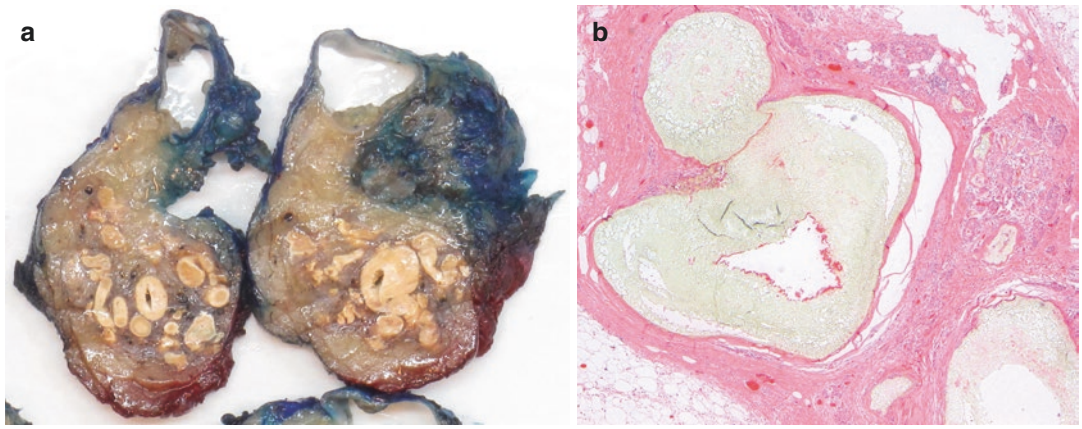

Fig. 3.13 Duct occlusion with non-biodegradable glue: the duct system of the pancreatic body and tail is occluded with a glue-like chemical substance (Neoprene ®) as a measure to prevent anastomotic leakage following pancreatoduodenectomy (**a**). The opaque material occludes pancreatic ducts, including small intralobular ducts. Note the complete atrophy of the acinar parenchyma with clustering of islets (**b**)

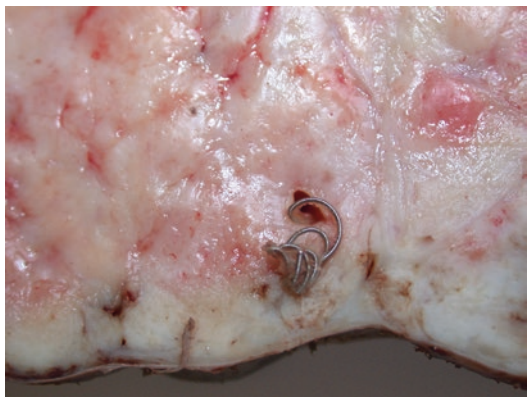

Fig. 3.14 Embolization coil: a metal coil protrudes from a blood vessel in a large, locally advanced pancreatic endocrine tumor. Emergency embolization for fulminant bleeding had been performed prior to distal pancreatectomy

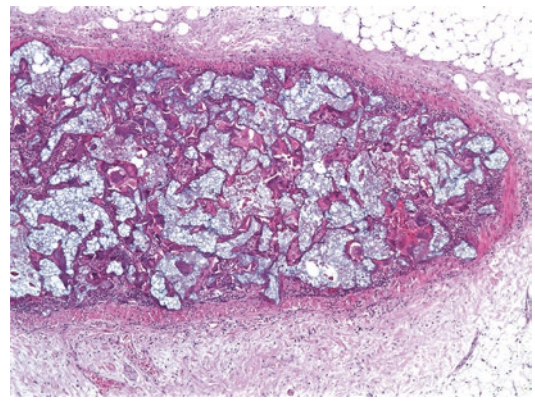

Fig. 3.15 Embolization material: histology reveals occlusion of the arterial lumen by injected embolization material

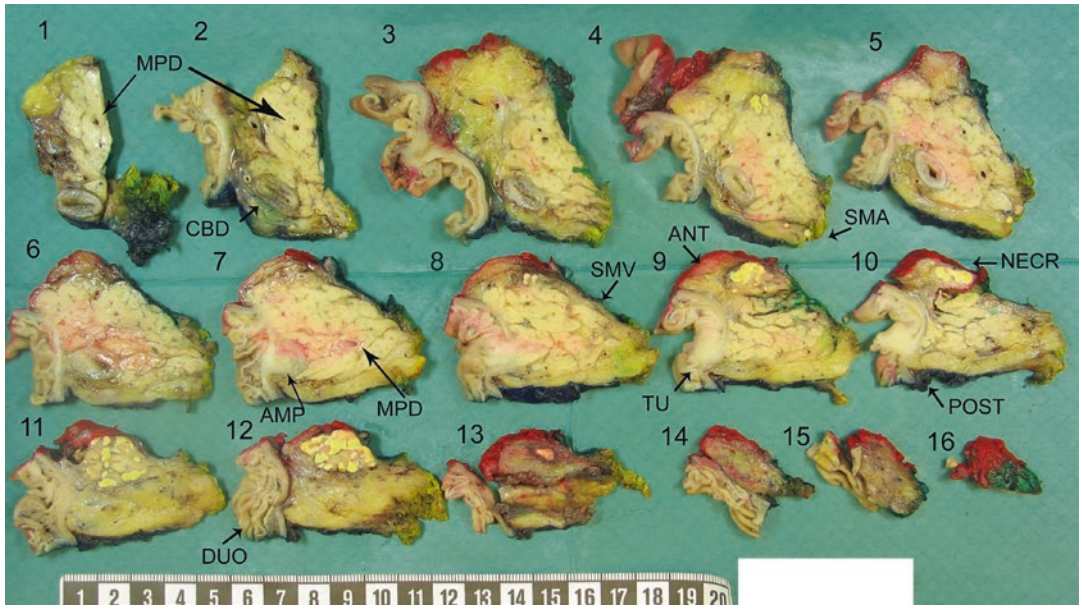

Fig. 3.16 Overview of specimen slices: following axial slicing of a pancreatoduodenectomy specimen, the slices are laid out in sequential order, from cranial to caudal, the inferior cut surface looking upward. The common bile duct (*CBD*) is seen in extrapancreatic position (slice 1–3) and in the posterior part of the pancreatic head (slices 4–6). The main pancreatic duct (*MPD*) can be followed from the pancreatic neck (slice 1) to the ampulla (slice 8). The ampulla (*AMP*) is represented in slices 7–8. In this case, a tumor involves the papilla of Vater (*TU*). Note the presence of multifocal fat necrosis (*NECR*). *ANT*: anterior surface, *DUO*: duodenum, *POST*: posterior surface, *SMA*: SMA-facing surface, *SMV*: SMV groove

knife is recommended, as it allows slicing in one swoop through the full width of the pancreatic head. As the axial specimen slices are produced, they can be laid out in sequential order from cranial to caudal, in a rectangular format that fills the camera viewer (Fig. 3.16) (see Sect. 3.3.6). To allow optimal correlation with preoperative imaging, the slices are best placed with the caudal surface showing up ('looking up to the slices from below').

3.3.5 Identification of Anatomy and Margins in Axial Specimen Slices

An important advantage of the axial dissection technique is that the pancreatoduodenectomy specimens are always sliced in the same (axial) plane and that therefore anatomical structures are present at the same position within the specimen slices. This greatly facilitates identification of anatomical structures, especially if these are altered in appearance or localization due to disease or anatomical variation. This section provides guidance on where in the specimen slices, the key anatomical structures can be found and, if appropriate, which specific macroscopic features allow their correct identification.

3.3.5.1 Pancreatic Duct System, Bile Duct, and Ampullae

The main pancreatic duct can be seen along its oblique descent from the pancreatic transection margin to the ampulla as an up to 3 mm wide, round or slightly collapsed, oval-shaped cross section (Fig. 3.17). Towards its distal end, the main pancreatic duct changes direction and runs in a nearly axial plane towards the ampulla, with the result that this particular part of the main pancreatic duct may be displayed as a more longitudinal section (see Chap. 1, Sect. 1.3.1.3, Figs. 1.2 and 1.6). If the main pancreatic duct is dilated significantly, the distal end of the duct

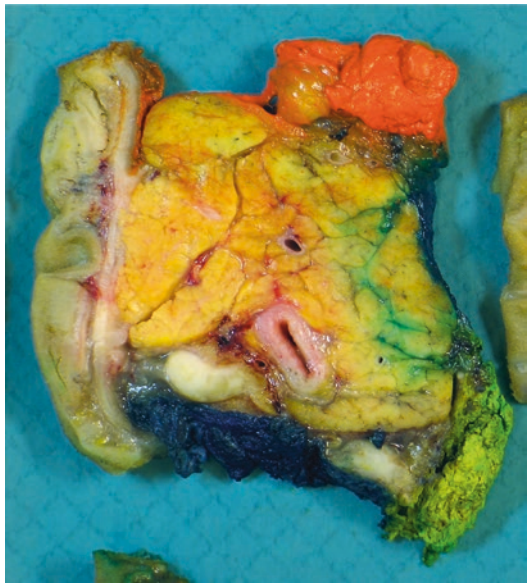

Fig. 3.17 Main pancreatic duct and common bile duct: the main pancreatic duct is small, has a membranous wall, and is located relatively centrally in the pancreatic head. The common bile duct is larger, has a thicker wall, and is located in the posterior aspect of the pancreatic head. Note the presence of two suspicious lymph nodes in the posterior pancreatoduodenal and SMA-facing fat

Fig. 3.18 Dilated pancreatic branch ducts: under normal conditions the pancreatic branch ducts are not visible macroscopically. This specimen slice contains multiple dilated branch ducts, whose diameter ranges from pinpoint to 2–3 mm. Cause of the branch duct dilatation in this case was focal chronic pancreatitis with stone formation

may be represented in a longitudinal fashion in more than one specimen slice. However, if the duct is of a normal caliber and the slices are thicker than 3 mm, this part of the pancreatic duct may remain hidden within a single specimen slice. In contrast to the intrapancreatic common bile duct, which runs through the posterior part of the pancreatic head, the main pancreatic duct is located more centrally within the pancreatic parenchyma. Santorini's duct may be visible close to the minor ampulla (see Chap. 1, Sect. 1.3.1.3, Fig. 1.7). Pancreatic branch ducts are not visible on gross inspection, unless they are pathologically dilated (Fig. 3.18), for example, in cases with duct obstruction or involvement by intraductal papillary mucinous neoplasia (see Chaps. 7 and 17).

The ampulla of Vater is usually present midway along the craniocaudal length of the pancreatic head, i.e., in one of the middle axial specimen slices, but there is considerable variation and in some cases, the ampulla of Vater may be found towards the caudal end of the pancreatic head. The full length of the ampulla—from its superficial part in the duodenal submucosa to its deep portion joining the distal common bile duct—is usually represented in two or three consecutive slices (Figs. 3.19 and 3.20) (see Chap. 1, Sect. 1.3.3, Fig. 1.9). Due to the configuration of the pancreatic and bile ducts as they approach the ampulla (see Fig. 1.2), the junction of the latter with the main pancreatic duct is usually represented in the slice caudal to the one containing the junction with the common bile duct.

In most pancreatic specimens the minor ampulla is visible as a nodular structure straddling the duodenal muscle layer. The size of the minor ampulla can vary, and prominence of this structure is often due to the presence of ectopic pancreatic tissue (see Chap. 1, Sect. 1.4.8). The minor ampulla (and associated Santorini's duct) is present in the specimen slice located approximately two levels above the slice containing the junction of the ampulla with the common bile duct.

The common bile duct can be followed over its entire extrapancreatic and intrapancreatic course, from the transection at the junction of the common hepatic duct with the cystic duct down to the junction with the ampulla (Fig. 3.20). The

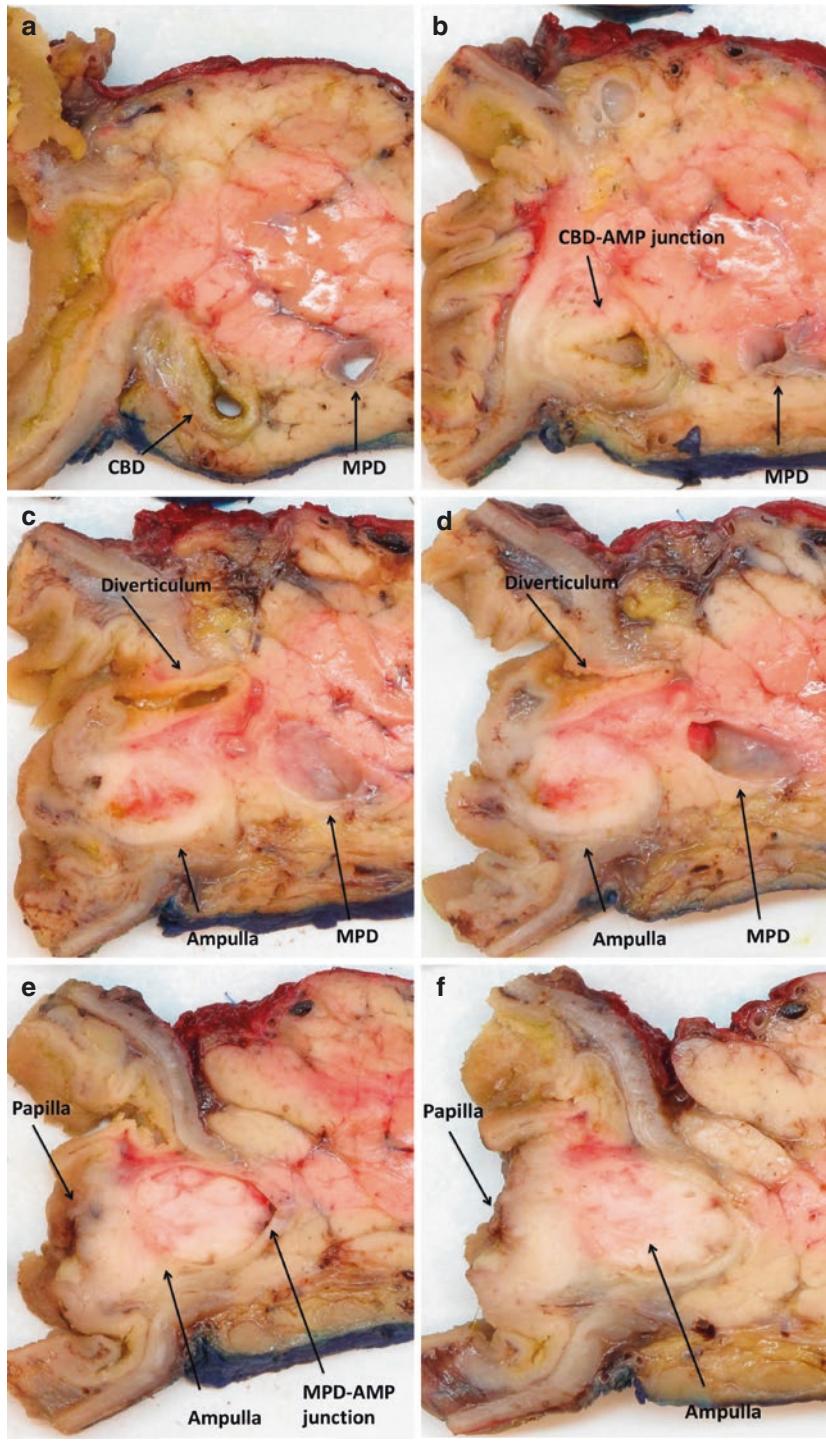

Fig. 3.19 Ampulla of Vater: in consecutive axial slices (in cranial-to-caudal sequence), the distal end of the main pancreatic duct (*MPD*) and common bile duct (*CBD*) can be seen to approach (**a**) and join the ampulla of Vater (*CBD-AMP junction*, **b**; *MPD-AMP junction*; **e**). Both ducts are dilated due to a tumor, which occludes the ampulla (**c**–**f**), protrudes into the distal pancreatic duct (**e**), and infiltrates the papilla of Vater (**f**). Note the presence of a small duodenal diverticulum that is located anterior to the ampulla (**c**, **d**) (Reproduced with permission from Verbeke and Gladhaug [2], Elsevier)

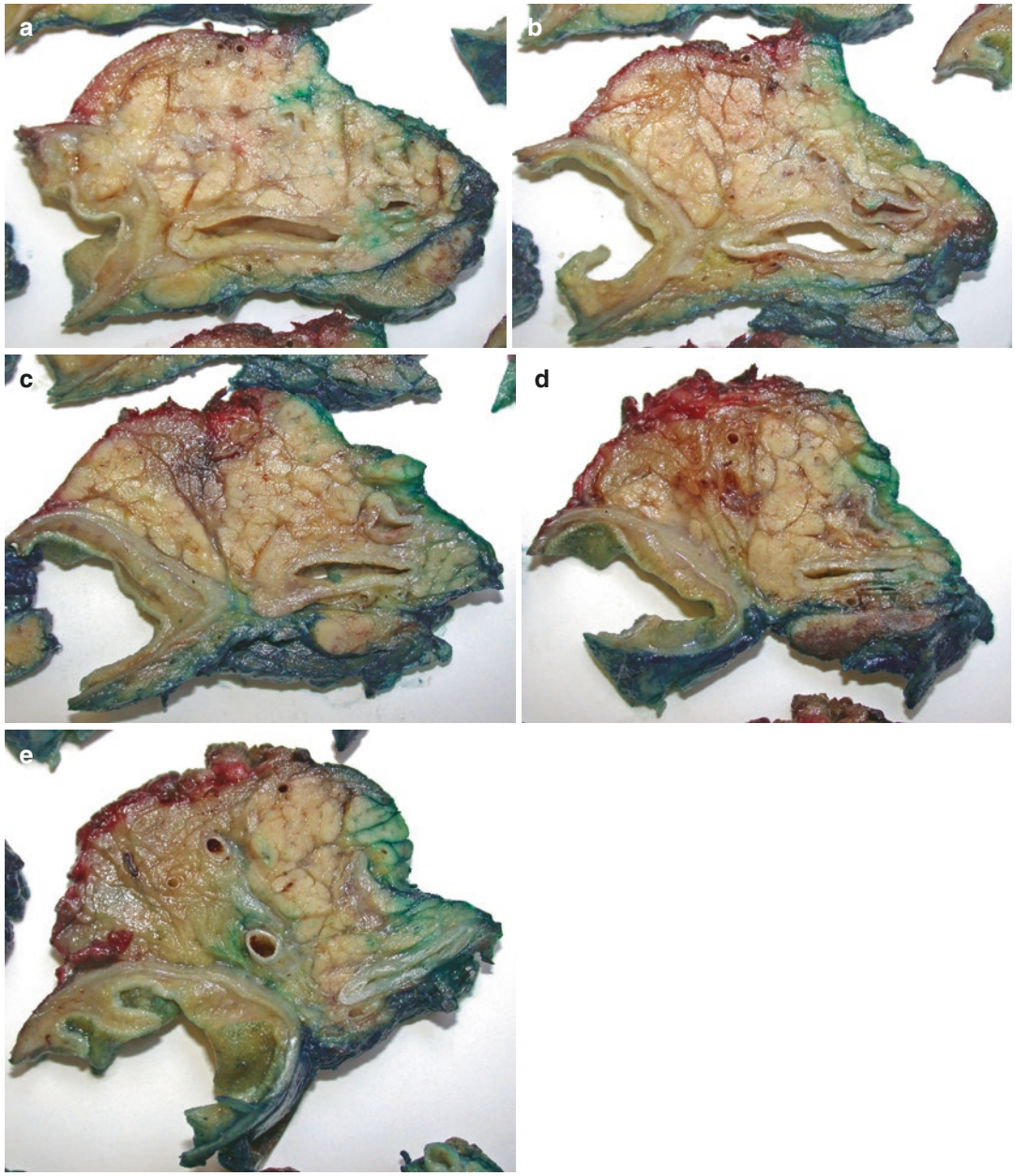

Fig. 3.20 Common bile duct: the course of the common bile duct can be followed in consecutive slices: close to the junction with the ampulla (**a**), in the posterior aspect of the pancreatic head (**b**–**c**), at the point of entry of the bile duct into the pancreas (**d**), and outside the pancreas (**e**). In this case the duct is dilated and only partially surrounded by pancreatic tissue

extrapancreatic part of the bile duct is contained in the most cranial specimen slices (Fig. 3.16), whereas the distal end of the bile duct is represented in the slice located above the one containing the ampulla of Vater and the junction with the main pancreatic duct (Fig. 3.19). The common bile duct runs through the posterior aspect of the pancreatic head and is therefore always located relatively close to the posterior specimen surface (Figs. 3.17 and 3.20). Large lymph nodes are

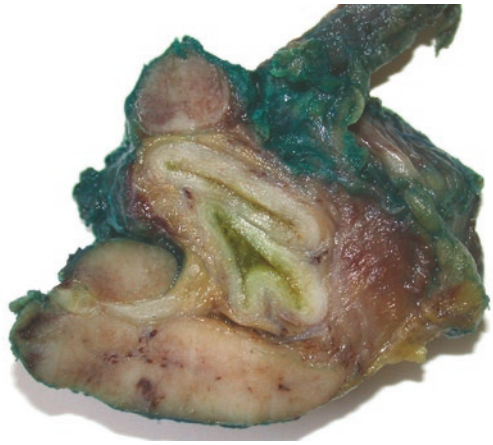

Fig. 3.21 Lymph nodes around the extrapancreatic common bile duct: the extrapancreatic bile duct at the junction with the cystic duct is surrounded by large reactive lymph nodes

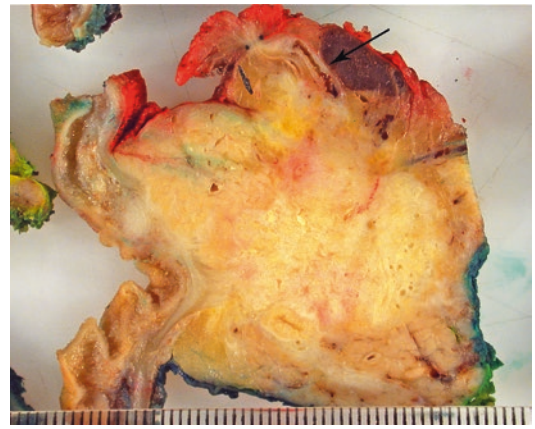

Fig. 3.22 Gastroduodenal artery: this artery is always included in the anterior peripancreatic fat of pancreatoduodenectomy specimens (*arrow*). In this case, pancreatic cancer grows close to the artery

often present in the soft tissue cuff surrounding the extrapancreatic common bile duct (Fig. 3.21).

3.3.5.2 Arteries and Veins

The gastroduodenal artery, which provides the main blood supply to the pancreatic head (see Chap. 1, Sect. 1.3.5), is the only large-caliber artery that is always contained in pancreatoduodenectomy specimens. It can be readily seen in the anterior peripancreatic soft tissue, where it runs over most of the craniocaudal length of the pancreatic head, and is thus represented in many of the axial specimen slices. (Fig. 3.22). Another artery that is contained in pancreatoduodenectomy specimens is the inferior pancreatoduodenal artery. It can be found in the caudal part of the pancreatic head, close to the SMA surface, where it sometimes appears as a small plexus of arterial cross sections (see Figs. 1.11 and 1.12). In selected patients, a segment of the superior mesenteric artery (SMA) may be resected, in isolation or in combination with a part of the superior mesenteric vein (SMV), and is then found adherent to the SMA-margin.

Surgical resection of a part of the superior mesenteric or portal vein during pancreatoduodenectomy (or total pancreatectomy) has become well established. Venous resections are found adherent to the SMV groove. They can vary in size from just a few millimeters across to several centimeters in length, and can be tangential or segmental (Figs. 3.8 and 3.23). Venous resections may be surrounded by irregular, tumor-infiltrated soft tissue (Fig. 3.24).

3.3.5.3 Specimen Surfaces and Margins

The contour of the axial specimen slices has a shape and configuration that is characteristic for each aspect of the pancreatic head (Fig. 3.25).

The anterior surface of the pancreatic head is typically curved in a convex fashion. Particularly in the more cranial slices, it can contain a rather copious amount of adipose tissue, which includes the gastroduodenal artery and some lymph nodes, and often blends with the peripyloric/perigastric fat. The junction of the anterior pancreatic surface with the anterior duodenal wall lies in a natural crevice, caused by the narrowing of the anteroposterior dimension of the pancreatic head as it adheres to the duodenal wall. The ‘anterior pancreatoduodenal crevice’ represents a site of possible margin involvement by tumors infiltrating the duodenal wall and ampullary area (Fig. 3.26) (see Chap. 9, Sect. 9.11.4, Figs. 9.44 and 9.45).

The surface facing the superior mesenteric vein and its junction with the portal vein has a shallow concave contour, the SMV groove.

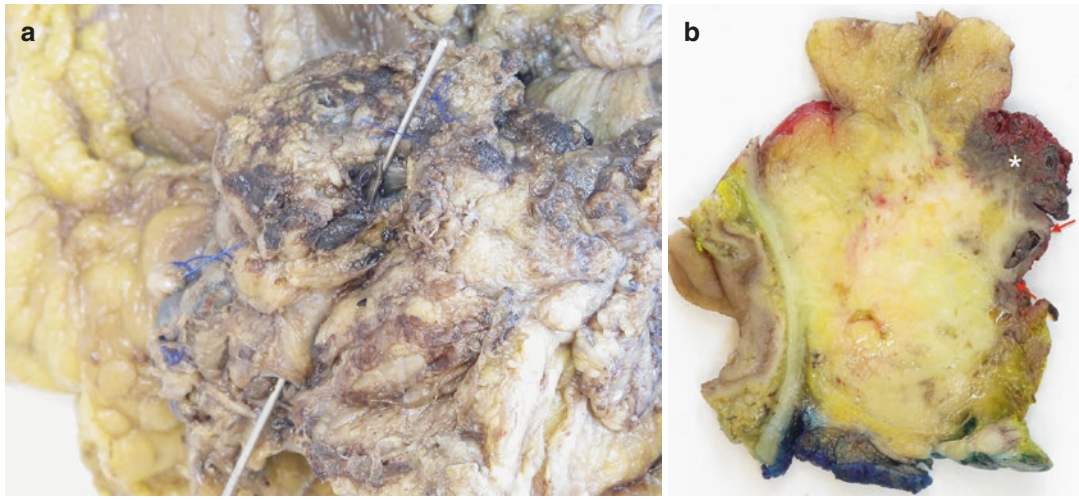

Fig. 3.23 Resection of the SMV: a 3 cm-long segment of the SMV is firmly adherent to the SMV groove just caudal to the transected pancreatic neck (**a**). An axial specimen slice shows that the segment of SMV is occluded with thrombus and its wall semicircumferentially infiltrated with tumor (*arrows*). Note the irregular, tumor-infiltrated soft tissue that flanks the venous resection (*asterisk*) (**b**)

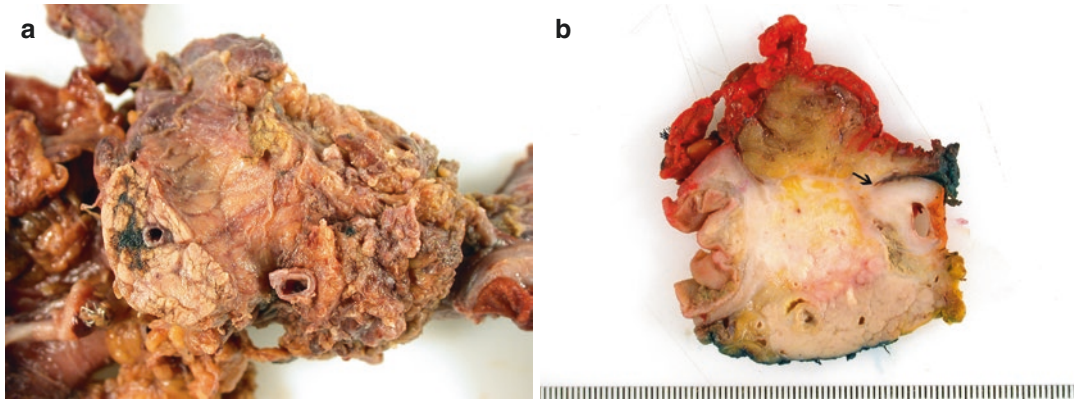

Fig. 3.24 Resection of the SMV: a segment of SMV, located caudal to the level of the pancreatic neck, is adherent to the SMV groove and surrounded by irregular tissue. Note the smooth surface of the SMV groove cranial to the venous resection (**a**). Full thickness of the venous wall is infiltrated by tumor and the segment of vein is drawn into the tumor mass. Note extension of tumor onto the SMV groove (*arrow*; **b**)

Peripancreatic soft tissue is very scanty or almost absent in this area, and consequently, pancreatic parenchyma lies almost immediately at this specimen surface (Fig. 3.25).

The surface facing the superior mesenteric artery (SMA margin) usually has an irregular outline, as this is a true surgical resection margin, where soft tissue is dissected from the artery. The adipose tissue at this specimen surface contains lymph nodes and is particularly rich in peripheral nerves and small lymphovascular channels (see Chap. 1, Sect. 1.4.6, Fig. 1.25).

The posterior margin has a flat contour and extends from the roughly textured SMA-margin to the posterior duodenal wall. Similar to the anterior pancreatoduodenal crevice, the posterior

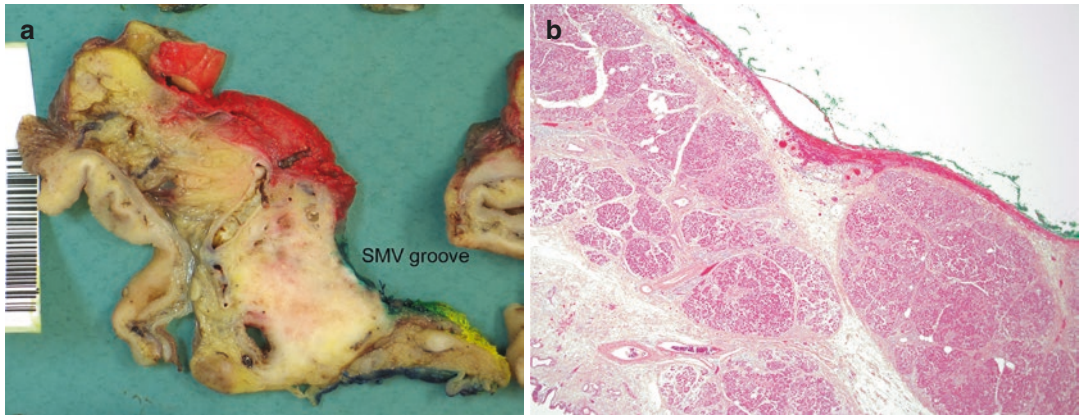

Fig. 3.25 Peripancreatic soft tissue: relatively copious adipose tissue can overlie the anterior (*red*), SMA-facing (*yellow*) and posterior surfaces (*blue*; **a**). In contrast, there is hardly any soft tissue between the pancreas and the SMV groove (**b**). Note the green ink on the SMV-facing surface, which is visible macro- and microscopically

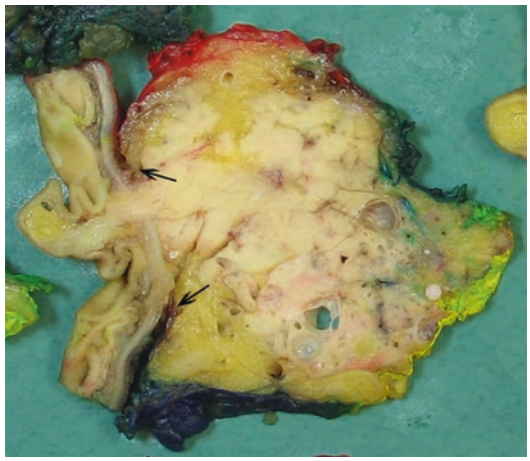

Fig. 3.26 Anterior and posterior pancreatoduodenal crevices: the pancreatic head narrows in the anteroposterior dimension where it meets the duodenum, resulting in a deep crevice anteriorly and posteriorly (*arrows*)

pancreatic margin turns often inward to meet the duodenal wall at the posterior pancreatoduodenal crevice (Fig. 3.26). Although less deep than the anterior crevice, this also represents a site of potential margin involvement, in particular for cancer developing in the ampullary region [8]. Lymph nodes are usually present in the posterior peripancreatic adipose tissue, which contains less numerous peripheral nerves and lymphovascular channels than are found in the neighboring SMA-facing soft tissue.

3.3.5.4 Lymph Nodes

Lymph nodes are present throughout the layer of soft tissue that envelops the pancreatic head and the extrapancreatic common bile duct. In Whipple's resection specimens, lymph nodes may also be contained in the infrapyloric and perigastric adipose tissues. The International Union Against Cancer (UICC) and the Japan Pancreas Society (JPS) have each proposed a system of lymph node allocation to different stations [1, 9, 10]. While (some of) the lymph node stations defined by JPS are often used in pancreatic surgery, pathology staging of lymph nodes is usually performed according to the UICC. Both lymph node systems differ in two aspects. First, the JPS system is more detailed than the UICC and allocates the lymph nodes to a larger number of different stations. A comparison of the stations as defined by both systems, and guidance on where these stations can be found in axial specimen slices, are summarized in Table 3.2 (Figs. 3.16 and 3.27). Second, the JPS uses a system of lymph node groups (group 1–3), which indicates whether certain lymph node stations are regional or distant to the primary tumor in the pancreatic head or body/tail. The UICC includes only lymph nodes that are regarded as regional (for cancer of the pancreatic head, body/tail, or both), but does not provide a grouping system for distant lymph node sites (see Table 9.4).

Table 3.2 Lymph node stations according to Japan Pancreas Society (JPS) [1, 10], their corresponding stations according to UICC [9], and their position in slices from pancreatoduodenectomy or distal pancreatectomy specimens

JPS lymph node stations	Corresponding UICC lymph node stations	Position in specimen slices from PDE	Position in specimen slices from DPE
6 Infrapyloric	Infrapyloric	In slice(s) cranial to top end of pancreatic head	NI
7 Left gastric artery	NM	NI (may be received separately)	
8 Common hepatic artery **a**: anterosuperior **p**: posterior	Common hepatic artery		
9 Celiac trunk	Celiac		
10 Splenic hilum	Splenic hilum	NI	At splenic hilum; in slices at distal end of pancreatic tail
11 Along splenic artery **p**: proximal **d**: distal	Splenic artery	NI	Along cranial border of pancreatic body/tail
12 Hepatoduodenal ligament **a**: along hepatic artery **p**: along portal vein **b**: along bile duct	12a: Common hepatic artery 12p: Portal vein 12b: Common bile duct	12a, 12p: NI (may be received separately) 12b: Around extrapancreatic bile duct in cranial specimen slices	NI
13 On posterior aspect of pancreatic head **a**: superior **b**: inferior	Posterior	Along posterior surface of pancreatic head	NI
14 Along SMA **p**: proximal **d**: distal	14p: Proximal mesenteric 14d: Right lateral wall of SMA	In peripancreatic soft tissue along SMA margin	NI
15 Along middle colic artery	NM	NI (may be received separately)	
16 Para-aortic **a1**: around aortic hiatus of diaphragm **a2**: from celiac trunk to LRV **b1**: from LRV to IMA **b2**: from IMA to aortic bifurcation	NM (Lateral aortic? Retroperitoneal?)		
17 On anterior aspect of pancreatic head **a**: superior **b**: inferior	Anterior	Along anterior surface of pancreatic head	NI
18 Along inferior border of body and tail of pancreas	Inferior	NI	Along caudal border of pancreatic body/tail

Abbreviations: *DPE* distal pancreatectomy, *IMA* inferior mesenteric artery, *JPS* Japan Pancreas Society, *LRV* left renal vein, *NI* not included in specimen, *NM* not mentioned in UICC staging system, *PDE* pancreatoduodenectomy, *SMA* superior mesenteric artery, *UICC* International Union Against Cancer

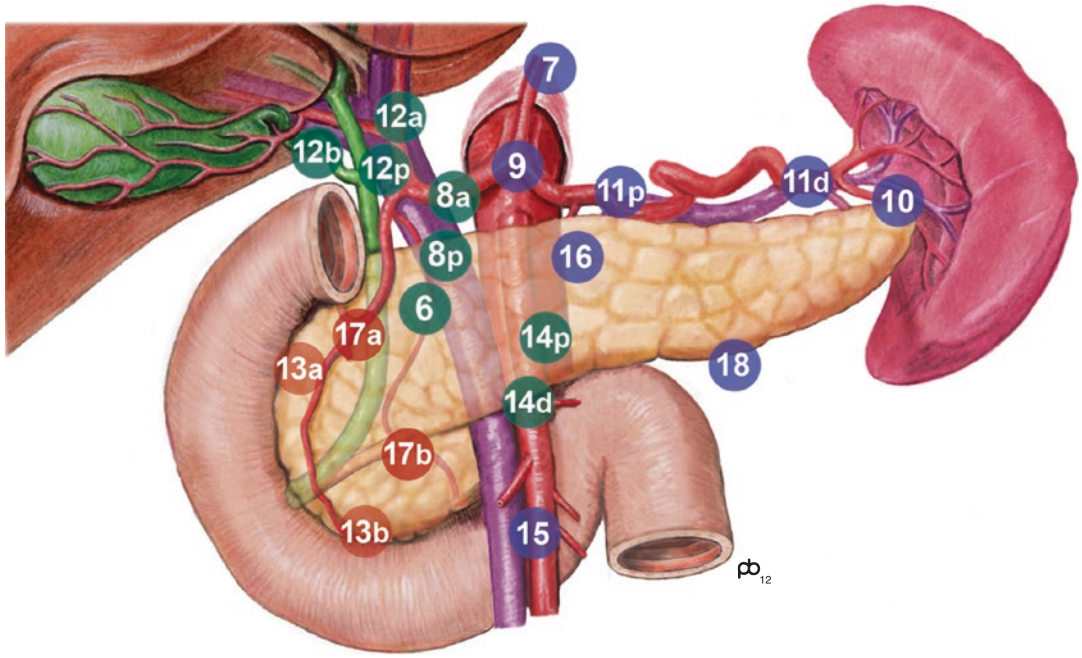

Fig. 3.27 Peripancreatic lymph node stations according to the Japan Pancreas Society (JPS) [1, 10]: lymph nodes are allocated to various stations (Table 3.2). *Red circles* indicate lymph nodes of group 1, i.e., lymph nodes that are removed by conventional pancreatoduodenectomy. Lymph nodes of group 2 (*green*) and 3 (*blue*) are more distant. Involvement of group 3 lymph nodes is regarded as distant metastasis (Image courtesy and copyright of Paul Brown, The Leeds Teaching Hospitals NHS Trust, Leeds, UK)

3.3.6 Photodocumentation

Photographs of the intact pancreatic resection specimen are usually uninformative, unless there are visible lesions on the gastroduodenal mucosa or at the specimen surface. However, overview photographs may be helpful in the case of multivisceral en bloc resections, enucleations, or central pancreatectomies.

Irrespective of the specimen type or the pathology encountered, photodocumentation of the specimen slices is of key importance as a permanent record of the macroscopic findings. As such, it allows retrospective review of the macroscopic part of the diagnostic process, which is equally important as and complements histological slide review for the provision of second opinion on an individual case or for systematic quality assurance. Photographs of specimen slices also provide useful guidance during microscopic assessment and allow re-consideration of macroscopic findings in the light of the histology, which is a powerful self-learning tool. Last but not least, the photographs are ideal for demonstration at clinicopathological conferences, as they allow direct comparison with radiological findings (see Chap. 4).

Photodocumentation should include an overview picture of all specimen slices along with close-up photographs of the slices that contain the main pathology and/or any other findings. Photographs—whether in overview or close-up—should always be taken as close as possible, that is, by filling the entire viewer area of the camera. A ruler and the specimen identification number should be included in all pictures.

3.3.7 Macroscopic Description: How and What to Record

As a general rule, during macroscopic inspection, any abnormality should be recorded with a description of its size, appearance, and exact localization. In addition, basic information should be provided regarding the main constituting specimen parts. A reporting checklist is provided in Table 3.3.

The *measurements* that can or should be recorded prior to specimen dissection include the length of the duodenum and distal stomach (along the greater and lesser curvature), and the length and maximum diameter of the gallbladder, cystic duct, and extrapancreatic common bile duct. The size of the pancreatic head is measured in three dimensions, that is, craniocaudal, mediolateral, and anteroposterior. The size, location, and appearance of any other tissues or organs that are included in the specimen, for example, a segmental resection of the superior mesenteric vein, should be recorded. Any abnormalities identified on external specimen inspection should also be included.

Table 3.3 Checklist for macroscopic reporting

• Specimen type
• Specimen dimensions: – Pancreas: craniocaudal, mediolateral, anteroposterior – Duodenum – Stomach – Extrapancreatic common bile duct: length and diameter – Gallbladder and cystic duct – Omentum – SMV resection (if present) – Other organs
• Stent: plastic/metal/none
• Total number of axial specimen slices
• Tumor: – Appearance: solid/cystic, color, texture, secondary phenomena (e.g., hemorrhage, calcification) – Size: craniocaudal (number of slices involved by tumor x slice thickness) and maximum axial dimensions – Localization: slices that are involved, which part of the pancreas (e.g., lateromedial, anteroposterior) – Relationship to key anatomical structures – Relationship to margins: which margins are close, minimum clearance
• Other findings: in pancreas or other structures and tissues
• Block key

Abbreviation: *SMV* superior mesenteric vein

The lesion that has been revealed by specimen dissection is described in terms of *appearance* (e.g., solid/cystic, color, texture, demarcation), size, and localization. The latter is important for accurate clinicopathological correlation and for identification of the cancer origin (i.e., pancreas, ampulla, or common bile duct) (see Chap. 9, Sect. 9.12.3). Using the axial slicing technique, *localization* in the craniocaudal dimension can be conveniently described by recording the number of the specimen slices that contain the lesion (e.g., slices 3-8). The localization in the anteroposterior and mediolateral dimension can be stated in form of a description of the quadrant that is involved (e.g., posterior-left lateral) or the proximity to anatomical structures (e.g., around the bile duct, flanking the SMV groove).

Similarly, the craniocaudal *size* of the lesion can be calculated from the number of slices that are involved, multiplied by the slice thickness. Both dimensions in the axial plane can be measured on the specimen slice where the lesion has reached its maximum extent. In the case of ductal adenocarcinoma of the pancreas, the characteristically poor delineation of the tumor requires that macroscopic 3-dimensional size assessment is verified and, if required, corrected by microscopic measurement.

Closely related to the localization and size of a lesion is its extension into neighboring tissues and structures. If possible, which structures and the extent to which these are involved, should be included in the description (e.g., the deep part of the ampulla, the anterior half of duodenal wall up to the submucosa, the entire circumference of the common bile duct from slice 2 to 5).

The goal is to provide an assessment of the lesion's localization and extent that mirrors the information in the radiology report, and, together with an accurate size measurement, allows a 3-dimensional reconstruction of the lesion within the pancreatic head [2, 8].

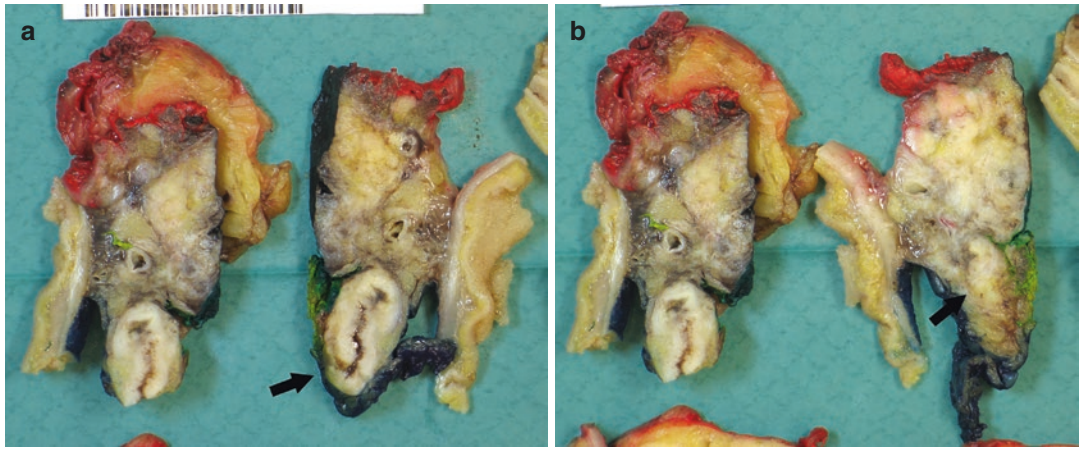

Fig. 3.28 Difference between the front and back of specimen slices: within the width of a single specimen slice of 3 mm thickness, the common bile duct (*arrow*) changes from being clearly identifiable (**a**) to being totally effaced by tumor (**b**)

The minimum distance of the tumor to the nearest specimen margins and surfaces is also part of the macroscopic assessment. However, this always requires microscopic measurement to determine the exact clearance.

Finally, it should be remembered that the most important structures in the pancreatic head—the ampulla, main pancreatic duct, and bile duct—are small, and, therefore specimen slices should be inspected on both sides. There may be significant differences in the appearances on either side, even if slices are thin (Fig. 3.28).

3.3.8 Tissue Sampling

The general rules for tissue sampling apply also to pancreatic resection specimens. The lesion of interest should be sampled adequately, and blocks should also be taken from the background pancreas and from any incidental findings. Specific guidance for the sampling of cystic tumors is discussed elsewhere (see Chap. 14, Sect. 14.2). This section provides a few practical recommendations that may facilitate tissue sampling from pancreatoduodenectomy specimens. Aspects of tissue sampling that are specific for distal pancreatectomy specimens and multivisceral resection specimens are described below (see Sects. 3.4 and 3.6).

Sampling is best performed following the *sequential order* of the specimen slices. The microscopic findings, and in particular the 3-dimensional reconstruction of the tumor location, size, and extent, are easier to capture and report, if the microscopic slides are lined up with the serial specimen slices (and macroscopic pictures). Therefore, sampling according to the tissue type (e.g., tumor first, then lymph nodes, followed by background tissue), as is best practice for many other cancers, is not recommended for pancreatic specimens. Tissue samples are best taken to include the lesion of interest together with neighboring anatomical structures, lymph nodes, or resection margins, such that both the nature of the lesion and its extent can be assessed in the same microscopic section. The structures or margins surrounding the lesion can also be used as anatomical points of reference, which allow unequivocal orientation of the microscopic slide.

Lymph nodes are not to be dissected out from the peripancreatic soft tissue, but left in situ and sampled together with the overlying specimen surface and, if appropriate, with other surrounding tissues. The color of the ink on the specimen surface together with the number of the specimen slice from which the sample was taken, allows unequivocal assignment of the lymph node to the various lymph node stations as defined by the UICC or the Japan Pancreas Society [1, 9], as

described above (see Sect. 3.3.5.4) (Fig. 3.27, Table 3.2). The localization or 'station' from which the lymph node stems does therefore not need to be recorded in the block key. Multiple counting of a lymph node that is represented in several consecutive specimen slices can be avoided by considering the shape, size, and location of the lymph node in both the microscopic section and the close-up photographs of the corresponding specimen slices. All lymph nodes should be sampled, not just the suspicious ones. An average minimum yield of 12 or 15 lymph nodes from pancreatoduodenectomy specimens has been suggested as a quality benchmark (see Chap. 9, Sect. 9.11.2). It is to be noted that perigastric lymph nodes are not represented in the axial specimen slices from the pancreatic head. Hence, they have to be dissected from the perigastric adipose tissue and embedded separately. On occasion, a few lymph nodes may be found in the sparse mesentery attached to the duodenum.

Considering the issues discussed above, it is recommended to divide axial specimen slices by simple rectilinear incisions into 4 or 5 parts, such that they can be accommodated in standard tissue cassettes (Fig. 3.29). Only the number of the specimen slice from which samples are taken needs to be included in the *block key*, while information regarding the site of tissue sampling does not require recording, because this will be obvious from the inked surfaces and the anatomical reference points, as outlined above. Overall, this sampling technique together with the help of close-up photographs from the specimen slices, provides maximum information for tissue orientation and macroscopic-microscopic correlation, thereby facilitating detailed reporting and case review. It also allows accurate microscopic measurement of the distance from the tumor to the various margins.

If possible, it is advisable to take (at least) one *whole mount sample* from the specimen slice that is most representative of the lesion in terms of size and extent. Alternatively, if whole mount block sampling is not available, the entire specimen slice can be embedded by dividing it into four to five parts, as described above.

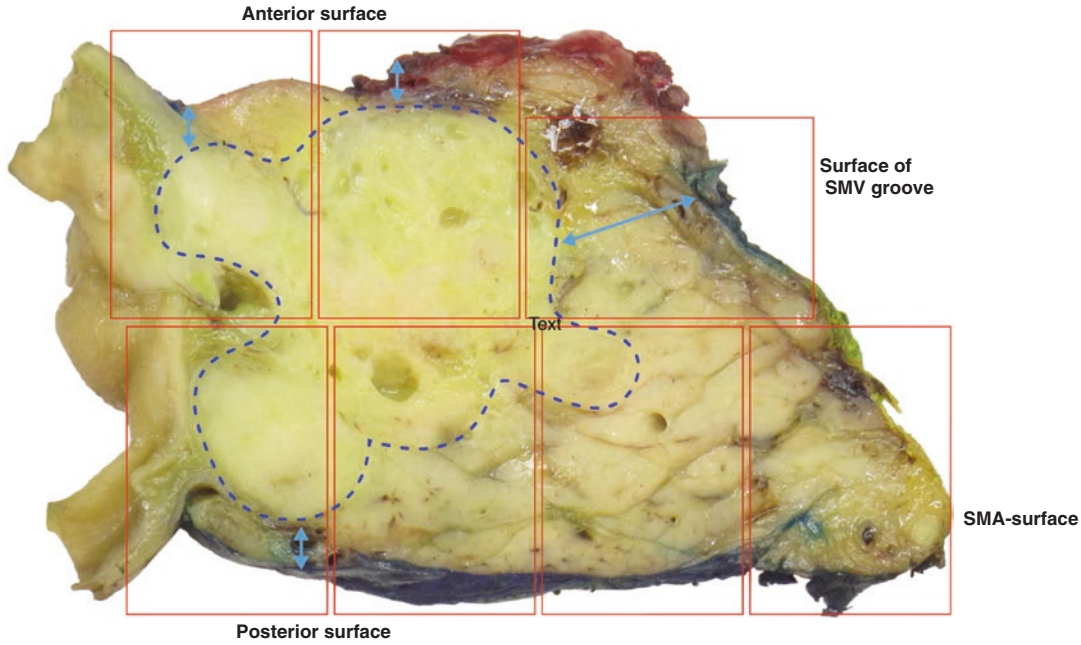

Fig. 3.29 Tissue sampling from a pancreatoduodenectomy specimen: an axial specimen slice is divided by rectilinear incisions into seven pieces that fit in standard tissue cassettes (*boxes*). The tissue samples allow accurate measurement of the tumor dimensions (*dotted line*) and the minimum distance to the various specimen surfaces (*double arrows*). The color of the ink on the specimen surface ensures unequivocal orientation of the tissue samples

In view of the generally poor delineation of pancreatic head cancers and the difficulty this poses for the macroscopic assessment of the tumor size and infiltration of anatomical structures and margins, the *extent of specimen sampling* is an important issue. This is particularly true for specimens from patients who have undergone neoadjuvant treatment, in which the tumor periphery is often even more blurred due to treatment-induced changes, such that subtotal or total embedding of the pancreas together with relevant adjacent tissues is required.

To allow microscopic verification and correction of the craniocaudal dimension of the tumor, samples should be taken from the specimen slices cranial and caudal to those containing the macroscopically apparent top and bottom end of the tumor. Regarding the assessment of the *margin* status, it has been shown that this is directly influenced by the number of samples taken from the tumor and the nearest circumferential margin [3]. The transection margins of pancreatoduodenectomy specimens are sampled en face, and in particular the margin at the pancreatic neck, is best sampled prior to axial specimen slicing.

Further samples may be required if the specimen includes additional tissues or structures. When a segment of superior mesenteric or portal *vein* is part of the surgical specimen, samples should be taken to assess whether and how deep the cancer has infiltrated the venous wall. Equally important is the examination of the margins of the resected vein and the adjacent SMV groove (see Chap. 9, Sect. 9.11.4). The resected vein is best sampled en bloc with the adjacent SMV groove and flanking pancreatic parenchyma, as this allows both accurate examination of the depth of tumor invasion of the venous wall and identification of involvement of the SMV margin and the circumferential margin of the resected venous tissue (Figs. 3.8, 3.23, and 3.24). In case of a long segmental venous resection, which is not adherent to the SMV groove over its entire length, both ends (i.e., transection margins) of the vein may be sampled separately as en face tissue slices.

Finally, tissue samples should also be taken from the background pancreatic parenchyma, ampulla, and bile duct to allow detection of microscopic pathological changes.

3.4 Dissection of Distal Pancreatectomy Specimens

Distal pancreatectomy specimens are best dissected by serial sectioning in 3 mm thick slices along a sagittal plane, that is, perpendicular to the longitudinal axis of the pancreatic body. Orientation of distal pancreatectomy specimens is based on the position of the splenic vessels, which run along the posterior surface of the pancreatic body and tail, the splenic artery cranial to the splenic vein (Fig. 3.30). Margins in this specimen type consist of the pancreatic transection margin, and the anterior and posterior surfaces of the pancreatic body and tail, which should also be

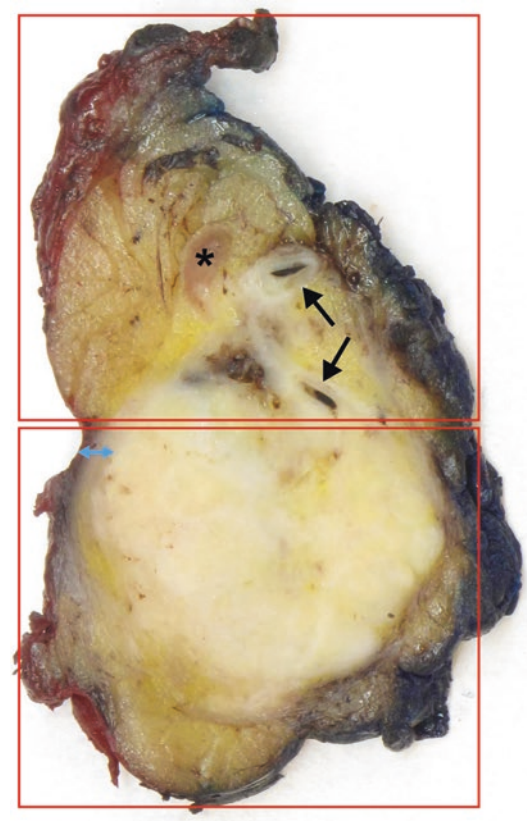

Fig. 3.30 Tissue sampling from a distal pancreatectomy specimen: in most cases, dividing the sagittal specimen slices in two results in tissue samples that fit in standard tissue cassettes. Note the tumor infiltration around the splenic artery and vein (*arrows*), the narrow clearance to the anterior surface (*double arrow*), and the presence of a small lymph node (*asterisk*)

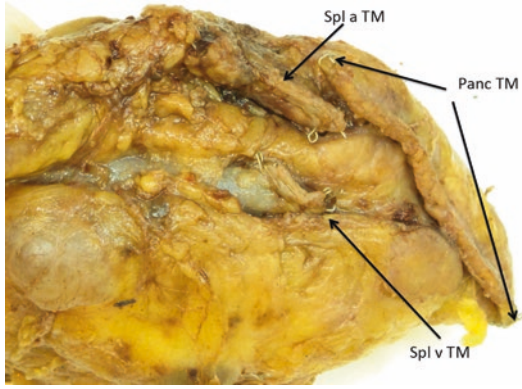

Fig. 3.31 Pancreatic and vascular transection margins: a view onto the posterior aspect of a distal pancreatectomy specimen shows the transection margin of the pancreatic body (*Panc TM*), the splenic artery (*Spl a TM*) and splenic vein (*Spl v TM*). All transection margins are stapled (laparoscopic procedure) (Reproduced with permission from Verbeke [11], Springer)

inked according to an agreed color-code. In addition, the transection margin of the splenic vessels may be of relevance in resection specimens with malignancy, in which case these structures are best inked with a different color and sampled en face (Fig. 3.31). The approach to photodocumentation, macroscopic description, and tissue sampling as described for pancreatoduodenectomy specimens can also be applied to distal pancreatectomy specimens.

3.5 Dissection of Total Pancreatectomy Specimens

For total pancreatectomy specimens a combined approach of axial slicing of the pancreatic head and sagittal slicing of the pancreatic body and tail is recommended. The point of transition between axial and sagittal slicing lies in principle at the level of the pancreatic neck but may be extended to either side if the tumor is located at or close to the pancreatic neck.

3.6 Dissection of Multivisceral En Bloc Resection Specimens

Extended surgical resection procedures are usually performed for tumors occurring in the pancreatic body and tail, and may include part of the stomach, the left adrenal, left kidney, or part of the colon (Figs. 3.32 and 3.33) (see Figs. 2.7, 2.8, and 9.3). Less frequently, a pancreatoduodenectomy may be extended by resection of the transverse mesocolon or a segment of small bowel (Fig. 3.34). Dissection is best undertaken following the standard protocol, that is, serial slicing in the sagittal plane for extended distal pancreatectomy specimens and axial slicing for extended pancreatoduodenectomy specimens. Important is prior inking of the various additional structures and organs in a color-coded fashion (Fig. 3.32) as well as meticulous recording of the relationship of the tumor to the various additional structures and their margins. En bloc tissue sampling of the tumor onto the additional structures and surfaces is key to the provision of an accurate record of the extent of the tumor and the margin status (Fig. 3.35). This information is also highly valuable for correlation with preoperative imaging and intraoperative surgical assessment.

3.7 Dissection of Other Pancreatic Specimen Types

Central pancreatectomy specimens (see Chap. 2, Sect. 2.6) are dissected in a similar fashion as distal pancreatectomy specimens, but require sampling and examination of both transection margins of the pancreas.

Resection specimens for chronic pancreatitis (see Chap. 2, Sect. 2.8) following the surgical procedures according to Frey may consist of irregular tissue fragments, which cannot be orientated, but whose entire surface can be

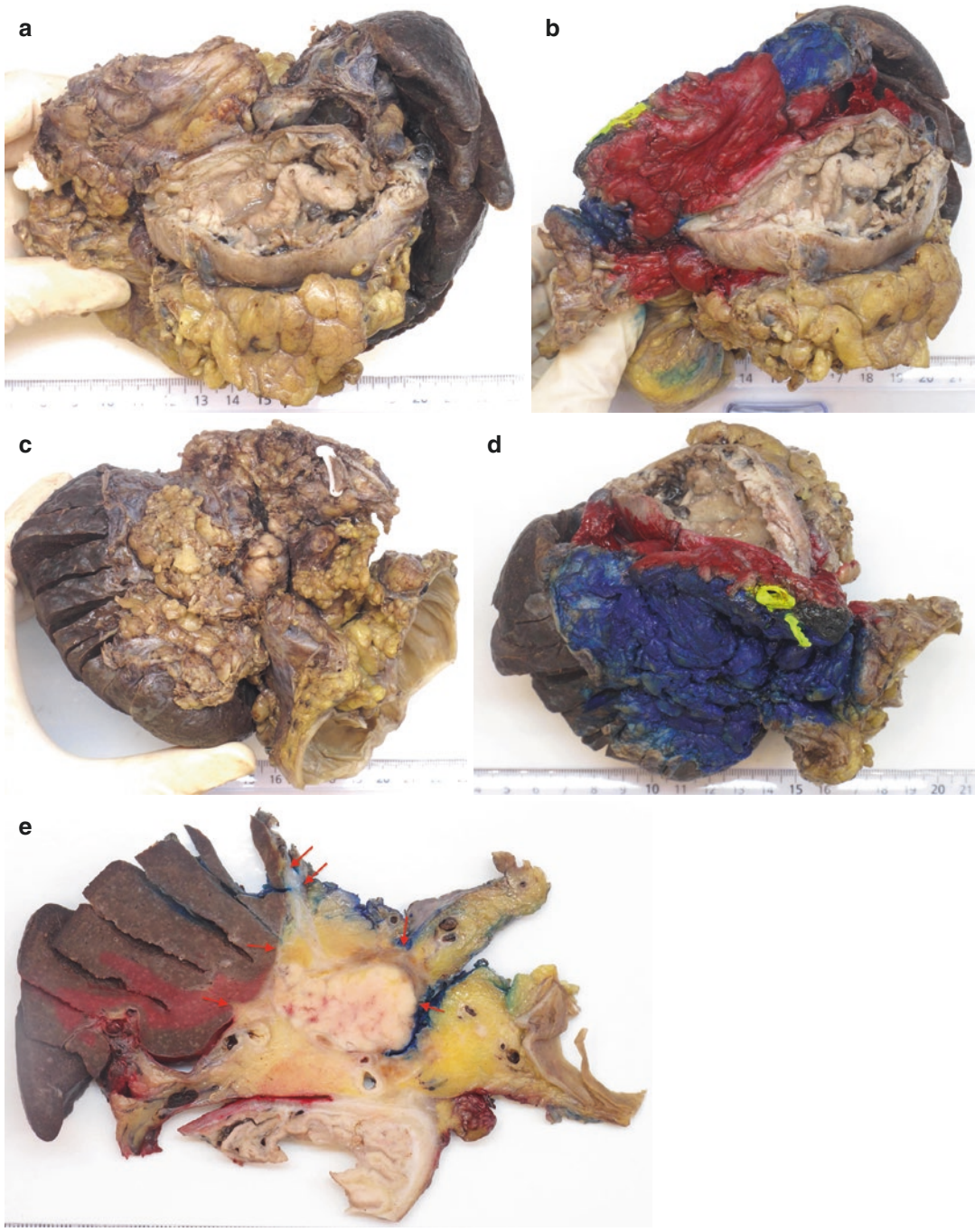

Fig. 3.32 Extended distal pancreatectomy specimen: this multivisceral distal pancreatectomy specimen includes a part of the stomach, which is adherent to the anterior surface of the tumor-bearing pancreatic tail (**a**). The anterior pancreatic surface is inked red (**b**). The posterior aspect of the specimen is irregular, and pale tumor tissue protrudes from it. A segment of colon that is adherent to the tumor is resected. Note the plastic clip and staple lines on the splenic artery and vein (**c**). The posterior surface of the specimen is inked blue, while the transection margins of the pancreatic body and splenic vessels are inked black and yellow, respectively (**d**). A sagittal specimen slice shows the close relationship of the tumor to the posterior margin and spleen (*arrows*), while the stomach and colon are clear (**e**)

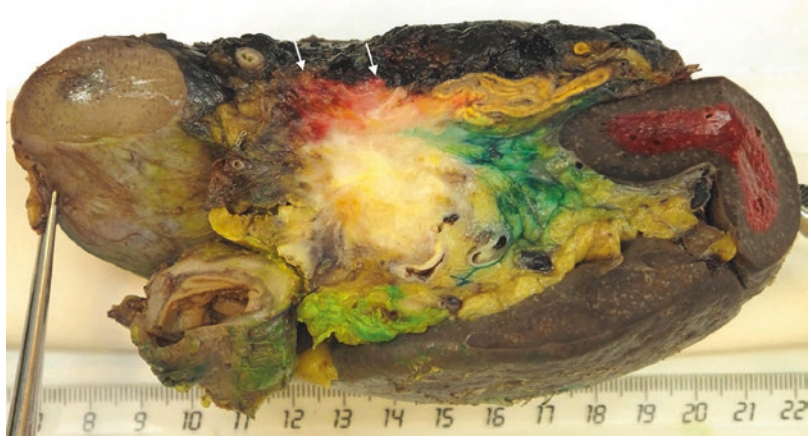

Fig. 3.33 Extended distal pancreatectomy specimen: sagittal slicing of this multivisceral specimen shows the spatial relationship of a tumor that arose in the tip of the pancreatic tail to the spleen, adrenal gland, left colon, and kidney. Note that tumor extends close to the posterior margin, which is inked black (*arrows*). Same specimen as shown in Fig. 2.7

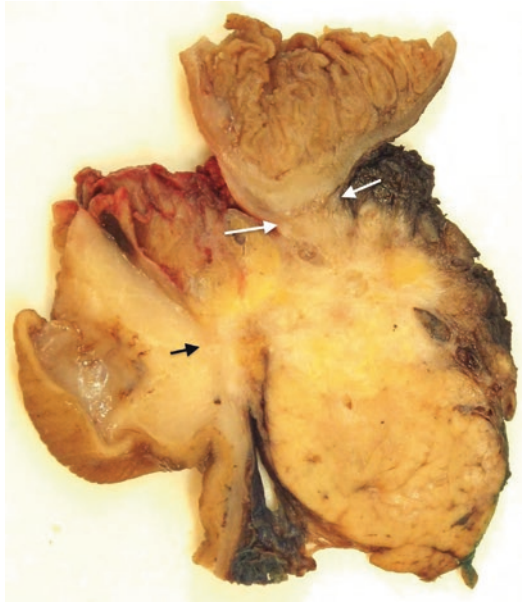

Fig. 3.34 Extended pancreatoduodenectomy specimen: an axial specimen slice reveals a tumor, which occupies nearly the entire mediolateral width of the pancreatic head and infiltrates the wall of the pylorus (*black arrow*) and the soft tissue adhesion to the small bowel (*white arrows*) (Reproduced with permission from Verbeke [2], Elsevier)

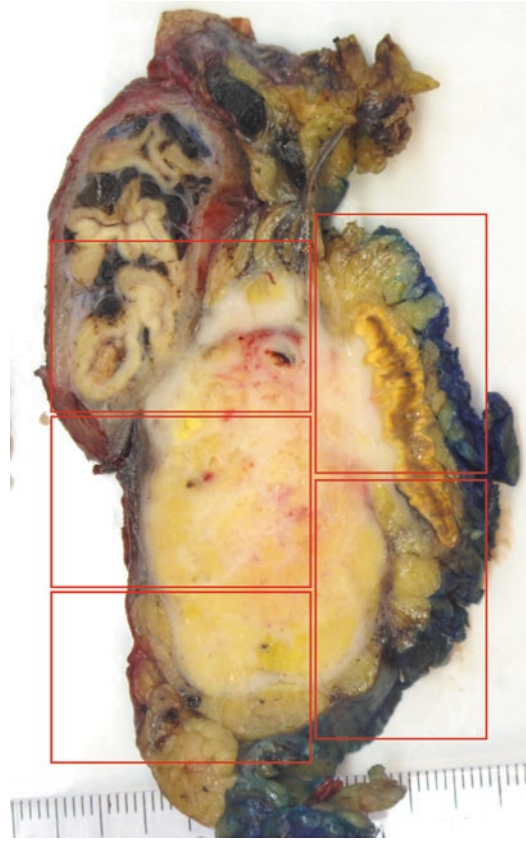

Fig. 3.35 Tissue sampling from an extended resection specimen: to allow meticulous assessment of the size of this pancreatic cancer and the relationship to the stomach, left adrenal gland, and specimen margins, the sagittal specimen slice is divided into rectangular samples (*boxes*) that fit into standard tissue cassettes

inked with a single color. The specimen from a procedure according to Beger results in a segment of pancreatic head and body, which may be received as one single or multiple smaller tissue fragments that, depending on size, should be serially sliced. All specimens from patients with chronic pancreatitis should be extensively sampled or, depending on the specimen size, embedded in their entirety, to exclude the presence of invasive ductal adenocarcinoma.

Enucleation specimens are best serially sliced after inking of the specimen surface. The extent of sampling from these specimens depends on the type of the lesion. However, as these specimens tend to be small, embedding the entire lesion may be considered.

3.8 Handling of Pancreatic Biopsies

The number and length of the trucut biopsies should be recorded. The biopsy sample is embedded in paraffin, sectioned, and stained with hematoxylin and eosin (H&E). In view of the small size of the biopsies and the sometimes limited representation of diagnostic lesions, cutting multiple spare sections at the time of the initial H&E(s) is good practice to safeguard tissue that may be needed for ancillary techniques.

3.9 Reporting Checklist of Macroscopic Findings

A list of data items to be recorded in the macroscopic description of pancreatic specimens is summarized in Table 3.3. The use of reporting proformas, which include the macroscopic findings, may be helpful to allow comprehensive, uniform, and time efficient reporting [6, 7, 12, 13].

References

1. Japan Pancreas Society. Classification of pancreatic carcinoma. 4th ed. (English). Tokyo: Kanehara; 2017.
2. Verbeke CS, Gladhaug IP. Dissection of pancreatic resection specimens. Surg Pathol. 2016;9:523–38.
3. Verbeke CS, Leitch D, Menon KV, McMahon MJ, Guillou PJ, Anthoney A. Redefining the R1 resection in pancreatic cancer. Br J Surg. 2006;93:1232–7.
4. Esposito I, Kleeff J, Bergmann F, Reiser C, Herpel E, Friess H, Schirmacher P, Büchler MW. Most pancreatic cancer resections are R1 resections. Ann Surg Oncol. 2008;15:1651–60.
5. Chandrasegaram MD, Goldstein D, Simes J, Gebski V, Kench JG, Gill AJ, Samra JS, Merrett ND, Richardson AJ, Barbour AP. Meta-analysis of radical resection rates and margin assessment in pancreatic cancer. Br J Surg. 2015;102:1459–72.
6. Campbell F, Cairns A, Duthie F, Feakins R. Dataset for the histopathological reporting of carcinomas of the pancreas, ampulla of Vater and common bile duct. London: The Royal College of Pathologists; 2017.
7. Björnstedt M, Franzén L, Glaumann H, Nordlinder H, Palmqvist R, Rissler P, Öst Å, Verbeke C. Gastrointestinal pathology—pancreas and periampullary region. Recommendations from the KVAST Study Group of the Swedish Society for Pathology. http://svfp.se/kvastdokument%5E8. Last accessed January 8, 2020.
8. Verbeke CS, Gladhaug IP. Resection margin involvement and tumour origin in pancreatic head cancer. Br J Surg. 2012;99:1036–49.
9. Brierly JD, Gospodarowicz MK, Wittekind C, editors. UICC: TNM classification of malignant tumors. 8th ed. Oxford: Wiley-Blackwell; 2016.
10. Matsuno S, Egawa S, Fukuyama S, Motoi F, Sunamura M, Isaji S, Imaizumi T, Okada S, Kato H, Suda K, Nakao A, Hiraoka T, Hosotani R, Takeda K. Pancreatic cancer registry in Japan. 20 years of experience. Pancreas. 2004;28:219–30.
11. Verbeke CS. Operative specimen handling and evaluation of resection margins. In: Kim S-W, Yamaue H, editors. Pancreatic cancer. Berlin Heidelberg: Springer; 2017.
12. Kakar S, Shi C, Adsay NV, Fitzgibbons P, Frankel WL, Klimstra DS, et al. Protocol for the examination of specimens from patients with carcinoma of the exocrine pancreas. College of American Pathologists (CAP); 2017. http://www.cap.org, web posting date June, 2012. Last accessed August 28, 2020.
13. ICCR (International Collaboration on Cancer Reporting). Carcinoma of the exocrine pancreas. Histopathology reporting guide. http://www.iccr-cancer.org/datasets/published-datasets/digestive-tract. Last accessed August 28, 2020.

Check for updates

4 The Pancreatic Multidisciplinary Team

In recent years, the role of the pathologist has changed dramatically from a pure provider of histological diagnoses to an active participant in the decision-making of pre- and postoperative patient management. To date, close collaboration between clinicians and pathologists is seen as the basis for optimal patient management.

In pancreatic cancer centers world-wide, regular multidisciplinary team meetings are held during which diagnostic investigations, treatment, and follow-up are discussed and planned for every individual patient. In many countries, the existence of a functioning pancreatic multidisciplinary team has become an integral part of the organisation of health care for patients with pancreatic disease, and as such it is now included in various national cancer care accreditation and quality review schemes. The unique and complex morphology and prognostic features of pancreatic neoplastic and non-neoplastic lesions require the participation of one or several pathologists with a special interest in pancreatic pathology. If the competence of the attending pancreatic pathologist does not cover that of pancreatic cytology, that is, the reporting of fine needle aspiration and brushing samples, additional experienced cytology representation is required, if not routinely then at least when cases with difficult cytological findings are discussed.

In most pancreatic multidisciplinary team meetings, both pre- and postoperative cases will be discussed. In the following, the pathologist's contribution to the discussion of these and to further roles and responsibilities of the multidisciplinary team are outlined.

4.1 Discussion of Postoperative Cases

Depending on local arrangements, patients who underwent surgery may be discussed again at the multidisciplinary team meeting either shortly after their surgery or several months later, when adjuvant treatment may have been completed and the patient had a first follow-up appointment. As the time for discussion of each individual patient is unavoidably limited, it is important that all information that is key to the future management of the patient is presented in a concise and structured way. This usually includes the following essentials:

- Morphological diagnosis: tumor entity, type, grade of differentiation/dysplasia, invasive or non-invasive, etc.
- Staging: all TNM descriptors (pTNMLVPnR) according to TNM UICC [1] or, if indicated, other staging systems.
- Features of relevance for prognosis, post operative treatment or follow-up: e.g., proliferation index in pancreatic endocrine tumors, presence of high-grade precursor lesions, issues regarding completeness of resection.
- Findings that may indicate the existence of a genetic predisposition to pancreatic neoplasia:

© Springer Nature Switzerland AG 2021
F. Campbell, C. S. Verbeke, *Pathology of the Pancreas*,
https://doi.org/10.1007/978-3-030-49848-1_4

for example, endocrine microadenomatosis or a combination of (pancreatic) lesions that are suspicious for von Hippel-Lindau disease.

In addition to the information that is key for optimal patient management, the pathologist may occasionally wish to demonstrate certain abnormalities, unusual tumor entities or anatomical variants, or unexpected but prognostically irrelevant findings, the discussion of which is more of an educational value.

Discussion of the pathology findings should be based first and foremost on the demonstration of the macroscopic photographs of the surgical specimen, in particular the close-up pictures of the specimen slices. For the majority of the multidisciplinary team members, macroscopic findings are more easily understandable than the rather 'abstract' histomorphology. Surgeons can readily relate to their intraoperative findings and the specimen they delivered, while radiologists are able to directly correlate the findings on CT- or MRI-imaging with those in the axial specimen slices. Demonstration of the exact location of the tumor, for example, within the pancreatic head, its relationship to adjacent structures, including venous resections, the site(s) of margin involvement, and the implications in terms of staging, are important findings that can be clearly explained on the macroscopic photographs. Ideally, preoperative imaging should be reviewed and discussed prior to the pathology demonstration, such that the various aspects of the radiological assessment can be directly compared with the actual morphological findings. Demonstration of microscopic features should be limited to findings that are not visible at a macroscopic level (e.g., tumor type, grade of differentiation, or vascular invasion) or to confirm macroscopic findings (e.g., tumor involvement of a resection margin or venous resection). On occasion, pathology may be demonstrated to illustrate a recurrent issue at the multidisciplinary team meetings. For example, demonstration of a case with tumor growth within 1–2 mm to, but not into, the wall of a venous resection may help clinical colleagues with understanding the apparent discrepancy between preoperative imaging showing involvement of the vein, and pathology examination not confirming this.

4.2 Discussion of Pretreatment Cases

These discussions usually relate to patients who undergo diagnostic investigations and whose further management—surgery, nonsurgical oncology, endoscopy, medical treatment, or follow-up—is to be decided upon. Histological biopsies or cytological samples—fine needle aspirations or brushings—are usually required in two settings: (1) pancreatic cancer patients who are either unfit for surgery or have unresectable, advanced disease and need histological tumor confirmation before receiving chemo- and/or radiotherapy and (2) pancreatic lesions that need further diagnostic clarification in order to identify optimal treatment or follow-up. In particular the diagnosis of autoimmune pancreatitis requires discussion in a multidisciplinary setting, during which morphological findings, imaging, and the clinical scenario are correlated (see Chap. 7, Sect. 7.2.7).

The pathologist's contribution to the discussion of these cases is essentially threefold:

- Review of pancreatic biopsies or cytology specimens: irrespective of whether the primary diagnosis had been made in-house or at a different pathology laboratory, the slides should be reviewed and the diagnosis communicated. In case the findings allow only a differential diagnosis, the range of this and the degree of certainty with which various lesions can be included or excluded from the differential should be discussed. In case the opinion of the reviewing pathologist differs from the primary diagnosis, the reasons for and implications of that should be explained and fed back to the pathologist who issued the original report.
- Advice on the use of tissue samples in the diagnostic work-up: the pathologist should advise the multidisciplinary team on the timing, site, and usefulness of the different types of tissue samples—true-cut tissue biopsies, fine needle aspirations or brushings—in obtaining a definitive diagnosis in view of the particularities of the individual case. Advice on whether specific clinical questions can be answered by the various tissue samples and the diagnostic limitations of each may be helpful in identifying the best approach and

avoiding investigational procedures with a low chance of providing useful information. Similarly, advice on the usefulness of intraoperative frozen section examination may be helpful in the planning for patients undergoing (explorative) surgery.

- Input in the radiological diagnostic considerations: with his/her experience regarding the macroscopic appearances of pancreatic neoplastic and nonneoplastic lesions and wide knowledge about clinicopathological features of the various entities, the pathologist can significantly contribute to the discussions that ensue from the radiologist's demonstration of findings. Many if not most of the diagnostic criteria used for assessment of CT- or MRI-imaging—for example, size, solid/cystic appearance, calcification, demarcation, localization, communication with the pancreatic duct system, type, and extent of regressive changes—are also part of the pathology macroscopic diagnostic tool kit; hence the pathologist's experience in this area can be valuable in narrowing down the differential diagnosis or excluding lesions that would require a different management approach.

4.3 Other Roles and Responsibilities

In addition to the diagnostic and advisory role outlined above, the pathologist has further responsibilities to the multidisciplinary team and beyond. Some of these roles can be the following:

- Audit of performance parameters: continuous quality monitoring should be performed by regular audit of key benchmarks, such as the concordance between pre- and postoperative diagnosis (cytological and/or histological), the concordance between diagnosis of intraoperative frozen section and paraffin-embedded tissue, the concurrence of primary diagnosis and (internal or external) second opinion, lymph node yield, completeness of reporting on minimum data set items, and reporting times. To allow retrospective case review, it is essential for key macroscopic findings to be documented by high-quality close-up photographs.
- Submission of data to regional or national registries: submission of pathology data to the cancer registry or other databases should be performed preferably with pathologist input. Where appropriate, pathologists may wish to advise on the design of the pathology part of the cancer data registration or on amendments that are required due to changes in staging or tumor classification systems.
- Provision and organisation of second opinion: the pathologist should be willing to give second opinion on referral cases, and at the same time ensure that difficult in-house cases will be appropriately referred to reference centers with specialist pathology expertise.
- Assistance in genetic counseling: the pathologist should support the multidisciplinary team in identifying patients who require specialist genetic counselling in case of suspected hereditary syndromes and/or familial pancreatic cancer (see Chap. 6). The pathologist should also ensure that all information on tissue samples and diagnoses is made available to the specialist center.
- Up-to-date information on changes in pancreatic tumor classification or staging systems, terminology, or diagnostic criteria: the pathologist should inform the multidisciplinary team of any of these changes that are of clinical importance and should explain the potential implications of these changes.
- Quality assurance: in many countries, regular and continued participation in regional or national external quality assurance schemes for pancreatic pathology, is considered best practice. Equally important for quality assurance is the accreditation of the pathology laboratory, which in certain countries can be obtained specifically for pancreatic pathology.

Reference

1. Brierley JD, Gospodarowicz MK, Wittekind C. UICC: TNM classification of malignant tumors. 8th ed. Oxford: Wiley-Blackwell; 2016.

Part II

Exocrine Pancreas: Non-Cystic

Check for updates

5 Common Minor Changes

This chapter describes a range of minor changes that can be observed relatively frequently in the pancreas. Most of these alterations are believed to develop in response to physiological changes, mild injury or ageing. The significance of these changes lies therefore in their correct identification and distinction from clinically more relevant lesions. However, recently, a few of these common changes have been implicated in the development of ductal adenocarcinoma of the pancreas, either as a possible risk factor, progenitor lesion, or a sentinel change. The molecular mechanisms underlying the development of these apparently minor changes are currently being actively researched.

5.1 Acinar Cell Nodules

Acinar cell nodules represent an incidental microscopic finding, which is more commonly observed in adults. They are characterized by sharply circumscribed nodules that stand out from the surrounding acinar parenchyma by their divergent tinctorial quality. They can be of an unusually prominent eosinophilic appearance, which is caused by loss of the normal basal basophilia of acinar cells. Less commonly, the acinar cell nodules may exhibit greater cellular basophilia than normal due to an increased nuclear to cytoplasmic ratio and the loss of apical zymogen granules. In addition, the cytoplasm of the lesional cells may be increased, decreased, or occasionally vacuolated; the nuclei may appear hyperchromatic or pyknotic; and the normal polarity of the acinar cells may be lost. Acinar cell nodules range in size from 100 to 1100 μm, and they may occur as solitary or multiple lesions. They have been previously reported under a variety of terms, including focal acinar transformation, eosinophilic degeneration, atypical acinar cell nodule, focal acinar cell dysplasia, or pseudoislet. The latter term refers to the superficial similarity of the less basophilic acinar cell nodules with Langerhans' islets (Fig. 5.1). The etiology and clinical significance—if any—of this lesion are unknown. However, there is no evidence to suggest that acinar nodules represent a neoplastic change.

5.2 Acinar Dilatation

Acinar dilatation (or acinar ectasia) is a common finding in autopsy and surgical material. It may affect a single acinus or multiple acini, sometimes an entire lobule. The dilated acinar lumen may be empty or contain eosinophilic, stringy or occasionally laminated, material. The acinar cells are flattened, the cytoplasm may become homogeneously eosinophilic and the nucleus compressed, such that the affected acinus resembles a ductule (Fig. 5.2). The etiology is poorly understood, and an association with a variety of conditions, including uremia, dehydration, intestinal obstruction, sepsis, congestive heart failure, intracranial lesions, ulcerative colitis, and malignancy, has been described.

© Springer Nature Switzerland AG 2021
F. Campbell, C. S. Verbeke, *Pathology of the Pancreas*,
https://doi.org/10.1007/978-3-030-49848-1_5

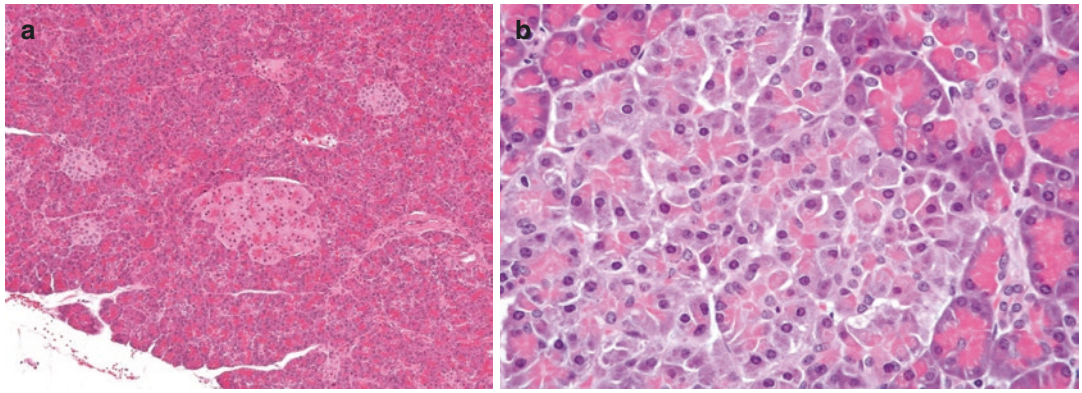

Fig. 5.1 Acinar cell nodule: a sharply circumscribed nodular cluster of acini stands out from the remainder of the acinar parenchyma. Note the superficial resemblance with islets (**a**). The acinar cells are paler and lack the characteristic basophilia at the basal pole of the cytoplasm (**b**)

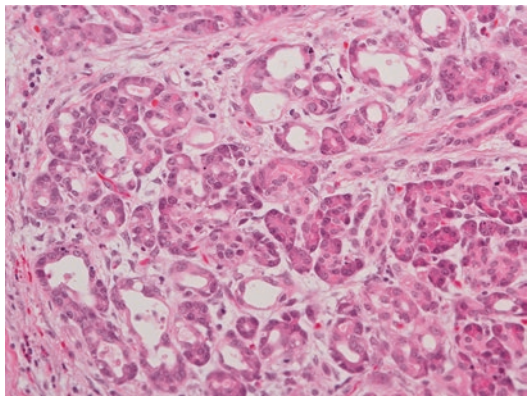

Fig. 5.2 Acinar dilatation: multiple acini within a lobule have a dilated lumen and the lining acinar cells are flattened. A small amount of eosinophilic secretion is present in some of the lumina

The main diagnostic significance of acinar dilatation lies in its distinction from well-differentiated adenocarcinoma, which on occasion is a differential to be considered in small biopsies or on frozen section examination.

5.3 Acinar to Ductal Metaplasia

Acinar cells in the adult pancreas show high plasticity, and under certain circumstances they can undergo transdifferentiation to a cell type with ductal characteristics, a phenomenon called acinar to ductal metaplasia. This alteration is characterized by the dilatation of an acinus (or, more commonly, a cluster of acini) with formation of a duct-like tubular structure that has a clearly visible patent lumen and is lined by flatter epithelial cells. The latter have a phenotype intermediate between acinar and duct-epithelial cells, morphologically and in terms of immunohistochemical marker expression (Fig. 5.3). Acinar to ductal metaplasia is a common and reversible process during acute pancreatitis, and the resulting cells are believed to contribute to the regeneration of acini and repopulation of the pancreas. However, experiments with transgenic mouse models show that acinar to ductal metaplasia may become irreversible when cells acquire oncogenic *Kras* mutations and/or persistent aberrant growth factor signaling, and that these cells may progress to low-grade pancreatic intraepithelial neoplasia (PanIN).

Acinar to ductal metaplasia is often associated with a degree of acinar atrophy and low-grade PanIN of the newly formed, small ducts, and as such it is often part of so-called lobulocentric atrophy (see Sect. 5.5). Acinar to ductal metaplasia is commonly identified in chronic pancreatitis and in resection specimens for ductal adenocarcinoma. Despite its emerging role in pancreatic carcinogenesis in mice, the proof that acinar to ductal metaplasia is linked to the development of human pancreatic cancer, either by preceding the PanIN progression model or through the initiation of dysplastic lesions other than PanIN, is still awaited [1]. Therefore, acinar

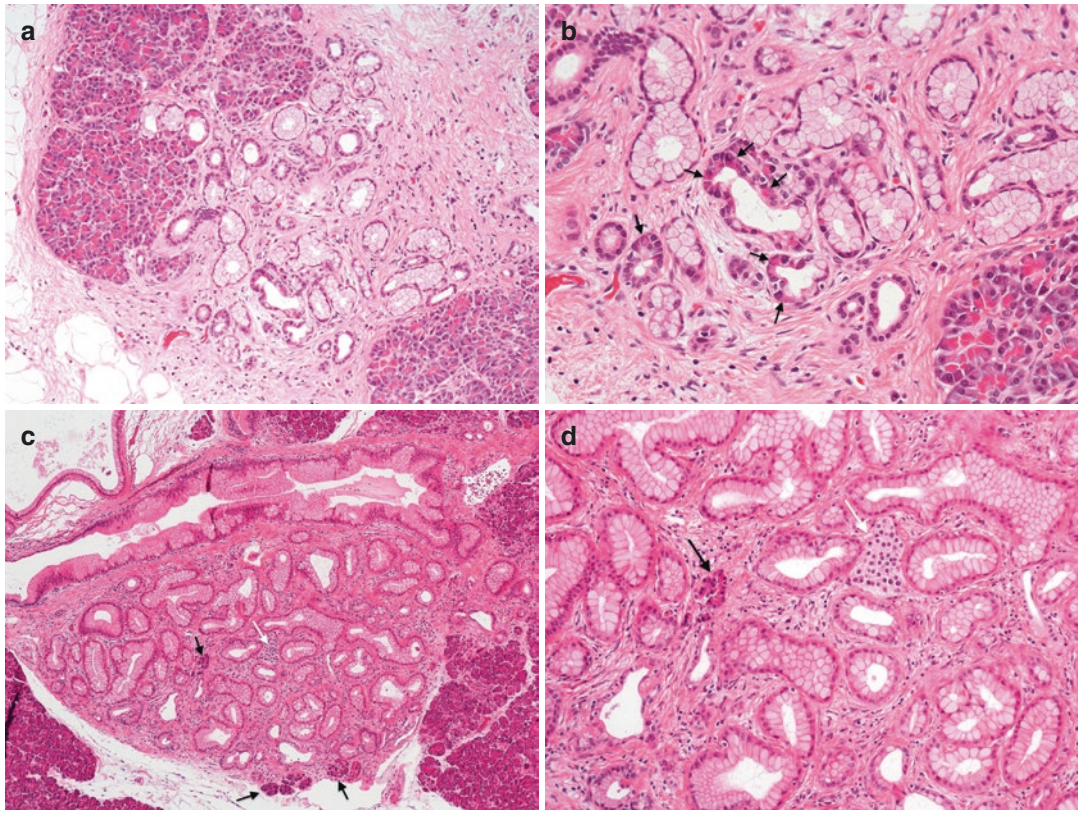

Fig. 5.3 Acinar to ductal metaplasia: some of the acini in this lobule have changed into small ductular structures (**a**). The latter are lined with mucin-rich columnar epithelium, consistent with low-grade PanIN, but some have retained cytoplasmic eosinophilia (*arrows*) (**b**). Almost the entire lobule has undergone acinar to ductal metaplasia, with only a few acini remaining (*black arrows*). Note the presence of a residual islet *(white arrow*) and the extensive low-grade PanIN changes in both the newly formed ductules and the adjacent interlobular duct (**c, d**)

to ductal metaplasia is currently not regarded as a core data item that should be included in diagnostic pathology reports.

5.4 Duct Epithelial Metaplasia

Several forms of metaplasia may affect the duct-lining epithelium (Fig. 5.4).

Squamous metaplasia is a common finding, which can occur anywhere in the pancreatic duct system. It is most commonly associated with chronic pancreatitis, in particular in the presence of intraductal calculi (see Chap. 7, Sect. 7.2.4). *Goblet cell (intestinal) metaplasia* may occasionally be identified as an isolated finding, usually in larger ducts in the vicinity of the ampulla of Vater. Goblet cells may occasionally be part of pancreatic intraepithelial neoplasia (PanIN), in which case the presence of cytological and architectural atypia should allow distinction from a mere metaplastic process (see Chap. 8, Sect. 8.3). *Oncocytic metaplasia* affects centroacinar cells and smaller duct ramifications and can be seen in the context of chronic pancreatitis or in otherwise unremarkable pancreatic tissue.

Probably the most common change exhibited by duct epithelium consists of a higher mucin content associated with a tall columnar cell shape. In the older literature this was reported as mucinous metaplasia or mucinous cell hypertrophy. However, currently it is regarded as a manifestation of low-grade PanIN (see Chap. 8, Sect. 8.2.1).

On rare occasion, in the context of sustained injury and inflammation, the main pancreatic duct

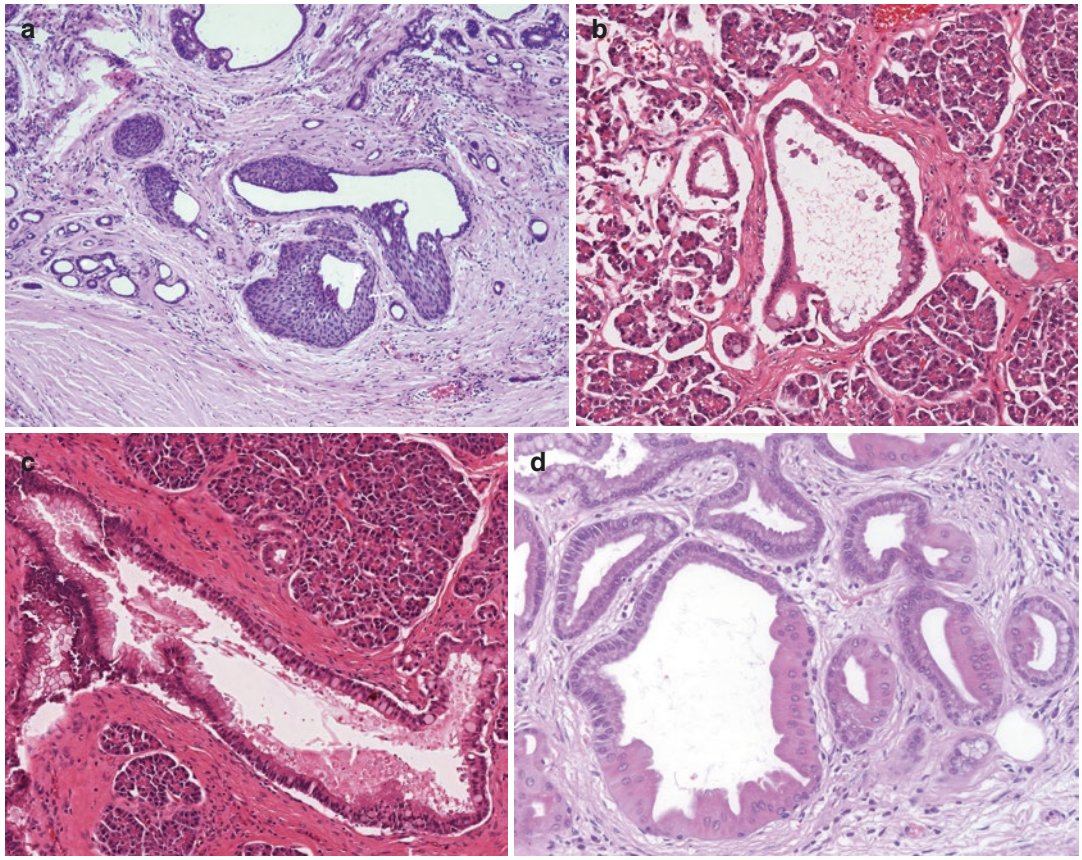

Fig. 5.4 Duct epithelial metaplasia: the lining of a cluster of mildly dilated ducts is replaced by mature squamous epithelium (**a**). Intestinal metaplasia is characterized by the presence of goblet cells within the duct-lining epithelium (**b**). Intestinal metaplasia with goblet cells is seen within an interlobular duct showing low-grade PanIN changes (**c**). In oncocytic metaplasia, the epithelial cells have copious eosinophilic cytoplasm (**d**)

and first-generation, large branch ducts may contain clusters of tightly packed, small glands that are located immediately underneath the surface epithelium. The glands resemble those of the pylorus and are lined with mucinous epithelial cells that are MUC5AC-positive (Fig. 5.5; see also Fig 7.11). These reparative changes are believed to result from hyperplasia of the pancreatic duct glands, i.e., the small blind-ending outpouches that are present in the large ducts of the pancreatic duct system (see Chap. 1, Sect. 1.4.3). While this rare change may at first glance resemble low-grade PanIN, the localization of the glands somewhat deeper below the surface epithelium, the absence of PanIN-like changes in the overlying duct-lining epithelium, and the context of heavy inflammation, will enable distinction from PanIN.

5.5 Lobulocentric Atrophy

Lobulocentric atrophy refers to a combination of changes, including atrophy of acinar parenchyma, acinar to ductal metaplasia, and fibrosis. 'Lobulocentric' indicates that the changes affect the center of the pancreatic lobules. The degree of changes can vary from only partial acinar atrophy with a small focus of acinar to ductal metaplasia to nearly complete acinar atrophy with replacement of most of the affected lobule by acinar to ductal metaplasia, fibrosis, and clustered islets. The changes are usually patchy, such that one lobule can be affected, while a neighboring lobule remains unaltered (Fig. 5.6). Lobulocentric atrophy is often associated with low-grade PanIN of

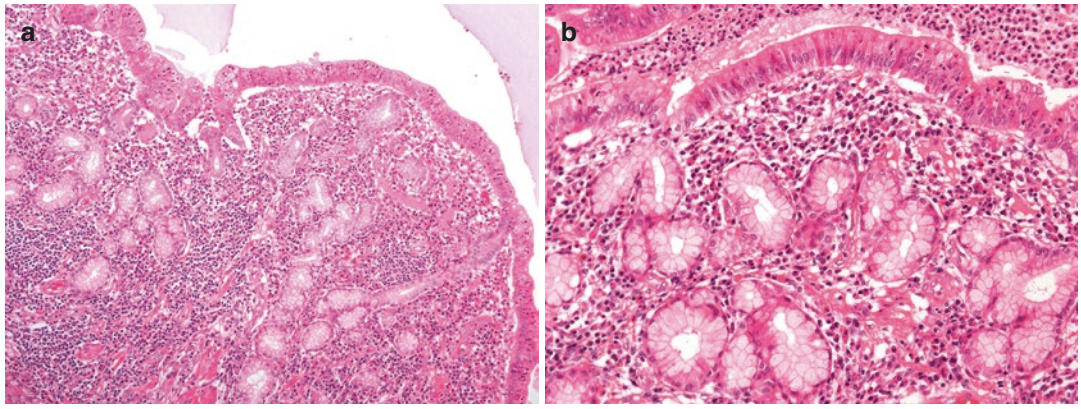

Fig. 5.5 Hyperplasia of periductal glands: the wall of this heavily inflamed main pancreatic duct contains clusters of small glands that are lined with mucinous columnar epithelium and resemble pyloric glands (**a**). In contrast to low-grade PanIN, the surface epithelium is free of PanIN-like changes (**b**). Inflammation in this case was due to actinomyces infection (same specimen as illustrated in Fig. 7.11)

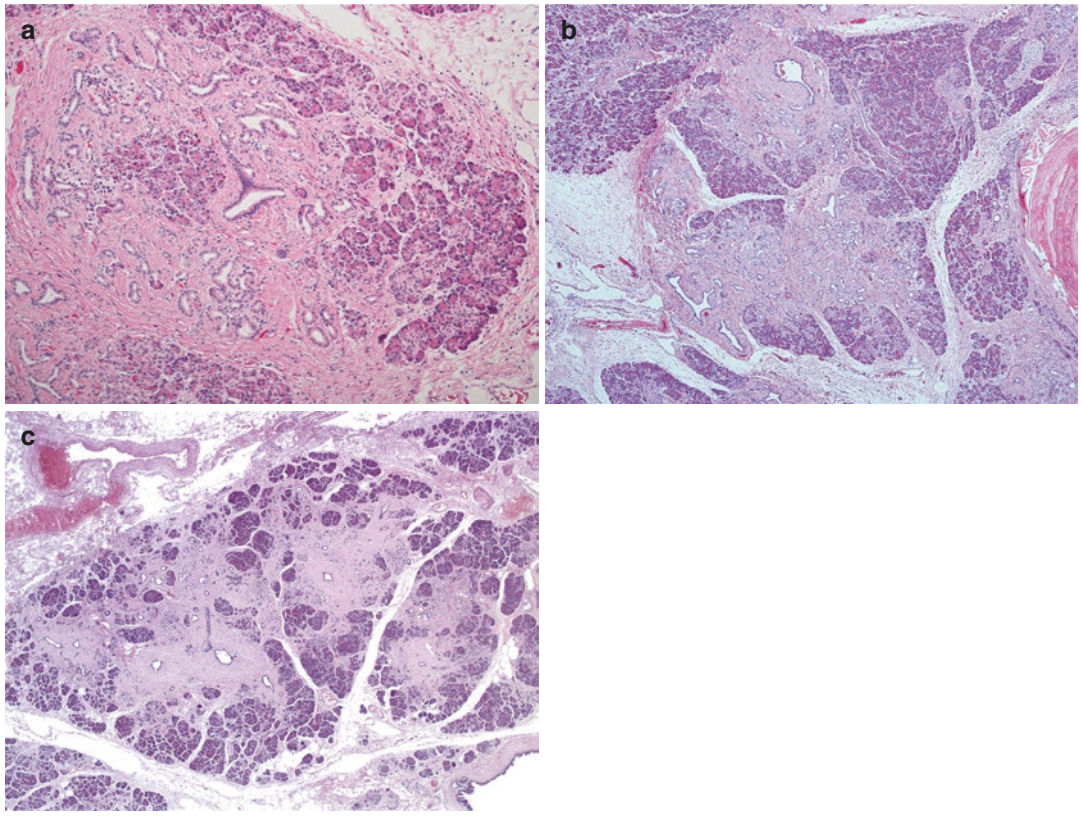

Fig. 5.6 Lobulocentric atrophy: in this lobule, acinar to ductal metaplasia is associated with marked atrophy and fibrosis of the central lobular area (**a**). Similar changes affect several neighboring lobules. Note the rim of residual acini at the periphery of the affected lobules (**b**). Most of the acinar parenchyma in the center of multiple lobules has been effaced and replaced by fibrosis with scattered ducts (**c**)

the intralobular ducts within the affected lobules, but the relationship between lobulocentric atrophy, acinar to ductal metaplasia, and PanIN, and the underlying pathogenetic mechanisms remain unclear. Because lobulocentric atrophy can measure a few millimeters in size and is therefore possibly detectable on endoscopic ultrasound (EUS) investigation, it has been suggested as a surrogate marker for PanIN in individuals who are at a high risk for developing ductal adenocarcinoma of the pancreas (see Chap. 6, Sect. 6.6) [2–4]. However, occurrence of lobulocentric atrophy is not limited to high-risk individuals and may also be found in chronic pancreatitis, in resection specimens with pancreatic ductal adenocarcinoma, in fatty atrophy of the pancreas, and in a variety of other conditions.

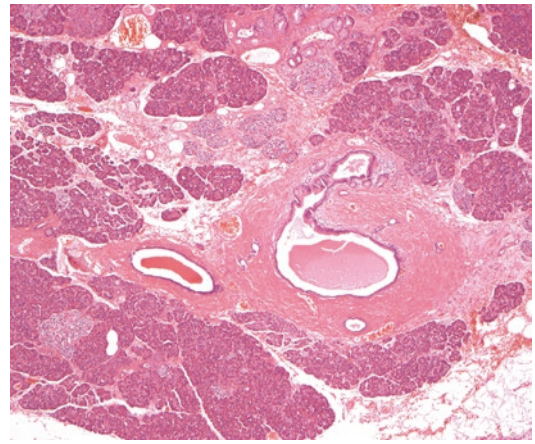

Fig. 5.7 Ageing pancreas: pancreas of a healthy octogenarian with mild duct dilatation and inspissated secretion, discrete periductal and inter-/intralobular fibrosis, as well as focal mild acinar atrophy

5.6 Age-Related Alterations

A range of histological changes in the pancreas has been associated with advancing age. None of these are specific, and similar changes may be seen in a different context. Various studies have shown that the pancreatic volume decreases with age, and concomitant with this change, the pancreatic exocrine function is gradually reduced with age. However, only 5% of otherwise healthy individuals older than 70 years of age develop exocrine pancreatic insufficiency [5]. In contrast, in healthy (non-diabetic) elderly individuals the β-cell mass remains preserved.

Fatty replacement or lipomatosis is increasingly frequent with advancing age (see Sect. 5.7) [6]. Pancreatic fat increases with age until approximately the age of 60, when this process reaches a plateau, while atrophy of the acinar parenchyma continues, resulting in an increased fat/parenchymal ratio in elderly individuals. Probably as a result of parenchymal atrophy and the replacement by adipose or fibrous tissue, lobulation of the pancreatic tissue may become more prominent both on imaging and macroscopic inspection.

Mild focal or segmental *duct ectasia*, of the main pancreatic duct or smaller branch ducts, can also be part of the spectrum of age-related pancreatic changes. Dilatation of the main pancreatic duct to over 4 mm in diameter was found at autopsy in 16% of cases [7]. In addition, small amounts of inspissated secretion may be present in the dilated ducts, and there may be a mild degree of periductal fibrosis (Fig. 5.7). Squamous metaplastic changes of the duct epithelium and low-grade PanIN may be seen (see Chap. 8). Acinar dilatation and prominence of centroacinar cells and intercalated ducts may also be part of the spectrum of alterations. All of these changes are neither strictly defined nor specific for advancing age, and similar alterations may also be seen in association with a variety of conditions and factors, including uremia, duct obstruction of any cause, ductal adenocarcinoma, excessive alcohol consumption, or cigarette smoking. The distinction from changes of early chronic pancreatitis may be difficult on morphological grounds only (see Chap. 7, Sect. 7.2.4).

5.7 Fatty Replacement

Fatty replacement of the pancreas, also known as adipose atrophy or lipomatosis of the pancreas, is a relatively common condition. The presence of adipocytes in the pancreas can vary from the common scattering of a few fat cells to the subto-

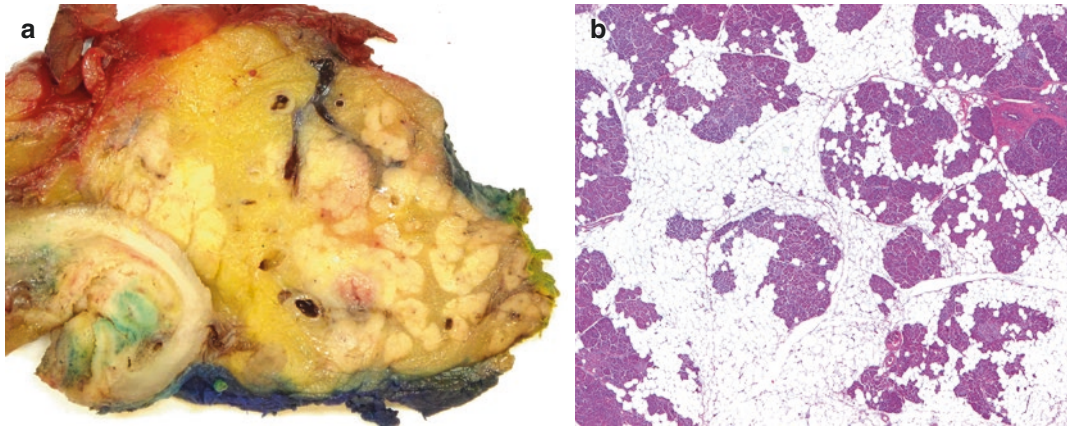

Fig. 5.8 Lipomatosis: the pancreatic lobules are reduced in number and separated by expanses of adipose tissue (**a**). Adipose tissue is present within and in between lobules. The amount of acinar parenchyma is markedly reduced (**b**)

tal replacement of the pancreatic parenchyma by adipose tissue (Fig. 5.8). Adipocytes can be seen within the parenchymal lobules and/or they accumulate in the interlobular space. The islets and ducts usually remain unaffected. While previously regarded as a finding of little if any importance, fatty replacement has recently become the subject of research, because epidemiological studies have shown that fat accumulation in the pancreas (and other viscera) is associated with obesity and type 2 diabetes mellitus, which are known risk factors for pancreatic cancer [8]. The pathophysiological role of the accumulation of adipocytes in the development of pancreatic ductal adenocarcinoma is poorly understood. Animal experiments suggest that through the release of pro-inflammatory and growth-promoting cytokines, adipocytes may promote cancer development and progression [9]. At the same time, obesity could be a risk factor for pancreatic cancer through the association with the development of diabetes mellitus. Meanwhile, a range of other conditions are known to be associated with fatty replacement of the pancreas, including dyslipidemia, arterial hypertension, steatosis of the liver, metabolic syndrome, human immunodeficiency virus-1 infection and/or antiretroviral therapy, and obstruction of the pancreatic duct. On rare occasions, fatty replacement may be seen in the context of cystic fibrosis (see Chap. 6, Sect. 6.1), hereditary pancreatitis (see Chap. 6, Sect. 6.3), Shwachman-Diamond syndrome, or Johanson-Blizzard syndrome, but these patients may present with clinical signs and symptoms of exocrine insufficiency. The clinical implications of fatty replacement are currently not clear and diagnostic criteria are lacking, both for radiological and histological diagnosis [10].

Fatty replacement of the pancreas is usually a diffuse process, although the degree of the fatty change may vary at the microscopic level. Occasionally, fatty replacement may appear as a single, focal, well-circumscribed lesion that is surrounded by normal pancreatic parenchyma, does not cause deformation of the organ countours, and may be difficult to correctly diagnose on preoperative imaging (Fig. 5.9).

5.8 Changes in Islets

The presence of endocrine cells within pancreatic ducts, often referred to as *ductulo-insular complexes* (see Chap.1, Sect. 1.4.4) can be seen in the context of chronic pancreatitis or endocrine cell hyperplasia (see Chaps. 7 and 21, Sects. 7.2.4 and 21.1).

Deposition of *amyloid* within islets may occur in older individuals, in particular in patients with type 2 insulin-independent diabetes mellitus (Fig. 5.10). There is no association between islet and systemic amyloidosis. Hyaline fibrosis

of islets, for example, in the context of chronic pancreatitis, may mimic islet amyloidosis, but distinction can easily be made with the help of a Congo red stain.

Cystic dilatation of islets is sometimes encountered in normal pancreatic tissue or in resection specimens for pancreatic cancer. It is of no known clinical significance, and the cause of the dilatation is usually not identifiable. The resulting cyst is an incidental microscopic finding, as the cyst diameter rarely exceeds 1–2 mm. The wall of the cyst is lined with endocrine cells, which in some areas may appear flattened. Immunostaining for chromogranin or synaptophysin can easily demonstrate the endocrine nature of this lesion (Fig. 5.11), which is helpful in distinguishing it from a small acinar cystic transformation (acinar cell cystadenoma), with which it may share superficial similarity (see Chap. 19, Sect. 19.1).

Focal reactive endocrine cell hyperplasia, a common finding in the context of acinar atrophy, is described in Chap. 21, Sect. 21.1.

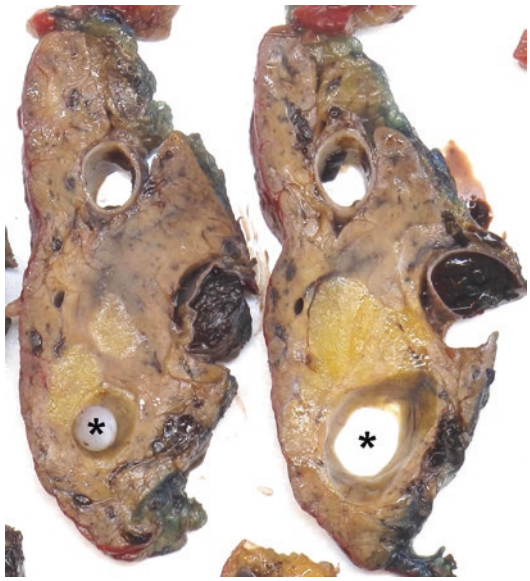

Fig. 5.9 Segmental fatty replacement: a sharply circumscribed area of fatty replacement is surrounded by unremarkable pancreatic parenchyma. Note the presence of a retention cyst (*asterisk*)

5.9 Autolytic Change

Pancreatic tissue is susceptible to autolytic change, and affected parenchymal areas may vary in extent from small randomly scattered foci to large expanses, in which case microscopic examination may be hampered (Fig. 5.12). Autolytic change should not be misinterpreted as genuine tissue necrosis, from which it can be distinguished first and foremost by the absence of an inflammatory reaction, that is, infiltration of leukocytes.

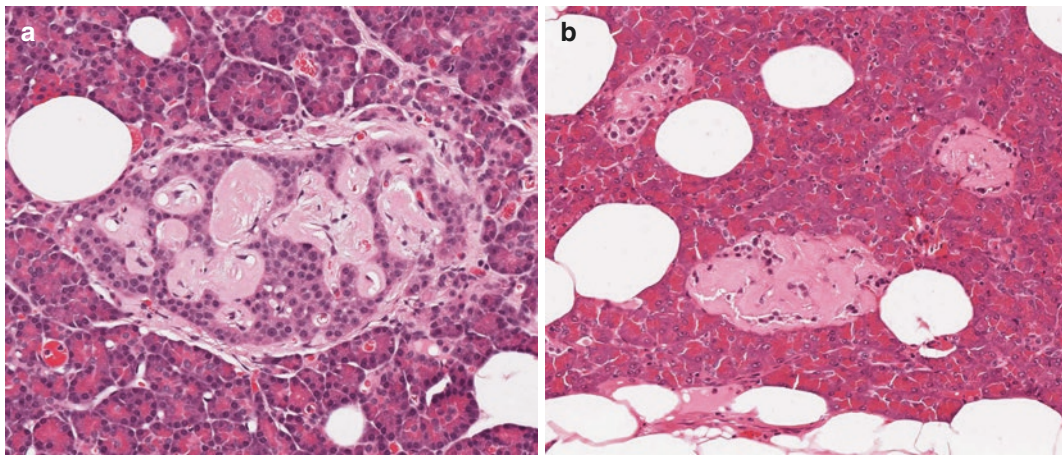

Fig. 5.10. Islet amyloidosis: extracellular deposits of amorphous eosinophilic material expand the space between islet cells (**a**). Several islets are nearly obliterated by amyloid deposits (**b**)

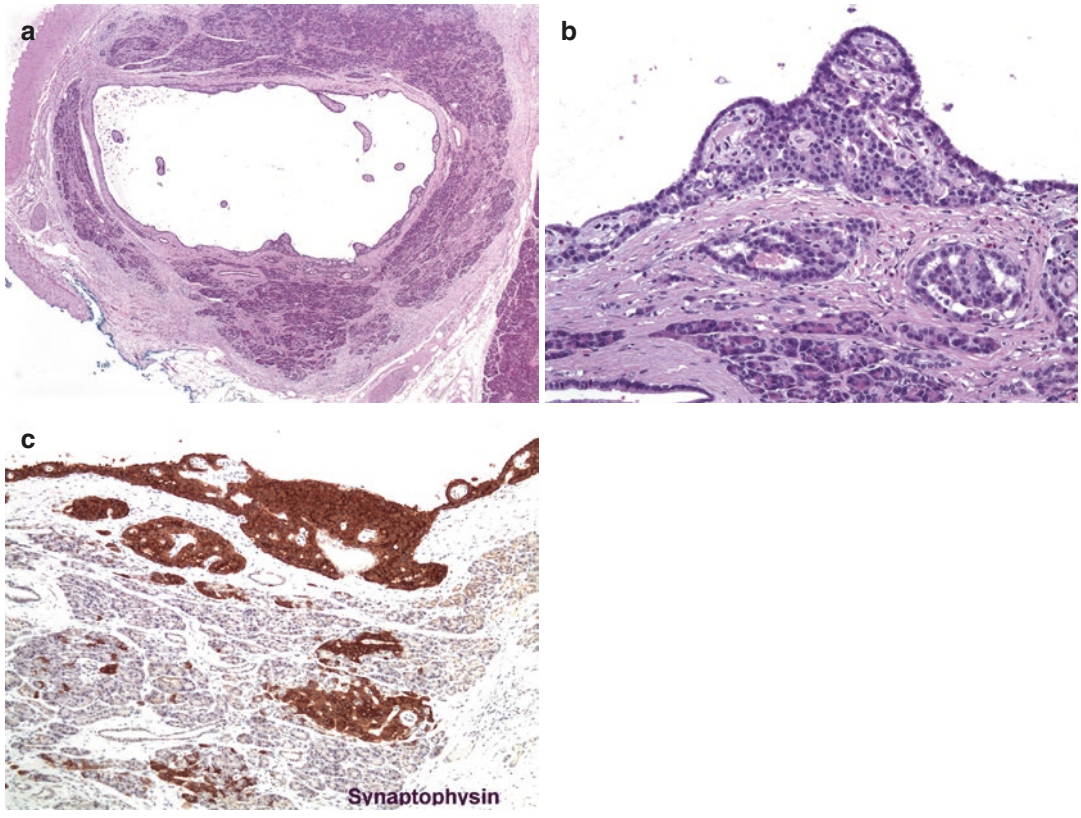

Fig. 5.11 Cystic islet dilatation: a small simple cystic space within an otherwise intact lobule (**a**) is surrounded by unremarkable islet cells (**b**) showing positive immunostaining for synaptophysin (**c**)

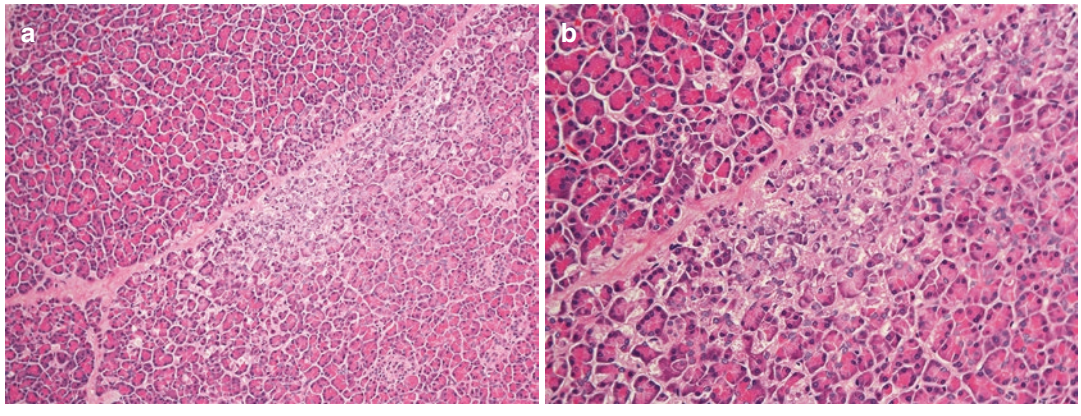

Fig. 5.12 Artefact mimicking necrosis: foci of acinar parenchyma of varying size and random localization show loss of normal cellular structures and staining (**a**). The absence of an inflammatory response distinguishes this artefactual change from necrosis, with which it bears superficial resemblance (**b**)

References

1. Storz P. Acinar cell plasticity and development of pancreatic ductal adenocarcinoma. Nat Rev Gastroenterol Hepatol. 2017;14:296–304.
2. Brune K, Abe T, Canto M, O'Malley L, Klein AP, Maitra A, et al. Multifocal neoplastic precursor lesions associated with lobular atrophy of the pancreas in patients having a strong family history of pancreatic cancer. Am J Surg Pathol. 2006;30:1067–76.
3. Shi C, Hruban RH, Klein AP. Familial pancreatic cancer. Arch Pathol Lab Med. 2009;133:365–74.
4. Goggins M, Overbeek KA, Brand R, Syngal S, Del Chiaro M, Bartsch DK, et al. Management of patients with increased risk for familial pancreatic cancer: updated recommendations from the International Cancer of the Pancreas Screening (CAPS) Consortium. Gut. 2020;69:7–17.
5. Löhr J-M, Panic N, Vujasinovic M, Verbeke CS. The ageing pancreas: a systematic review of the evidence and analysis of the consequences. J Intern Med. 2018;283:446–60.
6. Matsuda Y. Age-related morphological changes in the pancreas and their association with pancreatic carcinogenesis. Pathol Int. 2019;69:45062.
7. Stamm BH. Incidence and diagnostic significance of minor pathologic changes in the adult pancreas at autopsy: a systematic study of 112 autopsies in patients without known pancreatic disease. Hum Pathol. 1984;15:677–83.
8. Sreedhar UL, DeSouza SV, Park B, Petrov MS. A systematic review of intra-pancreatic fat deposition and pancreatic carcinogenesis. J Gastrointest Surg. 2019 Nov 20. https://doi.org/10.1007/s11605-019-04417-4. [Epub ahead of print]
9. Chang H-H, Eibl G. Obesity-induced adipose tissue inflammation as a strong promotional factor for pancreatic ductal adenocarcinoma. Cells. 2019;8:673.
10. Khoury T, Asombang AW, Berzin TM, Cohen J, Pleskow DK, Mizrahi M. The clinical implications of fatty pancreas: a concise review. Dig Dis Sci. 2017;62:2658–67.

Hereditary Exocrine Disorders

6

There are a number of inherited disorders that can affect the exocrine and/or endocrine function of the pancreas. These include inborn errors of metabolism such as hyperlipidemia, glycogen storage disorders, or maple syrup urine disease, which can be associated with pancreatitis (see review by Simon et al.) [1]. The autosomal dominant disorder hereditary pancreatitis will be discussed in this chapter, together with cystic fibrosis, which may only present in late adolescence or early adulthood, and hereditary hemochromatosis. There are also a number of inherited syndromes that are associated with an increased risk of pancreatic cancer, which will be briefly mentioned. Familial pancreatic cancer will be discussed in more detail, particularly with reference to the role of screening in high-risk individuals. Inherited endocrine disorders are discussed in Chap. 20, Sect. 20.12.

6.1 Cystic Fibrosis

Cystic fibrosis is an autosomal recessive disease caused by mutations in the cystic fibrosis transmembrane conductance regulator (*CFTR*) gene, located on chromosome 7q31.2. More than 1500 mutations have been described in the *CFTR* gene, but not all result in cystic fibrosis. This variation in genotype may account for the different phenotypes of cystic fibrosis and variation in disease severity. The *CFTR* gene encodes a protein that functions as a cell membrane chloride channel. Disruption of CFTR function leads to defective electrolyte transport across the cell membrane, particularly affecting the lung and pancreas. In the normal pancreas, the acinar cells secrete a relatively low volume of fluid rich in enzymes while the duct system secretes a relatively large volume of bicarbonate rich fluid. In cystic fibrosis, the volume of pancreatic fluid secreted is markedly lower than normal with resultant abnormally thick mucus in the pancreatic ducts, which leads to obstruction.

The incidence of cystic fibrosis in the Caucasian population is estimated to be 1 in 2000 to 1 in 3000. Males and females are affected equally, and most present in childhood with chronic sinopulmonary disease. Involvement of the pancreas manifests as pancreatic insufficiency and pancreatic abnormalities on imaging. Pancreatitis may be the first manifestation of cystic fibrosis. The sweat chloride test remains the gold standard for cystic fibrosis diagnosis, but does not always give a clear answer. Moreover, genetic testing does not always provide clarity [2].

6.1.1 Macroscopy

Pancreatic involvement in cystic fibrosis is characterized by varying degrees of fibrosis, fatty replacement, and cyst formation. There may be narrowing of the pancreatic ducts due to the

© Springer Nature Switzerland AG 2021
F. Campbell, C. S. Verbeke, *Pathology of the Pancreas*,
https://doi.org/10.1007/978-3-030-49848-1_6

fibrosis. The cysts, which represent dilated ducts, may vary from 1 to 3 mm in diameter up to 3–5 cm diameter. These cysts may contain cloudy fluid or inspissated protein-rich secretions, which can undergo mineralization and stone formation. In some cases, the pancreas may be almost entirely replaced by adipose tissue (lipomatosis) (see Chap. 5, Sect. 5.7).

6.1.2 Microscopy

The earliest change in cystic fibrosis is dilatation of acini and ductules with accumulation of eosinophilic secretions within them. Larger ducts may also contain inspissated secretions and show varying degrees of dilatation and periductal fibrosis. The secretions may show concentric lamellations resembling corpora amylacea. The cells lining the dilated ductules and acini may be flattened, and there may also be squamous metaplasia.

With progression of the disease, there is acinar and lobular atrophy, with increasing intralobular and interlobular fibrosis, typical of chronic pancreatitis (see Chap. 7, Sect. 7.2.4). There may be abundant islets, including enlarged islets, within the fibrous tissue, and fatty replacement of the pancreas. There may be marked cystic dilatation of ducts filled with eosinophilic secretions (Fig. 6.1) and, when ducts rupture, an associated periductal acute and chronic inflammatory cell infiltrate. In advanced disease, there may be extensive fatty replacement with only scattered residual ducts and islets within this adipose tissue.

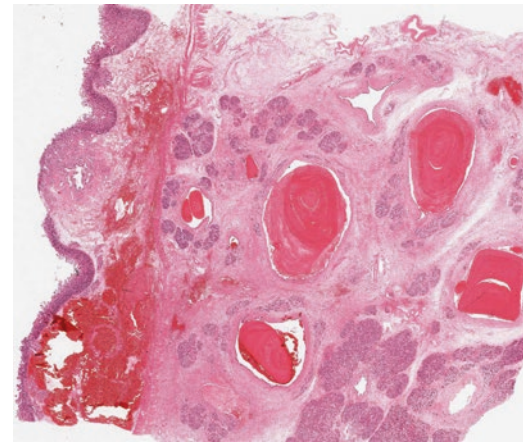

Fig. 6.1 Cystic fibrosis: cystic dilatation of ducts filled with eosinophilic secretions showing concentric lamellation. There is associated periductal fibrosis and a varying degree of lobular atrophy, but not the typical acinar dilatation

6.2 Hereditary Hemochromatosis

Hereditary hemochromatosis is an autosomal recessive disorder affecting the Caucasian population with a prevalence of between 1 in 200 and 1 in 300. The gene responsible for classic hereditary hemochromatosis is the *HFE* gene. Mutations in other iron genes, however, may be associated with hereditary iron overload syndromes and can cause all of the phenotypic features of classical hereditary hemochromatosis. The present definition of hereditary hemochromatosis, therefore, embraces the classic disorder related to HFE C282Y homozygosity and the rare disorders attributed to loss of transferrin receptor 2, hepcidin, hemojuvelin, or in very rare cases, ferroportin [3].

Hereditary hemochromatosis is characterized by inappropriately increased iron absorption from the duodenum and small intestine, with consequent deposition in various organs, notably the liver, endocrine glands, joints, heart, and skin, with resultant organ damage. Clinical features may be nonspecific and include lethargy and malaise, or reflect target organ damage and present with abnormal liver tests, cirrhosis, diabetes mellitus, arthropathy, cardiomyopathy, skin pigmentation, and hypogonadism. The classical description is that of cutaneous hyperpigmentation, diabetes mellitus, and hepatomegaly. Clinical manifestations often occur at 40 to 60 years of age, and men

tend to present earlier, due to the protective mechanism of menstrual blood loss in women.

6.2.1 Macroscopy

The descriptions of pancreatic pathology in hereditary hemochromatosis are almost invariably restricted to autopsy studies [4]. Macroscopically, the pancreas can be enlarged and may be a light brown or chocolate color with distinct lobulation, due to hemosiderin-laden lobules standing out from fibrous or fatty tissue.

6.2.2 Microscopy

On microscopy, hemosiderin deposition occurs throughout the pancreas and may be intracellular or extracellular. There is hemosiderin deposition within the acinar cells (Fig. 6.2), islets of Langerhans, and within the interstitium. There may be marked fibrosis, but the amount of fibrous tissue varies considerably and may be unevenly distributed throughout the pancreas. There may also be increased adipose tissue within the pancreas.

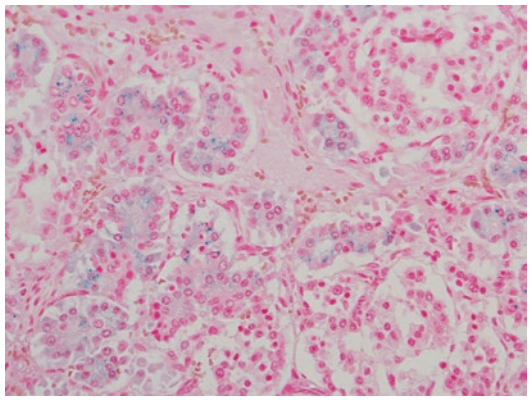

Fig. 6.2 Hereditary hemochromatosis: post-mortem pancreas showing hemosiderin deposition within the acini (Perls)

6.3 Hereditary Pancreatitis

Hereditary pancreatitis (HP), a rare form of early onset chronic pancreatitis (accounting for 1–2% of cases of chronic pancreatitis), was first described in 1952 [5], as hereditary chronic relapsing pancreatitis. It is an autosomal dominant disorder with incomplete (80%) penetrance and variable disease expression. In affected individuals, the disease may vary from very mild to severe, and there is an increased risk of pancreatic cancer (see Sect. 6.3.4).

In 1996, the gene for HP was mapped to the long arm of chromosome 7 (7q35) and the p.R122H mutation was identified in the serine protease 1 (*PRSS1*) gene, which encodes cationic trypsinogen [6, 7]. Cationic trypsinogen (*PRSS1*) gene mutations account for approximately 60–80% of all cases of HP, with no mutation having been identified in the other 20–40% of families. More than 30 mutations/polymorphisms in the *PRSS1* gene have now been described. With the exception of the p.R122x and p.N29x gain-of-function mutations, most of the mutations are not thought to be associated with chronic pancreatitis in an autosomal dominant manner. The p.R122H and p.N29I mutations in the *PRSS1* gene account for the majority of patients with HP. These mutations are thought to prevent the deactivation of inappropriately activated intrapancreatic trypsinogen or to increase trypsinogen activation, resulting in acinar cell autodigestion and subsequent pancreatitis. Mutation in the *PRSS1* gene can also induce misfolding of cationic trypsinogen, resulting in intracellular retention and decreased secretion [8]. This mutation-induced misfolding leads to endoplasmic reticulum stress and consequent acinar cell damage and pancreatitis.

Other genetic factors linked to chronic pancreatitis include mutations in the serine protease inhibitor Kazal type 1 (*SPINK1*) gene on chromosome 5q32, which encodes the pancreatic secretory trypsin inhibitor (PSTI). Although vari-

ous loss-of-function mutations in the *SPINK1* gene have been found in chronic pancreatitis, only the p.N34S mutation is believed to be associated with the disease. p.N34S is rare in HP but may act as a disease modifier.

6.3.1 Clinical Features

The typical presentation is with recurrent attacks of acute pancreatitis (without antecedent factors) before the age of 20 years (median age of onset about 10 years). There is subsequent progression to chronic pancreatitis (over a decade) in about half of the patients. The clinical features resemble those of idiopathic pancreatitis, but the clinical course may be more severe.

6.3.2 Diagnostic Criteria

The diagnosis of HP can only be considered after exclusion of other causes of chronic pancreatitis in childhood, e.g., anatomical anomalies (see Chap. 13), metabolic disorders, cystic fibrosis, trauma, and viruses. The diagnostic criteria for HP include two first-degree relatives, or at least three second-degree relatives, in two or more generations, with recurrent acute pancreatitis and/or chronic pancreatitis for which there are no precipitating factors. Detection of p.R122H or p.N29I mutations in the cationic trypsinogen (*PRSS1*) gene is diagnostic.

6.3.3 Pathology

There are limited publications on the histopathological features of HP [9–11]. There may be dilated ducts containing protein plugs and calculi, periductal fibrosis, pseudocysts, and diffuse atrophy of the pancreas, which may be detected on radiological imaging. The finding of a mutation does not predict the onset or severity of the disease. Patients may have entirely normal pancreas (Fig. 6.3), the classic histological features of chronic pancreatitis described above (Fig. 6.4), or may show extensive fatty replacement (Fig. 6.5 and see Chap. 5, Sect. 5.7).

Pancreatic intraepithelial neoplasia (PanIN—see Chap. 8) is frequently found in patients with hereditary pancreatitis [12], and includes both grades of PanIN. These PanINs occur at a younger age than in the general population (median age of 24 years), and the frequency is much higher than in the pancreata of normal subjects at the same age, or in patients with alcoholic chronic pancreatitis.

6.3.4 Cancer Risk

Patients with HP have an estimated 50–80 fold increased relative risk for developing pancreatic cancer and develop pancreatic cancer at a younger age than sporadic patients. This compares with a 2.5–3.8 fold increased risk of pancreatic cancer with cigarette smoking, and a 2–20 fold increased

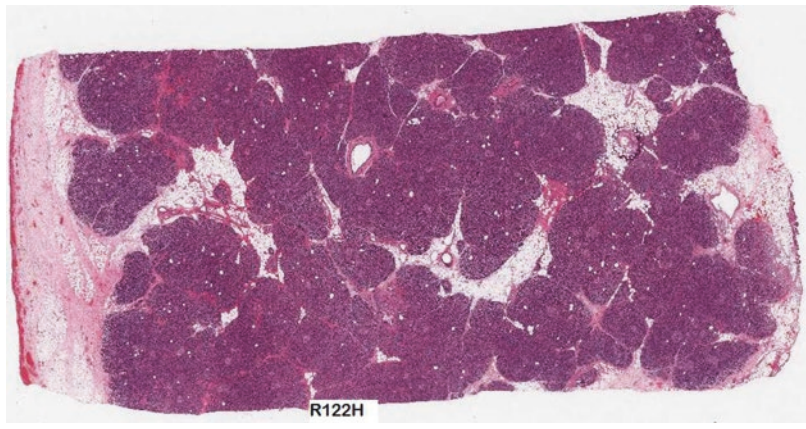

Fig. 6.3 Hereditary pancreatitis: the pancreas from this patient with a p.R122H mutation in the *PRSS1* gene shows normal histology

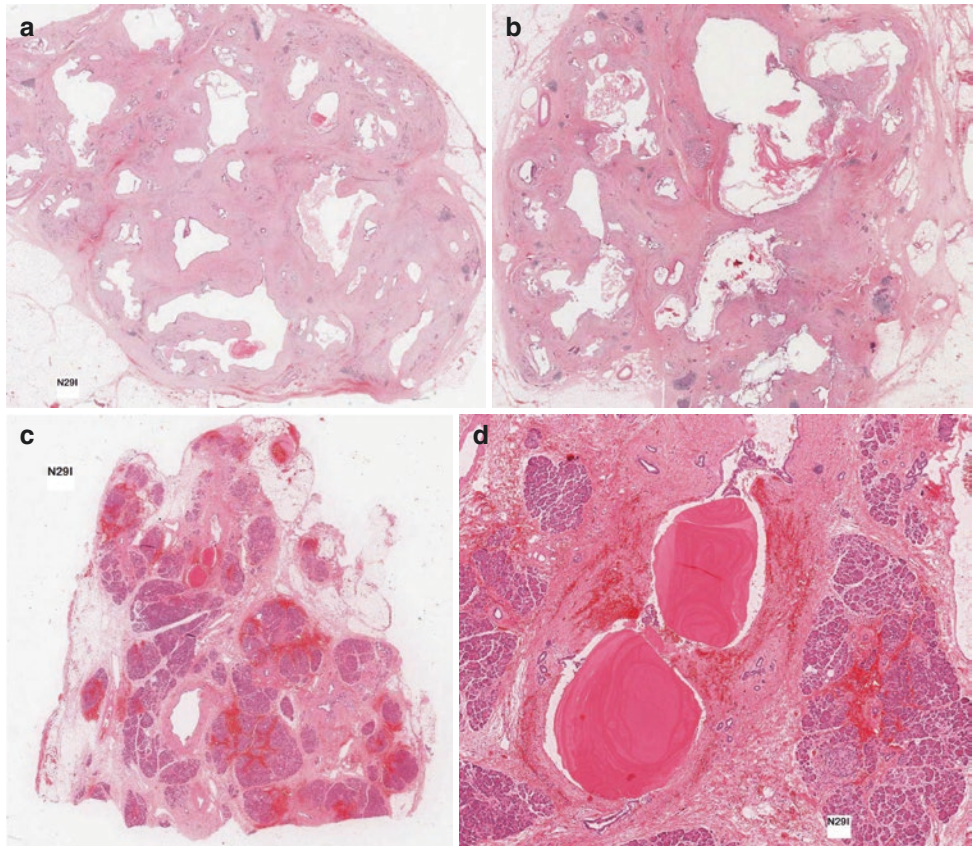

Fig. 6.4 Hereditary pancreatitis: the pancreas from this patient with a p.N29I mutation in the *PRSS1* gene shows dilated ducts and marked pancreatic atrophy and fibrosis (**a**). Calcified inspissated secretions are present in some of the dilated ducts, which also show disruption and associated inflammatory reaction (**b**). Pancreas from another patient with a p.N29I mutation in the *PRSS1* gene only shows focal duct dilatation and periductal fibrosis (**c**), with lamellated secretions in the lumen (**d**)

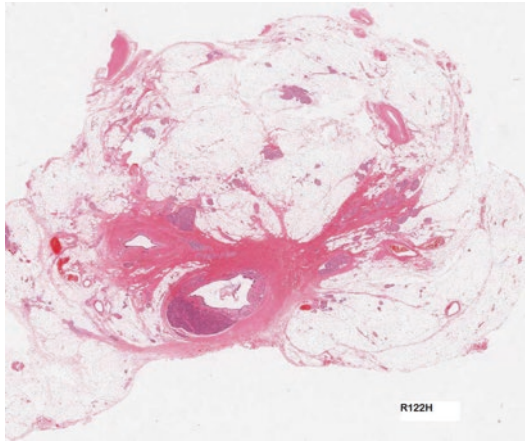

Fig. 6.5 Hereditary pancreatitis: the pancreas from this patient with a p.R122H mutation in the *PRSS1* gene shows severe fatty replacement (lipomatosis)

risk in chronic alcoholic pancreatitis (see below). Smoking also increases the risk of pancreatic cancer in HP and seems to lower the age of onset of the cancer by nearly two decades. There is no difference in the risk of pancreatic cancer based on the type of *PRSS1* gene mutation. Up to 40% of patients with hereditary pancreatitis may develop pancreatic cancer (conventional ductal type—see Chap. 9).

6.3.5 Management

HP should always be considered in the differential diagnosis when chronic pancreatitis occurs in a child or young adult. If HP is confirmed, then

patients should be advised not to smoke, because of the increased risk of pancreatic cancer, and should avoid alcohol since it is a risk factor for acute and chronic pancreatitis. A screening programme for the identification of HP patients and screening for early cancer, using multimodality imaging and molecular analysis of pancreatic juice obtained at endoscopic retrograde cholangiopancreatography (ERCP), combined with clinical genetic counselling and consultation with a pancreatologist, has been implemented by the European Registry of Hereditary Pancreatitis and Pancreatic Cancer (EUROPAC).

6.4 Inherited Pancreatic Cancer

Familial forms of pancreatic cancer account for approximately 10% of pancreatic carcinomas, and inherited predisposition to pancreatic cancer occurs in three distinct clinical settings:

(1) hereditary tumor predisposition syndromes, such as familial atypical multiple mole melanoma (FAMMM), familial adenomatous polyposis (FAP), hereditary breast and ovarian cancer (HBOC) syndrome, Lynch syndrome, Peutz-Jeghers syndrome (PJS),
(2) associated with chronic inflammation of the pancreas (cystic fibrosis and hereditary pancreatitis), and
(3) familial pancreatic cancer (FPC—see Sect. 6.5), which accounts for the largest proportion of families with autosomal dominant predisposition for pancreatic carcinoma.

The penetrance of pancreatic cancer is highly variable in these inherited disorders with relative risks ranging from 2 to 132 compared to the general population (Table 6.1) [13, 14]. These inherited risks of pancreatic cancer are generally much higher than the risks associated with cigarette smoking (2.5–3.8 fold increase), diabetes melli-

Table 6.1 Pancreatic cancer risk in inherited syndromes and disorders

	Inheritance	Location	Genes	Pancreas cancer risk (-fold)	Histology
Ataxia-telangiectasia	Autosomal recessive	11q22.3	*ATM*	Unknown	PDAC
Familial atypical multiple mole melanoma (FAMMM)	Autosomal dominant	9p21	*CDKN2A (p16)*	13–22	PDAC
Familial adenomatous polyposis (FAP)	Autosomal dominant	5q21	*APC*	4–5	PDAC IPMN
Hereditary breast and ovarian cancer syndrome	Autosomal dominant	13q12–13 & 17q21–24	*BRCA1* *BRCA2* *PALB2*	2.3 3.5–10 Unknown	PDAC
Li Fraumeni syndrome	Autosomal dominant	17p13.1	*TP53*	Unknown	PDAC
Lynch syndrome	Autosomal dominant	2p22–21 & 3p21.3	Mismatch repair genes	4.5–8.6	Medullary subtype of PDAC
Peutz-Jeghers syndrome	Autosomal dominant	19p13.3	*STK11/LKB1*	132	PDAC IPMN
Cystic fibrosis	Autosomal recessive	7q31.2	*CFTR*	2.6–5.3	PDAC
Hereditary pancreatitis	Autosomal dominant	7q35	*PRSS1*	53–87	PDAC
Familial pancreatic cancer (FPC)	Autosomal dominant (in 58–80%)	Unknown	Unknown	14–32	PDAC IPMN

Abbreviations: *PDAC* pancreatic ductal adenocarcinoma, *IPMN* intraductal papillary mucinous neoplasm, in which invasive carcinoma may be conventional PDAC or colloid carcinoma subtype of PDAC

tus (2.1–2.6 fold increase), and nonhereditary pancreatitis (2–20 fold increase).

6.4.1 Pathology

The pancreatic cancers in patients with these inherited syndromes are usually conventional, pancreatic ductal adenocarcinomas, but they may arise in a background of intraductal papillary mucinous neoplasm (IPMN), which can give rise to colloid carcinomas as well as conventional type ductal carcinoma (see Chap. 17). Whenever a medullary subtype of pancreatic ductal adenocarcinoma (see Chap. 9, Sect. 9.14.4) is diagnosed, the possibility of Lynch syndrome should be highlighted in the pathology report (Table 6.1).

6.5 Familial Pancreatic Cancer

Familial pancreatic cancer (FPC) applies to families with two or more first-degree relatives with pancreatic cancer that do not fulfill the criteria of any other inherited tumor syndrome (Table 6.1). A pattern indicative of an autosomal dominant trait of inheritance has been identified in 58–80% of FPC families. Germline mutations in *BRCA2*, *PALB2* (partner and localizer of *BRCA2*) and *ATM* are thought to be causative in 20% of FPC families [13], but the genetic basis of the majority of FPC cases has yet to be determined.

6.5.1 Cancer Risk

Most families with one or two cases of pancreatic carcinoma will be the result of chance or environmental factors, rather than due to an inherited predisposition. Families with many cases of pancreatic carcinoma are more likely to have FPC, so the prospective risk of pancreatic cancer progressively increases with the number of pancreatic cancers in a family. Thus, the risk for pancreatic cancer in individuals with one first-degree relative with pancreatic cancer is 4.6 fold higher than that for an individual without an affected first-degree relative; individuals with two affected first-degree relatives have a 6.4 fold increased risk; and individuals with three or more affected first-degree relatives have a 14- to 32-fold increased risk for pancreatic cancer [15].

6.5.2 Clinical Features, Pathology, and Prognosis

Patients with FPC develop their cancers at a similar age to those with sporadic forms of disease [16]. The sex distribution, pathology of the pancreatic carcinoma, and prognosis are also similar to the sporadic form. The majority of patients develop conventional pancreatic ductal adenocarcinoma or subtypes of pancreatic ductal adenocarcinoma, including adenosquamous carcinoma, undifferentiated carcinoma, and signet ring cell carcinoma (see Chap. 9, Sect. 9.14). They may develop invasive carcinoma arising from intraductal papillary mucinous neoplasm (IPMN with associated invasive carcinoma—see Chap. 17). However, it has recently been shown that IPMNs are probably not a specific feature of FPC [17].

6.6 Screening High-Risk Individuals

Patients with a family history of pancreatic cancer are significantly more likely to harbor widespread pancreatic cancer precursor lesions, namely pancreatic intraepithelial neoplasia (PanIN—see Chap. 8) and intraductal papillary mucinous neoplasia (IPMN—see Chap. 17), than those patients with sporadic pancreatic cancer. Furthermore, these pancreatic cancer precursors are more likely to contain high-grade dysplasia [18] than those present in pancreata from patients without a family history. This has led to the use of radiological imaging to detect these pre-invasive lesions (or asymptomatic small cancers) in high-risk individuals with an inherited predisposition to pancreatic cancer (Table 6.1), ultimately aiming to improve patient outcome [16].

PanIN can be associated with lobulocentric atrophy (see Chap. 5, Sect. 5.5), which may be detected on endoscopic ultrasound (EUS) [19].

However, lobulocentric atrophy occurs with low-grade and high-grade dysplasia and, therefore, there is a risk of overtreatment if pancreata are resected for lobulocentric atrophy which is only associated with low-grade dysplasia.

EUS and magnetic resonance imaging (MRI) can detect small cystic pancreatic lesions, which are often multiple and multifocal, and the majority of which are branch-duct-type IPMNs. CT is not as good as MRI or EUS for detecting these small cysts (see Chap. 14). Magnetic resonance cholangiopancreatography (MRCP) provides the best visualization of cystic communication (for IPMNs) with the main pancreatic duct [19]. Most sporadic branch-duct IPMNs have low risk for malignancy and can be observed safely if they do not meet standard internationally accepted consensus criteria for resection (see Chap. 17, Sect. 17.7). However, because these criteria have been validated only in patients with sporadic pancreatic cysts, it is unclear if they are appropriate for high-risk individuals [16].

The prevalence of PanINs and IPMNs increases with age; the likelihood of a prevalent lesion is much higher in patients over 50 years of age. Therefore, the recently published international guidelines on the management of patients with an inherited predisposition to pancreatic cancer [20] recommend that screening should start at 50–55 years of age. For patients with hereditary pancreatitis (see Sect. 6.3), screening typically should begin at 40 years of age, because of the younger age of onset of pancreatic cancer in these patients. These guidelines also propose that initial screening should include EUS and/or MRI/MRCP but not CT.

References

1. Simon P, Weiss FU, Zimmer KP, Koch HG, Lerch MM. Acute and chronic pancreatitis in patients with inborn errors of metabolism. Pancreatology. 2001;1:448–56.
2. Farrell PM, White TB, Ren CL, Hempstead SE, Accurso F, Derichs N, et al. Diagnosis of cystic fibrosis: consensus guidelines from the cystic fibrosis foundation. J Pediatr. 2017;181S:S4–S15.
3. Pietrangelo A, Torbenson M. Disorders of iron overload. In: Burt A, Ferrell L, Hubscher S. MacSween's pathology of the liver. Edinburgh: Churchill Livingstone Elsevier; 2017, p. 279–289, chapter 4.
4. Lack EE. Cystic fibrosis and selected disorders with pancreatic insufficiency. In: Pathology of the pancreas, gallbladder, extrahepatic biliary tract, and ampullary region. Oxford: Oxford University Press; 2003, p. 63–80, chapter 3.
5. Comfort MW, Steinberg AG. Pedigree of a family with hereditary chronic relapsing pancreatitis. Gastroenterology. 1952;21:54–63.
6. Whitcomb DC, Gorry MC, Preston RA, Furey W, Sossenheimer MJ, Ulrich CD, et al. Hereditary pancreatitis is caused by a mutation in the cationic trypsinogen gene. Nat Genet. 1996;14:141–5.
7. Le Bodic L, Bignon JD, Raguénès O, Mercier B, Georgelin T, Schnee M, et al. The hereditary pancreatitis gene maps to long arm of chromosome 7. Hum Mol Genet. 1996;5:549–54.
8. Kereszturi E, Szmola R, Kukor Z, Simon P, Weiss FU, Lerch MM, et al. Hereditary pancreatitis caused by mutation-induced misfolding of human cationic trypsinogen: a novel disease mechanism. Hum Mutat. 2009;30:575–82.
9. Klöppel G, Detlefsen S, Feyerabend B. Fibrosis of the pancreas: the initial tissue damage and the resulting pattern. Virchows Arch. 2004;445:1–8.
10. Felderbauer P, Stricker I, Schnekenburger J, Bulut K, Chromik AM, Belyaev O, et al. Histopathological features of patients with chronic pancreatitis due to mutations in the PRSS1 gene: evaluation of *BRAF* and *KRAS* mutations. Digestion. 2008;78:60–5.
11. Singhi AD, Pai RK, Kant JA, Bartholow TL, Zeh HJ, Lee KK, et al. The histopathology of *PRSS1* hereditary pancreatitis. Am J Surg Pathol. 2014;38:346–53.
12. Rebours V, Lévy P, Mosnier JF, Scoazec JY, Soubeyrand MS, Fléjou JF, et al. Pathology analysis reveals that dysplastic pancreatic ductal lesions are frequent in patients with hereditary pancreatitis. Clin Gastroenterol Hepatol. 2010;8:206–12.
13. Matsubayashi H, Takaori K, Morizane C, Maguchi H, Mizuma M, Takahashi H, et al. Familial pancreatic cancer: concept, management and issues. World J Gastroenterol. 2017;23:935–48.
14. Hong SM, Park JY, Hruban RH, Goggins M. Molecular signatures of pancreatic cancer. Arch Pathol Lab Med. 2011;135:716–27.
15. Klein AP, Brune KA, Petersen GM, Goggins M, Tersmette AC, Offerhaus GJ, et al. Prospective risk of pancreatic cancer in familial pancreatic cancer kindreds. Cancer Res. 2004;64:2634–8.
16. Canto MI, Hruban RH, Fishman EK, Kamel IR, Schulick R, Zhang Z, et al. American Cancer of the Pancreas Screening (CAPS) Consortium. Frequent detection of pancreatic lesions in asymptomatic high-risk individuals. Gastroenterology. 2012;142:796–804.
17. Sheel ARG, Harrison S, Sarantitis I, Nicholson JA, Hanna T, Grocock C, et al. Identification of cystic lesions by secondary screening of Familial Pancreatic Cancer (FPC) kindreds is not associated

with the stratified risk of cancer. Am J Gastroenterol. 2019;114:155–64.
18. Shi C, Klein AP, Goggins M, Maitra A, Canto M, Ali S, et al. Increased prevalence of precursor lesions in familial pancreatic cancer patients. Clin Cancer Res. 2009;15:7737–43.
19. Brune K, Abe T, Canto M, O'Malley L, Klein AP, Maitra A, et al. Multifocal neoplastic precursor lesions associated with lobular atrophy of the pancreas in patients having a strong family history of pancreatic cancer. Am J Surg Pathol. 2006;30:1067–76.
20. Goggins M, Overbeek KA, Brand R, Syngal S, Del Chiaro M, Bartsch DK, et al. Management of patients with increased risk for familial pancreatic cancer: updated recommendations from the International Cancer of the Pancreas Screening (CAPS) Consortium. Gut. 2020;69:7–17.

Check for updates

Inflammatory Disorders

7

Inflammatory processes affecting the pancreas present clinically as two distinct entities: acute and chronic pancreatitis. Although both exhibit characteristic morphological features, there is a certain overlap, in particular in the pathology of a common complication of both diseases, the pancreatic pseudocyst.

In recent years, new types of chronic pancreatitis have been characterized, and attempts are made at using a more etiology-based terminology, such as hereditary pancreatitis, autoimmune pancreatitis, paraduodenal pancreatitis, and obstructive chronic pancreatitis. Following the increasing insight into the lesions that precede the development of pancreatic cancer, the link between ductal adenocarcinoma and chronic pancreatitis has been an area of research activity. In clinical practice, reliable identification of cancer in patients with known chronic pancreatitis is of key importance and can be occasionally a diagnostic challenge to the reporting pathologist.

In addition to the prototypical acute and chronic pancreatitis, other inflammatory processes may affect the pancreas, either primarily or, more often, as part of a multi-organ or systemic disease, such as collagen vascular disease or sarcoidosis.

7.1 Acute Pancreatitis

7.1.1 Definition and Clinical Features

Acute pancreatitis is an acute inflammatory disorder of the pancreas, characterized clinically by abdominal pain and raised serum levels of pancreatic enzymes. From a clinical viewpoint, acute pancreatitis is usually described as mild, with recovery within 5–7 days, or severe, with prolonged hospitalization due to complications and a significant mortality rate. Corresponding with both clinical disease courses, morphology traditionally distinguishes between interstitial or edematous pancreatitis (mild) and acute hemorrhagic pancreatitis (severe). Because the pancreas can completely normalize following acute pancreatitis and surgery is performed only in a proportion of severe cases, the pathologist barely ever sees acute pancreatitis outside the context of animal experiments, except for the rare autopsy case or surgical specimen of grave disease. Occasionally, acute pancreatitis may be present in surgical resection specimens for neoplasia, in which the pancreatitis is often a complication of preoperative endoscopic retrograde cholangiopancreatography (ERCP) or, less commonly, secondary to tumor obstruction of the pancreatic duct system. Furthermore, morphological changes secondary to acute pancreatitis may sometimes be seen in extrapancreatic tissues, for

© Springer Nature Switzerland AG 2021
F. Campbell, C. S. Verbeke, *Pathology of the Pancreas*,
https://doi.org/10.1007/978-3-030-49848-1_7

example, in omental, retroperitoneal, bone marrow, or even subcutaneous adipose tissue that is affected by necrosis due to the elevated levels of circulating lipase.

7.1.2 Etiology

The list of possible causes of acute pancreatitis is extensive, and a summary is provided in Table 7.1. In the Western world, cholelithiasis and alcohol abuse are by far the most common causes. In 10–25% of patients, acute pancreatitis is idiopathic, that is, without identifiable etiology.

The morphological findings during acute pancreatitis are essentially the same, irrespective of the etiology, and in the majority of cases the underlying cause can be identified neither macroscopically nor microscopically. Infectious acute pancreatitis may be an exception to this. While a long list of infectious agents has been reported to cause acute pancreatitis, infectious pancreatitis as such is exceedingly rare, and may either occur as part of disseminated infectious disease or affect the pancreas in isolation. Primary bacterial pancreatitis is extremely rare, whereas secondary bacterial infection occurs in 40–70% of patients with necrotizing pancreatitis. The clinical presentation of infectious acute pancreatitis can vary from entirely asymptomatic with merely biochemical evidence (elevated serum amylase, lipase, or trypsin) to fulminant disease with fatal outcome. The damage caused to the pancreas depends on the specific infectious agent and can range from abscess formation to necrosis, development of an inflammatory mass, or peripancreatic lymphadenitis. The latter three types of lesions—observed, for example, in mycobacterial infection—may clinically mimic pancreatic cancer and occasionally result in pancreatic resection (Fig. 7.1). Some viruses (e.g., coxsackie- and enteroviruses) may affect the islet cells more than the acinar cell population and therefore present clinically as type 1 diabetes rather than acute pancreatitis. Opportunistic infections should always be considered in human immunodeficiency virus (HIV)-positive

Table 7.1 Etiology of acute pancreatitis

- Mechanical
  - Gallstones, biliary sludge
  - Pancreatic duct (or duodenal) stricture or obstruction
  - Pancreas divisum
  - Pancreas annulare
  - Long common channel
  - Periampullary duodenal diverticulum
  - Pancreatic tumor
- Toxic
  - Alcohol
  - Methanol
  - Organophosphate poisoning
  - Scorpion and snake venom
- Drug-induced
  - Thiazide diuretics
  - Angiotensin converting enzyme inhibitors
  - Estrogens
  - Corticosteroids
  - Azathioprine
- Metabolic
  - Hyperparathyroidism
  - Hyperlipidemia
  - Hypercalcemia
- Genetic
  - Mutations of *PRSS1, SPINK1, CFTR*
- Vascular
  - Ischemia
  - Hemorrhagic shock
  - Intraoperative hypotension
  - Vasculitis
  - Atheroembolism
- Trauma
  - Blunt or perforating abdominal injury
  - Iatrogenic injury (e.g., ERCP)
- Infectious
  - Viral: mumps, coxsackievirus, cytomegalovirus, varicella-zoster virus, herpes simplex virus, HIV
  - Bacterial: salmonella, leptospira, campylobacter, mycobacteria, yersinia
  - Fungal: candida, aspergillus, actinomyces (Fig. 7.11)
  - Parasitic: nematodes, cestodes, trematodes, toxoplasma, cryptosporidium
- Miscellaneous
  - Radiotherapy
  - Immunotherapy
  - Pregnancy and post-partum period
  - Renal insufficiency
  - Choledochal cyst
- Idiopathic

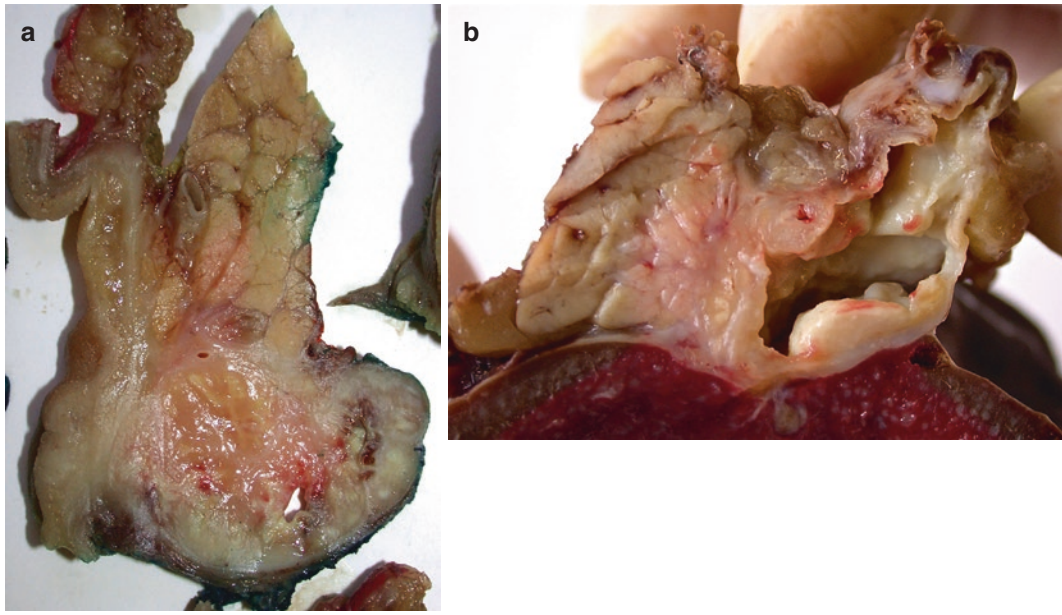

Fig. 7.1 Tuberculosis of the pancreas: necrotizing inflammation affects the posterior aspect of the pancreatic head and an adjacent enlarged peripancreatic lymph node. Pancreatic cancer was suspected on preoperative imaging (**a**). Tuberculosis involving the pancreatic tail has resulted in a cold abscess, which extends into the peripancreatic and perisplenic soft tissue (**b**)

Table 7.2 Etiology of acute pancreatitis in HIV-positive patients

• Viral
– Cytomegalovirus
– Herpes simplex
– Herpes zoster
• Fungal
– Cryptococcus neoformans
– Histoplasma capsulatum
– Candida
– Aspergillus
• Mycobacterial
– Mycobacterium tuberculosis
– Mycobacterium avium-intracellulare
• Other infectious agents
– Toxoplasma gondii
– Cryptosporidia
– Microsporidia
– Pneumocystis carinii
• Drugs
– Pentamidin (pneumocystis treatment)
– Antiretroviral treatment
• Neoplasms (involving pancreas)
– Kaposi sarcoma
– Malignant lymphoma

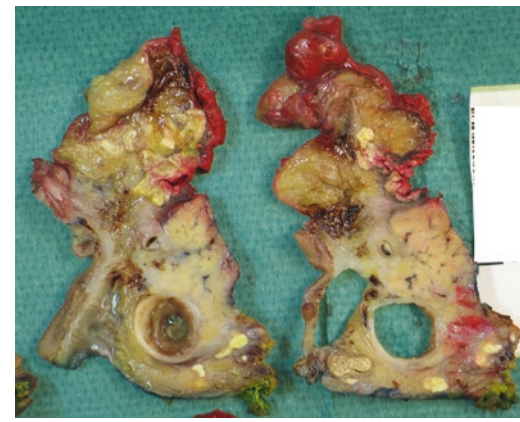

Fig. 7.2 Acute pancreatitis with fat necrosis: foci of fat necrosis are characterized by pale-yellow chalk-like material. Note the abundance of fat necrosis around the pancreas, in this case as a complication of endoscopic retrograde cholangiopancreatography (ERCP)

patients, immunocompromised individuals, and occasionally also in neonates (cytomegalovirus infection) presenting with acute pancreatitis (Table 7.2). On rare occasion, focal acute pancreatitis may be a complication of radiotherapy or immunotherapy.

7.1.3 Macroscopy

In *mild acute pancreatitis* the gland is swollen and there may be scattered foci of lipolytic fat necrosis (Fig. 7.2). The latter consist of chalk-like white-yellowish material containing calcium soaps, which precipitate when calcium binds to glycerol that has been freed up by lipase-mediated cleavage of fatty acids. Hemorrhage and necrosis are absent, and changes may resolve partially or completely over the course of several weeks.

In *severe acute pancreatitis* the key gross features are necrosis and hemorrhage (Figs. 7.3 and 7.4). The former rarely affects the entire organ but is usually patchy in distribution, with confluent areas of varying extent and foci of relatively spared pancreatic tissue flanking zones of necrosis and hemorrhage. It is not uncommon for the peripancreatic tissue and peripheral pancreatic parenchyma to be involved, while a core of tissue remains viable in the center of the gland. Foci of fat necrosis, often confluent, are present in and around the pancreas and occasionally at a distance from the pancreas (e.g., in the omentum). Necrosis is often associated with hemorrhage, which on rare occasion may dominate the gross findings and eclipse the presence of pancreatic or fat necrosis. Bleeding may extend into the surrounding tissues, for example, the mesentery and pararenal space, and from there to the subcutaneous tissues leading to bruising of the flank (Grey Turner's sign) or periumbilical area (Cullen's sign). Peripancreatic fluid collections, sometimes of considerable volume and flocculent appearance due to the suspension of necrotic tissue debris, may be present. The macroscopic appearance of pseudocysts, a key complication of acute pancreatitis, is described below.

Fig. 7.3 Early severe acute pancreatitis: an area of pancreatic parenchyma between the duodenal wall and common bile duct has lost the usual lobulation due to marked edema and early patchy necrosis

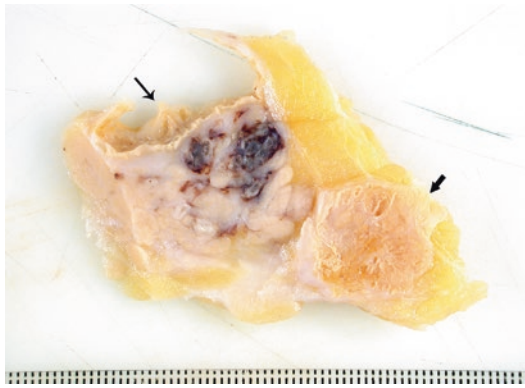

Fig. 7.4 Severe acute pancreatitis: pancreatic parenchyma shows extensive hemorrhage and necrosis. Note the presence of part of a pseudocyst (*arrow*) and a focus of fat necrosis (*block arrow*). Tissue was sampled at autopsy following gallstone-induced severe acute pancreatitis

7.1.4 Microscopy

In mild acute pancreatitis the pancreas is edematous, and collections of fibrin and neutrophils may be present in the widened interlobular septa (Fig. 7.5). There may be focal or more widespread duct dilatation. Necrosis of pancreatic parenchyma is not present, but scattered foci of

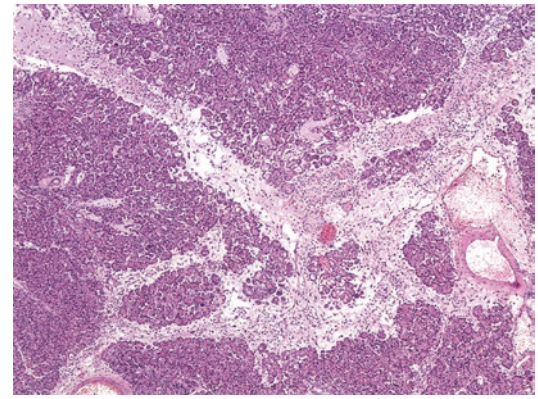

Fig. 7.5 Mild acute pancreatitis: interlobular septa are expanded by marked edema and neutrophilic infiltration. Note the absence of parenchymal necrosis

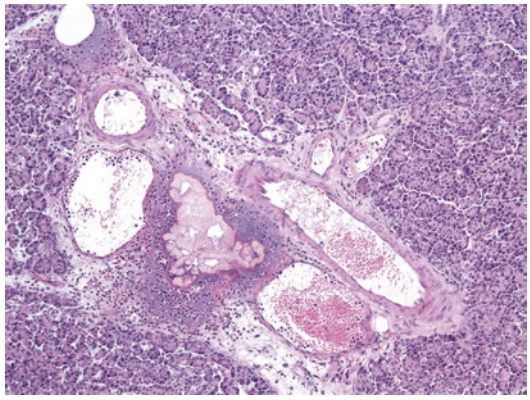

Fig. 7.6 Mild acute pancreatitis: an interlobular septum is widened by edema and neutrophilic infiltration. It also contains a focus of lipolytic fat necrosis

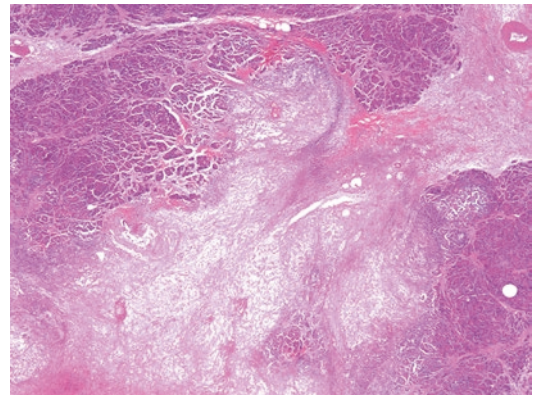

Fig. 7.8 Severe acute pancreatitis: pancreatic parenchyma shows extensive necrosis and patchy hemorrhage

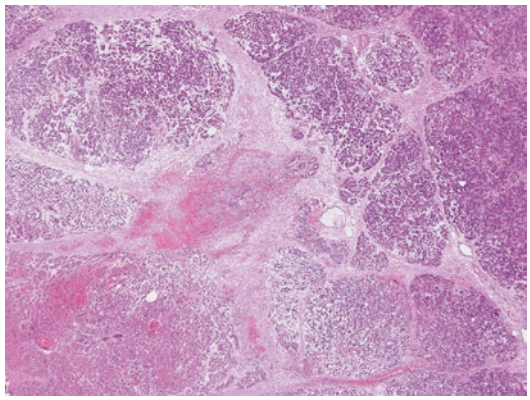

Fig. 7.7 Early severe acute pancreatitis: in addition to interlobular edema and neutrophilic infiltration, there is focal necrosis and hemorrhage in both the interlobular septa and acinar parenchyma

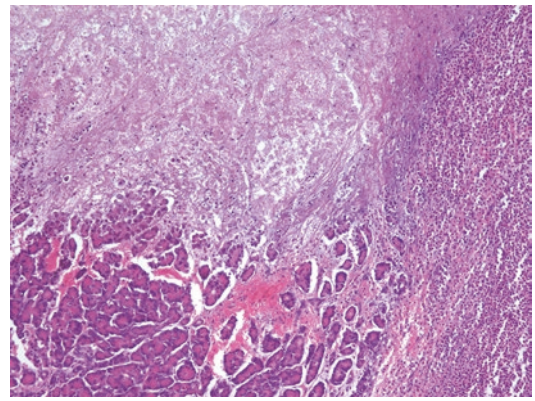

Fig. 7.9 Severe acute pancreatitis: necrosis of the acinar parenchyma is associated with hemorrhage and dense neutrophilic infiltration

fat necrosis may be seen in and around the pancreas (Fig. 7.6). The latter are microscopically characterized by ghost-like outlines of necrotic adipocytes, which contain opaque material consisting of birefringent saponification crystals.

In severe acute pancreatitis any of the constituent cells and tissues of the pancreas can be affected. Necrosis of pancreatic parenchyma, including islets and ducts, is the key feature, which in severe cases can lead to loss of considerable parts of the organ (Figs. 7.7, 7.8, 7.9, and 7.10). Hemorrhage from necrotic blood vessels or vascular thrombosis are relatively common findings in severely affected areas. As time progresses, the inflammatory cell infiltrate, which

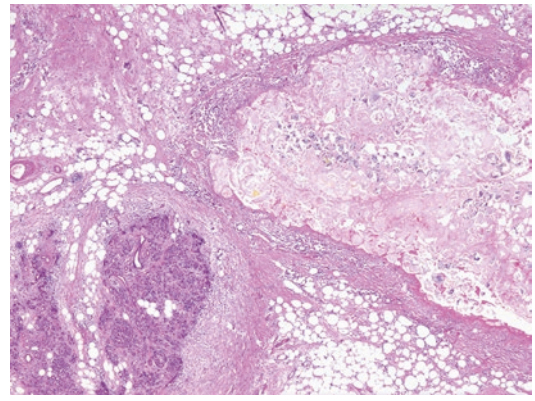

Fig. 7.10 Fat necrosis in severe acute pancreatitis: microscopically, fat necrosis is characterized by ghost-like outlines of necrotic adipocytes, which contain opaque or slightly basophilic material

is composed mainly of neutrophils, increases in intensity and spreads through interlobular septa, around areas of parenchymal necrosis, and occasionally within or around pancreatic ducts.

Microscopic changes are nonspecific and not related to the cause of the acute pancreatitis. An exception to this may be infectious pancreatitis. Certain morphological details, such as the specific cell populations that are affected, the nature of the inflammatory cell infiltrate, or the presence of intranuclear inclusions or other organism-specific features may allow identification of the causative infectious agent (Fig. 7.11). This may require confirmation by immunohistochemistry or PCR-analysis.

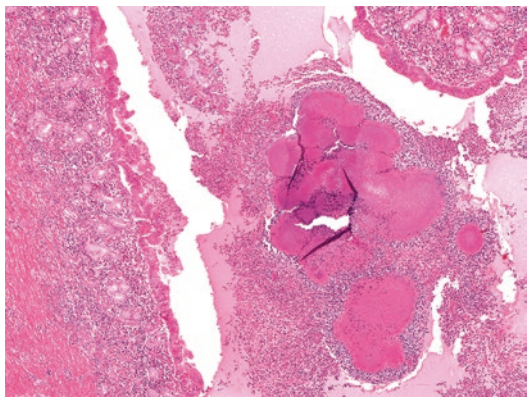

Fig. 7.11 Pancreatitis due to actinomyces infection: the dilated lumen of the main pancreatic duct contains numerous neutrophils and actinomyces colonies with the characteristic radiating arrangement of branched hyphae. Note the dense, chronic inflammatory cell infiltrate in the duct wall (see also Fig. 5.5)

Fig. 7.12 Acute pancreatitis with pseudocyst: this collapsed pseudocyst has a thin membranous capsule with a small focus of fresh necrosis

7.1.5 Complications

Systemic complications of acute pancreatitis, including shock and intravascular coagulopathy, may be life threatening, but have no morphological correlate within the pancreas. The most frequent local complications are hemorrhage, pseudocyst formation, and bacterial infection.

Pseudocysts represent collections of pancreatic juice secondary to duct rupture. Continuity of the pseudocysts with the pancreatic duct system is therefore a defining (albeit not always morphologically identifiable) feature and explains the continuous filling of the pseudocyst cavity with amylase-rich fluid. Pseudocysts are usually unilocular, often single, and can reach a considerable size of up to and over 10 cm. They are filled with turbid fluid and floating debris. The inner surface is often covered with necrotic tissue and exudate (Fig. 7.12).

Microscopically, the wall of a pseudocyst is characteristically devoid of epithelial lining but instead often covered with fibrinous exudate. It consists of granulation tissue, which contains a mixed inflammatory cell infiltrate and imperceptibly blends with the surrounding inflamed pancreatic tissue. Over time, granulation tissue transforms into less cellular, more compact fibrous tissue.

Pseudocysts can by themselves be the cause of further complications, the most significant of which are *hemorrhage, fistulating inflammation, and infection*. Vascular damage with—on occasion significant—bleeding into the pseudocyst cavity is caused by the combination of local inflammation and proximity of the blood vessels to the digestive enzymes in the lumen of the pseudocyst. Erosion of a vein or artery by a pseudocyst (see Fig. 7.41), or formation of a fistula between the aorta and a pseudocyst may result in life-threatening hemorrhage. Occasionally, a pseudocyst can extend by fistulization into adjacent tissues and organs such as the bowel, peritoneal or pleural cavities, or the portal vein.

The necrotic debris, which is abundantly present in severe acute pancreatitis, constitutes an ideal medium for bacterial or fungal growth. Infection may occur by blood-borne distribution, by spread via lymphatics draining tissues with bacterial colonization, or through direct spread from the adjacent transverse colon, which may be hypoperfused in severe acute pancreatitis and therefore permissible to bacterial transmigration. *Bacterial or fungal infection* of pancreatic necrosis is a serious complication of acute pancreatitis, which is associated with a significant mortality rate. In contrast, infection of a pseudocyst with formation of an abscess is a localized and demarcated infectious process with a less severe impact on outcome.

7.2 Chronic Pancreatitis

7.2.1 Definition and Clinical Features

Chronic pancreatitis is a progressive inflammatory disease of the pancreas, which leads to irreversible morphological changes of the gland, most notably parenchymal atrophy and fibrosis, along with a gradual impairment of exocrine and endocrine function. The process is chronic, it usually evolves slowly over many years. Acute pancreatitis and especially recurrent acute pancreatitis commonly initiate the development of chronic pancreatitis and are therefore considered significant risk factors for the disease [1].

Abdominal pain is usually the leading clinical symptom, along with gradually worsening impairment of the exocrine function, which leads to malabsorption, steatorrhea, and weight loss. Diabetes mellitus is often a late consequence of endocrine dysfunction. Pseudocysts are a frequent complication of chronic pancreatitis and affect up to 60% of all patients. Other common complications include stenosis of the common bile duct or duodenum and portal hypertension.

Treatment of patients with chronic pancreatitis is mainly conservative or endoscopic. It aims at the removal of the underlying cause, the alleviation of pain, and the management of the exocrine and endocrine insufficiency and any of the various complications. Pain alleviation can also be achieved through surgical decompression of the pancreatic duct system, and several procedures to accomplish this have been established. The various surgical procedures that exist and the corresponding pancreatic specimen types are discussed in Chap. 2, Sect. 2.8.

Because surgical resection is generally performed only for intractable pain in late-stage disease, tissue samples of chronic pancreatitis represent only a small proportion of the overall pancreatic workload, and pathologists see almost exclusively the so-called burnt-out chronic pancreatitis, when inflammatory cell infiltration is scanty and pancreatic parenchyma is nearly completely lost and replaced by fibrous tissue. An exception to this can be seen in autoimmune pancreatitis, a special form of pancreatitis, which is often diagnosed and biopsied at an earlier stage (see Sect. 7.2.7).

7.2.2 Etiology

Over the past five decades, several classification schemes for chronic pancreatitis have been proposed, each of which has put a different focus on clinical, imaging, and morphological features [2, 3]. Etiology has become an increasingly important criterion for the characterization of the disease, in particular as the genetics of pancreatitis are gradually elucidated. Whereas formerly, chronic pancreatitis was believed to be almost exclusively induced by environmental factors, the relationship between genetic predisposition and exposure to the environment has become a central concept in the understanding of the pathogenesis of this disease (see Chap. 6, Sect. 6.3).

In all continents, alcohol overconsumption is the most frequent cause of chronic pancreatitis. About 70% of pancreatitis cases are attributable to chronic heavy alcohol drinking. Tobacco smoking contributes to the risk of chronic pancreatitis, and smoking and alcohol consumption are suspected to act synergistically with regard to the pancreatitis-associated risk for pancreatic cancer (see Sect. 7.2.10). Chronic obstruction is a further not uncommon cause of chronic pancreatitis, and the nature of the obstruction can be manifold. Hereditary pancreatitis, that is, pancre-

atitis with a genetic pathogenesis, is discussed further in Chap. 6, Sect. 6.3. Tropical pancreatitis forms a small subgroup in which the exclusive geographical distribution is the main characteristic feature, while the underlying etiology is possibly a complex interaction between environmental and genetic factors. Autoimmune pancreatitis and paraduodenal pancreatitis have a distinct etiological basis. Other rare causes of chronic pancreatitis include radiation injury, metabolic diseases (many of which are hereditary, see Chap. 6), and medication. In approximately 25% of patients, a cause cannot be identified, and the disease is classified as idiopathic chronic pancreatitis. Where appropriate, more detailed information on the etiology of the different forms of chronic pancreatitis is provided in the corresponding sections within this chapter.

Several attempts at establishing a morphological classification of chronic pancreatitis in terms of etiology have mostly proven unsuccessful, as the correlation of the latter with gross and microscopic findings is generally poor. In most cases, morphological features do not allow conclusions regarding the underlying cause, except for autoimmune and paraduodenal pancreatitis, which have pathognomonic features, and are described separately in this chapter.

7.2.3 Macroscopy

Chronic pancreatitis involves the pancreas most commonly in a diffuse fashion, but segmental or focal involvement may also be seen. In case of focal involvement of the pancreas, chronic pancreatitis may be tumefactive and as such it may occasionally mimic neoplasia on imaging. As an exception, paraduodenal pancreatitis is by definition a segmental form of chronic pancreatitis, which is limited to the duodenum-flanking part of the pancreatic head. Even if the gland is affected diffusely by chronic pancreatitis, the changes tend to be patchy in distribution, with some areas being more severely altered than others. In early disease stages, the gland is usually indurated and enlarged. With disease progression and worsening of fibrosis and parenchymal atrophy, the pancreas becomes typically rock-hard and shrunken (Figs. 7.13, 7.14, and 7.15).

On slicing, pancreatic ducts are often irregularly dilated. Calculi may be present, which are typically of a white color due to their calcium carbonate content (Figs. 7.16 and 7.17). The size of the stones can vary from just a few millimeters to well over a centimeter. The largest stones are often found in tropical pancreatitis (see Sect. 7.2.6.3). While calculi are always present within ducts, the latter may rupture, and ensuing inflammation and fibrosis can result in incorporation

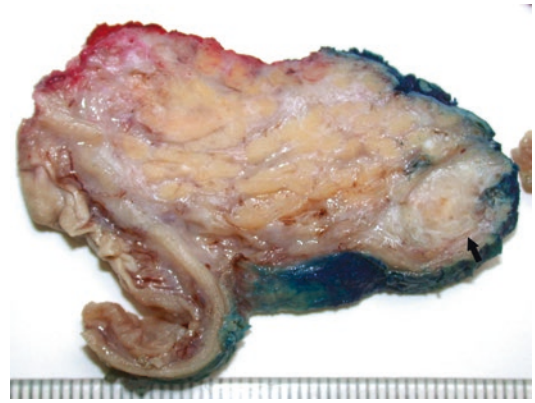

Fig. 7.13 Early chronic pancreatitis: interlobular septa are widened by fibrosis. A small area of parenchymal loss and scarring is present at the uncinate process (*arrow*)

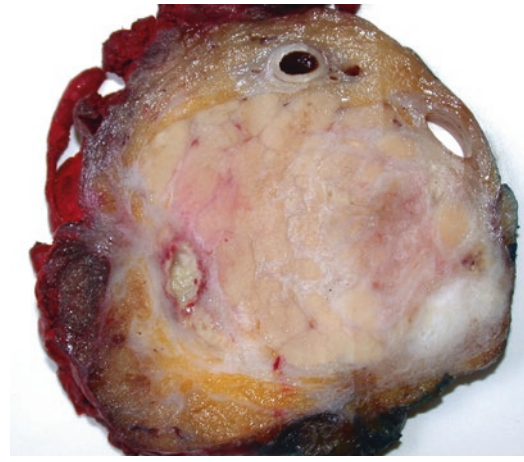

Fig. 7.14 Chronic pancreatitis: in some areas, fibrosis is still confined to the thickened interlobular septa, while in others it has become confluent and there is patchy parenchymal loss. Note the focus of frank necrosis

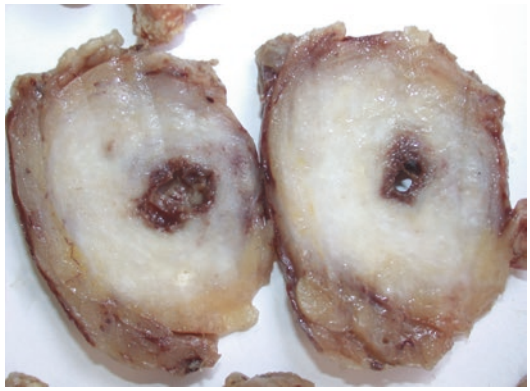

Fig. 7.15 End-stage chronic pancreatitis: the pancreas has been replaced by scar tissue without residual parenchyma. The main pancreatic duct is dilated and contains inflammatory detritus due to stone incarceration

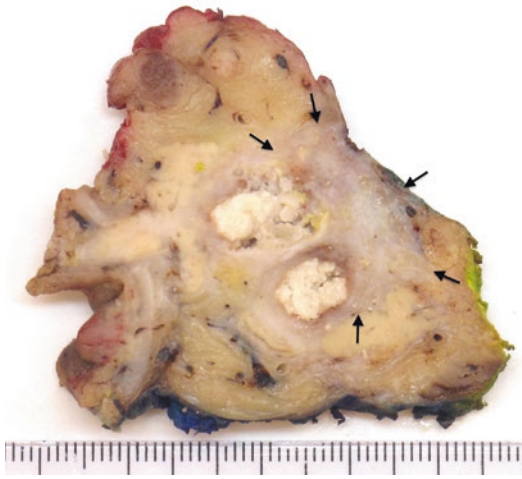

Fig. 7.16 Chronic pancreatitis with calcification: two dilated ducts are obliterated by large, pale concrements. Note the fibrosis and atrophy of pancreatic parenchyma in one area (*arrows*), whereas elsewhere, parenchyma is better preserved

Fig. 7.17 Calculi in chronic pancreatitis: stones are typically white and vary in size and shape (stones from same specimen as illustrated in Fig. 7.15)

of concretions in scar tissue, making it difficult to extract the stones during specimen dissection without disruption of the surrounding tissue. Occasionally, probably most commonly in obstructive chronic pancreatitis, intraluminal inspissated secretions may not be calcified but rather appear as soft, white, rounded mozzarella-like bodies (see Sect. 7.2.6.4). Calcified deposits may occasionally be found in intrapancreatic or peripancreatic soft tissue, and these represent the calcified residua of previous fat necrosis. Areas of acute parenchymal and fat necrosis may be seen (Fig. 7.14), especially in early stage chronic pancreatitis, which is often characterized by recurrent episodes of acute pancreatitis.

7.2.4 Microscopy

All constituent tissues and cell populations of the pancreas are affected by the progressive inflammatory process of chronic pancreatitis, although changes may not occur synchronously and homogenously throughout the gland. Acinar atrophy, fibrosis, and pancreatic duct changes represent the cardinal triad of microscopic features. No less important, however, are gradual changes to the islets of Langerhans, nerves, and blood vessels, which find their clinical correlate in glucose intolerance, pain, and vascular complications, respectively.

In the following sections, the microscopic features common to all forms of chronic pancreatitis are described, except for autoimmune pancreatitis and paraduodenal pancreatitis, which have different, pathognomonic morphological features and will be discussed separately.

Progressive atrophy of the acinar parenchyma is a constant feature of chronic pancreatitis (Figs. 7.18, 7.19, and 7.20). Distribution is often patchy, with near normal lobules flanking severely atrophic ones. Initially, atrophy of individual acini is characterized by loss of zymogen granulation and flattening of the acinar cells with formation of a central lumen, a phenomenon referred to as acinar to ductal metaplasia (see Chap. 5, Sect. 5.3). In subsequent stages, acini gradually disappear, and eventually much of the

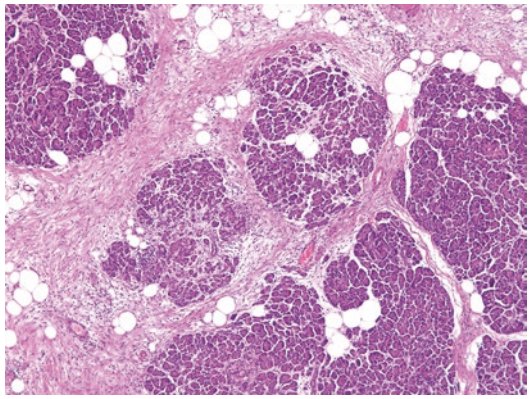

Fig. 7.18 Early chronic pancreatitis: interlobular septa are expanded by fibrosis. Note the 'rounding off' of the acinar lobules

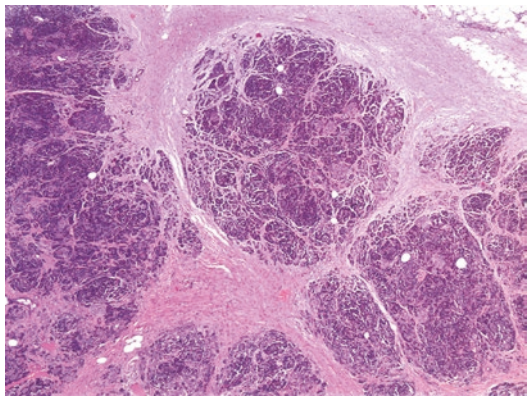

Fig. 7.19 Chronic pancreatitis: fibrosis has widened the interlobular septa and begins to extend into the lobules. Acinar atrophy affects mainly the periphery of the lobules

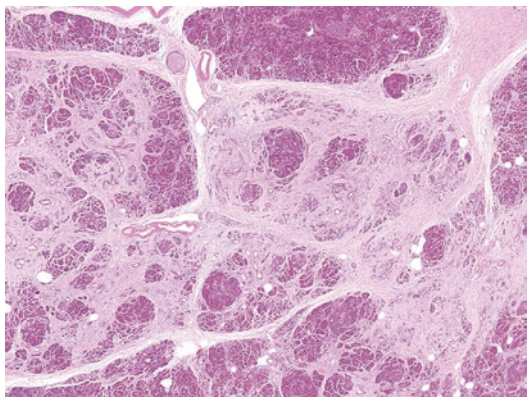

Fig. 7.20 Advanced chronic pancreatitis: inter- and intralobular fibrosis is associated with marked, in some areas subtotal lobular atrophy. Note the patchiness of changes, with some lobules remaining nearly intact

acinar compartment is lost and the lobular architecture becomes effaced (Fig. 7.21).

Fibrosis goes hand in hand with the gradual acinar atrophy. In early stages of the disease, fibrosis is more cellular and shows a patchy, mainly interlobular distribution. As the disease progresses, fibrosis extends between and within atrophic lobules, and may become confluent, forming vast sheets of fibrosis and scar tissue with low cellularity and a high collagen content.

Pancreatic ducts of all caliber are frequently dilated (Fig. 7.22). Duct dilatation can vary within the same specimen, ranging from areas with mild concentric dilatation to foci of irregular saccular ectasia. The ducts, whether or not dilated, commonly contain protein plugs. The latter represent inspissated secretions, which have an eosinophilic and often concentrically laminated appearance and may be calcified (Figs. 7.23 and 7.24). The epithelium lining dilated ducts is often flattened, and occasionally it can be eroded or ulcerated, especially in the vicinity of intraluminal calculi. Intraluminal collections of neutrophils may accompany these changes. Duct dilatation and ulceration can lead to duct rupture with associated nonspecific acute and chronic inflammation in the surrounding tissue (Fig. 7.25). Probably as a late complication of duct erosion and rupture, duct strictures may also develop in chronic pancreatitis (Fig. 7.26). Squamous metaplasia or PanIN-lesions of varying extent and severity can be present in both dilated and non-dilated ducts (Fig. 7.27), and they may be accompanied by foci of lobulocentric atrophy (see Chap. 5, Sect. 5.5, and Chap. 8, Sect. 8.5). Sheath-like fibrosis often surrounds ducts, especially if these are dilated.

The *inflammatory cell infiltrate* in chronic pancreatitis is usually rather mild and patchy. It consists of chronic inflammatory cells, mainly lymphocytes admixed with small numbers of macrophages and occasional plasma cells. The composition of the inflammatory cell population is nonspecific, and immunohistochemical characterization of the lymphoid cells is of no diagnostic value for the distinction between the different forms of chronic pancreatitis. Focal concentration of chronic inflammatory cells around pancreatic ducts or peripheral nerves is common (Fig. 7.28).

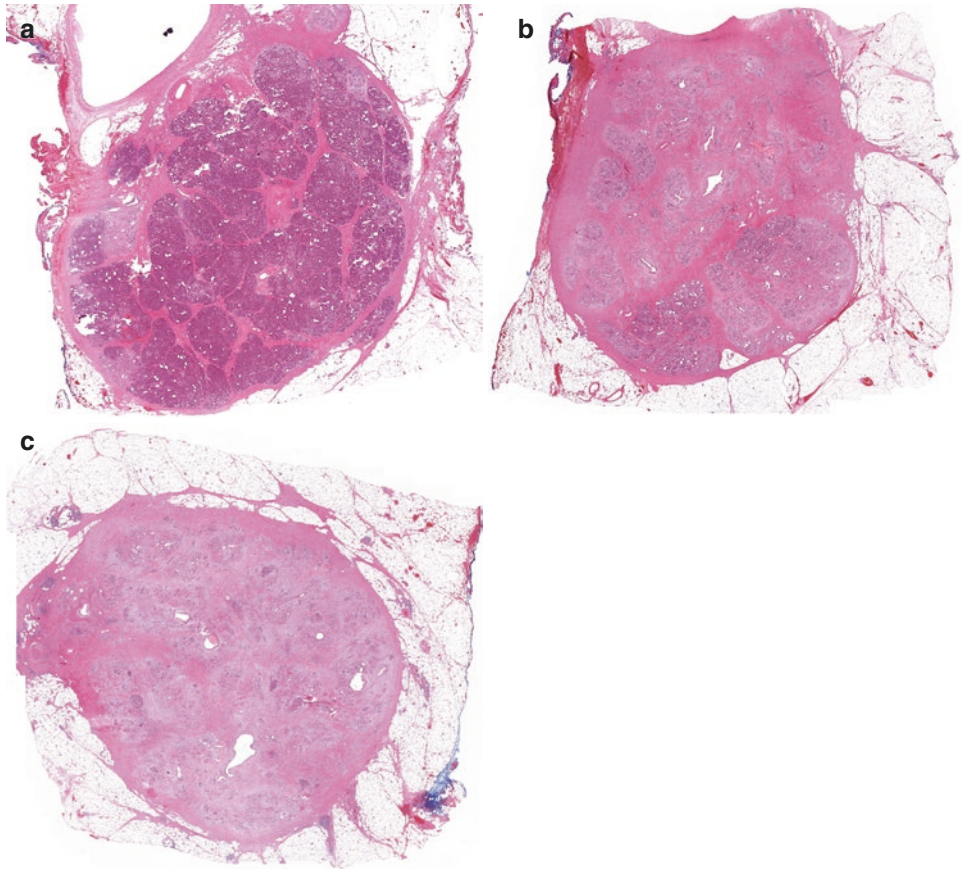

Fig. 7.21 Progression of chronic pancreatitis over time: in earlier stages, much of the acinar parenchyma is still preserved, while interlobular septa have become significantly wider (**a**). In a more advanced stage, the lobular architecture is still preserved, but much of the acinar parenchyma is lost. Note the broad fibrous septa that surround the atrophic lobules (**b**). In end-stage chronic pancreatitis with near-complete acinar atrophy, the lobular architecture is partially effaced. Where preserved, the preexisting lobules can be identified based on the looser, more delicate intralobular stroma that differs from the collagen-rich fibrous bands and sheets that characteristically develop in chronic pancreatitis (**c**)

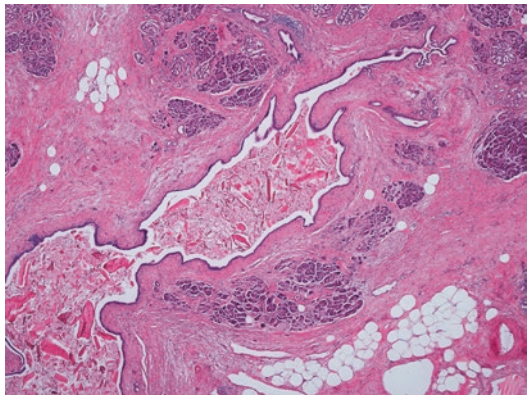

Fig. 7.22 Duct dilatation in chronic pancreatitis: a larger caliber pancreatic duct shows irregular saccular dilation and contains numerous protein plugs. Note the advanced acinar atrophy and extensive fibrosis

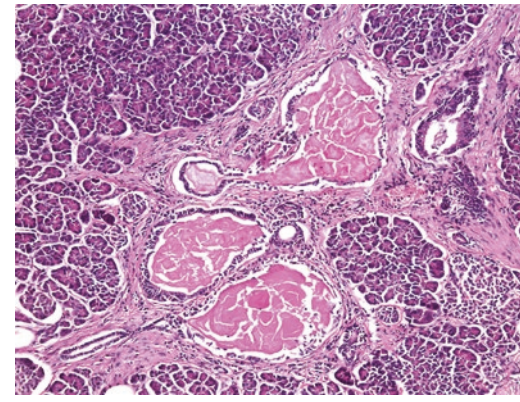

Fig. 7.23 Protein plugs in chronic pancreatitis: inspissated secretions consist typically of deeply eosinophilic material, which occasionally has a whorled or laminated inner structure

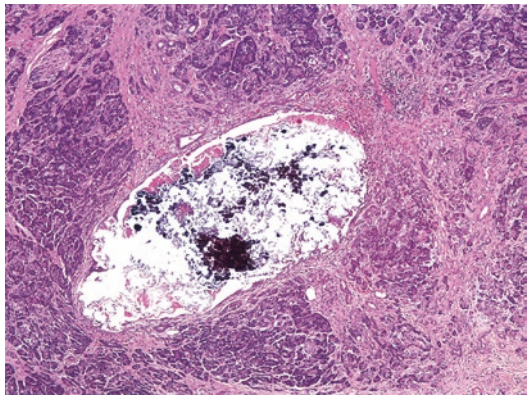

Fig. 7.24 Intraductal calcification in chronic pancreatitis: a calculus fills the lumen of a dilated duct. The lining epithelium is eroded by the stone. Note the artefactual fragmentation of the calcified material in this section

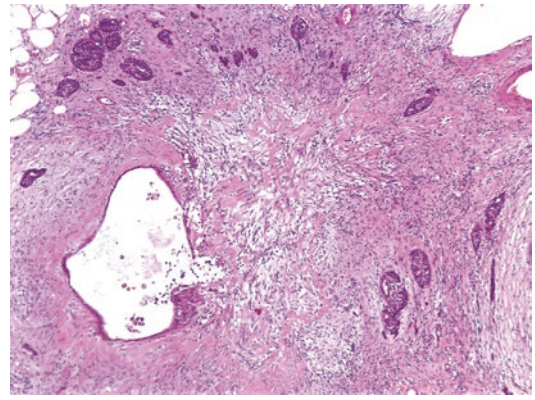

Fig. 7.25 Duct rupture in chronic pancreatitis: focal rupture of this dilated branch duct has elicited periductal inflammation and scarring

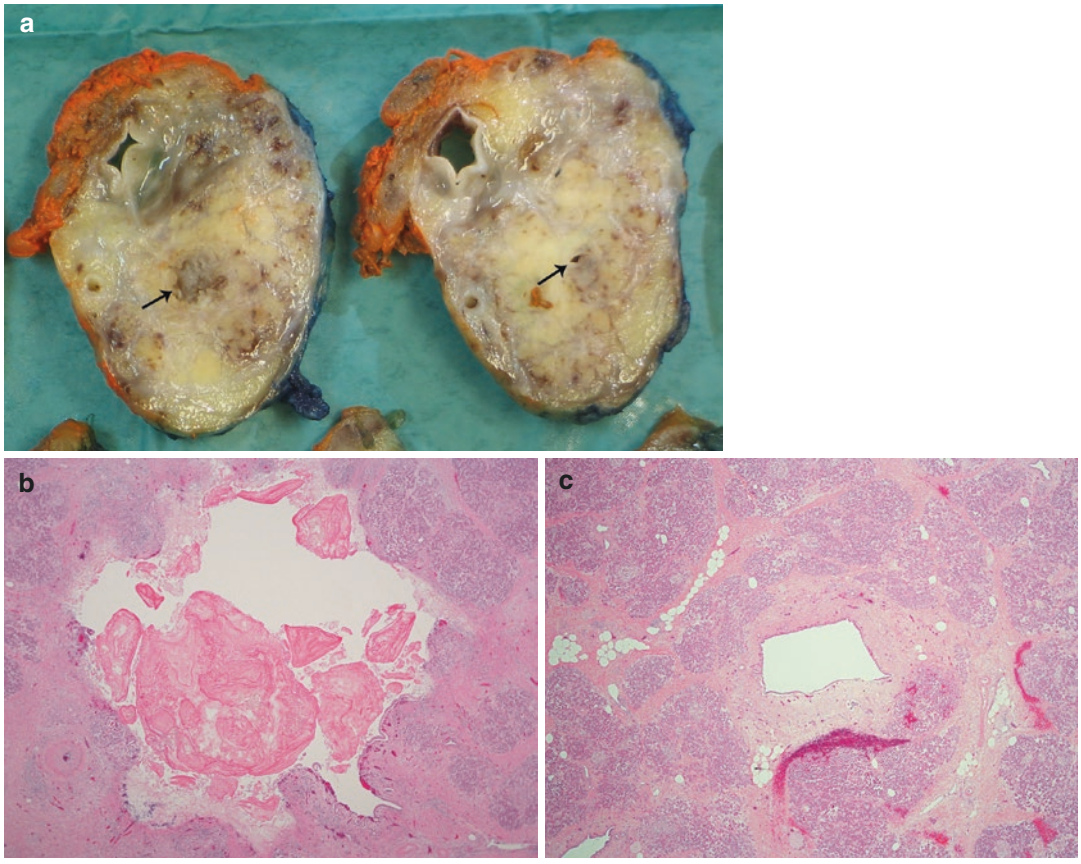

Fig. 7.26 Duct stricture in chronic pancreatitis: the main pancreatic duct appears inflamed and dilated in one specimen slice, and narrowed in the adjacent slice (*arrows*). Note the lobular atrophy and fibrosis of the surrounding parenchyma (**a**). Histologically, the dilated duct in figure (**a**) contains large protein plugs, its epithelial lining is partially eroded, and there is periductal inflammatory cell infiltration (**b**). Microscopy confirms stricturing of the main pancreatic duct shown in figure (**a**), along with periductal fibrosis (**c**; same magnification as in **b**)

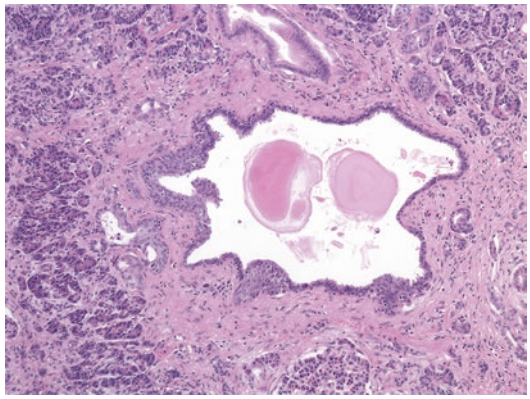

Fig. 7.27 Squamous metaplasia in chronic pancreatitis: a dilated pancreatic branch duct is lined by metaplastic squamous epithelium. Note the presence of intraductal protein plugs and periductal fibrosis

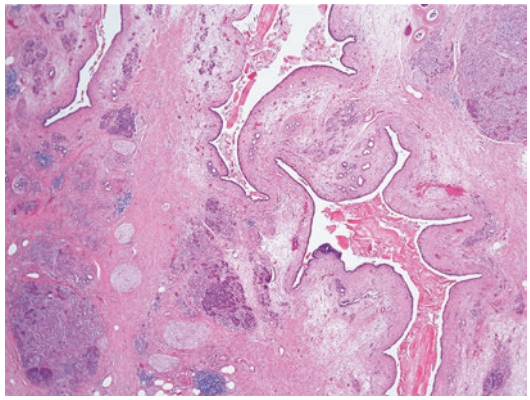

Fig. 7.28 Duct dilatation in end-stage chronic pancreatitis: several interlobular pancreatic ducts are markedly dilated and contain protein plugs. Note the panoply of microscopic changes characteristic of end-stage chronic pancreatitis: subtotal acinar atrophy, sheet-like fibrosis, prominence of peripheral nerves, and focal mild chronic inflammatory cell infiltration

Prominent chronic inflammatory cell infiltration centered on pancreatic ducts, with or without neutrophilic involvement, is a feature characteristic of autoimmune pancreatitis (see Sect. 7.2.7).

The *islets of Langerhans* seem rather resistant to the chronic inflammatory process, as they remain present well into late stages of the disease, albeit in reduced numbers and probably with reduced functionality. As a result of the gradual loss of acinar parenchyma and the collapse of preexisting lobular structure, residual islets often occur in aggregates. They may partially fuse and on rare occasion show pseudoperineural invasion, features which may cause differential diagnostic consideration of endocrine neoplasia (Figs. 7.29 and 7.30). While islets persist over a long period of the disease, they undergo subtle structural changes, in particular in their cellular composition. Glucagon- and pancreatic polypeptide-producing cells tend to increase in relative numbers, while insulin-producing cells become gradually less numerous (see Chap. 21, Sect. 21.1 and Fig. 21.1). Small clusters of islets cells are not uncommonly seen in association with small ductules, forming ductulo-insular complexes, which are not normally seen in the adult pancreas (Fig. 7.31) (see Chap 1, Sect. 1.4.4, and Chap. 5, Sect. 5.8). Eventually, the endocrine compartment will undergo atrophy to the extent that diabetes mellitus develops as a late clinical complication of chronic pancreatitis.

A further common finding in chronic pancreatitis is the presence of more numerous and frequently enlarged *peripheral nerves* (Fig. 7.28). In burnt-out pancreata, the organ may be reduced to expanses of fibrous tissue with hypertrophic, often clustered peripheral nerves and a few intervening residual acini, ducts, and islets of Langerhans. The nerves are often associated with focal chronic inflammatory cell infiltration and exhibit a range of subtle changes that are usually not appreciated on routine H&E staining, for example, reduction of the sympathetic nerve fiber content, changes in the glia cells, and damage of the perineurium. The severity of this 'pancreatic neuropathy' has been correlated with the patient's pain sensation.

Blood vessels of any caliber, both venous and arterial, within or outside the pancreas, can show marked fibrous mural thickening and luminal stenosis. These changes lie at the basis of the occasionally catastrophic vascular complications of chronic pancreatitis as described below (see Fig. 7.42).

The above-described parenchymal and stromal changes result in gradual effacement of the pancreatic lobule as an architectural unit. In general, lobular architecture is still identifiable well into late stages of the disease, even though by

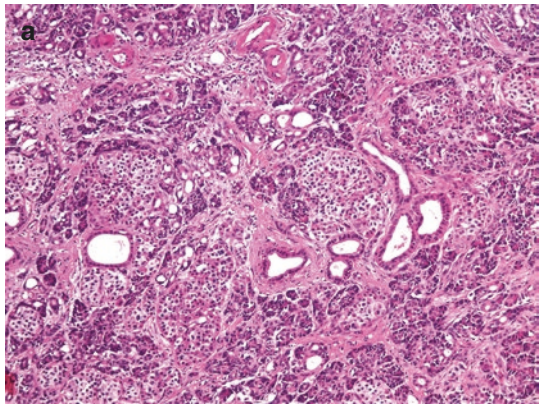

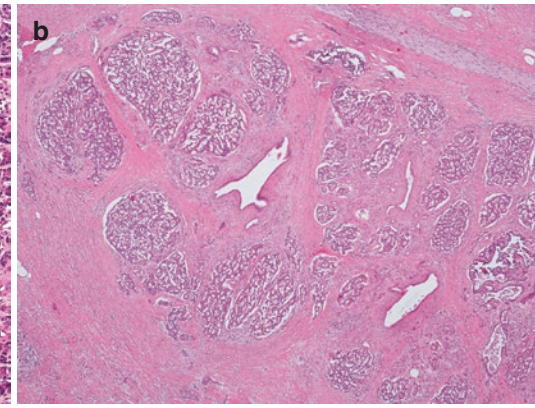

Fig. 7.29 Islet aggregation in chronic pancreatitis: due to atrophy of the acinar parenchyma, islets appear more numerous (**a**). In end-stage disease, aggregates of enlarged islets admixed with ductular structures may be found in vast expanses of fibrosis (**b**)

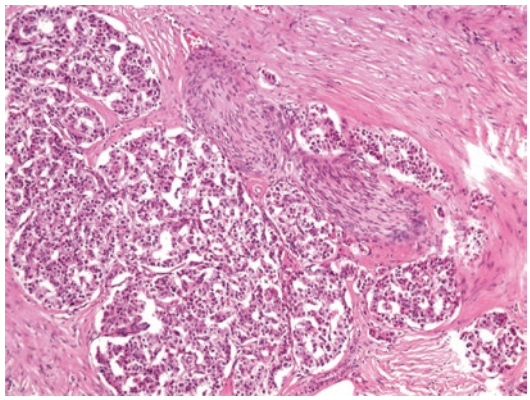

Fig. 7.30 Pseudoperineural invasion of islets in chronic pancreatitis: due to acinar atrophy and collapse of the normal microanatomy of the pancreas, aggregated islets may appear to invade peripheral nerves

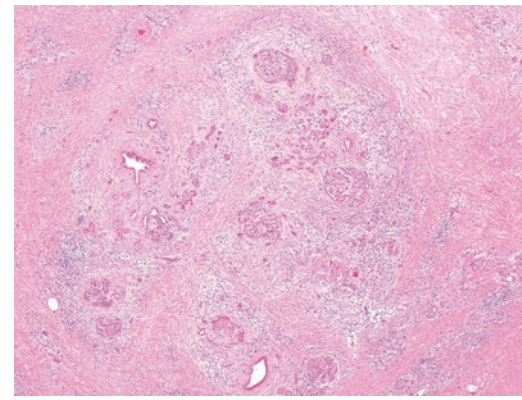

Fig. 7.32 Preservation of lobular architecture in chronic pancreatitis: over a long time, the boundaries of pancreatic lobules and their looser stroma are preserved, even if acinar atrophy is advanced

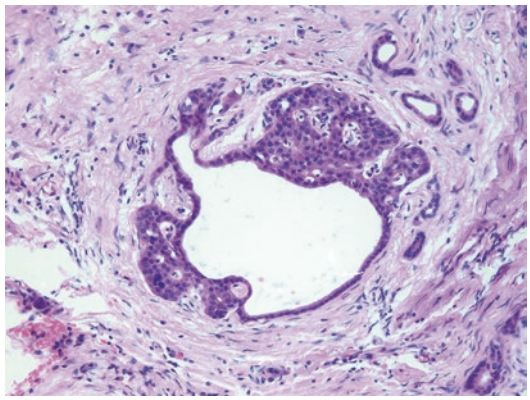

Fig. 7.31 Ductulo-insular complex in chronic pancreatitis: in chronic pancreatitis islets may associate with small duct structures, whereas in normal adult pancreas, they are separated from the latter

then lobules may be reduced to a number of ductular structures and a few scattered acinar cells and islets. These scanty residual structures are for a long time still embedded in the normally loose intralobular stroma, which ultimately will be replaced by dense fibrous tissue (Figs. 7.32 and 7.33). Due to the parenchymal atrophy, the gradual passive collapse of structures, and the diffuse extension of a collagen-rich fibrous stroma, the lobular outlines become effaced, and the spatial separation between pancreatic ducts and muscular blood vessels is reduced (Figs. 7.34 and 7.35) [4, 5]. In addition, residual ductular structures may exhibit a degree of (reactive) cytological atypia (Fig. 7.36). In view of this combination of

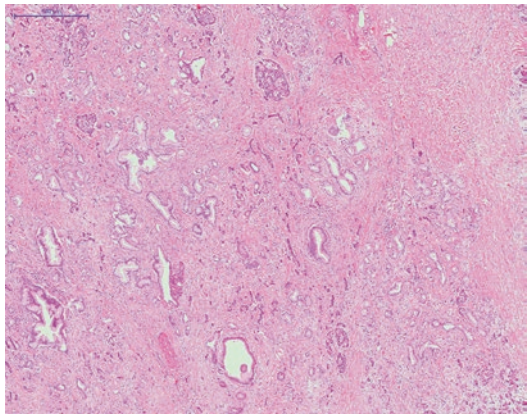

Fig. 7.33 Loss of lobular architecture in chronic pancreatitis: in end-stage disease, the lobular outlines are eventually effaced, and residual ducts, islets, and occasional acini seem randomly distributed within the fibrotic stroma

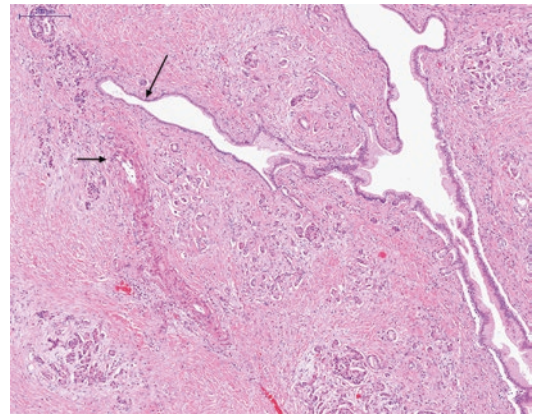

Fig. 7.34 Approximation of ducts and blood vessels in chronic pancreatitis: due to the structural collapse in end-stage chronic pancreatitis, the normal spatial separation of pancreatic ducts (*long arrow*) and muscular blood vessels (*short arrow*) by acinar parenchyma is lost

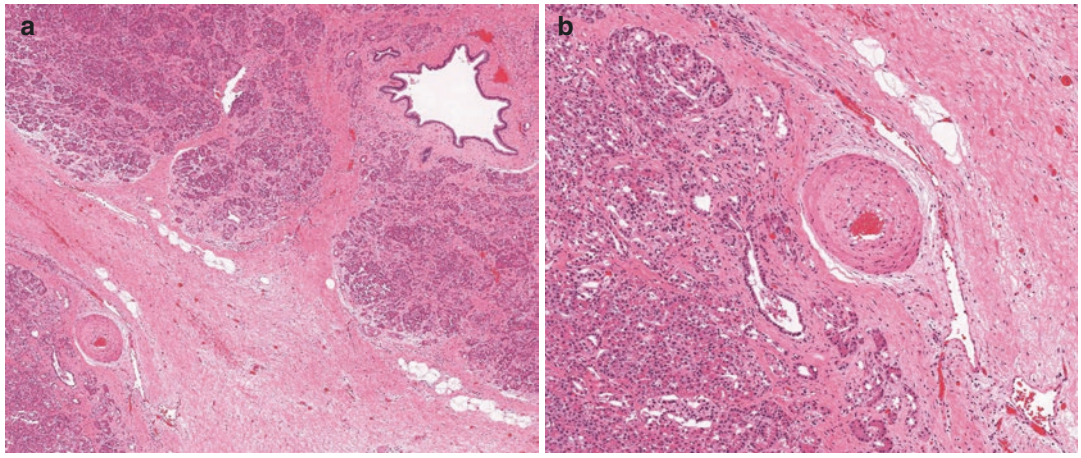

Fig. 7.35 Approximation of ducts and blood vessels in chronic pancreatitis: collapse of an atrophic lobule in the lower left corner (**a**) leads to approximation of ductular structures to a muscular artery (**b**)

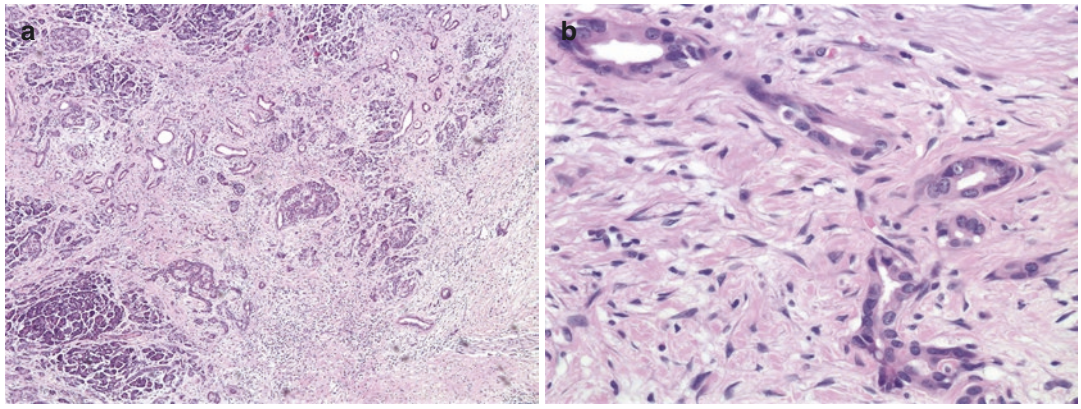

Fig. 7.36 Atypical ducts in chronic pancreatitis: numerous ductular structures varying in shape and size are scattered amongst residual islets and acini (**a**). Some small ducts show mild architectural and cytological atypia (**b**)

changes, in particular the loss of cardinal structural features, the distinction between chronic pancreatitis and ductal adenocarcinoma may be problematic, especially in biopsy material or on frozen section. For a more detailed discussion of this differential diagnosis see Chap. 9, Sect. 9.12.1, and Chap. 23, Sect. 23.2.

To date, there is no agreement regarding the diagnostic histological criteria for chronic pancreatitis [1, 6]. In particular, it is not clear whether the entire triad of changes—fibrosis, acinar atrophy, duct abnormalities—should be present to reach a diagnosis of chronic pancreatitis. Also lacking is a universally accepted grading system for the histological assessment of the severity of chronic pancreatitis. Scoring systems that have been used for research purposes are based exclusively on the extent and distribution of fibrosis. Because surgery is usually indicated for patients with end-stage chronic pancreatitis, histological diagnosis and grading of the disease is in practice straightforward in most cases.

Knowledge about the histological changes in *early chronic pancreatitis* is limited, but according to published data, patchy interlobular fibrosis and mild, patchy or diffuse chronic inflammatory cell infiltration, together with preserved acinar parenchyma and islets, seem to characterize the early stages of the disease (Fig. 7.37) [6]. In addition, the histological changes that occur during recurrent acute pancreatitis and the transition to early chronic pancreatitis are not well characterized (Fig. 7.38). Given the nonspecific nature of the changes in early chronic pancreatitis, the distinction from focal fibrosis that may be seen in elderly asymptomatic individuals or in chronic alcoholics without clinical evidence of chronic pancreatitis, may be difficult if not impossible (see Chap. 5, Sect. 5.6). As a general rule, chronic pancreatitis should be considered a clinicopathological diagnosis, that is, pathologists should consider clinical and radiological findings when making the diagnosis. The fibroinflammatory changes and acinar atrophy that are commonly seen in the vicinity of pancreatic tumors should not be reported as chronic pancreatitis, because they represent local, secondary changes. In that context, *peritumoral pancreatitis* is a more appropriate term. It should be noted that inflammation and fibrosis can also be seen as a result of renal disease, medication (e.g., cyclosporin), and long-standing diabetes mellitus (see Chap. 5, Sect. 5.6) [1]. Finally, there are no histomorphological features that allow identification of the etiology of chronic pancreatitis. Instead, clinical history and laboratory investigation, including genetic testing, are the diagnostic mainstay [6].

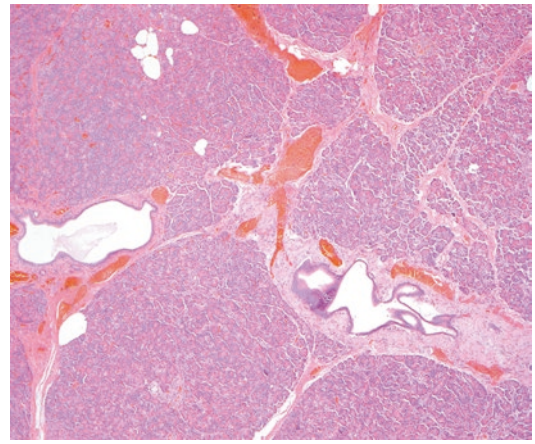

Fig. 7.37 Early chronic pancreatitis: the interlobular septa are slightly more prominent than in normal pancreas. Focally, there is discrete intralobular fibrosis but little if any acinar atrophy. Note the mild duct dilatation and periductal fibrosis together with a small amount of inspissated secretion in this case of early obstructive chronic pancreatitis

7.2.5 Complications

Complications of chronic pancreatitis tend to occur in later stages of the disease.

Pancreatic *pseudocysts* complicate not only acute pancreatitis, but may also develop in chronic pancreatitis, in particular if alcohol-related. The morphology is essentially identical to that of pseudocysts associated with acute pancreatitis, that is, unilocular fluid-filled cavities, which usually have no septations, mural nodules, or excrescences and are devoid of an epithelial lining. In contrast to pseudocysts developing in acute pancreatitis, the wall of pseudocysts in chronic pancreatitis is generally thicker and com-

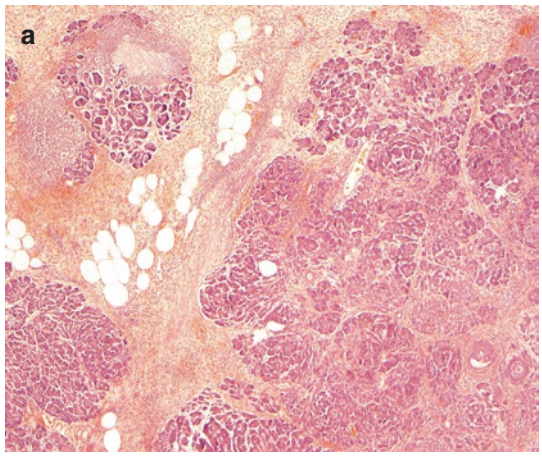

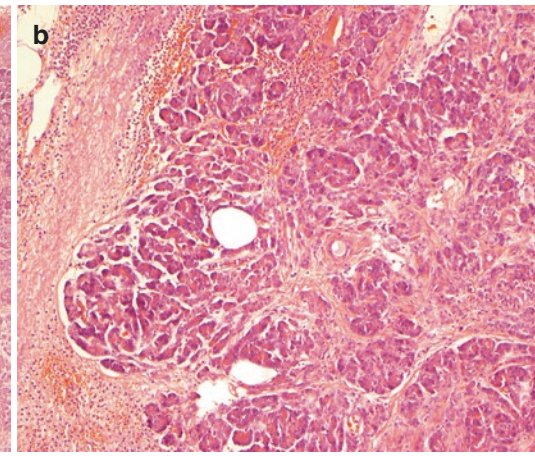

Fig. 7.38 Recurrent acute pancreatitis: interstitial edema, neutrophilic infiltration, focal necrosis, and hemorrhage are characteristic of an episode of acute pancreatitis. In addition, the presence of discrete acinar atrophy along with intra- and interlobular fibrosis is evidence of previous tissue damage (**a**, **b**)

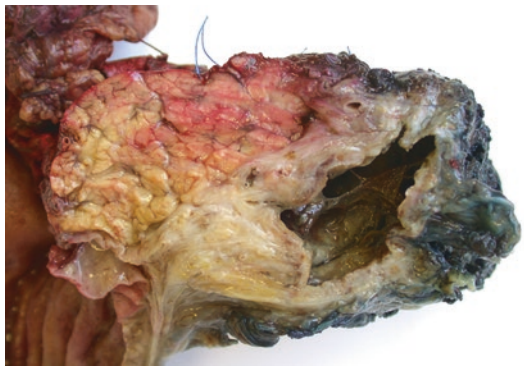

Fig. 7.39 Pseudocyst in chronic pancreatitis: a large unilocular cystic cavity with a thick firm wall is surrounded by scar tissue. Note the debris within the pseudocyst lumen

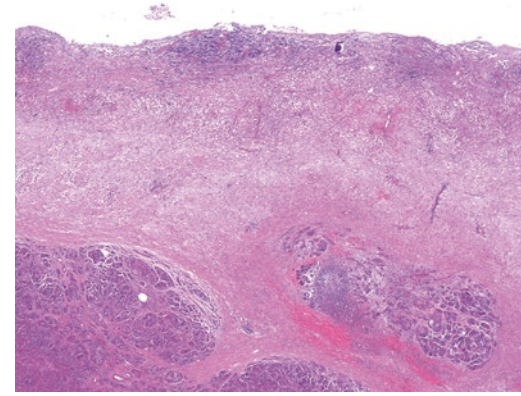

Fig. 7.40 Pseudocyst in chronic pancreatitis: the wall of the pseudocyst depicted in Fig. 7.39 consists of granulation and scar tissue, and is flanked by pancreatic parenchyma showing fibrosis and atrophy. The cyst has no epithelial lining

posed of mature granulation tissue and fibrous tissue (Figs. 7.39 and 7.40). As they are unlikely to resolve spontaneously and can reach a large size (see Fig. 14.1), pseudocysts may require endoscopic, percutaneous, or surgical drainage. Although communication with the pancreatic duct system is a defining feature of pancreatic pseudocysts, this is often difficult to confirm morphologically. With cystic neoplasia of the pancreas being the main differential diagnosis, examination of the entire lesion is required to confirm the diagnosis of a pseudocyst and to exclude neoplasia.

Not uncommon and potentially life-threatening are *vascular complications*. Erosion of a pseudocyst into a neighboring blood vessel can lead to thrombosis, formation of a pseudoaneurysm, or hemorrhage (Figs. 7.41, 7.42, and 7.43). Large blood vessels at risk are the splenic, gastroduodenal, dorsal pancreatic, and right gastroepiploic arteries. Thrombosis of the superior mesenteric vein or portal vein due to chronic pancreatitis may result in bleeding varices in the absence of liver cirrhosis. Occasionally, bleeding from the pancreatic duct system, referred to as

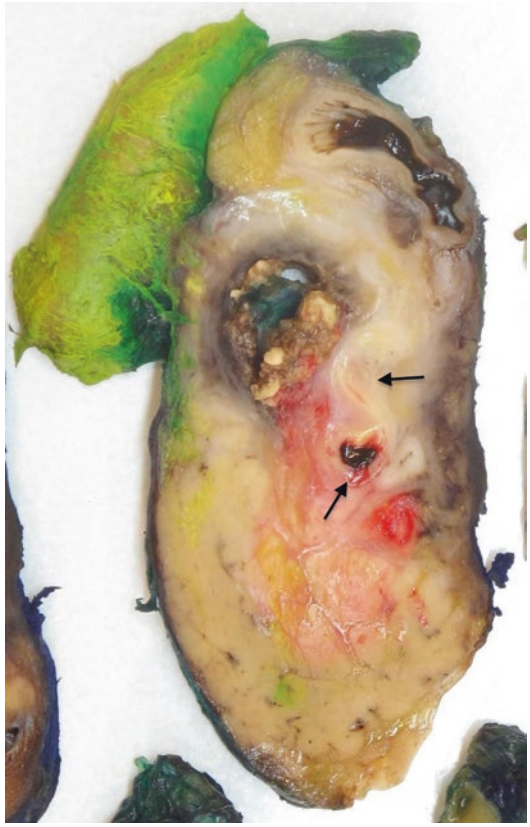

Fig. 7.41 Pseudocyst and risk of vascular complication: a pseudocyst is located in the cranial part of the pancreatic tail, close to the splenic vein (*arrows*). The latter shows fibrous thickening of the venous wall and luminal narrowing as a consequence of the adjacent necro-inflammatory process. Further expansion of the pseudocyst bears the risk of thrombosis or erosion of the splenic vein

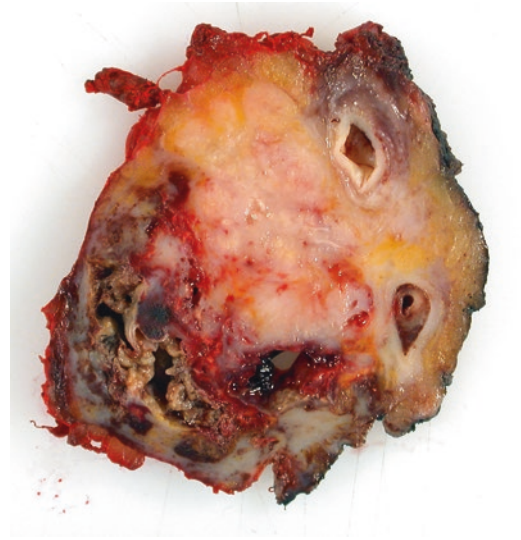

Fig. 7.42 Hemorrhage in chronic pancreatitis: fulminant hemorrhage with disruption and necrosis of (peri-)pancreatic tissue required emergency distal pancreatectomy in a patient with known chronic pancreatitis

Fig. 7.43 Vascular thrombosis in chronic pancreatitis: the splenic vein is occluded by thrombosis (*arrows*). Note the shrinkage and loss of lobulation of the pancreas as signs of chronic pancreatitis

hemosuccus pancreaticus, may be caused by pancreatic stones, which can develop in chronic pancreatitis. Fistulating inflammation into the colon or pleural cavity has also been described in chronic pancreatitis.

7.2.6 Forms of Chronic Pancreatitis with Nonspecific Morphology

7.2.6.1 Alcohol-Related Pancreatitis

The development of alcohol-related chronic pancreatitis is a multistep process that starts with recurrent episodes of acute pancreatitis, which progressively develop into a more chronic presentation with continuous pain and a gradual loss of pancreatic function. As only a minority of heavy drinkers (<10%) develop pancreatitis, it is likely that individual genetic factors also play

a role. Alcohol-related chronic pancreatitis is associated with the macroscopic and microscopic changes that are outlined above and lacks characteristic features that would allow identification of the association with alcohol abuse. The histological features that distinguish alcohol-related pancreatitis from autoimmune pancreatitis are discussed below (see Table 7.6).

7.2.6.2 Hereditary Pancreatitis

This is a rare form of chronic pancreatitis with a proven genetic basis, which usually begins in childhood and leads to the development of chronic pancreatitis in early adulthood. The morphology of hereditary pancreatitis is similar to that of alcohol-related chronic pancreatitis, and does not correlate with the exact gene mutation. Hereditary pancreatitis is discussed in detail in the chapter on hereditary disease of the exocrine pancreas (see Chap. 6, Sect. 6.3).

7.2.6.3 Tropical Pancreatitis

Occasionally also referred to as tropical calculous pancreatitis, this type of chronic pancreatitis is confined to equatorial regions in Central Africa, Brazil, and Southern Asia. It is particularly frequent in India. Patients present at a young age with recurrent abdominal pain and develop diabetes earlier than other chronic pancreatitis patients, often before the age of 30. For many years, environmental factors such as cassava consumption, malnutrition, and micronutrient deficiency were believed to be causative. Recently, however, at least two genes known to be involved in chronic pancreatitis, *SPINK* and *CTRC*, have also been implicated in tropical pancreatitis. Morphologically, tropical pancreatitis is similar to alcohol-related chronic pancreatitis, with particularly prominent interlobular and intralobular fibrosis and numerous calculi, some of which may reach considerable size (Fig. 7.44).

7.2.6.4 Obstructive Pancreatitis

Chronic obstruction of the pancreatic duct system leads to upstream duct dilatation, acinar atrophy, and fibrosis, in keeping morphologically and clinically with chronic pancreatitis. The causes for obstruction can be manifold: stones, benign or malignant tumors, abundant production of viscous mucus such as in intraductal papillary mucinous neoplasia, acquired duct strictures, or anatomical anomalies such as pancreas annulare, pancreas divisum, or a so-called long common channel (see Chap. 13, Sects. 13.1, 13.2, and 13.3, Fig. 13.4).

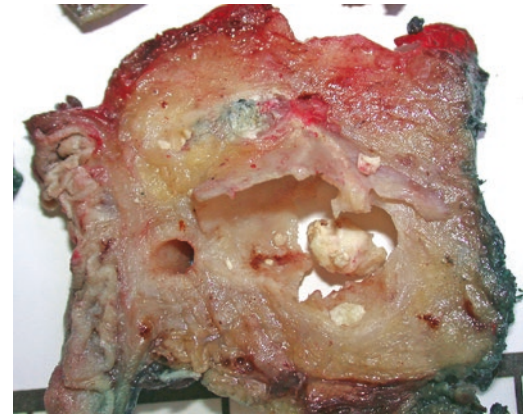

Fig. 7.44 Tropical pancreatitis: the pancreatic ducts are grossly dilated and some contain large stones. There is no macroscopically visible residual pancreatic parenchyma

The morphological features are essentially similar to those of alcohol-related chronic pancreatitis, although the changes tend to be more homogenous and synchronous throughout the entire gland. In some cases, inspissated pancreatic secretions can be visible macroscopically in form of white soft mozzarella-like or firmer, pearl-like roundish bodies with a smooth surface (Fig. 7.45).

7.2.7 Autoimmune Pancreatitis

7.2.7.1 Definition, Epidemiology, and Clinical Features

The concept of autoimmune pancreatitis (AIP) was introduced as recently as 1995, following earlier descriptions of a 'lymphoplasmacellular sclerosing pancreatitis'. AIP is a chronic relapsing fibroinflammatory disease of the pancreas with characteristic features, including pathognomonic morphological changes, a presumed autoimmune etiopathogenesis, and a clinical response to steroid treatment [7].

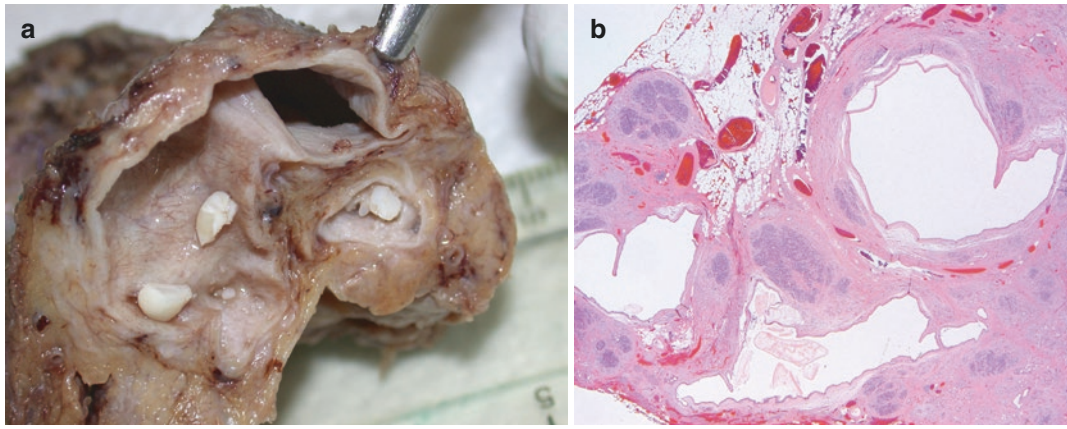

Fig. 7.45 Obstructive pancreatitis: the main pancreatic duct and some branch ducts show prominent, baggy dilatation and contain soft white, mozzarella-like protein plugs (**a**). Note the advanced parenchymal atrophy and fibrosis (**b**)

In view of the recent introduction of AIP as a separate pancreatitis entity, robust epidemiological data are still lacking. While the incidence appears to be gradually increasing, this is most likely due to the growing awareness of the disease and refined diagnostic criteria. It is estimated that AIP represents approximately up to 10% of all patients with chronic pancreatitis. While the age distribution is wide, ranging from childhood to old age, the majority of AIP patients are 50 years of age or older.

The clinical presentation of AIP is variable [8]. The most frequent symptom is abdominal pain, which is generally described as less severe than in other forms of chronic pancreatitis and does not require narcotic treatment. Weight loss is reported by up to a third of the patients, and 48–86% of patients present with painless obstructive jaundice. In view of this triad of most common presenting symptoms, pancreatic cancer, which is much more frequent, is the key clinical differential diagnosis. Recurrent cholangitis can precede the diagnosis of AIP by several months, whereas recurrent acute pancreatitis without biliary involvement is uncommon at presentation.

As information accumulates, it becomes increasingly apparent that AIP is in fact a heterogenous disease with two subtypes—type 1 and type 2—that have distinct histological and clinical features. Most of the existing literature represents information on AIP type 1, while the understanding and description of type 2 is more recent. Table 7.3 provides a summary of the main clinical differences between both types in terms of presentation, association with extrapancreatic disease, and relapse. Type 1 is more common worldwide: it is the predominant form in

Table 7.3 Clinical features of type 1 and type 2 autoimmune pancreatitis (adapted from [8])

	Type 1 AIP	Type 2 AIP
Age at presentation	7th decade	5th decade
Gender distribution (male:female)	Predominantly male (3:1)	Equal
Presentation:		
– Obstructive jaundice	75%	50%
– Acute pancreatitis	15%	33%
Imaging:		
– Diffuse sausage-like swelling, rim enhancement	40%	15%
– Focal changes	60%	85%
Elevated IgG4:		
– Serum	Usually	No
– Tissues	Usually	Scarce
Extrapancreatic organ involvement	Yes	No
Associated idiopathic inflammatory bowel disease	2–5%	10–30%
Disease relapse	Common	Rare

Abbreviation: *AIP* autoimmune pancreatitis

the United States of America and Europe and is almost exclusively prevalent in Japan and Korea.

AIP type 1 is associated with an elevated level of IgG4, both in the serum and in the affected tissues, and with involvement of one or possibly multiple extrapancreatic organs. This has led to the concept of a multiorgan chronic fibroinflammatory disease, coined 'IgG4-related systemic disease'. A small subset of type 1 patients may be seronegative, but this observation alone does not suffice for a reclassification as type 2 (see below). AIP type 1 is sometimes also referred to as 'lymphoplasmacytic sclerosing pancreatitis' (LPSP), indicative of its characteristic histological features, which will be discussed below. While in many patients the clinical findings (elevated serum IgG4, imaging, extrapancreatic involvement) are sufficiently characteristic to allow a diagnosis of AIP type 1 without the need for histology, in the case of localized AIP, histological confirmation and exclusion of other lesions may be required. In addition to elevated serum levels of IgG4, levels of IgG or IgE are also abnormally high in more than 50% of patients, and increased titers of antinuclear antibody and rheumatoid factor may be seen in some patients. Moreover, elevated levels of circulating plasmablasts can support the diagnosis of AIP type 1, independent of the serum IgG4 value [9].

Patients with *AIP type 2* tend to have a normal IgG4 serum level, and they rarely develop extrapancreatic IgG4-related disease. As such, a definitive diagnosis of type 2 AIP currently still requires histology. AIP type 2 is sometimes referred to as 'idiopathic duct-centric pancreatitis' (IDCP).

In several recent international consensus meetings, sets of diagnostic criteria for type 1 and type 2 AIP have been established [7, 10–13], which include or focus on histological features. The defining morphological features of AIP type 1 and type 2 are outlined below.

7.2.7.2 Etiology

Most of the current knowledge about the etiopathogenesis of AIP relates to type 1 AIP. While potential ductal and acinar autoantigens (e.g., carbonic anhydrase II, amylase, trypsinogens, SPINK1) have been proposed as autoimmunity antigens, the autoimmune etiopathogenesis of AIP type 1 is still controversial, also because men older than 50 years are predominantly affected by the disease. The likely pathogenetic mechanism for AIP type 1 (and IgG4-related disease) is the repetitive exposure of genetically susceptible individuals to unidentified antigens (such as microbes or chemicals) that induce immune reactions. Complex interactions between T and B cells have been proposed to result in a tissue-destructive process that is mediated by activated lymphocytes, macrophages, and fibrosis. The extensive infiltration of the pancreas is dominated by CD4-positive T cells, while circulating regulatory (Treg) and follicular helper T cells (Tfh) are likely to induce the IgG4 class switch and the increased eosinophilia and production of IgE that are often detected in patients with AIP type 1. B cells are also part of the complex pathophysiology of IgG4-related disease, as evidenced by the increased number of circulating, oligoclonal, IgG4-positive plasmablasts. However, to date, the role of the plasmablasts and the IgG4 molecule remains unclear: it has been suggested that they may represent reactive phenomena secondary to cytokine production rather than being intrinsically related to the tissue damage that characterizes AIP type 1 and IgG4-related disease in other organs [14].

7.2.7.3 Macroscopy

The pancreas is usually diffusely enlarged and indurated, and its normal lobulation appears effaced (Figs. 7.46 and 7.47). However, in a proportion of patients suffering from AIP, the organ is affected only focally, which may result in a mass-forming lesion that mimics pancreatic cancer (Fig. 7.48). In contrast to other forms of chronic pancreatitis, the main pancreatic duct is diffusely or segmentally narrowed. In some cases, the duct-centric leukocytic infiltrate that is characteristically found in AIP, may be visible macroscopically as a thin, white, periductal cuff (Fig. 7.46). In up to 60% of patients, the pancreatic head is involved, and the intrapancreatic common bile duct may be narrowed and its wall thickened by the same fibroinflammatory process. The peripancreatic adipose tissue may also

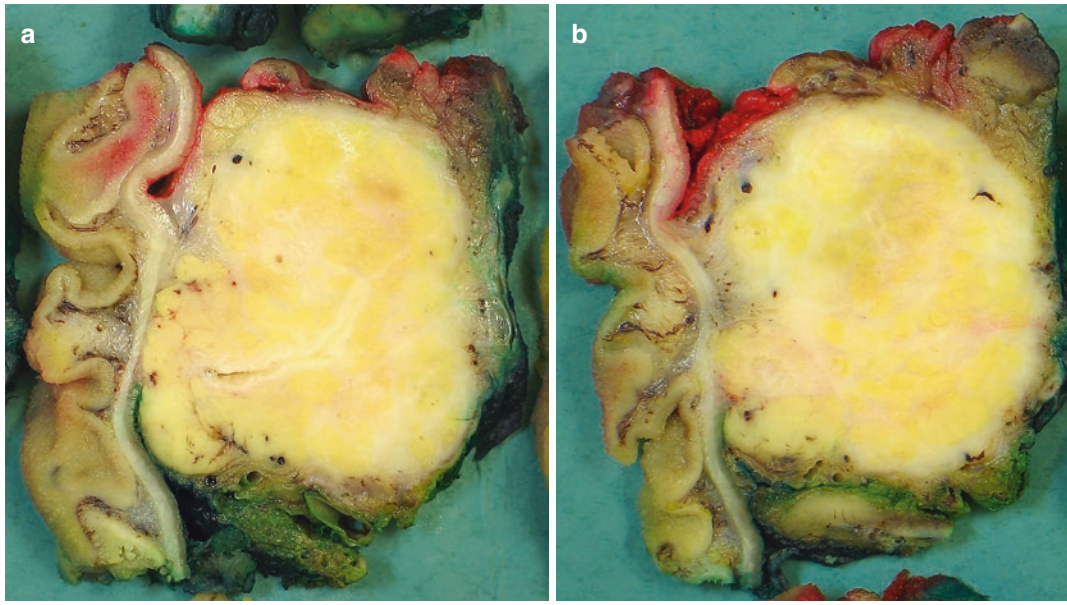

Fig. 7.46 Macroscopy of early autoimmune pancreatitis: the lobular architecture of the pancreatic parenchyma is largely effaced. The main pancreatic duct shows an irregular, partially narrowed lumen, while the duct wall appears thickened by a cream-colored periductal cuff (**a**). More advanced changes are seen in this case: the lobular architecture is entirely effaced, and the parenchyma is partially replaced by irregular white tissue (**b**)

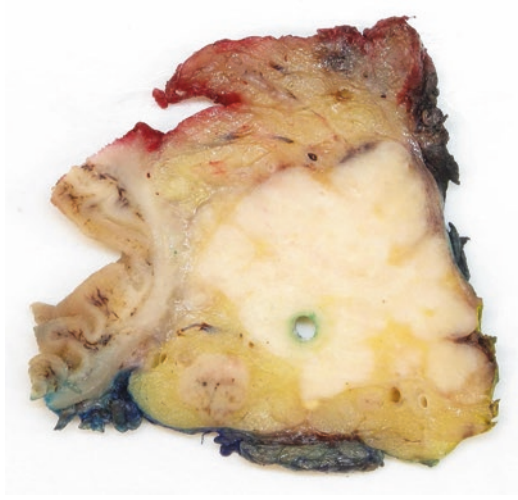

Fig. 7.47 Macroscopy of advanced autoimmune pancreatitis: the pancreatic parenchyma has lost its lobular architecture and is replaced by white, firmer tissue. The main pancreatic duct is narrowed to the point of no longer being visible. Note the punched-out lumen of the common bile duct due to a plastic stent (removed)

be involved, in particular in type 1 disease, and peripancreatic lymph nodes are often enlarged. Many of these macroscopic changes may, on imaging, raise the suspicion of malignancy. In longstanding untreated AIP, advanced parenchymal atrophy and fibrosis, and rare intraductal calcification may resemble the macroscopic features of chronic pancreatitis [15].

7.2.7.4 Microscopy

The pathognomonic features of AIP are well established and can be used to distinguish AIP from other forms of chronic pancreatitis. In contrast, the distinction between type 1 and type 2 is based on more recent observations (Table 7.4). Guidance on the histomorphological (and clinical) diagnosis of type 1 and 2 AIP is likely to require revision, when additional data and new biomarkers will become available. Currently, IgG4 is the only available biomarker, and its diagnostic use is discussed in detail below.

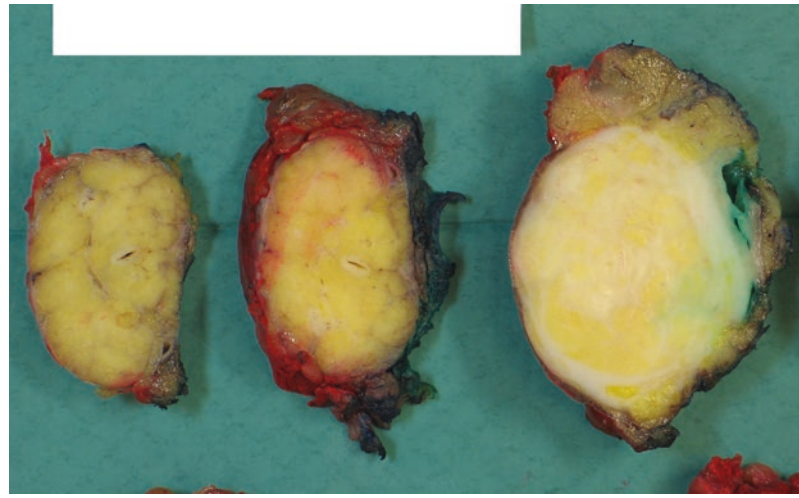

Fig. 7.48 Segmental AIP: there is an abrupt transition from near-normal pancreatic tissue in the first two specimen slices to atrophic and fibrotic pancreatic tissue in the third specimen slice. Note that the main pancreatic duct is strictured to the point of being macroscopically invisible

Table 7.4 Diagnostic microscopic features of type 1 and type 2 autoimmune pancreatitis (adapted from [12])

	Type 1 AIP	Type 2 AIP
Periductal lymphoplasmacytic infiltrate	Present	Present
Inflammatory cellular stroma	Present	Present
Storiform fibrosis	Prominent	Occasional
Obliterative phlebitis	Yes	Rare
Lymphoid follicles	Prominent	Occasional
IgG4+ plasma cell infiltration	Marked	Scant or absent
GEL	Absent	Present
Inflammation of lobules	Present	Patchy, less marked, commonly admixed with neutrophils
Inflammation of peripancreatic fat	Possible	Rare

Abbreviations: *AIP* autoimmune pancreatitis, *GEL* granulocytic epithelial lesion

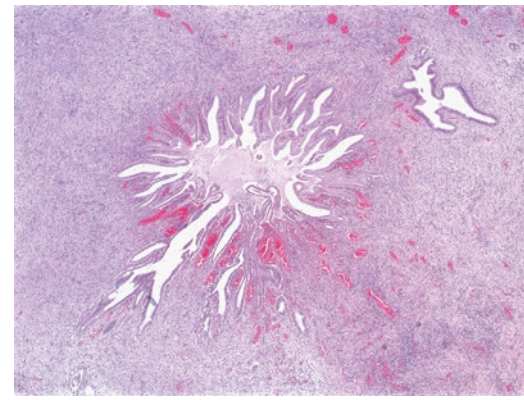

Fig. 7.49 Periductal inflammation in AIP: dense inflammatory cell infiltration is present immediately around a large pancreatic duct, which shows star-shaped deformation and luminal narrowing. Periductal inflammation extends into the surrounding parenchyma, which is atrophic

The three *cardinal features of AIP, common to both type 1 and type 2,* are the periductal lymphoplasmacytic infiltration, the inflammation of the acinar parenchyma, and the patchy distribution of the inflammatory changes. The usually dense and conspicuous *periductal chronic inflammation* involves medium-sized to large interlobular pancreatic ducts. The inflammatory cells infiltrate the wall of the duct and are present immediately underneath, but rarely within, the duct epithelium. The lumen of the affected duct is often narrow and irregularly star-shaped (Figs. 7.49, 7.50, and 7.51). The inflammatory infiltrate consists predominantly of T lymphocytes and scattered or aggregated B cells (Fig. 7.52). Plasma cells are always present and may occasionally predominate. Eosinophils are usually present in low

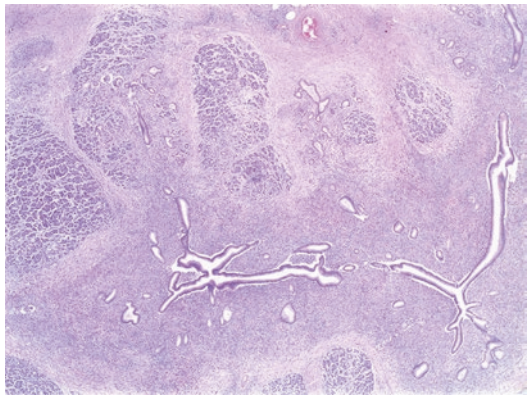

Fig. 7.50 Periductal inflammation in AIP: extensive periductal inflammation involves a large pancreatic duct and several of its tributaries. Note the deformation of the ducts and fibroinflammatory changes of surrounding pancreatic tissue

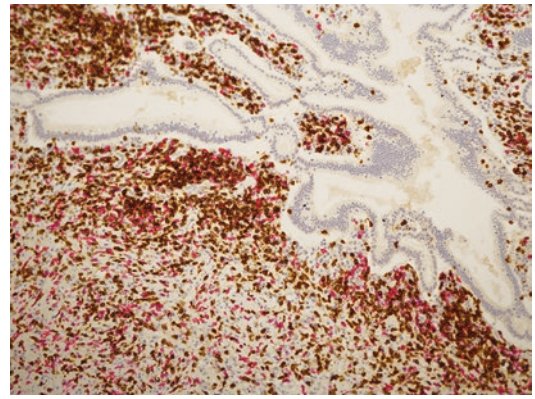

Fig. 7.52 Periductal inflammation in AIP: the periductal chronic inflammatory cell infiltrate consists mainly of T cells (*brown*) with scattered B cells (*red*; immunohistochemical double staining for CD3 and CD20)

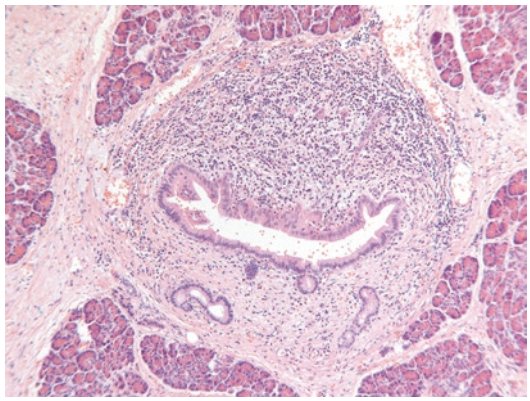

Fig. 7.51 Periductal inflammation in AIP: a medium-sized interlobular pancreatic duct shows semicircumferential infiltration of the thickened periductal fibrous cuff by chronic inflammatory cells. The latter lie immediately underneath the duct epithelium, and only few inflammatory cells infiltrate the epithelial lining

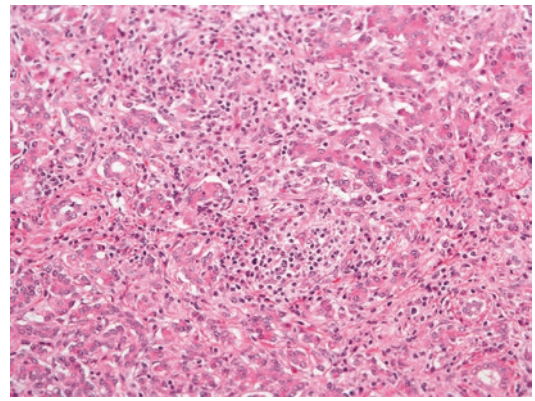

Fig. 7.53 Acinar inflammation in AIP: patchy, but in some areas fairly dense infiltration by lymphocytes, plasma cells, and scattered eosinophils is seen within the acinar parenchyma

to moderate numbers, but may be numerous in rare cases. Scattered macrophages are often also present. The inflammatory cell infiltrate usually extends into the immediate periductal soft tissue plane, which in many instances is widened by periductal fibrosis. The latter may vary in intensity and is possibly more pronounced in later disease stages.

Inflammation of the acinar parenchyma is a further characteristic feature of AIP (Fig. 7.53). While the inflammatory cell infiltrate consists mainly of lymphocytes—T cells more than B cells (Fig. 7.54)—and plasma cells, patchily distributed eosinophils and neutrophils may also be included. The latter are present especially in AIP type 2, in which the lobular inflammation is usually less prominent and significantly more patchy in distribution. The parenchymal inflammation may be associated with gradual acinar atrophy and fibrosis (Fig. 7.55).

A third hallmark of AIP is the *patchy distribution of the inflammatory changes*. While involvement of the pancreas at the macroscopic level may be diffuse or segmental, microscopically, the distribution is patchy, and the intensity and

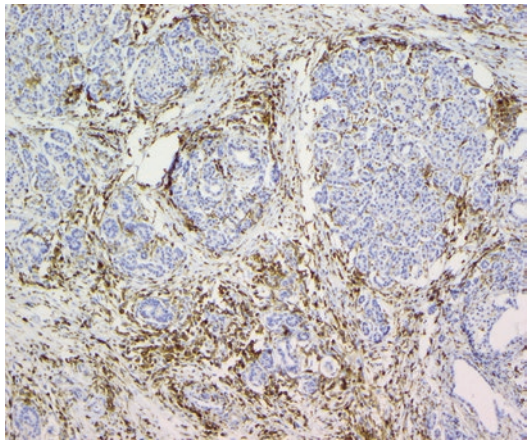

Fig. 7.54 Acinar inflammation in AIP: the lymphocytic infiltration of the acinar parenchyma consists predominantly of CD4-positive T cells (immunostaining for CD4)

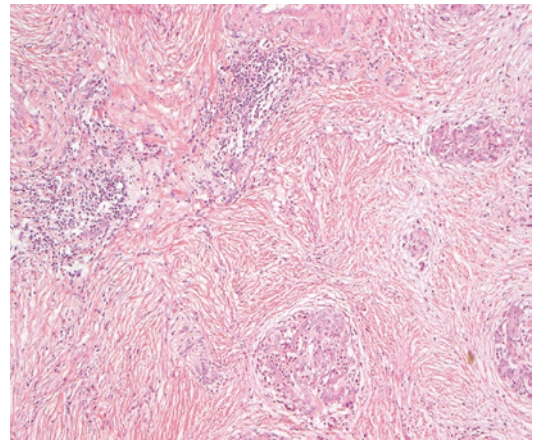

Fig. 7.56 Storiform fibrosis in AIP type 1: dense fibrosis shows an irregular cartwheel arrangement, characterized by fibers radiating out from a center

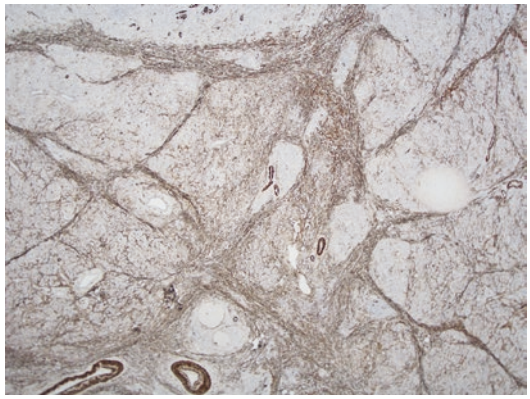

Fig. 7.55 Parenchymal fibrosis in autoimmune pancreatitis: thick fibrous bands accentuate and widen the interlobular septa and periductal stromal sheaths (elastica van Gieson stain)

extent of inflammatory changes can vary significantly between areas.

In addition to the histological changes that are common to both types of AIP, there are several specific *diagnostic features for type 1 disease* (Table 7.4). *Storiform fibrosis* refers to fibrotic changes that are characterized by irregularly whorled collagen bundles and fibroblasts, which radiate out from a center, like the spokes of a cartwheel (Figs. 7.56 and 7.57). In addition, dense chronic inflammatory cell infiltration is present in between the stromal fibers. Storiform fibrosis is usually not a diffuse phenomenon, but develops focally, such that it may not be present in limited tissue samples, for example, needle biopsies. The swirling fibrosis is often centered on ducts and veins, but not uncommonly, it is most prominent in the peripancreatic soft tissue. *Involvement of the peripancreatic tissue* by the fibroinflammatory changes is a further distinguishing feature of type 1 AIP (Fig. 7.58).

Obliterative phlebitis is a relatively frequent finding in type 1 AIP (Fig. 7.59). It probably starts as a perivenulitis, that is, a lymphocytic infiltrate around and in the outermost layers of the venous wall. Over time, inflammatory infiltration of the vessel wall may become gradually deeper and result in destruction and fibrosis. Luminal obliteration of the affected veins may be partial or total. The detection of an orphan artery that is flanked by a nodular focus of fibroinflammatory change may be helpful in identifying a vein that is totally effaced by obliterative phlebitis. Remnants of the venous wall may be more easily appreciated on elastica van Gieson staining.

Lymphoid follicles are often numerous in AIP type 1. They can cluster around affected pancreatic ducts or may be found elsewhere inside or outside the pancreas. However, it should be borne in mind that the presence of numerous large germinal center-containing lymphoid follicles is a feature of follicular pancreatitis (see Sect. 7.3.1, Figs. 7.82 and 7.83).

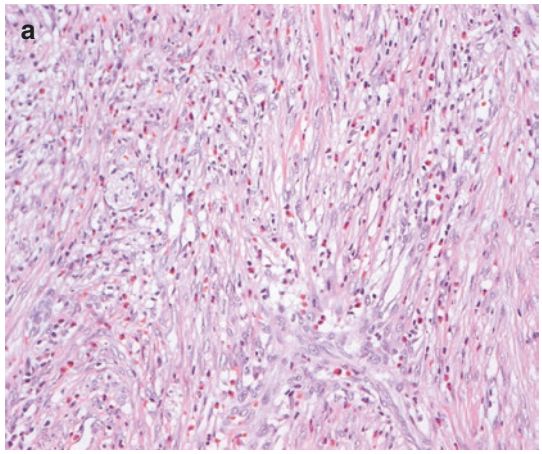

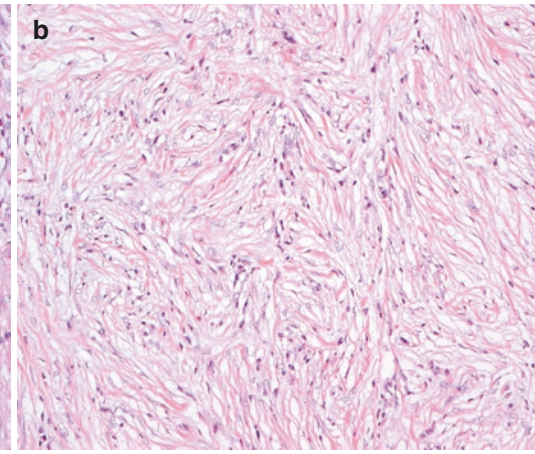

Fig. 7.57 Storiform fibrosis in AIP type 1: storiform fibrosis is commonly densely infiltrated by numerous lymphocytes and plasma cells. The number of eosinophils can vary and is high in this case (**a**). In some areas, and especially in patients who were treated, storiform fibrosis may contain fewer inflammatory cells (**b**)

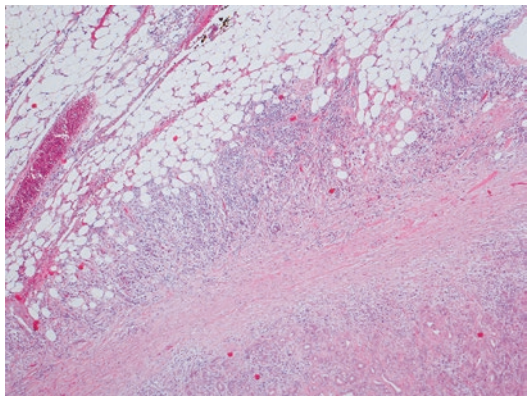

Fig. 7.58 Peripancreatitis in AIP type 1: chronic inflammatory cell infiltration and associated fibrosis extend into the peripancreatic fat

Amongst the *diagnostic features of type 2 disease* (Table 7.4), the *granulocytic epithelial lesion* (GEL) is the most distinctive (Figs. 7.60, 7.61, and 7.62). It affects small to medium-sized pancreatic ducts and is characterized by the presence of neutrophilic granulocytes. The latter are not only admixed with the chronic periductal infiltrate but typically also infiltrate the duct epithelial lining. As a consequence, the epithelium undergoes degenerative changes: it is thrown into tufts, may show reactive atypia, is often detached, and lies in the duct lumen admixed with neutrophils and cellular detritus. Occasionally, the changes may lead to formation of an intraluminal microabscess. The neutrophils in GELs are usually present in prominent numbers. The significance of rare neutrophils is not known. Granulocytes are also part of the intralobular and perilobular inflammatory cell infiltrate, but microabscesses are usually not present in this location.

7.2.7.5 Unusual Histological Features in AIP

Vasculitic changes in AIP are characteristically those of obliterative phlebitis. Arteritis with features similar to those of obliterative phlebitis (i.e., non-necrotizing lymphoplasmacytic infiltration with or without luminal obliteration) can occasionally be observed and does not exclude a diagnosis of AIP.

Granulomatous inflammation does not belong to the spectrum of histological appearances of AIP. However, on occasion, one or a small number of granulomas may be present, and this finding in itself does not exclude AIP, if it is present in an otherwise specific setting. Recently, perifollicular granulomas have been reported in a few cases of IgG4-related disease [16]. Giant cells are usually not seen.

Necrosis is not a feature of AIP, and the combination of neutrophils, granulomas, necrosis, and vasculitis should raise the suspicion of Wegener's granulomatosis (see Sect. 7.3.3).

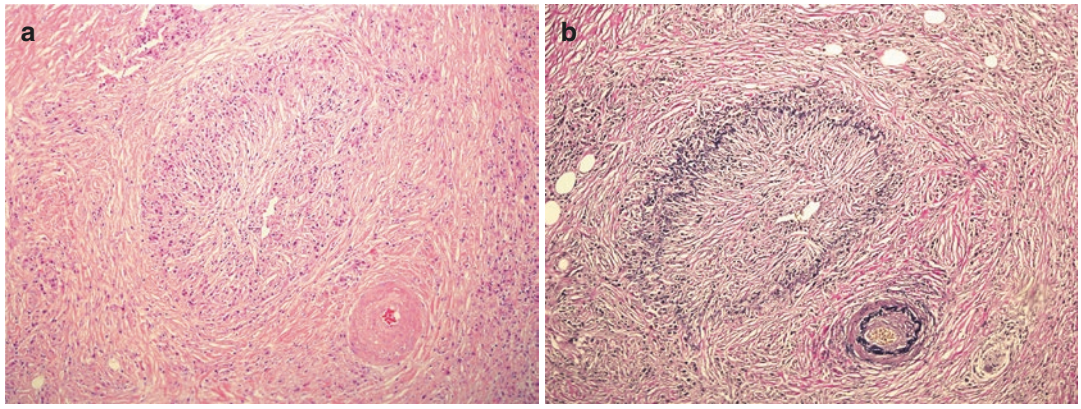

Fig. 7.59 Obliterative phlebitis in AIP type 1: chronic inflammation and fibrosis of the venous wall cause severe mural thickening and subtotal lumen stenosis. Note the unaffected associated artery (**a**). The intensity of fibrosis is highlighted by elastica van Gieson staining (**b**)

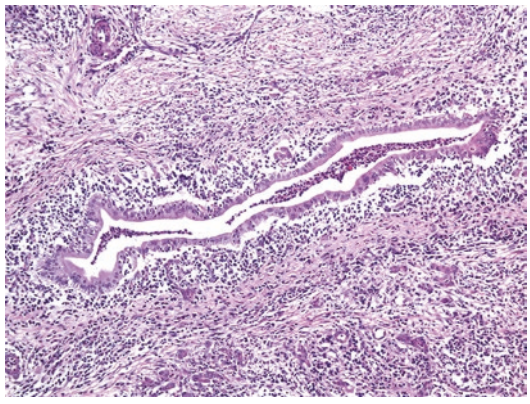

Fig. 7.60 GEL in AIP type 2: a medium-sized pancreatic duct shows neutrophil-rich inflammatory infiltration of the periductal stroma. Neutrophils are present in the duct epithelium and lumen. Note the marked inflammation of adjacent pancreatic parenchyma

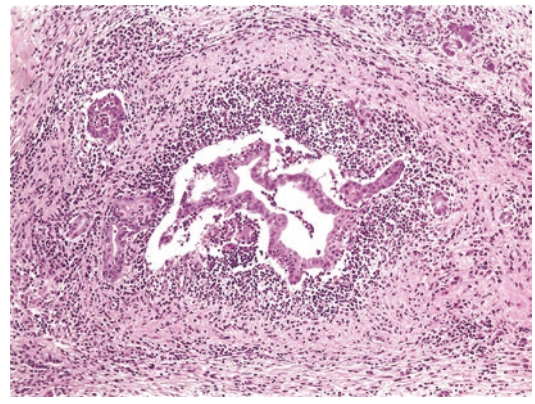

Fig. 7.62 GEL in AIP type 2: duct epithelium is detached and lies in the lumen. There is dense inflammatory infiltration, including neutrophils, of epithelium and periductal stroma

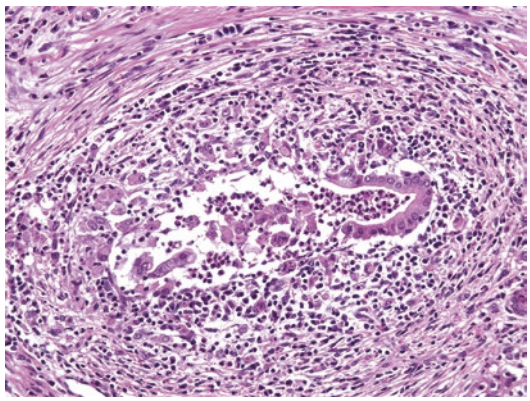

Fig. 7.61 GEL in AIP type 2: dense inflammation, including numerous neutrophils, is seen in and around this small pancreatic duct. The duct epithelium shows reactive atypia and is partially detached and fragmented

7.2.7.6 AIP Not Otherwise Specified (NOS)

Occasionally, an unequivocal case of AIP may not be classifiable as type 1 or type 2. A possible constellation would be an IgG4-seronegative patient without extrapancreatic organ involvement, but with radiologically characteristic pancreatic change and histological features common to both types, while GELs and IgG4 positive plasma cells are lacking. It has been suggested to classify these patients as AIP not otherwise specified and to proceed with steroid treatment.

7.2.7.7 IgG4 Immunohistochemistry

Immunohistochemical detection of IgG4⁺ plasma cells in pancreatic or extrapancreatic tissues is an important part of the diagnostic process. Not all AIP patients whose pancreas contains IgG4⁺ plasma cells have an elevated IgG4⁺ serum level, and therefore, IgG4⁺ immunohistochemical staining may be of particular importance in suspected cases of AIP without biochemical evidence.

While the diagnostic usefulness of IgG4 immunohistochemistry is meanwhile accepted, the debate continues as to which cut-off value is most appropriate. Different threshold values, ranging from >10 to >50 IgG4⁺ plasma cells/HPF, have been proposed by various studies. These are obviously associated with different levels of sensitivity (43–84%) and specificity (70–100%), depending on the type of tissue (pancreatic or extrapancreatic) and specimen sample (resection specimen or biopsy). While the optimal cut-off value has yet to be identified, most consensus guidelines for AIP include >10 IgG4⁺ plasma cells/HPF as one of the histological criteria (Fig. 7.63). Recently, a higher threshold value of >50 IgG4⁺ plasma cells/HPF has been recommended when assessment is performed on a surgical resection specimen (Table 7.5).

This section discusses in more detail some practical considerations regarding the diagnostic use of IgG4 immunohistochemistry for the

Table 7.5 IgG4⁺ plasma cell count cut-off values for IgG4-related disease (adapted from [13])

	IgG4⁺ plasma cells/HPF	
Site	Cases with ≥2 diagnostic features	Cases with 1 diagnostic feature
Meningus	>10	>10
Lacrimal gland	**>100**	**>100**
Salivary gland	**>100**	>100
Lymph node	>100	>50
Lung (surgical specimen)	**>50**	>50
Lung (biopsy)	>20	>20
Pleura	**>50**	>50
Pancreas (surgical specimen)	**>50**	>50
Pancreas (biopsy)	**>10**	>10
Bile duct (surgical specimen)	**>50**	>50
Bile duct (biopsy)	>10	>10
Liver (surgical specimen)	**>50**	>50
Liver (biopsy)	>10	>10
Kidney (surgical specimen)	**>30**	>30
Kidney (biopsy)	**>10**	>10
Aorta	**>50**	>50
Retroperitoneum	**>30**	>30
Skin	>200	>200

Histological diagnostic features of IgG4-related disease:

- dense lymphoplasmacytic infiltration
- fibrosis, usually storiform
- obliterative phlebitis

Bold values: highly suggestive of Ig4-related disease
Unbold values: probable IgG4-related disease
Abbreviation: *HPF* high power fields

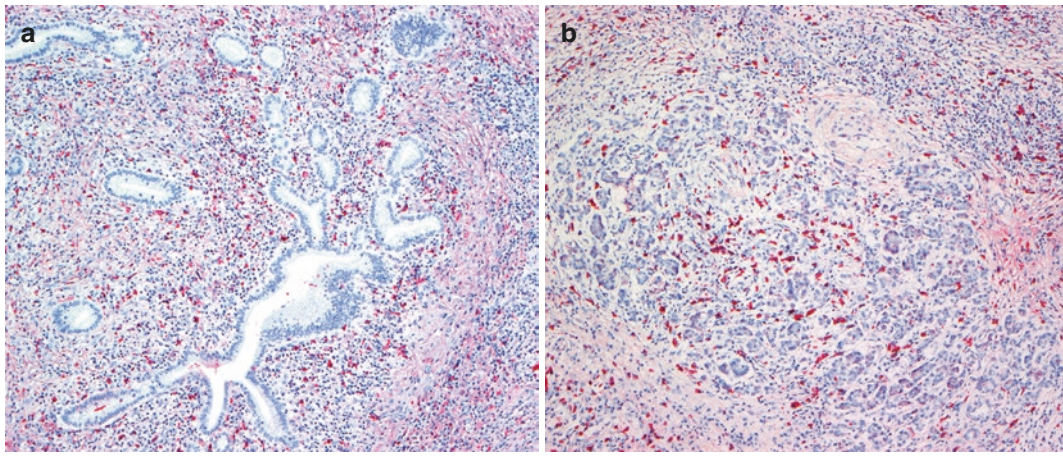

Fig. 7.63 IgG4⁺ plasma cells in AIP type 1: immunostaining for IgG4 reveals the presence of numerous positive cells in the periductal inflammatory cell infiltrate (**a**) and the acinar parenchyma (**b**)

assessment of both pancreatic and extrapancreatic tissue samples.

While an agreed standard for the assessment of the *number of IgG4⁺ plasma cells* is currently lacking, a few recommendations have been made. As the distribution of IgG4⁺ plasma cells tends to be patchy, the IgG4⁺ plasma cell count is best performed in the so-called hot spots. It has been suggested to derive the IgG4⁺ plasma cell count from the average value of the number of positive plasma cells counted in three x40 objective microscopic fields within the hot spot.

The interpretation of the IgG4⁺ plasma cell count needs careful consideration. A low IgG4⁺ plasma cell count does not exclude AIP, especially not in type 2, but neither in type 1. The possible reasons for a low IgG4⁺ plasma cell count in tissues from an AIP patient are essentially threefold. First, sampling artefact has to be taken into account. As the distribution of IgG4⁺ plasma cells may be patchy, in samples of limited size such as needle biopsies, the count may be low. This is partially accounted for by the consensus diagnostic criteria, in as far as the cut-off values are lower for biopsy material (>10 IgG4⁺ plasma cells/HPF) than for surgical resection specimens (>50 IgG4⁺ plasma cell/HPF) (Table 7.5). Second, the stage of the disease has to be considered. As AIP evolves, fibrosis becomes more pronounced, and this tends to be associated with a decrease in IgG4⁺ plasma cells. Finally, previous (trial) therapy with steroids may result in reduced IgG4⁺ plasma cell numbers.

Conversely, however, it should be borne in mind that a high IgG4⁺ plasma cell count per se does not allow an unequivocal diagnosis of AIP. A range of non-IgG4-related disorders may be associated with elevated numbers of IgG4⁺ plasma cells: primary sclerosing cholangitis, anti-neutrophil cytoplasmic antibody-associated vasculitis, rheumatoid arthritis, Rosai-Dorfman disease, multicentric Castleman's disease, certain low-grade B-cell lymphomas, and pancreatobiliary cancer.

Because a mere abundance of IgG⁺ plasma cells may result in elevated IgG4⁺ plasma cell numbers, including in inflammatory diseases other than AIP, the *IgG4⁺/IgG⁺ ratio* has been proposed as a more powerful diagnostic tool than the IgG4⁺ plasma cell count. An IgG4⁺/IgG⁺ ratio of >40% has been recommended as a valid cut-off value for both AIP and extrapancreatic IgG4-related disease. However, the finding of an IgG4⁺/IgG⁺ ratio above 40% is not, in isolation, sufficient for a diagnosis of AIP or IgG4-related disease. This applies in particular to cases with a low overall plasma cell count per HPF. For instance, in a case with only 5 IgG4⁺plasma cells/HPF and 10 IgG⁺ plasma cells/HPF, the IgG4⁺/IgG⁺ ratio would be 50%. However, the IgG4⁺ plasma cell count clearly does not reach the (lowest suggested) cut-off value. Furthermore, an IgG4⁺/IgG⁺ ratio >40% can be observed in inflammatory disorders other than AIP or IgG4-related disease, such as in multicentric Castleman's disease and rheumatoid arthritis [17].

Because IgG immunohistochemistry may suffer from background staining and a wide variation in the intensity of staining of plasma cells, in situ hybridisation for IgG (and possibly IgG4) has been recommended [16]. Alternatively, MUM1, a marker of mature plasma cells, is used in some pathology departments as an alternative to IgG. However, the diagnostic value of this combination has not been formally validated.

IgG4 immunohistochemistry on extrapancreatic tissues may be performed in two settings. First, it may be helpful to establish a diagnosis of IgG4-related disease in patients with a suspected lesion in one or more extrapancreatic tissues (see Sect. 7.2.7.10). Second, it may be considered as a substitute for a pancreatic biopsy in patients with suspected AIP. In the latter scenario, forceps biopsies from a swollen major duodenal ampulla have been proposed as more easily retrievable surrogate diagnostic samples (Fig. 7.64). While storiform fibrosis or obliterative phlebitis have never been reported in the ampulla, immunostaining for IgG4 and IgG may provide supportive diagnostic evidence with acceptable accuracy (73%), based on a cut-off value of >10 IgG4⁺ plasma cells/HPF) and >40% IgG4+/IgG+ counted in at least one HPF [18] (Fig. 7.65). Overall, it seems that IgG4 immunostaining of a biopsy from the major ampulla may provide supportive diagnostic evi-

dence, especially in patients with a normal IgG4 serum level [19].

7.2.7.8 Differential Diagnosis

From a clinical point of view, the most important differential of AIP is *ductal adenocarcinoma of the pancreas*. The inflammatory and fibrotic changes associated with pancreatic ductal adenocarcinoma, which are often referred to as 'peritumoral pancreatitis', can have overlapping features with AIP. In the absence of diagnostic findings such as duct-centered inflammation or phlebitis, the distinction may be problematic. It is especially in this context that IgG4 immunostaining may prove useful. Although the number of $IgG4^+$ plasma cells can vary from area to area in both AIP and ductal adenocarcinoma, within the most affected areas, the $IgG4^+$ plasma cell count is usually significantly higher in AIP than in peritumoral pancreatitis. In a recent study based on a cut-off value of 50 $IgG4^+$ plasma cells/HPF, averaged over three fields in the hot spot, the sensitivity of IgG4 staining for AIP (type 1) was 84%, the specificity 100% [20].

Fig. 7.64 Swollen ampulla of Vater in AIP type 1: a grossly swollen ampulla of Vater raises the suspicion of IgG4-related disease, and biopsy samples may aid in establishing the diagnosis

The distinction of AIP from *other forms of chronic pancreatitis*, such as alcoholic pancreatitis or chronic obstructive pancreatitis, can be based on the following observations. Pancreatic ducts in the latter two conditions are usually dilated and display a rounded contour, whereas in AIP the ducts are commonly narrowed and have an irregular star-shaped lumen. Protein plugs or stones may fill the duct lumina in alcoholic or chronic obstructive pancreatitis, whereas pancreatic ducts are either empty (type 1) or contain neutrophils possibly admixed with strips of inflamed duct epithelium (type 2) in AIP. Pancreatic calcification can be found on rare occasions, but only in patients with end-stage AIP. Periductal fibrosis is prominent in the three conditions, but it is less cellular and more bland collagenous in alcoholic or chronic obstructive pancreatitis. Similarly, inflammatory cell infiltration is significantly less

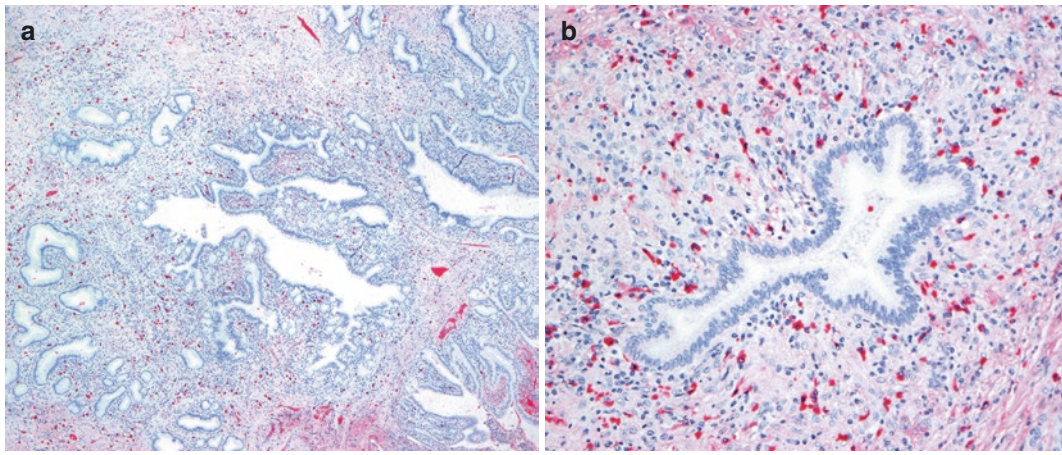

Fig. 7.65 $IgG4^+$ plasma cells in a swollen ampulla of Vater: immunostaining for IgG4 reveals the presence of numerous positive plasma cells in the ampullary mucosa (**a**, **b**)

Table 7.6 Autoimmune pancreatitis versus alcohol-related chronic pancreatitis (adapted from [10])

	AIP	Alcohol-related pancreatitis
General description	Fibroinflammatory process focussing on pancreatic ducts	Fibrosis and duct changes more prominent than inflammatory cell infiltration
Infiltrate	Predominantly lymphoplasmacytic infiltration, often admixed with eosinophils; neutrophils in and around ducts mainly in type 2	Sparse infiltration of lymphocytes, plasma cells, and macrophages
Pancreatic ducts	Dense periductal inflammation without (type 1) or with (type 2) epithelial destruction Cellular periductal fibrosis Often star-shaped narrowing of duct lumen	Rarely surrounded by inflammatory cells Periductal fibrosis blends in with inter- and intralobular fibrosis Dilated and distorted ducts
Intraductal protein plugs and stones	Absent	Frequently present
Lobules	Patchy lymphoplasmacytic inflammation, without (type 1) or with (type 2) neutrophils Acinar atrophy and fibrosis	Patchy lobular atrophy with fibrosis and sparse chronic inflammatory cell infiltrate
Obliterative phlebitis	Common in type 1	Absent
Pseudocysts	Absent	May be present
Peripancreatic fat	Fibroinflammatory process may extend into peripancreatic tissues (mainly type 1)	Frequent peripancreatic fat necrosis and pseudocysts
IgG4 immunostaining	Abundant $IgG4^+$ plasma cells (type 1)	Scant/absent $IgG4^+$ plasma cells

Abbreviation: *AIP* autoimmune pancreatitis

dense than in AIP. While nonspecific intimal fibrosis and mural thickening may be seen in arteries and veins in non-autoimmune pancreatitis, obliterative phlebitis is a feature in AIP only. Acinar atrophy and loss of lobular arrangement occur in all three conditions, but focal complete effacement of lobular architecture is more frequently seen in badly affected areas of AIP than in alcoholic or chronic obstructive pancreatitis. Table 7.6 summarizes the histological features that allow distinction between AIP and alcoholic chronic pancreatitis.

Inflammatory pseudotumor is currently regarded as a nonneoplastic tumefactive process, which clinically and radiologically mimics a neoplastic process. It has been reported under different designations, including fibrous pseudotumor, plasma cell granuloma, localized lymphoplasmacellular pancreatitis or lymphoplasmacytic sclerosing pancreatitis. The common features of the reported cases form a triad that is similar to that of AIP: diffuse infiltration by lymphocytes and plasma cells, myofibroblastic proliferation, and phlebitis. Based on this morphological resemblance, evidence in support of an association with autoimmune diseases (Sjögren's syndrome, sclerosing cholangitis, retroperitoneal fibrosis), and the occasional regression of the tumor following corticosteroid treatment, at least in a subset of lesions with a $IgG4^+/IgG4^+$ ratio >40%, inflammatory pseudotumor is currently believed to be part of the spectrum of lesions encountered in AIP and IgG4-related disease [21]. The main differential diagnosis of inflammatory pseudotumor is inflammatory myofibroblastic tumor (see Chap. 11, Sect. 11.1.4). While histological features, in particular the presence of a lymphoplasmacytic infiltrate and cellular fibrosis, are shared with inflammatory pseudotumor, positive immunolabeling for ALK1 and P53 is found significantly more frequently in inflammatory myofibroblastic tumors, Ki67-immunolabeling is considerably higher, less than 5% show obliterative phlebitis, and the $IgG4^+$ plasma cell count and $IgG4^+/IgG^+$ ratio are mostly below 10/HPF and 40%, respectively [22, 23].

Rosai-Dorfman disease, though extremely rare in the pancreas, may show two or more of the cardinal features of AIP, that is, dense lymphoplasmacytic infiltration, storiform fibrosis, and (some degree of) vasculitis. The number of $IgG4^+$ plasma cells is increased in some,

but not all, cases. Rosai-Dorfman disease can be distinguished from AIP based on the detection of sheets of histiocytes (plump or spindle-shaped) that are immunopositive for S100 and/or CD163, and the presence of emperipolesis, i.e., the engulfment of inflammatory cells in the cytoplasm of the lesional histiocytes [24]. Unlike AIP, Rosai-Dorfman disease is not treated with steroids.

On rare occasions, malignant lymphoma may have to be considered, especially since the publication of reports on malignant lymphoma (mainly of marginal zone type) in patients with IgG4-related disease [25]. However, to date, the relationship between IgG4-related disease and the subsequent development of malignant lymphoma remains unclear. Most lymphomas occurring in patients with IgG4-related disease are IgG4-negative, and conversely, most of the sporadic IgG4-positive lymphomas and plasma cell neoplasms that have been reported, did not occur in patients with IgG4-related disease. Currently, the implication for diagnostic practice is that there should be a low threshold for the use of immunohistochemistry of kappa and lambda light chains when the diagnosis of AIP type 1 or IgG4-related disease is considered. It should be noted, however, that increased intrafollicular monotypic IgG4$^+$ plasma cells may occasionally occur within hyperplastic germinal centers of reactive lymph nodes in individuals without known IgG4-related disease or lymphoma [26].

7.2.7.9 Diagnostic Criteria and Algorithms

Several diagnostic algorithms for the clinical diagnosis of AIP have been formulated by international expert panels. The approach is necessarily probabilistic, and therefore a system is endorsed that indicates the strength of the histological evidence in support of a diagnosis of AIP and classifies the diagnosis as 'definite' or 'probable'.

In the algorithm proposed by the International Association of Pancreatology [11] (Table 7.7), the histological criteria for type 1 AIP are periductal inflammation, storiform fibrosis, obliterative phlebitis, and an IgG4$^+$ plasma cell count >10/HPF. Presence of at least three of the four criteria is regarded as a 'definite' diagnosis of AIP type 1, whereas the presence of only two of the criteria amounts to a 'probable' diagnosis. For type 2 AIP, the presence of GEL in combination with

Table 7.7 International consensus diagnostic criteria for autoimmune pancreatitis—histological criteria for level 1 (definite) and level 2 (probable) type 1 and type 2 disease (adapted from [11])

Type 1 AIP	
Level 1	Level 2
LPSP (pancreatic core biopsy/resection specimen)	*LPSP (pancreatic core biopsy)*
At least 3 of the following:	Any 2 of the following:
1. Periductal lymphoplasmacytic infiltrate without granulocytic infiltration 2. Obliterative phlebitis 3. Storiform fibrosis 4. Abundant (> 10 cells/HPF) IgG4$^+$ cells	
Extrapancreatic organs	*Extrapancreatic organs, including endoscopy biopsies from the bile duct/ampulla of Vater*
Any 3 of the following:	Both of the following:
1. Marked lymphoplasmacytic infiltration with fibrosis and without granulocytic infiltration 2. Obliterative phlebitis 3. Storiform fibrosis 4. Abundant (> 10 cells/HPF) IgG4$^+$ cells	1. Marked lymphoplasmacytic infiltration without granulocytic infiltration 2. Abundant (> 10 cells/HPF) IgG4$^+$ cells
Type 2 IAP	
Level 1	Level 2
IDCP (core biopsy/resection specimen)	
Both of the following:	
Granulocytic infiltration of duct wall (GEL) with or without granulocytic acinar inflammation	Granulocytic and lymphoplasmacytic acinar infiltrate
Absent or scant (0–10 cells/HPF) IgG4$^+$ cells	Absent or scant (0–10 cells/HPF) IgG4$^+$ cells

Abbreviations: *AIP* autoimmune pancreatitis, *IDCP* idiopathic duct-centric pancreatitis, *GEL* granulocytic epithelial lesions, *HPF* high power fields, *LPSP* lymphoplasmacytic sclerosing pancreatitis

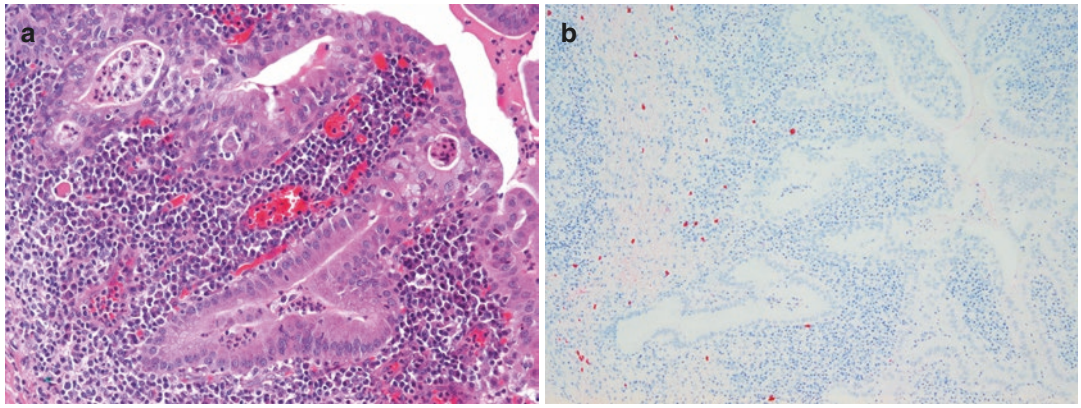

Fig. 7.66 AIP type 2: dense periductal infiltration of lymphocytes and plasma cells is associated with a so-called granulocytic epithelial lesion (GEL), that is, the presence of neutrophils in the duct epithelium (**a**). Unlike in AIP type 1, very few IgG4$^+$ plasma cells are present (**b**)

low or absent IgG4$^+$ plasma cells is regarded as confident histological evidence (Fig. 7.66). The presence of an acinar infiltrate including neutrophils, in the absence of GEL or an elevated IgG4$^+$ plasma cell count ($\leq$ 10/HPF), is considered as a probable diagnosis of type 2.

Alternative diagnostic algorithms have been proposed, which, regarding the histopathological diagnosis, do not significantly differ [13], but may include additional criteria such as eosinophilic infiltration and both periductal and diffuse lymphoplasmacytic infiltration, the latter occupying more than a third of the total area of the biopsy specimen [27]. It should be emphasized that in the case of a 'probable' diagnosis of AIP, additional clinical, serological, or radiological evidence is required to reach a final diagnosis. Such evidence may include, but is not limited to, elevated IgG4 serum levels and extrapancreatic involvement. Furthermore, it should be borne in mind that histological evidence falling short of a 'probable' diagnosis does not necessarily exclude AIP.

While the cardinal diagnostic criteria have mainly been identified in, and validated on, surgical resection specimens, they are also applicable on *biopsy material*. Histopathology is the single best test for the diagnosis of IgG4-related disease, irrespective of the organ site, and a biopsy also helps exclude the many mimics of this disease. EUS-guided fine needle biopsies using a 19- and even 22-gauge needle can provide sufficient tissue for histological assessment, while fine needle aspiration cytology is usually diagnostically uninformative [27, 28]. The main problem with biopsy samples is obviously the limited sample size, which is of concern in view of the natural patchy distribution of the fibroinflammatory lesions in AIP. Pancreatic branch ducts may be very limited in number in pancreatic biopsies and of a smaller caliber than those that are usually affected in AIP, in particular in type 1 disease. A statement in the pathology report on this important issue may, therefore, be helpful, especially in case the cardinal diagnostic features are absent. Similar limitations apply to IgG4 immunostaining since, away from areas of inflammation, the number of positive plasma cells may be below the diagnostic threshold of >10 cells/HPF. Importantly, however, a biopsy showing little or no evidence of AIP cannot be used in isolation to exclude this diagnosis, unless a positive alternative diagnosis can be made [29]. Biopsies from tumefactive lesions with lymphoplasmacytic infiltration should be immunostained for IgG4 and IgG, and elevated counts should trigger clinical evaluation for AIP, irrespective of the presence or absence of storiform fibrosis or obliterative phlebitis [16].

Reaching a definitive clinical *diagnosis of AIP type 2* can be challenging, because of the lack of a serum marker, the absence of

extrapancreatic IgG4-related lesions, and the low incidence (10%) of concurrent inflammatory bowel disease. Therefore, supportive histology is usually required, but GELs as the main distinguishing feature may not be represented in a biopsy sample. Recently, immunostaining for PD-L1 in pancreatic ductal and acinar epithelium has been proposed as a potentially specific diagnostic test for AIP type 2 [30]. Further studies are awaited to validate these findings.

The diagnostic algorithms apply to adult patients. In *children*, the approach to a pancreatic mass with biliary obstruction is different because of the markedly lower probability of an underlying neoplasm compared to the situation in adults (see Sect. 7.4). AIP may be more common in children than hitherto believed, because many of the cases previously reported as fibrosing pancreatitis would fulfill the current diagnostic criteria of AIP [31].

Despite international guidelines for diagnosing AIP, distinguishing the disease from its many mimics, in particular pancreatic cancer, remains challenging [32]. It cannot be emphasized sufficiently that *careful correlation* of the histological and immunohistochemical findings with the clinical scenario and features on imaging are paramount to reaching a correct diagnosis. Any apparent discrepancies between the different diagnostic aspects should be resolved in a multidisciplinary setting (see Chap. 4).

7.2.7.10 IgG4-Related Systemic Disease

To date, IgG4-related disease has been described in virtually every organ system. Several of these lesions were previously recognized and described under various disease entities, for example, Mickulicz's syndrome, Küttner tumor, multifocal fibrosclerosis, or eosinophilic angiocentric fibrosis.

Over half of the patients with IgG4-related disease have more than two organs involved. The pancreas is involved in 45% of patients and hence the most common site of IgG4-related disease. The relative order of frequency of organ involvement is the pancreas and hepatobiliary system (Figs. 7.67, 7.68, 7.69, 7.70, and 7.71), followed by the salivary glands, lymph nodes, lacrimal glands, soft tissue, lungs, and kidneys [33]. Taken together, these organs are affected in 85% of cases [34]. In cases with pancreatobiliary involvement, the ampulla of Vater may also be affected and appear grossly enlarged (Fig. 7.64).

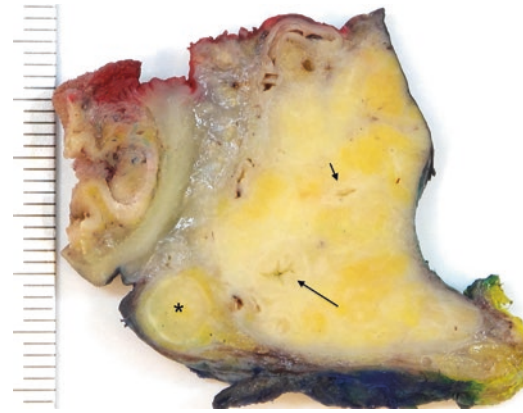

Fig. 7.67 IgG4-related disease: an axial specimen slice from a pancreatoduodenectomy specimen shows changes of AIP type 1 in the acinar parenchyma and a periductal cuff around the narrowed main pancreatic duct (*short arrow*). In addition, the intrapancreatic common bile duct (*long arrow*) has a thickened wall and narrowed lumen as a result of involvement by IgG4-related disease. Also affected is a posterior pancreatoduodenal lymph node (*asterisk*), which is enlarged and shows an abnormal cut surface

Fig. 7.68 IgG4-related cholangitis: the wall of the common bile duct and cystic duct is inflamed and thickened. The pancreas in this case was diffusely affected by AIP type 1

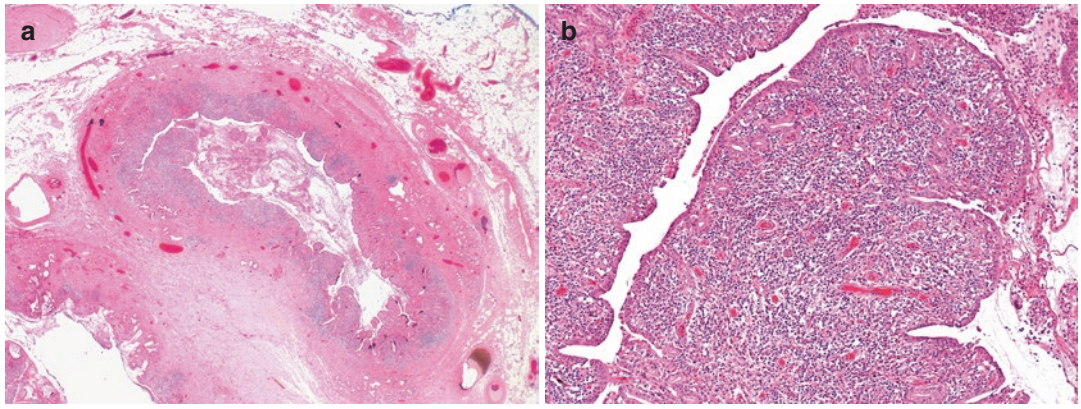

Fig. 7.69 IgG4-related cholangitis: the wall of the common bile duct is concentrically thickened by inflammatory cell infiltration and fibrosis (**a**). The dense inflammatory cell infiltrate consists mainly of lymphocytes and plasma cells (**b**) (same case as in Fig. 7.68)

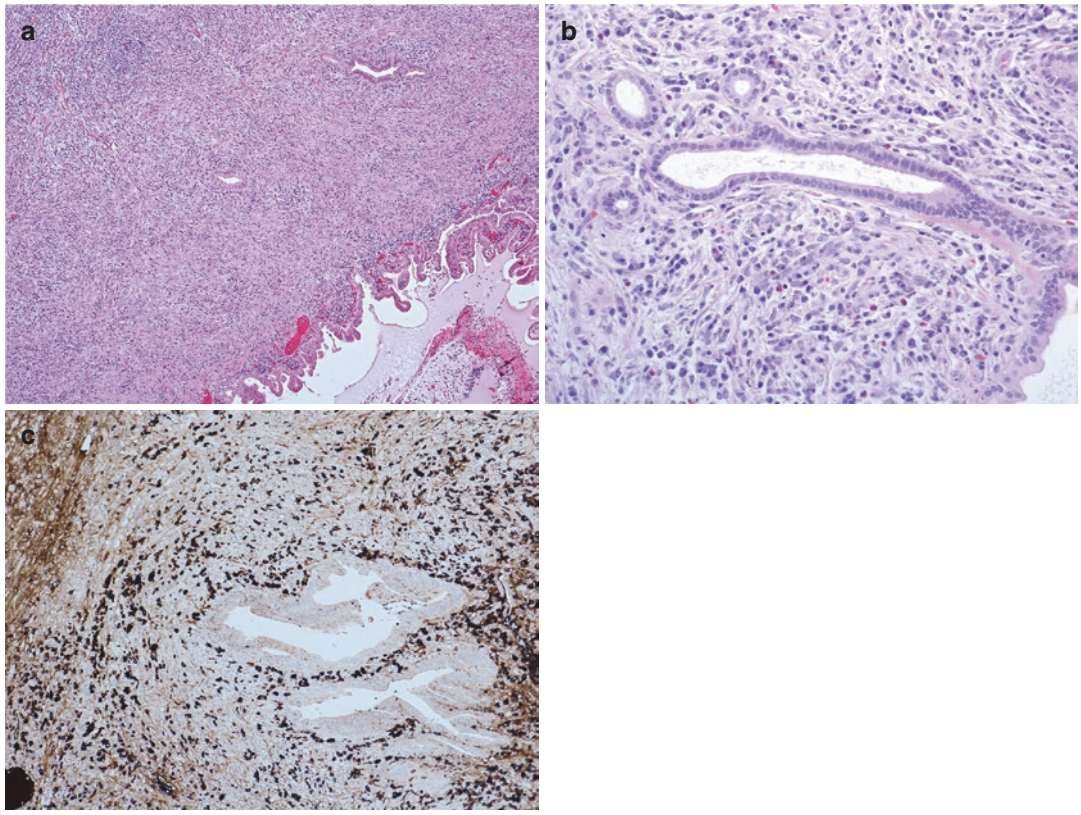

Fig. 7.70 IgG4-related cholangitis: the bile duct wall and surrounding fibrous tissue are densely infiltrated by lymphocytes, plasma cells, and scattered eosinophils (**a**, **b**). There are numerous $IgG4^+$ plasma cells (**c**; immunohistochemistry) (same case as in Fig. 7.69)

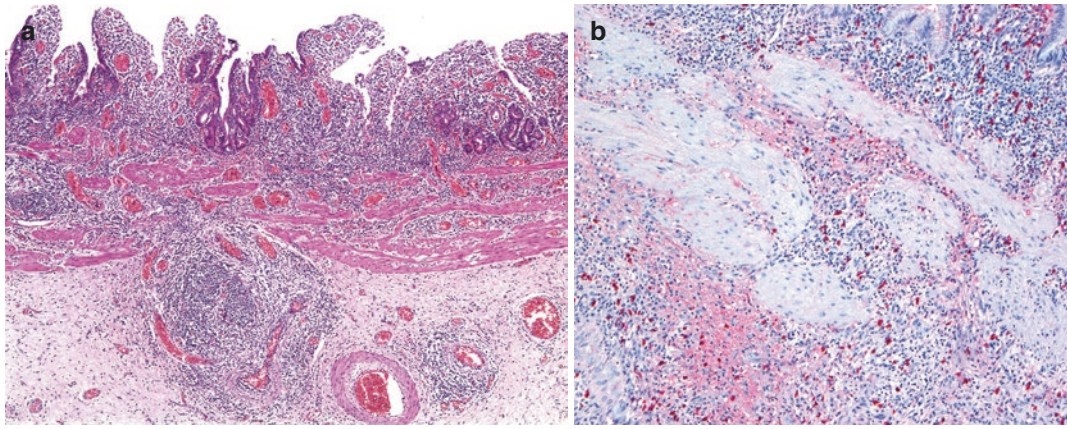

Fig. 7.71 IgG4-related cholecystitis: the gallbladder wall shows chronic inflammatory cell infiltration, which is denser and more deep-seated than in gallstone-related cholecystitis. Note the focus of phlebitis with incipient lumen obliteration (**a**). Immunostaining for IgG4 confirms the presence of numerous IgG4$^+$ plasma cells (**b**)

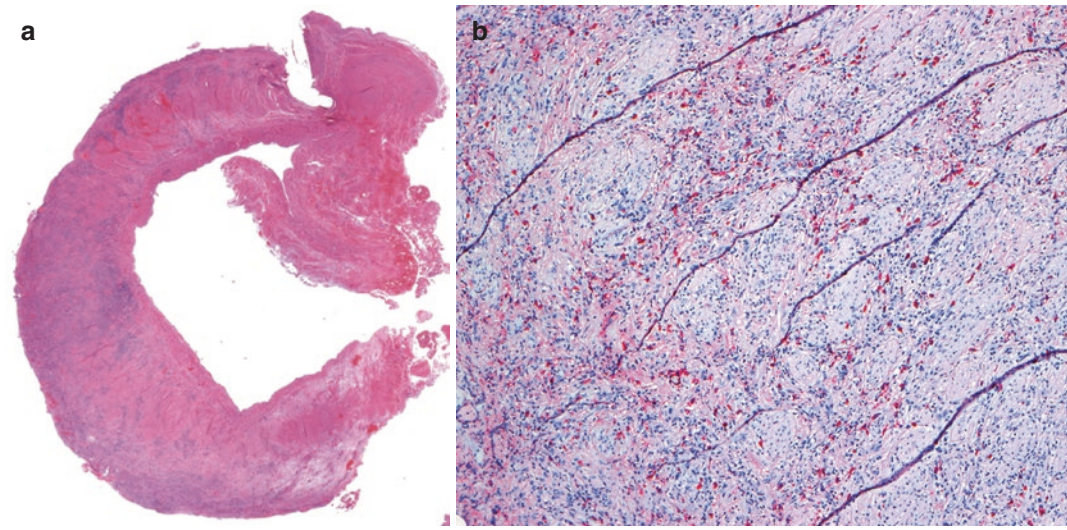

Fig. 7.72 IgG4-related involvement of large blood vessels: during a pancreatoduodenectomy procedure for presumed ductal adenocarcinoma, a fragment of the thickened wall of the superior mesenteric vein was sent for intraoperative frozen section examination. Histological examination showed dense inflammatory cell infiltration and absence of neoplasia (**a**). Subsequent immunostaining revealed dense infiltration with IgG4$^+$ plasma cells (**b**). The pancreas in this case showed features characteristic of AIP type 1

Importantly, large peripancreatic blood vessels, for example, the superior mesenteric vein or portal vein, may also be affected (Fig. 7.72) and lead to vascular wall thickening, a finding that on preoperative imaging is bound to be misconstrued as evidence of malignancy. In both locations, ampulla and portal/superior mesenteric vein, a significantly increased number of IgG4$^+$ plasma cells confirms involvement by IgG4-related disease. Interestingly, the organs that are affected most commonly differ between the sexes: while AIP is the most common manifestation in men, the salivary glands are most frequently affected in women. The difference in sex predilection and the divergence in histological and clinical features between organ sites indicate that the causes

of IgG4-related disease differ between patients, with different antigens or autoantibodies potentially initiating similar immune reactions in different organs.

Lesions in the various organs may occur synchronously or metachronously with AIP. Although they share the common cardinal triad of marked lymphoplasmacytic inflammation, storiform fibrosis, and obliterative phlebitis, these histological features vary among organs: they are most prevalent in the pancreas and biliary system, while IgG4-related disease of the lacrimal or salivary glands, breast, and skin often lacks significant fibrosis. Conversely, involvement of the retroperitoneum, mediastinum, and orbit is often characterized by dominant fibrosclerosis and less conspicuous lymphoplasmacytic infiltration.

IgG4-related disease of the lymph nodes may demonstrate a number of patterns: follicular hyperplasia, interfollicular expansion, progressive transformation of germinal centers, Castleman disease-like, and inflammatory pseudotumor. Awareness of these patterns is important to avoid diagnosing histological mimics that are not associated with IgG4-related disease, e.g., true Castleman or Rosai-Dorfman disease, syphilitic lymphadenitis, or intranodal inflammatory myofibroblastic tumor [35]. While the inflammatory-pseudotumor pattern is rare but specific, the others are relatively nonspecific. True IgG4-related lymphadenitis is likely characterized by $IgG4^+$ plasma cells in the interfollicular region, whereas intrafollicular $IgG4^+$ plasma cells may represent a nonspecific finding [26]. A summary of the inflammatory lesions considered to date to be part of IgG4-related disease is provided in Table 7.8, and the organ-specific cut-off values for $IgG4^+$ plasma cell counts are listed in Table 7.5.

Table 7.8 Organs and tissues affected by IgG4-related systemic disease (adapted from [14] and [36])

Organ, tissue, site	Clinicopathological features
Pancreas	Autoimmune pancreatitis (type 1 or type 2)
Bile duct	Sclerosing cholangitis or IgG4-associated cholangitis
	Inflammatory pseudotumor
Liver	Sclerosing cholangitis involving intrahepatic ducts
	Portal inflammation, with or without interface hepatitis
	Large bile duct obstruction
	Portal sclerosis
	Lobular hepatitis
	Canalicular cholestasis
	Inflammatory pseudotumor
Gallbladder	Diffuse acalculous lymphoplasmacytic cholecystitis
Gastrointestinal tract	Increased $IgG4^+$ positive cells in mucosa
	Inflammatory bowel disease
Salivary and lacrimal glands	Küttner tumor (chronic sclerosing sialadenitis)
	Mikulicz disease
	Chronic sclerosing dacryoadenitis
Kidney	Membranous glomerulopathy, with IgG4 immune complex deposits
	Inflammatory pseudotumor
Retroperitoneum and mesentery	Retroperitoneal fibrosis
	Sclerosing mesenteritis
Thyroid	Hypothyroidism/Riedel thyroiditis
	Multifocal fibrosclerosis
Breast	Inflammatory pseudotumor
Lung	Interstitial pneumonia
	Inflammatory pseudotumor
Aorta	Periaortitis
	Inflammatory abdominal aortic aneurysm
Orbit	Inflammatory pseudotumor
	Eosinophilic angiocentric fibrosis
	Multifocal fibrosclerosis
Mediastinum	Sclerosing mediastinitis
Pituitary gland	Hypophysitis
	Inflammatory pseudotumor
Meninges	Hypertrophic pachymeningitis
Prostate	IgG4-associated prostatitis

(continued)

7.2.8 Paraduodenal (Groove) Pancreatitis

7.2.8.1 Definition and Nomenclature

This distinct form of chronic pancreatitis occurs in the 'pancreatoduodenal groove', the anatomical compartment composed of the soft tissue at

Table 7.8 (continued)

Organ, tissue, site	Clinicopathological features
Lymph nodes	Castleman disease-like lymphadenopathy Lymphadenopathy with follicular hyperplasia Lymphadenopathy with interfollicular expansion by immunoblasts and plasma cells

the pancreatoduodenal interface, and the flanking duodenal wall and pancreatic parenchyma. Paraduodenal pancreatitis is characterized by the presence of inflamed cysts or pseudocysts within the duodenal muscle layer, which develop from ectopic pancreatic tissue. It is usually associated with inflammation of the duodenum-flanking pancreatic parenchyma.

Paraduodenal pancreatitis has been reported under various other names: groove pancreatitis, cystic dystrophy of heterotopic pancreas, cystic dystrophy of the duodenum, pancreatic hamartoma of the duodenum, myoepithelial hamartoma, adenomyoma, adenomyomatosis, and paraduodenal wall cyst (see also Chap. 13, Sect. 13.4). Paraduodenal pancreatitis is currently the more favored terminology.

7.2.8.2 Etiopathogenesis

The underlying cause of paraduodenal pancreatitis is the presence of ectopic pancreatic tissue within the wall of the duodenum. Usually this is found most prominently in the duodenum between the ampulla of Vater and the minor ampulla, and not uncommonly further proximally. Due to the abnormal localization, drainage of pancreatic secretions from the ectopic tissue is impaired. Over time this can lead to duct dilatation, cyst formation and rupture, and ensuing prominent inflammation in the surrounding tissues, that is, the duodenal wall, the adjacent pancreatic parenchyma, and the soft tissue between the duodenum and pancreas. Chronic consumption of alcohol has been identified as a further pathogenetic factor, which increases pancreatic secretion, also in the ectopic tissue, and therefore amplifies the problem of impaired drainage and subsequent complications. The need for both pathogenetic factors to coincide explains the rarity of this condition, despite the fact that ectopic pancreatic tissue within the duodenal wall is a fairly common finding in the general population.

7.2.8.3 Clinical Findings

Patients are mainly young to middle-aged male adults with a history of alcohol abuse. They usually present with abdominal pain, which can be severe, nausea and vomiting due to duodenal stenosis, and weight loss. Obstructive jaundice is rare. In typical cases, the diagnosis can be made based on imaging, in particular endoscopic ultrasound (EUS), which reveals multiple cysts within the thickened pancreas-facing duodenal wall. When findings on imaging are less pathognomonic, the main clinical differential diagnosis is pancreatic cancer. While abstention from alcohol is the obvious measure to take, complemented with conservative treatment, pancreatoduodenectomy may be the only treatment option for severe cases.

7.2.8.4 Macroscopy

Cystic spaces, usually multiple, are a constant feature, but the size of the cysts may vary from hardly noticeable to large (0.1–4.0 cm) (Figs. 7.73, 7.74, and 7.75). The content of the cysts ranges from watery clear fluid to thick or occasionally purulent material. The cysts are typically located within the duodenal wall and

Fig. 7.73 Paraduodenal pancreatitis: large cystic spaces are present in the duodenal muscularis propria (*arrows*) and extend into the pancreatic tissue

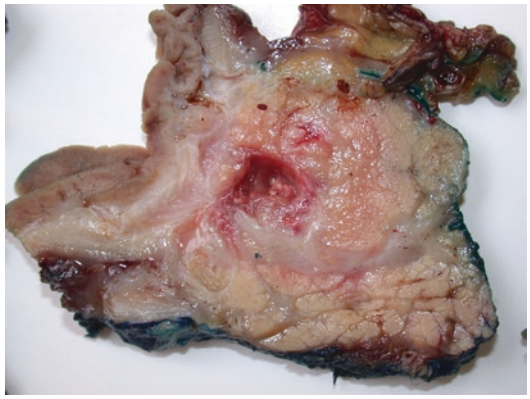

Fig. 7.74 Paraduodenal pancreatitis: an inflamed cystic cavity is present within the duodenal muscle layer and adjacent pancreatic tissue. There is marked fibrosis and scarring of the duodenual wall and surrounding pancreas. Away from the cystic lesion, the pancreas is well preserved

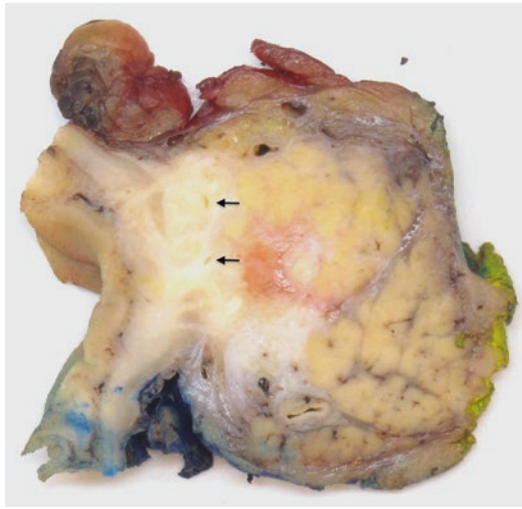

Fig. 7.75 Paraduodenal pancreatitis: there is marked fibrosis and scarring of the pancreatoduodenal groove, but cyst formation (*arrows*) is minimal

pancreatoduodenal groove, that is, the soft tissue plane between the duodenum and pancreatic head, and they can extend into the pancreatic parenchyma. The duodenal wall is thickened and shows a varying degree of inflammation, fibrosis, and scarring. Inflammation and fibrosis can also affect the adjacent pancreas, but pancreatic parenchyma is usually normal at a distance from the duodenal wall, except in the rare case of coincidental chronic (alcohol-related) pancreatitis. The duodenal mucosa overlying the pancreatic head is usually irregular and thickened, often thrown into irregular polypoid folds, and occasionally ulcerated (Fig. 7.76). On slicing, hyperplasia of the Brunner's glands is often apparent as a yellow-brownish layer, which expands the duodenal submucosa (Fig. 7.77).

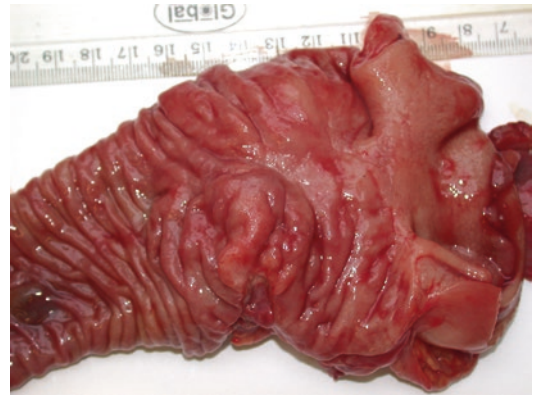

Fig. 7.76 Duodenal stenosis in paraduodenal pancreatitis: the duodenum overlying the pancreatic head is lined by irregular mucosa with coarse, 'bumpy' folds

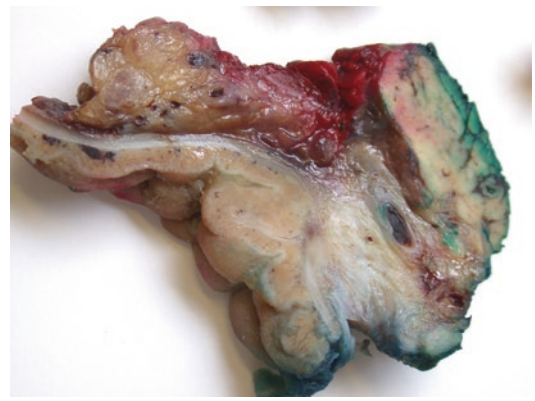

Fig. 7.77 Brunner's gland hyperplasia in paraduodenal pancreatitis: the duodenal submucosa is changed into a thick ochre-colored tissue layer due to Brunner's gland hyperplasia. Note the marked fibrosis and scarring of the deeper duodenal wall

7.2.8.5 Microscopy

As the cystic spaces in the duodenal wall and groove represent dilated ectopic pancreatic ducts, they are lined with ductal epithelium, which may be flattened, atrophic, or absent. Not uncom-

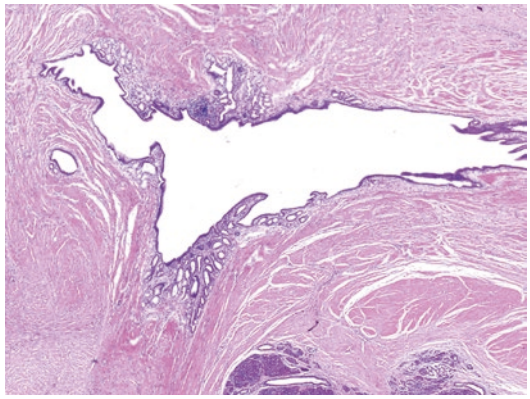

Fig. 7.78 Ectopic pancreatic tissue in paraduodenal pancreatitis: scattered foci of ectopic pancreatic tissue, including acini, islets, and numerous ducts, are present in the duodenal muscle layer. Several ducts are dilated. Note the disarray of the surrounding smooth muscle

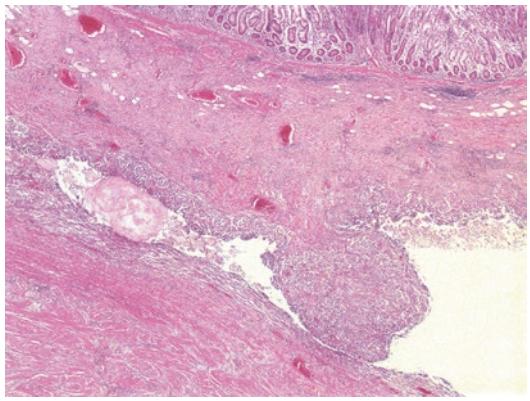

Fig. 7.79 Cysts in paraduodenal pancreatitis: this cystic cavity has no epithelial lining and is demarcated by granulation tissue. The presence of a protein plug indicates that this is in fact a dilated (ectopic) pancreatic duct

monly, smaller dilated pancreatic ducts may be found around the gross cystic cavities, along with lobules of ectopic acini and scattered islets (Fig. 7.78). Protein plugs are commonly found within the lumina of the cysts and dilated ectopic ducts. When cysts rupture, the epithelial lining may be replaced by granulation tissue with dense mixed inflammatory cell infiltration (Figs. 7.79 and 7.80). Acute and chronic inflammation, occasionally with abscess formation, necrosis, and loss of native tissue structures, may involve the duodenal wall and pancreas adjacent to the cystic cavities.

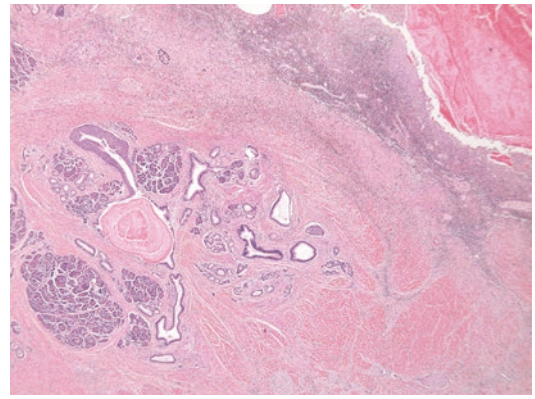

Fig. 7.80 Cysts in paraduodenal pancreatitis: ectopic pancreatic tissue within the duodenal muscle layer contains a dilated duct with a protein plug and squamous metaplasia. Part of the wall of a large neighboring cavity is present in the right-upper corner. There is dense inflammatory cell infiltration of the wall and a large protein plug fills the lumen

The duodenal muscularis propria is often thickened and composed of irregularly arranged muscle bundles. It commonly contains additional small foci of ectopic pancreatic tissue. This intermingling of irregular smooth muscle tissue and ectopic glandular lobules lies at the origin of 'duodenal adenomyoma' or 'duodenal adenomyomatosis' as an earlier terminology for paraduodenal pancreatitis. Fibrosis and scarring extend from the inflamed cysts and often result in focal atrophy or effacement of the duodenal muscle layer and/or pancreatic parenchyma. Occasionally, acute and chronic inflammation may involve large caliber pancreatic ducts or the distal intrapancreatic common bile duct. Brunner's glands are commonly hyperplastic and present as a continuous layer of densely packed voluminous glands that expand the duodenal submucosa and extend into the lamina propria (Fig. 7.81).

7.2.8.6 Differential Diagnosis

Paraduodenal pancreatitis is by definition a localized disease and, based on its limitation to the part of the pancreatic head that flanks the duodenal wall, distinction from other forms of pancreatitis, in particular alcohol-related pancreatitis which affects the pancreas diffusely, is usually

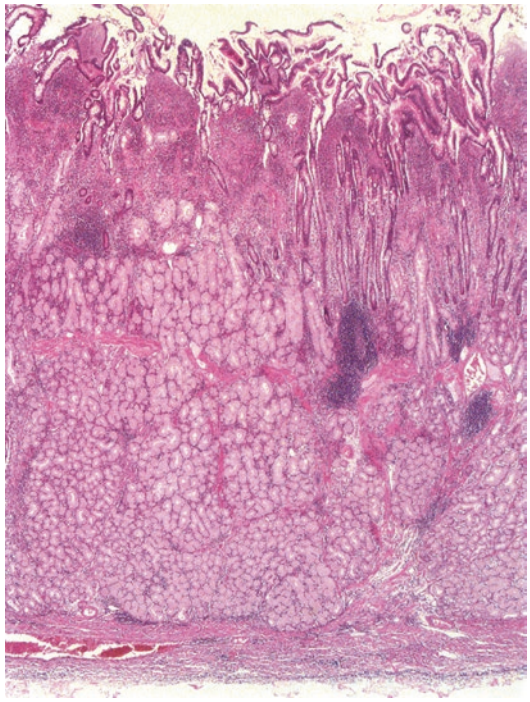

Fig. 7.81 Brunner's gland hyperplasia in paraduodenal pancreatitis: voluminous and densely packed Brunner's glands fill and expand the duodenal submucosa and extend into the lamina propria

straightforward. Clinically, however, it may be difficult to distinguish paraduodenal pancreatitis from cancer if cyst formation is minimal (see Fig. 9.21). In cases of paraduodenal pancreatitis containing larger cystic spaces, foregut (duplication) cysts or inflamed diverticula may be considered clinically, but these differentials are readily excluded based on the lining of the cysts (see Chap. 13, Table 13.1, and Chap. 19).

7.2.9 Eosinophilic Pancreatitis

Eosinophilic pancreatit*s* is an extremely rare form of chronic or acute recurrent pancreatitis, which currently lacks a clear definition both clinically and morphologically. It is characterized by a dense infiltration of eosinophils or of predominantly eosinophils, which is usually diffuse and involves the periductal, acinar, and interlobular tissue [37, 38]. The etiology of eosinophilic pancreatitis is diverse. In some patients it occurs in conjunction with eosinophilic gastroenteritis or hypereosinophilic syndrome, in which case it is associated with elevated serum immunoglobulin E levels, an elevated eosinophil count, and eosinophilic infiltration in parts of the gastrointestinal tract. Hypersensitivity responses to medication and allergy (e.g., to food stuffs) have also been described as possible etiologies. A peculiar form of eosinophilic infiltration of hypertrophic islets has been described in infants born to type 1 diabetic mothers [39]. In some patients, the eosinophilic infiltration may be localized, in which case pseudocyst formation may be present, while eosinophilia in the peripheral blood and involvement of other organs are absent. Localized eosinophilic pancreatitis may mimic malignancy, especially if it is associated with obstruction of the common bile duct. Eosinophilic vasculitis (phlebitis and arteritis) has been described in some but not all cases. Eosinophilic pancreatitis should be distinguished from processes that may rarely affect the pancreas and have a prominent eosinophil component in the inflammatory cell infiltrate, for example, pancreatic allograft rejection (see Chap. 22), parasitic infection, systemic mastocytosis, histiocytosis X, eosinophilic granulomatosis with polyangiitis (Churg-Strauss syndrome) and inflammatory myofibroblastic tumor (see Chap. 11, Sect. 11.1.4). Moderately dense eosinophilic infiltration of the pancreas, with or without associated peripheral eosinophilia, may also be seen in patients with autoimmune pancreatitis, who may also have an elevated peripheral eosinophil count, elevated serum IgE, and a history of allergy. The presence of storiform fibrosis, obliterative phlebitis, and an elevated IgG4-count may help in making the distinction. Some of the cases of eosinophilic pancreatitis reported in the older literature may in fact represent autoimmune pancreatitis according to the current diagnostic criteria.

7.2.10 Chronic Pancreatitis and Pancreatic Cancer

Multiple studies have confirmed a strong link between chronic pancreatitis and pancreatic cancer, although the lifetime risk varies depend-

ing on the cause of the chronic pancreatitis. The highest risk, amounting to a lifetime risk of 40%, is observed in the small group of patients with hereditary pancreatitis (see Chap. 6, Sect. 6.3). In view of the risk of pancreatic cancer in patients with chronic pancreatitis, malignancy and precursor lesions should always be actively looked for in cytology, biopsy, or surgical specimens. In small biopsies or frozen sections during intraoperative consultation, the distinction between chronic pancreatitis and ductal adenocarcinoma can be a diagnostic challenge. The differential diagnostic criteria are discussed in Chap. 9, Sect. 9.12.1, and Chap. 23, Sect. 23.2.

The risk of developing malignancy, including pancreatic cancer, is reported to be increased in patients with IgG4-related disease by some studies, while others do not find an association. To date, it is not clear whether the increased cancer incidence may be the result of more careful surveillance of patients diagnosed with IgG4-related disease.

7.3 Other Inflammatory Diseases of the Pancreas

7.3.1 Follicular Pancreatitis

Follicular pancreatitis is a recently described clinicopathological entity that is characterized by the presence of numerous lymphoid follicles in the pancreas, resulting in a tumefactive lesion [40]. The lymphoid follicles are of variable size, often large, and they contain a reactive germinal center and an intact follicle mantle zone. The lymphoid follicles are diffusely distributed in the pancreatic parenchyma (Fig. 7.82). A periductal arrangement may also be found, but the duct epithelium is usually intact and spared from lymphocytic infiltration (Fig. 7.83). Plasma cells are present around the lymphoid follicles, though usually in moderate numbers. Scattered eosinophils may also be seen, but neutrophils are usually absent. Mild interlobular and periductal fibrosis may be observed. The intrapancreatic

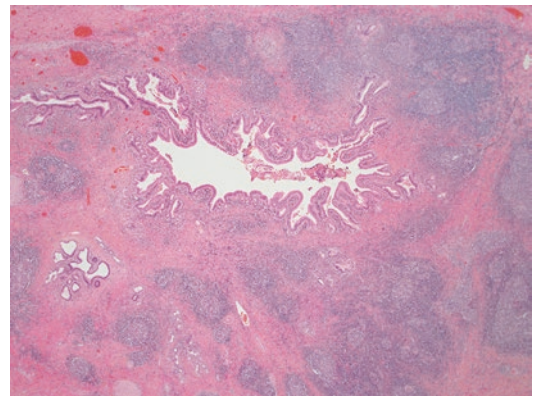

Fig. 7.83 Follicular pancreatitis: lymphoid follicles may be present around pancreatic ducts, which may show an irregular, slightly narrowed lumen. The duct epithelium is free of inflammatory cell infiltration

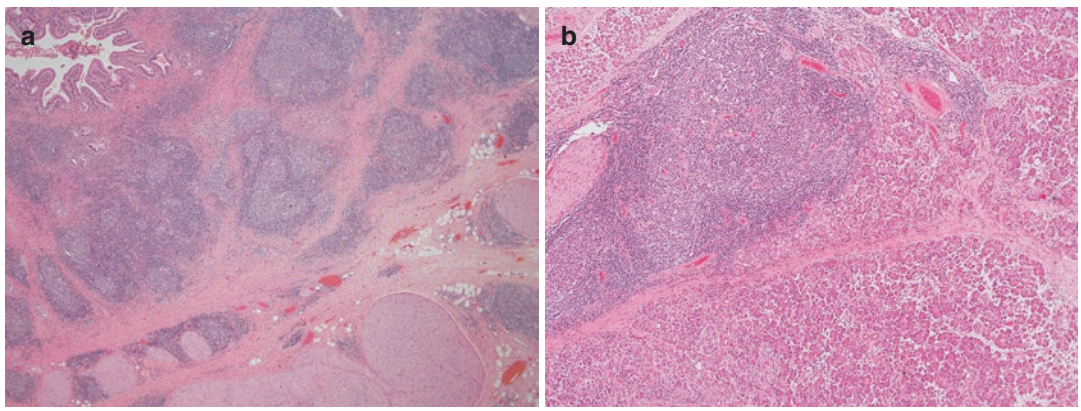

Fig. 7.82 Follicular pancreatitis: numerous, often large, lymphoid follicles are present in the pancreatic parenchyma (**a**). Most lymphoid follicles contain a germinal center and an intact mantle zone (**b**)

common bile duct can be involved by similar albeit less prominent inflammatory changes.

In some of the reported cases, an identical inflammatory process was found to affect the large bile ducts at the liver hilus, without apparent involvement of the pancreas. These cases were reported as *follicular cholangitis* [41, 42]. Based on the clinicopathological similarities, it is presumed that pancreatic or biliary involvement are both a manifestation of a single underlying condition *follicular pancreatocholangitis* (Figs. 7.84 and 7.85).

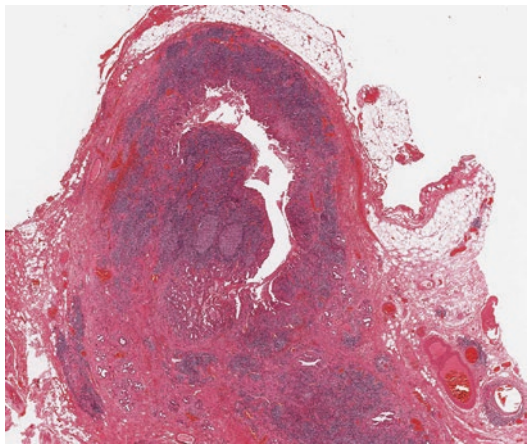

Fig. 7.84 Follicular cholangitis: the wall of the common bile duct is thickened by dense chronic inflammatory infiltration. Numerous lymphoid follicles are lined up along the circumference of the duct

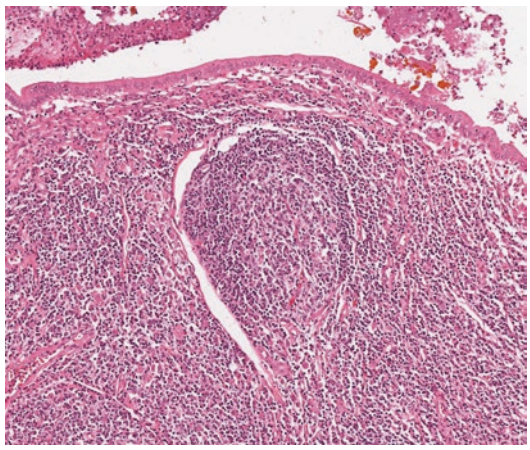

Fig. 7.85 Follicular cholangitis: a large lymphoid follicle is positioned underneath the duct epithelium

While follicular pancreatitis resembles autoimmune pancreatitis in some aspects, it differs from it by the prominence of lymphoid follicles and the absence of obliterative phlebitis, storiform fibrosis, or increased IgG4+ plasma cells (see Sects. 7.2.7.4 and 7.2.7.7). The latter are present only in small numbers, well below the values considered diagnostic for autoimmune pancreatitis or IgG4-associated cholangitis. Serum markers indicative of autoimmune disease and serum IgG4 levels are not elevated.

Based on the few cases of follicular pancreatitis that have been reported to date, the disease affects mainly middle-aged to elderly patients (mean age 62 years) with a male predilection. Any part of the pancreas may be affected. Most patients with follicular pancreatitis are asymptomatic, and the pancreatic lesion is detected incidentally, unless involvement of the common bile duct has resulted in duct obstruction, which then often raises the clinical suspicion of malignancy. Single cases of 'pancreatic pseudolymphoma' reported in the older literature may well represent follicular pancreatitis.

7.3.2 Malakoplakia

Malakoplakia involving the pancreas is exceedingly rare, and affected patients present clinically with a pancreatic mass mimicking carcinoma. Macroscopically, the lesion consists of a yellow-brown nonencapsulated mass that may be several centimeters in size. The histological features are the same as for malakoplakia in other, more commonly affected organs. The diagnostic hallmark is a large collection of PAS-positive histiocytes (von Hansemann histiocytes), some of which contain characteristic Michaelis-Gutmann bodies. The latter are small intracytoplasmic and interstitial targetoid spherules, which label with von Kossa's and Perls' stains. A mixed inflammatory cell infiltrate is usually present, and bundles of fibroblasts and myofibroblasts may be seen in between the histiocyte collections. The differential diagnosis includes histiocyte-rich inflammatory lesions, myofibroblastic inflammatory tumor, and histiocytic neoplasms.

The etiology of malakoplakia is still not entirely clear, but an association with bacterial infection has been described. Two reported patients with malakoplakia of the pancreas suffered from concomitant chronic pancreatitis with ductal adenocarcinoma and diabetes mellitus [43, 44]. A further patient presented with abdominal pain, while in a fourth patient a pancreatic mass due to malakoplakia was detected during elective cholecystectomy [45]. Secondary pancreatic involvement by malakoplakia of the colon, adrenal gland, and retroperitoneum has been reported in patients with immunodeficiency.

7.3.3 Vasculitis and Vasculogenic Pancreatitis

Pancreatic involvement by vasculitis is rare. It may result in acute 'vasculogenic' pancreatitis (Figs. 7.86 and 7.87), which in most cases is accompanied by other clinical symptoms that are related to the underling systemic vasculitis. Only on rare occasion is pancreatitis the main clinical manifestation.

Vasculitides are classified based on the size of the affected blood vessels. Table 7.9 provides a summary of the relatively more common vasculitic disorders that may affect the pancreas, with their main morphological and clinical features.

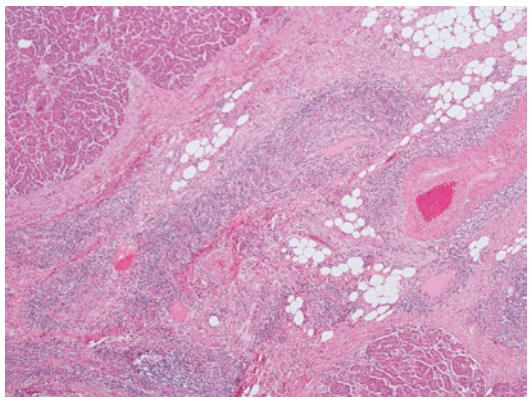

Fig. 7.86 Vasculitis affecting the pancreas: in this case both arteries and veins are heavily infiltrated by a mainly lymphocytic cell population. The affected vein is occluded

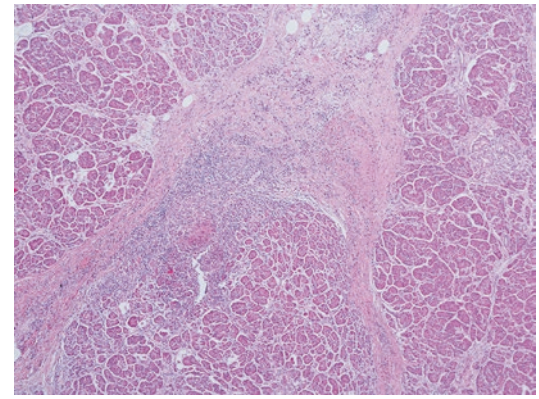

Fig. 7.87 Vasculogenic pancreatitis: same case as in Fig. 7.86. Inflammation also extends into parenchymal lobules. Note the interlobular fibrosis and mild acinar atrophy

Pancreatic involvement has also been reported as a rare complication of a range of vasculitic conditions associated with medication, drug abuse, human immunodeficiency virus (HIV) infection, hemolytic uremic syndrome, and thrombotic thrombocytopenic purpura.

7.3.4 Collagen Vascular Diseases

The pancreas is one of the organs that can be affected by collagen vascular disease. The clinical manifestation is usually that of acute pancreatitis, while chronic pancreatitis is much more uncommon. Pancreatitis is usually secondary to the vasculitis that is part of the collagen vascular diseases. Occasionally, damage to the pancreas may also be caused by the medication for the treatment of these disorders.

Acute pancreatitis is a complication of *lupus erythematosus* in <5% of the patients. While it is only rarely the presenting symptom, 44% of patients develop pancreatitis within the first year of the diagnosis. The mortality rate of acute lupus pancreatitis is 27%. Only a few case reports of chronic pancreatitis associated with lupus erythematosus have been published. Bleeding from a ruptured pseudoaneurysm related to lupus erythematosus pancreatitis has been documented.

An autopsy study of patients with *rheumatoid arthritis* revealed that morphological features of

Table 7.9 Vasculitides affecting the pancreas (adapted from [46])

Affected vessel	Disease	Histological features	Clinical features	Pancreatic involvement
Large arteries	Takayasu's arteritis	Granulomatous inflammation	Patient age < 50 years, predominantly women	Rare Acute pancreatitis, if involvement of descending aorta (10% of patients)
	Giant cell arteritis		Patient age > 50 years	
Small and medium-sized arteries	Polyarteritis nodosa	Focal or segmental, transmural necrotizing vasculitis, preferentially at arterial branching points	Adults Usually systemic; can rarely be limited to the gallbladder and/or pancreas	In up to 25% of patients Acute pancreatitis or pancreatic mass [47]
	Wegener's granulomatosis	Granulomatous inflammation	Lung and kidney involvement c-ANCA positivity	Exceedingly rare Pancreatitis or pancreatic mass [48]
	Eosinophilic granulomatosis with polyangiitis-like necrotising vasculitis (Churg-Strauss syndrome)	Granulomatous and necrotizing inflammation; eosinophils	Asthmatic patients c-ANCA positivity	Rare Pancreatitis
	Thrombangiitis obliterans (Buerger's disease)	Segmental acute and chronic inflammation with thrombosis and vaso-occlusion	Young smokers	Rare Acute pancreatitis and pancreatic infarction if involvement of celiac trunk [49]
	Kawasaki's disease	Mononuclear infiltration of blood vessels and other organs, including pancreas	Infants and young children Ex-/enanthema, fever, lymphadenopathy, polyarteritis Most serious complication: coronary arteriitis	Rare Acute pancreatitis, diabetes mellitus
	Behçet's syndrome	Lymphocytic arteritis/phlebitis with occasional fibrinoid necrosis	Classical triad: oral and genital ulcers, uveitis	Rare Acute pancreatitis
Small vessels	Microscopic polyangiitis	Necrotising leukocytoclastic vasculitis	Lung, kidney, gastrointestinal involvement p-ANCA positivity	Rare Acute pancreatitis or pancreatic mass [50]
	Henoch-Schönlein purpura	Immune complex vasculitis, leukocytoclastic with possible transition into lymphoplasmacytic vasculitis	Mainly children >60% gastrointestinal involvement; usually self-limiting	Rare Acute pancreatitis [51]
	Cryoglobulinemia		Possible association with hepatitis C virus infection	Rare Acute pancreatitis [52]

multifocal vasculogenic pancreatitis were often found in patients without clinically apparent acute pancreatitis. These relatively subtle morphological changes are thought to be responsible for unexplained recurrent abdominal symptoms and spontaneous remissions, which over time may compromise the metabolic function of the gland [53]. Blood vessels of all calibers can be affected by vasculitis in the context of rheumatoid arthritis, and the inflammatory changes of the vessels may range from acute to chronic. Depending on the extent of the vasculitis and the size of the vessels that are affected, changes to the pancreas can vary from necrosis with acute inflammation to regressive changes. AA amyloid deposition in both vasculature and pancreatic parenchyma of patients with rheumatoid arthritis has been suggested as an aggravating factor, resulting in a high risk of mortality of associated acute pancreatitis [54].

Pancreatic involvement is possibly not so uncommon in *Sjögren's syndrome*, although it often remains clinically silent, while acute pancreatitis and pancreatic insufficiency are rare.

7.3.5 Sarcoidosis

Sarcoidosis is a chronic multiorgan granulomatous disease of unknown etiology. Involvement of the pancreas is rare and often asymptomatic. At autopsy, pancreatic involvement is discovered in 1–3% of patients with systemic sarcoidosis [55]. There are only a small number of case reports on symptomatic pancreatic sarcoidosis. Patients present mainly with abdominal pain, weight loss, and obstructive jaundice, while a clinical picture of acute pancreatitis is rare. In some cases, sarcoidosis may present as a carcinoma-mimicking circumscribed mass (Fig. 7.88) [56]. Histology reveals the characteristic features of sarcoidosis, i.e., noncaseating epithelioid granulomas with Langerhans histiocytic giant cells and fibrosis.

7.4 Pancreatitis in Children

Over the past two decades, knowledge about pediatric pancreatitis has significantly increased. Acute pancreatitis is almost as common in children as it is in adults, but it has a lower complication and mortality rate. Etiologies and risk factors are strikingly different and more varied in the pediatric compared to the adult patient groups with acute, recurrent acute, and chronic pancreatitis. In over 20% of the pediatric cases, pancreatitis results from more than one contributing factor [57].

Genetic causes account for less than 10% of children with acute pancreatitis, but for more than 50% and around 75% of cases with recurrent acute pancreatitis and chronic pancreatitis, respectively (see Chap. 6, Sect. 6.3). Up to 20% of children with acute pancreatitis have anomalies of the pancreas, most commonly pancreas divisum (see Chap. 13, Sect. 13.1). Children with recurrent acute or chronic pancreatitis have a higher frequency of pancreas divisum than the general population, and many of these patients have additional risk factors, in particular genetic mutations. Gallstones and sludge are currently the most common cause of acute pancreatitis in children, representing 30% of all cases. In up to 25% of children with acute pancreatitis, medication is the underlying cause, the most common drugs being antiepileptics (in particular valproic acid), the cancer drug asparaginase, and immunomodulators (e.g., thiopurines and corticosteroids). In a considerable proportion of children with medication-associated pancreatitis, additional risk factors are present, and recently, HLA subtypes (DQA1, DRB1) were found to confer susceptibility to thiopurine pancreatitis.

A large and varied group of less common, additional risk factors also needs to be considered: abdominal trauma, metabolic disorders (e.g., diabetic ketoacidosis, hypertriglyceridemia, hypercalcemia), infections (e.g., mumps, herpes, hepatitis, influenza viruses), and systemic diseases (e.g., hemolytic uremic syndrome, Henoch-Schönlein purpura, Kawasaki disease, inflammatory bowel disease).

Autoimmune pancreatitis can affect children, but published reports are scarce. Clinical presentation and histological changes are predominantly akin type 2, while classical type 1 with elevated IgG4 in serum and tissues and IgG4-related systemic disease is only rarely diag-

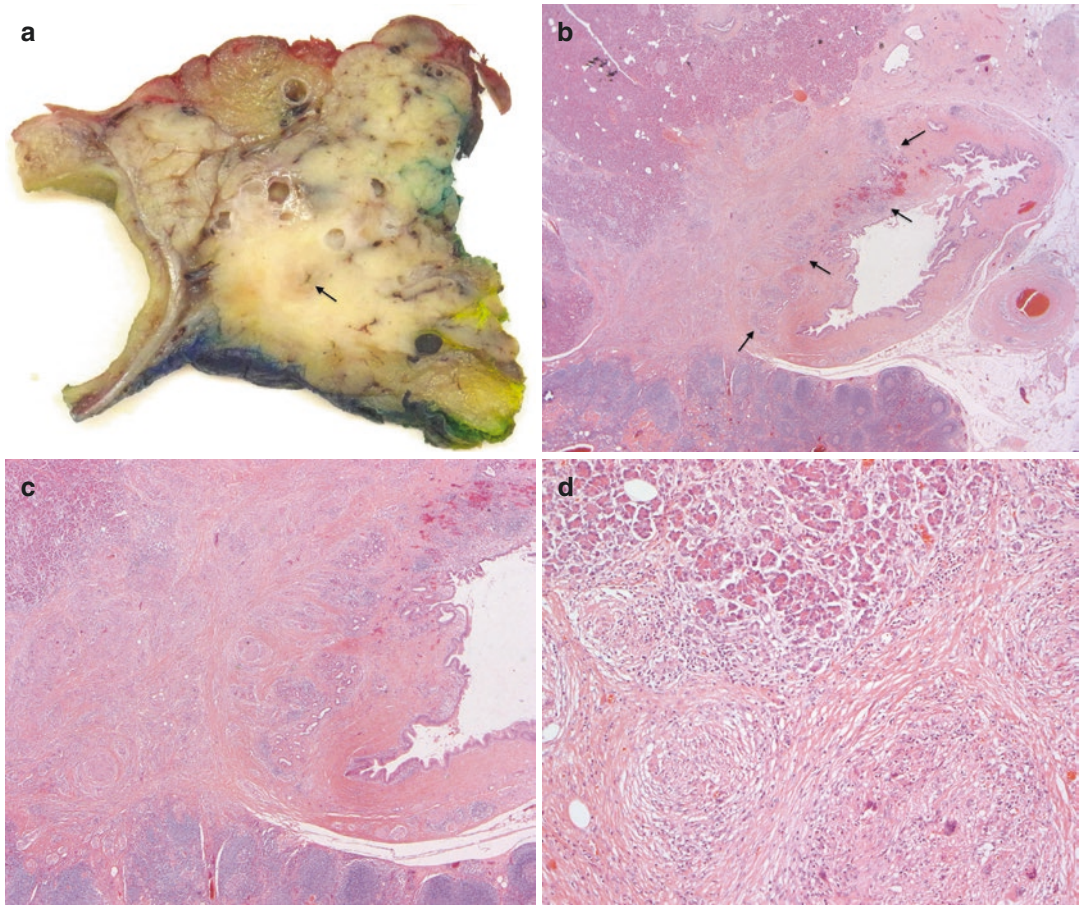

Fig. 7.88 Sarcoidosis of the pancreas: tumefactive involvement of the pancreas by sarcoidosis resulted in obstruction of the intrapancreatic common bile duct (*arrow*) and raised the preoperative suspicion of bile duct cancer (**a**). Microscopic examination reveals the inflammatory nature of the mass-forming lesion, with involvement of the common bile duct (*arrows*) and adjacent pancreatic parenchyma (**b**). At higher magnification, numerous, partially confluent, noncaseating, epithelioid granulomas and scattered multinucleated giant cells can be seen (**c**, **d**)

nosed in childhood. In some children, disease presentation does not fall into either category. Up to 30% of children have concurrent immune or inflammatory disease, in particular ulcerative colitis [58].

7.5 Reporting Checklist

The key items to be considered when reporting on the macroscopic and microscopic findings in chronic pancreatitis are listed in Table 7.10.

Table 7.10 Reporting checklist for chronic pancreatitis

Macroscopic assessment
• Specimen type (e.g., pancreatoduodenectomy, distal/total pancreatectomy, following Frey/Beger/Puestow procedure)
• Distribution of changes: – Diffuse – Segmental or focal: localization and size
• Pancreatic ducts: – Dilatation/stricture – Stones
• Cystic lesions? – Number, size, localization – Wall, content
• Cause of duct obstruction (tumor, stones, lesion at ampulla/papilla)?
• Suspicion of carcinoma?
Microscopic assessment
• Extent and degree of: – Acinar atrophy – Fibrosis – Inflammation
• Pancreatic ducts: – Dilatation/stricture – Rupture/periductal inflammation – Content – Epithelial changes: PanIN, IPMN, other
• Features specific of autoimmune pancreatitis? – Periductal inflammation/GEL – Storiform fibrosis – Obliterative phlebitis – Increased IgG4$^+$ plasma cells
• Features specific of paraduodenal pancreatitis? – (Pseudo-)cysts within pancreatoduodenal groove – Ectopic pancreatic tissue within duodenal wall/pancreatoduodenal groove
• Evidence of infectious etiology?
• Vasculitis, granulomas, eosinophilia?
• Evidence of malignancy?

Abbreviations: *GEL* granulocytic epithelial lesion, *IPMN* intraductal papillary mucinous neoplasia, *PanIN* pancreatic intraepithelial neoplasia

References

1. Whitcomb DC, Shimosegawa T, Chari ST, Forsmark CE, Frulloni L, Pramod G, et al. International consensus statements on early chronic pancreatitis: recommendation from the working group for the international consensus guidelines for chronic pancreatitis in collaboration with the International Association of Pancreatology, American Pancreatic Association, Japan Pancreas Society, PancreasFest Working Group and European Pancreatic Club. Pancreatology. 2018; S1424-3903(18)30113-3. https://doi.org/10.1016/j.panc.2018.05.008. [Epub ahead of print].
2. Andrén-Sandberg Å. Chapter 7. Classification of pancreatitis. In: Löhr M, Andrén-Sandberg Å, editors. Pancreatitis – diagnosis and therapy. Bremen; London; Boston: Uni-Med Verlag AG; 2011. p. 73–81.
3. Löhr JM, Dominguez-Munoz E, Rosendahl J, Besselink M, Mayerle J, Lerch MM, et al. United European Gastroenterology evidence-based guidelines for the diagnosis and therapy of chronic pancreatitis (HaPanEU). UEG J. 2017;5:153–99.
4. Sharma S, Green KB. The pancreatic duct and its arteriovenous relationship. An underutilized aid in the diagnosis and distinction of pancreatic adenocarcinoma from pancreatic intraepithelial neoplasia. A study of 126 pancreatectomy specimens. Am J Surg Pathol. 2004;28:613–20.
5. Wachtel MS, Miller EJ. Focal changes of chronic pancreatitis and duct-arteriovenous relationships. Avoiding a diagnostic pitfall. Am J Surg Pathol. 2005;29:1521–3.
6. Esposito I, Hruban R, Verbeke C, Terris B, Zamboni G, Scarpa A, et al. International consensus guidelines on the histopathology of chronic pancreatitis. Recommendations from the working group for the international consensus guidelines for chronic pancreatitis in collaboration with the International Association of Pancreatology, the American Pancreatic Association, the Japan Pancreas Society, and European Pancreatic Club. Pancreatology. 2020;20:586–93.
7. Löhr J-M, Beuer U, Vujasinovic M, Alvaro D, Frøkjær JB, Buttgereit F, et al. European guideline on IgG4-related digestive disease - UEG and SGF evidence-based recommendations. United European Gastroenterol J. 2020;8:637–66.
8. Raghuwansh PS, Chari ST. Autoimmune pancreatitis: an update on classification, diagnosis, natural history and management. Curr Gastroenterol Rep. 2012;14:95–105.
9. Wallace ZS, Mattoo H, Carruthers M, Mahajan VS, Della Torre E, Lee H, et al. Plasmablasts as a biomarker for IgG4-related disease, independent of serum IgG4 concentrations. Ann Rheum Dis. 2015;74:190–5.
10. Chari ST, Klöppel G, Zhang L, Notohara K, Lerch MM, Shimosegawa T, the Autoimmune Pancreatitis International Cooperative Study Group (APICS). Histopathologic and clinical subtypes of autoimmune pancreatitis: the Honolulu consensus document. Pancreas. 2010;39:549–54.
11. Shimosegawa T, Chari ST, Frulloni L, Kamisawa T, Kawa S, Mino-Kenudson M, et al. International consensus diagnostic criteria for autoimmune pancreatitis. Guidelines of the International Association of Pancreatology. Pancreas. 2011;40:352–8.
12. Zhang L, Chari S, Smyrk TC, Deshpande V, Klöppel G, Kojima M, et al. Autoimmune pancreatitis (AIP) type 1 and type 2. An international consensus study

on histopathological diagnostic criteria. Pancreas. 2011;40:1172–9.
13. Deshpande V, Zen Y, Chan JKC, Yi EE, Sato Y, Yoshino T, et al. Consensus statement on the pathology of IgG4-related disease. Mod Pathol. 2012;25:1181–92.
14. Kamisawa T, Zen Y, Pillai S, Stone JH. IgG4-related disease. Lancet. 2015;385:1460–71.
15. Maryama M, Arakura N, Ozaki Y, Watanabe T, Ito T, Yoneda S, et al. Type 1 autoimmune pancreatitis can transform into chronic pancreatitis: a long-term follow-up study of 73 Japanese patients. Int J Rheumatol. 2013;2013:272595.
16. Arora K, Rivera M, Ting DT, Deshpande V. The histological diagnosis of IgG4-related disease on small biopsies: challenges and pitfalls. Histopathology. 2019;74:688–98.
17. Strehl JD, Hartmann A, Agaimy A. Numerous IgG4-positive plasma cells are ubiquitous in diverse localised non-specific chronic inflammatory conditions and need to be distinguished from IgG4-related systemic disorders. J Clin Pathol. 2011;64:237–43.
18. Yamashita H, Naitoh I, Nakazawa T, Hayashi K, Miyabe K, Shimizu S, et al. A comparison of the diagnostic efficacy of type 1 autoimmune pancreatitis based on biopsy specimens from various organs. Pancreatology. 2014;14:186–92.
19. Moon S-H, Kim M-H, Park DH, Song TJ, Eum J, Lee SS, Seo DW, Lee SK. IgG4 immunostaining of duodenal papillary biopsy specimens may be useful for supporting a diagnosis of autoimmune pancreatitis. Gastrointest Endosc. 2010;71:960–6.
20. Dhall D, Suriawinata AA, Tang LH, Shia J, Klimstra DS. Use of immunohistochemistry for IgG4 in the distinction of autoimmune pancreatitis from peritumoral pancreatitis. Hum Pathol. 2010;41:643–52.
21. Chougule A, Bal A. IgG4-related inflammatory pseudotumor: a systematic review of histopathological features of reported cases. Mod Rheumatol. 2017;27:320–5.
22. Yamamoto H, Yamaguchi H, Aishima S, Oda Y, Kohashi K, Oshiro Y, Tsuneyoshi M. Inflammatory myofibroblastic tumor versus IgG4-related sclerosing disease and inflammatory pseudotumor: a comparative clinicopathologic study. Am J Surg Pathol. 2009;33:1330–40.
23. Mizukami H, Yajima N, Wada R, Matsumoto K, Kojima M, Klöppel G, Yagihashi S. Pancreatic malignant fibrous histiocytoma, inflammatory myofibroblastic tumor, and inflammatory pseudotumor related to autoimmune pancreatitis: characterization and differential diagnosis. Virchows Arch. 2006;448:552–60.
24. Tracht J, Reid MD, Tue Y, Madrigal E, Sarmiento JM, Kooby D, Alese OB, Krasinskas AM. Rosai-Dorfman disease of the pancreas shows significant histologic overlap with IgG4-related disease. Am J Surg Pathol. 2019;43:1536–46.
25. Ferry J. IgG4-related lymphadenopathy and IgG4-related lymphoma: moving targets. Diagn Histopathol. 2013;19:128–39.
26. Bledsoe JR, Wallace ZS, Deshpande V, Richter JS, Klapman J, Cowan A, et al. Atypical IgG4+ plasmacytic proliferations and lymphomas. Characterization of 11 cases. Am J Clin Pathol. 2017;148:215–34.
27. Detlefsen S, Drewes AM, Vyberg M, Klöppel G. Diagnosis of autoimmune pancreatitis by core needle biopsy: application of six microscopic criteria. Virchows Arch. 2009;454:531–9.
28. Kanno A, Masamune A, Fujishima F, Iwashita T, Kodama Y, Katanuma A, et al. Diagnosis of autoimmune pancreatitis by EUS-guided FNA using a 22-gauge needle: a prospective multicenter study. Gastrointest Endosc. 2016;84:797–804.
29. Bateman AC, Culver EL. IgG4-related disease - experience of 100 consecutive cases from a specialist centre. Histopathology. 2017;70:798–813.
30. Gupta R, Neyaz A, Chougule A, Akita M, Zen Y, Forcione D, et al. Autoimmune pancreatitis type 2. Diagnostic utility of PD-L1 immunohistochemistry. Am J Surg Pathol. 2019;43:898–906.
31. Friedlander J, Quiros JA, Morgan T, Zhang Z, Tian W, Kehr E, Shackleton DV, Zigman A, Stenzel P. Diagnosis of autoimmune pancreatitis vs neoplasms in children with pancreatic mass and biliary obstruction. Clin Gastroenterol Hepatol. 2012;10:1051–5.
32. Dickerson LD, Farooq A, Bano F, Kleeff J, Baron R, Raraty M, et al. Differentiation of autoimmune pancreatitis from pancreatic cancer remains challenging. World J Surg. 2019;43:1604–11.
33. Li PH, Ko KL, Ho CT, Lau LL, Tsang RK, Cheung TT, Leung WK, Lau CS. Immunoglobulin G4-related disease in Hong Kong: clinical features, treatment practices, and its association with multi system disease. Hong Kong Med J. 2017;23:446–53.
34. Miyabe K, Zen Y, Cornell LD, Rajagopalan G, Chowdhary VR, Roberts LR, Chari ST. Gastrointestinal and extra-intestinal manifestations of IgG4-related disease. Gastroenterology. 2018;155:990–1003.
35. Wick MR, O'Malley DP. Lymphadenopathy associated with IgG4-related disease: diagnosis & differential diagnosis. Sem Diagn Pathol. 2018;35:61–6.
36. Zhang L, Smyrk TC. Autoimmune pancreatitis and IgG4-related systemic diseases. Int J Clin Exp Pathol. 2010;3:491–504.
37. Abraham SC, Leach S, Yeo CJ, Cameron JL, Murakata LA, Boitnott JK, Albores-Saavedra JL, Hruban RH. Eosinophilic pancreatitis and increased eosinophils in the pancreas. Am J Surg Pathol. 2003;27:334–42.
38. Reppucci J, Chang M, Hughes S, Liu X. Eosinophilic pancreatitis: a rare cause of recurrent acute pancreatitis. Case Rep Gastroenterol. 2017;11:120–6.
39. George ER, Patel SS, Sen P, Sule N. A unique case of eosinophilic pancreatitis and anencephaly in the fetus of a type I diabetic mother. Gastroenterol Res. 2011;4:174–6.
40. Ryota H, Ishida M, Satoi S, Yanagimoto H, Yamamoto T, Kosaka H, et al. Clinicopathological and immuno-

logical features of follicular pancreatitis - a distinct disease entity characterised by Th17 activation. Histopathology. 2019;74:709–17.
41. Fujita T, Kojima M, Kato Y, Gotohda N, Takahashi S, Konishi M, Kinoshita T. Clinical and histopathological study of "follicular cholangitis". Sclerosing cholangitis with prominent lymphocytic infiltration masquerading as hilar cholangiocarcinoma. Hepatol Res. 2010;40:1239–47.
42. Zen Y, Ishikawa A, Ogiso S, Heaton N, Portmann B. Follicular cholangitis and pancreatitis – clinicopathological features and differential diagnosis of an under-recognized entity. Histopathology. 2012;60:261–9.
43. Zuk RJ, Neal JW, Baithun SI. Malakoplakia of the pancreas. Virchows Arch Pathol Anat. 1990;417:181–4.
44. Nuciforo PG, Moneghini L, Braidotti P, Castoldi L, De Rai P, Bosari S. Malakoplakia of the pancreas with diffuse lymph-node involvement. Virchows Arch. 2003;442:82–5.
45. Kulatunga A, Kyllönen AP, Dammert K. Malakoplakia of the pancreas. A case report. Acta Pathol Microbiol Immunol Scand A. 1987;95:127–9.
46. Mitchell KA, West AB. Chapter 10. Vascular disorders of the gastrointestinal tract. In: Odze RD, Goldblum JR, editors. Surgical pathology of the GI tract, liver, biliary tract, and pancreas. 3rd ed. Philadelphia: Saunders; 2015. p. 215–55.
47. Yokoi Y, Nakamura I, Kaneko T, Sawayanagi T, Watahiki Y, Kuroda M. Pancreatic mass as an initial manifestation of polyarteritis nodosa: a case report and review of the literature. World J Gastroenterol. 2015;21:1014–9.
48. Kontis E, Paplexopoulou N, Zen Y, Prachalias AA. Isolated primary pancreatic Wegener's granulomatosis: report of two cases. J Pancreas (Online). 2014;15:403–6.
49. Sobel RA, Ruebner BH. Buerger's disease involving the celiac artery. Hum Pathol. 1979;10:112–5.
50. Iida T, Adachi T, Tabeya T, Nakagaki S, Yabana T, Goto A, et al. Rare type of pancreatitis as the first presentation of anti-neutrophil cytoplasmic antibody-related vasculitis. World J Gastroenterol. 2016;22:2383–90.
51. Helbling R, Lava RAG, Simonetti GD, Camozzi P, Bianchetti MG, Milani GP. Gallbladder and pancreas in Henoch-Schönlein purpura: review of the literature. J Pediatr Gastroenterol Nutr. 2016;62:457–61.
52. Tada M, Naruse S, Arai A, Sato A, Tanaka K, Piao YS, et al. An autopsy case of systemic vasculitis associated with hepatitis C virus-related mixed cryoglobulinemia presenting severe peripheral neuropathy. Rinsho Shinkeigaku. 2004;44:686–90.
53. Bély M, Apáthy Á. Recurrent pancreatic arteritis and vasculogenic relapsing pancreatitis in rheumatoid arthritis – a retrospective clinicopathologic and immunohistochemical study of 161 autopsy patients. Pathol Oncol Res. 2008;14:473–80.
54. Kuroda T, Sato H, Hasegawa H, Wada Y, Murakami S, Saeki T, Nakano M, Narita I. Fatal acute pancreatitis associated with reactive AA amyloidosis in rheumatoid arthritis with end-stage renal disease: a report of three cases. Intern Med. 2011;50:739–44.
55. Iwai K, Tachibana T, Hosoda Y, Matsui Y. Sarcoidosis autopsies in Japan. Frequency and trend in the last 28 years. Sarcoidosis. 1988;5:60–5.
56. Caceres M, Sabbaghian MS, Braud R, Wilks S, Boyle M. Pancreatic sarcoidosis: unusual presentation resembling a periampullary malignancy. Curr Surg. 2006;63:179–85.
57. Uc A, Husain SZ. Pancreatitis in children. Gastroenterology. 2019;156:1969–78.
58. Scheers I, Palermo JJ, Freedman S, Wilschanski M, Shas U, Abu-El-Haija M, et al. Autoimmune pancreatitis in children: characteristic features, diagnosis, and management. Am J Gastroenterol. 2017;112:1604–11.

Pancreatic Intraepithelial Neoplasia

8

The pancreatic intraepithelial neoplasia (PanIN) nomenclature and classification system, used to describe the microscopic epithelial precursor lesions of pancreatic ductal adenocarcinoma, was first proposed in 1994 [1], modified in 1999 [2], and further refined in 2004 [3]. This PanIN nomenclature replaced at least 70 different diagnostic terms for the same entities [3]. Such previous descriptive terms included mucinous hyperplasia, mucinous cell hypertrophy, papillary hyperplasia, mucinous metaplasia, atypical hyperplasia, and dysplasia.

It is now well recognized that the morphological progression of PanIN to invasive ductal adenocarcinoma mirrors the molecular progression, which is often referred to as the 'PanINgram' [4]. The average time taken for genetic progression from an initiating mutation in a normal ductal epithelial cell, through PanIN, to invasive ductal adenocarcinoma has been estimated to be 11.7 years (see Chap. 9, Sect. 9.13) [5]. However, most low-grade PanINs never progress to invasive carcinoma. A recent study has suggested that PanIN may seed along the ductal system [6].

PanIN is one of the three main precursors of pancreatic invasive adenocarcinoma. The two other precursors are mucinous cystic neoplasm (see Chap. 16) and intraductal papillary neoplasm (see Chap. 17). These are both macroscopic lesions, in contrast to the microscopic nature of PanIN.

PanINs may arise in any part of the pancreatic duct system, including the main pancreatic duct, and until recently were classified into PanIN-1A, PanIN-1B, PanIN-2, and PanIN-3, according to the degree of architectural and cytological atypia [2]. The normal ductal lining of nonmucinous, cuboidal to low-columnar epithelial cells (see Chap. 1, Sect. 1.4.3) is replaced initially by tall columnar mucinous epithelium showing minimal cytological atypia (PanIN-1A). In PanIN-1B, this minimally atypical tall columnar mucinous epithelium is thrown into micropapillae or papillae. PanIN-2 is characterized by increasing cytological atypia, and in PanIN-3 there is a more complex architecture and severe cytological atypia. More than one type of PanIN may be seen in a single duct. Although PanIN-1 may show an abrupt transition with normal ductal epithelium (Fig. 8.1), this does not occur with high-grade PanIN.

Following a consensus meeting in Baltimore, it was recommended that this three-tiered grading system should be replaced by a two-tiered system [7], with PanIN-1 and PanIN-2 being categorized as low-grade PanIN, and PanIN-3 as high-grade PanIN. This two-tiered system has now been included in the 2019 WHO classification of tumors of the pancreas, where it is also referred to as 'glandular intraepithelial neoplasia, low grade' and 'glandular intraepithelial neoplasia, high grade' [8].

© Springer Nature Switzerland AG 2021
F. Campbell, C. S. Verbeke, *Pathology of the Pancreas*,
https://doi.org/10.1007/978-3-030-49848-1_8

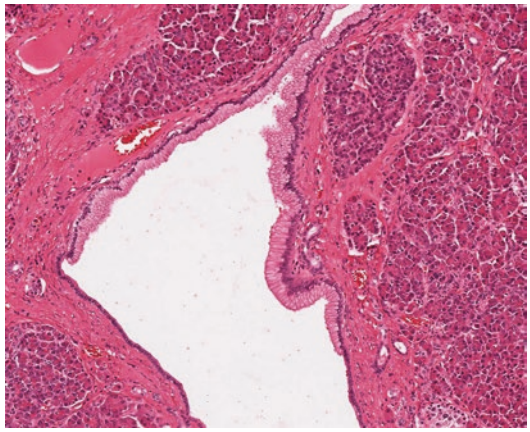

Fig. 8.1 Low-grade PanIN (formerly PanIN-1A): there is abrupt transition between the normal duct epithelium (*bottom*) and this flat lesion lined by tall columnar cells with supranuclear mucin and small round basal nuclei

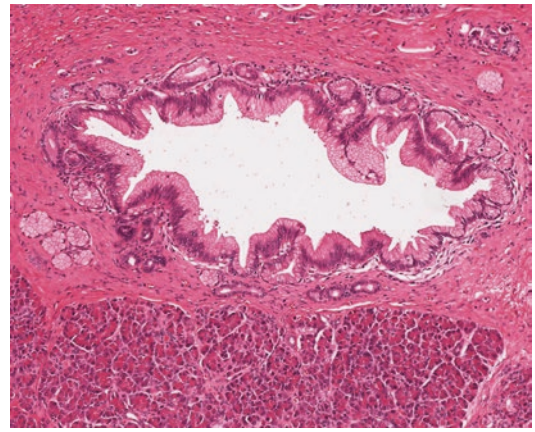

Fig. 8.2 Low-grade PanIN (formerly PanIN-1B): this papillary/micropapillary lesion is lined by tall columnar cells identical to those seen in Fig. 8.1

8.1 WHO Classification

Pancreatic (glandular) intraepithelial neoplasia (low grade and high grade) is included in 'benign epithelial tumors and precursors' in the 2019 WHO classification of tumors of the pancreas [8].

8.2 Classification and Microscopy

8.2.1 Low-grade PanIN (Figs. 8.1–8.3)

These are epithelial lesions composed of tall columnar cells with varying amounts of supranuclear mucin and mild-to-moderate cytological atypia. The epithelium may be flat or have a papillary or micropapillary architecture. The nuclei may be small, uniform, round to oval, and basally located (formerly PanIN-1) or show some nuclear abnormalities, including loss of nuclear polarity, nuclear crowding and pseudostratification, nuclear enlargement, hyperchromatic nuclei, and small nucleoli (formerly PanIN-2). Mitotic figures are rare, but when present are basal and not atypical.

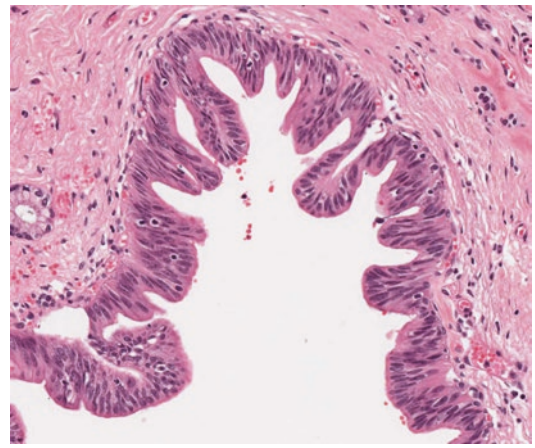

Fig. 8.3 Low-grade PanIN (formerly PanIN-2): this micropapillary lesion is lined by columnar cells that lack intracytoplasmic mucin and show nuclear crowding and pseudostratification with mild-to-moderate nuclear atypia

8.2.2 High-grade PanIN (Fig. 8.4)

This is also known as carcinoma in situ. These epithelial lesions are usually papillary and/or micropapillary, but rarely may be flat. They may show a cribriform architecture, there may be luminal necrosis, and small clusters of epithelial cells may bud off into the lumen. There is significant cytological atypia with loss of nuclear

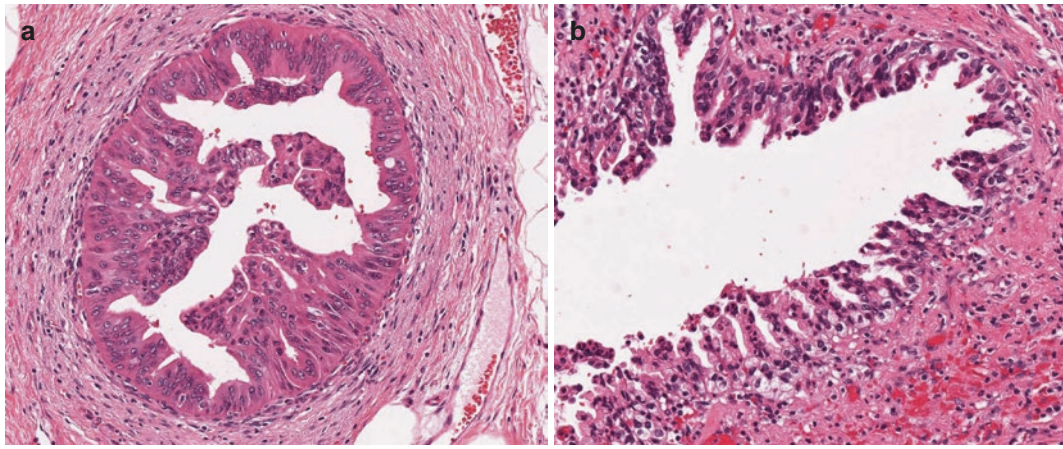

Fig. 8.4 High-grade PanIN (formerly PanIN-3): there is a complex papillary, almost cribriform, architecture with loss of nuclear polarity and marked nuclear pleomorphism with prominent nucleoli (**a**). Single cells and occasional clusters of cells can be seen budding off the numerous micropapillae in this lesion (**b**)

polarity, marked nuclear pleomorphism, and prominent nucleoli. Mitotic figures can be present and may occasionally be abnormal.

8.3 Variants of PanIN

Three variants of PanIN have been described, *intestinal PanIN*, *oncocytic PanIN* [9] and *foamy variant of PanIN* [10]. However, all were described in pancreata with associated invasive adenocarcinoma of the same phenotype, namely intestinal-type adenocarcinoma, oncocytic carcinoma, and foamy gland pattern of adenocarcinoma, respectively (see Chap. 9, Sects. 9.6.2 and 9.8). Therefore, it is possible that some cases may represent cancerization of ducts (see Sect. 8.6.2) and/or (for the intestinal and oncocytic variants) residual intraductal papillary neoplasia (see Sect. 8.6.1 and Chap. 17), rather than PanIN.

In intestinal PanIN, the duct lining shows an intestinal phenotype with pseudostratified tall columnar cells, scattered goblet cells, and elongated cigar-shaped nuclei. In oncocytic PanIN, the small ducts are lined by cuboidal or columnar cells with pale or eosinophilic granular cytoplasm and large vesicular nuclei with prominent nucleoli. The foamy variant of PanIN (Fig. 8.5) differs from conventional PanIN in that involved small ducts may be markedly dilated and the lining cells have abundant foamy cytoplasm, often with small irregular hyperchromatic nuclei. Foamy cells alternate with non-foamy cuboidal or columnar cells in the same duct. On mucin histochemistry (alcian blue, PAS-diastase, or mucicarmine), the foamy cells show band-like staining

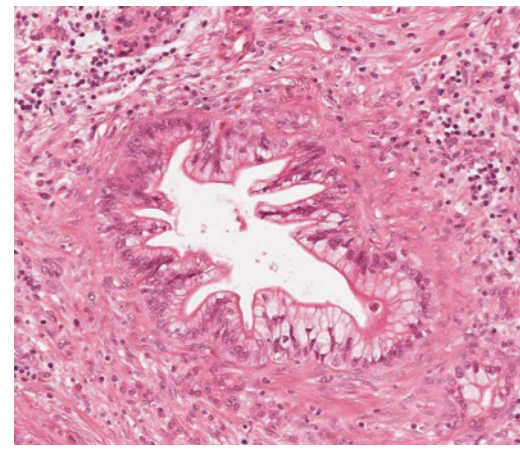

Fig. 8.5 Foamy variant of PanIN: the columnar cells have abundant foamy cytoplasm with luminal cytoplasmic condensation

in the apical cytoplasm, while the rest of the cytoplasm only shows focal staining.

8.4 Associations

Low-grade PanIN may occur in normal pancreas (including heterotopic pancreas) and diseased pancreata. The frequency appears to correlate with age: low-grade PanIN is rare in patients younger than 40 years but increases in frequency after 40 years of age. Low-grade PanIN may be seen in chronic pancreatitis and in the background of pancreata with ductal adenocarcinoma or ampullary neoplasia, as well as less common neoplasms such as mucinous cystic neoplasm, serous cystic neoplasm, solid pseudopapillary neoplasm, pancreatic endocrine neoplasm, and acinar cell carcinoma.

In contrast, high-grade PanIN is very rare in the normal pancreas but may occasionally be seen in (nonhereditary) chronic pancreatitis and in fatty replacement of the pancreas [11]. High-grade PanIN is most commonly described in the background of pancreata with invasive ductal adenocarcinoma. However, this may represent intraductal extension of the invasive carcinoma along the duct (so called cancerization of ducts—see Sect. 8.6.2) and not high-grade PanIN [12]. One study has shown that such duct cancerization can extend for more than 2cm along the ducts [13].

8.4.1 Hereditary Pancreatitis and Familial Pancreatic Cancer

PanINs are frequently found in patients with hereditary pancreatitis (see Chap. 6, Sect. 6.3) and includes both grades of PanIN. They occur at a younger age (median age of 24 years), and their frequency is much higher than in the pancreata of normal subjects at the same age or in patients with alcoholic chronic pancreatitis [14].

PanINs are also more common in patients with familial pancreatic cancer (see Chap. 6, Sect. 6.5) than in patients with sporadic pancreatic cancer [15].

8.5 Lobulocentric Atrophy

Pancreatic parenchyma adjacent to PanINs often shows varying degrees of atrophy and/or fibrosis referred to as lobulocentric atrophy [16]. Lobulocentric atrophy (Fig. 8.6) is characterized by loss of acinar parenchyma in the lobule surrounding the PanIN, acinar to ductal metaplasia, fibrosis, and aggregates of islets (see Chap. 5, Sect. 5.5). It occurs with both grades of PanINs and is seen particularly in elderly patients and in those with a strong family history of pancreatic cancer (see Chap. 6, Sects. 6.4 and 6.5).

8.6 Differential Diagnosis

8.6.1 Intraductal Papillary Mucinous Neoplasm

PanIN lesions are too small to be seen grossly or by imaging techniques. In contrast, intraductal papillary mucinous neoplasms (IPMNs) can be detected clinically and radiologically (see Chap. 17). IPMNs involve the main pancreatic duct and branch ducts, and produce copious amounts of mucin, which may be seen oozing from the ampulla of Vater. In addition, the papillae of IPMN can be grossly visible and are taller and more complex than the papillae of PanIN (Table 8.1).

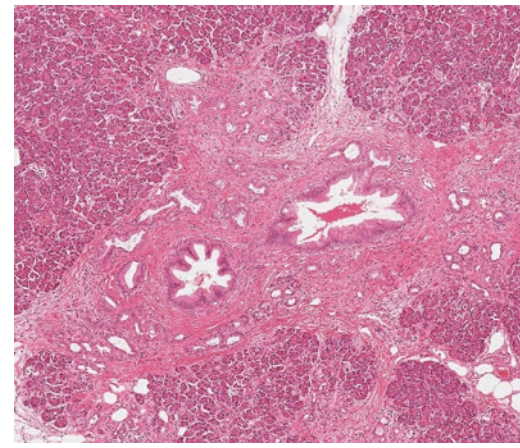

Fig. 8.6 Lobulocentric atrophy associated with low-grade PanIN: there is acinar to ductal metaplasia and fibrosis in the lobule around the PanIN

Table 8.1 Potential criteria for distinguishing pancreatic intraepithelial neoplasia (PanIN) from intraductal papillary mucinous neoplasia (IPMN)

	PanIN	IPMN
Clinically detected	No	Yes
Grossly visible	No	Yes
Mucus oozes from ampulla of Vater	No	Yes
Duct size	Usually <5 mm diameter	Usually >5 mm diameter
Intraluminal mucin	Minimal	Abundant
Growth pattern	Flat or papillae	Predominantly papillary, rarely flat
Papillae	Microscopic	Taller, more complex, and grossly visible
Associated invasive adenocarcinoma	Conventional type	Conventional type or colloid carcinoma

PanIN lesions are defined as involving ducts less than 5 mm in diameter, whereas IPMNs involve the main pancreatic duct or branch ducts and usually produce a lesion greater than 5 mm in diameter. The epithelium in PanIN almost always shows gastric foveolar differentiation. In contrast, the epithelium in IPMN can show gastric, intestinal, or pancreatobiliary differentiation, and the epithelium in intraductal oncocytic papillary neoplasm (IOPN) shows oncocytic differentiation. Therefore, lesions with intestinal or oncocytic differentiation are most likely to be IPMN or IOPN, respectively.

It is worth noting that low-grade PanIN may be found in retention cysts (see Fig. 19.10b and Chap. 19, Sect. 19.3.1), which can mimic gastric-type IPMN, whereas, conversely, IPMNs may extend into the adjacent smaller ducts and mimic PanIN (see Fig. 17.10 and Chap. 17). In retention cysts, there is usually normal ductal epithelium as well as the PanIN in the same cyst, but IPMN can give rise to similar appearances. Moreover, the cause for obstruction and formation of retention cysts is not always apparent. Step-sections can be used to determine whether or not a lesion in a small duct is in continuity with, and shares the same lining epithelium as, a larger lesion that fulfills the criteria for IPMN.

The distinction between a large, low-grade PanIN and a small gastric-type IPMN may not always be possible, both of which can involve branch ducts, share similar morphological features, and have similar mucin profiles. It may be helpful to use the term 'intraductal/intraepithelial neoplasm of low grade, either PanIN or IPMN' in such circumstances (see Chap. 23, Sect. 23.3.2) [17]. However, the distinction between PanIN and gastric-type IPMN appears not to be prognostically significant if the lesion is low grade and has been completely excised.

8.6.2 Cancerization of Ducts

Invasive pancreatic ductal adenocarcinoma and, on occasion, metastatic adenocarcinoma can invade and grow along the lumina of nonneoplastic ducts (see Chap. 9, Sect. 9.10), so called 'cancerization' of ducts [12, 13], and may mimic high-grade PanIN (Fig. 8.7). There is usually a sharp transition between the normal duct epithelium and the cancer, whereas high-grade PanIN usually either involves the whole duct or merges with low-grade PanIN in the same duct. The presence of invasive cancer nearby readily helps establish the diagnosis.

8.6.3 Intravascular Invasion of Pancreatic Ductal Adenocarcinoma

When pancreatic ductal adenocarcinoma invades into vessels it may grow along the luminal surface of the vessel and mimic high-grade PanIN (see Chap. 9, Sect. 9.10 and Figs. 9.35 and 9.36). Elastica van Gieson (EVG) stain may be used to identify the vessel wall, but be aware that the normal pancreatic ductal system also contains elastin fibers in the wall, but not smooth muscle (see Chap. 1, Sect. 1.4.3 and Fig. 1.17). Therefore, when ducts are involved by PanIN (Fig. 8.8), be careful not to mistake this for vascular invasion on EVG stain.

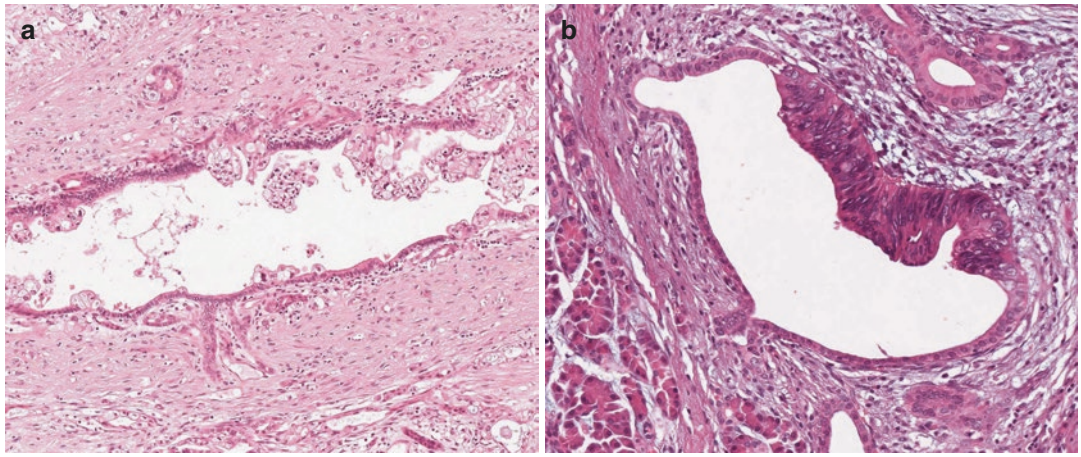

Fig. 8.7 Cancerization of ducts: there is luminal growth along a benign duct by invasive ductal adenocarcinoma (**a**). Duct cancerization may be mistaken for high-grade PanIN (**b**). However, the sharp transition seen here between the highly atypical epithelium and the normal epithelium indicates that this is cancerization

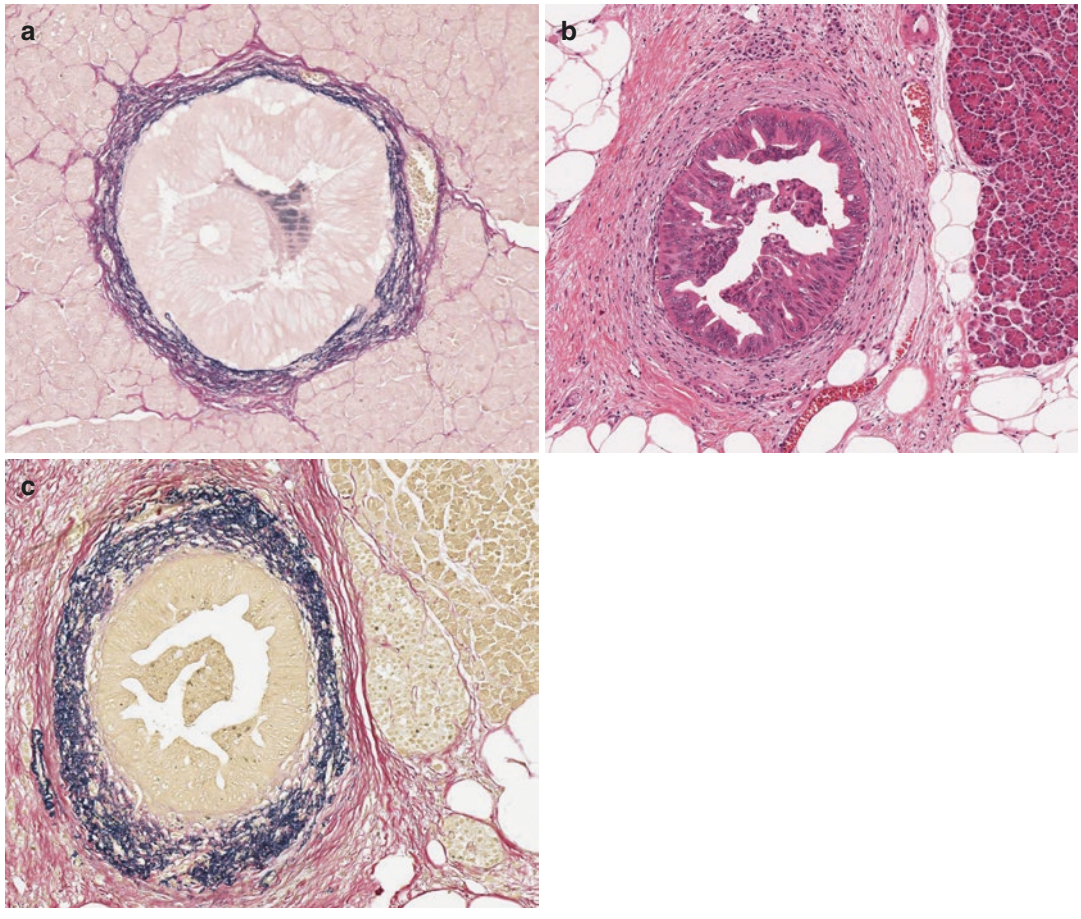

Fig. 8.8 Elastin fibers around PanIN: there are elastin fibers around normal ducts, which may then be involved by low-grade PanIN (**a**). Note the normal acinar tissue around this PanIN. In this example of (**b**) high-grade PanIN (shown at higher power in Fig. 8.4a), the normal periductal elastin fibers (**c**) should not be mistaken for vascular invasion. Elastica van Gieson (EVG) stain

References

1. Klimstra D, Longnecker DS. K-ras mutations in pancreatic ductal proliferative lesions. Am J Pathol. 1994;145:1547–50.
2. Hruban RH, Adsay NV, Albores-Saavedra J, Compton C, Garrett ES, Goodman SN, et al. Pancreatic intraepithelial neoplasia: a new nomenclature and classification system for pancreatic duct lesions. Am J Surg Pathol. 2001;25:579–86.
3. Hruban RH, Takaori K, Klimstra DS, Adsay NV, Albores-Saavedra J, Biankin AV, et al. An illustrated consensus on the classification of pancreatic intraepithelial neoplasia and intraductal papillary mucinous neoplasms. Am J Surg Pathol. 2004;28:977–87.
4. Maitra A, Adsay NV, Argani P, Iacobuzio-Donahue C, De Marzo A, Cameron JL, et al. Multicomponent analysis of the pancreatic adenocarcinoma progression model using a pancreatic intraepithelial neoplasia tissue microarray. Mod Pathol. 2003;16:902–12.
5. Yachida S, Jones S, Bozic I, Antal T, Leary R, Fu B, et al. Distant metastasis occurs late during the genetic evolution of pancreatic cancer. Nature. 2010;467:1114–7.
6. Makohon-Moore AP, Matsukuma K, Zhang M, Reiter JG, Gerold JM, Jiao Y, et al. Precancerous neoplastic cells can move through the pancreatic ductal system. Nature. 2018;561:201–5.
7. Basturk O, Hong SM, Wood LD, Adsay NV, Albores-Saavedra J, Biankin AV, et al. A revised classification system and recommendations from the Baltimore consensus meeting for neoplastic precursor lesions in the pancreas. Am J Surg Pathol. 2015;39:1730–41.
8. Lokuhetty D, White VA, Watanabe R, Cree IA, editors. Digestive system tumours. WHO classification of tumours 5th edition. Lyon: IARC Press; 2019. p. 296.
9. Albores-Saavedra J, Wu J, Crook T, Amirkhan RH, Jones L, Hruban RH. Intestinal and oncocytic variants of pancreatic intraepithelial neoplasia. A morphological and immunohistochemical study. Ann Diagn Pathol. 2005;9:69–76.
10. Albores-Saavedra J, Weimersheimer-Sandoval M, Chable-Montero F. Montante-Montes de Oca D, Hruban RH, Henson DE. The foamy variant of pancreatic intraepithelial neoplasia. Ann Diagn Pathol. 2008;12:252–9.
11. Rebours V, Gaujoux S, d'Assignies G, Sauvanet A, Ruszniewski P, Levy P, et al. Obesity and fatty pancreatic infiltration are risk factors for pancreatic precancerous lesions (PanIN). Clin Cancer Res. 2015;21:3522–8.
12. Hisa T, Suda K, Nobukawa B, Ohkubo H, Shiozawa S, Ishigame H, et al. Distribution of intraductal lesions in small invasive ductal carcinoma of the pancreas. Pancreatology. 2007;7:341–6.
13. Ishii M, Kimura Y, Sugita S, Imamura M, Ito T, Nobuoka T, et al. Surgical and oncological impact of main pancreatic duct spread in invasive ductal adenocarcinoma: a clinicopathological study of 184 resected cases. Pancreatology. 2015;15:681–7.
14. Rebours V, Lévy P, Mosnier JF, Scoazec JY, Soubeyrand MS, Fléjou JF, et al. Pathology analysis reveals that dysplastic pancreatic ductal lesions are frequent in patients with hereditary pancreatitis. Clin Gastroenterol Hepatol. 2010;8:206–12.
15. Shi C, Klein AP, Goggins M, Maitra A, Canto M, Ali S, et al. Increased prevalence of precursor lesions in familial pancreatic cancer patients. Clin Cancer Res. 2009;15:7737–43.
16. Detlefsen S, Sipos B, Feyerabend B, Klöppel G. Pancreatic fibrosis associated with age and ductal papillary hyperplasia. Virchows Arch. 2005;447:800–5.
17. Tanaka M, Castillo F-d, Kamisawa T, Jang JY, Levy P, Ohtsuka T, et al. Revisions of international consensus Fukuoka guidelines for the management of IPMN of the pancreas. Pancreatology. 2017;17:738–53.

Further Reading

Basturk O, Esposito I, Fukushima N, Furukawa T, Hong SM, Klöppel G, et al. Pancreatic intraepithelial neoplasia. In: Lokuhetty D, White VA, Watanabe R, Cree IA, editors. Digestive system tumours. WHO classification of tumours 5th edition. Lyon: IARC Press; 2019. p. 307–9.

Check for updates

Ductal Adenocarcinoma

9

9.1 Definition and Terminology

Ductal adenocarcinoma is a malignant epithelial neoplasm arising in the pancreas, which exhibits glandular differentiation and does not contain a predominant component of another type of neoplasia (see Chap. 20).

The name 'ductal adenocarcinoma' implies that the neoplasm originates from the pancreatic duct system. Although the exact cellular origin is still debated, current data indicate that ductal adenocarcinoma is likely to develop from a cell type in the peripheral ramifications of the duct system. Therefore, topographical association of ductal adenocarcinoma with the main pancreatic duct or large caliber branch ducts is more likely to reflect secondary tumor involvement than the site of cancer origin, except in the context of intraductal papillary neoplasia (see Chap. 17).

Tubular adenocarcinoma, infiltrating duct carcinoma, and duct cell carcinoma are occasionally used as synonyms for ductal adenocarcinoma. The term mucinous adenocarcinoma refers to ductal adenocarcinoma of the pancreas with intracellular or intraluminal mucin production and should not be confounded with colloid carcinoma (syn. mucinous noncystic carcinoma), which is a subtype of ductal adenocarcinoma characterized by large extracellular mucin pools containing suspended neoplastic cells (see Sect. 9.14.2).

In clinical practice, and also throughout this chapter, the term 'pancreatic cancer' is used as a shorthand for ductal adenocarcinoma. The term 'pancreatic head cancer' is ambiguous, as it either indicates ductal adenocarcinoma of the pancreas arising in the pancreatic head or can be used as a more generic term for adenocarcinoma of ampullary, common bile duct, or pancreatic origin.

9.2 Epidemiology

Ductal adenocarcinoma accounts for 85–90% of all pancreatic neoplasms. It is a fairly common cancer, although its incidence varies between different parts of the world. Overall, pancreatic cancer is more common in higher-income than in lower-income countries (age-adjusted incidence rate for both sexes 6.2 versus 1.5 cases per 100,000 person-years), which may reflect a difference in both genuine cancer incidence and pancreatic cancer reporting due to unequal accessibility to advanced medical diagnostics. A further reason for the geographical variation in incidence is the possible existence of racial differences. Epidemiological data show, for instance, that native Hawaiians, Alaskans, and African-Americans are more frequently affected than white Americans, and that the incidence in the Maori population is higher than in the remainder of the population in New Zealand. How far these differences between various population groups can be explained by differences in expo-

© Springer Nature Switzerland AG 2021
F. Campbell, C. S. Verbeke, *Pathology of the Pancreas*,
https://doi.org/10.1007/978-3-030-49848-1_9

sure to etiological factors such as tobacco smoking, is yet to be determined. Studies of migrant populations moving from low- to high-risk regions suggest an important role of environmental exposure, because after 15–20 years the risk of the first generation migrants has increased above the level of the country of origin.

Between the 1950s and the 1980s, the incidence rates of pancreatic cancer rose in high-income countries but leveled off or slightly declined thereafter, particularly in men. In 2007, the highest mortality rates in men were observed in the Baltics, the Nordic, and some Eastern European countries (over 9/100,000), while the lowest rates were recorded in Latin America and Hong Kong [1]. Recent reports indicate an increasing incidence rate in Europe and North America, which may be the result of ageing populations and increasing risk factors, in particular obesity. It has been predicted that by 2030, pancreatic cancer will become the second-leading cause of cancer-related death in the Western world, which is mainly due to the continued improvement of prognosis for cancers in other organs.

Due to its poor prognosis, ductal adenocarcinoma of the pancreas is one of the few cancers for which the incidence nearly equals the mortality rate. It ranks as the 7th leading cause of cancer-related death worldwide but takes up position 4 in the Western world.

Pancreatic cancer affects mainly the middle-aged to elderly, age being an important risk factor. It is rare before the age of 40 and extremely uncommon before age 20. There is only a mild male predilection (male:female ratio: 1.1–1.3:1.0).

9.3 Etiology

Our knowledge of the etiology of pancreatic cancer is limited. However, intense research in recent years, both in the epidemiological and molecular biological fields, has brought to light a number of extrinsic and genetic risk factors, as well as a possible interaction between both.

Hereditary risk factors for ductal adenocarcinoma of the pancreas, believed to play a role in an estimated 10% of patients, are covered in the chapter on hereditary disease (see Chap. 6, Sect. 6.4). In addition to the relatively rare, inherited diseases and syndromes, the ABO blood type has been shown to be related to the risk of pancreatic cancer (lower in individuals with O blood type compared to type A or B).

Only a small number of extrinsic risk factors have been convincingly identified. Tobacco smoking is by far the strongest risk factor, the risk for current smokers compared to never smokers being increased 2- to 3-fold. Heavy (but not mild or moderate) alcohol consumption is a possible, weak etiological factor, which may have genetic and epigenetic effects in addition to potentiating other risk factors such as smoking, poor nutrition, and the inflammatory pathways that are related to chronic pancreatitis. The role of diet-related factors in the development of pancreatic cancer has been studied intensely, but the results are conflicting. Overall, the consumption of red or processed meat, especially when cooked at high temperatures, the intake of N-nitrosamines or nitrates, high intake of (saturated) fats, low consumption of fruits and vegetables, and a low dietary folate intake are associated with an increased risk. Several occupational exposures have also been linked to ductal adenocarcinoma of the pancreas, in particular those connected to industrial areas such as car manufacturing, coal gas industries, hide tanning, and metalworking.

Chronic pancreatitis, particularly if hereditary, is the most important medical condition that is associated with an increased risk of ductal adenocarcinoma (see Chap. 6, Sect. 6.4 and Chap. 7, Sect. 7.2.10). Longstanding diabetes type 2 and obesity, in particular obesity during adolescence, are likely further risk factors, although the associated increase in risk is estimated at only 1.5- to 2-fold. The risk associated with previous cholecystectomy or partial gastrectomy has not been confirmed by all studies.

The link between these established or possible risk factors and the morphologically defined precursor lesions of invasive ductal adenocarcinoma (pancreatic intraepithelial neoplasia, intraductal papillary mucinous neoplasia, mucinous cystic neoplasia) is left largely unexplored, except for familial pancreatic cancer, in which precursor

lesions are the target of screening and surveillance programmes for high-risk individuals (see Chap. 6, Sect. 6.6).

9.4 Clinical Features

Recent studies indicate that—at least in some patients—pancreatic cancer may already have been present for close to a decade before the disease becomes clinically manifest [2]. As the initial clinical symptoms are frequently nonspecific, the diagnosis of pancreatic cancer may be delayed even further. Weight loss and epigastric pain, often radiating towards the back, are the most common symptoms. Some patients may also develop nausea and symptoms of biliary obstruction, that is, pruritus, dark urine, and clay-colored stools. However, in the majority of patients, it is only painless jaundice that will be sufficiently alarming to lead them to seek medical advice. Diabetes mellitus type 2 is a further known clinical manifestation of pancreatic cancer that may precede the cancer diagnosis by 24 months. The sudden onset of this type of diabetes as well as the association with weight loss rather than weight gain differ from the usual type 2 diabetes that is common in the elderly age group and should alert the clinician to the possibility of pancreatic cancer-associated diabetes [3]. Two further clinical signs related to ductal adenocarcinoma usually develop at a later disease stage and only in a proportion of patients: Trousseau syndrome (migratory thrombophlebitis) and the Sister Mary Joseph nodule. The latter refers to a palpable periumbilical nodule, which represents a subcutaneous metastasis of pancreatic cancer. Other, less common presentations include acute pancreatitis, hypoglycemia, hypercalcemia, metastatic carcinoma of unknown origin, and endocarditis.

The clinical presentation depends on the location of the tumor. While painless jaundice is the main presenting sign of cancer arising in the pancreatic head, there is no comparable sign for tumors developing in the body or tail of the pancreas. Consequently, ductal adenocarcinoma in the body or tail often presents at an even more advanced stage than pancreatic head cancer. General symptoms such as weight loss and fatigue, pain, and possibly a palpable tumor mass are the main alarming features for this group of pancreatic cancers.

The mainstay of pancreatic cancer diagnostics nowadays is abdominal imaging, in particular computerized tomography (CT), magnetic resonance imaging (MRI), and endoscopic ultrasound (EUS). Pancreatic ductal adenocarcinoma is usually identified as a hypodense mass that may deform or expand the pancreatic outlines and often involves the peripancreatic soft tissue or other surrounding structures. Dilatation and abrupt cut-off of the main pancreatic duct, common bile duct, or both (the so-called double duct sign) are highly suggestive of cancer of the pancreatic head. The degree of local and regional tumor extension, which is paramount to decisions regarding the resectability of the cancer, can be assessed with the three modalities. EUS offers the additional advantage of fine needle aspiration (FNA) or biopsy (FNB) from the lesion. FNA/FNB is particularly important for the management of patients with unresectable pancreatic cancer, whose cytotoxic treatment usually requires a positive tissue diagnosis (see Chap. 24). Endoscopic retrograde cholangiopancreatography (ERCP) is more invasive and associated with the risk of acute pancreatitis, which makes it less attractive as a first-line diagnostic investigation but may be required for stent insertion to relieve biliary obstruction.

Serum carcinoembryonic antigen (CEA) and CA19.9 have insufficient sensitivity and specificity to be useful as screening markers. However, they are used for follow-up to monitor treatment effect and identify tumor recurrence.

9.5 Macroscopy

Ductal adenocarcinoma of the pancreas usually presents as a poorly circumscribed tumor mass with an ill-defined, highly infiltrative margin (Fig. 9.1), although occasionally, tumors may be more sharply demarcated (Fig. 9.2). It has a characteristic firm, ‘wooden’ consistency. The tumor is most commonly of a pale greyish-white color, and occasionally a yellow-orange tinge may be seen where the cancer infiltrates adipose tissue.

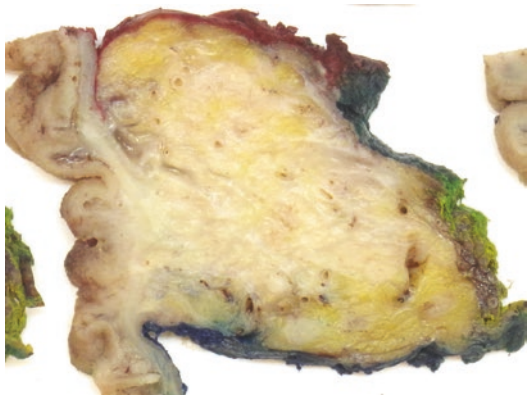

Fig. 9.1 Macroscopy: the tumor consists of pale tissue and is poorly circumscribed

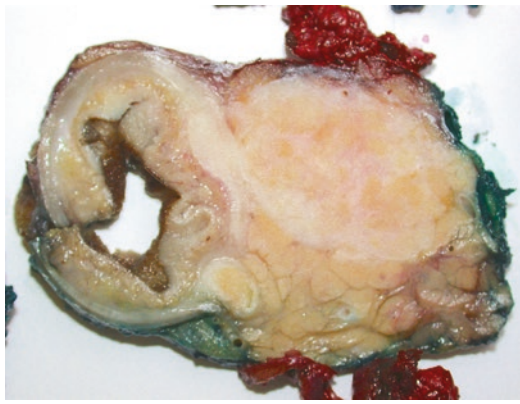

Fig. 9.2 Macroscopy: white tumor tissue is relatively well demarcated from the lobulated, ochre-colored pancreatic parenchyma

The tumor is usually of an irregular spherical shape and can reach a size of up to or over 10 cm. Most commonly, the tumor size ranges between 2 and 4 cm. Ductal adenocarcinomas smaller than 1 cm are highly uncommon, except for those arising in the context of intraductal papillary mucinous neoplasia, mucinous cystic neoplasia, tumors picked up during screening of high-risk patients, or so-called incidentalomas (see Fig. 9.38). Ductal adenocarcinoma of the body and tail is usually larger in size than that arising in the pancreatic head, because obstructive jaundice is a common, earlier presenting sign of the latter (Fig. 9.3). Due to the characteristically ill-defined outlines of ductal adenocarcinoma, the tumor size is often underestimated on naked-eye inspection, and microscopic assessment is required to establish the tumor dimensions and identify the correct tumor stage (see Chap. 3, Sect. 3.3.8).

Fig. 9.3 Macroscopy: a large tumor of the pancreatic body and tail infiltrates the spleen, gastric wall (*arrow*), and colon (*block arrow*). Note the unusual hemorrhagic sponge-like appearance of the tumor where it infiltrates the retroperitoneal soft tissue (same tumor as shown in Figs. 2.6 and 9.63)

Ductal adenocarcinomas are solid tumors. A cystic component due to tumor necrosis may be present. However, in most tumors necrosis is too limited in extent to cause gross cavitation (Fig. 9.4). Smaller cystic areas, measuring up to several millimeters in size, may be seen in subtypes of ductal adenocarcinoma, such as large duct adenocarcinoma or colloid carcinoma (see Sects. 9.8.3 and 9.14.2), in which large tumor glands or mucinous collections, respectively, can reach a macroscopically visible size. Not infrequently associated with pancreatic cancer are small retention cysts, that is, native pancreatic ducts that are cystically dilated due to tumor-related outflow obstruction (see Chap. 19, Sect. 19.3.2). The presence of significant cystic areas in a ductal adenocarcinoma, in particular if containing mucin, should raise the suspicion of underlying mucinous cystic neoplasia or intraductal papillary mucinous neoplasia (see Chaps. 16 and 17).

Hemorrhage is an uncommon finding in pancreatic cancer, with the exception of undifferentiated carcinoma with osteoclast-like giant cells, a subtype of ductal adenocarcinoma, which differs from the typical macroscopic morphology of pancreatic cancer in several aspects (see Sect. 9.14.8).

Ductal adenocarcinoma is commonly associated with marked fibrosis of the surrounding

Fig. 9.4 Cystic degeneration: this ductal adenocarcinoma of the pancreatic body contains multiple irregular cystic areas due to tumor necrosis

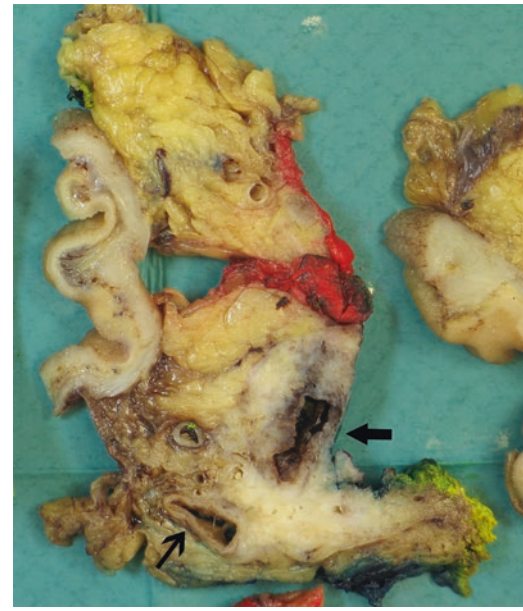

Fig. 9.5 Double duct dilatation: a ductal adenocarcinoma seated in the cranial part of the pancreatic head causes obstruction and prestenotic dilatation of the extrapancreatic common bile duct (*arrow*) and the main pancreatic duct (*block arrow*) close to the pancreatic neck transection margin

pancreas. This phenomenon further obscures the ill-defined invasive tumor front and renders the macroscopic identification of the tumor extent even more difficult. Fibrosis of the pancreas is often associated with a degree of parenchymal atrophy around and upstream from the tumor site, and this characteristic combination of features is often referred to as obstructive pancreatitis or peritumoral pancreatitis (see Chap. 7, Sects. 7.2.4 and 7.2.6.4). Dilatation of the main pancreatic duct due to tumor obstruction is common (Fig. 9.5). Dilatation of the common bile duct, in isolation or in combination with pancreatic duct dilatation is a frequent finding. A metal or plastic stent may be introduced to alleviate the biliary obstruction (see Chap. 3, Sect. 3.3.3).

The vast majority of ductal adenocarcinomas extend beyond the confines of the pancreas and infiltrate surrounding structures such as the duodenal wall, ampulla, common bile duct, peripancreatic soft tissue, and the adjacent large vessels, that is, the superior mesenteric, portal, or splenic vein (Fig. 9.6). Especially when located in the very top (i.e., most cranial) part of the pancreatic head, ductal adenocarcinoma, even of fairly small size, commonly involves multiple neighboring structures, that is, the common bile duct, portal vein, or gastroduodenal artery (Fig. 9.7). Pancreatic cancer developing in the pancreatic body or tail may infiltrate the spleen, stomach, (meso-)colon, small bowel, adrenal gland, Gerota's fascia, perirenal fat, renal hilum, or renal parenchyma (Fig. 9.3). Metastatic deposits in peripancreatic lymph nodes are not uncommonly macroscopically visible (see Fig. 3.17).

Ductal adenocarcinoma of the pancreas is usually a solitary lesion, but multifocal tumors have been reported. Diffuse cancer involvement of the pancreas is exceedingly rare. The majority of pancreatic cancers develop in the pancreatic

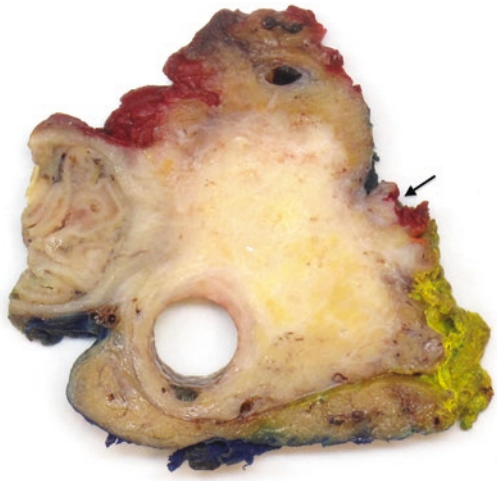

Fig. 9.6 Duodenal invasion: tumor tissue spans the full width of the pancreatic head and infiltrates both the duodenal wall and SMV groove, necessitating a small resection of the SMV (*arrow*)

Fig. 9.7 Invasion of bile duct and portal vein: the tumor is located in the cranial part of the pancreatic head. The invasive front of the tumor shows segmental invasion of the common bile duct (*short arrows*) and focal infiltration of a segment of resected portal vein (*long arrow*)

head (60–70%). As carcinoma in this location is more often resectable than adenocarcinoma arising in the pancreatic body or tail, it is usually overrepresented in surgical series.

Adenocarcinoma in the pancreatic head with macroscopic features as outlined above is not always of pancreatic origin but may have arisen from the ampulla, distal common bile duct, or duodenum. Distinction between these cancers, which are often collectively referred to as 'periampullary cancers', is of paramount significance, and detailed macroscopic assessment of the tumor location, epicenter, and extension is key to correct cancer origin attribution (see Sect. 9.12.3).

9.6 Microscopy

Ductal adenocarcinoma of the pancreas consists of highly infiltrative neoplastic epithelial tumor cells, which show a degree of gland formation and are embedded in a prominent desmoplastic stroma. The tumor glands are distributed haphazardly, irrespective of the lobular architecture of the pancreas and the organized spatial distribution of ducts and muscular blood vessels. This is an important diagnostic feature, which is particularly helpful in distinguishing pancreatic cancer from reactive glandular structures (see Sect. 9.12.1).

9.6.1 Pancreatobiliary Type

The vast majority of ductal adenocarcinomas are of the so-called pancreatobiliary type, which is characterized by the formation of small to medium-sized simple or branched glands (Fig. 9.8). The glands often have irregular and angulated contours and may seem incomplete or

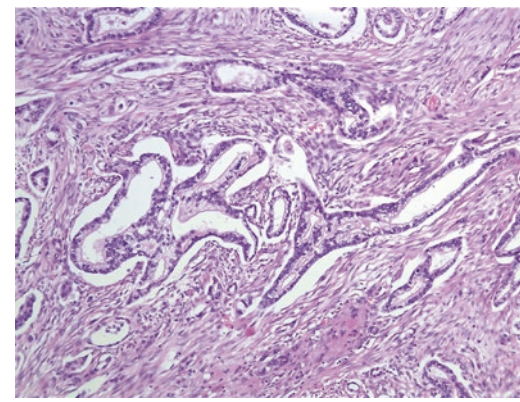

Fig. 9.8 Microscopy: pancreatobiliary type ductal adenocarcinoma typically consists of simple or branching glands, which are lined by columnar epithelium with pale-staining cytoplasm and a roundish basally located nucleus. Note the presence of dense desmoplastic stroma

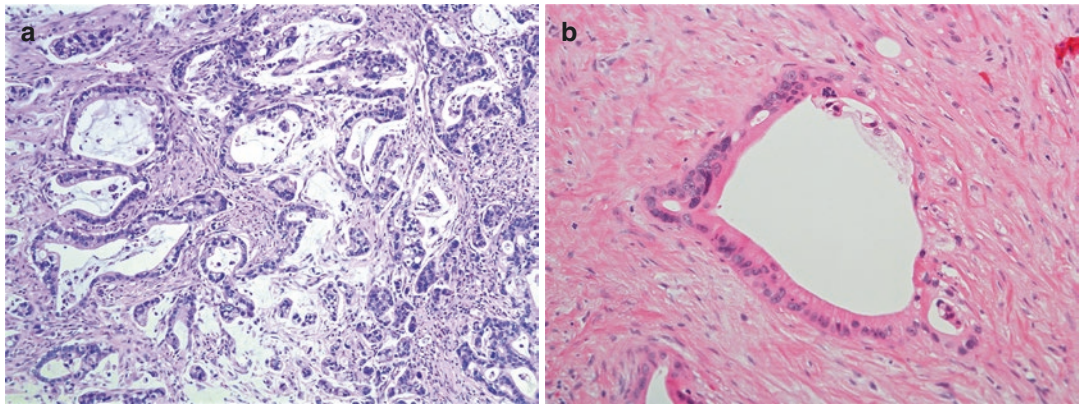

Fig. 9.9 Microscopy: pancreatobiliary type ductal adenocarcinoma consists of irregularly spaced glands, many of which show spillage of mucus into the stroma (so-called ruptured glands) (**a**). This tumor gland has an incomplete appearance, as part of the neoplastic epithelium consists of significantly flattened tumor cells (**b**)

'ruptured', when a part of the glandular wall is composed of highly flattened tumor cells or is focally apparently missing (Fig. 9.9). Complex glandular or cribriform patterns may occasionally be seen as well as intraluminal micropapillary projections (see Fig. 9.17). The lumen of the tumor glands is usually empty, and collections of mucus or cellular detritus admixed with neutrophils—so-called dirty necrosis—are not common. Intracellular mucin production is present to a varying degree, and if prominent, the cytoplasm may be copious. Consequently, the nuclear to cytoplasmic ratio may not always be high. Extracellular mucin, if present, is usually found within the lumina of the tumor glands and confined to a focus or limited area of the tumor, whereas extensive pool-like extracellular mucin collections are considered a feature of a special subtype of ductal adenocarcinoma, the so-called colloid (or mucinous noncystic) carcinoma (see Sect. 9.14.2). The term mucinous adenocarcinoma, which refers to a conventional ductal adenocarcinoma with intracellular and intraluminal mucin, should be avoided, as it may cause confusion with colloid carcinoma or pancreatic cancer arising in a mucinous cystic neoplasm.

The tumor cells are usually cuboidal to low columnar in shape, but irregular to bizarre cell shapes may be observed in poorly differentiated cancers. Nuclear morphology is commonly characterized by enlargement and a varying degree of pleomorphism. As a rule of thumb, a four-fold variation in nuclear size between cells lining the same gland can be regarded as diagnostic of carcinoma. However, the absence of this finding does not exclude carcinoma, because well-differentiated tumors may show markedly uniform, round, and basally orientated nuclei with one or two inconspicuous nucleoli. The cytoplasm may vary in tinctorial quality from pale eosinophilic to slightly basophilic or clear.

Ductal adenocarcinoma is characterized by a highly invasive growth pattern. Infiltration by tumor cell singletons, a single tumor gland, or a small number of tumor cell clusters is commonly present at a considerable distance from the main tumor mass. Tumor glands often extend along interlobular septa deeply into otherwise uninvolved pancreatic parenchyma and intermingle with islets, acini, and nonneoplastic pancreatic ducts (Fig. 9.10). A similar pattern of tumor infiltration may be observed along interlobular septa of the peripancreatic adipose tissue (Fig. 9.11).

The desmoplastic stroma that accompanies ductal adenocarcinoma is nearly as characteristic as the cancer proper. It is composed of fibroblasts, collagen fibers, and a scattering of inflammatory cells, mainly lymphocytes and histiocytes. The tumor stroma can vary from rather cellular with more densely packed tumor glands (Fig. 9.12), to collagen-rich and less cellular. The latter is often present in the tumor periphery,

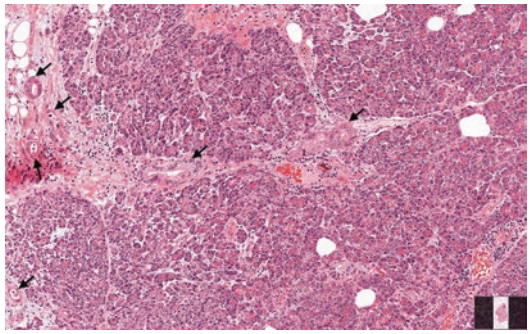

Fig. 9.10 Infiltrative growth: single tumor glands spread along interlobular septa (*arrows*)

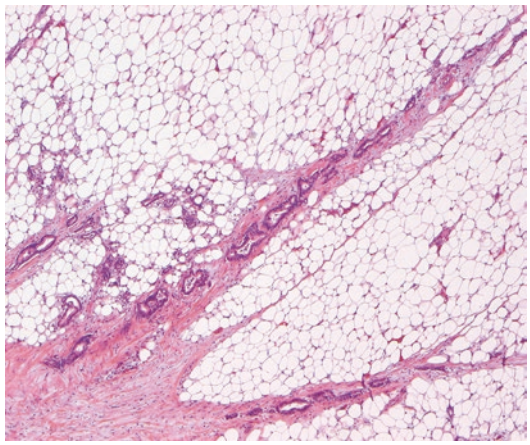

Fig. 9.11 Infiltrative growth: tumor glands spread along septa of the peripancreatic adipose tissue

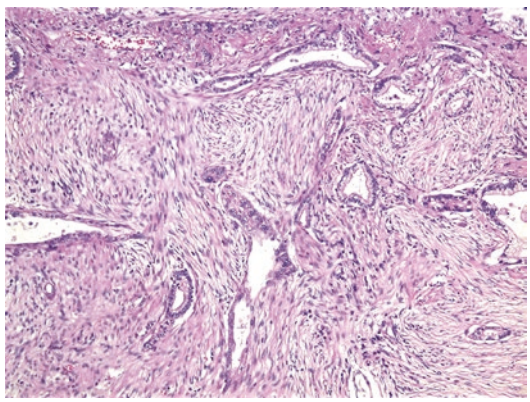

Fig. 9.12 Tumor stroma: branching tumor glands of pancreatobiliary type are embedded in a cellular desmoplastic stroma

where the cancer glands tend to be spaced more widely (Fig. 9.13). Especially at the invasive front, tumor glands may be separated from each

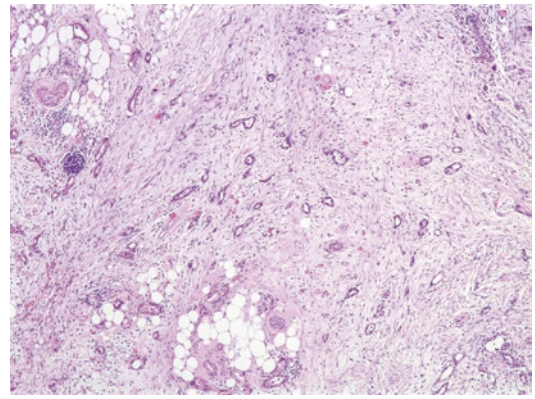

Fig. 9.13 Tumor stroma: tumor glands at the cancer periphery are widely spaced in a vast expanse of desmoplastic stroma, which is collagen-rich and less cellular

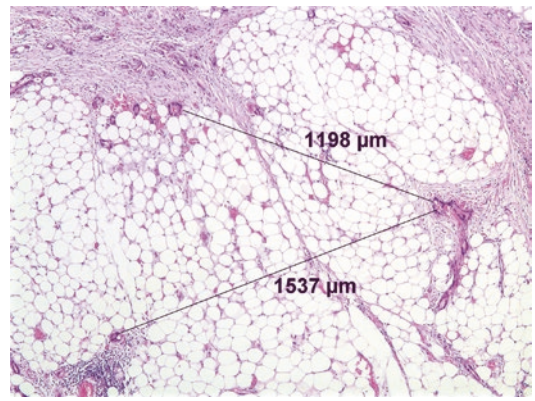

Fig. 9.14 Dispersed growth: infiltrating glands at the tumor periphery grow at a marked distance from each other (exceeding 1.5 mm in this figure)

other by considerable distances—1.5 mm or more—and therefore they can be easily missed on cursory microscopic examination (Fig. 9.14). The desmoplastic reaction extends in a carpet-like fashion along with, and often slightly ahead of, the invasive cancer, entrapping residual acini, islets, and pancreatic ducts along its way. The prominent stromal component of pancreatic cancer accounts for the characteristic macroscopic appearance of the tumor, its grey-white color, and wooden consistency. However, invasive tumor glands are not always accompanied by the desmoplastic stroma. The presence of 'naked' tumor glands, which are often found within pristine peripancreatic adipose tissue without evidence of a stromal reaction, is a well-recognized feature at

the invasive front of ductal adenocarcinoma (Fig. 9.15). Lacking an associated stromal reaction and occurring in small numbers, these naked glands escape macroscopic inspection or radiographical imaging and account amongst other factors for the frequent underestimation of tumor size and extent in pancreatic cancer.

9.6.2 Intestinal Type

Up to 5–10% of ductal adenocarcinomas have been reported to exhibit an intestinal type morphology. As indicated by the name, the morphology of these tumors resembles that of intestinal cancer. Compared to the pancreatobiliary type of ductal adenocarinoma, the glands of the intestinal type are usually larger and well defined. Moderately or poorly differentiated tumors of this type may show a cribriform growth pattern. The glandular lumina can contain 'dirty necrosis', and they are lined by a high-columnar epithelium with cigar-shaped, often pseudo-palisaded nuclei (Fig. 9.16).

While several recent reports claim a more favorable outcome for intestinal type compared to pancreatobiliary type ductal adenocarcinoma, this observation awaits definitive confirmation. For this reason and the fact that the diagnostic criteria lack validation in terms of reproducibility, the intestinal type has not been included in the WHO classification 2019 of pancreatic tumors [4].

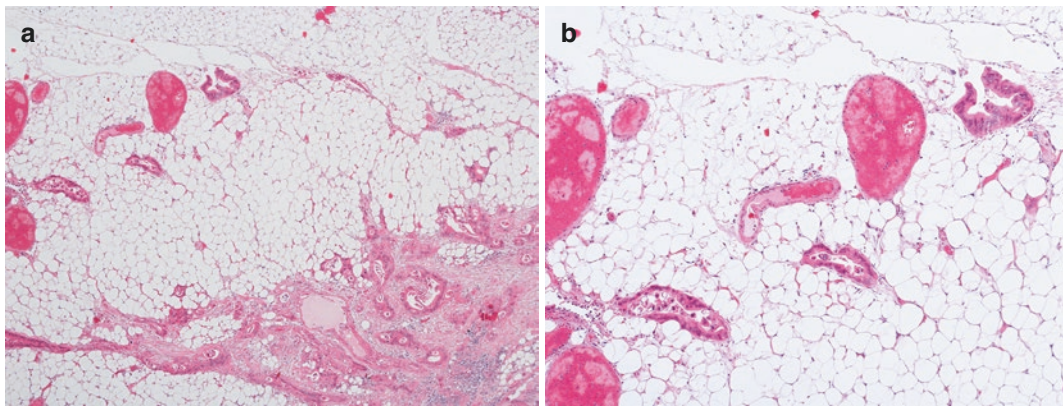

Fig. 9.15 Naked glands: at the invasive tumor front, a few single tumor glands infiltrate the peripancreatic fat (**a**). They are not associated with a stromal reaction, and tumor cells are flanked by adipocytes (**b**)

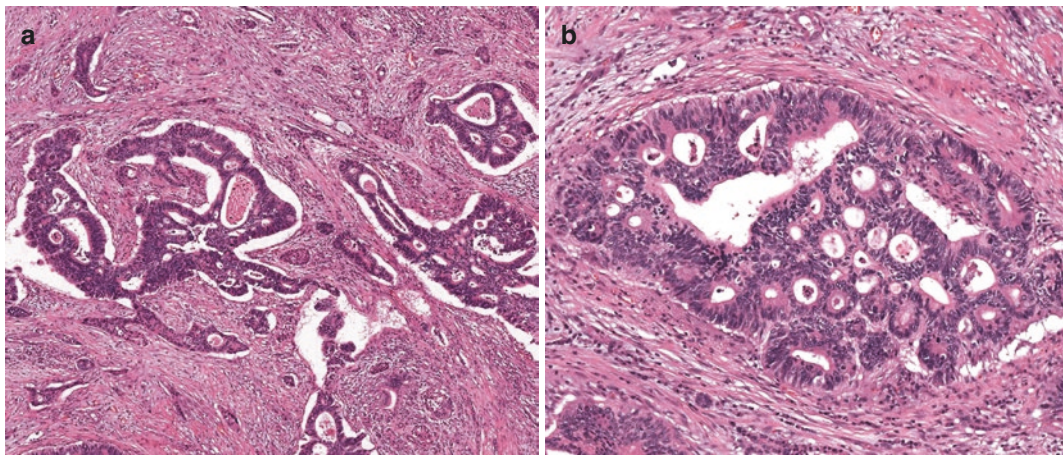

Fig. 9.16 Intestinal type: tumor glands are large and often of a complex or cribriform architecture (**a**). The neoplastic epithelium is high columnar and has cigar-shaped nuclei, which are orientated perpendicularly to the basement membrane (**b**). Note the presence of small amounts of necrotic detritus in some lumina

9.6.3 Intratumor Heterogeneity

The histomorphology of invasive ductal adenocarcinoma is not uncommonly characterized by a marked degree of intratumor heterogeneity, such that a variety of growth patterns and cytological appearances may be seen in different parts of the same tumor (Fig. 9.17). The morphology of both the carcinoma proper and the associated tumor stroma may differ, resulting in a wide range of different morphological phenotypes that are not represented in the WHO classification 2019 (see Fig. 9.23) [5]. In addition, in many pancreatobiliary type cancers, there is a tendency towards a more intestinal morphology in areas where the tumor involves the duodenum. When infiltrating the duodenal muscularis propria, tumor glands commonly become larger and elongated, align with the smooth muscle bundles, show a more intestinal-type cytomorphology, and appear moderately to well-differentiated (Figs. 9.18 and 9.19). Furthermore, when infiltrating the mucosa of the duodenum or papilla of Vater, the cancer cells may grow along the basement membrane of the native crypts and villi, creating the impression of in situ neoplasia (Fig. 9.20). In endoscopic biopsy material this intestinal mimicry may occasionally lead to an erroneous diagnosis of a primary duodenal carcinoma (see below). On occasion, the tumor glands infiltrating the duodenal wall may enlarge to the point of being macroscopically visible cysts (Fig. 9.21), a finding that may erroneously raise the suspicion of paraduodenal (groove) pancreatitis (see Chap. 7, Sect. 7.2.8 and Fig. 7.75).

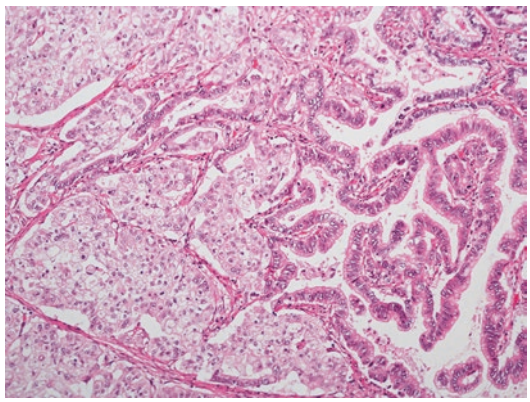

Fig. 9.17 Intratumor heterogeneity: ductal adenocarcinoma changes abruptly from a solid to a papillary growth pattern. The tumor cells have a clear cell appearance only in the solid area

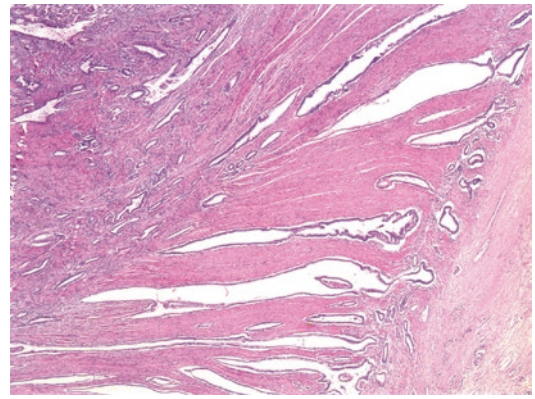

Fig. 9.18 Intestinal mimicry: when infiltrating the duodenal muscularis propria, the usually small angulated or branching glands of pancreatobiliary type ductal adenocarcinoma become large and elongated, and align with the muscle bundles. Note the lack of prominent desmoplasia

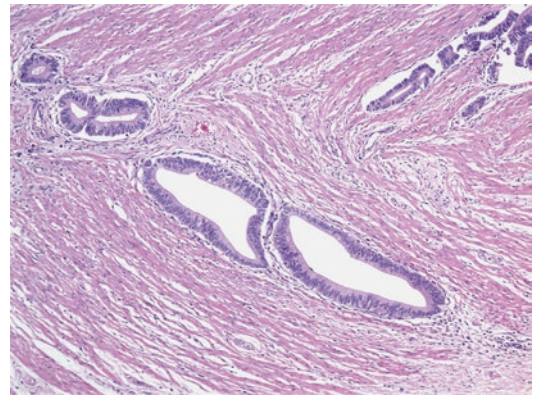

Fig. 9.19 Intestinal mimicry: pancreatobiliary type carcinoma can acquire an intestinal phenotype when infiltrating the duodenal muscle layer. Glands are larger, elongated, and lined by high-columnar cells with cigar-shaped, slightly pseudostratified nuclei. Note the lack of prominent desmoplasia

9.7 Grading

Different systems have been proposed for the grading of ductal adenocarcinoma of the pancreas. Grading according to TNM UICC (eighth

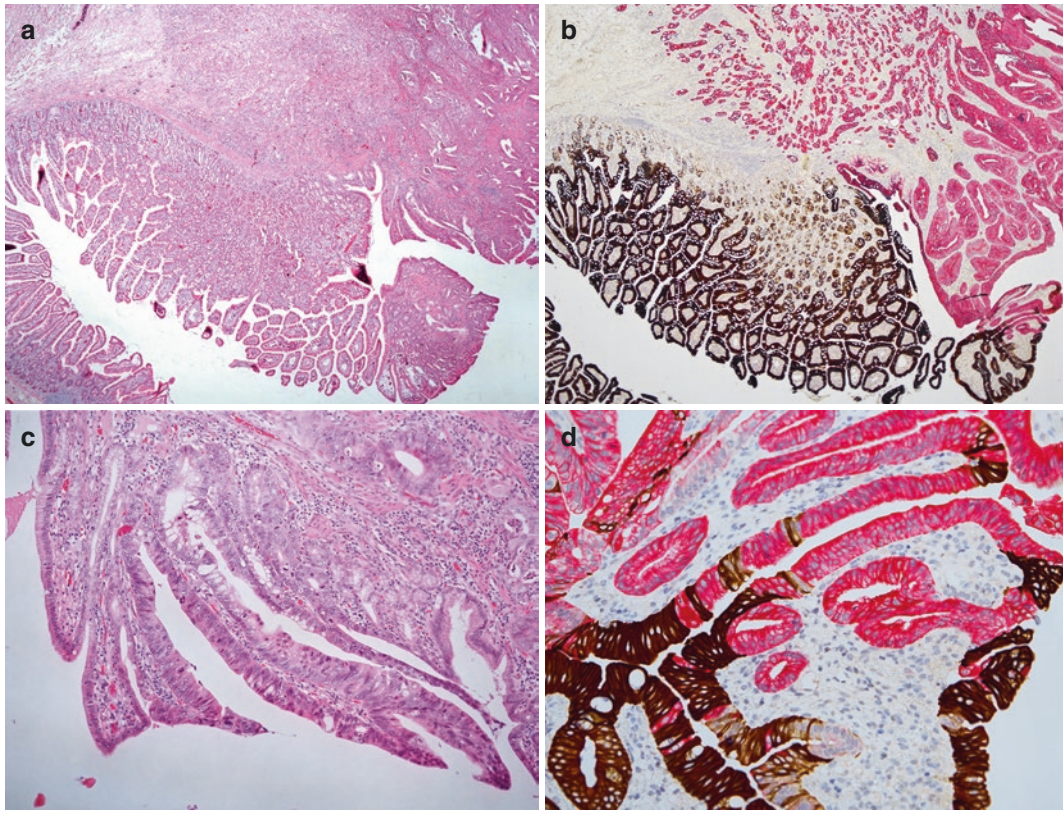

Fig. 9.20 Intestinal mimicry: pancreatobiliary type ductal adenocarcinoma infiltrates the duodenal wall and reaches the mucosal surface (**a**). Immunohistochemical double staining shows a sharp demarcation between invasive ductal adenocarcinoma (*red*; MUC1) and duodenal mucosa (*brown*; MUC2). Note the change in size and shape of the tumor glands as they reach the mucosa (**b**). Invasive tumor cells grow along the basement membrane of duodenal villi and crypts, mimicking in situ neoplasia (**c**). Immunostaining shows clear distinction between tumor cells (*red*; MUC1) and native epithelium (*brown*; MUC2) (**d**)

edition) follows a general four-tiered system, which is also applicable to other gastrointestinal adenocarcinomas (Table 9.1) [6]. The grading system proposed by the WHO classification is based on the degree of glandular differentiation, mucin production, nuclear atypia, and the mitotic activity (Table 9.2) [4]. It is more elaborate and therefore more onerous to apply than the grading system proposed by TNM UICC. Grading is highly concordant between both systems and has a similar predictive value [7].

Most tumors exhibit a range of histopathological grades, in which case the highest grade should be reported, irrespective of its extent. In practice, the majority of ductal adenocarcinomas comprise a poorly differentiated component, which consists of a rather inconspicuous population of tumor cell singletons or small solid clusters, which contain little mucin and may show marked nuclear atypia (Fig. 9.22).

9.8 Morphological Patterns

Conventional ductal adenocarcinoma may include areas with variant growth patterns, which are of no known biological, genetic, or clinical relevance. The significance of these patterns lies mainly in their distinction from benign structures, that is, normal pancreatic ducts or precursor lesions such as pancreatic intraepithelial neoplasia and intraductal papillary mucinous neoplasia (see Chaps. 8 and 17). In addition to the patterns that are included in the WHO classi-

Fig. 9.21 Paraduodenal pancreatitis-like invasion of the duodenal wall: occasionally, ductal adenocarcinoma infiltrating the duodenal muscularis propria may assume a cystic appearance, which may mimic paraduodenal (groove) pancreatitis

Table 9.1 Histological grading of ductal adenocarcinoma of the pancreas according to the UICC TNM classification (8th edition) [6]

Grade of differentiation	
Grade X	Grade of differentiation cannot be assessed
Grade 1	Well differentiated
Grade 2	Moderately differentiated
Grade 3	Poorly differentiated
Grade 4	Undifferentiated

fication and further described below, there is a wide range of histomorphologies that have been neither assigned a nomenclature nor further characterized (Fig. 9.23) [5].

9.8.1 Foamy Gland Pattern

Tumor cells of this variant pattern of ductal adenocarcinoma acquire a foamy appearance due to their microvesicular mucin-rich cytoplasm. The luminal border of the tumors cells is often particularly well defined by linear cytoplasmic condensation, which resembles the enterocytic brush border. The nuclei are typically basally

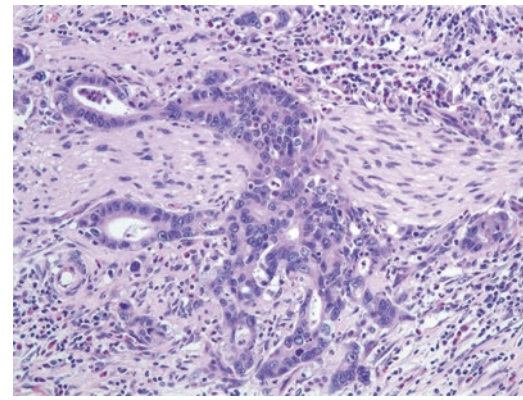

Fig. 9.22 Grading: fairly well formed tumor glands are admixed with complex, nearly solid tumor cell groups showing moderate nuclear pleomorphism. In addition, there are scattered small solid tumor cell clusters and a few single cells, some of which exhibit marked nuclear atypia. Note the presence of mitotic activity. The tumor is graded as poorly differentiated (grade 3)

Table 9.2 Histological grading of ductal adenocarcinoma of the pancreas according to the WHO classification 2019 [4]

Grade of differentiation	Glandular differentiation	Mucin production	Mitoses/10 HPF	Nuclear features
Grade 1	Well-differentiated glands	Intensive	5	Little pleomorphism, polar arrangement
Grade 2	Moderately differentiated ductular or tubular glands	Irregular	6–10	Moderate pleomorphism
Grade 3	Poorly differentiated glands, abortive mucoepidermoid and pleomorphic structures	Abortive	>10	Marked pleomorphism and increased size

Abbreviation: *HPF* high power fields

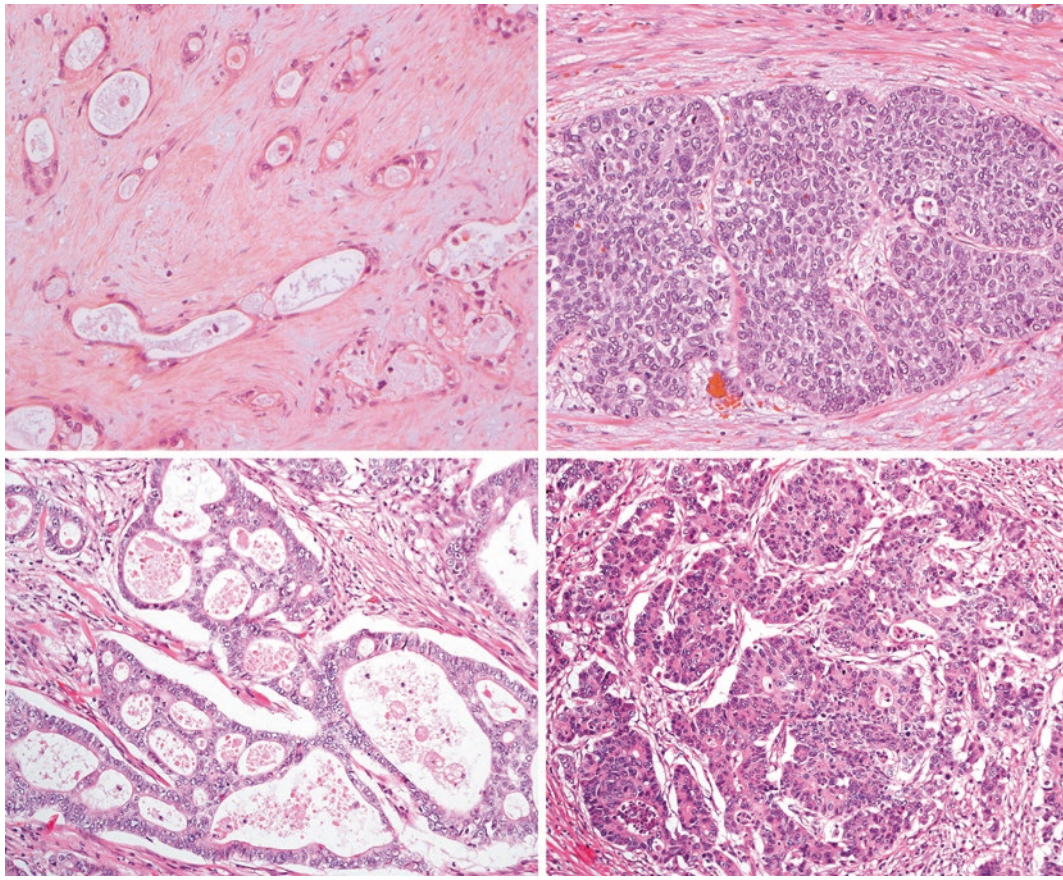

Fig. 9.23 Morphological heterogeneity: ductal adenocarcinoma *not otherwise specified* encompasses a wide range of growth patterns and histomorphological appearances, four examples of which are shown

located, round, hyperchromatic, and often raisinoid in shape. Ductal adenocarcinoma with foamy gland features is usually well differentiated to the point that the deceptively bland tumor glands may be misinterpreted as benign ducts (Fig. 9.24).

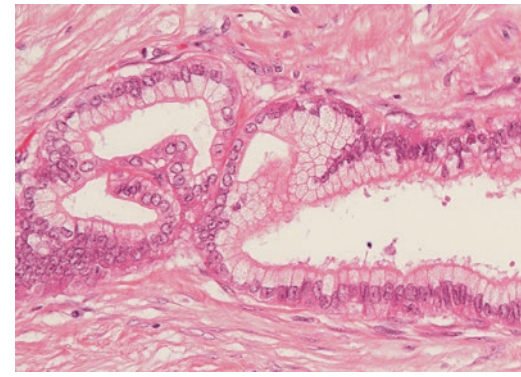

Fig. 9.24 Foamy gland pattern: the presence of cytoplasmic mucin-filled microvesicules gives the tumor cells a foamy appearance. The apical cell border is well delineated by linear cytoplasmic condensation. Round or raisinoid nuclei showing little pleomorphism are basally located

9.8.2 Clear Cell Pattern

Some ductal adenocarcinomas have abundant clear cytoplasm, which differs from that of the foamy gland pattern, because it is homogeneous and non-vesicular (Fig. 9.25). Given the fact that these tumors often display a solid growth pattern, ductal adenocarcinoma with clear cell features may resemble metastatic renal cell carcinoma,

from which it can be distinguished with the aid of immunohistochemistry (see Chap. 12, Sect. 12.5). Clear cell ductal adenocarcinoma stains positively for mucin and for other immunohistochemical markers of ductal adenocarcinoma (see Sect. 9.9).

9.8.3 Large Duct Pattern

In this variant, tumor glands are dilated (> 0.5 mm) up to a size that may be macroscopically apparent as small cysts (Fig. 9.26). While the tumor cells may show a mild degree of intraluminal tufting, this is never a prominent feature. Devoid of prognostic significance, the importance of this variant lies in the occasional difficult distinction between single such large invasive tumor glands and native pancreatic ducts with or without pancreatic intraepithelial neoplasia. Because these large glands are often deceptively bland-looking, their abnormal localization outwith the normal lobular architecture or within the duodenal wall may help reaching the correct diagnosis.

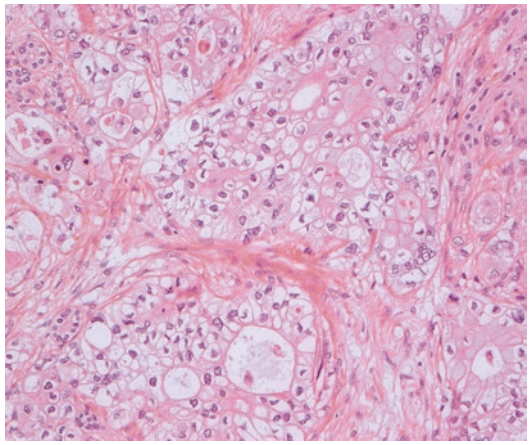

Fig. 9.25 Clear cell pattern: tumor cells are characterized by abundant, homogeneously clear cytoplasm. The clear cytoplasm and solid growth pattern bear resemblance with renal cell cancer of clear cell type

9.8.4 Cystic Papillary Pattern

This variant is characterized by large-caliber neoplastic glands, which—in contrast to the large duct variant—show prominent and often complex intraluminal papillary projections. The neoplastic tumor cells are high-columnar and contain intracellular mucin. The lumina of the large tumor glands contain mucin and can be dilated, occasionally reaching grossly cystic dimensions (Fig. 9.27). This variant pattern shows resemblance with intraductal papillary mucinous neoplasia, but the neoplastic proliferation is stroma-invasive and not intraductal, as evidenced by the absence of elastin fibers around the neoplastic glands (see Chap. 1, Sect. 1.4.3). Furthermore, the distribution of the neoplastic glands is haphazard, independent of the branching architecture of the pancreatic duct system. The presence of the cystic papillary

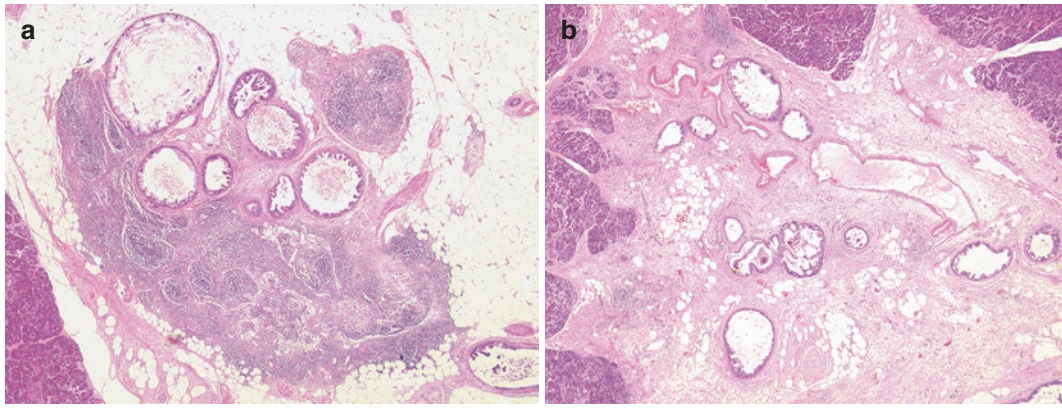

Fig. 9.26 Large duct pattern: this tumor forms large glands with mild intraluminal tufting and mild to moderate atypia. While the invasive nature of the glands is obvious when found within a lymph node (**a**), the distinction from pancreatic intraepithelial neoplasia is more difficult within the confines of the pancreas. The proximity of the suspicious glands to muscular blood vessels indicates the invasive nature (**b**)

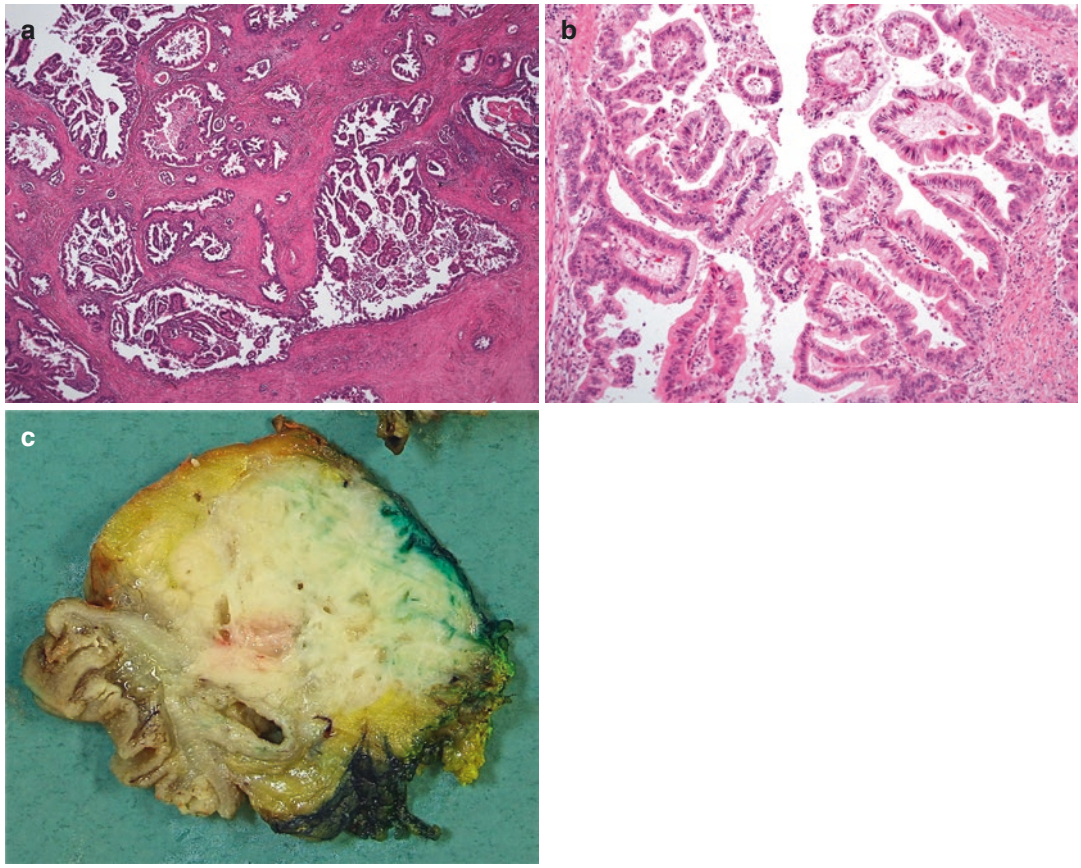

Fig. 9.27 Cystic papillary pattern: the tumor grows as large duct-like structures with prominent intraluminal papillary projections (**a**). The tumor cells are high-columnar and contain mucus (**b**). Macroscopically, the tumor is mainly solid but contains small, slightly mucinous, cystic areas (**c**)

neoplastic formations within the duodenal wall, lymphovascular channels, or perineural clefts further indicates their invasive nature. Tumors with this variant microscopic pattern usually contain areas of conventional ductal adenocarcinoma, although these may be less prominent.

9.9 Immunohistochemistry

Intensive research in recent years has uncovered a rapidly expanding range of markers—over 2500—that are aberrantly expressed in pancreatic cancer [8]. However, not all of these are specific for pancreatic cancer, and for many the diagnostic value in distinguishing invasive ductal adenocarcinoma from nonneoplastic pancreatic ducts, other primary pancreatic neoplasms, or extrapancreatic cancer has not been validated. Data on the few markers that have been tested are not uncommonly divergent, if not conflicting, due to—amongst several other factors—differences in the immunoscoring system that has been used. In this section, the discussion is limited to markers that may be of some proven diagnostic value.

9.9.1 Immunohistochemical Profile

Ductal adenocarcinoma expresses the same keratins as normal pancreatic duct epithelium, that is, cytokeratins (CK) 7, 8, 18, and 19. Expression of CK20 is absent or less extensive than that of CK7, except in pancreatic cancer of intestinal type or in certain subtypes of ductal adenocarcinoma, for example, colloid carcinoma. However,

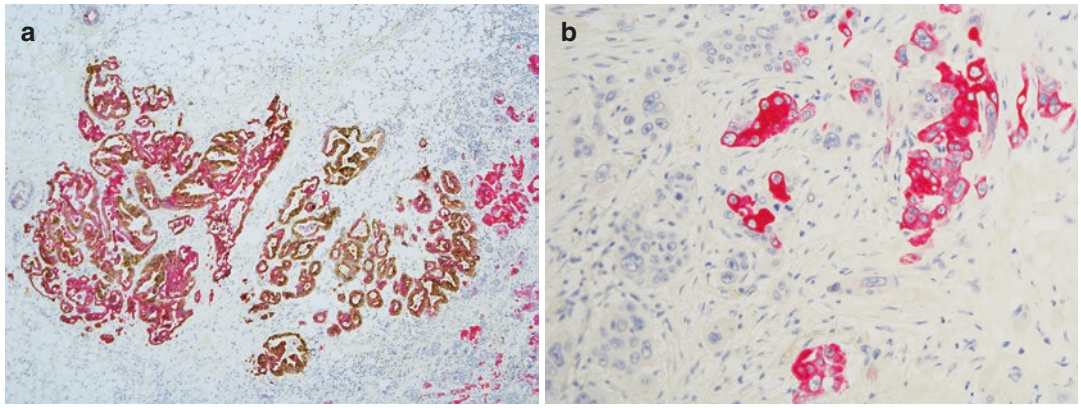

Fig. 9.28 Cytokeratin immunostaining: this pancreatobiliary type tumor shows staining for both CK7 (*red*) and CK20 (*brown*) (**a**). Some of the poorly differentiated tumor cells are negative for both markers (**b**)

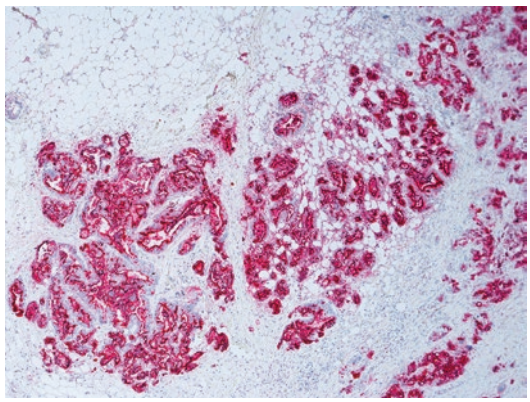

Fig. 9.29 Mucin immunostaining: the entire tumor cell population shows immunolabeling for MUC1 (*red*), while MUC2 (*brown*) expression is absent (same tumor as in Fig. 9.28)

expression of both CK7 and 20 can be lacking in poorly differentiated ductal adenocarcinoma (Fig. 9.28). Over 50% of tumors also stain for CK4.

Most ductal adenocarcinomas express mucin (MUC) 1 and 5AC, while 20–25% are positive for MUC6. Immunostaining for MUC2 is observed in less than 10% of ductal adenocarcinomas, mainly those with an intestinal or colloid morphology (Fig. 9.29). The vast majority of ductal adenocarcinomas also express CEA, CA19-9, and maspin, whereas CA125 and mesothelin are found in approximately 50% and 49–71% of cases, respectively [9–11]. Vimentin is usually absent, except in the undifferentiated subtypes (see Sects. 9.14.7 and 9.14.8). Immunolabeling for synaptophysin and chromogranin A highlights scattered endocrine cells that may be present in a proportion of ductal adenocarcinomas. If more than 30% of the cancer cells stain positively, the tumor is to be regarded as a pancreatic mixed neuroendocrine–non-neuroendocrine neoplasm (MiNEN) (see Chap. 20, Sect. 20.10). Immunostaining for neuroendocrine markers may also pick up a small number of entrapped nonneoplastic endocrine cells. Ductal adenocarcinoma is usually negative for the pancreatic exocrine enzymes trypsin, chymotrypsin, amylase, lipase, and the acinar marker BCL10. Nuclear staining for SMAD4 (DPC4) is lost in approximately 55% of pancreatic cancers, while staining is positive for p53 in 50–75% of cases. Overexpression of a number of other markers has been reported recently, including EGF and its receptor ERRB2, TGFα, TGFβ, PDGF, VEGF, CD44v6, claudin 4 and 18, B72.3, IMP-3, members from the S100 group of proteins (S100A4, S100A6, S100P), and many more.

9.9.2 Distinction from Other Pancreatic or Extrapancreatic Neoplasms

Despite the abundance of information on the immunohistochemical staining patterns in ductal adenocarcinoma, there is as yet not a single

marker or an immunohistochemical signature that can be used to unequivocally diagnose pancreatic ductal adenocarcinoma and distinguish it from nonneoplastic reactive ductular pancreatic structures or adenocarcinoma of ampullary and bile duct origin. The use of immunohistochemistry for the distinction of ductal adenocarcinoma from other primary pancreatic neoplasms and metastasis from extrapancreatic malignant tumors is discussed elsewhere (see Chaps. 12 and 20, Sects. 12.5 and 20.9, Tables 12.1 and 20.5).

9.9.3 Distinction from Reactive Pancreatic Ductules

In some cases, immunohistochemistry for CEA, CA125, mesothelin, S100P, SMAD4, and p53 may be helpful in the distinction between invasive ductal adenocarcinoma and reactive pancreatic ductules. However, results should be interpreted with great caution, because—as outlined above—immunostaining for the first three markers is neither entirely sensitive nor specific. The absence of immunostaining for CEA, CA125, S100P, or mesothelin does not definitively exclude a diagnosis of ductal adenocarcinoma, especially if applied to only a small number of glandular structures, for example, on biopsy material. Furthermore, a normal nuclear immunolabeling pattern for p53 and SMAD4 may be found in 25–50% of ductal adenocarcinomas. Conversely, reactive ducts may occasionally show focal positivity for CEA, CA125, mesothelin, S100P, or p53. However, absence of nuclear staining for SMAD4 is not observed in reactive glands.

9.10 Tumor Propagation

Ductal adenocarcinoma is characterized by a highly infiltrative growth pattern and a propensity for propagation along preformed channels, be it perineural clefts, lymphatics, blood vessels, pancreatic ducts, or preformed structures such as fibrous septa between lobules of the acinar parenchyma or the peripancreatic adipose tissue (Figs. 9.10 and 9.11).

The vast majority (>90%) of tumors show evidence of *perineural tumor propagation* (Fig. 9.30). This may be especially prominent in pancreatic cancers that infiltrate the peripancreatic soft tissue, in particular the tissue plane facing the superior mesenteric artery and the soft tissue sheath around the extrapancreatic common bile duct, because these areas contain numerous peripheral nerves of various calibers (see Chap. 1, Figs. 1.25 and 1.28). Perineural tumor propagation is commonly also seen in the periarterial neural plexus (see Chap. 1, Figs. 1.26 and 1.27) that surrounds the gastroduodenal and splenic artery (Fig. 9.31), or the celiac trunk and superior

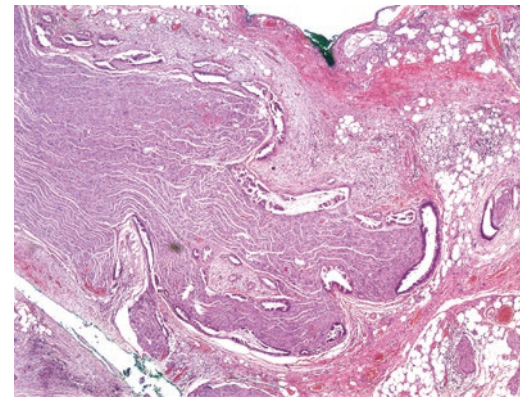

Fig. 9.30 Perineural invasion: numerous tumor glands involve a large peripheral nerve in peripancreatic adipose tissue flanking the superior mesenteric vessels

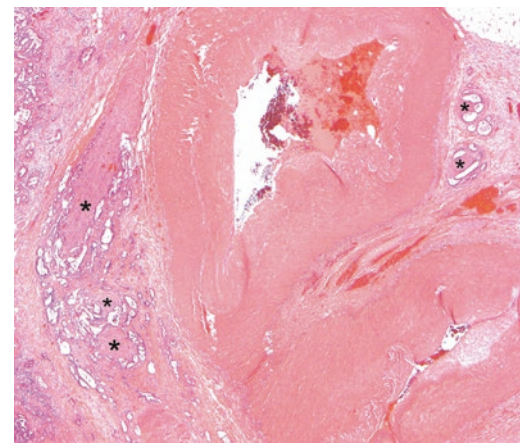

Fig. 9.31 Perineural invasion: the neural plexus surrounding the splenic artery shows multifocal perineural tumor propagation (*asterisks*)

mesenteric artery in the rare case that these large arteries are resected. Benign glandular inclusions have been described in peripheral nerves in and around the pancreas (see Chap. 1, Fig. 1.29), but these are so extremely rare that they hardly represent a differential diagnosis. Maybe more problematic is the rare occurrence of pseudoneural inclusion of nonneoplastic islet cells in chronic pancreatitis (see Chap. 7, Sect. 7.2.4, Fig. 7.30), a finding that in combination with other atypical features in this setting may raise the suspicion of invasive adenocarcinoma.

Tumor *invasion of lymphatic channels* is also common in ductal adenocarcinoma of the pancreas, and this may be found both within and outside the pancreas. The duodenal wall and ampullary region are particularly rich in lymph vessels, and therefore, these areas must be scrutinized with great care to identify lymphatic tumor propagation (Fig. 9.32). Immunostaining for podoplanin/D2-40, a marker of lymphatic endothelium, may be helpful, in particular in distinguishing lymphatic from vascular tumor invasion (Fig. 9.33). However, in pancreatic cancers that have metastasized to the lymph nodes—over 70% of all cases—the histological identification of lymphatic tumor propagation provides no additional prognostic information.

Vascular tumor propagation is another frequent mode of tumor spread. It is of particular prognostic importance, as distant metastasis—most commonly to the liver—is the cause of death in the majority of pancreatic cancer patients (see Sect. 9.13). Vascular invasion may be less easy to identify than perineural tumor propagation. Because arterial branches are paired with the venous ramifications of the vasculature and tumor invasion usually affects the latter, it may be helpful to search for arterial blood vessels that are not accompanied by a venous counterpart (‘orphan arteries’), but instead are flanked by a tumor cell cluster that is located within and thereby obscures the accompanying vein (Fig. 9.34). Detailed inspection of the tumor

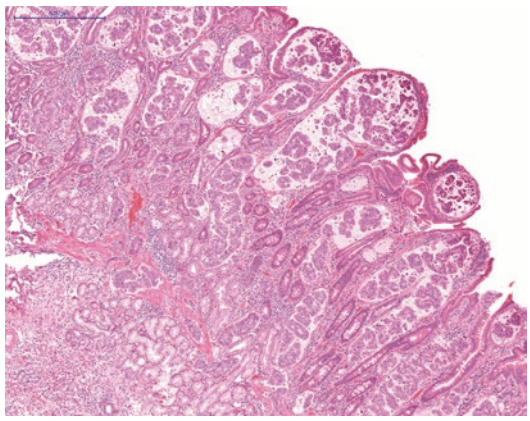

Fig. 9.32 Lymphatic channel permeation: countless lymphatic channels in the duodenal lamina propria are dilated and filled with invasive adenocarcinoma

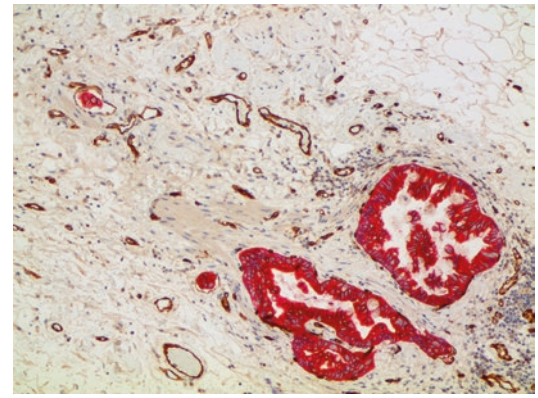

Fig. 9.33 Lymphatic channel permeation: immunohistochemical double-staining for D2–40 (*brown*) and CK7 (*red*) reveals the presence of numerous lymphatic channels, two of which contain a small tumor cell cluster. In addition, there are two larger stroma-invasive tumor glands

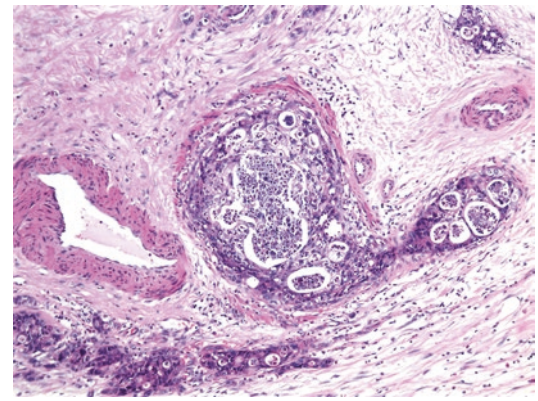

Fig. 9.34 Vascular invasion: a medium-sized vein is completely occluded by adenocarcinoma. Note the unaltered flanking artery, whose presence aids in identifying venous tumor occlusion

focus may reveal residual structures of the venous wall, and elastica van Gieson staining is most valuable in identifying residua of both elastin and smooth muscle fibers within and around such intravascular tumor foci (Fig. 9.35). Occasionally, the invasive tumor cells seem to replace the endothelial cells such that the vascular lumen is surrounded by neoplastic cells, resulting in a mimicry of a nonneoplastic duct or, if atypia is more pronounced, a pancreatic duct involved by pancreatic intraepithelial neoplasia (see Chap. 8). The presence of a smooth muscle layer surrounding the structure, detected on van Gieson staining or by immunohistochemistry, leads to the correct diagnosis of vascular invasion (Fig. 9.36). It should be borne in mind that a collar of elastin fibers can be seen in association with both blood vessels and pancreatic ducts (see Chap. 1, Sect. 1.4.3). Immunostaining for endothelial markers (e.g., CD31) allows identification of intravascular tumor cell clusters in a smaller proportion of affected blood (and lymphatic) vessels, whose wall and endothelial lining have remained intact. Thrombosed veins deserve particular attention, as thrombosis is commonly the result of intravascular tumor spread. While blood vessels are obviously present throughout the entire pancreas and surrounding tissues, they are particularly

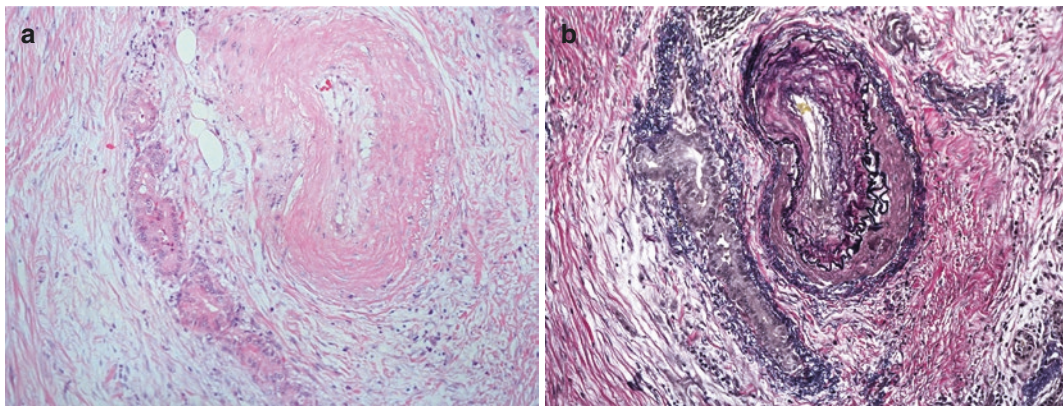

Fig. 9.35 Vascular invasion: an orphan artery is flanked by a tumor gland cluster (**a**). Elastica van Gieson staining reveals residua of the elastin membrane and smooth musculature of the tumor-occluded associated vein (**b**)

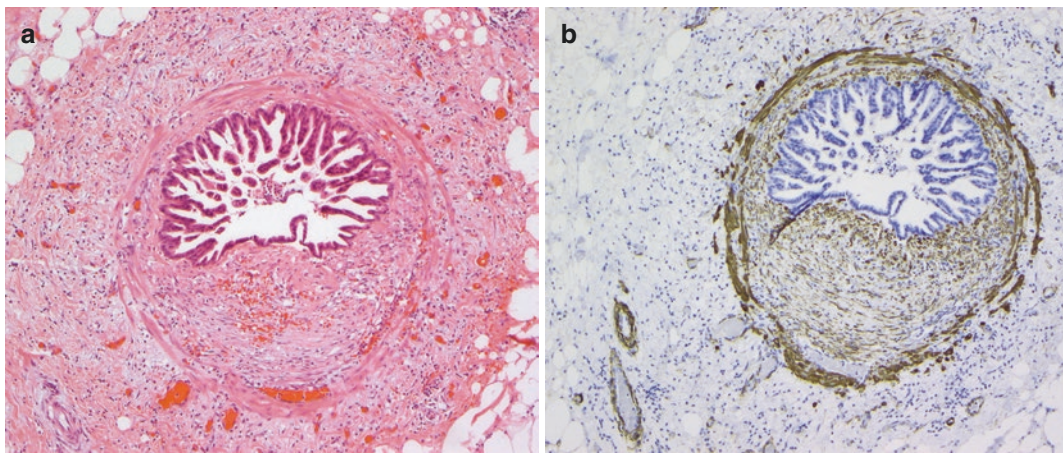

Fig. 9.36 Vascular invasion mimicking PanIN: invasive adenocarcinoma growing along the luminal surface of a vein resembles high-grade PanIN (**a**). The presence of a smooth muscle layer encircling the neoplastic epithelium confirms that the latter is present within a vein, not a pancreatic duct (**b**, immunohistochemical stain for smooth muscle actin)

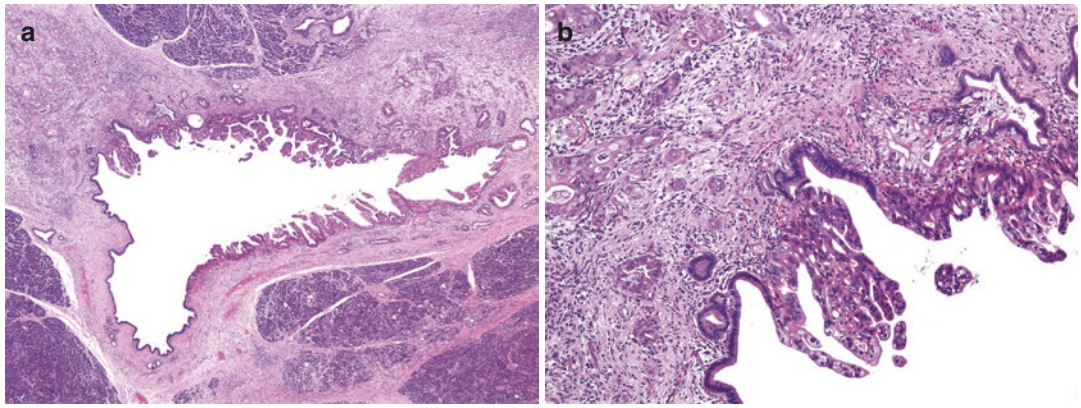

Fig. 9.37 Duct cancerization: this large interlobular duct is partially involved by intraductal tumor propagation (**a**). The abrupt transition between the highly atypical epithelium and the normal epithelial lining, together with the presence of invasive adenocarcinoma around the duct, allow the distinction from high-grade PanIN (**b**)

prominent and therefore easier to examine near the anterior and posterior pancreatoduodenal crevices, in the anterior adipose tissue, and in the soft tissue facing the superior mesenteric artery. For tumors involving any of these areas, the search for vascular invasion may be most promising here.

Intraductal tumor propagation is a further common mode of pancreatic cancer spread, which is found in up to 70% of tumors and may result in tumor spread up to several centimeters beyond the main tumor mass [12]. It is often a multifocal finding, and ducts of any caliber, in particular medium-sized interlobular ducts, can be involved. Occasionally, intraductal tumor spread or so-called duct cancerization may also be seen along the common bile duct or ampulla. At times, the distinction between duct cancerization and high-grade PanIN may be problematic (see Chap. 8, Sect. 8.6.2). Overall, the presence of invasive tumor glands in the vicinity of the pancreatic duct in question, and the abrupt transition from atypical to normal epithelium are clues in favor of duct cancerization (Fig. 9.37).

9.11 Staging

The UICC TNM (eighth edition) staging system [6] applies to cancer derived from the exocrine pancreas, that is, ductal adenocarinoma and its subtypes as well as acinar cell carcinoma. It may also be used for staging of mixed neuroendocrine-non-neuroendocrine neoplasms (MiNENs) with a ductal adenocarcinoma or acinar cell carcinoma as the exocrine tumor component (see Chap. 10, Sect. 10.10.3 and Chap. 20, Sect. 20.10), for intraductal papillary mucinous neoplasia and mucinous cystic neoplasia with high-grade dysplasia or invasive carcinoma, for pancreatoblastoma, and solid pseudopapillary neoplasia. In 2018, the eighth edition of the UICC TNM classification of tumors published a revised version of the staging of primary tumor (pT) and lymph node (pN) status. The reason to change staging criteria for pT1–3 from tumor size and extent (seventh edition) [13] to tumor size only (eighth edition) [6] was prompted by the following observations and concerns. First, extension beyond the pancreas was found to be a criterion with suboptimal reproducibility, because the pancreas has no capsule and the outline of the gland may not always be well defined. In addition, tumor infiltration of the common bile duct was also interpreted differently by individual pathologists and national guidelines. Second, extrapancreatic tumor extension occurs in more than 80% of tumors that are smaller than 20 mm in size, and yet, there is no associated decrease in survival compared to size-matched tumors without extrapancreatic extension. Third, extrapancreatic extension is present in up to 90% of cases, such that the vast majority of pancreatic cancers fall into the same stage category of pT3. The

implementation of exclusively size-based criteria for pT1–3 in the eighth edition of UICC TNM results in a more even stratification of patients across stages without sacrificing prognostic accuracy and with a presumed improved reproducibility [14]. When it comes to staging of the lymph node status, an N2 category has been added, similar to the pN-staging for other gastrointestinal cancer sites. Several studies have validated the eighth edition of the UICC/AJCC staging systems and found the revised N-stage to be highly prognostic, while only a modest improvement is observed for the revised T-stage, which still remains a fairly weak predictor of survival [14–17].

The prefix 'p' indicates that staging is based on pathology findings. The descriptors L, V, Pn, and R can be used to report the cancer stage in terms of lymphatic, vascular, and perineural tumor propagation as well as residual disease.

Staging is an essential part of the diagnostic work-up and key to the patient management. The pathology report on resection specimens should therefore always explicitly state the staging for pT, pN, and the various other descriptors.

The staging system for pancreatic cancer issued by the American Joint Committee on Cancer (AJCC) [18] is identical to the UICC TNM system, with exception of the assignment of celiac lymph nodes (see Sect. 9.11.2).

Table 9.3 Staging of carcinoma of the exocrine pancreas according to the UICC TNM classification (8th edition) [6]

Stage	Staging criteria
T-primary tumor	
• TX	• Primary tumor cannot be assessed
• T0	• No evidence of primary tumor
• Tis	• Carcinoma in situ[a]
• T1	• Tumor 2 cm or less in greatest dimension
– T1a	– Tumor 0.5 cm or less in greatest dimension
– T1b	– Tumor greater than 0.5 cm and no more than 1 cm in greatest dimension
– T1c	– Tumor greater than 1 cm but no more than 2 cm in greatest dimension
• T2	• Tumor more than 2 cm but no more than 4 cm in greatest dimension
• T3	• Tumor more than 4 cm in greatest dimension
• T4	• Tumor involves celiac axis, superior mesenteric artery, and/or common hepatic artery
N-regional lymph nodes	
• NX	• Regional lymph nodes cannot be assessed
• N0	• No regional lymph node metastasis
• N1	• Metastasis in 1–3 regional lymph node(s)
• N2	• Metastasis in 4 or more regional lymph nodes
M-distant metastasis	
• M0	• No distant metastasis
• M1	• Distant metastasis

[a]Includes high-grade pancreatic intraepithelial neoplasia (PanIN)

9.11.1 Staging of the Primary Tumor

The criteria for staging of the primary tumor (pT-stage) are based on tumor size and extent (Table 9.3), the latter criterion pertaining only to stage pT4. Incorrect pT-assessment, and in particular underestimation of tumor size, is the main pitfall in staging of ductal adenocarcinoma. This is likely to happen, if macroscopic size measurement is not checked and corrected by microscopic assessment. As explained above, the highly infiltrative pattern of pancreatic cancer, its markedly dispersed growth, and the occurrence of 'naked glands' can only be appreciated on histology. Because these phenomena are particularly prominent at the tumor periphery, their identification is important for accurate assessment of tumor size (and extent) and, consequently, for assignment to the correct T-stage.

The majority of ductal adenocarcinomas are stage pT2, that is, measure between 2 cm and 4 cm in size. Outside the context of intraductal papillary mucinous neoplasia or mucinous cystic neoplasm, ductal adenocarcinoma smaller than 2 cm, that is, stage pT1, is rarely diagnosed because of the lack of specific symptoms (Fig. 9.38).

While tumor invasion of the wall of the superior mesenteric vein (SMV) or portal vein does not affect the T-stage, accurate microscopic assessment of the relationship of the tumor to the vein is nevertheless important, because several—but not all—studies observed that tumor invasion of the named veins (Fig. 9.39) (see Figs. 3.8, 3.23, and 3.24) portends worse patient outcome [19–22] and that the depth of invasion into the vessel wall (tunica adventitia, media, intima, or vascular lumen) is prognostically relevant [23,

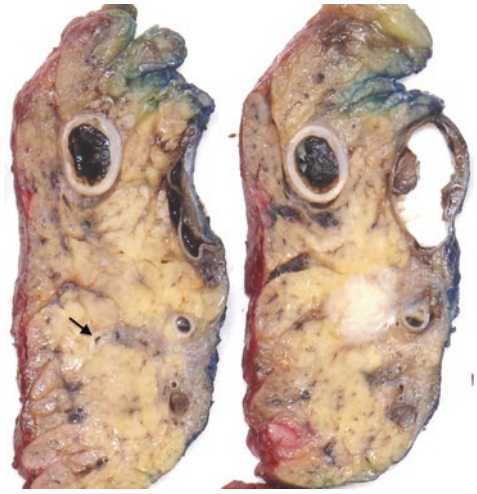

Fig. 9.38 Ductal adenocarcinoma detected at an early stage: this ductal adenocarcinoma measuring 11 mm in maximum diameter occludes the main pancreatic duct (*arrow*), which resulted in recurrent attacks of acute pancreatitis and early detection of the small cancer

24]. Furthermore, accurate pathology reporting on the presence or absence of tumor invasion of the large veins is important for correlation with preoperative imaging and intraoperative surgical assessment during multidisciplinary case discussion (see Chap. 4). As discussed in Chap. 3, the entire fragment of resected vein should be subjected to microscopic examination, and the depth of tumor invasion into the vein—adventitia, media, intima or lumen—should be recorded. Because the tunica adventitia blends with the surrounding soft tissue, it has been defined by some as the layer of fibrous tissue within 1 mm from the outer limit of the tunica media. Assessment of the resection margins of the resected fragment of vein and the adjacent margin at the SMV groove is described below (see Sect. 9.11.4).

Ductal adenocarcinoma located in the anterior-cranial part of the pancreatic head may surround

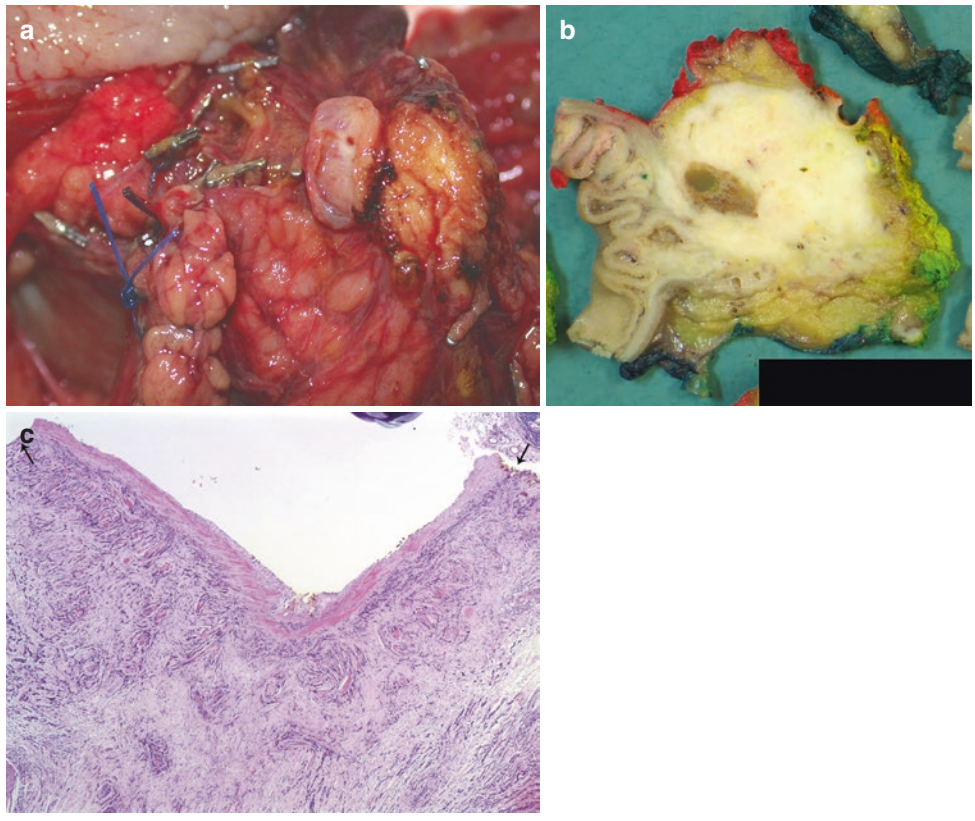

Fig. 9.39 Invasion of SMV: an ellipse of the superior mesenteric vein (SMV) is tightly adherent to the SMV groove opposite to the pancreatic transection margin (with blue suture; **a**). Axial specimen slicing reveals a large tumor, which invades the SMV wall (inked orange; **b**). Microscopically, poorly differentiated adenocarcinoma infiltrates the full thickness of the SMV wall and reaches the transection margins of the vein (*arrows*, **c**)

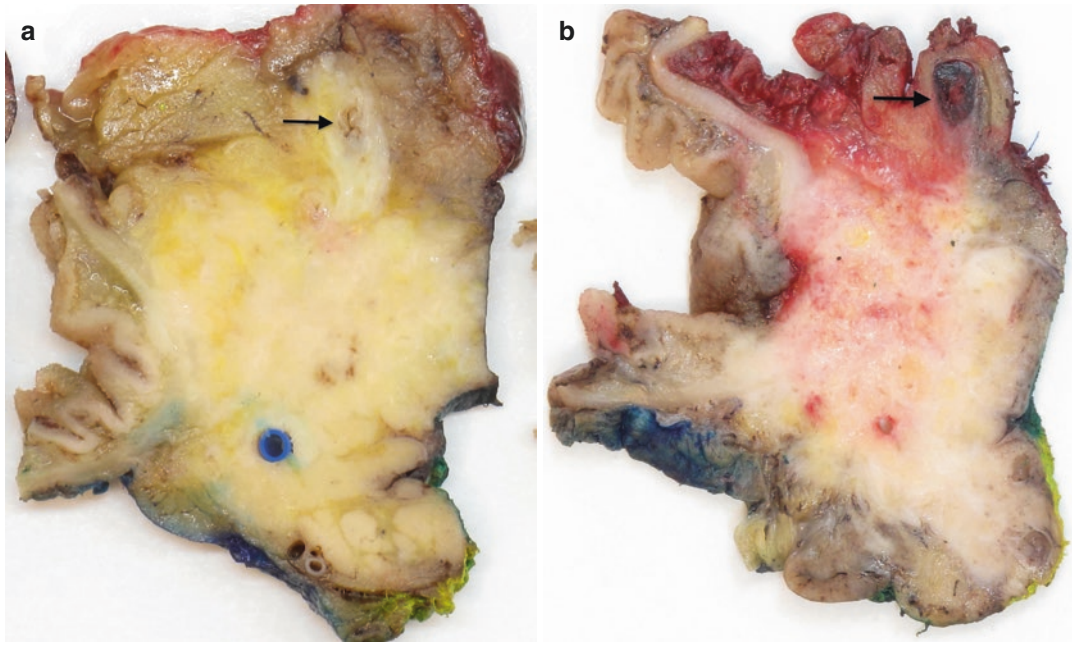

Fig. 9.40 Involvement of the gastroduodenal artery: tumor infiltrates the anterior peripancreatic adipose tissue and surrounds the gastroduodenal artery (*arrow*, **a**). In this case, tumor involvement of the gastroduodenal artery has resulted in thrombosis (*arrow*, **b**)

the gastroduodenal artery and occasionally lead to thrombosis of that blood vessel (Fig. 9.40).

9.11.2 Staging of Lymph Node Metastasis

Tumor involvement of one or more regional lymph nodes, either by metastatic seeding or direct tumor invasion, is observed in 70% or more of resected ductal adenocarcinomas and is present even when the primary tumor is small (<2 cm). Lymph node status is one of the strongest predictors of survival for ductal adenocarcinoma of the pancreas. Based on outcome data, node-positive disease has now been subdivided in pN1 (1–3 positive regional lymph nodes) and pN2 (4 or more positive regional lymph nodes) [6, 14–16].

The lymph node stations that are regarded by UICC TNM (eighth edition) as regional for pancreatic cancer arising in the pancreatic head and neck or body and tail are listed in Table 9.4, and their position is explained in Fig. 3.27 and Table 3.2. It should be mentioned that the UICC and AJCC (eighth edition) staging systems differ regarding the assignment of celiac lymph nodes [6, 18]. While UICC considers these as regional lymph nodes for cancer in the head of the pancreas, they are regarded as regional lymph nodes exclusively for tumors in the body and tail of the pancreas by the AJCC. Current knowledge about the topographic distribution of lymph node metastases depending on the site of the primary cancer within the pancreas is limited. Overall, tumors arising in the pancreatic head metastasize most frequently to the anterior and posterior pancreatoduodenal lymph nodes and those along the superior mesenteric artery. Pancreatic cancer in the uncinate process spreads most frequently to the latter group of lymph nodes. Carcinoma of the body and tail metastasizes mainly to the lymph nodes along the splenic artery and celiac trunk. Lymph node grouping according to the Japan Pancreas Society is discussed in Chap. 3.

Tumor metastasis to other, more distant lymph node stations, for example, the aortocaval lymph

Table 9.4 Regional lymph nodes for carcinoma of the head/neck and body/tail of the pancreas according to the UICC TNM classification (eighth edition) [6]

Anatomical localization	For tumors of pancreatic
Common bile duct	Head/neck
Common hepatic artery	Head/neck and body/tail
Portal vein	Head/neck
Pyloric	Head/neck
Infrapyloric	Head/neck
Subpyloric	Head/neck
Anterior pancreatoduodenal vessels	Head/neck
Posterior pancreatoduodenal vessels	Head/neck
Superior mesenteric vein	Head/neck
Right lateral wall of superior mesenteric artery	Head/neck
Celiac	Head/neck and body/tail
Proximal mesenteric	Head/neck
Retroperitoneal	Body/tail
Lateral aortic	Body/tail
Splenic artery	Body/tail
Hilum of spleen	Body/tail

nodes, is to be reported as distant metastasis, stage pM1.

The accuracy of the pN-stage depends on the lymph node yield [25, 26], which according to UICC TNM (eighth edition) is set at an average of 10 lymph nodes in pancreatoduodenectomy specimens [6]. The AJCC requires a minimum of 12 lymph nodes [18]. A higher lymph node yield of 15 lymph nodes has been suggested and is meanwhile accepted as a national pathology standard in some countries [27]. There are currently no recommendations for the lymph node yield from distal pancreatectomy specimens.

The clinical significance of lymph node micrometastasis is controversial, although an increasing body of literature suggests that the presence of micrometastatic spread is an adverse prognostic factor. One reason for the divergence in observations between studies is the existence of controversial definitions of lymph node micrometastasis. The UICC introduced the concept of isolated tumor cells, which are defined as single tumor cells or small cell clusters that measure no more than 0.2 mm in greatest extent and can be detected on routine H&E staining or by immunohistochemistry [6]. It is proposed to classify lymph nodes with isolated tumor cells as negative, but to indicate the presence of isolated tumor cells by adding a specific suffix, i.e., pN0(i+). At present there is insufficient evidence regarding the clinical significance of micrometastasis to recommend the examination of multiple section levels, or the use of immunohistochemical or molecular analysis for the identification of isolated tumor cells within lymph nodes.

Lymph node metastasis should be distinguished from benign glandular lymph node inclusions, which are extremely rare in peripancreatic lymph nodes, but not so uncommon in abdominal lymph nodes of females (see Chap. 13, Sect. 13.6).

9.11.3 Lymphatic, Vascular, and Perineural Tumor Spread

The presence of tumor within lymphatic channels, blood vessels, or perineural clefts is staged as pL1, pV1, or pPn1. These descriptors are binary, hence they describe only the presence or absence of the particular mode of tumor spread, but do not reflect whether this is a common or rare finding within a given tumor. The accuracy of reporting depends on multiple factors, including the number of sections examined and whether ancillary techniques (elastica van Gieson staining or immunohistochemistry for CD31, D2-40, or S100) are used to identify blood and lymphatic vessels or peripheral nerves. These modes of tumor propagation are not as strong prognostic factors as tumor stage. On occasion, tumor growth within a large vessel, most commonly the splenic vein, may be visible macroscopically and should then be reported as pV2 (Fig. 9.41).

9.11.4 Resection Margin Status

The R descriptor refers to the presence or absence of residual disease. However, in clinical practice, the R-stage is usually regarded as synonymous to the resection margin status. To date there is no

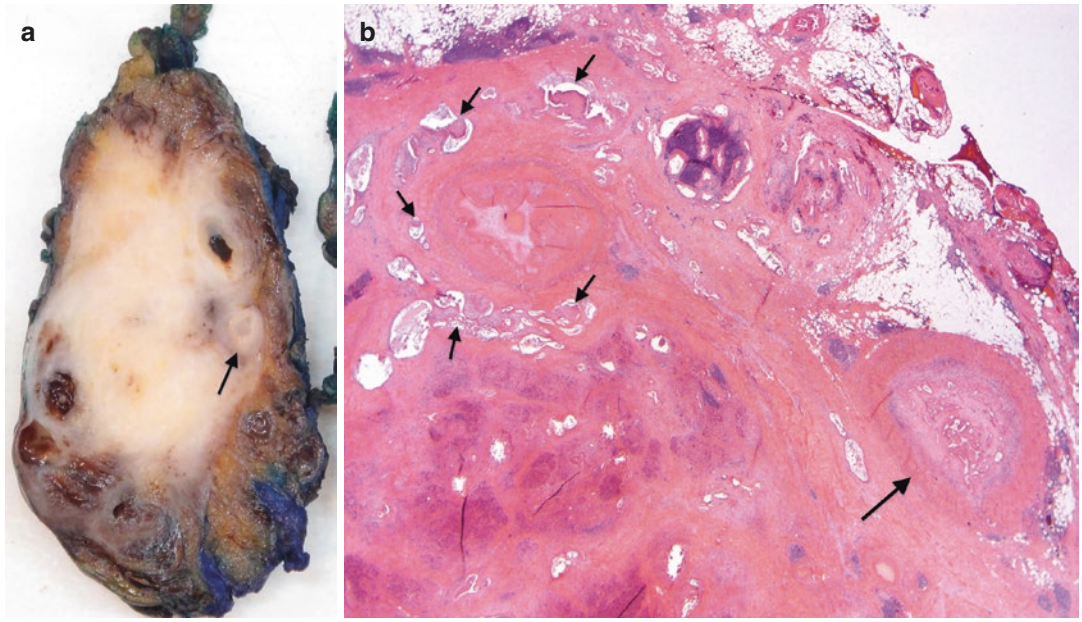

Fig. 9.41 Tumor occlusion of the splenic vein: the splenic vein is occluded by tumor (*arrow*, **a**). Histology confirms venous tumor occlusion (*long arrow*). Note the presence of a small lymph node metastasis and extensive tumor propagation along the neural plexus surrounding the splenic artery (*short arrows*, **b**)

universally accepted, evidence-based definition of microscopic margin involvement (pR1) in pancreatic cancer. In most countries, pR1 is defined as the presence of tumor cells within 1 mm of a margin (Fig. 9.42). However, this '1 mm rule' is a mere adoption from rectal cancer, for which clinicopathological correlation studies have shown a significant association between a clearance of up to 1 mm and an increased risk of local tumor recurrence. Such studies have not been performed for pancreatic cancer, and consequently, the minimum clearance appropriate for this malignancy is not known. In view of the more dispersed growth pattern in pancreatic compared to rectal cancer, the 1 mm rule may underestimate the presence of microscopic residual disease [28].

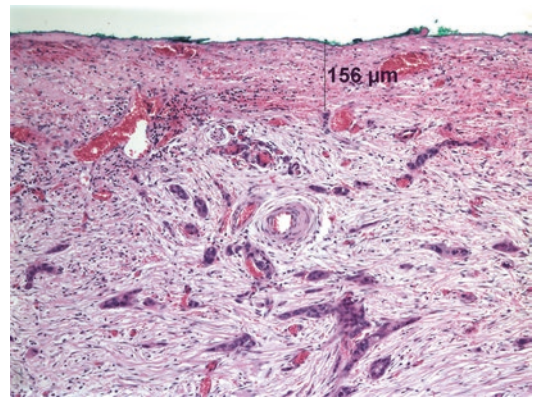

Fig. 9.42 Microscopic margin involvement: invasive adenocarcinoma lies within 1 mm of the inked circumferential resection margin

Further controversy exists as to whether microscopic margin involvement relates only to direct tumor growth or whether it can also be applied to tumor cells within lymphovascular channels or perineural clefts that are present within 1 mm to the margin. Regarding lymph node metastasis, it seems sound to record microscopic margin involvement only if there is extranodal tumor growth within 1 mm of the margin (Fig. 9.43). In practice, however, microscopic margin involvement will be identified in the majority of cases (over 75%), even if based exclusively on direct tumor growth, provided the specimen has been properly dissected and sampled.

Tumor involvement of the transection margins of the pancreatic neck or common bile duct is often assessed intraoperatively by frozen section examination (see Chap. 23, Sect. 23.3). In con-

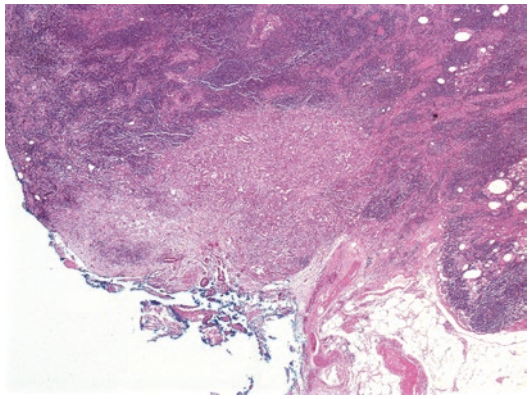

Fig. 9.43 Microscopic margin involvement: a lymph node metastasis with tumor extension into the perinodal fat is present at the inked circumferential resection margin

trast, there is no clear indication for assessment of the circumferential resection margins, because involvement of any of these margins has usually no surgical implication, since the resection in these areas cannot be extended, provided the surgery is performed according to current standards [29]. Microscopic tumor involvement is reported most frequently at the posterior margin and the margins facing the superior mesenteric vein (SMV) and artery (SMA) (see Fig. 3.5). Amongst the various circumferential resection margins, the SMA-facing margin is the only true resection margin, that is, the only area where the surgeon transects tissue, in this case the soft tissue adjacent to the SMA. The posterior margin and the margins at the SMV and around the extrapancreatic bile duct are so-called dissection margins, where the surgeon bluntly dissects tissue along an anatomical plane. It remains to be seen whether involvement of either type of margin—resection or dissection—is of similar prognostic significance [30].

Involvement of the anterior surface is rather uncommon, but occasionally it may be suspected already during macroscopic inspection, when the tumor protrudes and is visible on the anterior surface of the pancreas (Fig. 9.44). In pancreatoduodenectomy specimens, involvement of the anterior surface is often detected at the anterior pancreatoduodenal crevice, the anatomical narrow where the anterior surface curves inward before reaching the anterior duodenal wall (see Fig. 3.26). Because the anterior surface is a true anatomical surface rather than a surgical resection margin, reporting of R1 should be based on a clearance of 0 mm, i.e., tumor cells should be present at the surface (Fig. 9.45).

Special attention should be given to the margins of tangential or segmental resections of the superior mesenteric or portal vein. While the transection margin of the venous tissue is usually clear of tumor, microscopic tumor infiltration up to the specimen surface where the vein is adherent to the SMV groove is commonly seen (Figs. 9.46 and 9.47) [31].

According to the UICC definition, R2 denotes the presence of macroscopic residual disease. However, in clinical practice R2 is usually interpreted as macroscopic margin involvement. An R2 surgical resection usually suggests underestimation of local tumor extent and resectability on preoperative imaging. Discussion sometimes arises as to who should make the diagnosis of R2—the surgeon or the pathologist—and where the difference between microscopic and macroscopic margin involvement exactly lies. The distinction between R1 and R2 seems indeed to be important, as the prognosis is significantly worse after R2 resection. In many pancreatic cancer centers it has been agreed that a diagnosis of R2 resection depends on the surgeon's assessment. In practice, it may be more objective and informative if the pathologist refrains from using the R2 terminology, but instead simply states the extent over which the specimen surface is involved by tumor (Fig. 9.48).

9.12 Differential Diagnosis

The diagnosis of ductal adenocarcinoma of the pancreas may on occasion require differential diagnostic considerations to distinguish it from reactive pancreatic changes (especially in the context of chronic pancreatitis) and from primary pancreatic or metastatic tumors. Distinction of ductal adenocarcinoma from this variety of lesions is of paramount importance, because the treatment, follow-up, and prognosis for the various entities differ significantly. Immunohistochemistry may be helpful on many

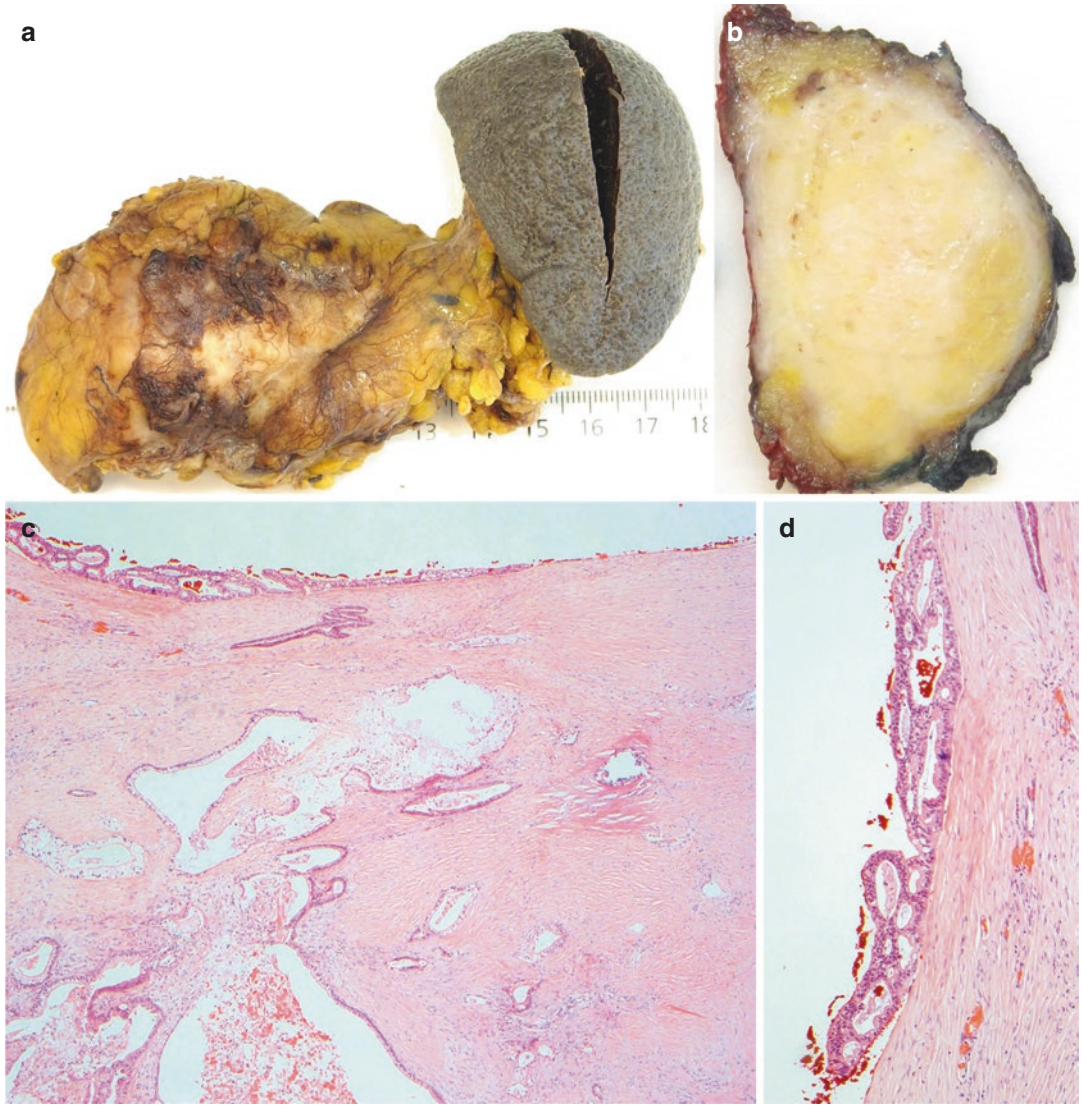

Fig. 9.44 Involvement of the anterior pancreatic surface: a large tumor protrudes from the anterior pancreatic surface (**a**). On cut section, tumor tissue lies directly underneath the red-inked anterior surface (**b**). Histologically, the well-differentiated ductal adenocarcinoma grows extensively on the anterior surface (**c**). Note the red ink on the anterior specimen surface (**d**)

occasions, but meticulous macroscopic and microscopic examination remains the backbone of the differential diagnosis.

9.12.1 Chronic Pancreatitis and Reactive Duct Changes

The distinction between ductal adenocarcinoma and reactive ducts, for example, in the context of chronic pancreatitis, can be problematic, especially in biopsy material or on frozen section. However, even in surgical resection material from patients with known chronic pancreatitis, definitive exclusion or diagnosis of ductal adenocarcinoma may be difficult, as both diseases can share multiple microscopic features. In chronic pancreatitis, gradual atrophy and fibrosis of the gland result in a vast fibrous stroma with a small number of scattered ductular structures, some of

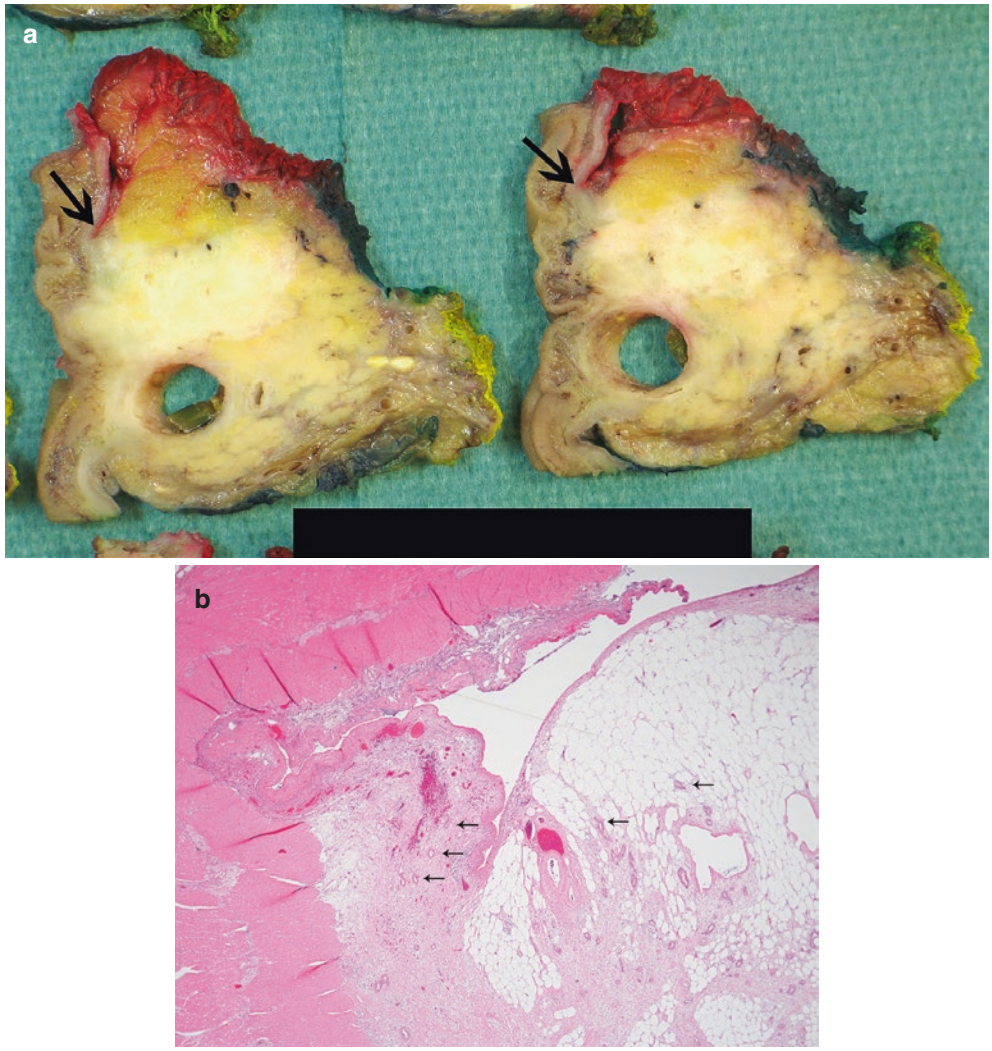

Fig. 9.45 Microscopic involvement of anterior surface: ductal adenocarcinoma located in the anterior part of the pancreatic head infiltrates the anterior peripancreatic fat and extends close to the anterior pancreatoduodenal crevice (*arrows*; **a**). Microscopically, tumor glands (*arrows*) lie close to, but do not breach the anterior surface (pR0; **b**)

which may show architectural and cytological atypia (see Chap. 7, Sect. 7.2.4, Fig. 7.36). This microscopic picture is not dissimilar from that of ductal adenocarcinoma, in which invasive tumor glands, exhibiting only mild atypia in case of a well-differentiated tumor, are spread out in the desmoplastic tumor stroma. Interspersed residual islets, acini, and unequivocal normal pancreatic ducts may be found in both chronic pancreatitis and ductal adenocarcinoma.

The resolution of this differential diagnosis is first and foremost based on the assessment of two architectural features: lobular architecture and segregation of blood vessels and pancreatic ducts. Lobular architecture is mainly preserved in chronic pancreatitis. Even if acinar atrophy is advanced, the outline of the lobules can remain identifiable by the distinct quality of the intralobular stroma, which is looser and slightly more basophilic than the dense collagen-rich fibrous stroma that surrounds the lobules (see Chap. 7, Sect. 7.2.4, Fig. 7.32). In contrast, in ductal adenocarcinoma, tumor glands are haphazardly distributed, across lobular boundaries, and irrespective of the branching system of the pancreatic ducts (Fig. 9.49).

In the normal pancreas, muscular blood vessels and pancreatic ducts take a different course

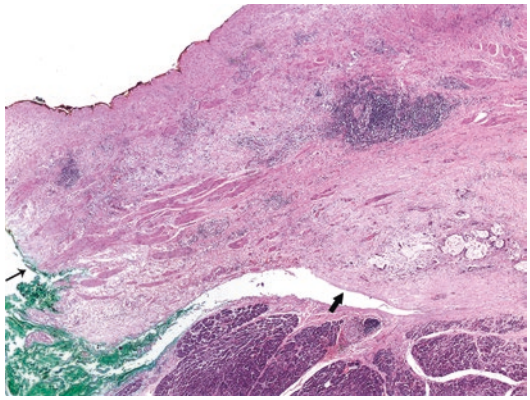

Fig. 9.46 Microscopic margin involvement around SMV resection: adenocarcinoma infiltrates the SMV groove and tunica adventitia of the SMV. While the transection margin of the vein is clear (*arrow*), tumor is present within 1 mm of the SMV margin (*block arrow*)

and are separated by acinar parenchyma (see Chap. 1, Sect. 1.4.5, Fig. 1.23). Therefore, the finding of a ductular structure in close approximation of a muscular blood vessel is highly suggestive of invasive adenocarcinoma (Figs. 9.50 and 9.51a). While this architectural feature is usually retained well into later stages of chronic pancreatitis, due to the gradual acinar atrophy and subsequent collapse, the separation of residual pancreatic ducts and muscular blood vessels will ultimately become reduced [32, 33]. Therefore, the use of this architectural feature should be circumspect in cases with advanced acinar atrophy (Fig. 9.51b) (see Figs. 7.33, 7.34, and 7.35). In contrast, even in advanced fatty infiltration of the

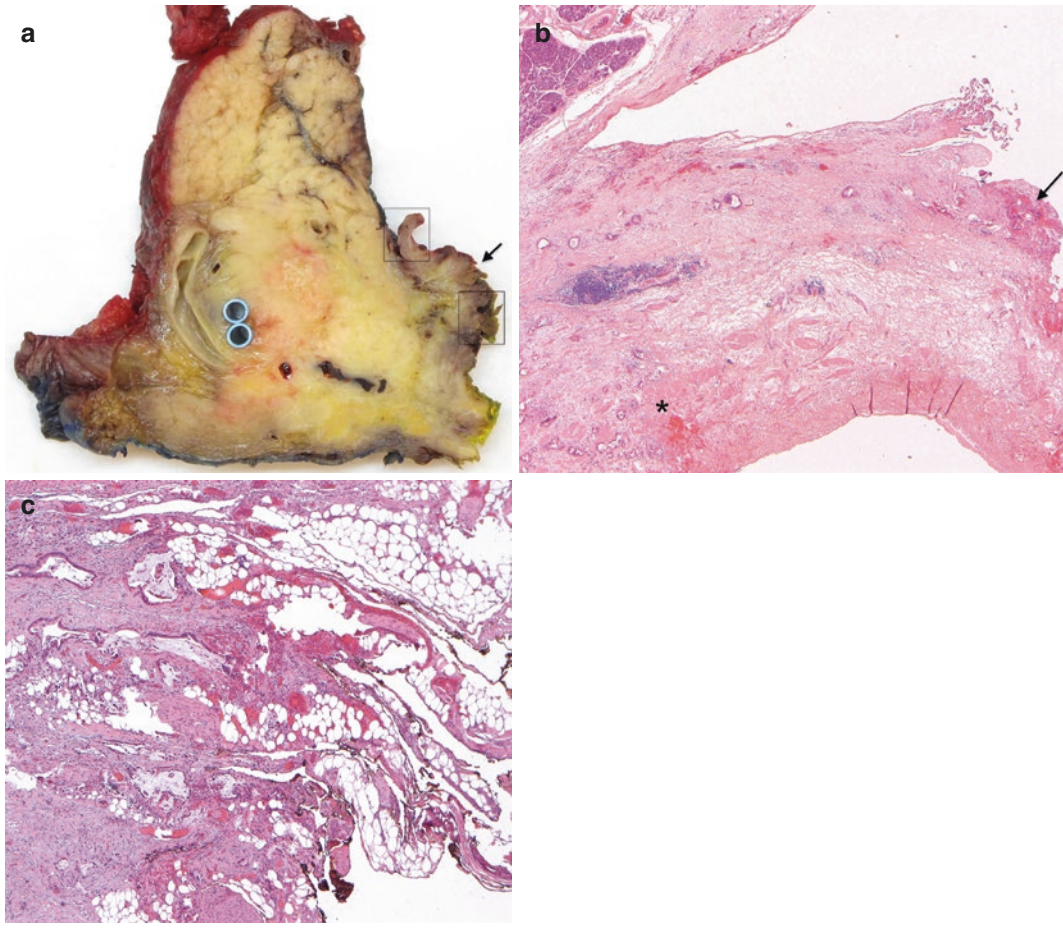

Fig. 9.47 Microscopic margin involvement around SMV resection: an ill-circumscribed ductal adenocarcinoma infiltrates the uncinate process. Note the irregular soft tissue flanking one side of the venous resection (*arrow*). The *boxes* indicate the areas that are shown at higher magnification in (**b**) and (**c**). Microscopically, tumor infiltrates the tunica media (*asterisk*) and adventitial soft tissue up to the transection margin of the venous sleeve (*arrow*, **b**). There is broad tumor infiltration of the irregular peripancreatic soft tissue that flanks the SMV-resection, with involvement of the overlying, inked margin (**c**)

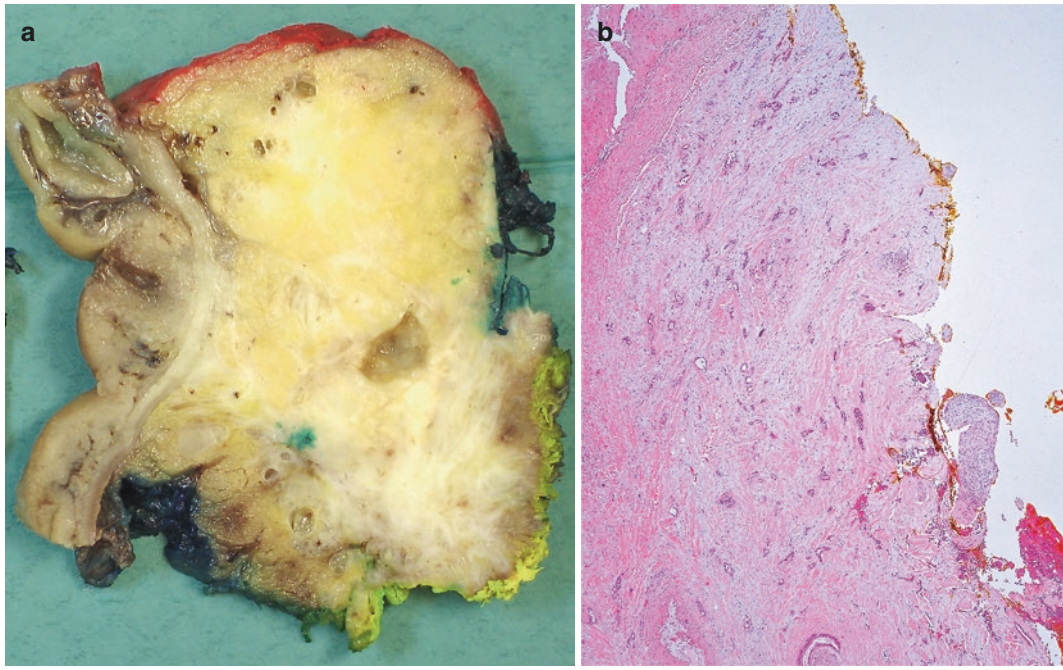

Fig. 9.48 Extensive microscopic margin involvement: there is broad tumor growth onto the SMA margin, which is inked yellow (**a**). Microscopically, there is extensive tumor growth within 1 mm to that margin (**b**)

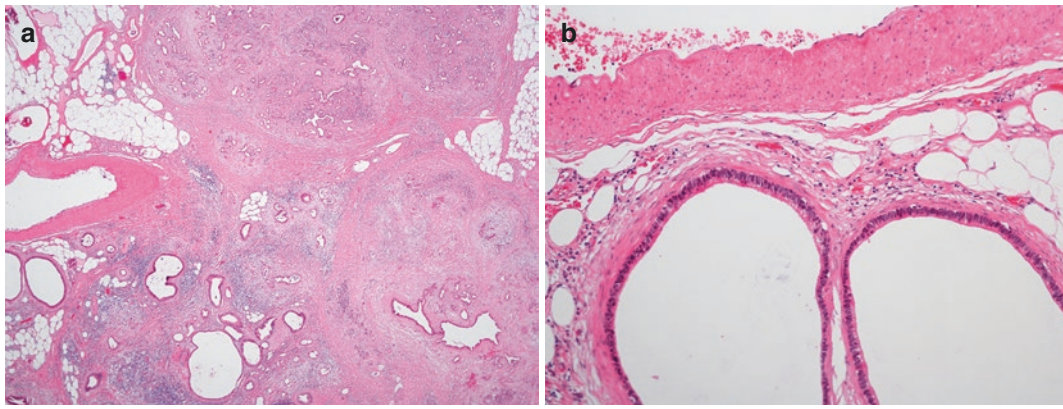

Fig. 9.49 Loss of normal tissue architecture: lobular boundaries are clearly outlined in the upper-right of the picture, whereas in the lower-left corner, large ductular structures efface the lobular architecture (**a**). Despite the rather bland cytology of some ducts, their presence adjacent to a muscular artery confirms this is adenocarcinoma (**b**)

pancreas, individual glands in chronic pancreatitis are usually surrounded by a small amount of stroma, whereas so-called naked glands, devoid of any associated stroma, can be seen at the invasive front of ductal adenocarcinoma (see Sect. 9.6.1).

Cytological features are also important in the distinction between pancreatic cancer and reactive ductular structures, and these criteria are discussed in detail in Chap. 23. The use of immunohistochemical staining has been discussed earlier in this chapter (see Sect. 9.9.3).

Chronic pancreatitis also causes changes to the endocrine compartment that may require careful consideration. Islet cells may exhibit marked nuclear atypia, which may raise the sus-

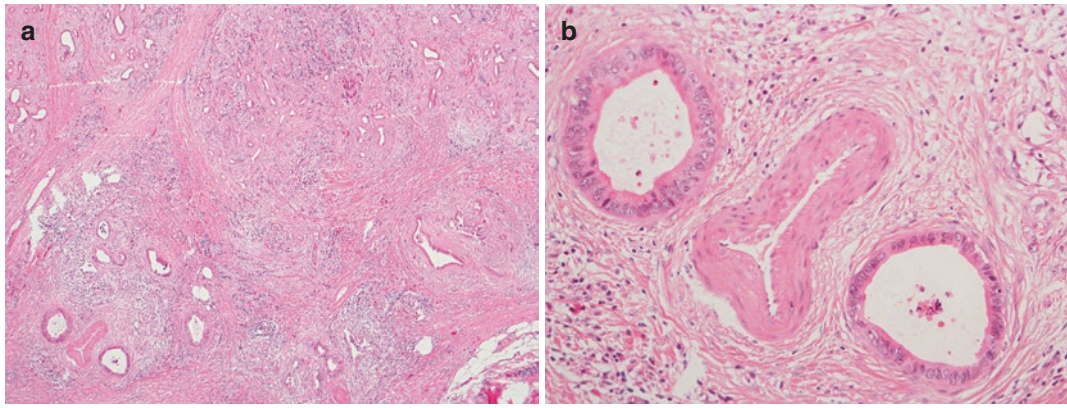

Fig. 9.50 Loss of normal tissue architecture: the loss of lobular architecture, presence of glandular structures next to a muscular artery (**a**), and cytological atypia (**b**) confirm that this is invasive ductal adenocarcinoma

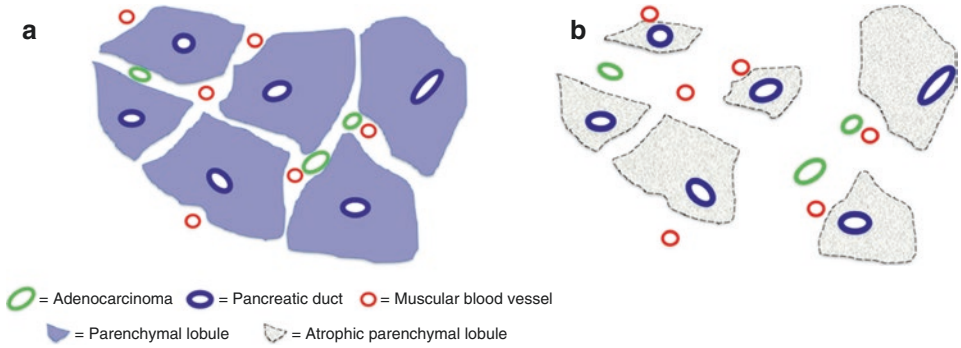

Fig. 9.51 Altered spatial relationship between intralobular ducts and muscular blood vessels following acinar atrophy: in normal pancreas, intralobular ducts and muscular blood vessels are separated by acinar parenchyma. Ductlike structures flanking muscular blood vessels are therefore suspicious of invasive carcinoma (**a**). As acinar atrophy progresses and lobules become smaller, gradual collapse of the tissue architecture may result in the proximity of intralobular ducts and muscular blood vessels, which should not be mistaken as evidence of malignancy (**b**)

picion of ductal adenocarcinoma if these atypical islet cells are present in any of the three following scenarios: (i) if islets are fragmented and small solid nests and strands of residual islets cells are scattered in dense fibrous stroma (Fig. 9.52); (ii) if islets are intimately associated with nonneoplastic glands; (iii) if, on rare occasion, islet cells associate intimately with peripheral nerves and thus mimic perineural invasion (see Fig. 7.30).

9.12.2 Other Pancreatic Neoplasms

A summary of the main differential diagnostic features of the primary solid pancreatic neoplasms is presented in Table 20.5.

9.12.2.1 Acinar Cell Carcinoma

The distinction between acinar cell carcinoma and ductal adenocarcinoma is usually straightforward. A lobulated appearance, high cellularity, scanty stroma within the tumor lobules, and an acinar growth pattern are features of acinar cell carcinoma. In addition, cytological detail and preserved nuclear uniformity, despite a high proliferative activity, are further findings in favor of acinar cell carcinoma (see Chap. 10). Careful consideration should be given to cancers with a signet ring or clear cell morphology, as these can be variants of both ductal adenocarcinoma and acinar cell carcinoma. Immunostaining for the enzymes trypsin and chymotrypsin and for the acinar cell marker BCL10 is the most useful

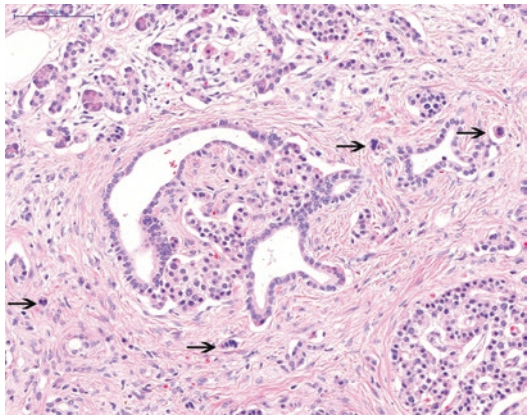

Fig. 9.52 Altered islets mimicking ductal adenocarcinoma: fragmented residual islets composed of small endocrine cell clusters showing nuclear atypia (*arrows*) should not be confounded with poorly differentiated adenocarcinoma

ancillary test to make the distinction, while immunolabeling for CEA can be focally present, and expression of cytokeratins 7 and 19 can also be seen in a proportion of acinar cell carcinomas.

9.12.2.2 Pancreatic Neuroendocrine Neoplasia

Pancreatic neuroendocrine tumors grade 1–3 (PanNETs) are always to be included in the differential diagnosis of ductal adenocarcinoma, as the former may assume a tubular, glandular, or cribriform growth pattern. The stroma of PanNETs can vary, but may be extensive and hyaline, and as such not entirely different from the desmoplastic stroma in ductal adenocarcinoma. With the exception of the pleomorphic variant, PanNETs usually exhibit less cytological atypia than ductal adenocarcinoma, and the uniformity of their centrally placed nuclei, the stippled chromatin pattern, and the absence of prominent nucleoli are distinguishing features. Because the mitotic activity in ductal adenocarcinoma may vary considerably, this is not usually a reliable criterion to distinguish ductal adenocarcinoma from PanNETs. Further morphological and immunohistochemical criteria on which to base this important differential diagnosis are discussed in detail in Chap. 20, Sect. 20.9.

Less obvious may be the distinction between adenocarcinoma and pancreatic neuroendocrine carcinoma (PanNEC) of large cell type, which usually lacks the above-described distinctive morphological features of grade 1–3 PanNETs. Immunostaining for neuroendocrine markers is usually needed to ascertain the correct diagnosis.

Special attention is required for the distinction between ductal adenocarcinoma and mixed neuroendocrine-non-neuroendocrine neoplasm (MiNEN), as by definition, these neoplasms exhibit ductal differentiation in at least one third of the tumor mass. The confirmation of neuroendocrine differentiation in the remainder of the tumor will indicate the correct diagnosis.

9.12.2.3 Solid Pseudopapillary Neoplasm

While solid pseudopapillary neoplasms have a strong predilection for young females, they may also be found in males and at an older age. However, both the macroscopic and microscopic features of these tumors are usually distinct from ductal adenocarcinoma, and both tumors have different immunohistochemical profiles (see Chap. 18 and Table 20.5). The rare solid pseudopapillary neoplasms that exhibit prominent cytoplasmic vacuolization may mimic the signet ring cell subtype of ductal adenocarcinoma (see Sect. 9.14.3). However, the intracytoplasmic vacuoles are—unlike those in adenocarcinoma—devoid of mucin. Poorly differentiated tumor areas lacking the characteristic features of solid pseudopapillary neoplasm have been reported in a few patients with an unusually short survival (see Chap. 18). While, in isolation, these areas may be more difficult to distinguish from (poorly differentiated) ductal adenocarcinoma, they are usually found in only a part of the tumor mass, the remainder of which exhibits features characteristic of solid pseudopapillary neoplasia.

9.12.3 Adenocarcinoma of Ampullary, Distal Bile Duct, or Duodenal Origin

Pancreatic, ampullary, and distal bile duct cancer are often collectively denoted as periampullary cancers or pancreatic head cancers. The reason for this grouping is the anatomical proximity of

the parent tissues, which can render pathological identification of the cancer origin difficult, especially in tumors of a large size. Some authors define periampullary cancer as a carcinoma arising within 2 cm of the major duodenal papilla. While this term may be useful as a clinical working diagnosis, it is inaccurate and should be avoided in pathology reports.

Duodenal adenocarcinoma can usually be excluded from the group of pancreatic head cancers based on its extensive, not uncommonly circumferential, involvement of the bowel wall, which is highly unusual in primary pancreatic, ampullary, or distal bile duct carcinoma. Because duodenal carcinoma may show a range of morphologies, including pancreatobiliary and gastric-like features, in addition to the intestinal type [34], microscopic and immunohistochemical examination may be of limited help to distinguish it from primary pancreatic cancer. Furthermore, pancreatic cancer may occasionally mimic duodenal carcinoma at a microscopic level, as it can acquire a more intestinal phenotype when infiltrating the duodenal wall, and it may simulate duodenal intramucosal neoplasia by spreading within the lamina propria (see Sect. 9.6.3; see Figs. 9.19 and 9.20).

Rigorous distinction between the different pancreatic head cancers is of direct relevance to individual patient management. First and foremost, clinical evidence suggests that these cancers differ in prognosis. Hence, careful distinction is essential for accurate prediction of outcome. Second, cancer origin determines to a major extent the indication for and selection of adjuvant treatment as well as the patient's participation in clinical trials. Furthermore, accurate identification of the tumor origin is important for correct staging, as the T-staging criteria differ between the pancreatic head cancers. In the long term and irrespective of individual patient management, exact diagnostic distinction between the cancer groups is a prerequisite for identification of possible differences in epidemiology, etiology, and molecular biology.

Identification of the cancer origin is based on (i) the anatomical relationship of the center of the tumor mass to the ampulla, common bile duct, and pancreas, and (ii) the presence of a neoplastic precursor lesion. The localization of the center of the tumor is the most important diagnostic criterion, as precursor lesions are often lacking or may be present fortuitously (see below). Careful gross examination of the three-dimensional relationship of the cancer to the key anatomical structures as outlined in Chap. 3 is of paramount importance and cannot be substituted by histomorphological or immunohistochemical investigations, because the microscopic features and immunoprofiles are largely shared among the three cancer groups (Fig. 9.53). While intestinal type adenocarcinoma is more common in the group of ampullary cancers compared to primary pancreatic and common bile duct carcinoma, the difference in relative incidence is not helpful for the correct diagnosis in the individual case. Furthermore, the suggested immunohistochemical signature to distinguish between intestinal and pancreatobiliary type ampullary adenocarcinomas based on a panel, including MUC1, MUC2, CDX2, and CK20 [35], may at times be useful, although subtyping is not always straightforward, and a significant proportion of carcinomas has hybrid features [36].

In *adenocarcinoma arising from the ampulla*, the center of the tumor will be located at mid-level of the craniocaudal length of the pancreatic head. As the tumor increases in size, it will involve the adjacent duodenal wall and pancreatic parenchyma and eventually extend into the peripancreatic soft tissue of the anterior and/or posterior pancreatoduodenal crevice (Figs. 9.54 and 9.55). In contrast, due to the location of the common bile duct in the posterior aspect of the pancreatic head (see Chap. 1, Sect. 1.3.2), *cancer developing from the intrapancreatic common bile duct* will predominantly involve the posterior part of the pancreatic head and peripancreatic soft tissue in the cranial half of the pancreatic head (Fig. 9.56). In *adenocarcinoma arising in the extrapancreatic common bile duct*, tumor involvement will be found mainly in the soft tissue sheath around the common bile duct stump and in the superior part of the pancreatic head (Fig. 9.57). As ductal adenocarcinoma can originate anywhere within the pancreatic head, it may involve any part of the pancreas and/or surrounding tissues (Fig. 9.53), including the common bile duct,

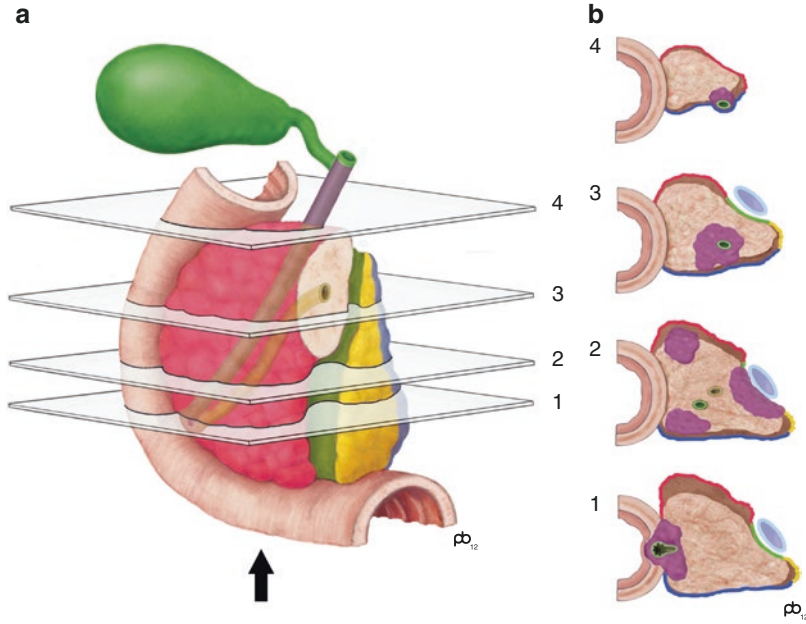

Fig. 9.53 Localization of periampullary cancers: the craniocaudal localization of a tumor (**a**) and its position within the axial specimen slices (**b**) is key to identification of the cancer origin. Ampullary carcinoma is located at and around the ampulla at mid craniocaudal height (1). Pancreatic carcinoma can be located anywhere within the pancreatic head (2). Cancer of the intrapancreatic bile duct is seated in the posterior part of the pancreatic head, above the level of the ampulla (3). Carcinoma arising from the extrapancreatic common bile duct is located in the cranial part of a pancreatoduodenectomy specimen and centers on the short extrapancreatic bile duct stump (4). (Image courtesy and copyright of Paul Brown, The Leeds Teaching Hospitals NHS Trust, Leeds, UK)

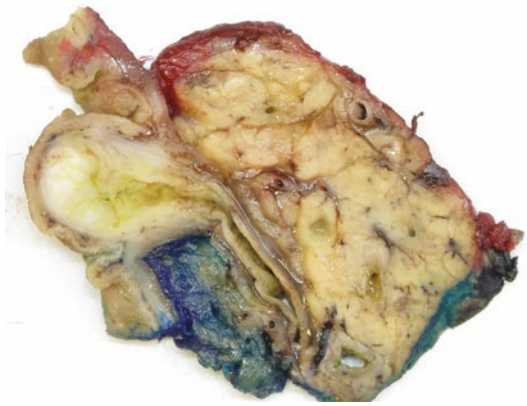

Fig. 9.54 Ampullary carcinoma: a well-circumscribed carcinoma involves the ampulla of Vater. Note the dilated main pancreatic duct

which is then secondarily involved and therefore does not lie in the center of the tumor mass (Fig. 9.58). If a tumor is located caudal to the level of the ampulla and in the part of the pancreatic head that is close to the superior mesenteric artery, origin from the ampulla, duodenum, or common bile duct can be excluded.

Meticulous assessment of the local anatomical landmarks is also important for the correct identification of the localization of precursor lesions. The latter are most frequently found in association with ampullary cancer, the reported incidence amounting to over 80%. In contrast, precursor neoplasia of the bile duct is much less commonly observed in association with distal bile duct carcinoma (10%–33%), and it usually presents as flat dysplasia rather than an adenomatous polypoid lesion. The diagnostic usefulness of pancreatic intraepithelial neoplasia (PanIN) as evidence of the pancreatic origin of an adenocarcinoma is limited, because low-grade PanIN is a common finding in the general population, especially over the age of 40, and it can be fortuitously coexistent with non-pancreatic cancer (see Chap. 8). If PanIN changes are high-grade, distinction from secondary duct cancerization may be problematic (see Fig. 9.37).

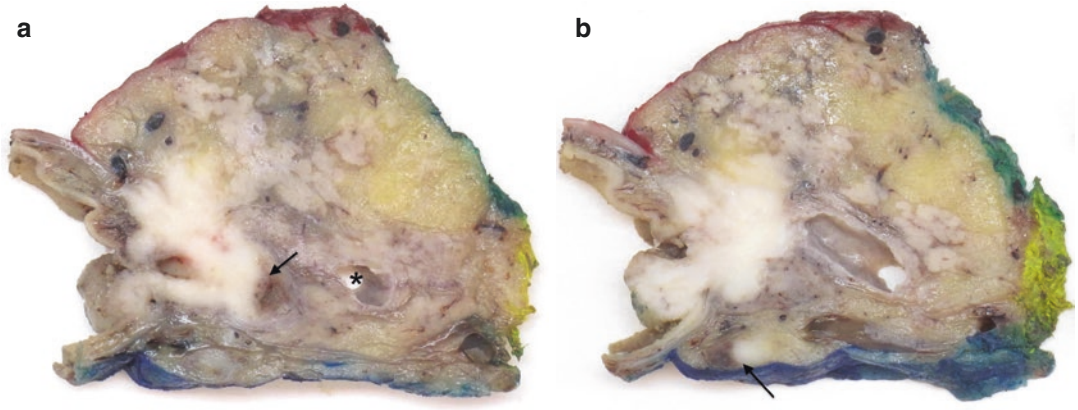

Fig. 9.55 Ampullary carcinoma: a locally advanced carcinoma infiltrates the ampulla of Vater and extends into the dilated distal common bile duct (*arrow*). Note the dilated main pancreatic duct (*asterisk*, **a**). There is also tumor invasion of the duodenal papilla and early infiltration of the pancreas. Note the presence of a peripancreatic lymph node metastasis (*arrow*, **b**)

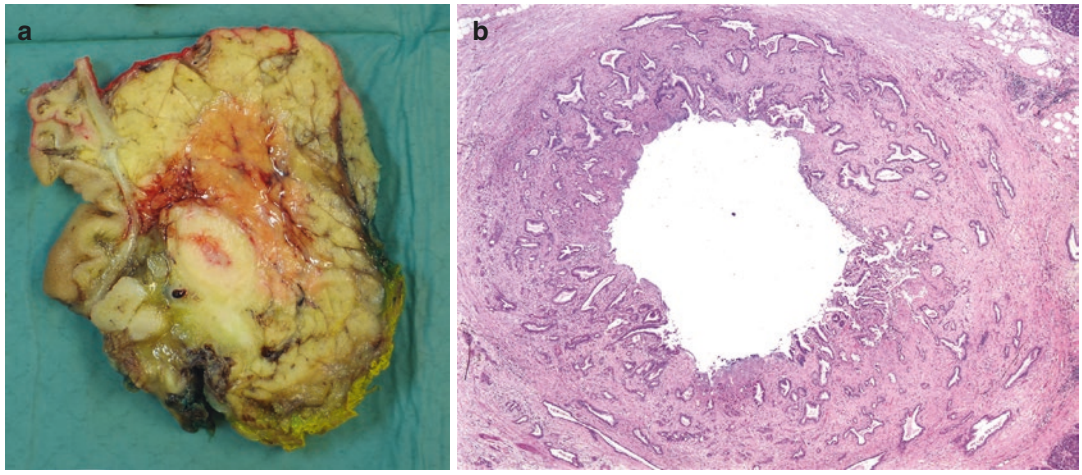

Fig. 9.56 Carcinoma of the intrapancreatic bile duct: the wall of the bile duct is thickened and its lumen narrowed by tumor, which extends into the surrounding pancreatic tissue (**a**). Microscopically, adenocarcinoma encircles the bile duct wall and infiltrates the periductal stroma (**b**)

9.12.4 Metastasis from Extrapancreatic Primaries

The distinction between ductal adenocarcinoma of the pancreas and metastasis from extrapancreatic primary cancers is discussed in Chap. 12.

9.13 Treatment and Prognosis

Ductal adenocarcinoma is fatal in almost all patients. This dire outcome is the combined result of the intrinsic aggressiveness of the cancer, the lack of effective cytotoxic treatment, and the late stage at which these tumors are usually detected. In line with the carcinogenesis model of ductal

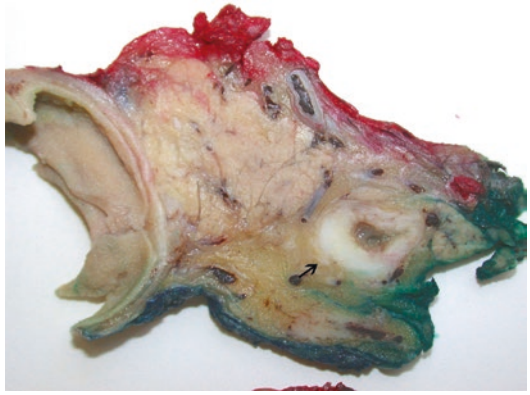

Fig. 9.57 Carcinoma of the extrapancreatic bile duct: white tumor tissue shows segmental infiltration of the extrapancreatic common bile duct. Note early tumor extension into the periductal soft tissue (*arrow*) and the proximity to the periductal circumferential margin (inked green)

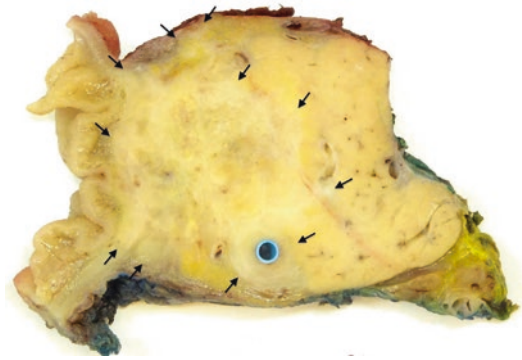

Fig. 9.58 Pancreatic cancer with secondary involvement of the common bile duct: this large pancreatic cancer involves mainly the anterolateral part of the pancreatic head and the duodenal wall (*arrows*). At its periphery, the tumor also infiltrates half of the circumference of the (stented) common bile duct

adenocarcinoma that is based on a linear progression through the various stages of pancreatic intraepithelial neoplasia (PanIN) and the concomitant accumulation of mutations (see Chap. 8), it has been estimated that more than a decade has elapsed between the occurrence of the initiating mutations and the establishment of the first metastasis. According to this computational model, patients die on average 2 years thereafter [2]. While in theory this offers a large window of opportunity for diagnosis of pancreatic cancer at a curative stage, the early and rapid metastatic spread that characterizes the disease as well as the fact that even small tumors (< 2 cm) have already metastasized, argue against gradual pancreatic cancer progression. Recently, an alternative "cataclysmic" model has been suggested, according to which large-scale and complex, simultaneous rather than sequential, genomic errors occur that lead within a short time span to aggressive invasive and metastasizing tumors [37]. Further knowledge about the progression of ductal adenocarcinoma is essential to guide more effective screening and treatment strategies.

Surgical resection is currently the only potentially curative treatment option. However, only 15–20% of patients are eligible for surgery at the time of diagnosis. In the remaining 80% of patients, the tumor is locoregionally too advanced to be resected or has metastasized to distant sites, mainly to the liver. Despite recent advances in surgical techniques allowing, for example, safe resection of ductal adenocarcinomas with a degree of involvement of the superior mesenteric vessels or portal vein, the mean survival after surgical resection is only 10–20 months [38]. In comparison, for patients who do not undergo surgical resection, the mean survival is 3 to 5 months. Even after successful surgical resection with curative intent, the majority of patients (70–90%) develop disease recurrence, most within 2 years after surgery. Correspondingly, the 5-year survival rate for patients following surgical resection is approximately 10–25%, compared to 8% for patients with inoperable disease [38]. Distant metastasis—in decreasing order to the liver, peritoneum, and lung—and local recurrence develop with a similar frequency [39]. However, patients rarely die of the latter but rather of distant metastasis, which usually exerts its fatal effect before local tumor recurrence becomes the determinant of outcome.

Since most pancreatic cancers that are surgically resected show a full house of adverse prognostic factors—the typical stage being pT2N1L1V1Pn1R1—it is difficult to assess the prognostic impact of each individual factor. Furthermore, many published data are based on retrospective analysis of series that date back to

before the late 1990s, when specimen handling and microscopic reporting were not standardized and pathology assessment was less meticulous than what is currently regarded as good practice. Hence, not surprisingly, key pathology data from various centers differ significantly. Overall, however, pT-, pN-, and pM-stage are strong prognostic factors, while vascular and perineurial invasion, and the grade of differentiation seem to be of weaker predictive value.

Adjuvant treatment has become part of the standard therapy for ductal adenocarcinoma of the pancreas; its survival benefit is statistically significant but limited, increasing the median survival by a few months. The discussion of whether adjuvant treatment should be based on chemotherapy or chemoradiotherapy is still ongoing [38].

Despite adjuvant treatment, most patients die of distant metastasis, and some do after such a short postoperative time interval that the presence of occult metastasis at the time of surgery must be assumed. Since pancreatic disease seems to be a systemic disease at presentation in most patients, moving chemo(radio)therapy to the preoperative setting seems to be appropriate. Indeed, neoadjuvant chemo(radio)therapy offers systemic treatment at the earliest possible moment rather than at a later time point (if and) when the patient has recovered from surgery, which offers ultimately only a local form of treatment. In addition, patients may manifest clinically detectable metastasis or an aggressive disease course during the neoadjuvant treatment period, that is, before unnecessary surgery is undertaken. Finally, with preoperative chemo(radio)therapy, the risk of R1 resection may be reduced, and treatment is delivered to tissues that are not yet rendered less receptive to cytotoxic treatment due to surgery-induced inflammation and hypoxia.

In recent years, chemo(radio)therapy is also considered for patients with locally advanced pancreatic cancer with the intention to reduce tumor size and extent, such that the cancer becomes resectable. For the approximately 20% of patients whose tumor can be surgically removed, survival improves to a level that is comparable with that of patients with primary operable disease [38].

Limited data are available regarding the prognosis and response to (neo-)adjuvant treatment of the subtypes of ductal adenocarcinoma, which are discussed in the next section. While most subtypes have an equally poor or even worse outcome, colloid and medullary carcinoma seem to portend a better prognosis.

9.14 Histological Subtypes of Ductal Adenocarcinoma

This diagnostic group encompasses tumors that are regarded as subtypes of pancreatic cancer, because they exhibit significant other features of differentiation in addition to the morphology of conventional ductal adenocarcinoma. These subtypes do not only exhibit a distinct morphological appearance but differ also clinically and in terms of patient outcome. Staging of the variant tumors follows the TNM UICC system (eighth edition) for carcinoma of the exocrine pancreas (Table 9.3). The subtypes of ductal adenocarcinoma are rare tumors, which overall account for up to 3–4% of all malignancies of the exocrine pancreas. Colloid carcinoma may be slightly less uncommon, as it can develop in association with intraductal papillary mucinous neoplasia (see Chap. 17). Occasionally, ductal adenocarcinomas with a distinct histomorphology—for example, oncocytic—that differs from the below-described subtypes, have been reported. However, because their clinical and biological features are currently not well defined, they are currently not considered separate subtypes by the WHO classification.

9.14.1 Adenosquamous Carcinoma and Squamous Cell Carcinoma

This subtype shows significant ductal and squamous differentiation. The latter should represent at least 30% of the entire tumor mass. While this cut-off is arbitrary, it is useful in distinguishing this subtype from the occasional presence of small foci of squamous differentiation within otherwise conventional ductal adenocarcinoma, a

finding that is of no clinical significance. Tumors with predominant squamous differentiation and only focal evidence of ductal differentiation should also be reported as adenosquamous carcinoma. True squamous cell carcinoma with pure squamous differentiation is extremely rare in pancreatic cancer, and if ductal differentiation is not identified despite thorough tumor sampling, metastasis from an extrapancreatic primary (e.g., lung cancer) should be excluded. Adenosquamous carcinoma does not usually differ from conventional ductal adenocarcinoma in its clinical presentation and macroscopic appearance. There is no known association with any specific clinical syndrome.

Microscopically, the areas of squamous differentiation are usually intimately admixed with those of conventional ductal adenocarcinoma. They show the usual characteristic features of squamous cell carcinoma, including a growth pattern of solid sheets and clusters with often a layered or swirling cellular arrangement, and polygonal tumor cells with distinct cellular borders, intercellular junctions, deeply eosinophilic cytoplasm, and a varying degree of keratinization (Fig. 9.59). Immunostaining for the markers p63, p40, and cytokeratins (CKs) 5/6 and 14 may be helpful in confirming the presence and evaluating the extent of squamous differentiation. Immunolabeling for CK7, CK20, and CA19-9 is usually limited to the ductal component, which may also be highlighted by mucin stains. The molecular signature and immunohistochemical profile of adenosquamous carcinoma showing loss of p16 and SMAD4, and strong nuclear staining for p53 are similar to those found in conventional ductal adenocarcinoma. Limited evidence suggests that adenosquamous carcinoma falls into the basal-like subtype of the transcription-based classification of pancreatic ductal adenocarcinoma (see Sect. 9.18) [40].

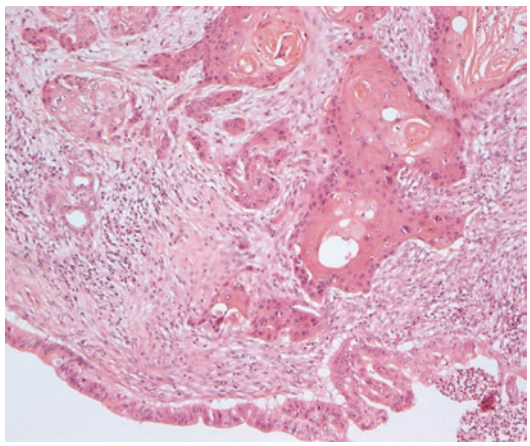

Fig. 9.59 Adenosquamous carcinoma: the carcinoma is mainly composed of solid cell sheets with squamoid features and contains, in addition, foci of glandular differentiation

In addition to metastatic spread from extrapancreatic adenosquamous carcinoma, the differential diagnosis also includes pancreatoblastoma. The latter contains squamoid nests and may include areas of ductal differentiation, but is predominantly composed of acinar cell neoplasia, which stains for pancreatic enzymes (see Chap. 10, Sect. 10.11.3).

Patients with resected adenosquamous carcinoma have a poorer prognosis (median survival less than 1 year) than those with a conventional, pure ductal adenocarcinoma. Both the ductal and squamous components of this variant may be found in metastatic deposits.

9.14.2 Colloid Carcinoma

This subtype, also denoted as mucinous noncystic carcinoma, has been defined by the WHO classification as a ductal adenocarcinoma containing features of a colloid carcinoma, that is, large extracellular mucin pools, in at least 80% of the tumor mass (Fig. 9.60). The latter are partially lined with neoplastic epithelium and contain free-floating tumor cells, which are often fairly well differentiated and have a prominent mucin content. Tumor cells suspended in the mucin pools can acquire signet ring morphology. Colloid carcinoma should be distinguished from mucinous adenocarcinoma, which is a conventional ductal adenocarcinoma containing abundant intracellular or intraluminal mucin collections, but lacking the extracellular mucin pools characteristic of colloid cancer.

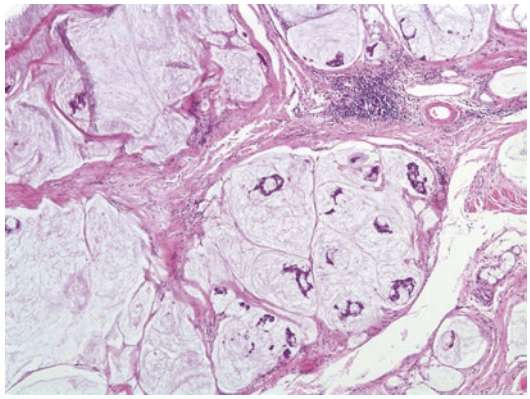

Fig. 9.60 Colloid carcinoma: the tumor is composed of large extracellular mucin pools containing free-floating strips of tumor cells

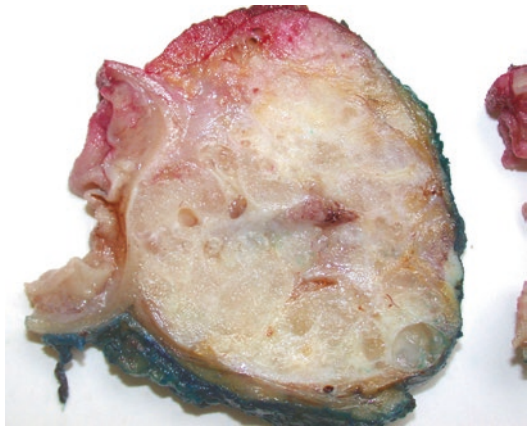

Fig. 9.61 Colloid carcinoma: the tumor shows a glistening mucinous cut surface, contains small cystic areas, and has pushing type margins

Macroscopically, colloid carcinomas are usually large and well circumscribed. They consist, at least in some parts, of friable solid tumor tissue with a gelatinous appearance (Fig. 9.61). Mucin is abundant and of a viscous, jelly-like consistency. Colloid carcinomas occur almost exclusively in association with intraductal papillary mucinous neoplasia (IPMN), which may be identifiable macroscopically as cystically dilated ducts (see Chap. 17). In this context, it is important to distinguish invasive colloid carcinoma from spillage of mucin into the stroma following rupture of a pancreatic duct involved by IPMN. The presence of free-floating neoplastic cells within the mucin pools or in abnormal location, for example, in perineural clefts, may help in making the distinction. The location of the mucin pools proper is a further diagnostic feature, as these are found in the periductal stroma in case of duct rupture, whereas in colloid carcinoma they can be present at a distance from the duct system. Furthermore, the inflammatory reaction is usually more prominent in duct rupture than in invasive colloid carcinoma. A further differential of colloid carcinoma is mucinous cystic neoplasia, which occurs almost exclusively in women and has a characteristic ovarian-type stroma (see Chap. 16).

Immunohistochemically, colloid carcinoma cells express markers of intestinal differentiation, in particular CDX2 and MUC2, in addition to cytokeratins (including CK20), CEA, and CA19-9. Immunostaining for MUC1 is usually negative. Unlike conventional ductal adenocarcinoma, nuclear staining for p53 is positive in only a quarter of cases, and expression of SMAD4 is usually retained.

Colloid carcinoma is rare in the pancreas and occurs more commonly in the ampulla and duodenum. Therefore, the diagnosis of colloid carcinoma of the pancreas requires careful exclusion of a tumor origin in the GI tract.

Colloid carcinoma is reported to portend a more favorable prognosis compared to conventional ductal adenocarcinoma, despite the overall larger tumor size of this subtype. Pseudomyxoma peritonei is a rare complication of colloid carcinoma.

9.14.3 Signet-Ring Cell (Poorly Cohesive Cell) Carcinoma

This is a very rare subtype with histomorphological features similar to signet ring cell carcinoma originating in the stomach. Infiltration by individual, poorly cohesive rounded tumor cells containing a large intracytoplasmic mucin vacuole and a peripherally placed, flattened nucleus is characteristic of these tumors (Fig. 9.62). A com-

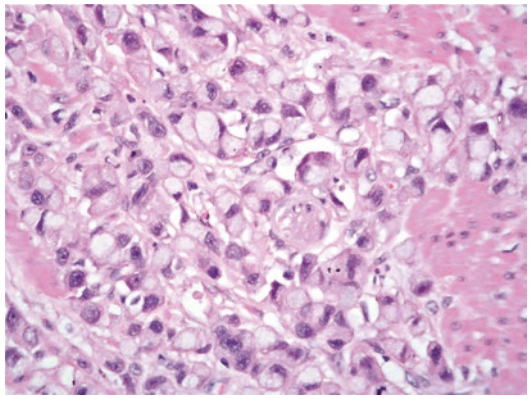

Fig. 9.62 Signet ring cell carcinoma: the tumor cells are poorly cohesive and grow in ill-defined clusters. Many cells have a signet ring appearance

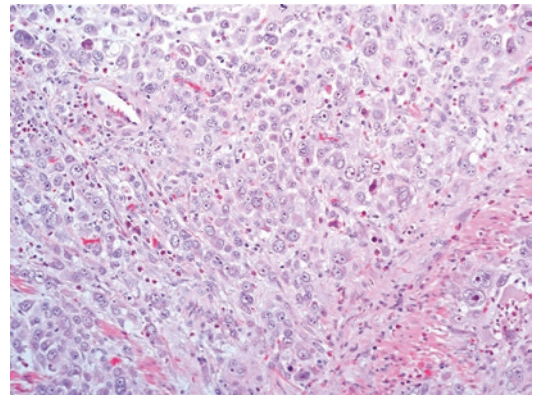

Fig. 9.63 Medullary carcinoma: large tumor cells with ill-defined borders grow in a syncytium-like solid sheet. The macroscopy of this pancreatic cancer is illustrated in Figs. 2.6 and 9.3

ponent of conventional ductal adenocarcinoma is usually present, and it has been recommended to report this variant only if at least 50% of the tumor mass shows signet ring cell differentiation. While extracellular mucin collections can be present, they do not form the large pools that are characteristic of colloid carcinoma. Individual tumor cells, or small clusters, infiltrating the stroma are a feature of signet ring cell carcinoma that is not observed in colloid carcinoma. Unlike the latter, signet ring cell carcinoma is not associated with intraductal papillary mucinous neoplasia.

While survival data for this rare subtype are limited, prognosis seems to be extremely poor. The differential diagnosis includes metastatic carcinoma from the stomach or breast (see Chap. 12, Table 12.1). In addition, signet ring morphology due to non-mucinous cytoplasmic accumulations may occasionally be seen in pancreatic endocrine neoplasia with rhabdoid features, acinar cell carcinoma with signet ring change, and rare lymphomas with signet ring morphology. Prominent cytoplasmic vacuolization mimicking signet ring morphology may also be seen in solid pseudopapillary neoplasia, but the lack of highly infiltrative tumor cell growth and desmoplastic stroma, along with a distinct immunohistochemical profile, allow an unequivocal distinction between both tumors (see Chaps. 10, 18 and 20, Table 20.5).

9.14.4 Medullary Carcinoma

This rare subtype of ductal adenocarcinoma shares some, but not all, morphological features with medullary carcinoma of the large bowel. The tumor is characterized by poor differentiation with limited glandular differentiation and the appearance of a syncytial growth pattern, due to the indistinct borders of individual tumor cells (Fig. 9.63). Tumor-infiltrating T lymphocytes may be numerous and at least focal necrosis is commonly observed. A Crohn's-like lymphoid reaction is usually not present in pancreatic tumors, which also lack the mucinous component that has been described in colonic medullary tumors. Unlike conventional ductal adenocarcinoma, medullary carcinoma is macroscopically characterized by soft tumor tissue with well-demarcated pushing type borders.

Medullary carcinoma can occur sporadically or in patients with Lynch syndrome (see Chap. 6, Sect. 6.4). Many but not all tumors are wild-type for the *KRAS* gene and microsatellite instable (MSI+), and immunostaining for one or more of the mismatch repair proteins is lost in some of these cancers. The diagnosis of medullary carcinoma of the pancreas may be a clue to an inherited cancer syndrome, including Lynch syndrome, and may justify genetic counseling of the patient. Pancreatic ductal adenocarcinoma with Epstein-Barr virus infection of the

cancer cells may morphologically mimic medullary carcinoma [41].

The differential diagnosis of medullary carcinoma includes poorly differentiated acinar cell carcinoma and conventional ductal adenocarcinoma. Immunohistochemistry is usually helpful, in particular the loss of nuclear staining for MLH1 or MSH2, and the absence of labeling for trypsin, other acinar enzymes, and BCL10.

Prognosis for medullary carcinoma of the pancreas seems more favorable than that for conventional ductal adenocarcinoma (mean survival 62 months versus 10–20 months in surgically resected patients). In analogy with medullary colorectal carcinoma, pancreatic tumors may not respond to 5-fluouracil treatment, while immunotherapy may be effective.

9.14.5 Hepatoid Carcinoma

This extremely rare subtype shows morphological and immunohistochemical evidence of hepatocellular differentiation in >50% of the tumor mass. The tumor is composed of large polygonal cells with abundant eosinophilic cytoplasm that show immunolabeling for HepPar1 (Hepatocyte-Paraffin 1). The tumor cells have a centrally placed nucleus with a single nucleolus, and they are arranged in a trabecular pattern, often with a sinusoidal type of vascularization. Some cases may exhibit a canalicular pattern of staining for CEA (polyclonal) and CD10. Bile production may be present in well-differentiated tumors. Periodic acid-Schiff (PAS)-positive diastase-resistant hyaline globules, similar to those seen in liver parenchyma, may occasionally be present. Alpha-fetoprotein (AFP) is expressed in some but not all tumors. Hepatoid differentiation occurs not only in pancreatic cancer with ductal differentiation, but also in association with neuroendocrine neoplasia (see Chap. 20, Sect. 20.5.1, Fig. 20.11). The macroscopic appearance of hepatoid carcinoma is non-distinct, although some tumors have been reported to exhibit an unusual tan to red-brown color.

The main differential diagnosis is the pancreatic metastasis of an occult hepatocellular carcinoma, which should be excluded primarily on clinical grounds. Acinar cell carcinoma can mimic hepatoid carcinoma morphologically and may also express AFP and markers of hepatocellular differentiation, including HepPar1 and glypican 3. Immunostaining for arginase 1 and FISH for albumin are likely more specific markers of hepatocellular differentiation. Positive immunostaining for AFP can also be seen in a minority of ductal adenocarcinomas, pancreatic endocrine neoplasms, and pancreatoblastomas as well as in extrapancreatic malignancies, including germ cell tumors. Therefore, immunolabeling for AFP is by itself insufficient evidence for a diagnosis of hepatoid carcinoma. Moreover, HepPar1 expression may also be seen in intraductal oncocytic papillary neoplasia (see Chap. 17, Sect. 17.3).

Information on the prognosis for hepatoid carcinoma of the pancreas is currently too limited to allow a confident statement.

9.14.6 Invasive Micropapillary Carcinoma

The micropapillary component in this subtype is characterized by small clusters of cancer cells that closely adhere to each other and are located in a distinct empty space that may resemble a dilated lymphatic channel (Fig. 9.64). Invasive micropap-

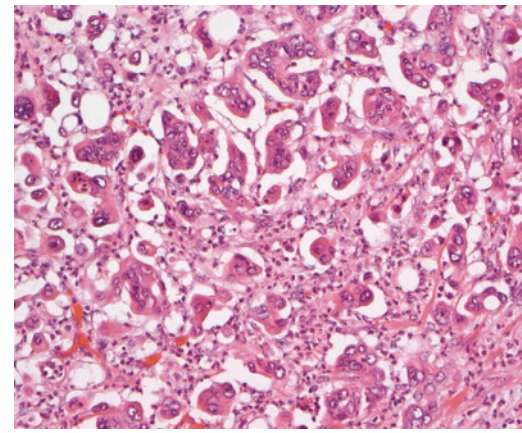

Fig. 9.64 Invasive micropapillary carcinoma: small cohesive cancer cell clusters are surrounded by an empty space. Note the presence of scattered neutrophils

illary carcinoma is defined by the occurrence of micropapillae in >50% of the tumor mass, which is a rare finding. Slightly more frequently, micropapillary morphology may be seen focally in conventional ductal adenocarcinoma. Invasive micropapillary carcinoma is often associated with dense intraepithelial infiltration of neutrophils and shows a more aggressive behavior. It should be noted that invasive micropapillary carcinoma is slightly more common in the ampulla [42].

9.14.7 Undifferentiated Carcinoma

Undifferentiated carcinoma has also been denoted as anaplastic carcinoma, pleomorphic large cell carcinoma, spindle cell carcinoma, sarcomatous carcinoma, and carcinosarcoma. It is defined as a malignant epithelial neoplasm in which a significant tumor component does not show a definitive direction of differentiation. Necrosis and hemorrhage are commonly present and may be extensive. Most tumors are large and widely invasive and exhibit lymphovascular and perineural propagation.

Undifferentiated carcinomas exhibit a spectrum of morphological features. Three patterns can be distinguished, but individual tumors may contain a combination of patterns. *Anaplastic undifferentiated carcinoma* consists at least to 80% of pleomorphic mononuclear cells admixed with bizarre, often multinucleated giant cells showing copious eosinophilic cytoplasm. Cell cannibalism of tumor cells, erythrocytes, or inflammatory cells may be seen. Nuclear pleomorphism is usually prominent, and mitotic figures, including atypical ones, are numerous. The neoplastic cells are usually non-cohesive, and desmoplastic stroma is scanty (Fig. 9.65).

In *sarcomatous undifferentiated carcinoma*, neoplastic cells are mainly spindle-shaped and may be arranged in a vague fascicular or herringbone pattern in at least 80% of the tumor. While cytological atypia is usually less prominent than in anaplastic giant cell carcinoma, pleomorphism is nonetheless significant (Fig. 9.66).

Carcinosarcomas contain in addition to the atypical spindle cell component, areas of unequivocal adenocarcinomatous differentiation. Arbitrarily, either component should represent at least 30% of the tumor mass.

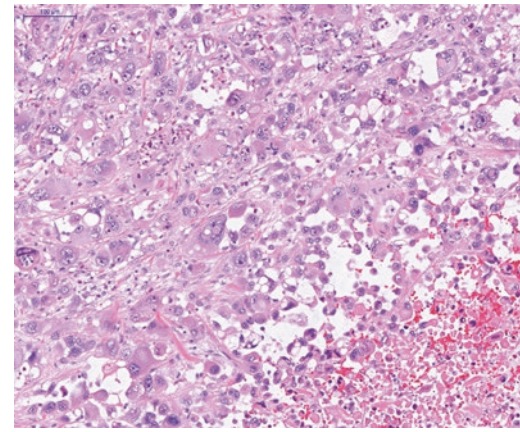

Fig. 9.65 Undifferentiated carcinoma, anaplastic giant cell variant: large, highly pleomorphic tumor cells grow in poorly cohesive solid sheets. Note the scanty tumor stroma and presence of an atypical mitotic figure

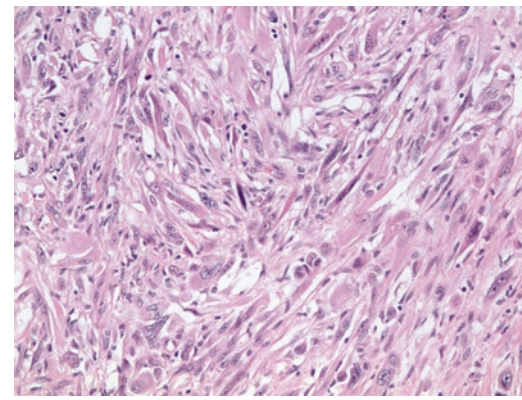

Fig. 9.66 Undifferentiated carcinoma, sarcomatoid variant: tumor spindle cells with pleomorphic nuclei are arranged in vague short bundles

Mesenchymal tumor differentiation in the latter two variants may sometimes lead to the presence of heterologous stromal elements, including bone, cartilage, or skeletal muscle. Squamous differentiation and rhabdoid features have also been reported.

Immunohistochemical evidence of an epithelial histogenesis is found in all undifferentiated carcinomas, although labeling for epithelial markers may be very focal. CK7, 8, 18, and 19

are among the cytokeratins that can be expressed. Immunolabeling for E-cadherin is typically absent. Most tumors also express vimentin, CEA, MUC1, and CA19-9. Spindle cells may stain for actin but usually not desmin. Immunolabeling for neuroendocrine markers is absent in most tumors.

The differential diagnosis of this group of neoplasms is wide and depends on the morphological features of the individual tumor. Overall, metastatic melanoma, poorly differentiated germ cell tumors, and hematopoietic neoplasms should be included in the differential diagnosis. Immunostaining for melanocytic markers (HMB45, melan-A, S100), human chorionic gonadotropin-beta (β-HCG) and leukocyte common antigen or other leukocyte markers may be helpful. Primary sarcomas of the pancreas are extremely rare, and the absence of a specific line of mesenchymal differentiation (morphologically and/or immunohistochemically), the marked degree of cytological atypia, and the positive staining for cytokeratins, even if only focal, favor carcinosarcoma. However, it has to be noted that keratin positivity can occur in the rare case of pancreatic synovial sarcoma (see Chap. 11, Sect. 11.1.12). Undifferentiated carcinoma metastatic to or originating from the pancreas cannot be distinguished immunohistochemically. However, the presence of extensive and high-grade PanIN or the association with a mucinous cystic neoplasm may make a pancreatic primary more likely (see Chap. 16). Distinction from undifferentiated carcinoma with osteoclast-like giant cells is discussed below.

The prognosis for undifferentiated carcinoma of the pancreas is extremely poor. Metastasis is often already present at the time of diagnosis. The reported mean survival is less than 6 months.

9.14.8 Undifferentiated Carcinoma with Osteoclast-Like Giant Cells

This subtype of ductal adenocarcinoma is composed of round or spindle-shaped, highly pleomorphic neoplastic tumor cells that are non-cohesive. In addition, it contains a second population of nonneoplastic multinucleated histiocytic giant cells (Fig. 9.67). The latter are believed to represent an unusual stromal reaction and are often found in areas of necrosis or hemorrhage (Fig. 9.68). They typically have 20 or more uniform small nuclei and may occasionally contain hemosiderin or other phagocytosed material within their copious eosinophilic cytoplasm.

Immunohistochemistry highlights the different character of both cell populations. Most of the pleomorphic neoplastic cells stain for vimentin, while some show labeling for epithelial markers (MNF116, cytokeratins, AE1/AE3, EMA, CEA). Nuclear staining for p53 may be found in some tumors, while Ki67 labeling

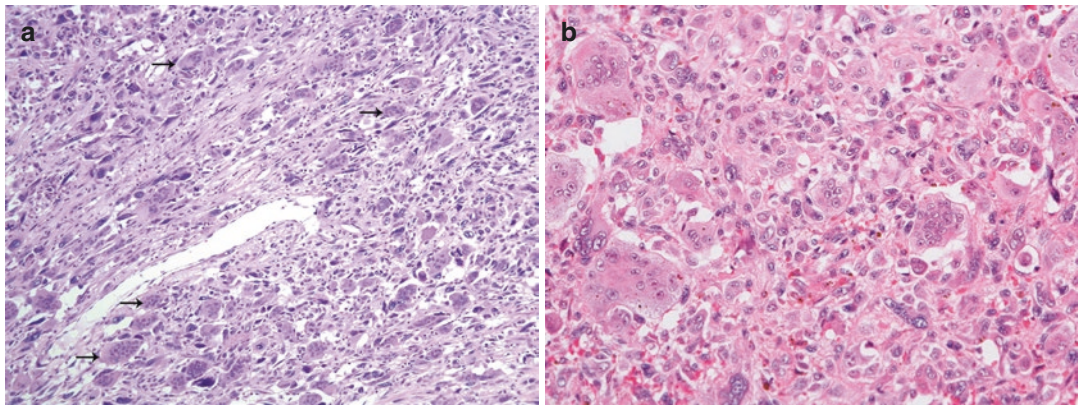

Fig. 9.67 Undifferentiated carcinoma with osteoclast-like giant cells: cellular tumor tissue is composed of large, highly pleomorphic tumor cells admixed with multinucleated osteoclast-like cells (*arrows*; **a**). The latter contain copious cytoplasm and numerous uniform vesicular nuclei with a single nucleolus (**b**)

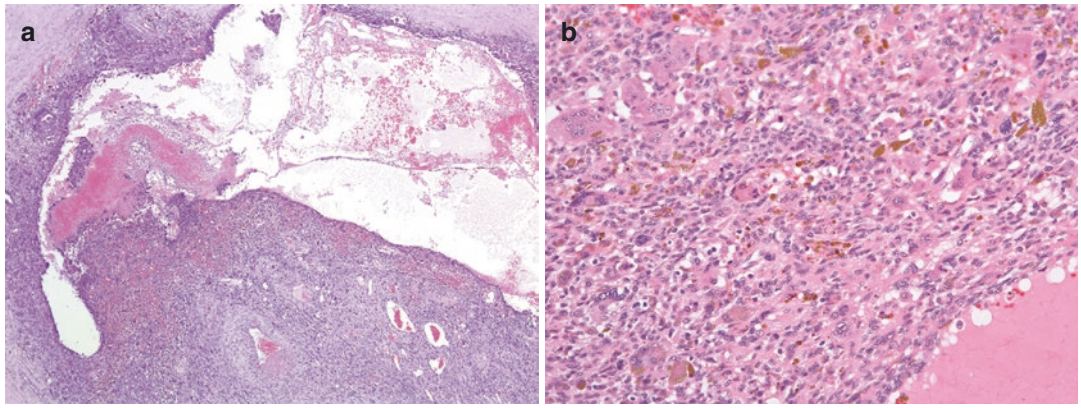

Fig. 9.68 Undifferentiated carcinoma with osteoclast-like giant cells: hemorrhage and necrosis result in gross pseudocystic change (**a**). Osteoclast-like giant cells are particularly numerous in areas of hemorrhage (**b**)

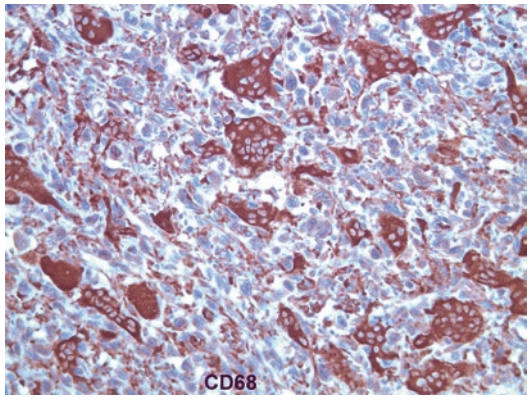

Fig. 9.69 Undifferentiated carcinoma with osteoclast-like giant cells: immunostaining for CD68 labels the osteoclast-like giant cells while the tumor cells remain negative

always reflects a high proliferation rate. In contrast, the osteoclast-like giant cells do not express epithelial markers, have a low proliferative activity, lack nuclear immunolabeling for p53, and stain for markers of leukocytic/histiocytic differentiation (CD45, CD68) (Fig. 9.69). The nonneoplastic nature of the osteoclast-like giant cell population has also been confirmed by molecular analysis: in contrast to the pleomorphic tumor cells, these are diploid and do not contain *KRAS* mutations. Expression of osteonectin and cathepsin K by the osteoclast-like giant cells has been reported in areas of osteoid or bone formation, which may be present in some tumors (Fig. 9.70). Focal chondroid differentiation has also been described.

A significant proportion of undifferentiated carcinomas with osteoclast-like giant cells include areas of conventional ductal adenocarcinoma, which is a further line of evidence supporting the classification of the former as a rare subtype of the latter. While the components of undifferentiated carcinoma and adenocarcinoma are intimately admixed, the transition between the two is usually abrupt (Fig. 9.71), and the characteristic osteoclast-like giant cells are limited to the areas of undifferentiated carcinoma. Some tumors have been reported to arise in association with high-grade PanIN or mucinous cystic neoplasia (see Chap. 16).

The presence of the benign-appearing osteoclast-like giant cells allows distinction of this rare subtype of ductal adenocarcinoma from other neoplasms with pleomorphic tumor cells, first and foremost undifferentiated carcinoma. Multinucleated osteoclast-like histiocytic giant cells may also be present in other malignant tumors, including trophoblastic neoplasia, malignant fibrous histiocytoma, and various forms of Hodgkin or non-Hodgkin lymphoma.

The gross appearance of undifferentiated carcinoma with osteclast-like giant cells differs significantly from that of conventional ductal adenocarcinoma and indeed other primary pancreatic neoplasms. The tumors are usually large

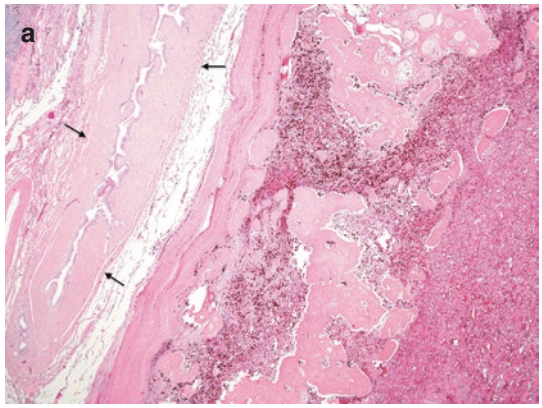

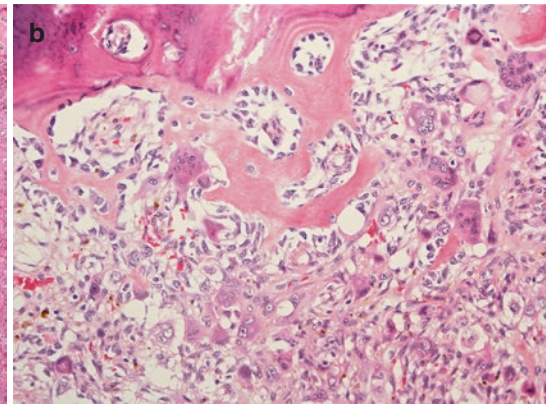

Fig. 9.70 Undifferentiated carcinoma with osteoclast-like giant cells: extensive osteoid and bone formation are present within the tumor. Note the expansile border of the tumor, which is sharply demarcated from the adjacent common bile duct (*arrows*, **a**). Tumor cells are intimately associated with the tumor osteoid and bony formations (**b**)

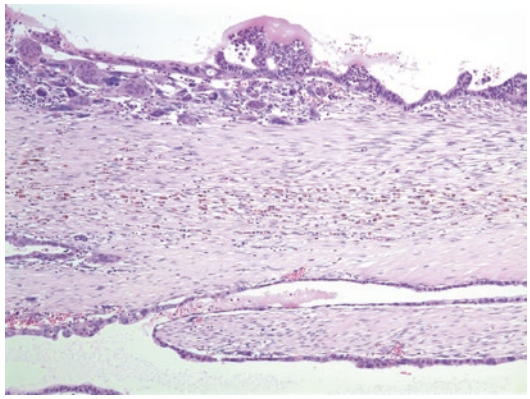

Fig. 9.71 Undifferentiated carcinoma with osteoclast-like giant cells: the transition to conventional ductal adenocarcinoma is abrupt

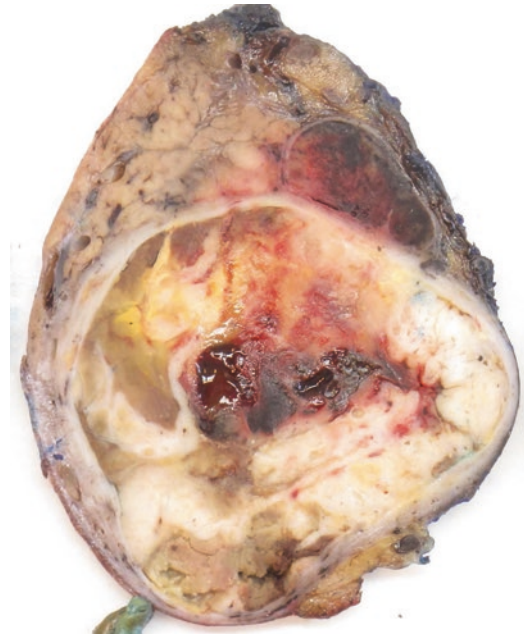

Fig. 9.72 Undifferentiated carcinoma with osteoclast-like giant cells: this large tumor with sharply demarcated expansile margins shows prominent hemorrhage and cystic change

at the time of presentation. They have well-defined pushing borders, and despite the considerable tumor size, the flanking pancreatic parenchyma is often remarkably well preserved. The tumor is essentially solid, but cystic cavities, often of considerable dimensions, are common and may occasionally be the dominant macroscopic feature. Hemorrhage is usually extensive but patchy in distribution (Fig. 9.72). The tumor tissue is of an unusually soft consistency and may show areas of necrosis. In rare cases, bone formation may be extensive to the point of being macroscopically visible as irregular whitish 'spiky' formations (Fig. 9.73). The tumors have a propensity to extend in a polypoid fashion along the main pancreatic duct, branch ducts, or exceptionally, the distal common bile duct (Figs. 9.74 and 9.75).

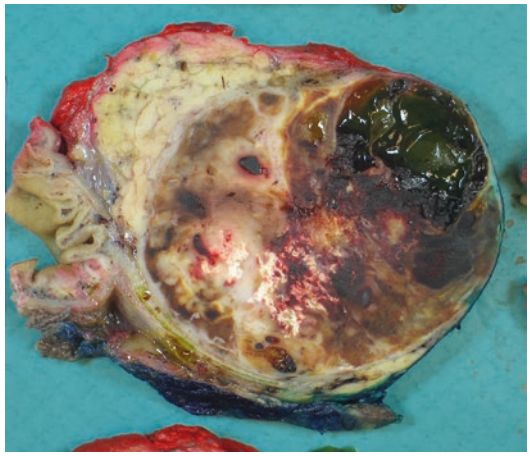

Fig. 9.73 Undifferentiated carcinoma with osteoclast-like giant cells: this large tumor has sharply defined expansile margins and shows extensive hemorrhage. Note the spiky white bone depositions. The adjacent pancreas is well preserved

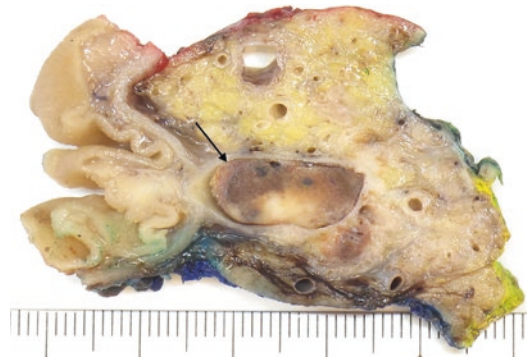

Fig. 9.75 Undifferentiated carcinoma with osteoclast-like giant cells: the tumor extends in a polypoid fashion into the dilated main pancreatic duct (*arrow*)

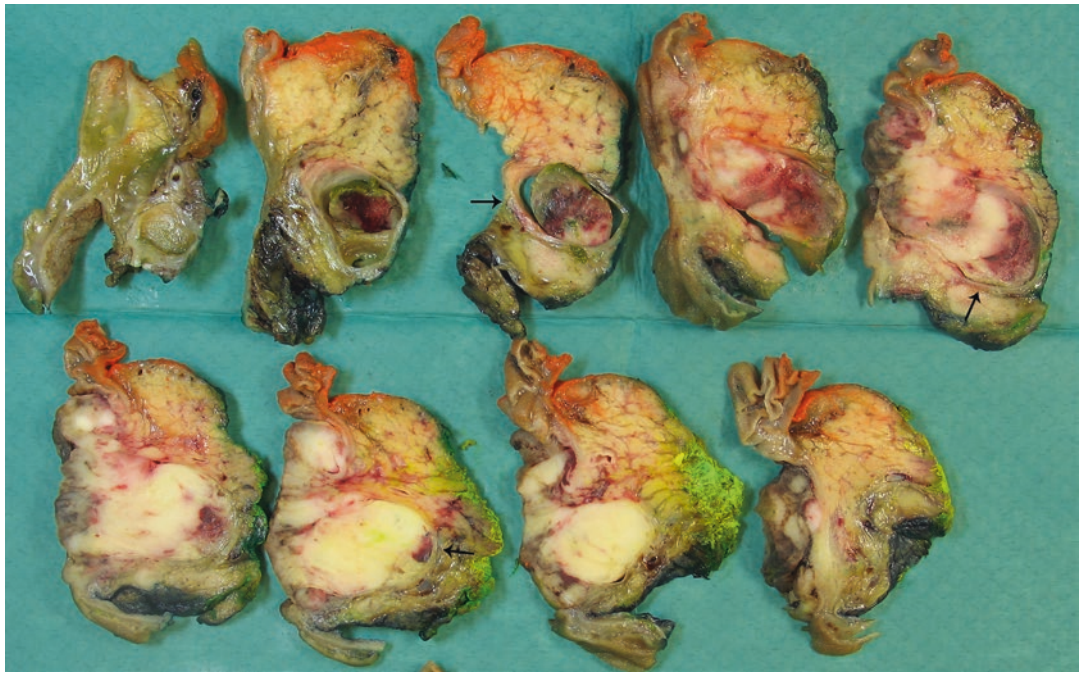

Fig. 9.74 Undifferentiated carcinoma with osteoclast-like giant cells: the bulk of this tumor grows within and dilates the common bile duct (*arrows*)

The prognosis of this subtype seems to be unpredictable, with a protracted clinical course and in some cases survival beyond 5 years being recorded. It has been suggested that the extent of conventional ductal adenocarcinoma in these tumors has an adverse prognostic impact, but this correlation awaits confirmation [43].

9.15 Carcinoma with Mixed Differentiation

Carcinomas with mixed differentiation are defined as malignant epithelial neoplasms of the pancreas containing significant components of more than one distinct direction of differentiation. In addition to ductal adenocarcinoma, these mixed carcinomas may contain a component with neuroendocrine or acinar differentiation. Extremely rare is a combination of all three lines of differentiation within a single pancreatic cancer. By definition, each component of the mixed carcinoma should comprise at least 30% of the overall tumor mass, and there should be an intimate admixture of the various components. The so-called collision tumors, in which the components are topographically separated within the common tumor mass, are not included in this category.

9.15.1 Mixed Neuroendocrine—Non-Neuroendocrine Neoplasm (MiNEN)

These tumors are among the rarest pancreatic neoplasms. They should be carefully distinguished from the rather common finding of pancreatic neuroendocrine tumors with entrapped nonneoplastic ductules, or of ductal adenocarcinomas containing scattered endocrine cells or enlarged nonneoplastic islets. The diagnosis and clinical implications of these tumors are discussed in more detail in Chap. 20, Sect. 20.10.

9.16 Mixed Acinar-Ductal Carcinoma

Mixed carcinomas can also show a combination of ductal and acinar differentiation (see Chap. 10). The diagnosis is usually based on immunohistochemical identification of either component, unless the ductal adenocarcinoma part presents as a colloid carcinoma, for which no ancillary diagnostic investigations are required.

9.17 Ductal Adenocarcinoma Following Neoadjuvant Treatment

In recent years, neoadjuvant chemo(radio)therapy has become an established treatment option. The theoretical advantages of this form of treatment are discussed elsewhere (see Sect. 9.13). For the pathologist, the reporting of pancreatic resection specimens from patients who have undergone neoadjuvant treatment can pose a diagnostic challenge. The main difficulties in the macroscopic and microscopic assessment of such specimens are directly linked to the intended therapeutic effect. When the cancer has responded to preoperative treatment, the number of tumor cells has been reduced, but this process of tumor regression often occurs in a non-uniform fashion, affecting some parts of the tumor more than others. Tumor regression is usually associated with inflammation and fibrosis, although the former may be mild and patchy at the time of surgical resection. The net result of the treatment-induced changes is usually the presence of a reduced number of tumor cells within an expanded fibrous stroma.

This section discusses in more detail the issues that are of particular importance and the problems that may arise when reporting on pancreatic resection specimens following neoadjuvant treatment.

9.17.1 Macroscopic Examination

The combination of treatment-induced changes affecting both the carcinoma and the nonneoplastic pancreas renders the macroscopic assessment of these specimens even more difficult than is the case for tumors that have not undergone neoadjuvant treatment (Fig. 9.76). Reliable macroscopic distinction between (viable) tumor tissue and areas of fibrosis is sometimes not possible, and therefore the key principles of pancreatic specimen dissection—thin axial slicing, close-up photography, and extensive, that is, subtotal, sampling—are even more important.

Due to the seemingly random regression of the cancer, its relationship with the key anatomical

Fig. 9.76 Effect of neoadjuvant treatment: macroscopic examination can be problematic due to marked tissue shrinkage and distortion of the local anatomy. Fibrosis and residual tumor are often indistinguishable. Note the gross distortion of the specimen contours and irregularity of the circumferential margins

structures and the exact location of the center of the tumor mass may no longer be unequivocally recognizable. Hence, exact identification of the tumor origin—pancreatic, ampullary, or common bile duct—may occasionally be problematic. The effect of neoadjuvant treatment on precursor lesions has not been systematically studied.

9.17.2 Microscopic Examination

As a consequence of the effect of treatment, the density of the tumor cells will be reduced, that is, even lower than that typically found in untreated ductal adenocarcinoma (Fig. 9.77). Some tumor cells may show marked atypia, including occasional bizarre nuclei and cell shapes, whereas others may be cytologically deceivingly bland (Figs. 9.78 and 9.79). As treatment can have a significant effect on the tumor morphology, the grade of tumor differentiation is not reported in pancreatic cancer following neoadjuvant chemo(radio)therapy.

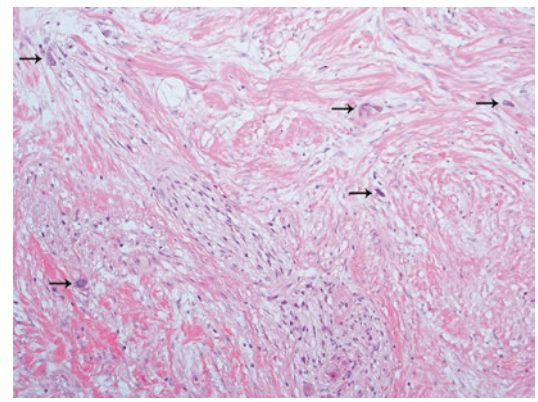

Fig. 9.77 Effect of neoadjuvant treatment: tumor cells may be present as inconspicuous singletons (*arrows*) lying widely dispersed in a desmoplastic stroma

In some cases, tumor regression may result in lake-like accumulations of mucin within the fibrous stroma (Fig. 9.80). Individual cells or small

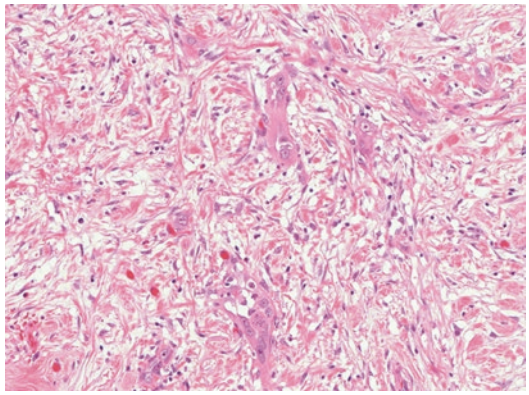

Fig. 9.78 Effect of neoadjuvant treatment: tumor cells may acquire bizarre shapes and nuclear features, which should not be mistaken as an indication of poor tumor differentiation. Note the abundant cellular stroma

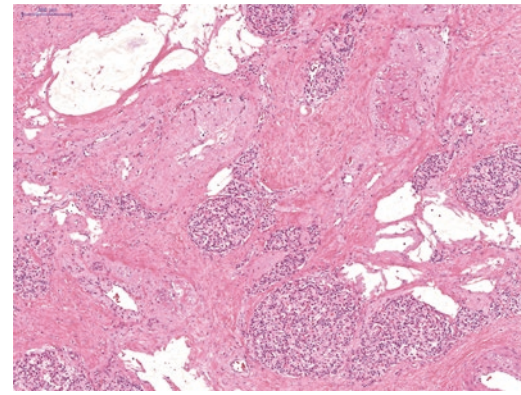

Fig. 9.80 Effect of neoadjuvant treatment: acellular mucin lakes indicate areas of tumor regression. Note the marked degenerative vascular changes and islet aggregation

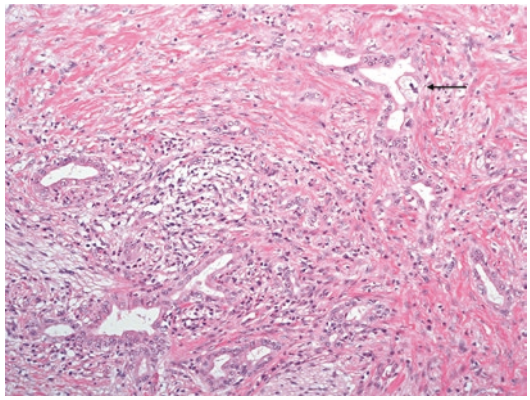

Fig. 9.79 Effect of neoadjuvant treatment: treatment-induced cytomorphological changes are patchy. A single bizarre tumor cell is present within relatively bland-looking tumor glands (*arrow*)

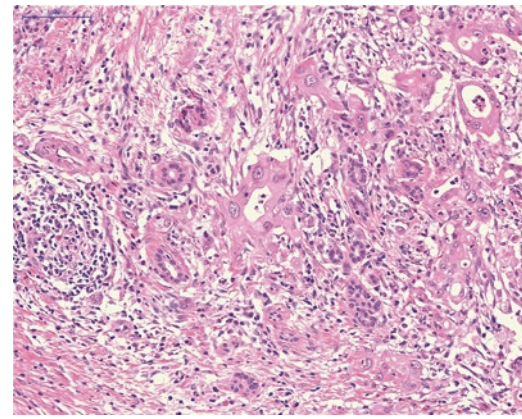

Fig. 9.81 Effect of neoadjuvant treatment: residual tumor glands are intimately admixed with nonneoplastic ducts

cell clusters may float in these pools, and occasionally distinction between viable tumor cells or macrophages may be difficult and require immunohistochemistry, particularly in case this represents the only focus of possible residual tumor.

Microscopic assessment is often hindered by the fact that tumor regression tends to be patchy and unpredictable in distribution. Hence, residual tumor foci may be found at a considerable distance from each other, scattered between areas of nonneoplastic pancreatic parenchyma (Fig. 9.81). The latter often exhibits marked atrophy and fibrosis with effacement of the lobular architecture, fragmentation or aggregation of islets, and reactive epithelial atypia, which in summation can make the distinction between nonneoplastic ductular structures and scanty residual tumor glands problematic. This is compounded by the fact that the morphology of the cancer can vary considerably throughout the specimen, such that comparison with microscopic appearances in areas of unequivocal residual cancer is not always helpful when having to decide on the nature of an individual focus showing atypical features. The presence of glandular structures flanking large blood vessels (Fig. 9.82), in lymphovascular or perineural spaces, or in structures adjacent to the pancreas (e.g., the duodenal wall, ampulla, common bile duct, or peripancreatic soft tissue) allows a confident diagnosis of residual cancer.

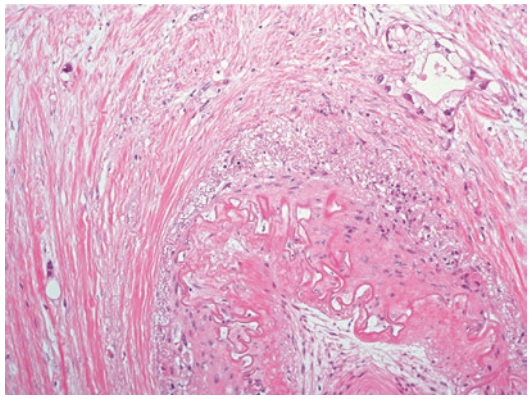

Fig. 9.82 Effect of neoadjuvant treatment: the presence of small ducts and atypical cell clusters adjacent to a muscular artery confirms their malignant nature

The usefulness of immunohistochemistry for the distinction between tumor glands and reactive ductules in posttreatment pancreatic resection specimens has not been well studied, and observations from untreated pancreatic cancer cases may not always be applicable to tumors that underwent neoadjuvant treatment.

9.17.3 Vascular Resection

Opinions on the indications for neoadjuvant therapy differ. While in some pancreatic cancer centers, patients with primarily resectable tumors are also offered preoperative treatment, this is usually limited to patients with borderline resectable tumors, with the intention to shrink the tumor such that it becomes resectable. Borderline resectability is defined, amongst other factors, by the involvement of the superior mesenteric vein or portal vein. Hence, venous resection is commonly included in the surgical procedures following neoadjuvant treatment. As outlined elsewhere (see Chap. 3, Sects. 3.3.5.2 and 3.3.8), the venous tissue should be carefully examined. Preliminary reports indicate that involvement of the wall of the resected vein predicts a shorter disease-free and overall survival.

In recent years, patients with locally advanced pancreatic cancer are also considered for chemotherapy, with the aim to reduce the size and extent of the tumor such that the cancer becomes resectable. These cases often present with involvement of one or several arteries (superior mesenteric artery, hepatic artery, celiac trunk), possibly in combination with venous involvement and/or tumor growth into neighboring viscera. Consequently, an extended surgical procedure is often required, and the resulting specimen may include, in addition to a venous resection, resection of an artery and/or (part of) the stomach, left adrenal, or colon (Figs. 9.83 and 9.84). As outlined in Chap. 3, the relationship of the (residual) cancer and these structures should be examined, together with the associated resection margins and surfaces.

9.17.4 Staging

Staging for the full set of descriptors (T N L V Pn R) requires meticulous scrutiny of all tissue sections. The prefix 'yp' should be used to indicate that staging was performed following neoadjuvant treatment. Because stages T1–3 are defined by tumor size according to the eighth edition of UICC/AJCC TNM [6, 18], exact measurement of the size of the residual cancer is essential to correct staging. However, following neoadjuvant treatment, measurement of the tumor dimensions may be difficult, especially because the residual cancer is often present in the form of two or more separate foci rather than a single residual tumor mass. Currently, there are two different approaches: (i) measurement of the length of the line that connects the tumor foci that lie furthest away from each other, including intervening noncancerous tissue, or (ii) measurement of the size of each separate residual cancer focus (excluding intervening nonneoplastic tissues) and addition of these sizes to obtain the overall tumor dimensions [44]. While the first approach is easier, it may result in considerable overestimation of tumor size in case there are only a few small residual cancer foci that are lying at larger distances from each other. The disadvantage with the second approach is that it may be difficult if not impossible to distinguish contiguous from separate tumor foci in multiple tissue sections through the tumor bed and to make the

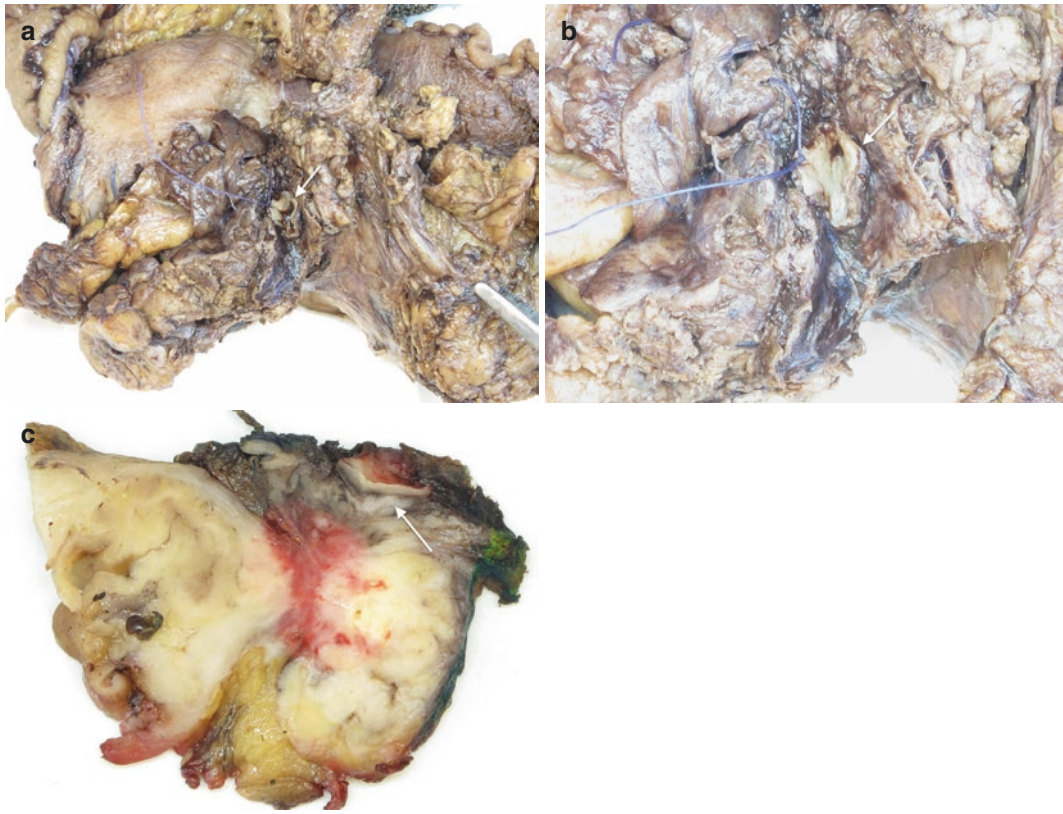

Fig. 9.83 Resection of hepatic artery following neoadjuvant treatment: a 1 cm long segmental resection of the hepatic artery is firmly adherent to the cranial part of the pancreatic head. Note the surgical marker suture (*arrow*; **a** and **b**). An axial specimen slice shows a longitudinal section through the small arterial resection (*arrow*), which is drawn into a large ductal adenocarcinoma that infiltrates the duodenal wall and the peripancreatic soft tissue (**c**)

measurements in two or more directions to identify the largest tumor dimension. To date, there is no consensus as to how measurement should best be done, and the decision is left at the discretion of the pathologist, depending on local practice, personal experience, and the individual case. While further studies to evaluate the prognostic significance of T-staging following neoadjuvant therapy are awaited, first reports suggest that T-staging according to the eighth edition of AJCC/UICC is not an independent predictor of patient survival [45]. In contrast, lymph node status following neoadjuvant treatment seems to remain a strong predictor of outcome. Treatment-induced regression of lymph node metastasis has hardly been studied, but seems to occur, because the overall rate of lymph node metastasis is lower in series following neoadjuvant therapy. However, in the individual case, tumor regression with associated fibroinflammatory changes is not a common finding in regional lymph nodes. The prognostic value of the lymph node rate following neoadjuvant treatment needs further validation, especially because the lymph node yield in preoperatively treated specimens is often lower. A minimum lymph node yield to ensure reliable assessment of the ypN-stage has not been identified yet.

While the margin status should be included in the pathology report, the assessment of the resection margins following neoadjuvant treatment is not without its problems. As preoperative treatment causes tumor cells to regress in a haphazard fashion, the absence of tumor cells within 1 mm of the specimen surface—the admittedly somewhat arbitrary, currently proposed definition of R1 used in treatment-naïve tumors—does not

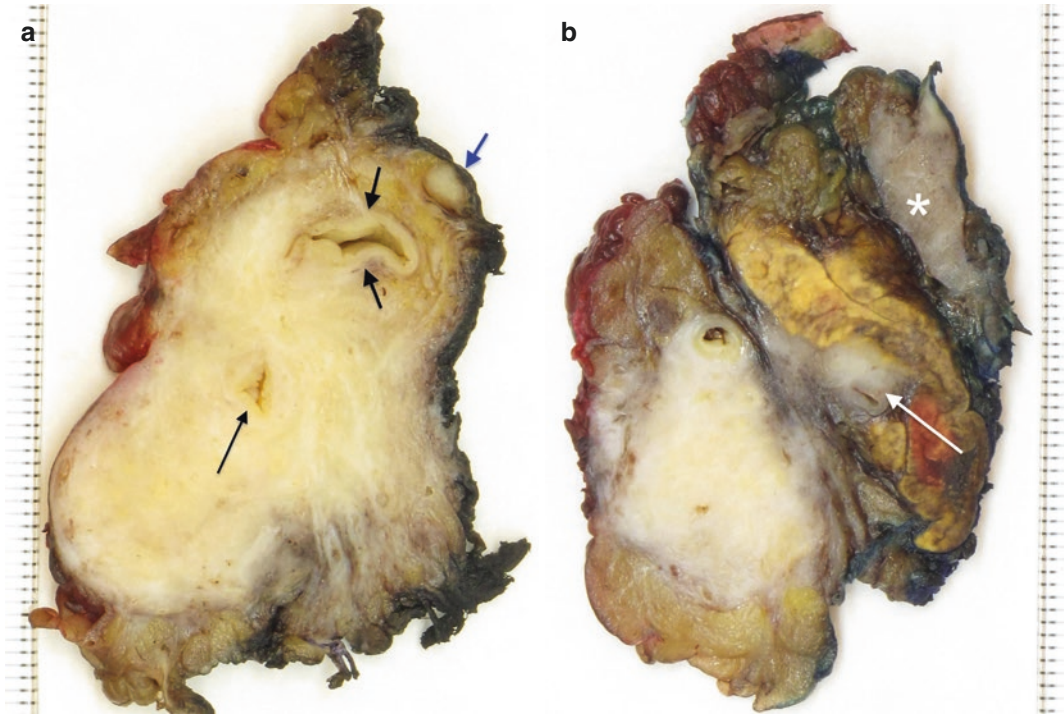

Fig. 9.84 Resection of celiac trunk and left adrenal gland following neoadjuvant treatment: a large ductal adenocarcinoma originating in the pancreatic body shows extensive infiltration of soft tissue posterior to the pancreas with 180 degrees involvement of the celiac trunk (*short arrows*). Note the high-grade tumor occlusion of the splenic artery (*long arrow*) and a small lymph node metastasis (*blue arrow*, **a**). There is direct tumor extension around the superior adrenal artery and invasion of the adrenal gland (*arrow*). Note the large aggregate of neural ganglia posterior to the adrenal gland (*asterisk*, **b**)

reliably predict that tumor cells were not left behind in the surgical bed (Fig. 9.85). Application of the current definition of microscopic margin involvement (see Sect. 9.11.4) is bound to underestimate the presence of microscopic residual disease following neoadjuvant treatment. Perhaps not surprisingly, preliminary reports seem to indicate that margin status following neoadjuvant treatment is of no prognostic value [45], but further studies are awaited.

9.17.5 Tumor Regression Grading

In recent years, various schemes for the histological grading of the degree of tumor regression have been proposed (Table 9.5) [44]. Most are based on an estimation of the proportion of tumor cells that have been destroyed or, conversely, cancer cells that have remained viable compared to the original tumor bulk or with respect to the extent of (treatment-induced) fibrosis. The scoring systems are typically three- or four-tiered. The main problem with these systems is that the original tumor bulk is neither known to the pathologist, nor can it be reliably identified in the surgical specimen. Furthermore, fibrosis is both common and extensive in pancreatic cancer, and there are no diagnostic features that allow distinction of treatment-induced fibrosis from fibrosis of other causes. Hence, a scoring system based exclusively on the amount of residual cancer—which is the only reliably assessable parameter—seems to be the most sound and is recommended by the College of American Pathologists [48]. A further advantage of this system is that it is based on semi-quantitative criteria rather than numeric cut-off values, which are both arbitrary and difficult to use in practice. Further adding to the difficulty of scoring tumor regression is the fact that the effect of treatment is often heterogenous within

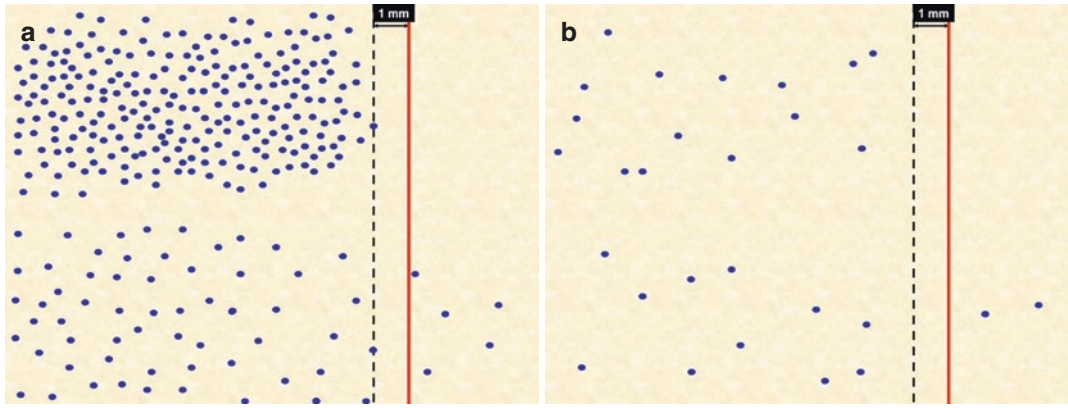

Fig. 9.85 Effect of neoadjuvant treatment: prediction of the presence or absence of residual tumor at the resection margin is determined by the tumor growth pattern. In the tumor with a less compact growth pattern (*lower half*), a clearance of 1 mm does not guarantee the absence of residual disease (**a**). As the growth pattern is altered by neoadjuvant treatment and tumor cells lie at greater distances from each other, the usual definition of R1 (<1 mm clearance) leads to underestimation of residual tumor (**b**) (*blue dots*: tumor cells, *red line*: resection margin, *dotted line*: 1 mm from margin)

Table 9.5 Tumor regression grading for ductal adenocarcinoma of the pancreas

	Evans et al. [46]	Chatterjee et al. [47]	College of American Pathologists [48]
Criterion	Percentage tumor cell destruction/viable cancer cells	Extent/percentage viable cancer cells	Extent residual cancer
Grade	I = 0–9% tumor cell destruction IIa = 10–50% tumor cell destruction IIb = 51–90% tumor cell destruction III = <10% viable cancer cells IV = 0% viable cancer cells	0 = No residual tumor 1 = Minimal residual tumor (<5%) 2 = ≥5% residual tumor	0 = Complete response (no residual cancer cells) I = Near-complete response (single cancer cells or rare small groups of cancer cells) II = Partial response (residual cancer with evident tumor regression but more than single cells or rare small groups of cancer cells) III = Poor or no response (extensive residual cancer with no evident tumor regression)

a tumor. Not surprisingly, interobserver agreement is low [49], and therefore a simplified, 3-tiered scoring system has been suggested, which discriminates only between complete regression, near-complete regression, and non-near-complete regression, the latter being defined as >5% residual cancer cells [47]. While interobserver agreement is better, the simplified system introduces an arbitrary, difficult to use numeric threshold value based on the unrealistic comparison of the residual cancer burden with the original cancer bulk. Moreover, as (near-) complete tumor regression is rare, the vast majority of patients fall in the same category, such that it has no predictive value in most cases. On the whole, at present, the tumor regression grading system that is recommended by the College of American Pathologists seems the better approach, despite the above-described shortcomings.

9.18 Diagnostic Molecular Pathology

Ductal adenocarcinoma is caused by a wide range of somatic and germline mutations. The latter are discussed in Chap. 6. The most common genetic

abnormalities in ductal adenocarcinoma are oncogenic mutations of *KRAS* and the loss-of-function and/or deletions of the tumor suppressor genes *TP53, SMAD4 (DPC4),* and *CDKN2A (P16)*. In addition, a large number of other genomic alterations are found at low prevalence. Of the vast knowledge that has been acquired over the past decades, little is currently of direct diagnostic application. Because the loss of expression of *SMAD4* is cancer-specific, immunohistochemistry may be of help to distinguish invasive carcinoma from reactive ducts in a pancreatic biopsy (see Sect. 9.9.3).

In recent years, expression profiling has resulted in several classification systems of ductal adenocarcinoma, which on the whole distinguish between two subtypes—classic and basal-like—that are characterized by distinct molecular signatures and differences in therapeutic response and patient outcome [50, 51]. Similarly, two subtypes of tumor stroma—normal and activated—have been proposed [52]. Ductal adenocarcinomas combining a basal-like cancer cell population with an activated stroma show a poorer response to chemotherapy and a worse survival compared to tumors of classic subtype with normal-type stroma. Development of improved taxonomy systems, especially in the face of marked intratumor heterogeneity, is awaited.

To date, detection of microsatellite instability (MSI+) and mutations of *BRCA* and related genes are the only analyses that, in a hitherto experimental setting, may be undertaken to identify patients who may benefit from immunotherapy or treatment with platinum-based chemotherapy and PARP (poly ADP ribose polymerase) inhibitors, respectively [53].

9.19 Reporting Checklist

Table 9.6 provides a summary of the data items that are to be included in the pathology reporting of ductal adenocarcinoma of the pancreas. A more detailed checklist for the reporting of the macroscopic examination is provided in Chap. 3 (see Table 3.3).

Table 9.6 Reporting checklist for ductal adenocarcinoma of the pancreas (including subtypes)

Macroscopic assessment
• Specimen type (e.g., pancreatoduodenectomy, distal/total pancreatectomy) – Type – Dimensions of main anatomical constituent parts – Other anatomical structures (e.g., venous resection)
• Appearance of tumor – Consistency, color, well/poorly circumscribed – Presence of cystic change, hemorrhage, necrosis
• Tumor size – Craniocaudal dimension – Axial dimensions
• Tumor site and extension – Localization in craniocaudal (specimen slices involved), mediolateral, and anteroposterior direction – Relationship to key anatomical structures – Invasion of other structures included in the specimen (e.g., venous resection) – Minimum distance to nearest resection margin(s)
• Other findings
• Background pancreas

Table 9.6 (continued)

Microscopic assessment
• Type, pattern, or subtype of ductal adenocarcinoma – Type: pancreatobiliary or intestinal – Pattern: foamy gland, clear cell, large duct, cystic papillary – Subtype: adenosquamous/squamous, colloid, signet ring cell, medullary, hepatoid, invasive micropapillary, undifferentiated, undifferentiated with osteoclast-like giant cells
• Grade of differentiation[a]
• Tumor size: corrected by microscopic measurement – Craniocaudal dimension – Axial dimensions
• Tumor extent – Confined to pancreas or infiltration of extrapancreatic tissues – Involvement of additionally resected tissues or organs, e.g., superior mesenteric/portal vein – Depth of tumor invasion
• Lymph nodes: number of involved lymph nodes/total number of lymph nodes – Regional (number and position of lymph nodes according to UICC TNM or JPS system) [6, 54] – Extraregional
• Tumor propagation – Lymphatic – Vascular – Perineural – Duct cancerization
• Resection margins – Transection margins: pancreatic neck, common bile duct, stomach/duodenum – Circumferential margins: facing SMV, facing SMA, posterior, anterior, around extrapancreatic common bile duct – Resection margins of additionally resected structures or organs (e.g., venous resection)
• Tumor regression grading[b]
• Tumor stage: (y[b])pT N M L V Pn R
• Precursor lesions: – Pancreatic intraepithelial neoplasia – Intraductal papillary mucinous neoplasia – Mucinous cystic neoplasia
• Background pancreas: – E.g., chronic pancreatitis
• Other findings

Abbreviations: *JPS* Japan Pancreas Society, *SMA* superior mesenteric artery, *SMV* superior mesenteric vein
[a]Not applicable to pancreatic ductal adenocarcinoma following neoadjuvant therapy
[b]For pancreatic ductal adenocarcinoma following neoadjuvant therapy

References

1. Bosetti C, Bertuccio P, Negri E, La Vecchia C, Zeegers MP, Boffetta P. Pancreatic cancer: overview of descriptive epidemiology. Mol Carcinog. 2012;51:3–13.
2. Yachida S, Jones S, Bozic I, Antal T, Leary R, Fu B, et al. Distant metastasis occurs late during the genetic evolution of pancreatic cancer. Nature. 2010;467:1114–8.
3. Andersen DK, Korc M, Petersen GM, Eibl G, Li D, Rickels MR, Chari ST, Abbruzzese JL. Diabetes, pancreatogeneic diabetes, and pancreatic cancer. Diabetes. 2017;66:1103–10.
4. Lokuhetty D, White V, Watanabe R, Cree IA, editors. Digestive system of malignant tumours. WHO classification of tumours. 5th ed. Lyon, France: IARC Press; 2019.
5. Verbeke C. Morphological heterogeneity in ductal adenocarcinoma of the pancreas—does it matter? Pancreatology. 2016;16:295–301.

6. Brierley JD, Gospodarowicz MK, Wittekind C, editors. UICC: TNM classification of malignant tumours. 8th ed. Oxford: Wiley-Blackwell; 2017.
7. Giulianotti PC, Oggi U, Fornaciari G, Bruno J, Rossi G, Giardino D, Di Candio G, Mosca F. Prognostic value of histological grading in ductal adenocarcinoma of the pancreas. Klöppel vs TNM grading. Int J Pancreatol. 1995;17:279–89.
8. Harsha HC, Kandasamy K, Ranganathan P, Rani S, Ramabadran S, Gollapudi S, et al. A compendium of potential biomarkers of pancreatic cancer. PLoS Med. 2009;6:e1000046.
9. Dennis JL, Hvidsten TR, Wit EC, Komorowski J, Bell AK, Downie I, et al. Markers of adenocarcinoma characteristic of the site of origin: development of a diagnostic algorithm. Clin Cancer Res. 2005;11:3766–72.
10. Liu H, Shi J, Anadan V, Wan HL, Diehl D, Blansfield J, Gerhard GI, Lin F. Reevaluation and identification of the best immunohistochemical panel (pVHL, maspin, S100P, IMP-3) for ductal adenocarcinoma of the pancreas. Arch Pathol Lab Med. 2012;136:601–9.
11. Winter JM, Tang LH, Klimstra DS, Brennan MF, Brody JR, Rocha FG, et al. A novel survival-based tissue microarray of pancreatic cancer validates MUC1 and mesothelin as markers. PLoS One. 2012;7:e40157.
12. Ishii M, Kimuar Y, Sugita S, Imamura M, Ito T, Nobuoka T, Meguro M, Hasegawa T, Mizuguchi T, Hirata K. Surgical and oncological impact of main pancreatic duct spread in invasive ductal adenocarcinoma: a clinicopathological study of 184 resected cases. Pancreatology. 2015;15:681–7.
13. Sobin LH, Gospodarowicz MK, Wittekind C, editors. UICC: TNM classification of malignant tumours. 7th ed. Oxford: Wiley-Blackwell; 2009.
14. Allen PJ, Kuk D, Castillo CF, Basturk O, Wolfgang CL, Cameron JL, et al. Multi-institutional validation study of the American Joint Commission on Cancer (8th edition) changes for T and N staging in patients with pancreatic adenocarcinoma. Ann Surg. 2017;265:185–91.
15. van Roessel S, Kasumova GG, Verheij J, Najarian RM, Maggino L, de Pastena M, et al. International validation of the eighth edition of the American Joint Committee on Cancer (AJCC) TNM staging system in patients with resected pancreatic cancer. JAMA Surg. 2018;153:e183617.
16. Park MY, Shin SH, Song KB, Hwang D, Lee JH, Lee YJ, Kim SC. Validation of the eighth edition of the American Joint Committee on Cancer staging system and proposal of an improved staging system for pancreatic ductal adenocarcinoma. Ann Hepatobiliary Pancreat Surg. 2019;23:46–55.
17. Kamarajah SK, Burns WR, Frankel TL, Cho CS, Nathan H. Validation of the American Joint Commission on Cancer (AJCC) 8th edition staging system for patients with pancreatic adenocarcinoma: a surveillance, epidemiology and end results (SEER) analysis. Ann Surg Oncol. 2017;24:2023–30.
18. Amin MB, Edge SB, Green FL, Byrd DR, Brookland RK, Washington MK, et al., editors. AJCC Cancer staging manual. 8th ed. New York: Springer; 2017.
19. Wang J, Estrella JS, Peng L, Rashid A, Varadhachary GR, Wang H, et al. Histologic tumor involvement of superior mesenteric vein/portal vein predicts poor prognosis in patients with stage II pancreatic adenocarcinoma treated with neoadjuvant chemoradiation. Cancer. 2012;118:3801–11.
20. Beltrame V, Gruppo M, Pedrazzoli S, Merigliano S, Pastorelli D, Sperti C. Mesenteric-portal vein resection during pancreatectomy for pancreatic cancer. Gastroenterol Res Pract. 2015;2015:659730.
21. Tseng JF, Raut CP, Lee JE, Pisters PW, Vauthey JN, Abdalla EK, et al. Pancreaticoduodenectomy with vascular resection: margin status and survival duration. J Gastroinstest Surg. 2004;8:935–49.
22. Yekebas EF, Bogoevski D, Cataldegirmen G, Kunze C, Marx A, Vashist YK, et al. En bloc vascular resection for locally advanced pancreatic malignancies infiltrating major blood vessels: preoperative outcome and long-term survival in 136 patients. Ann Surg. 2008;247:300–9.
23. Fukuda S, Oussoultzoglou E, Bachellier P, Rosso E, Nakano H, Audet M, Jaeck D. Significance of the depth of portal vein wall invasion after curative resection for pancreatic adenocarcinoma. Arch Surg. 2007;142:172–9.
24. Ravikumar R, Sabin C, Abu Hilal M, Aroori S, Bond-Smith G, Bramhall S, et al. Impact of portal vein infiltration and type of venous reconstruction in surgery for borderline resectable pancreatic cancer. Brit J Surg. 2017;104:1538–48.
25. Slidell MB, Chang DC, Cameron JL, Wolfgang C, Herman JM, Schulick RD, Choti MA, Pawlik TM. Impact of total lymph node count and lymph node ratio on staging and survival after pancreatectomy for pancreatic adenocarcinoma: a large, population-based analysis. Ann Surg Oncol. 2008;15:165–74.
26. Schwarz RE, Smith DD. Extent of lymph node retrieval and pancreatic cancer survival: information from a large US population database. Ann Surg Oncol. 2006;13:1189–200.
27. Campbell F, Cairns A, Duthie F, Feakins R. Dataset for the histopathological reporting of carcinoma of the pancreas, ampulla of Vater and common bile duct. 2019. https://www.rcpath.org. Accessed 01 Oct 2019.
28. Verbeke CS, Knapp J, Gladhaug IP. Tumour growth is more dispersed in pancreatic head cancers than in rectal cancer—implications for resection margin assessment. Histopathology. 2011;59:1111–21.
29. Verbeke C, Frankel W. Pathology. Operative standards for cancer surgery presented by the American College of Surgeons and the Alliance for Clinical Trials in Oncology. Volume I: Breast, lung, pancreas, colon. Edited by Katz MH, Posner M. Philadelphia, PA: Lippincott Williams & Wilkins; 2015, p. 181–272.
30. Jamieson NB, Foulis AK, Oien KA, Going JJ, Glen P, Dickson EJ, Imrie CW, McKay CJ, Carter R. Positive immobilization margins alone do not influence survival following pancreatico-duodenectomy

for pancreatic ductal adenocarcinoma. Ann Surg. 2010;251:1003–10.
31. Kleive D, Labori KJ, Line PD, Gladhaug IP, Verbeke CS. Pancreatoduodenectomy with venous resection for ductal adenocarcinoma rarely achieves complete (R0) resection. HPB (Oxford). 2020;22:50–7.
32. Sharma S, Green KB. The pancreatic duct and its arteriovenous relationship. An underutilized aid in the diagnosis and distinction of pancreatic adenocarcinoma from pancreatic intraepithelial neoplasia. A study of 126 pancreatectomy specimens. Am J Surg Pathol. 2004;28:613–20.
33. Wachtel MS, Miller EJ. Focal changes of chronic pancreatitis and duct-arteriovenous relationships. Avoiding a diagnostic pitfall. Am J Surg Pathol. 2005;29:1521–3.
34. Xue Y, Vanoli A, Balci S, Reid MM, Saka B, Bagci P, et al. Non-ampullary-duodenal carcinomas: clinicopathologic analysis of 47 cases and comparison with ampullary and pancreatic adenocarcinomas. Mod Pathol. 2017;30:255–66.
35. Ang DC, Shia J, Tang LH, Katabi N, Klimstra DS. The utility of immunohistochemistry in subtyping adenocarcinoma of the ampulla of Vater. Am J Surg Pathol. 2014;38:1371–9.
36. Xue Y, Reid MM, Balci S, Quigley B, Muraki T, Memis B, et al. Immunohistochemical classification of ampullary carcinomas. Critical reappraisal fails to confirm prognostic relevance for recently proposed panels, and highlights MUC5AC as a strong prognosticator. Am J Surg Pathol. 2017;41:865–76.
37. Notta F, Chan-Seng-Yue M, Lemire M, Li Y, Wilson GW, Connor AA, et al. A renewed model of pancreas cancer evolution based on genomic rearrangement patterns. Nature. 2016;538:378–82.
38. Neoptolemos JP, Kleeff J, Michl P, Costello E, Greenhalf W, Palmer DH. Therapeutic development in pancreatic cancer: current and future perspectives. Nature Rev Gastroenterol Hepathol. 2018;15:333–48.
39. Tanaka M, Mihaljevic AL, Probst P, Heckler M, Klaiber U, Heger U, et al. Meta-analysis of recurrence pattern after resection for pancreatic cancer. Brit J Surg. 2019;106:1590–601.
40. Kalimuthu SN, Wilson GW, Grant RC, Seto M, O'Kane G, Vajpeyi R, Notta F, Gallinger S, Chetty R. Morphological classification of pancreatic ductal adenocarcinoma that predicts molecular subtypes and correlates with clinical outcome. Gut. 2019;69:317–28.
41. Wilentz RE, Goggings M, Redston M, Marcus VA, Adsay NV, Sohn TA, et al. Genetic, immunohistochemical, and clinical features of medullary carcinoma of the pancreas. A newly described and characterized entity. Am J Pathol. 2000;156:1641–51.
42. Guzinska-Ustymowicz K, Niewiarowska K, Pryczynicz A. Invasive micropapillary carcinoma: a distinct type of adenocarcinoma in the gastrointestinal tract. World J Gastroenterol. 2014;20:4597–606.
43. Muraki T, Reid MD, Basturk O, Jang K-T, Bedolla G, Bagci P, et al. Undifferentiated carcinoma with osteoclastic giant cells of the pancreas: clinicopathological analysis of 38 cases highlights a more protracted clinical course than currently appreciated. Am J Surg Pathol. 2016;40:1203–16.
44. Verbeke C, Häberle L, Lenggenhager D, Esposito I. Pathology assessment of pancreatic cancer following neoadjuvant treatment: time to move on. Pancreatology. 2018;18:467–76.
45. Klaiber U, Schnaidt ES, Hinz U, Gaida MM, Heger U, Hank T, Strobel O, Neoptolemos JP, Mihaljevic AL, Büchler MW, Hackert T. Prognostic factors of survival after neoadjuvant treatment and resection for initially unresectable pancreatic cancer. Ann Surg. 2019; https://doi.org/10.1097/SLA.0000000000003270. Online ahead of print.
46. Evans DB, Rich TA, Byrd DR, Cleary KR, Connelly JH, Levin B, Chamsangavej C, Fenoglio CJ, Ames FC. Preoperative chemoradiation and pancreaticoduodenectomy for adenocarcinoma of the pancreas. Arch Surg. 1992;127:1335–9.
47. Chatterjee D, Katz MH, Rashid A, Varadhachary GR, Wolff RA, Wang H, et al. HIstologica grading of the extent of residual carcinoma following neoadjuvant chemoradiation in pancreatic ductal adenocarcinoma: a predictor for patient outcome. Cancer. 2012;118:3182–90.
48. Kakar S, Shi C, Adsay NV, Fitzgibbons P, Frankel WL, Klimstra DS, et al. Protocol for the examination of specimens from patients with carcinoma of the pancreas: College of American Pathologists (CAP).
49. Kalimuthu SN, Serra S, Dhani N, Hafezi-Bakhtiari S, Szentgyorgyi E, Vajpeyi R, Chetty R. Regression grading in neoadjuvant treated pancreatic cancer: an interobserver study. J Clin Pathol. 2017;70:237–43.
50. Bailey P, Chang DK, Nones K, Johns AL, Patch AM, Gingras MC, et al. Genomic analyses identify molecular subtypes of pancreatic cancer. Nature. 2016;531:47–52.
51. Collisson EA, Sadanandam A, Olson P, Gibb WJ, Truitt M, Gu S, et al. Subtypes of pancreatic ductal adenocarcinoma and their different responses to therapy. Nat Med. 2011;17:500–3.
52. Moffitt RA, Marayati R, Flate EL, Volmar KE, Loeza SG, Hoadley KA, et al. Virtual microdissection identifies distinct tumor- and stroma-specific subtypes of pancreatic ductal adenocarcinoma. Nat Genet. 2015;47:1168–78.
53. Singh RR, Goldberg J, Varghese AM, Yu KH, Park W, O'Reilly EM. Genomic profiling in pancreatic ductal adenocarcinoma and a pathway towards therapy individualisation: a scoping review. Cancer Treat Rev. 2019;75:27–38.
54. Japan Pancreas Society. Classification of pancreatic carcinoma. 4th ed. (English). Tokyo: Kanehara; 2017.

Check for updates

Acinar Cell Carcinoma

10

Acinar cell carcinoma is a rare malignant epithelial neoplasm composed of cells which morphologically resemble acinar cells and produce pancreatic enzymes. They may show a wide range of morphological appearances, ranging from well-differentiated acinar structures to solid sheets of poorly differentiated cells, which can cause diagnostic difficulty.

10.1 WHO Classification

Acinar cell carcinoma is classified as a 'malignant epithelial tumor' in the 2019 WHO classification of tumors of the pancreas [1].

10.2 Terminology

Acinar cell carcinoma is totally unrelated to acinar cell nodules (see Chap. 5, Sect. 5.1) or the benign entity acinar cystic transformation of the pancreas (see Chap. 19, Sect. 19.1).

10.3 Epidemiology

Acinar cell carcinoma accounts for 1–2% of pancreatic exocrine neoplasms in adults and for approximately 15% of pediatric pancreatic exocrine neoplasms. Most occur in late adulthood, mean age 60 years, but 6% occur in children usually 8–15 years of age. The age range is 3–90 years. Males are affected more often than females (male-to-female ratio of 2:1).

10.4 Clinical Features

Most patients present with nonspecific symptoms such as abdominal pain, nausea and vomiting, and weight loss. Jaundice is rare.

Up to 10–15% of patients may present with the lipase hypersecretion syndrome, a paraneoplastic syndrome characterized by elevated serum lipase, diffuse subcutaneous fat necrosis, and polyarthralgia, with or without blood eosinophilia. Patients may present with this syndrome or develop it after tumor recurrence. Symptoms may resolve after tumor resection. Up to 50% of patients with acinar cell carcinoma present with metastatic disease in lymph nodes, liver, lungs, or peritoneum.

10.4.1 Associations

There are case reports of acinar cell carcinoma arising in patients with Lynch syndrome (hereditary non-polyposis colorectal cancer) [2] or Familial Adenomatous Polyposis [3].

© Springer Nature Switzerland AG 2021
F. Campbell, C. S. Verbeke, *Pathology of the Pancreas*,
https://doi.org/10.1007/978-3-030-49848-1_10

10.4.2 Imaging

On CT and MRI, acinar cell carcinomas are generally large, well circumscribed, round or oval, solid, and homogeneous, but they may show necrosis and areas of degenerative cystic change.

10.5 Macroscopy

Acinar cell carcinomas are large, well-circumscribed, partially encapsulated, soft, solitary tumors with a pushing (expanding), rather than an infiltrative, border (Fig. 10.1). The cut-surface is tan to red-brown, white to grey, homogeneous, and multinodular (lobulated), but there may be foci of hemorrhage, necrosis, and degenerative cystic change (Fig. 10.2). They can occur anywhere within the pancreas, but are slightly more common in the head of the pancreas, and may show intraductal growth (Fig. 10.3) or invade adjacent structures (Fig. 10.1b). The mean size is 8 cm with a range of 2–30 cm.

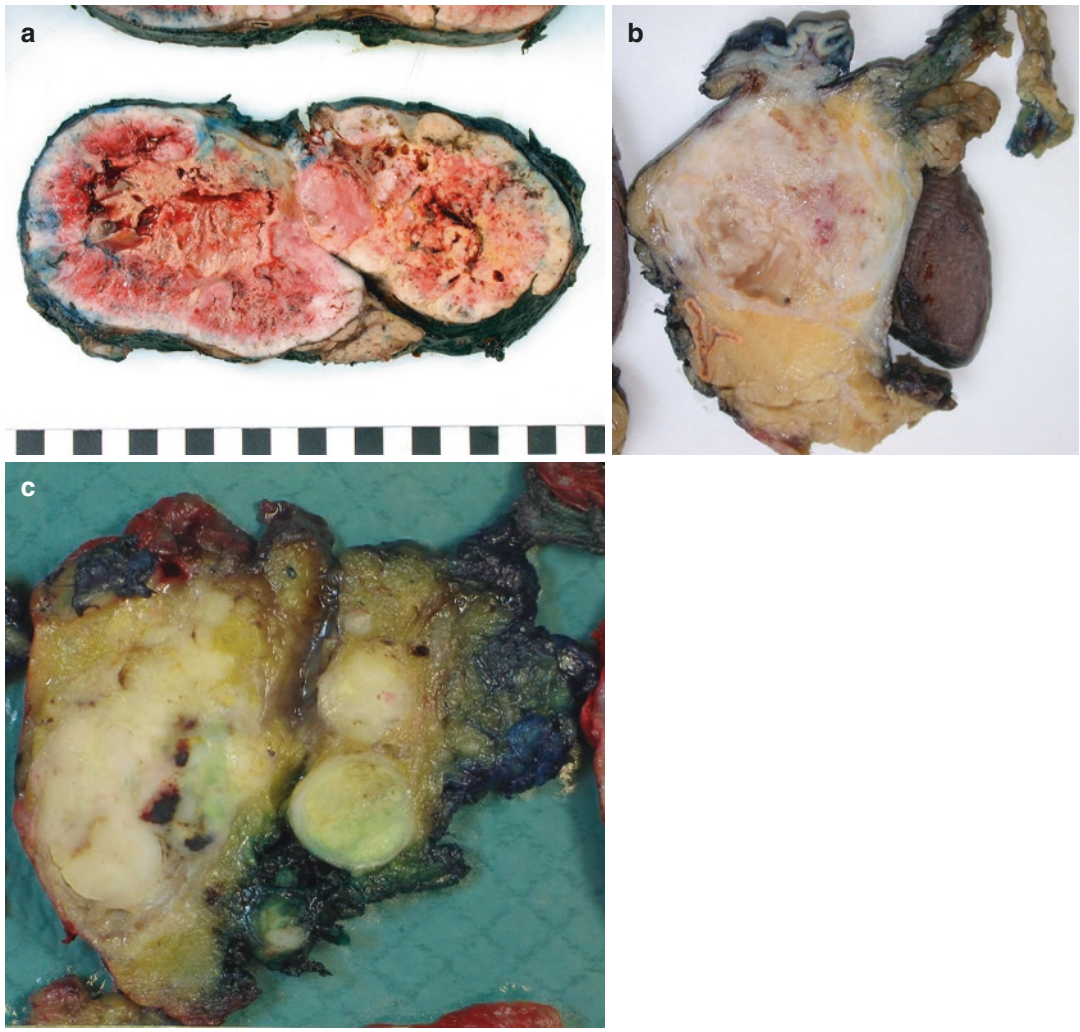

Fig. 10.1 Acinar cell carcinoma: the tumor is well circumscribed, nodular and shows areas of hemorrhage and cystic degeneration (**a**). The cut-surface of this tumor (**b**) shows partial encapsulation lowermost, near the uninvolved adrenal gland (*bottom left*), but does infiltrate the wall of the stomach (*top*). Vascular invasion is present at the periphery of this tumor as macroscopically visible 'satellite' nodules (**c**)

Fig. 10.2 Cystic degeneration in acinar cell carcinoma: this large, totally encapsulated tumor shows extensive cystic degeneration with residual soft, tan-brown tumor confined to the periphery

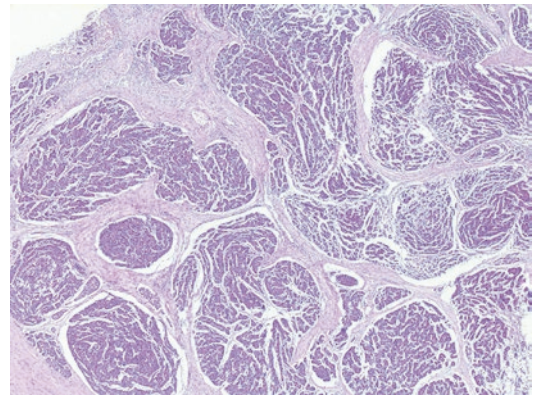

Fig. 10.4 Acinar cell carcinoma: this low-power view shows the lobulated nature of the tumor with lobules of cellular tumor separated by fibrous bands

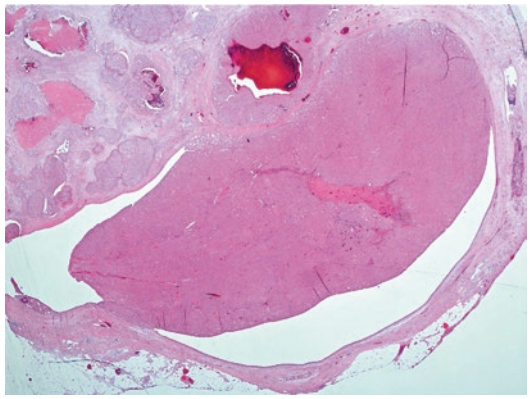

Fig. 10.3 Acinar cell carcinoma: this acinar cell carcinoma shows prominent intraductal growth, which was visible macroscopically

10.5.1 Sampling

Specimens containing an acinar cell carcinoma should be sampled thoroughly (see Chap. 3, Sect. 3.3.8) to ensure that all of the information required for accurate staging and margin status is obtained.

10.6 Microscopy

Acinar cell carcinomas consist of lobules of highly cellular tumor separated by hypocellular fibrous bands without desmoplasia (Fig. 10.4). The periphery of the carcinoma is usually well circumscribed but there may be irregular extension into the adjacent pancreas and peripancreatic structures. There may be extensive coagulative necrosis.

The carcinoma cells may be arranged in an acinar pattern (Fig. 10.5), solid sheets or, less commonly, a trabecular or gyriform pattern. A mixture of growth patterns can occur in the same carcinoma. There are often numerous small vessels around the nests of carcinoma cells (Fig. 10.5b).

In the acinar growth pattern, there are back-to-back acini with pyramidal cells clustered around small lumina. The cells have a moderate amount of cytoplasm and basally located nuclei (Fig. 10.5c). If the lumina become dilated, the architecture can become more glandular (Fig. 10.6). In the solid pattern, there are large sheets of cells, with minimal to moderate cytoplasm, separated by small blood vessels and scanty stroma (Fig. 10.7a). Occasionally, there may be palisading of the nuclei at the interface of these solid sheets with the vessels. In the trabecular pattern, there are interlacing ribbons or trabeculae, each consisting of two rows of cells with peripherally located nuclei. The gyriform pattern is rare and resembles that of pancreatic endocrine neoplasms.

The carcinoma cells have minimal to moderate amounts of amphophilic to eosinophilic, granular cytoplasm. The granularity is due to the presence of zymogen granules. The nuclei in acinar cell carcinomas are generally fairly uniform,

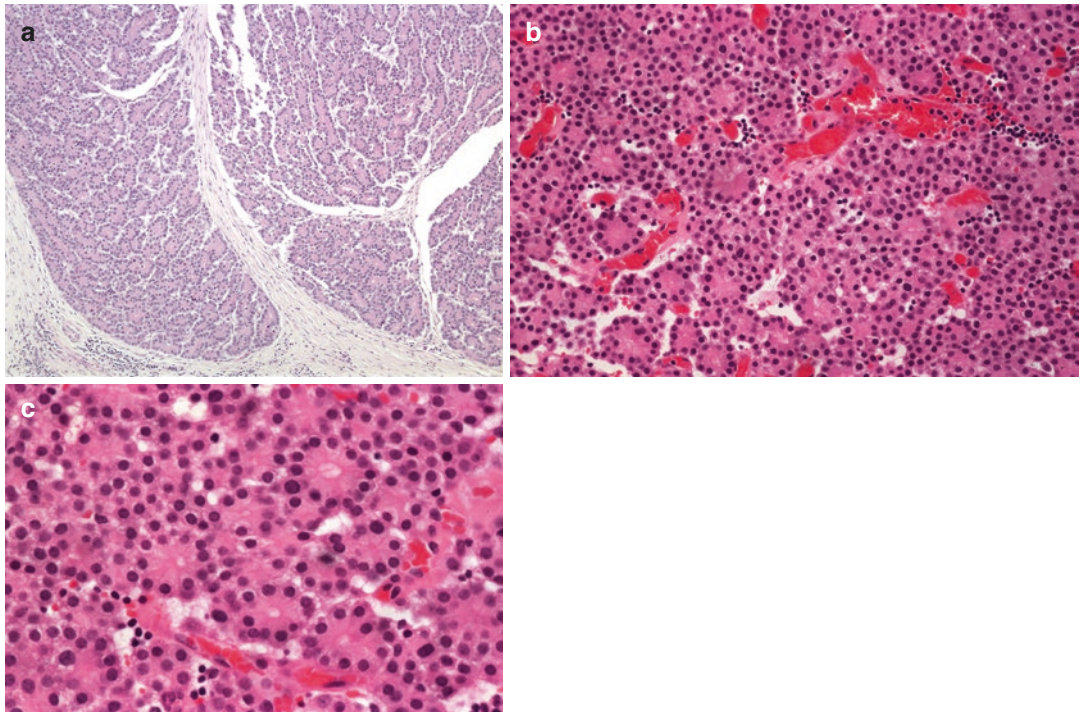

Fig. 10.5 Acinar cell carcinoma: the lobules show an acinar growth pattern with back-to-back acini (**a**). There are numerous small blood vessels between the acini, which are composed of pyramidal cells (with basally located nuclei) clustered around small lumina (**b**). In this example, nucleoli are inconspicuous (**c**)

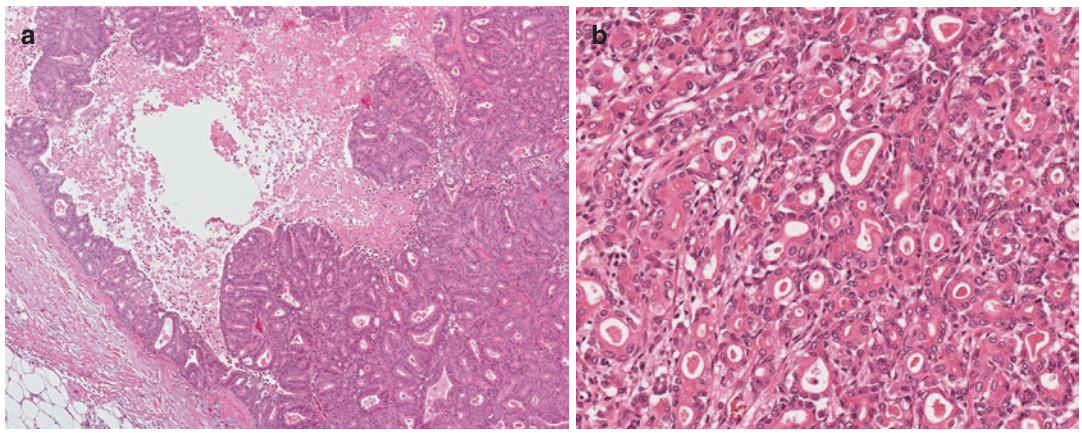

Fig. 10.6 Acinar cell carcinoma: there is a glandular growth pattern and necrosis (**a**). The gland lumina are clearly visible at higher power (**b**)

round to oval, and have a characteristic single, central nucleolus (Fig. 10.7). However, a nucleolus is not always present and there may be nuclear atypia, which La Rosa et al. [3] graded into three groups. In their grading system, well-differentiated carcinomas have cells with uniform, monomorphic nuclei with inconspicuous nucleoli (Fig. 10.5c), whereas poorly differentiated carcinomas have large vesicular nuclei with dispersed chromatin and eosinophilic nucleoli. A poor degree of differentiation was seen more commonly in carcinomas with a solid

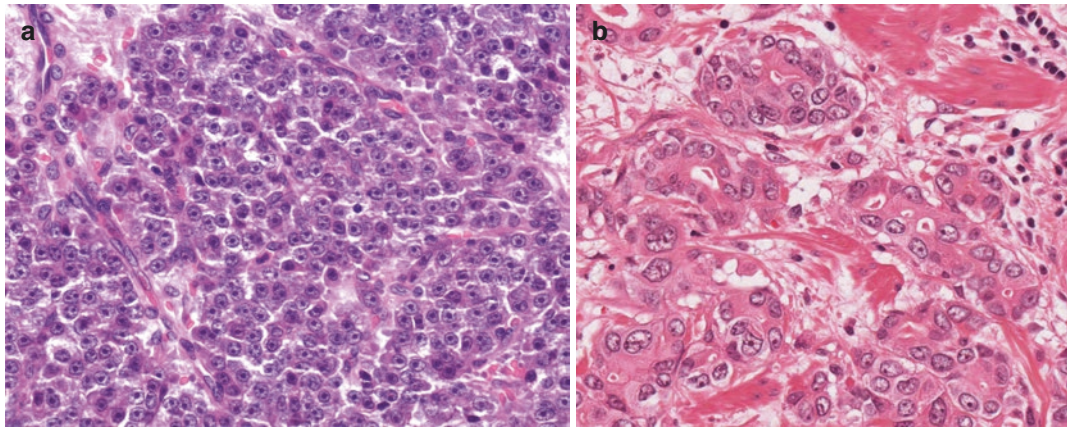

Fig. 10.7 Acinar cell carcinoma: there is a solid growth pattern with tumor cells showing a prominent central single nucleolus within uniform nuclei (**a**). In this example of glandular growth pattern, there is more variation in nuclear size and shape (**b**)

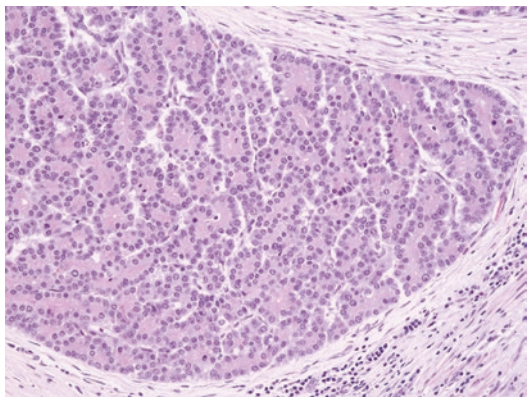

Fig. 10.8 Acinar cell carcinoma: acinar growth pattern with prominent mitotic figures

growth pattern. Moderately differentiated carcinomas show variation in nuclear size, with or without prominent nucleoli, but not to the same degree as that seen in poorly differentiated carcinomas. This grading scheme, however, has not been accepted into current diagnostic practice, and grading is not recommended by the College of American Pathologists and the International Collaboration on Cancer Reporting (ICCR).

Mitotic figures (Fig. 10.8) are readily found (with a mean of 10–15/10 high power fields). Vascular invasion is often present, outside (Fig. 10.1c) or within the capsule, whereas perineural invasion is less frequently found.

10.7 Histochemistry

The zymogen granules, which are present particularly in the apical aspect of the carcinoma cells, are weakly positive with periodic acid-Schiff (PAS) (Fig. 10.9) and PAS-diastase. However, there may be no staining if there are only scanty zymogen granules. The cytoplasm is negative for mucicarmine and alcian blue (mucin stains), but focal faint staining may be present on the apical surface of the cells.

10.8 Immunohistochemistry

Acinar differentiation can be confirmed by the use of antibodies against pancreatic enzymes such as trypsin (Fig. 10.10), chymotrypsin, and lipase. Pancreatic amylase is rarely detected, despite its presence in normal acinar cells. There may be diffuse cytoplasmic immunopositivity for these enzymes in solid areas or apical cytoplasmic staining in acinar areas (Fig. 10.10). In a large, multi-institutional series, trypsin was detected in 95% of cases, lipase in 26%, and amylase in 9% [3]. BCL10 was detected in 86% of cases. The cases that were negative for trypsin were positive for BCL10, leading the authors to conclude that antibodies directed against trypsin and BCL10 seem to be the best in terms of sensitivity.

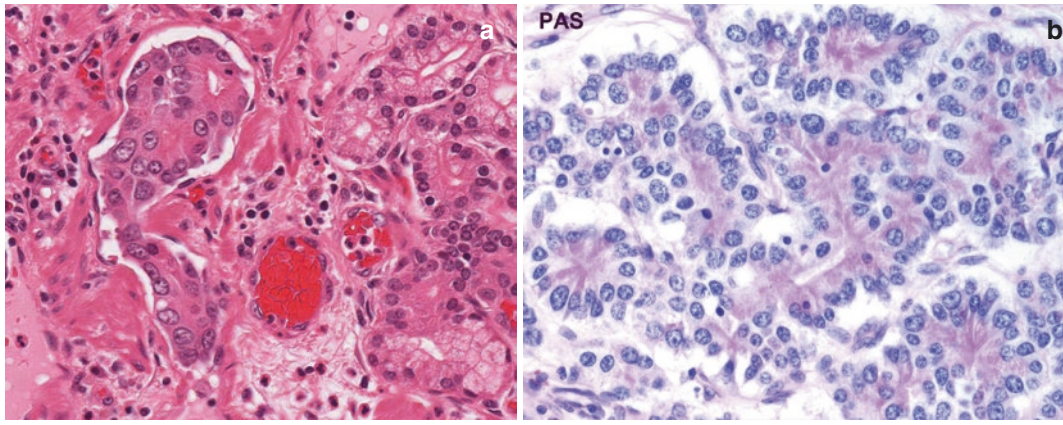

Fig. 10.9 Acinar cell carcinoma: eosinophilic zymogen granules can be seen in the apical cytoplasm of this intralymphatic tumor (present in the duodenal submucosa), which shows a glandular growth pattern (**a**). On histochemistry, the apical cytoplasm of the carcinoma cells is weakly positive with periodic acid-Schiff (**b**)

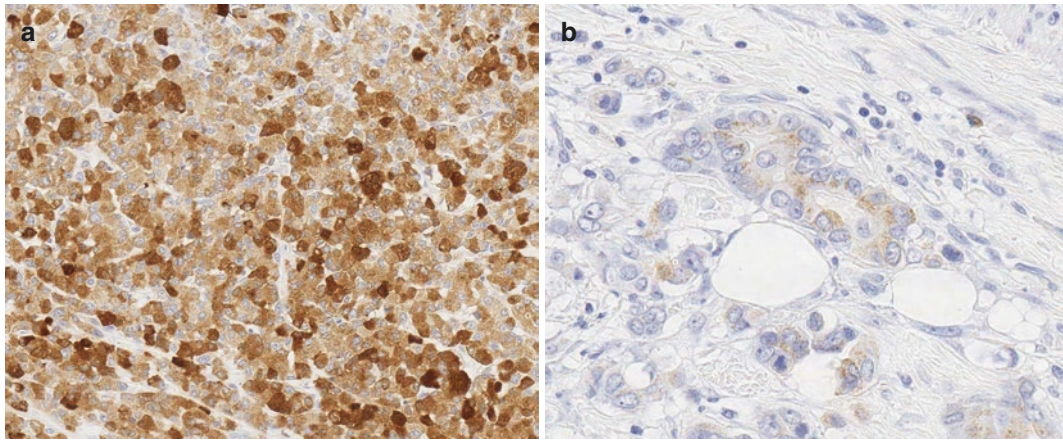

Fig. 10.10 Acinar cell carcinoma: on trypsin immunohistochemistry, there is some variation in intensity of cytoplasmic staining in this area of solid growth pattern (**a**). In the same tumor, a focus of glandular growth pattern, within peripancreatic fat, shows only fine granular immunopositivity in the apical cytoplasm (**b**)

Acinar cell carcinomas are generally immunopositive for alpha-1-antitrypsin (Fig. 10.11), AE1/AE3, CAM5.2, CK8, and CK18. Approximately 50% of cases express EMA. There are conflicting results with CK7 and CK19, which may relate to the different antibodies used in different studies. These are traditionally considered to be markers of ductal differentiation and, in some studies, have not been expressed by acinar cell carcinomas. However, in one large study, CK7 expression was found in 73% of cases and CK19 in 86% of cases [3]. The immunoreactivity for both of these cytokeratins was generally strong and present in a large number of carcinoma cells, but in some cases it was confined to groups of carcinoma cells, suggesting a clonal proliferation. Both of these cytokeratins are expressed in pancreatic ductal adenocarcinoma which, therefore, may need to be considered in the differential diagnosis on a small biopsy.

Immunohistochemistry may show patchy or diffuse, nuclear staining for beta-catenin, in a small number of cases. Immunohistochemistry for Ki67 will highlight the proliferative activity (Fig. 10.12); the mean Ki67 index was 32% in the study by La Rosa et al. [3].

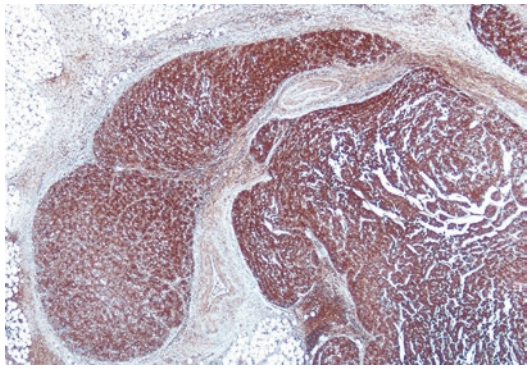

Fig. 10.11 Acinar cell carcinoma: there is diffuse cytoplasmic immunopositivity with alpha-1-antitrypsin throughout this tumor

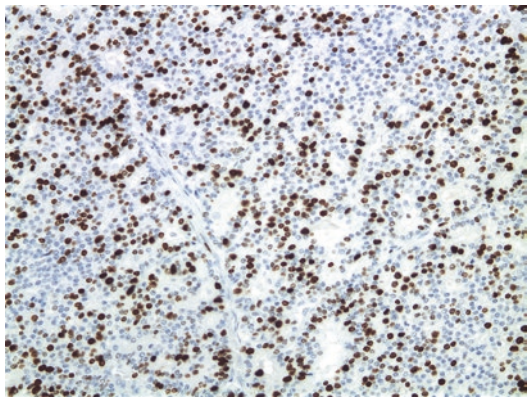

Fig. 10.12 Acinar cell carcinoma: there is a high Ki67 proliferative index

Occasionally, there may be immunopositivity for alpha-fetoprotein (in patients with and without elevated serum alpha-fetoprotein). There may be scattered endocrine cells or focal nodules of endocrine cells within an acinar cell carcinoma, which will express chromogranin A and/or synaptophysin. When more than 30% of the tumor shows such endocrine differentiation, then the tumor should be classified as a mixed acinar cell carcinoma-neuroendocrine carcinoma (see Chap. 20, Sect. 20.10).

10.9 Molecular Pathology

The typical genetic alterations observed in pancreatic ductal adenocarcinoma are found much less frequently in acinar cell carcinoma: mutations in *KRAS* are extremely rare, and alterations in *TP53*, *SMAD4,* and *CDKN2A* occur in no more than 25% of acinar cell carcinomas [4, 5]. Abnormalities in the APC/beta-catenin pathway are common, somatic alterations in *BRCA2* occur in about 12% of cases, and, although *BRAF* mutations are rare, 23% of acinar cell carcinomas harbor rearrangements of *BRAF* and *RAF1* [4, 6]. Acinar cell carcinomas, however, do have a high degree of genomic instability and frequent DNA repair defects [7, 8]. Although identification of these genetic alterations is not required for diagnosis, there may be a future role in treatment and personalized therapy.

10.10 Variants

Clear cell change, *signet ring cells,* and *oncocytic differentiation* have been described in acinar cell carcinomas. *Spindle cells* have also been described in two carcinomas with a solid growth pattern [3]. Signet ring cells have been described within the solid sheets of cells and show crescentic nuclei displaced by the abundant cytoplasm. The lack of single cell stromal infiltration or mucin within these cells will distinguish them from a signet ring cell subtype of pancreatic ductal adenocarcinoma (see Chap. 9, Sect. 9.14.3).

10.10.1 Intraductal Nodular and Papillary Variants

There are a small number of reported cases of acinar cell carcinoma which, in addition to solid areas, showed macroscopic cystic dilatation of the pancreatic ducts [9]. On microscopy, some of the tumors showed a nodular (lobular) growth pattern of acinar cells (solid or acinar pattern) with extension into ducts as macroscopically visible polypoid projections. In some tumors, there was a papillary or papillocystic growth pattern with papillae containing fibrovascular cores, again with intraductal growth. Both variants mimicked intraductal papillary neoplasia (see Chap. 17), but were readily distinguished by the neoplastic cells, which were histologically and immunohistochemically similar to conventional acinar cell carcinoma.

There has been one case report of diffuse involvement of the pancreatic duct system by intraductal acinar cell carcinoma [10]. In contrast to the above intraductal variants, which were solitary tumors with extension into ducts, there was no distinct tumor mass in this case.

10.10.2 Cystic Variant (Acinar Cell Cystadenocarcinoma)

There are extremely rare cases of acinar cell carcinoma showing macroscopic (non-degenerative) cyst formation, which have been reported as acinar cell cystadenocarcinoma. They are usually large (mean size 24 cm) and multilocular with a pseudocapsule [11]. The variably-sized cysts (ranging from a few millimeters to several centimeters) are separated by thin septa and, macroscopically, the tumor may resemble a microcystic serous cystadenoma. The cysts contain eosinophilic material, with a few concentric lamellae, and are lined by neoplastic cells similar to those seen in conventional acinar cell carcinoma with solid and cribriform areas. The clinical behavior appears to be the same as that for conventional acinar cell carcinoma.

10.10.3 Mixed Acinar Carcinomas

Acinar cell carcinomas may rarely have a component of ductal or neuroendocrine differentiation, either as topographically separate areas (so called collision tumor) or as intermingled coexisting, but distinct, populations (so called composite tumor). The different types of differentiation may require confirmation by immunohistochemistry. When each component accounts for more than 30% of the tumor, then the tumor may be called a mixed acinar-ductal carcinoma or a mixed acinar cell carcinoma-neuroendocrine carcinoma (Fig. 10.13), respectively. Very rarely, there may be all three components in the same tumor (each >30%), so-called mixed acinar cell carcinoma-ductal adenocarcinoma-neuroendocrine carcinoma. The collective term used for tumors composed of a mixture of morphologically recognizable carcinoma and neuroendocrine neoplasm is 'mixed neuroendocrine—non-neuroendocrine neoplasm' or MiNEN (see Chap. 20, Sect. 20.10). More commonly, however, there may be amphicrine differentiation, when individual tumor cells express both acinar cell markers and neuroendocrine markers, or acinar cell markers and mucin, on histochemistry and/or immunohistochemistry. These amphicrine tumors are not considered to meet the definition for MiNEN, which requires morphologically recognizable different components, and are referred to as mixed acinar carcinomas.

10.11 Differential Diagnosis

10.11.1 Pancreatic Neuroendocrine Neoplasia

Acinar cell carcinoma with a nested or trabecular growth pattern and small uniform nuclei may mimic a grade 1–3 pancreatic neuroendocrine tumor (see Chap. 20, Sect. 20.9.1). However, acinar cell carcinomas have readily identifiable mitotic figures, do not show the 'salt and pepper' chromatin pattern (typical of pancreatic neuroendocrine tumors), and show acinar differentiation on immunohistochemistry (see Table 20.5).

Poorly differentiated acinar cell carcinomas may mimic large cell type pancreatic neuroendocrine carcinoma (see Chap. 20, Sect. 20.9.2). Both can show extensive necrosis, prominent nucleoli, and a high mitotic count. Immunohistochemistry for acinar cell markers and for endocrine markers (chromogranin A, synaptophysin, and CD56) will help make the distinction (see Table 20.5). However, it is important to remember that acinar cell carcinomas can have an endocrine component (as scattered cells or focal nodules), and when this endocrine component accounts for >30% of the tumor, the tumor should be classified as a mixed acinar cell carcinoma-neuroendocrine carcinoma.

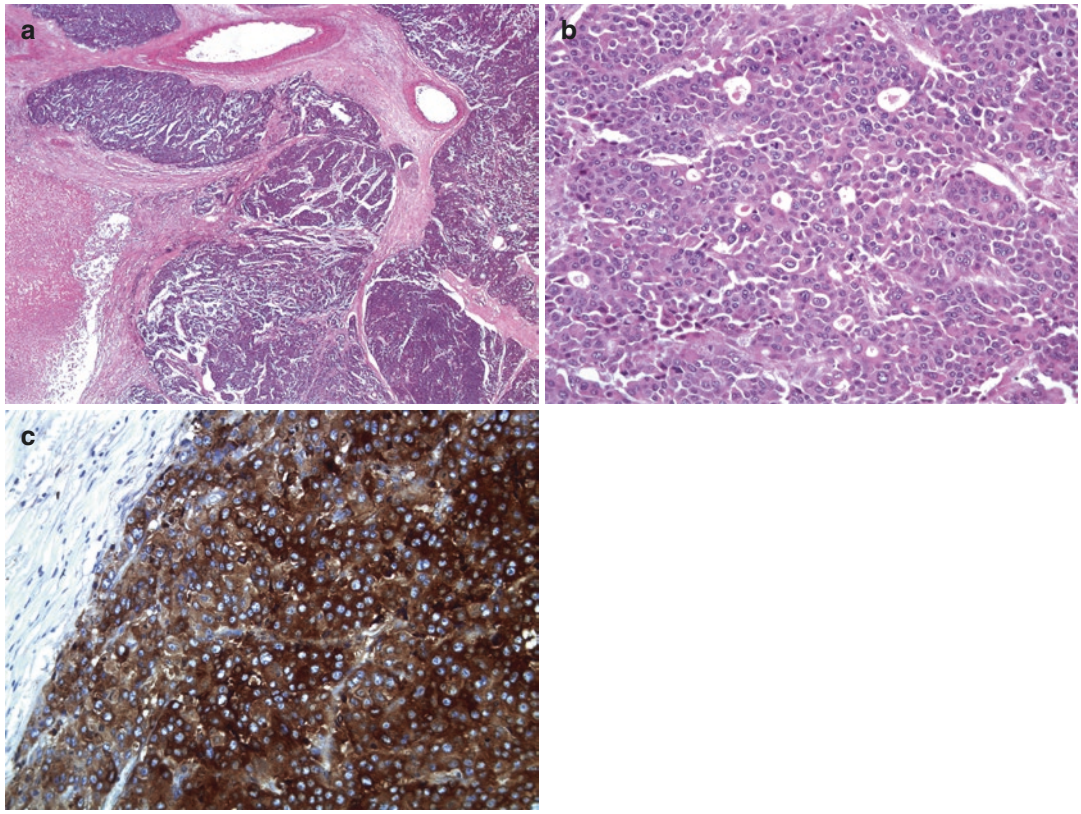

Fig. 10.13 Mixed acinar cell carcinoma-neuroendocrine carcinoma (MiNEN): the lobules of cellular tumor separated by fibrous septa are typical for acinar cell carcinoma (**a**). In some areas, the cytology of the tumor cells is typical for acinar cell carcinoma. However, in other areas, (**b**) the tumor nuclei are not uniform and lack the single central nucleolus. These areas are strongly positive for synaptophysin and represent a component of neuroendocrine carcinoma (large cell type) within this mixed tumor (**c**)

10.11.2 Solid Pseudopapillary Neoplasm

Acinar cell carcinoma may mimic the solid component of a solid pseudopapillary neoplasm, which typically occurs in young females (see Chap. 18). However, solid pseudopapillary neoplasms express vimentin, CD56, CD10, progesterone receptors, and beta-catenin (abnormal nuclear and cytoplasmic staining), and do not express trypsin or other acinar cell markers (see Table 20.5).

10.11.3 Pancreatoblastoma

Acinar cell carcinoma may mimic pancreatoblastoma, an extremely uncommon malignant epithelial neoplasm characterized by cells showing multiple lines of differentiation including prominent acinar differentiation and squamoid nests (morules). Ductal and endocrine differentiation can be seen, but are generally focal, and some pancreatoblastomas may have a primitive (small, monotonous, immature) cell component. There is also a distinct mesenchymal component.

Pancreatoblastoma occurs almost exclusively in infants and children, mean age 5 years [12], but cases have been described in adults 18–78 years of age [13]. Pancreatoblastomas may be large at presentation (mean 10 cm, range 1.5–20 cm) and are generally well-circumscribed, solid tumors composed of lobules of highly cellular tumor separated by fibrous bands, which can show varying degrees of cellularity. Gross

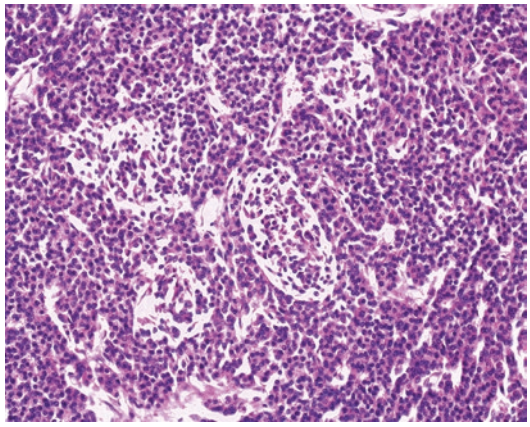

Fig. 10.14 Pancreatoblastoma: cellular tumor showing acinar cell differentiation and a central, non-keratinizing squamoid nest (Kindly provided by Professor Günter Klöppel, Department of Pathology, Technical University, Munich, Germany)

cystic change is described in congenital pancreatoblastomas associated with the Beckwith-Wiedemann syndrome.

Acinar cells predominate and merge with the squamoid nests (Fig. 10.14), which may show keratinization, and are usually located in the center of the epithelial lobules. The nuclei in these squamoid nests may be clear due to the presence of intranuclear biotin, which can result in nonspecific nuclear staining on immunohistochemistry. Endocrine cells are scattered among the acinar cells and may form trabeculae or solid nests. Focal ductal differentiation may be seen as columnar cells surrounding lumina. Mitotic figures may be frequent, and vascular and perineural invasion can also occur.

Immunohistochemistry is positive for Cam5.2, AE1-AE3, CK7, CK8, CK18, CK19, trypsin, chymotrypsin, lipase, and alpha-1-antitrypsin. The endocrine component (present in up to 70% of cases) is positive for chromogranin, synaptophysin, and neuron-specific enolase, and the ductal component is positive for cytokeratins and CEA. The squamous morules are positive for EMA, CK5/6, and nuclear and cytoplasmic beta-catenin [14]. Alpha-fetoprotein may be expressed by the acinar cells in up to a third of cases, and can be detected in the serum.

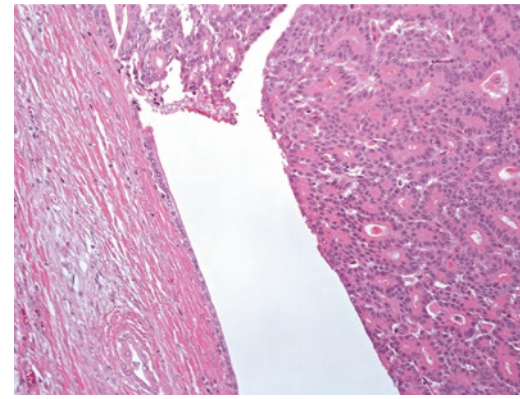

Fig. 10.15 Acinar cell carcinoma: there is intraductal growth of acinar cell carcinoma showing a glandular growth pattern. The duct epithelium can be seen on the left

The distinction between acinar cell carcinoma, which can occur in childhood, and pancreatoblastoma, which can occur in adulthood, can be difficult. The macroscopic and microscopic appearances are similar, but the presence of squamoid nests distinguishes these two entities. Moreover, pancreatoblastomas tend to have a more organoid growth pattern and also have hypercellular stroma, which is lacking in acinar cell carcinoma.

10.11.4 Intraductal Papillary Neoplasms

Acinar cell carcinoma may grow into ducts (Figs. 10.3 and 10.15) and mimic intraductal papillary neoplasms (see Chap. 17). In contrast to intraductal papillary mucinous neoplasms (IPMNs), however, acinar cell carcinoma does not contain mucin. The distinction from the oncocytic type of intraductal papillary neoplasm may be more difficult since it can also show solid growth and is composed of cells with abundant eosinophilic cytoplasm. However, acinar cell carcinoma is a more basophilic tumor and the cells have granular cytoplasm (representing the zymogen granules), which, on immunohistochemistry, stain for markers of acinar differentiation (see Sect. 10.8). Acinar cell carcinoma will not show

expression of mucin glycoproteins, which are found in the oncocytic type of IPMN (see Table 17.1).

10.12 Staging

Acinar cell carcinomas should be staged in the same way as conventional pancreatic ductal adenocarcinoma (see Chap. 9, Sect. 9.11 and Table 9.3).

10.13 Prognosis and Management

Acinar cell carcinoma is an aggressive tumor, but the prognosis is better than that for pancreatic ductal adenocarcinoma. Surgical resection is the treatment of choice but, similar to pancreatic ductal adenocarcinoma, local recurrence or distant metastases can occur following surgery. Epidemiological studies have shown a 5-year survival rate ranging from 36 to 72% for resected acinar cell carcinomas, and a 5-year survival rate of 9 to 22% for unresected cases. In the large, multi-institutional series, patients who underwent a tumor resection showed a statistically better survival compared to patients with unresectable tumors or patients who could not undergo surgery. At multivariate analysis, the only independent prognostic factor was stage [3].

There is no relationship between the histological architectural patterns and prognosis. Patients with acinar cell carcinoma showing intraductal growth appear to have improved survival [9], possibly due to earlier presentation and diagnosis or perhaps different biological behavior.

10.14 Reporting Checklist

A list of macroscopic and microscopic features to consider when reporting an acinar cell carcinoma is shown in Table 10.1.

Table 10.1 Reporting checklist for acinar cell carcinoma

Macroscopic assessment
• Specimen type
• Additional resected structures, e.g., spleen
• Tumor location
• Tumor size (3-dimensions)
• Cut-surface
• Involvement of adjacent organs
• Distance from resection margin(s)
Microscopic assessment
• Growth pattern
• Intraductal growth or not
• Vascular or perineural invasion
• Involvement of other organs/structures
• Completeness of excision/ resection margin status
• Metastases
• Immunohistochemical profile
• UICC TNM staging
• Background changes

References

1. Lokuhetty D, White VA, Watanabe R, Cree IA, editors. Digestive system tumours. WHO classification of tumours. 5th ed. Lyon: IARC Press; 2019. p. 296.
2. Lowery MA, Klimstra DS, Shia J, Yu KH, Allen PJ, Brennan MF, O'Reilly EM. Acinar cell carcinoma of the pancreas: new genetic and treatment insights into a rare malignancy. Oncologist. 2011;16:1714–20.
3. La Rosa S, Adsay V, Albarello L, Asioli S, Casnedi S, Franzi F, et al. Clinicopathologic study of 62 acinar cell carcinomas of the pancreas: insights into the morphology and immunophenotype and search for prognostic markers. Am J Surg Pathol. 2012;36:1782–95.
4. Chmielecki J, Hutchinson KE, Frampton GM, Chalmers ZR, Johnson A, Shi C, et al. Comprehensive genomic profiling of pancreatic acinar cell carcinomas identifies recurrent RAF fusions and frequent inactivation of DNA repair genes. Cancer Discov. 2014;4:1398–405.
5. La Rosa S, Bernasconi B, Frattini M, Tibiletti MG, Molinari F, Furlan D, et al. TP53 alterations in pancreatic acinar cell carcinoma: new insights into the molecular pathology of this rare cancer. Virchows Arch. 2016;468:289–96.
6. Furlan D, Sahnane N, Bernasconi B, Frattini M, Tibiletti MG, Molinari F, et al. APC alterations are frequently involved in the pathogenesis of acinar cell carcinoma of the pancreas, mainly through gene loss and promoter hypermethylation. Virchows Arch. 2014;464:553–64.

7. Bergmann F, Aulmann S, Sipos B, Kloor M, von Heydebreck A, Schweipert J, et al. Acinar cell carcinomas of the pancreas: a molecular analysis in a series of 57 cases. Virchows Arch. 2014;465:661–72.
8. Jakel C, Bergmann F, Toth R, Assenov Y, van der Duin D, Strobel O, et al. Genome-wide genetic and epigenetic analyses of pancreatic acinar cell carcinomas reveal aberrations in genome stability. Nat Commun. 2017;8:1323
9. Basturk O, Zamboni G, Klimstra DS, Capelli P, Andea A, Kamel NS, et al. Intraductal and papillary variants of acinar cell carcinomas. A new addition to the challenging differential diagnosis of intraductal neoplasms. Am J Surg Pathol. 2007;31:363–70.
10. Toll AD, Mitchell D, Yeo CJ, Hruban RH, Witkiewicz AK. Acinar cell carcinoma with prominent intraductal growth pattern: case report and review of the literature. Int J Surg Pathol. 2011;19:795–9.
11. Colombo P, Aizzi C, Roncalli M. Acinar cell cystadenocarcioma of the pancreas: report of rare case and review of the literature. Hum Pathol. 2004;35:1568–71.
12. Bien E, Godzinski J, Dall'igna P, Defachelles AS, Stachowicz-Stencel T, Orbach D, et al. Pancreatoblastoma: a report from the European cooperative study group for paediatric rare tumours (EXPeRT). Eur J Cancer. 2011;47:2347–52.
13. Cavallini A, Falconi M, Bortesi L, Crippa S, Barugola G, Butturini G. Pancreatoblastoma in adults: a review of the literature. Pancreatology. 2009;9:73–80.
14. Tanaka Y, Kato K, Notohara K, Nakatani Y, Miyake T, Ijiri R, et al. Significance of aberrant (cytoplasmic/nuclear) expression of beta-catenin in pancreatoblastoma. J Pathol. 2003;199:185–90.

Further Reading

La Rosa S, Klimstra DS, Wood LS. Pancreatic acinar cell carcinoma. In: Lokuhetty D, White VA, Watanabe R, Cree IA, editors. Digestive system tumours. WHO classification of tumours. 5th ed. Lyon: IARC Press; 2019. p. 333–6.

Ohike N, Rosa L, Pancreatoblastoma S. In: Lokuhetty D, White VA, Watanabe R, Cree IA, editors. Digestive system tumours. WHO classification of tumours. 5th ed. Lyon: IARC Press; 2019. p. 337–9.

Non-Epithelial Neoplasia

11

Primary mesenchymal neoplasms of the pancreas are extremely rare, accounting for less than 1% of all pancreatic tumors. The pancreas is more commonly involved by extrapancreatic mesenchymal neoplasia (e.g., from the stomach, duodenum, or retroperitoneum) invading directly into the pancreas (Fig. 11.1). However, it is not always possible to clearly determine the primary origin of a neoplasm on imaging techniques and, therefore, such extrapancreatic tumors may be mistaken for primary pancreatic neoplasms on radiology. Moreover, some mesenchymal neoplasms may undergo cystic degeneration (see Table 14.1) and mimic a pancreatic cystic neoplasm. Very occasionally, mesenchymal tumors can also metastasize to the pancreas. Therefore, whenever a mesenchymal neoplasm is found in the pancreas, it is essential to consider an extrapancreatic primary origin, including a metastasis.

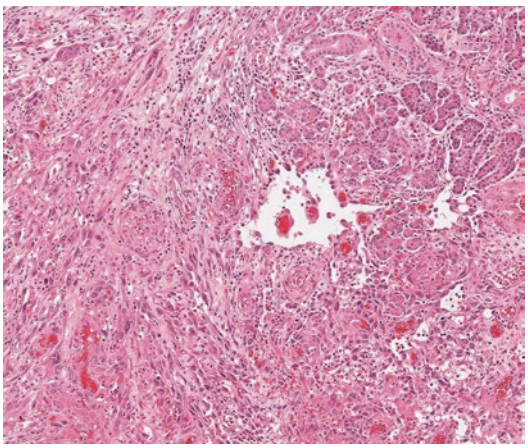

Fig. 11.1 Duodenal angiosarcoma: this primary duodenal angiosarcoma is seen infiltrating into the pancreas (*right of picture*)

Most of the mesenchymal neoplasms that occur primarily in soft tissues can arise in the pancreas, although many tumors are only described as single case reports. It is beyond the scope of this book to provide a comprehensive morphological description, immunohistochemical profile, and cytogenetic/molecular analysis for all of these entities. Those mesenchymal tumors that may mimic other primary pancreatic neoplasms will be discussed in this chapter. However, it should be emphasized that these mesenchymal neoplasms are extremely rare in the pancreas.

Non-Hodgkin lymphomas may also occur in the pancreas. However, secondary involvement of the pancreas by advanced stage lymphoma, from other sites, is much more common than primary pancreatic lymphoma. Primary pancreatic lymphoma will also be briefly discussed in this chapter.

© Springer Nature Switzerland AG 2021
F. Campbell, C. S. Verbeke, *Pathology of the Pancreas*,
https://doi.org/10.1007/978-3-030-49848-1_11

11.1 Mesenchymal Neoplasms of the Pancreas

11.1.1 Desmoplastic Small Round Cell Tumor

Desmoplastic small round cell tumor is a rare, highly aggressive, malignant intra-abdominal neoplasm composed of small round blue cells with a distinctive desmoplastic stroma. It occurs predominantly in young males. Desmoplastic small round cell tumors usually occur in the peritoneal cavity, but occasionally may arise in the retroperitoneum and, rarely, may predominantly involve the pancreas [1].

Macroscopically, desmoplastic small round cell tumor forms a solid, firm, tan-white tumor with areas of hemorrhage and central necrosis or cystic degeneration (see Table 14.1). Microscopically, the tumor is composed of well-defined nests and broad bands of small cells with scanty cytoplasm and round-to-oval, frequently moulded nuclei with inconspicuous nucleoli (see Fig. 20.29). Mitoses are frequent and individual tumor cell necrosis is also common. The nests of cells are separated by desmoplastic stroma.

On immunohistochemistry, the neoplastic cells express cytokeratins (AE1/AE3 and CAM 5.2), EMA, desmin (with a distinctive, dot-like, intracytoplasmic localization), vimentin, and neuron-specific enolase. Nuclear expression of WT1 is usually seen. Most neoplasms do not express CD99, and they do not stain with neuroendocrine markers. The desmoplastic stroma is positive for vimentin and smooth muscle actin.

Desmoplastic small round cell tumor is characterized by a specific reciprocal translocation, t(11;22)(p13;q12), involving the fusion of the Ewing sarcoma gene (*EWS)* on chromosome 22q12 with the Wilm's tumor gene (*WT1*) on chromosome 11p13 (*WT1-EWSR1*).

The differential diagnosis for desmoplastic small round cell tumor within the pancreas includes acinar cell carcinoma (see Chap. 10), pancreatic neuroendocrine carcinoma (see Chap. 20, Sect. 20.9.2), pancreatoblastoma (see Chap. 10, Sect. 10.11.3), solid pseudopapillary neoplasm (see Chap. 18), and primitive neuroectodermal tumor (see Sect. 11.1.10). The morphological appearances, immunohistochemical profile (immunopositive for desmin and WT1), and genetic analysis (for the t(11;22)(p13;q12) translocation) enable the diagnosis of desmoplastic small round blue cell tumor to be made and distinguish it from these other entities.

11.1.2 Gastrointestinal Stromal Tumor

Gastrointestinal stromal tumor (GIST) within the pancreas is usually secondary involvement of the pancreas from a primary gastric or duodenal GIST. There are case reports of primary pancreatic GISTs, which show the characteristic spindle and epithelioid cells that are immunopositive for CD117, DOG-1, and CD34 [2]. Primary pancreatic GISTs may undergo cystic degeneration (see Table 14.1) and appear to behave in an aggressive fashion.

The differential diagnosis for a pancreatic GIST includes leiomyosarcoma, schwannoma, and solitary fibrous tumor (see Sects. 11.1.5, 11.1.11, and 11.1.12). Cellular stroma that was immunopositive for CD117, CD34, and BCL-2 has been described in two cases of solid hamartoma [3] (also see Chap. 19, Sect. 19.5.1). However, the hamartomata could be distinguished from a GIST by the presence of pancreatic exocrine and endocrine tissue admixed within the stroma.

11.1.3 Granular Cell Tumor

Granular cell tumors are rare benign neoplasms of nerve sheath origin, which may occur in the pancreas and cause pancreatic duct obstruction [4]. They show identical features to those arising in other sites. They are composed of nests of large tumor cells with abundant eosinophilic granular PAS-positive cytoplasm and bland nuclei. The tumor cells are immunopositive for S100 protein.

11.1.4 Inflammatory Myofibroblastic Tumor

There are a few reports of inflammatory myofibroblastic tumor (IMT) occurring in the pancreas, mostly in children [5]. However, there is considerable morphological overlap with inflammatory pseudotumor and autoimmune pancreatitis (see Chap. 7, Sect. 7.2.7.8), which should always be taken into consideration before making the diagnosis of IMT [6].

Macroscopically, IMT forms a well-circumscribed firm white or tan mass with a whorled cut-surface. Occasionally, there may be hemorrhage or necrosis. On microscopy, IMTs are cellular tumors composed of fascicles of spindle cells (fibroblasts and myofibroblasts) with a prominent chronic inflammatory cell infiltrate composed of plasma cells, lymphocytes, and eosinophils. The spindle cells have plump atypical nuclei and mitotic figures may be present.

On immunohistochemistry, the spindle cells are diffusely positive for vimentin, focally or diffusely positive for smooth muscle actin, may be positive for desmin, and may also show focal expression of cytokeratin. Cytoplasmic ALK1 is present in approximately 30–40% of cases and correlates with the presence of *ALK1* gene rearrangements. IMT is negative for myogenin, myoglobin, S100 protein, and CD117.

11.1.5 Leiomyosarcoma

Leiomyosarcoma (Fig. 11.2) is the most common primary sarcoma of the pancreas and occurs in men and women equally (mean age at diagnosis 54 years, range 14–87 years). Pancreatic leiomyosarcomas are usually large at the time of diagnosis (mean size 11.4 cm, range 1–30 cm) and may show cystic degeneration (see Table 14.1) [7]. They are highly aggressive, invade adjacent organs, and commonly show hematogenous spread to the liver. Lymph node metastases are rare.

Histologically, primary pancreatic leiomyosarcomas resemble leiomyosarcomas at other sites. Immunohistochemistry shows diffuse immunopositivity for smooth muscle actin and desmin. CD117 is negative.

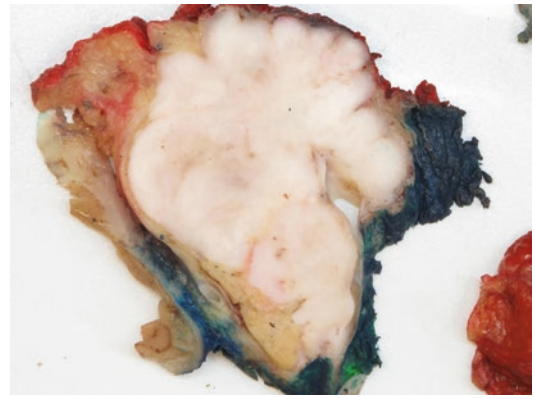

Fig. 11.2 Pancreatic leiomyosarcoma: this leiomyosarcoma replaces most of the pancreas. Duodenum is seen to the *left*, and residual pancreas at the *bottom*

The differential diagnosis includes gastrointestinal stromal tumor (GIST), sarcomatoid carcinoma, and other sarcomas, including fibrosarcoma, liposarcoma, malignant peripheral nerve sheath tumor, and angiosarcoma.

Primary pancreatic leiomyosarcomas are aggressive tumors and require extensive resection with wide margins [6]. Prognosis is poor with 5 and 10 year survival rates of 44% and 30%.

11.1.6 Lipoma

Pancreatic lipomas are well-circumscribed, multilobulated fatty tumors (Fig. 11.3) that range in size from 0.4 to 30 cm. The lipomatous nature of the tumor can be detected on MRI. Pancreatic lipomas are composed of mature adipocytes with thin fibrous septa and small blood vessels. If the blood vessels are large and form a prominent component of the neoplasm, then the term angiolipoma is used. Lipomas located in the head of the pancreas may originate from entrapped retroperitoneal or mesenteric fat between the dorsal and ventral pancreatic buds, during embryonic fusion (see Chap. 1, Sect. 1.2). The pathogenesis of lipomas within the body and tail of the pancreas is unclear [8].

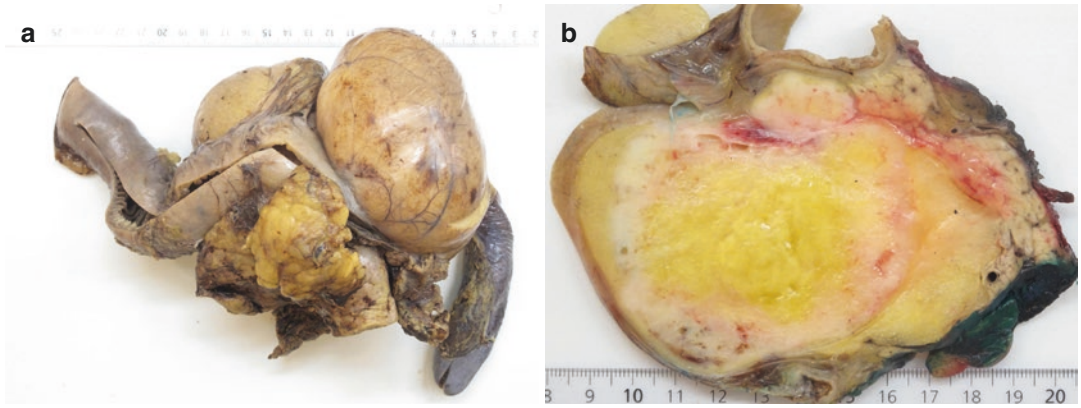

Fig. 11.3 Pancreatic lipoma: this lipoma replaces much of the head of the pancreas (**a**). The cut-surface shows the adipose tissue with residual normal pancreas on the right (**b**)

The differential diagnosis includes focal fatty replacement of the pancreas, which is much more common than a pancreatic lipoma and may be associated with obesity, aging, type 2 diabetes mellitus, chronic pancreatitis, and cystic fibrosis. In fatty replacement (lipomatosis), pancreatic elements are present within the fat and there is irregular extension of the fat into the surrounding pancreas (see Chap. 5, Sect. 5.7). Lipomas, in contrast, are well-circumscribed and do not usually contain entrapped pancreatic elements. Pancreatic liposarcoma has been reported, but retroperitoneal liposarcomas may also involve the pancreas. They can be distinguished from a lipoma by the presence of nuclear atypia and lipoblasts.

11.1.7 Lymphangioma

Pancreatic lymphangioma is a rare, benign neoplasm showing lymph vessel differentiation that can occur within the pancreatic parenchyma, adjacent to the pancreas, or be connected to the pancreas by a pedicle. Most lymphangiomas arise in the peripancreatic tissue (Fig. 11.4). They occur predominantly in young women (mean age 29 years, range 2–61 years) and are found most commonly within the tail of the pancreas.

Lymphangiomas are generally large (mean size 13 cm, range 2–15 cm), solitary, and multicystic with a thin fibrous capsule. They are smooth-lined cysts and contain straw-coloured or chylous fluid. On microscopy, the cysts are lined by endothelial cells with oval bland nuclei (Fig. 11.4c). The capsule and thin septa between the cysts may contain smooth muscle cells, lymphocytes, and foamy macrophages (Fig. 11.4d). On immunohistochemistry, the endothelial cells express CD31, CD34, and D2–40. Resection is usually curative. However, recurrence may follow incomplete resection.

The differential diagnosis includes hemangioma and serous cystic neoplasms. Hemangiomas are less common than lymphangioma and lack lymphocytes or foamy macrophages in the cyst wall. Serous cystic neoplasms express cytokeratins and do not express the vascular markers CD31, CD34, or D2–40.

11.1.8 Paraganglioma

Paragangliomas are rare neuroendocrine neoplasms arising in extra-adrenal chromaffin cells of the autonomic nervous system. Most paragangliomas are peripancreatic rather than intrapancreatic [9]. They may undergo cystic degeneration (see Table 14.1) and, therefore, be mistaken for a primary pancreatic cystic lesion.

On microscopy, paraganglioma is characterized by the typical ‘Zellballen’ arrangement of haphazardly arranged, chief cells

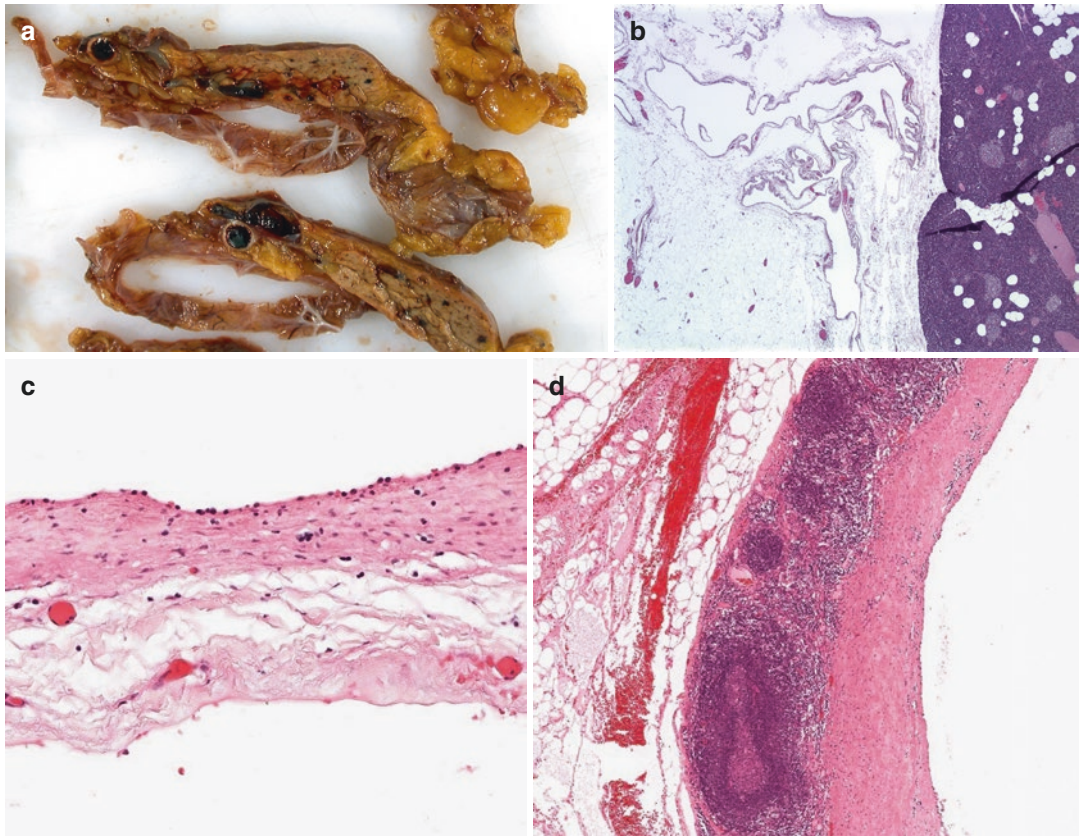

Fig. 11.4 Pancreatic lymphangioma: this lymphangioma can be seen in the peripancreatic tissue adjacent to normal pancreas (**a**). This wholemount picture shows the peripancreatic location and thin wall of the lymphangioma (**b**) which, on higher power (**c**), is lined by endothelial cells (*top* of picture). There is focally prominent lymphoid tissue in the fibrotic wall of this lymphangioma (**d**)

(see Fig. 20.26a). The chief cells have round, regular nuclei with basophilic cytoplasm. Immunohistochemistry can be used to identify the characteristic two cell populations; the chief cells are immunopositive for synaptophysin and chromogranin A, while the sustentacular cells are immunopositive for S100 protein (see Fig. 20.26b).

The main differential diagnosis for paraganglioma is a grade 1–3 pancreatic neuroendocrine tumor (PanNET), which can have similar morphology and will also be immunopositive for endocrine markers (see Chap. 20, Sect. 20.9.1). PanNETs, however, are much more common and express cytokeratins. Paragangliomas rarely express cytokeratins and, unlike PanNETs, contain S100 protein immunopositive sustentacular cells.

11.1.9 Perivascular Epithelioid Cell Neoplasm (PEComa)

Perivascular epithelioid cell neoplasm (PEComa), also known as clear cell sugar tumor or angiomyolipoma, is a benign, well-vascularized neoplasm composed of epithelioid smooth muscle cells with glycogen-rich clear cytoplasm. Mature adipocytes are also present but are not a major component in pancreatic PEComas. Although PEComas can occur in tuberous sclerosis,

pancreatic PEComa does not appear to be associated with this condition [10].

PEComas form well-demarcated, pale, variegated, focally hemorrhagic firm nodules that may undergo central cystic degeneration (see Table 14.1). The neoplastic cells have abundant, typically clear cytoplasm with eccentrically located reniform nuclei. The glycogen-rich cytoplasm stains with periodic acid-Schiff (PAS). On immunohistochemistry, the neoplastic cells express HMB45, Melan-A, CD31, and myogenic markers (smooth muscle actin and/or desmin). They do not express cytokeratins.

PEComas (see Fig. 20.28) may resemble a grade 1–3 pancreatic neuroendocrine tumor (PanNET) (see Chap. 20, Sect. 20.9.1), but do not express endocrine markers (e.g., synaptophysin and chromogranin A). PEComas may also resemble solid serous adenoma (see Chap. 15, Sect. 15.11.1), but serous neoplasms express epithelial markers and do not express HMB45, Melan-A, CD31, or smooth muscle actin.

11.1.10 Primitive Neuroectodermal Tumor

Primitive neuroectodermal tumor (PNET), a member of the Ewing's sarcoma family of tumors, is extremely rare in the pancreas [11]. Patients present at a mean age of 22 years (age range 2–60 years), typically with abdominal pain or jaundice. Most PNETs arise in the head of the pancreas (mean size 8.2 cm, range 3.5–22 cm), but they may also occur within the body or tail of the pancreas. They are usually solid, tan-white tumor masses, but they can occasionally show cystic degeneration (see Table 14.1). They typically invade the peripancreatic tissue or adjacent organs.

Microscopically, the neoplastic cells are arranged in sheets and lobules (Fig. 11.5a). The neoplastic cells are typically small, round, and blue with round-to-oval nuclei, coarse chromatin, and scanty cytoplasm. There is often nuclear moulding and prominent mitotic figures. The Homer-Wright rosettes that are typically seen in extrapancreatic PNETs have not been described in PNETs of the pancreas.

On immunohistochemistry (Fig. 11.5b), the neoplastic cells are strongly immunopositive for CD99 (membranous staining) and FLI-1. They may also express cytokeratins (AE1/AE3) and endocrine markers (synaptophysin and neuron-specific enolase). They do not usually express chromogranin A, nor do they express desmin, HMB45, or pancreatic hormones. The neoplastic cells have rearrangement of the *EWSR1* gene, usually a *EWSR1-FLI-1* fusion with t(11;22)(q24;q12) translocation.

The differential diagnosis includes pancreatic neuroendocrine carcinoma small cell type

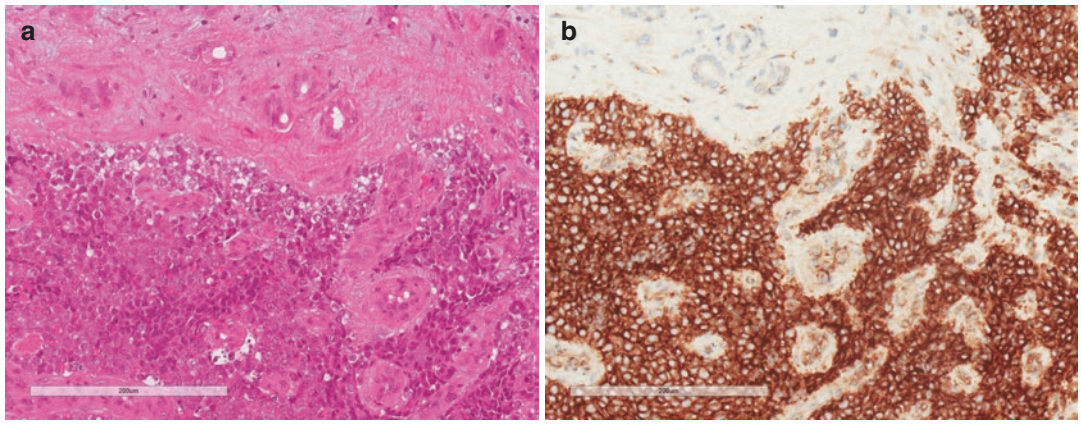

Fig. 11.5 Pancreatic primitive neuroectodermal tumor: small round blue tumor cells are seen infiltrating around vessels (**a**). Residual pancreas is present at the *top*. Diffuse CD99-immunopositivity is seen within the tumor (**b**)

(see Chap. 20, Sect. 20.9.2), desmoplastic small round cell tumor (see Sect. 11.1.1), and metastatic small cell malignancies. Pancreatic neuroendocrine carcinoma may show immunopositivity for CD99. Most pancreatic neuroendocrine carcinomas, however, show diffuse immunopositivity for synaptophysin and chromogranin, whereas PNETs only show focal immunopositivity for synaptophysin. FLI-1 immunopositivity may be used to distinguish PNET from a pancreatic neuroendocrine carcinoma. Genetic testing for the characteristic t(11;22)(q24;q12) chromosomal translocation will also help establish the diagnosis of PNET.

Desmoplastic small round cell tumors can be distinguished from PNETs by the presence of the distinctive desmoplastic stroma, the immunopositivity for desmin and WT1, the lack of expression of CD99, and by the detection of the *WT1-EWSR1* fusion product (see above).

11.1.11 Schwannoma

Schwannoma, a benign neoplasm with nerve sheath (Schwann cell) differentiation, may occur very rarely within the pancreas. Schwannomas frequently undergo cystic degeneration (see Table 14.1) and, therefore, can mimic other pancreatic cystic lesions. Pancreatic schwannoma occurs in adults (mean age 55 years), in women slightly more frequently than men, and may range in size from 1 to 30 cm [12]. Microscopy reveals the typical Antoni A and Antoni B areas, but a peripheral lymphoid cuff (typical of gastrointestinal schwannomas) is rare. On immunohistochemistry, there is diffuse positivity for S100 protein.

The majority of pancreatic schwannomas are benign and can be treated by enucleation. Malignant transformation is associated with larger size and neurofibromatosis type 1, and requires oncological pancreatic resection.

11.1.12 Solitary Fibrous Tumor

Solitary fibrous tumor, which is most common in the pleura, may occur on the serosal surfaces of the peritoneum or within the pancreas. It is a well-circumscribed, solitary, solid tumor (Fig. 11.6a) composed of bland spindle cells within collagenous stroma, which shows a characteristic hemangiopericytoma-like vascular growth pattern (Fig. 11.6b). The spindle cell nuclei are wavy and slender, with moderate pleomorphism. Mitotic figures are not present. Although the tumor is well circumscribed, pancreatic elements may be entrapped within it (Fig. 11.6c and d). On immunohistochemistry, the neoplastic cells show diffuse strong immunopositivity with CD34 (Fig. 11.7), CD99, and BCL-2. There is no expression of CD117, DOG-1, or S100.

The differential diagnosis includes other spindle cell neoplasms involving the pancreas. Synovial sarcoma may have a hemangiopericytoma-like vascular pattern, but is more uniformly cellular, mitotically active, and immunopositive for EMA and cytokeratins. Synovial sarcomas may be positive for S100 protein and CD99, but the majority are negative for CD34. Cytogenetically, synovial sarcoma shows the chromosome translocation t(X;18)(p11.2;q11.2).

11.2 Lymphoma

Primary non-Hodgkin lymphoma of the pancreas is very rare and occurs more frequently in the elderly (mean age 65 years, age range 37–86 years). It may be associated with immunodeficiency (e.g., HIV infection or follow solid organ transplantation). The lymphomas are usually B-cell non-Hodgkin lymphomas, although rare cases of T-cell lymphomas have been reported. Most primary pancreatic lymphomas are diffuse large B-cell lymphomas.

Primary pancreatic lymphomas present most frequently in the pancreatic head. Patients present with abdominal pain and, less frequently, jaundice. The tumor size ranges from 3 to 17 cm, with a mean of approximately 8 cm, and the tumors form a solid homogeneous fleshy pale tumor mass. The histological appearances and immunohistochemical profile are identical to those of non-Hodgkin lymphomas arising within lymph nodes and other primary sites. Lymphomatous

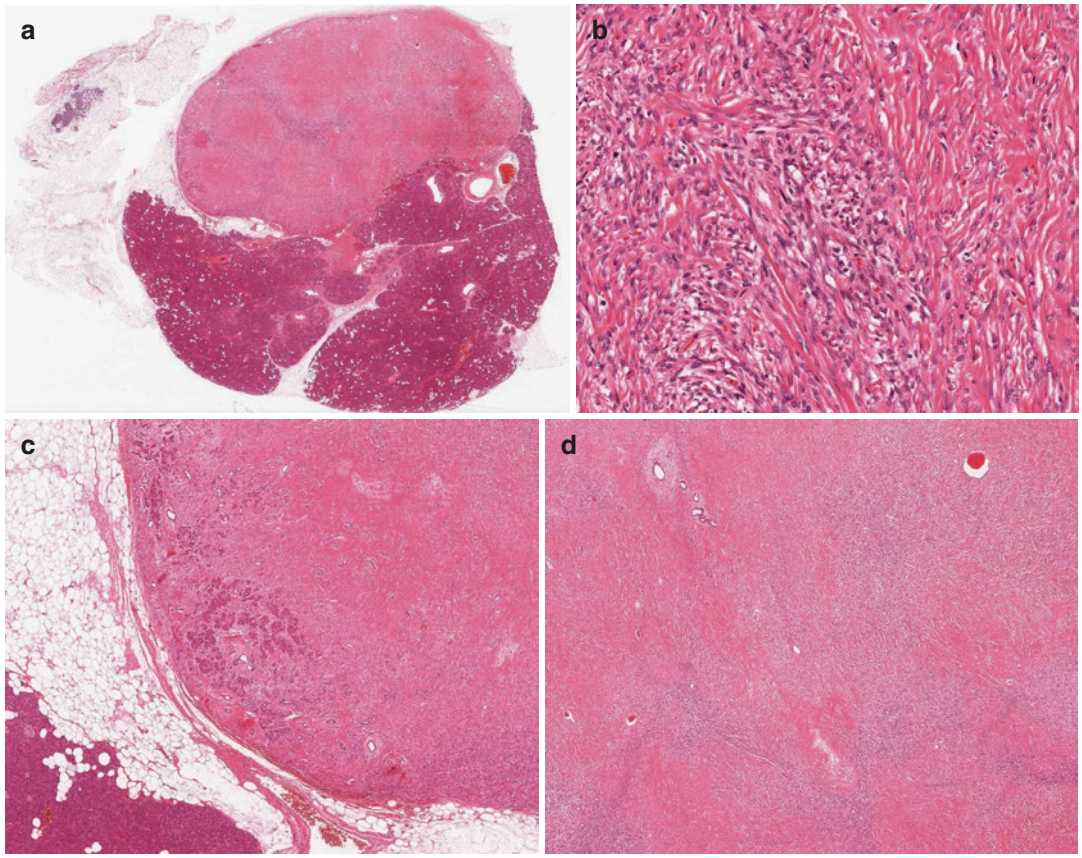

Fig. 11.6 Pancreatic solitary fibrous tumor: this whole-mount shows the well-circumscribed, solid nature of the tumor (**a**). The tumor is composed of bland spindle cells within collagenous stroma showing a characteristic hemangiopericytoma-like vascular growth pattern (**b**). There is a focus of entrapped acini and ductules at the tumor periphery (**c**), together with scanty entrapped ductules in the center of the tumor (**d**)

Fig. 11.7 Pancreatic solitary fibrous tumor: diffuse CD34 immunopositivity is seen within the tumor

cells may infiltrate widely through the pancreas entrapping normal pancreatic parenchymal elements.

Carcinoma is the main differential diagnosis. Immunohistochemistry with epithelial markers and lymphoid markers will help make the distinction. Other entities that may enter the differential diagnosis include follicular pancreatitis (see Chap. 7, Sect. 7.3.1), and IgG4-related disease within the pancreas (see Chap. 7, Sect. 7.2.7.8) and/or peripancreatic lymph nodes (see Chap. 7, Sect. 7.2.7.10).

The prognosis for primary pancreatic lymphomas is much better than that of pancreatic adenocarcinoma. Surgical resection is not required and, therefore, diagnosis on fine needle aspira-

tion or biopsy, using immunohistochemistry and molecular genetics, is important for clinical management. Once a pancreatic lymphoma has been diagnosed, the patient can be referred to the hematology multidisciplinary team for appropriate staging scans, exclusion of other primary sites, and consideration for chemotherapy.

References

1. Bismar TA, Basturk O, Gerald WL, Schwarz K, Adsay NV. Desmoplastic small cell tumor in the pancreas. Am J Surg Pathol. 2004;28:808–12.
2. Tian YT, Liu H, Shi SS, Xie YB, Xu Q, Zhang JW, et al. Malignant extra-gastrointestinal stromal tumor of the pancreas: report of two cases and review of the literature. World J Gastroenterol. 2014;20:863–8.
3. Pauser U, da Silva MTS, Placke J, Klimstra DS, Klöppel G. Cellular hamartoma resembling gastrointestinal stromal tumor: a solid tumor of the pancreas expressing c-kit (CD117). Modern Pathol. 2005;18:1211–6.
4. Kanno A, Satoh K, Hirota M, Hamada S, Umino J, Itoh H, et al. Granular cell tumor of the pancreas: a case report and review of literature. World J Gastrointest Oncol. 2010;2:121–4.
5. Liu HK, Lin YC, Yeh ML, Chen YS, Su YT, Tsai CC. Inflammatory myofibroblastic tumors of the pancreas in children: a case report and literature review. Medicine (Baltimore). 2017;96:e5870.
6. Yamamoto H, Yamaguchi H, Aishima S, Oda Y, Kohashi K, Oshiro Y, et al. Inflammatory myofibroblastic tumor versus IgG4-related sclerosing disease and inflammatory pseudotumor: a comparative clinicopathologic study. Am J Surg Pathol. 2009;33:1330–40.
7. Xu J, Zhang T, Wang T, You L, Zhao Y. Clinical characteristics and prognosis of primary leiomyosarcoma of the pancreas: a systematic review. World J Surg Oncol. 2013;11:290.
8. Lee JY Seo HI, Park EY, Kim GH, Park DY, Kim S. Histologic confirmation of huge pancreatic lipoma: a case report and review of literatures. J Korean Surg Soc. 2011;81:427–300.
9. Singhi AD, Hruban RH, Fabre M, Imura J, Schulick R, Wolfgang C, et al. Peripancreatic paraganglioma: a potential diagnostic challenge in cytopathology and surgical pathology. Am J Surg Pathol. 2011;35:1498–504.
10. Zizzo M, Ugoletti L, Tumiati D, Castro Ruiz C, Bonacini S, Panebianco M, et al. Primary pancreatic perivascular epithelioid cell tumor (PEComa): a surgical enigma. A systematic review of the literature. Pancreatology. 2018;18:238–45.
11. Komforti MK, Sokolovskaya E, D'Agostino CA, Benayed R, Thomas RM. Extra-osseous Ewing sarcoma of the pancreas: case report with radiologic, pathologic, and molecular correlation, and brief review of the literature. Virchows Arch. 2018;473:361–9.
12. Zhang X, Siegelman ES, Lee MK, Tondon R. Pancreatic schwannoma, an extremely rare and challenging entity: report of two cases and review of literature. Pancreatology. 2019;19:729–37.

Check for updates

Secondary Neoplasia

12

12.1 Definition

The pancreas can be involved secondarily by extrapancreatic neoplasms, either by direct invasion (e.g., from the colon, stomach, or duodenum), or by metastatic spread along lymphatic channels, perineural clefts, or the blood stream.

In principle, the possibility of a secondary neoplasm should always be considered as a differential when diagnosing a pancreatic cancer. The distinction between ductal adenocarcinoma of the pancreas and ampullary, distal bile duct, or duodenal carcinoma involving the pancreatic head is discussed in detail elsewhere (see Chap. 9, Sect. 9.12.3). This chapter focuses on metastatic spread to the pancreas.

12.2 Clinical Features

Patients with metastatic tumor spread to the pancreas often present with clinical signs and symptoms that are similar to those of primary pancreatic tumors: weight loss, early satiety, abdominal pain, and jaundice if the tumor is located in the pancreatic head. Occasionally, pancreatitis may be the initial symptom. In some patients, pancreatic metastasis is clinically occult and becomes apparent during follow-up examination for the known extrapancreatic cancer. Fulminant upper gastrointestinal hemorrhage is a rare presenting feature that can occur in patients with a metastatic tumor in the pancreatic head causing ulceration of the duodenal mucosa.

Patients are usually elderly, 60–70 years old, that is, the age distribution is similar to that for ductal adenocarcinoma of the pancreas. Depending on the type of the primary tumor, metastasis to the pancreas can occur many years after diagnosis and/or resection of the primary.

Only a small selected group of patients will undergo pancreatic resection, which is never curative but may significantly prolong survival with good quality of life [1]. In most patients, however, palliative nonsurgical treatment is the only option. Not infrequently, metastasis is not limited to the pancreas but manifest also in other sites.

Secondary neoplasms of the pancreas are rare. Because surgical resection is performed in only a small subset of patients with metastatic disease to the pancreas, the frequency and site of origin of the malignancy varies between postmortem and surgical series, the latter partially reflecting a selection bias for malignancies with a more protracted course. The reported incidence of secondary neoplasms of the pancreas ranges from 1.6 to 11% in autopsy studies. In surgical series, these lesions account for up to 4% of pancreatic specimens. About one-third of these are clinically mistaken as primary pancreatic tumors [2].

Overall, carcinomas and malignant melanomas spread more commonly to the pancreas than sarcomas or hematopoietic neoplasia. The latter

© Springer Nature Switzerland AG 2021
F. Campbell, C. S. Verbeke, *Pathology of the Pancreas*,
https://doi.org/10.1007/978-3-030-49848-1_12

may include both myeloproliferative and lymphoproliferative disease (Fig. 12.1). Carcinoma of the kidney, lung, breast, and large bowel together with malignant melanoma are amongst the most frequent malignancies that spread to the pancreas. Some of these are discussed in more detail below.

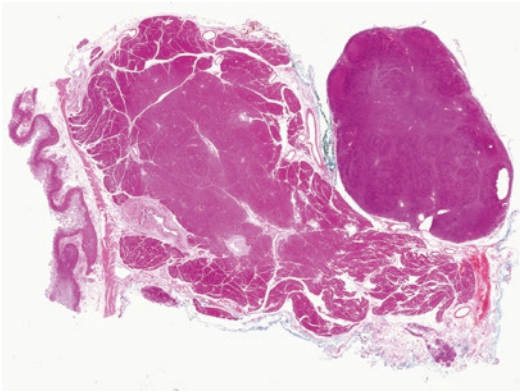

Fig. 12.1 Hodgkin lymphoma in a peripancreatic lymph node: a lymph node involved by Hodgkin lymphoma is prominently enlarged and indents the adjacent pancreas. On preoperative imaging this was misinterpreted as primary pancreatic cancer (whole-mount section)

12.3 Macroscopy

Metastatic tumor deposits in the pancreas tend to differ in their gross appearances from ductal adenocarcinoma of the pancreas, in as far as they are usually well-circumscribed, can exhibit significant hemorrhage, and may be partially cystic (Fig. 12.2). Although they are often of a considerable size, the surrounding pancreatic parenchyma is usually remarkably well preserved (Fig. 12.3). Metastasis can be solitary or multifocal (Fig. 12.4) and has usually no predilection for the head, body, or tail of the pancreas. Occasionally, the entire pancreas may be involved. Gross intraductal tumor growth, in the main pancreatic duct or common bile duct, may be seen and should not be interpreted as

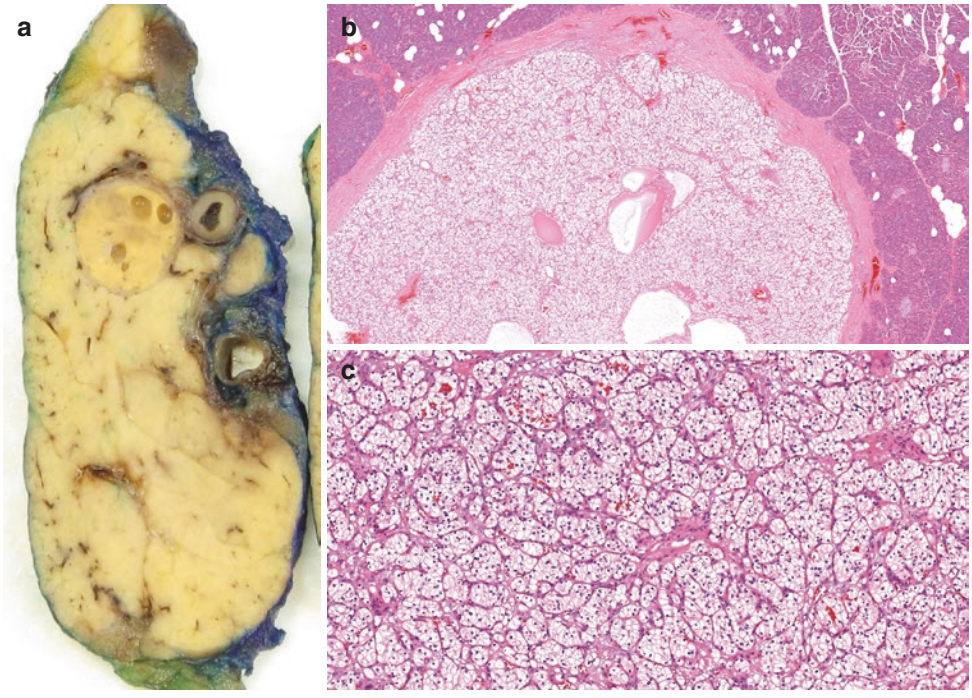

Fig. 12.2 Metastatic renal cell carcinoma: in contrast to primary pancreatic cancer, this metastatic deposit of renal cell carcinoma shows well-delineated pushing-type margins (**a**). Microscopically, the tumor has a fibrous capsule (**b**) and consists of densely packed clear cells (**c**)

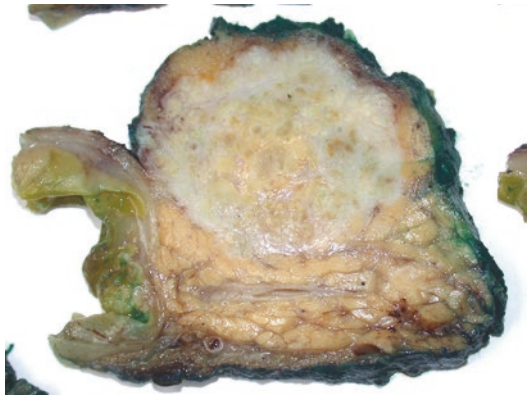

Fig. 12.3 Metastatic colonic adenocarcinoma: this metastasis of colonic cancer differs from primary pancreatic cancer by its remarkably well-defined contours. Note the normal appearance of the flanking pancreatic parenchyma and duct, despite the considerable size of the tumor

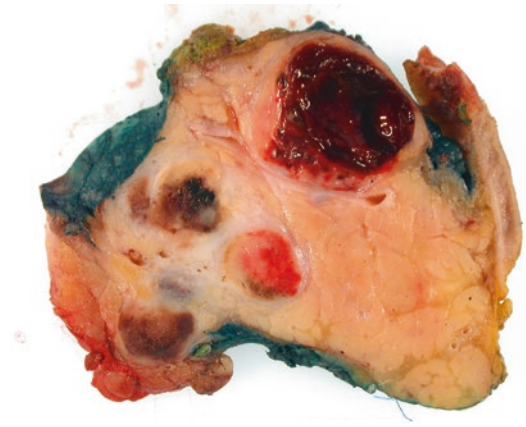

Fig. 12.4 Multifocal metastasis: the presence of multiple tumors within the pancreas raises the suspicion of metastatic rather than primary tumors

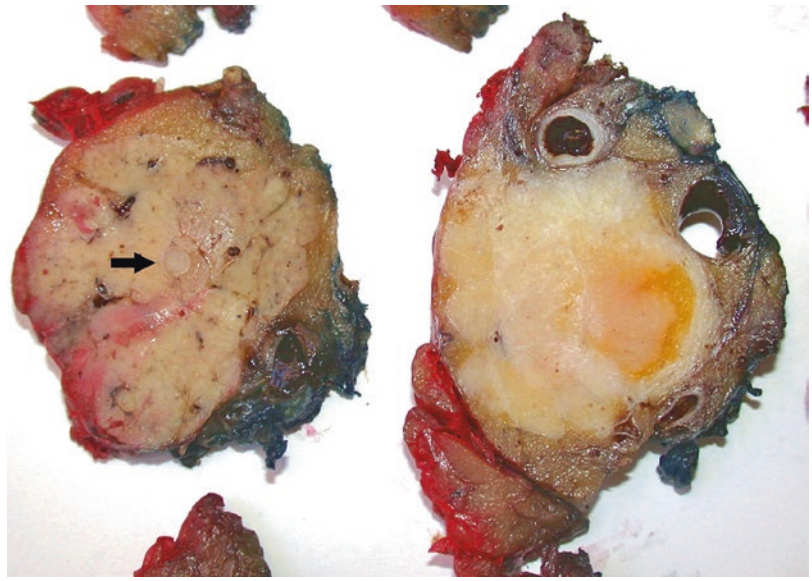

Fig. 12.5 Intraductal growth of metastatic tumor: this large metastatic deposit of colonic adenocarcinoma (*right*) extends beyond the main tumor mass by intraluminal growth within the main pancreatic duct (*left*, *arrow*)

an exclusion criterion for metastatic tumor (Figs. 12.5 and 12.6). Similarly, tumor occlusion of the splenic vein, which is commonly seen in pancreatic ductal adenocarcinoma, may occasionally also be found in metastatic cancer (Fig. 12.7).

Extensive hemorrhage and a yellow-orange color of the tumor tissue is characteristic of metastatic renal cell carcinoma, whereas dark brown-black pigmentation may be seen in the metastasis of malignant melanoma.

12.4 Microscopy

Depending on the type of the metastasis, the microscopic tumor appearances may by themselves raise the suspicion of metastatic rather than primary pancreatic neoplasia (Fig. 12.8). An abrupt transition from the neoplastic lesion to more or less pristine pancreatic parenchyma without convincing evidence of obstructive pancreatitis should also raise the suspicion of a metastatic process. Intraductal tumor propagation does not confirm a primary

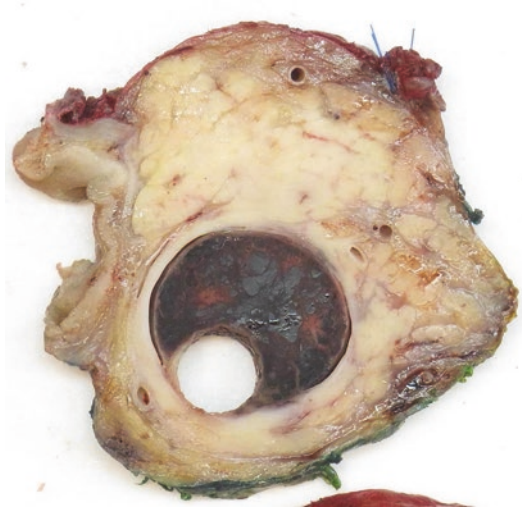

Fig. 12.6 Intraductal metastatic renal cell carcinoma: the common bile duct is grossly distended and obstructed by metastatic renal cell carcinoma growing within the duct lumen. Note the hemorrhagic tumor tissue and the punched-out hole due to a plastic biliary stent (removed)

Fig. 12.7 Metastatic renal cell carcinoma occluding the splenic vein: in this sagittal slice from a distal pancreatectomy specimen, the pancreatic body is almost entirely replaced by metastatic renal cell carcinoma, which also occludes and expands the splenic vein (*black arrows*). The splenic artery (*red arrow*) lies in contact with the tumor capsule but is not infiltrated

pancreatic origin, as metastastic tumor may also grow along pancreatic ducts of varying caliber, and on occasion mimic pancreatic intraepithelial neoplasia (PanIN).

12.5 Differential Diagnosis

Accurate information on the patient's medical history is essential to reach a correct diagnosis. Direct microscopic comparison of the pancreatic tumor with the previous extrapancreatic primary malignancy is helpful. However, the histomorphology of the primary tumor and metastasis may not always be entirely identical.

Immunohistochemistry may be helpful in many cases (Table 12.1) [3]. Probably the most difficult distinction to make is that between ductal adenocarcinoma of the pancreas and *metastatic colorectal cancer*, because a proportion of primary pancreatic cancers may exhibit an intestinal phenotype, both morphologically and immunohistochemically (see Chap. 9, Sect. 9.6.2). In addition, pancreatic ductal adenocarcinoma of pancreatobiliary type may assume intestinal features when infiltrating the duodenal wall, and in areas where it involves the duodenal mucosa, it may mimic dysplasia of the duodenal mucosa (see Chap. 9, Sect. 9.6.3, Fig. 9.20). *Metastatic breast cancer* of lobular type requires distinction from the rare signet ring cell subtype of ductal adenocarcinoma (Fig. 12.9) (see Chap. 9, Sect. 9.14.3). Distinction is important, because of the specific treatment options for metastatic breast cancer.

Renal cell carcinoma has a propensity to metastasize to the pancreas. If the *renal cell cancer* is *of clear cell type* (Fig. 12.2c), the differential diagnosis includes ductal adenocarcinoma with foamy gland or clear cell pattern, although the latter is usually only a focal feature within an otherwise conventional ductal adenocarcinoma. PAS-diastase staining or MUC1-immunohistochemistry may be helpful, as the clear cytoplasm in renal cell carcinoma contains glycogen, whereas in ductal adenocarcinoma it is mucin. Pancreatic endocrine neoplasia of clear cell type is a further important differential, which may be particularly difficult in patients with von Hippel-Lindau disease, who can also

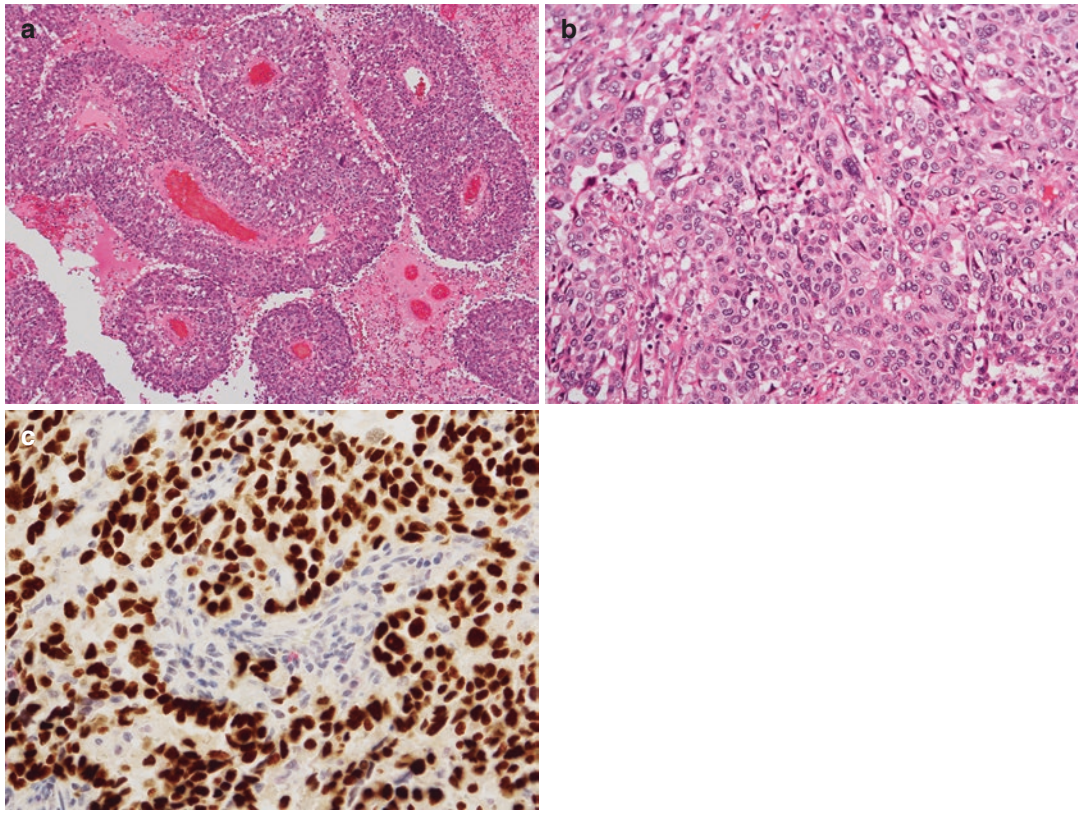

Fig. 12.8 Metastatic lung cancer: the growth pattern (**a**) and cytological features (**b**) of this tumor in the pancreatic body were not characteristic of ductal adenocarcinoma of the pancreas and raised the suspicion of metastasis in a patient with a history of lung cancer. Immunohistochemistry showed strong labeling for TTF-1 (**c**)

develop renal cell cancer (see Chap. 20, Sects. 20.9.1 and 20.12). PEComas, which are rare primary tumors of the pancreas, should also be distinguished. It should be borne in mind that the primary tumor and metastasis in renal cell carcinoma may differ in the extent of the clear cell features and the expression of various markers [4, 5]. For metastatic *renal cell carcinoma of non-clear cell morphology* (e.g., chromophobe), acinar cell carcinoma, pancreatic endocrine neoplasm, and solid pseudopapillary neoplasm are to be considered as a differential diagnosis, in particular if the metastatic renal cell carcinoma shows a trabecular or acinar growth pattern (Fig. 12.10). Very rarely, the renal cell carcinoma can be of a poorly differentiated or sarcomatoid morphology, in which case the pancreatic metastasis requires distinction from undifferentiated carcinoma of the pancreas (Fig. 12.11).

A further important differential diagnosis of poorly or undifferentiated pancreatic carcinoma is malignant melanoma. Diffuse sheets of noncohesive tumor cell growth, marked cellular atypia, and prominent nucleoli may be seen in both cancers (Fig. 12.12). Up to 10% of patients with malignant melanoma metastatic to the pancreas may not have a known primary. Immunohistochemistry usually aids in reaching the correct diagnosis (Table 12.1).

Table 12.1 Immunohistochemical staining of primary and secondary neoplasia of the pancreas [3–9]

	Ductal adenocarcinoma of pancreas	Pancreatic endocrine tumor	Renal cell carcinoma	Colorectal adenocarcinoma	Breast adenocarcinoma	Lung adenocarcinoma	Malignant melanoma
CK7	++	+	-/+ (clear cell, oncocytic) ++ (chromophobe, papillary)	-/+	++	++	-
CK20	-/+	-/+	-	++	-	-	-
CA125	+	-	-	-	-/+	-/+	-
CEA	++	-/+	-	++	-/+	+	-
CDX2	- (except intestinal type)	-/+	-	++	-	-	-
Pax8	-	++	++	-/+	-	-/+	ID
Mesothelin	-/+	-	-	-/+	-	-/+	-
Synaptophysin, Chromogranin	-	++	-	-	-	-	-
NSE, CD56	-	++	-/+ (except clear cell: +)	-	-	-	-
RCC	-	-	+ (except oncocytic:-)	-	-	-	-
TTF1	-	-	-	-	-	++	-
Napsin A	-	-	-/+	-	-	++	-
GATA3	-/+	-	-/+	-	++	-	-
GCDFP15	-	-	-	-	-/+	-	-
ER	-	-	-	-	+	-	-
WT1	-	-	-/+	-	-/+	-/+	++
Vimentin	- (except undifferentiated carcinoma)	-/+	++ (except chromophobe, oncocytic:-)	-	-/+	-/+	+
HMB45, Melan-A, S100	- -	- -/+	- -	- -	- -/+	- -	++ ++

Abbreviations: *ID* insufficient data, ++ >80% tumors stain positively, + 50-80% of tumors stain positively, -/+ 6-49% of tumors stain positively, - 0-5% of tumors stain positively

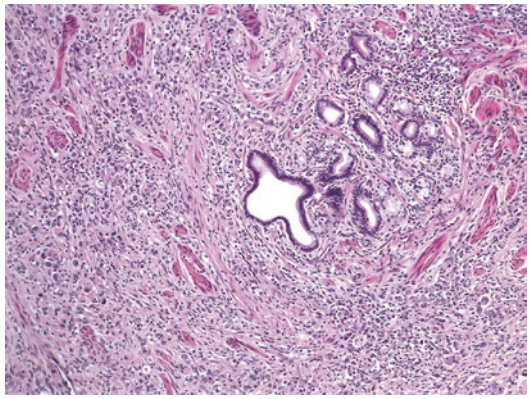

Fig. 12.9 Metastatic breast cancer: a metastatic deposit of lobular breast cancer shows microscopic similarity with the signet ring cell subtype of ductal adenocarcinoma

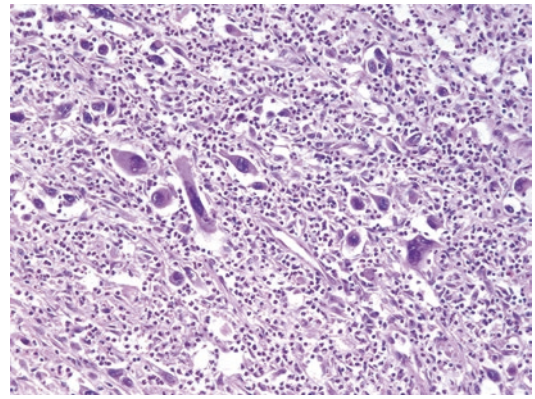

Fig. 12.11 Poorly differentiated metastatic renal cell carcinoma: the marked cytological atypia and nuclear pleomorphism, and the presence of bizarre tumor cells in this metastatic deposit of renal cell carcinoma may be mistaken as features of undifferentiated carcinoma of the pancreas

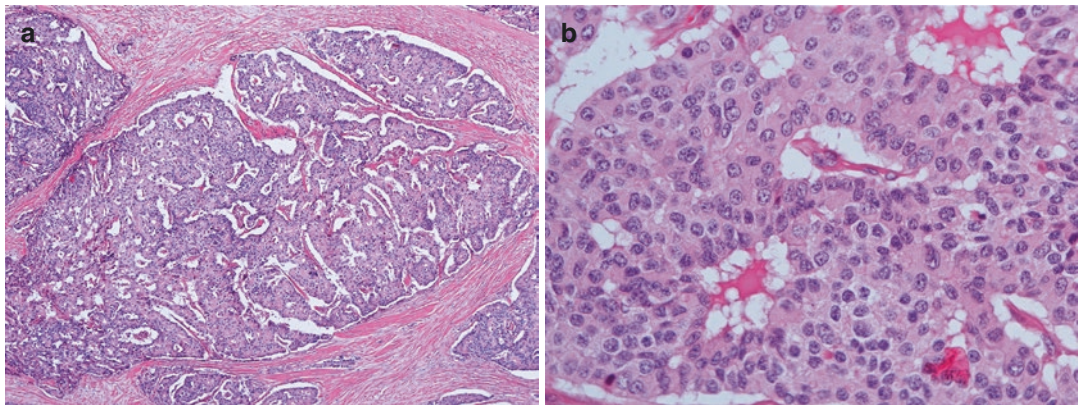

Fig. 12.10 Metastatic renal cell carcinoma of chromophobe type: the nearly organoid growth pattern of this tumor, its delicate vasculature, and cytomorphology raise the suspicion that this may be a pancreatic neuroendocrine tumor (**a**). However, the degree of nuclear pleomorphism, the irregular nuclear membranes, vesicular chromatin, and slightly prominent nucleoli are dissimilar from the nuclear features of endocrine tumors (**b**)

12.6 Synchronous Primary and Metastatic Cancer

On rare occasion, both primary pancreatic cancer and metastatic cancer of extrapancreatic origin may be present in the same resection specimen. This unusual finding may occur in patients with a hereditary cancer predisposition, for example, in patients with a germline *BRCA*-mutation, who may have both metastatic ovarian cancer and ductal adenocarcinoma of the pancreas. In such cases, the difference in tumor histomorphology and immunohistochemical profile, as well as the different location of both tumors (primarily intrapancreatic versus peripancreatic/peritoneal), will lead to a correct diagnosis (Fig. 12.13).

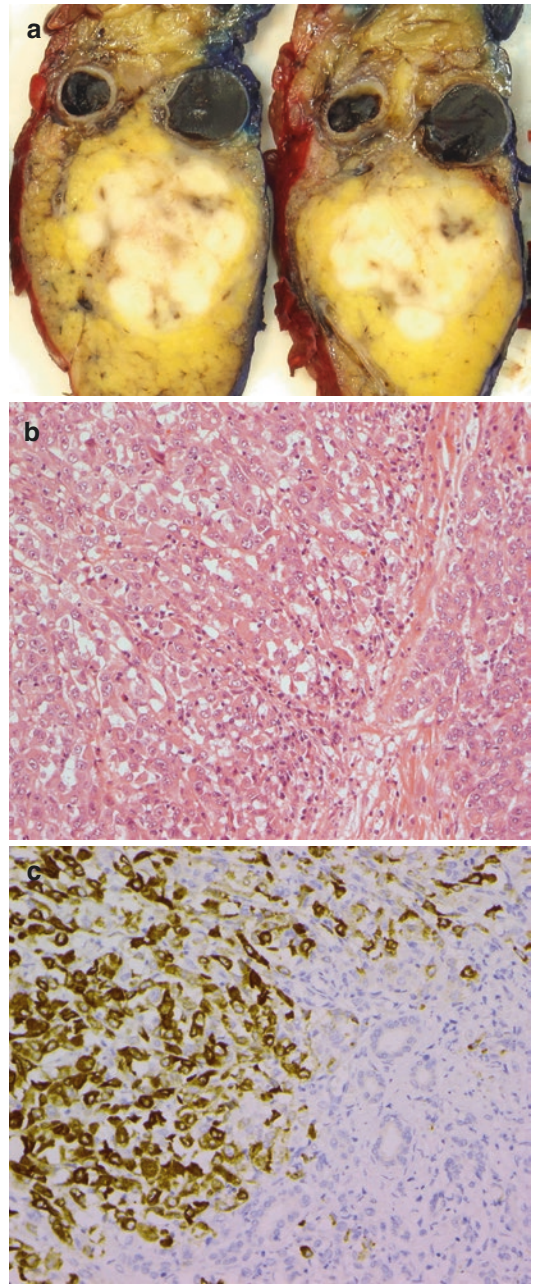

Fig. 12.12 Metastatic melanoma: a tumor in the body of the pancreas (**a**) consists of densely packed, large tumor cells with prominent nucleoli (**b**). Immunostaining for Melan-A shows strong labeling in the tumor cells, while the adjacent pancreatic parenchyma is negative (**c**)

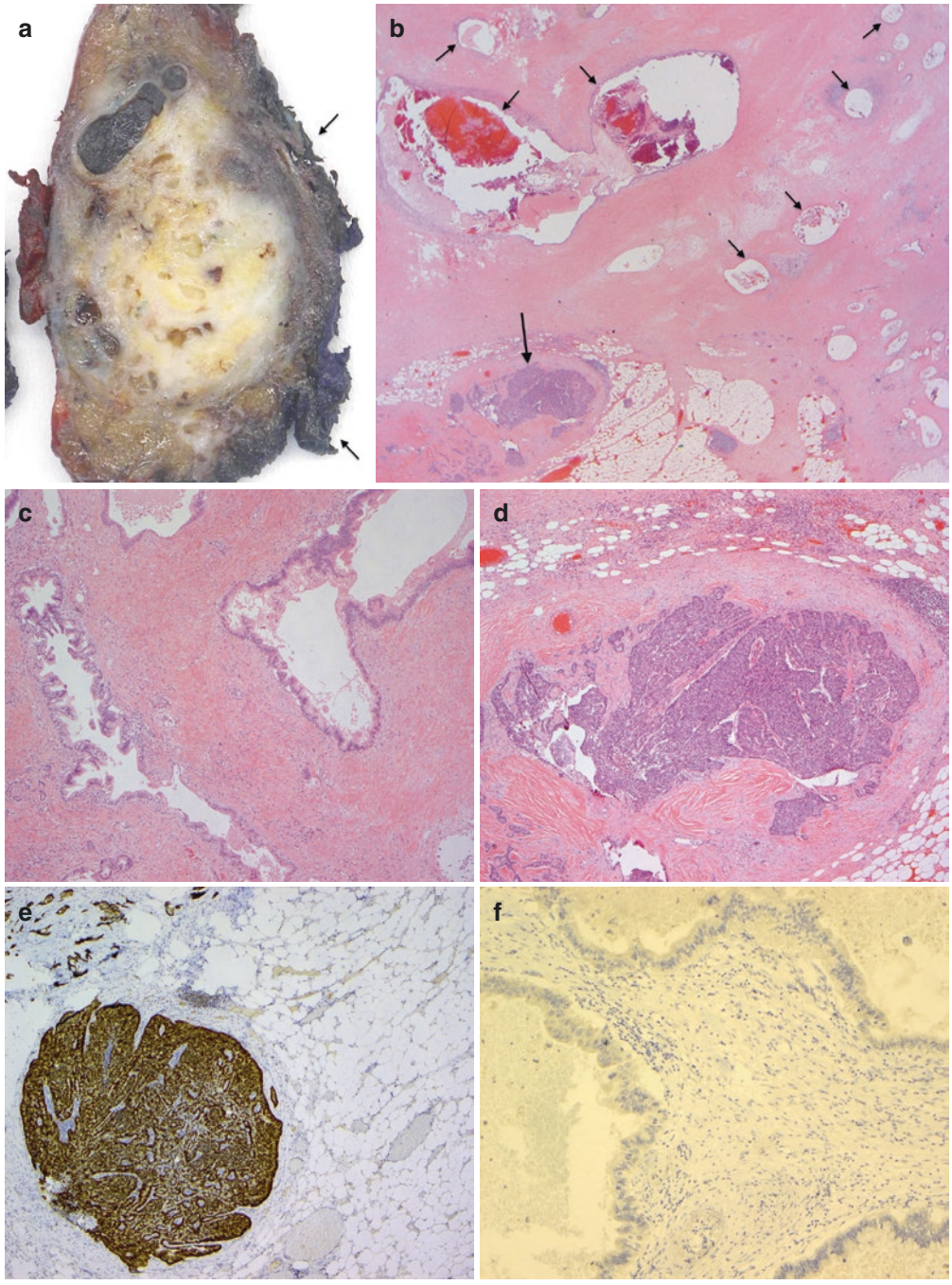

Fig. 12.13 Ductal adenocarcinoma and synchronous metastatic tubal cancer: a patient with a history of serous adenocarcinoma arising in the left fallopian tube underwent distal pancreatectomy for a tumor in the body of the pancreas. Note the irregular surface of the peripancreatic tissue posteriorly (*arrows*) (**a**). Histology revealed two tumors with distinct morphological features and a glandular (*short arrows*) and solid (*long arrow*) growth pattern (**b**). The former showed features characteristic of ductal adenocarcinoma of cystic-papillary pattern (**c**), while the latter consisted of compact solid and trabecular cell clusters suggestive of serous carcinoma (**d**). Immunostaining for PAX8 showed strong labeling of the compact tumor cell clusters, confirming the presence of metastatic tubal cancer in addition to primary ductal adenocarcinoma (**e**). PAX8 immunostaining was negative in the carcinoma with glandular growth pattern (**f**). Genetic analysis confirmed that the patient had a germline *BRCA1* mutation

References

1. Crippa S, Angelini C, Mussi C, Bonardi C, Romano F, Sartori P, Uggeri F, Bovo G. Surgical treatment of metastatic tumors to the pancreas: a single center experience and review of the literature. World J Surg. 2006;30:1536–42.
2. Adsay NV, Andea A, Basturk O, Kilinc N, Nassar H, Cheng JD. Secondary tumors of the pancreas: an analysis of a surgical and autopsy database and review of the literature. Virchows Arch. 2004;444:527–35.
3. Stelow EB, Yaziji H. Immunohistochemistry, carcinomas of unknown primary, and incidence rates. Semin Diagn Pathol. 2018;35:143–52.
4. Truong LD, Shen SS. Immunohistochemical diagnosis of renal neoplasms. Arch Pathol Lab Med. 2011;135:92–109.
5. Park S-Y, Kim B-H, Kim J-H, Lee S, Kang GH. Panels of immunohistochemical markers help determine primary sites of metastatic adenocarcinoma. Arch Pathol Lab Med. 2007;131:1561–7.
6. Dennis JL, Hvidsten TR, Wit EC, Komorowski J, Bell AK, Downie I, et al. Markers of adenocarcinoma characteristic of the site of origin: development of a diagnostic algorithm. Clin Cancer Res. 2005;11:3766–72.
7. Cai YC, Banner B, Glickman J, Odze RD. Cytokeratin 7 and 20 and thyroid transcription factor 1 can help distinguish pulmonary from gastrointestinal carcinoid and pancreatic endocrine tumors. Hum Pathol. 2001;32:1087–93.
8. Ordonez NG. Application of mesothelin immunostaining in tumor diagnosis. Am J Surg Pathol. 2003;27:1418–28.
9. Werling RW, Yaziji H, Bacchi CE, Gown AM. CDX2, a highly sensitive and specific marker of adenocarcinomas of intestinal origin. An immunohistochemical survey of 476 primary and metastatic carcinomas. Am J Surg Pathol. 2003;27:303–10.

Check for updates

13 Congenital and Developmental Abnormalities

Most developmental and congenital anomalies of the pancreas are very rare. They may or may not occur in association with other congenital abnormalities or as part of a congenital syndrome. This chapter describes in greater detail the three developmental anomalies that are not so uncommon: pancreas divisum, pancreas annulare, and pancreatic heterotopia. Less common conditions are summarized in Table 13.1.

13.1 Pancreas Annulare

In this condition, pancreatic tissue completely or partially encircles the second part of the duodenum following failed regression or rotation of the ventral anlage of the pancreas (see Chap. 1, Sect. 1.2). In the majority of affected individuals, pancreas annulare remains asymptomatic and may be detected incidentally. However, occasionally it can cause duodenal obstruction or chronic pancreatitis due to inappropriate drainage through the anomalous or distorted pancreatic duct system (Fig. 13.2). In approximately half of the patients with pancreas annulare, the anomaly becomes apparent only in adult life. The annular pancreas can be separated from the duodenum by a thin soft tissue plane, or may be buried in the duodenal wall without intervening soft tissue. Pancreas annulare has been reported in association with multiple other abnormalities, including pancreas divisum.

13.2 Pancreas Divisum

This congenital anomaly affects 5-10% of the population. It is caused by the failed fusion of the ventral and dorsal duct systems. However, because the fusion of the ventral and dorsal primordia is normal, the external appearance of the pancreas is normal (see Chap. 1, Sect. 1.2). Pancreas divisum is best demonstrated on endoscopic retrograde cholangiopancreatography (ERCP), and sphincterotomy of the minor papilla may decompress the pancreatic duct system. Three types of pancreas divisum can be distinguished (Fig. 13.3). While pancreas divisum can remain asymptomatic, a significant proportion of affected individuals develop pancreatitis, usually recurrent episodes of acute pancreatitis that may start in late childhood (Fig. 13.4). The pancreatitis in patients with pancreas divisum is traditionally believed to be due to the small size of the minor ampulla and papilla, which is usually insufficient to allow unhindered outflow of

© Springer Nature Switzerland AG 2021
F. Campbell, C. S. Verbeke, *Pathology of the Pancreas*,
https://doi.org/10.1007/978-3-030-49848-1_13

Table 13.1 Congenital and developmental abnormalities of the pancreas

Congenital anomaly	Morphological features
Agenesis and hypoplasia	
1. Complete agenesis	1. Extremely rare
2. Partial agenesis	2. Agenesis of either posterior or ventral pancreatic anlage
3. Hypoplasia ('congenital short pancreas')	3. Pancreas of reduced size and abnormal shape but without hypofunction; may be associated with polysplenia syndrome
Abnormal position	
1. Situs inversus	1. Portal vein located anterior to duodenum and pancreas
2. Splanchnoptosis	2. Abnormal descent of intestines and pancreas
3. 'Floating pancreas'	3. Pancreas suspended in mesentery
4. Intrathoracic	4. Associated with left-sided diaphragmatic hernia
Congenital/developmental pancreatic cysts	
• Von Hippel-Lindau syndrome • Infantile polycystic disease of kidney and liver • Meckel-Gruber syndrome • Trisomy 13	Cysts lined with single row of cuboidal serous epithelium
Duodenal anomalies	
1. Duodenal foregut (duplication) cyst	1. Lined by normal duodenal or ectopic gastric- or respiratory-type mucosa; no communication with duodenal lumen (Fig. 13.1)
2. Intraluminal duodenal diverticulum	2. Periampullary; communicates with pancreatic and bile duct and empties into duodenum through separate orifice
3. Juxta-ampullary bile-filled duodenal foregut (duplication) cyst	3. Communicates with common bile duct only
Hypertrophy and hyperplasia of islets of Langerhans	
• Infant of diabetic mother • Beckwith-Wiedemann syndrome • Erythroblastosis fetalis • Long-term parenteral nutrition • Persistent hyperinsulinemic hypoglycemia	Histology: see Chap. 21

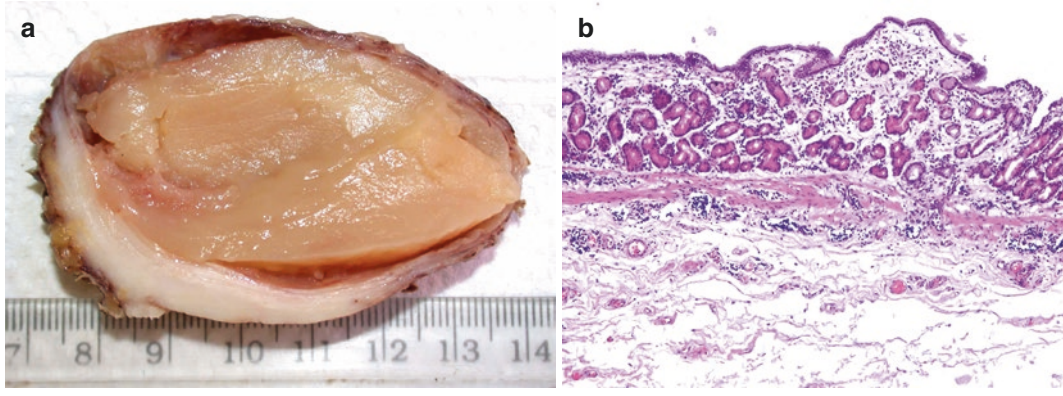

Fig. 13.1 Foregut (duplication) cyst: a unilocular cystic cavity with jelly-like content and a wall, which is firm and relatively thick (**a**). Microscopically, the cyst is lined by mucosa of gastric type, supported by a layer of muscularis mucosae (**b**). In deeper layers, the cyst wall consisted of a bilayered muscularis propria (not shown). The absence of other tissue components helps in distinguishing a duplication cyst from cystic mature teratoma

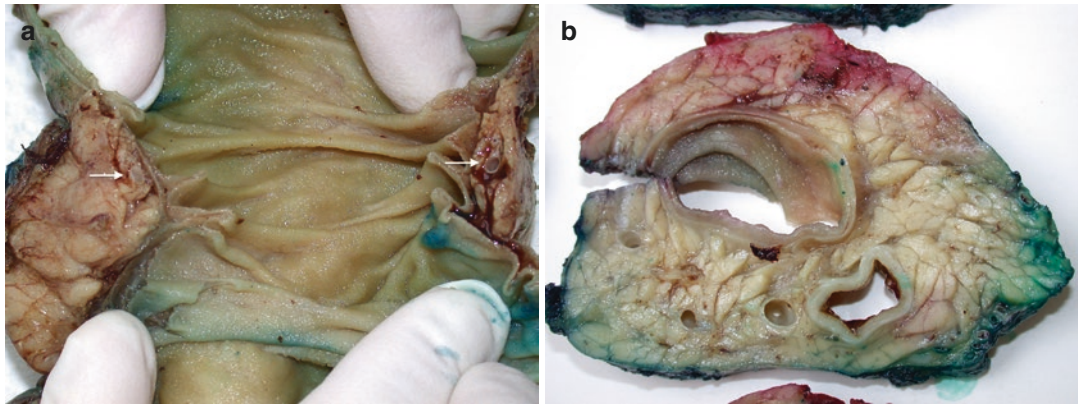

Fig. 13.2 Pancreas annulare: the duodenum is encircled by lobulated pancreatic tissue with a duct structure (*arrows*; **a**). The duodenum appears slightly narrowed, and the annular pancreatic tissue contains several dilated pancreatic ducts. Note the dilated common bile duct (**b**)

pancreatic secretion. However, recent research suggests that pancreas divisum by itself does not cause pancreatitis, but that it may be a co-factor in patients with hereditary pancreatitis [1] (see Chap. 6, Sect. 6.3, and Chap. 7, Sects. 7.2.6.2 and 7.4).

13.3 Pancreatobiliary Maljunction

Pancreatobiliary maljunction is a developmental anomaly characterized by the union of the pancreatic and common bile ducts outside the duodenal wall. Because of this abnormal configuration, the sphincter of Oddi cannot affect the flow of bile and pancreatic juice, and pancreatobiliary or biliopancreatic reflux can occur. Given that the pressure is usually greater in the pancreatic duct than in the bile duct, pancreatic juice can regurgitate through the abnormal junction into the bile duct. This is associated with an increased risk of biliary tract carcinoma, which often occurs at a much younger age than in individuals without underlying pancreaticobiliary maljunction. Biliopancreatic reflux can lead to acute or chronic pancreatitis. Reflux occurs in particular when the long common channel is temporarily obstructed for various reasons, for example, due to protein plugs or concrement [2].

13.4 Pancreatic Heterotopia

Pancreatic heterotopia (or ectopia) refers to the occurrence of pancreatic tissue in aberrant sites that are not anatomically connected to the pancreas proper. Ectopic pancreatic tissue is most frequently found in the upper gastrointestinal tract, in descending order in the duodenum (second part), ampulla, stomach (prepyloric antrum), and upper jejunum (Figs. 13.5 and 13.6). The size can vary from a microscopically small, incidentally identified focus to a lesion, which measures several centimeters in size (0.1—5 cm) and presents as a polypoid, plaque- or nipple-like, firm, pale-yellow lobulated lesion. The ectopic pancreatic tissue is usually located in the submucosa and/or the muscularis propria or subserosa. Sometimes there is a central umbilication of the overlying mucosa, where a small duct drains secretion from the ectopic pancreatic tissue into the main lumen.

Further relatively frequent sites of pancreatic ectopia are the liver (around the bile ducts), gallbladder, and Meckel's diverticulum. Rare occurrence has been reported in the esophagus, lung, mediastinum, thyroid, spleen, fallopian tube, umbilicus, and several other unusual sites. A single case report exists on ectopic pancreas within lymph nodes around the hepatic artery [3].

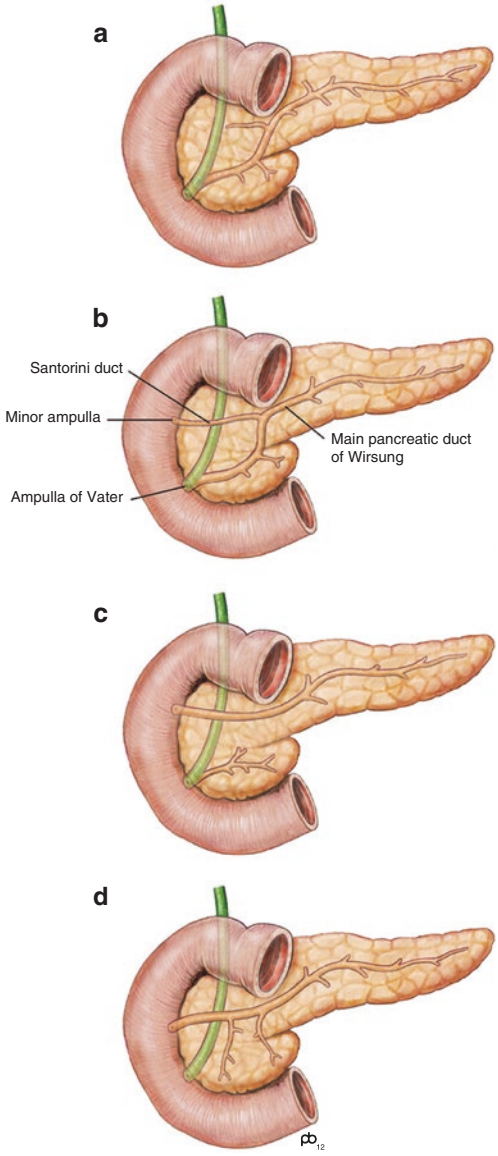

Fig. 13.3 Pancreas divisum and variants: complete regression of the distal part of the dorsal pancreatic duct leads to absence of Santorini's duct and the minor ampulla (**a**). The distal part of the dorsal pancreatic duct remains patent and forms Santorini's duct, which drains through the minor ampulla (**b**). Absence of fusion between the ducts of both buds results in drainage of the pancreatic tail, body, and cranial head through Santorini's duct and the minor ampulla, while the caudal part of the head drains through the ventral duct and major ampulla ('true' pancreas divisum (**c**)). The ventral duct fuses with the dorsal duct and drains through Santorini's duct and the minor ampulla, while only the bile duct joins the major ampulla (**d**) (Image courtesy and copyright of Paul Brown, The Leeds Teaching Hospitals NHS Trust, Leeds, UK)

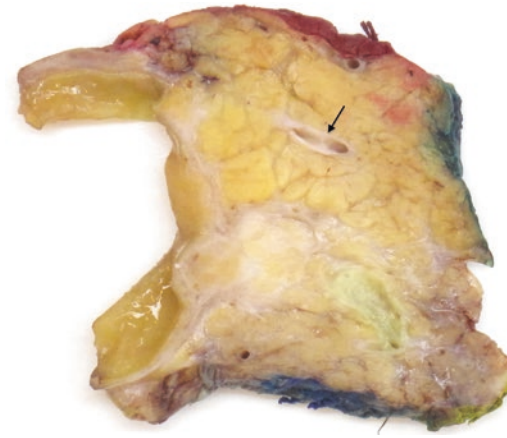

Fig. 13.4 Pancreas divisum with recurrent acute pancreatitis: axial specimen slice from the pancreatoduodenectomy specimen of a patient with known pancreas divisum and recurrent attacks of acute pancreatitis. Santorini´s duct is dilated (*arrow*) and the posterior part of the pancreatic head shows scarring, patchy atrophy, and duct dilatation

Histologically, ectopic pancreatic tissue consists in principle of its normal constituents, that is, ducts, acini, and islets. However, the latter two may be scanty or absent, such that ductular structures—true pancreatic ducts and dilated acini—predominate. When embedded in the muscle layer of the gastrointestinal tract, the combination of ductular structures and smooth muscle has given rise to the misnomer of adenomyosis or myoepithelial hamartoma (see Chap. 7, Sect. 7.2.8.1).

Ectopic pancreatic tissue is often an incidental finding. However, any of the pancreatic diseases can in principle affect the ectopic pancreatic tissue, and episodes of acute pancreatitis may cause local inflammation of the host tissue. Being a mass-forming lesion, pancreatic ectopia can occasionally clinically mimic carcinoma, cause symptoms related to mechanical obstruction or hemorrhage. Rare cases of pancreatic ductal adenocarcinoma developing from ectopic pancreas in the rectum, mediastinum, or a hiatus hernia have been reported [4–6]. Ectopic pancreatic tissue in the second part of the duodenum and ampulla of Vater can, in combination with alcohol abuse, lead to paraduodenal pancreatitis (see Chap. 7, Sect. 7.2.8).

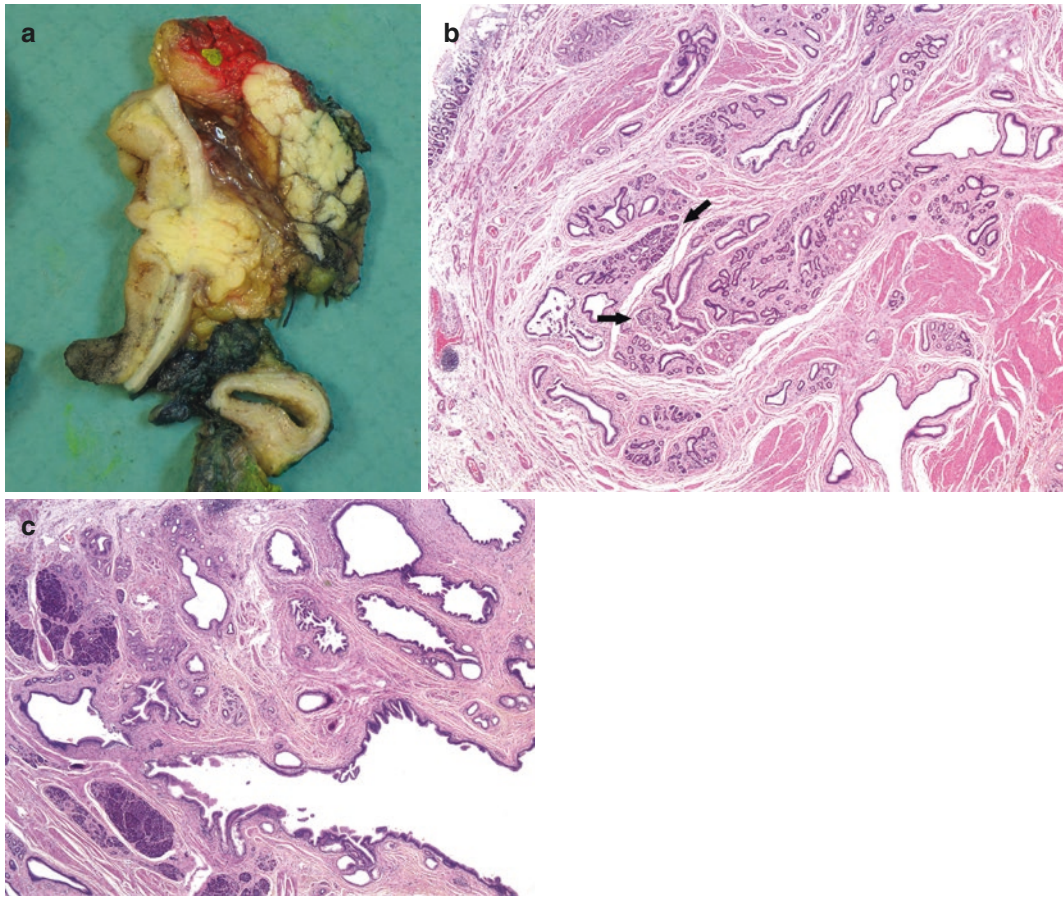

Fig. 13.5 Ectopic pancreas in duodenum: a well-circumscribed nodular structure of compact, slightly lobulated tissue is located astride the muscularis propria of the proximal duodenum, cranial to the pancreatic head (**a**). Microscopically, this focus consists of loosely aggregated pancreatic lobules embedded in the fibromuscular stroma of the duodenal muscularis mucosae and deep lamina propria. The lobules are mainly composed of ductular structures interspersed with an occasional islet and a few acini (*arrows*; **b**). Several ectopic lobules of pancreatic tissue are present around the mildly dilated Santorini's duct at the minor ampulla (**c**)

13.5 Ectopic Tissue in the Pancreas

Heterotopic spleen ('splenunculus') may occur within the pancreas. It is almost exclusively found in the region of the tail. To date, only a single case report on ectopic spleen in the pancreatic head has been published [7]. Heterotopic spleen is usually a small (up to 3 cm), well-circumscribed, soft, dark red-brown lesion (Fig. 13.7). Because intrapancreatic heterotopic spleen seldom causes symptoms, it is usually an incidental finding on imaging and may mimic a pancreatic tumor, in particular a neuroendocrine tumor or a metastatic lesion, due to its rich vascularization. Histologically, it consists of normal white and red splenic pulp. Occasionally, it may contain foci of pancreatic tissue that may be attenuated and embedded in fibrous stroma. In fine-needle biopsy or aspiration cytology material, the presence of CD8-positive sinusoidal endothelial cells (which are also positive for CD31), is usually helpful in reaching a diagnosis (Fig. 13.7d). Epithelial cysts may rarely occur within the intrapancreatic splenic tissue (see Chap. 19, Sect. 19.4.3). Intrapancreatic encapsulated heterotopic

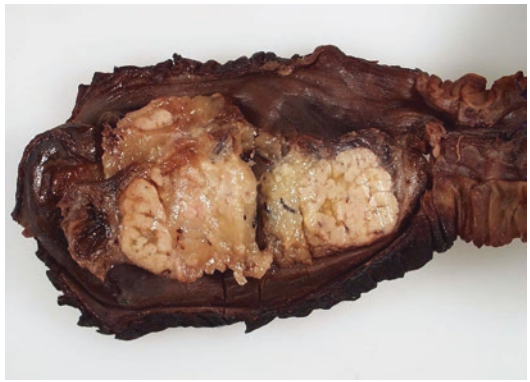

Fig. 13.6 Ectopic pancreas in small bowel mesentery: the small bowel mesentery contains a 2 cm nodular lesion, which is composed of well-demarcated lobulated tissue and shows no invasion of the surrounding tissues

spleen should be distinguished from the poorly encapsulated aggregates of splenic pulp that can be found in trisomy 13, together with the cystic changes of the exocrine pancreas (Table 13.1).

Ectopic adrenal cortical nodules may on rare occasion occur in the pancreas and, when large, may cause confusion with clear cell pancreatic endocrine neoplasia or metastatic renal cell carcinoma (see Chap. 12, Sect. 12.5 and Table 12.1; Chap. 20, Sects. 20.5.1 and 20.9.1) (Fig. 13.8). The histology is consistent with that of normal adrenal cortex, and immunostaining may be helpful in reaching the correct diagnosis (positive for synaptophysin and variable staining for cytokeratins; vimentin may be positive in some cells; negative for EMA, chromogranin, S100).

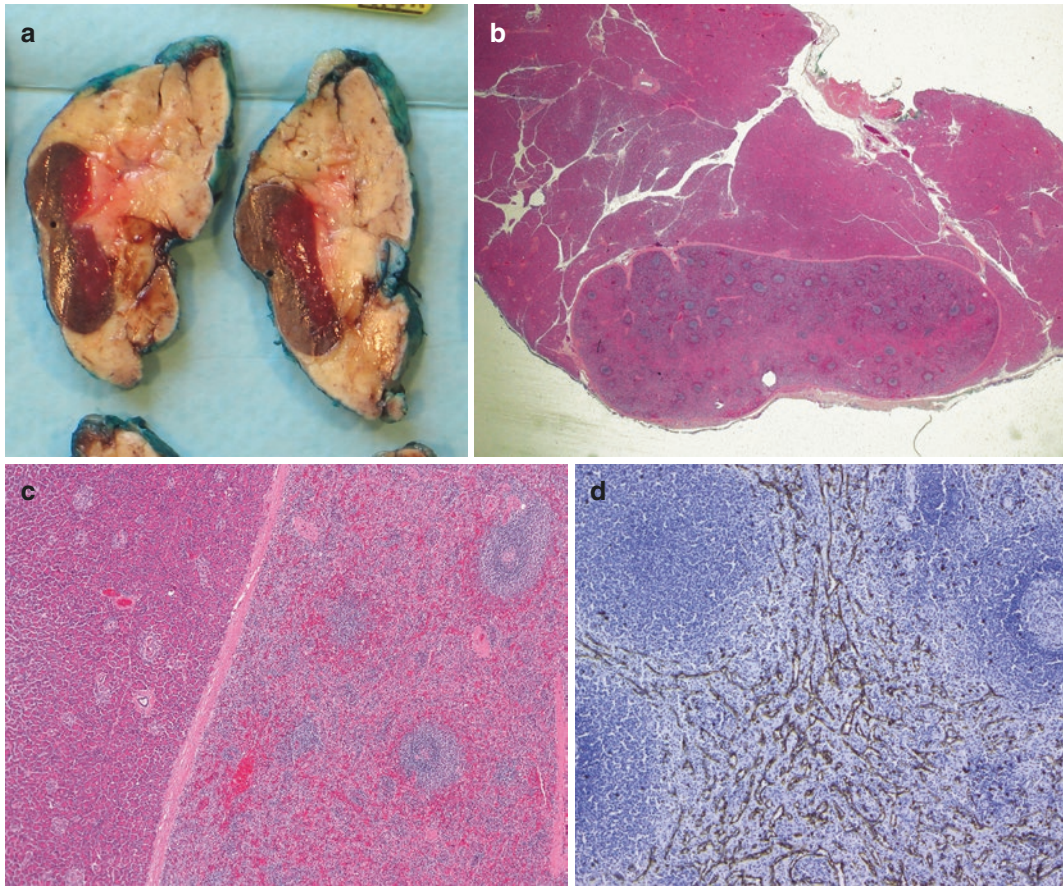

Fig. 13.7 Intrapancreatic ectopic spleen: an ovoid well-circumscribed nodular lesion consisting of dark red-brown soft tissue is present within normal pancreatic parenchyma (**a**). At low power, histological features are consistent with ectopic spleen (**b**), which comprises normal red and white pulp, and is separated from normal pancreas by a thin fibrous capsule (**c**). Immunostaining for CD8 shows labeling of the sinusoidal endothelial cells (**d**)

13.6 Benign Glandular Inclusions in Abdominal Lymph Nodes

Benign glandular inclusions are not an uncommon finding in abdominal lymph nodes of females. According to an autopsy study, they were identified in 14% of 50 random postmortems of females and in none of 50 autopsies of males. In most cases, the glandular inclusions are located in capsular or cortical sites. They have a ciliated epithelium that resembles tubal or endometrial epithelium (Fig. 13.9). If the glandular inclusions are surrounded by endometrial stroma, they qualify as endometriosis. Metastatic adenocarcinoma is the obvious differential, which can be excluded based on cytological atypia, mitotic activity and—for early metastases—predominant location within the marginal sinus [8]. Positive immunostaining for estrogen receptor protein in many of the benign glandular inclusions may help with the differential diagnosis.

As mentioned above, a single case of ectopic pancreatic tissue within upper abdominal lymph nodes has been reported [3].

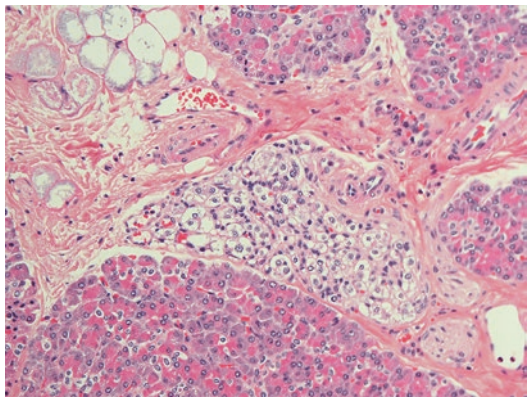

Fig. 13.8 Adrenal cortical nodule: a well-circumscribed nonencapsulated nodular cluster of clear-appearing cells with a vaguely trabecular arrangement is present within interlobular stroma. Adjacent pancreatic parenchyma is unremarkable

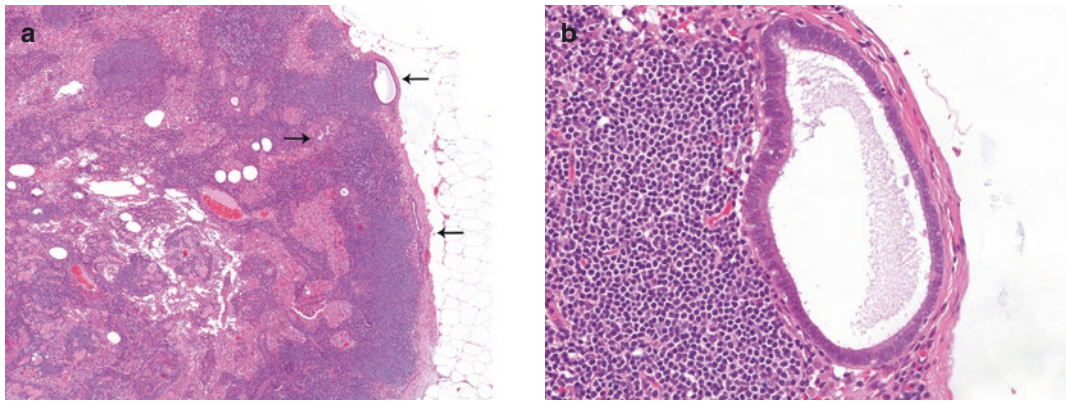

Fig. 13.9 Benign glandular lymph node inclusions: several simple glands of varying size are present in the marginal sinus and cortex of an aortocaval lymph node removed during pancreatoduodenectomy for pancreatic cancer in a middle-aged female (**a**). At high power magnification, the glands are lined by a tubal-type epithelium including ciliated cells. There is no cytological atypia (**b**)

References

1. Bertin C, Pelletier A-L, Vullierme MP, Bienvenu T, Rebours V, Hentic O, et al. Pancreas divisum is not a cause of pancreatitis by itself but acts as a partner of genetic mutations. Am J Gastroenterol. 2012;107:311–7.
2. Kamisawa T, Kaneko K, Itoi T, Ando H. Pancreaticobiliary maljunction and congenital billiary dilatation. Lancet Gastroenterol Hepatol. 2017;2:2610–8.
3. Muruyama H, Kikuchi M, Imai T, Yamamoto Y, Iwata Y. A case of heterotopic pancreas in lymph node. Virchows Arch A. 1978;377:175–9.
4. Guillou L, Nordback P, Gerber C, Schneider RP. Ductal adenocarcinoma arising in a heterotopic pancreas situated in a hiatal hernia. Arch Pathol Lab Med. 1994;118:568–71.
5. Goodarzi M, Rashid A, Maru D. Invasive ductal adenocarcinoma arising from pancreatic heterotopia in rectum: case report and review of literature. Hum Pathol. 2010;41:1809–13.
6. St Romain P, Muehlebach G, Damjanov I, Fan F. Adenocarcinoma arising in an ectopic mediastinal pancreas. Ann Diagn Pathol. 2012;16:494–7.
7. Landry ML, Sarma DP. Accessory spleen in the head of the pancreas. Hum Pathol. 1989;20:497.
8. Miranda RN, Khoury JD, Medeiros LJ. Epithelial inclusions in lymph node. In: Atlas of lymph node pathology, Atlas of anatomic pathology. New York, NY: Springer. p. 487–90.

Part III

Exocrine Pancreas: Cystic

Cystic Lesions: Classification and Sampling

14

Cystic lesions of the pancreas are now being diagnosed much more frequently due to the increased use of modern imaging techniques such as computed tomography (CT), magnetic resonance imaging (MRI), magnetic resonance cholangiopancreatography (MRCP), and endoscopic ultrasound (EUS). The majority (approximately 70%) are asymptomatic and diagnosed incidentally during investigation for other conditions. The prevalence of these incidentally detected pancreatic cystic lesions varies with the imaging methods employed and the population studied [1]. Prevalences of 2.4–49.1% have been reported on MRI and MRCP, but are only 0.2–5.4% on CT [1]. The prevalence, number, and mean size of the cysts increase with age [2]. In autopsy studies, pancreatic cysts have been found in up to 50% of the elderly population [2]. Most pancreatic cystic lesions are non-invasive and amenable to resection. However, not all pancreatic cysts require surgery and establishing the true nature of a cystic lesion on imaging can be difficult. In the study by Salvia et al. [3], the rate of inaccurate preoperative diagnoses for pancreatic cystic lesions was 22%. However, less than 10% of preoperative diagnostic errors appear to be clinically relevant [4]. In the future, analysis of molecular markers in pancreatic cyst fluid [5] in combination with cyst fluid cytology and biochemistry, imaging, and/or clinical features, may help to further improve preoperative diagnosis of pancreatic cystic lesions [6]. Endoscopic ultrasound-guided needle-based confocal laser endomicroscopy for in vivo evaluation of pancreatic cysts is also emerging as a potentially useful tool for improving preoperative diagnosis [7].

14.1 Classification

There are numerous types of pancreatic cystic lesion, the relative frequencies of which vary in different studies. Pseudocysts are the most common (see Chap. 7, Sects. 7.1.5 and 7.2.5), but are not often resected (Fig. 14.1) Intraductal papillary mucinous neoplasm (see Chap. 17) is the most commonly resected pancreatic cystic neoplasm [8]. Pancreatic cystic lesions can be classified in several ways:

- Congenital versus acquired
- True cysts versus cystic degeneration
- Epithelial versus non-epithelial
- Neoplastic versus nonneoplastic
- Benign or premalignant versus malignant

Congenital or developmental cysts include those of von Hippel-Lindau syndrome, duplication (foregut) cyst, duodenal diverticulum (see Table 13.1), and choledochal cyst of the common bile duct (see Chap. 19, Sect. 19.3.2). Pancreatic hamartoma with cystic features has also been described (see Chap. 19, Sect. 19.5.1).

© Springer Nature Switzerland AG 2021
F. Campbell, C. S. Verbeke, *Pathology of the Pancreas*,
https://doi.org/10.1007/978-3-030-49848-1_14

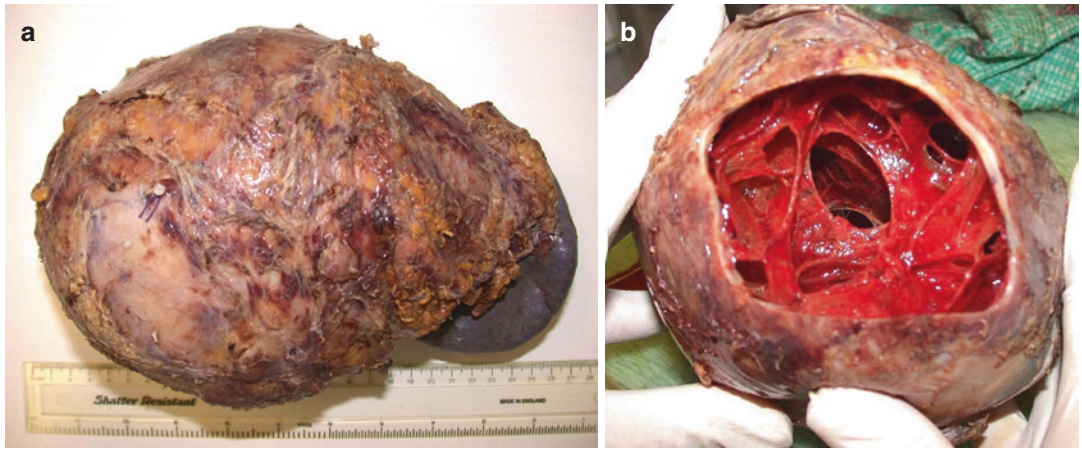

Fig. 14.1 Giant pseudocyst: this giant pseudocyst resembles many cystic lesions of the pancreas (**a**). Opening revealed a unilocular cyst with web-like membranes of hemorrhagic exudate and a firm fibrous wall (**b**)

Table 14.1 Pancreatic neoplasms with secondary cystic change (degeneration)

Epithelial
• Solid pseudopapillary neoplasm (see Chap. 18)
• Pancreatic neuroendocrine neoplasm (see Chap. 20)
• Pancreatic ductal adenocarcinoma (see Chap. 9)
• Undifferentiated carcinoma with osteoclast-like giant cells (see Chap. 9)
• Acinar cell carcinoma (see Chap. 10)
• Metastases (see Chap. 12)
• Pancreatoblastoma (see Chap. 10)
Non-epithelial (see Chap. 11)
• Cystic schwannoma
• Desmoplastic small round cell tumor
• Gastrointestinal stromal tumor (GIST)
• Leiomyosarcoma
• Malignant peripheral nerve sheath tumor (PNST)
• Paraganglioma
• Peripheral neuroectodermal tumor (PNET)
• Perivascular epithelioid cell neoplasm (PEComa)

Cystic degeneration and necrosis can occur in any typically solid pancreatic (epithelial or non-epithelial) tumor (Table 14.1), including ductal adenocarcinoma (see Chap. 9, Sect. 9.5) and pancreatic neuroendocrine tumor (see Chap. 20, Sect. 20.4), and may also occur in metastases to the pancreas (see Chap. 12, Sect. 12.3) [9, 10].

A commonly used classification system for pancreatic cystic lesions separates them into neoplastic or nonneoplastic cysts and then separates each of these two categories into those with and without an epithelial lining, resulting in four groups [11]. This classification into neoplastic epithelial, neoplastic non-epithelial, nonneoplastic epithelial, and nonneoplastic non-epithelial is shown in Table 14.2, which can be used as a quick reference to all of the cystic lesions of the pancreas and indicates where each entity is discussed in more detail in this book.

Another practical classification is based on the type of epithelial lining of the pancreatic cystic lesion, namely acinar, mucinous, pancreatobiliary, serous, or squamous. This classification is shown in Table 14.3, which, again, includes cross-references to those chapters where further discussion on each entity can be found.

14.2 Sampling of Cystic Lesions

As indicated above, establishing the true nature of a pancreatic cystic lesion on imaging can be difficult. Similarly, establishing the diagnosis on microscopy can be problematic. The epithelium of neoplastic cysts can become denuded and, with inadequate sampling, lead to a misdiagnosis of a pseudocyst. In the study by Warshaw et al. [13], the epithelial lining of cystic neoplasms was partially denuded in 40-72% of cases. The area of denuded epithelium averaged 40% of the wall (range 5-98%) in the denuded tumors. A more recent study has shown that 80% of pancreatic

Table 14.2 Classification of cystic lesions of the pancreas [11]

Neoplastic epithelial	Nonneoplastic epithelial
Serous cystic neoplasm (see Chap. 15)	Congenital cyst (in malformation syndromes)
Mucinous cystic neoplasm (see Chap. 16)	Duplication (foregut) cyst (see Chap. 13)
Intraductal papillary neoplasm (see Chap. 17)	Choledochal cyst (see Chap. 19)
Solid pseudopapillary neoplasm (see Chap. 18)	Cystic hamartoma (see Chap. 19)
Pancreatic endocrine neoplasm (see Chap. 20)	Lymphoepithelial cyst (see Chap. 19)
Acinar cell cystadenoma[a] (see Chap. 19)	Mucinous nonneoplastic cyst[b] (see Chap. 19)
Cystic acinar cell carcinoma (see Chap. 10)	Retention cyst (see Chap. 19)
Cystic teratoma (see Chap. 19)	Paraduodenal (groove) pancreatitis (see Chap. 7)
Cystic ductal adenocarcinoma (see Chap. 9)	Endometrial cyst (see Chap. 19)
Cystic pancreatoblastoma (see Chap. 10)	Epidermoid cyst in intrapancreatic heterotopic spleen
Cystic metastasis (see Chap. 12)	(see Chap. 19)
Neoplastic non-epithelial	**Nonneoplastic non-epithelial**
Lymphangioma (see Chap. 11)	Pseudocyst (see Chap. 7)
Hemangioma	Parasitic cyst (see Chap. 19)
Cystic schwannoma (see Chap. 11)	
Cystic degeneration in PNET (see Chap. 11)	
Cystic degeneration in leiomyosarcoma (see Chap. 11)	
Cystic degeneration in GIST (see Chap. 11)	
Cystic degeneration in malignant PNST	
Cystic degeneration in paraganglioma (see Chap. 11)	

[a] and [b]: In the WHO 2019 classification of tumors of the pancreas [12], these entities are now referred to as [a]acinar cystic transformation and [b]simple mucinous cyst (see Chap. 19).

Table 14.3 Classification of pancreatic cystic lesions according to type of epithelial lining

Acinar
- Acinar cystic transformation or acinar cell cystadenoma (see Chap. 19)
- Cystic change in acinar cell carcinoma (see Chap. 10)
- Acinar cell cystadenocarcinoma—a rare variant of acinar cell carcinoma with (non-degenerative) cyst formation (see Chap. 10)

Mucinous
- Mucinous cystic neoplasm (see Chap. 16)
- Intraductal papillary mucinous neoplasm (see Chap. 17)
- Simple mucinous cyst or mucinous nonneoplastic cyst (see Chap. 19)

Pancreatobiliary
- Retention cyst (see Chap. 19)
- Choledochal cyst (see Chap. 19)

Serous (see Chap. 15)
- Microcystic serous cystadenoma
- Macrocystic serous cystadenoma
- Von Hippel-Lindau syndrome-associated serous cystic neoplasm
- Serous cystadenocarcinoma

Squamous
- Lymphoepithelial cyst (see Chap. 19)
- Dermoid cyst/ mature cystic teratoma (see Chap. 19)
- Epidermoid cyst in intrapancreatic heterotopic spleen (see Chap. 19)
- Squamous cyst of pancreatic duct (see Chap. 19)
- Squamous metaplasia in dilated duct/retention cyst (see Chap. 19)
- Squamous metaplasia in mucinous cystic neoplasm (see Chap. 16)
- Squamous epithelial lining in foregut/duplication cyst (see Chap. 19)

cystic lesions had varying degrees of denuded epithelium [14]. For this reason, it is always prudent to consider sampling the entire wall of a pancreatic cyst to identify the lining epithelium (e.g., serous in a macrocystic serous cystadenoma or mucinous in mucinous cystic neoplasm and intraductal papillary mucinous neoplasm). Extensive sampling of the cyst wall is also particularly important in mucinous neoplasms, not just to confirm the diagnosis, but to establish the grade of dysplasia and to exclude invasive carcinoma.

In large mucinous cystic neoplasms (see Chap. 16), the capsule can be so sclerotic that it may be difficult to find the ovarian-type stroma to confirm the diagnosis and exclude an intraductal papillary mucinous neoplasm (see Chap. 17). Macroscopic papillary areas and solid areas in a mucinous cystic neoplasm (MCN) are most likely to show high-grade dysplasia or invasive carcinoma, and should always be sampled. However, both high-grade dysplasia and invasion may be focal and not apparent macroscopically.

Solid areas and mucoid areas in the wall of an intraductal papillary mucinous neoplasm should always be sampled, as they likely represent invasive carcinoma. However, high-grade dysplasia or invasive carcinoma in an intraductal papillary mucinous neoplasm (IPMN) may also be focal (or multifocal) and again not identifiable macroscopically.

In the absence of macroscopic invasive carcinoma, embedding the entire mucinous neoplasm (MCN or IPMN) may be considered, particularly if microscopic examination reveals high-grade dysplasia but no invasion.

References

1. Zerboni G, Signoretti M, Crippa S, Falconi M, Arcidiacono PG, Capurso G. Systematic review and meta-analysis: Prevalence of incidentally detected pancreatic cystic lesions in asymptomatic individuals. Pancreatology. 2019;19:2–9.
2. Komrey ML, Bulow R, Hubner J, Paperlein C, Lerch MM, Ittermann T, et al. Prospective study on the incidence, prevalence and 5-year pancreatic-related mortality of pancreatic cysts in a population-based study. Gut. 2018;67:138–45.
3. Salvia R, Malleo G, Marchegiani G, Pennacchio S, Paiella S, Paini M, et al. Pancreatic resections for cystic neoplasms: from the surgeon's presumption to the pathologist's reality. Surgery. 2012;152(3 Suppl 1):S135–42.
4. Del Chiaro M, Segersvard R, Pozzi Mucelli R, Rangelova E, Kartalis N, Ansorge C, et al. Comparison of preoperative conference-based diagnosis with histology of cystic tumors of the pancreas. Ann Surg Oncol. 2014;21:1539–44.
5. Singhi AD, McGrath K, Brand RE, Khalid A, Zeh HJ, Chennat JS, et al. Preoperative next-generation sequencing of pancreatic cyst fluid is highly accurate in cyst classification and detection of advanced neoplasia. Gut. 2018;67:2131–41.
6. The European Study Group on Cystic Tumours of the Pancreas. European evidence-based guidelines on pancreatic cystic neoplasms. Gut. 2018;67:789–804.
7. Krishna SG, Brugge WR, Dewitt JM, Kongkam P, Napoleon B, Robles-Medranda C, et al. Needle-based confocal laser endomicroscopy for the diagnosis of pancreatic cystic lesions: an international external interobserver and intraobserver study (with videos). Gastrointest Endosc. 2017;86:644–54.
8. Valsangkar NP, Morales-Oyarvide V, Thayer SP, Ferrone CR, Wargo JA, Warshaw AL, et al. 851 resected cystic tumors of the pancreas: a 33-year experience at the Massachusetts General Hospital. Surgery. 2012;152(3 Suppl 1):S4–12.
9. Adsay NV, Klimstra DS. Cystic forms of typically solid pancreatic tumors. Semin Diagn Pathol. 2000;17:81–8.
10. Kosmahl M, Pauser U, Anlauf M, Klöppel G. Pancreatic adenocarcinoma with cystic features: neither rare nor uniform. Mod Pathol. 2005;18:1157–64.
11. Kosmahl M, Pauser U, Peters K, Sipos B, Luttges J, Kremer B, et al. Cystic neoplasms of the pancreas and tumor-like lesions with cystic features: a review of 418 cases and a classification proposal. Virchows Arch. 2004;445:168–78.
12. Lokuhetty D, White VA, Watanabe R, Cree IA, editors. Digestive system tumours. WHO classification of tumours 5th edition. Lyon: IARC Press; 2019. p. 296.
13. Warshaw AL, Compton CC, Lewandrowski K, Cardenosa G, Mueller PR. Cystic tumors of the pancreas. New clinical, radiologic, and pathologic observations in 67 patients. Ann Surg. 1990;212:432–43.
14. Gomez V, Majumder S, Smyrk TC, Topazian MD, Chari ST, Gleeson FC, et al. Pancreatic cyst epithelial denudation: a natural phenomenon in the absence of treatment. Gastrointest Endosc. 2016;84:788–93.

Serous Cystic Neoplasia

15

Serous cystic neoplasms are composed of uniform cuboidal, glycogen-rich, epithelial cells lining cysts of varying sizes. These cysts contain watery serous fluid. In clinical practice, serous cystic neoplasms are considered entirely benign. There are, however, very rare examples of serous cystadenocarcinoma in the literature, but some question whether they represent multifocal disease rather than metastatic malignant neoplasm.

15.1 WHO Classification

Serous cystic neoplasms are included in 'benign epithelial tumors and precursors' in the 2019 WHO classification of tumors of the pancreas [1].

15.2 Terminology

Serous cystadenoma is also known as glycogen-rich cystadenoma, serous microcystic adenoma, or microcystic serous adenoma. The macrocystic variant is known as macrocystic serous cystadenoma, oligocystic serous cystadenoma, or serous oligocystic and ill-demarcated adenoma.

In this chapter, we will use the terms '*microcystic serous cystadenoma*' and '*macrocystic serous cystadenoma*' for the two commonest variants.

15.3 Epidemiology

Serous cystic neoplasms are uncommon, accounting for 1–2% of exocrine pancreatic neoplasms and for 10% of resected cystic pancreatic lesions. Microcystic serous cystadenoma is the most common variant. The mean age at presentation for microcystic serous cystadenoma is 60 years and for macrocystic serous cystadenoma is 50 years (range 18–93 years). The macrocystic variant has also been described in infants under 18 months of age. Serous cystic neoplasms are more common in females.

15.4 Clinical Features

The majority of patients with a serous cystic neoplasm are asymptomatic and the tumor is detected on imaging or at laparotomy. Symptoms include abdominal pain, nausea and vomiting, weight loss, or a palpable mass, and are usually related to location of the tumor in the head of the pancreas [2]. Serous cystic neoplasms may occasionally compress or obstruct the pancreatic duct or the common bile duct. However, jaundice is extremely unusual. Serum tumor markers are generally not raised.

© Springer Nature Switzerland AG 2021
F. Campbell, C. S. Verbeke, *Pathology of the Pancreas*,
https://doi.org/10.1007/978-3-030-49848-1_15

15.4.1 Associations

The etiology is unknown. A small minority of serous cystadenomas may be associated with von Hippel-Lindau (VHL) syndrome (see Chap. 20, Sect. 20.12). There are rare cases of serous cystic neoplasms co-existing with other neoplasms including pancreatic ductal adenocarcinoma and ampullary adenocarcinoma. Serous cystic neoplasms may also co-exist with grade 1–3 pancreatic neuroendocrine tumors (PanNETs); von Hippel-Lindau syndrome should always be considered when this occurs.

15.4.2 Imaging

On CT scan or endoscopic ultrasound scan, microcystic serous cystadenoma appears as a well-circumscribed mass composed of tiny (less than 1–2 cm in size) cysts separated by fine septa with a characteristic central stellate fibrous scar. In approximately a third of cases, there is a 'sunburst' pattern of calcification in the central scar.

Macrocystic serous cystadenoma is composed of larger cysts (1–3 cm in size, or larger) and may even be unilocular. On imaging, they are poorly circumscribed, do not have a central scar, and may mimic a mucinous cystic neoplasm (see Chap. 16) or a branch-duct-type intraductal papillary mucinous neoplasm (see Chap. 17).

Serous cystic neoplasms do not usually communicate with the pancreatic duct system. However, there are rare case reports in which microcystic and macrocystic serous cystadenomas have been found to communicate with the duct system [3].

The solid variant of serous cystic neoplasms (see Sect. 15.11.1) may be mistaken for a neuroendocrine tumor on imaging.

The newly emerging technique endoscopic ultrasound-guided needle-based confocal laser endomicroscopy can be used to identify serous cystic neoplasms on preoperative evaluation of pancreatic cysts, by visualizing the capillary plexus beneath the epithelial lining, which is characteristic of serous cystic neoplasms [4].

15.5 Classification

There are six types of serous cystic neoplasm:

1. Microcystic serous cystadenoma,
2. Macrocystic serous cystadenoma,
3. Solid serous adenoma,
4. von Hippel-Lindau syndrome-associated serous cystic neoplasm,
5. Mixed serous-neuroendocrine neoplasm, and
6. Serous cystadenocarcinoma.

15.6 Macroscopy

15.6.1 Microcystic Serous Cystadenoma

Microcystic serous cystadenomas may occur anywhere within the pancreas, but the majority arise in the body and tail of the pancreas. They are usually solitary, well-circumscribed, bosselated, round tumors with an incomplete fibrous pseudocapsule or, more commonly, no capsule at all. The adjacent pancreas is usually macroscopically normal. Multiple serous cystic neoplasms should always raise the possibility of von Hippel-Lindau syndrome. The mean size is 4–5 cm (range 1–30 cm) and they may compress or displace the main pancreatic duct or common bile duct (Fig. 15.1).

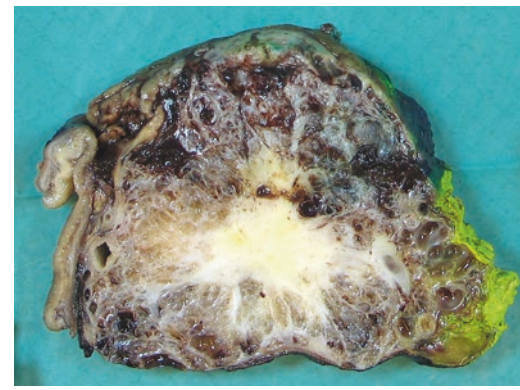

Fig. 15.1 Microcystic serous cystadenoma: there is a large central scar with radiating fibrous septa and small cysts. The neoplasm compresses the bile duct (*left* of picture)

The cut-surface is sponge-like (also referred to as honeycomb-like) with numerous tiny, thin-walled cysts (usually less than 2–10 mm in size) filled with clear watery fluid (Fig. 15.2). There is a central fibrous scar, which may be calcified, with fibrous septa radiating out towards the periphery (Figs. 15.1 and 15.2). The adjacent pancreas may be entirely normal or show obstructive changes, including chronic pancreatitis and fatty replacement (Figs. 15.2 and 15.3). There may be irregular extension of the neoplasm into the adjacent pancreas, duodenum (Fig. 15.4), peripancreatic lymph nodes, or large blood vessels, sometimes referred to as 'locally aggressive behavior' (see Sect. 15.11.6).

Fig. 15.2 Microcystic serous cystadenoma: there is a honeycomb or sponge-like cut-surface and central radiating scar. Note the surrounding pancreas is entirely normal

15.6.2 Macrocystic Serous Cystadenoma

Macrocystic serous cystadenomas occur most commonly in the head of the pancreas. They are usually solitary and may be well circumscribed but, more commonly, are ill-demarcated and extend into the adjacent pancreas. The mean size is 4 cm (range 2–15 cm).

The cut-surface reveals a few thin-walled cysts ranging in size from 1 to 8 cm and filled with

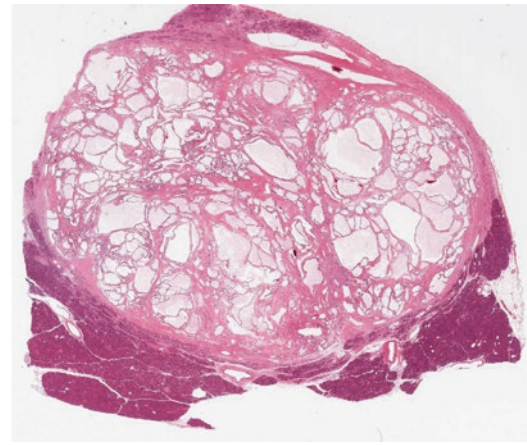

Fig. 15.3 Microcystic serous cystadenoma: this whole-mount cross-section shows a well-circumscribed neoplasm that is associated with fibrosis and atrophy of only the peritumoral pancreatic parenchyma

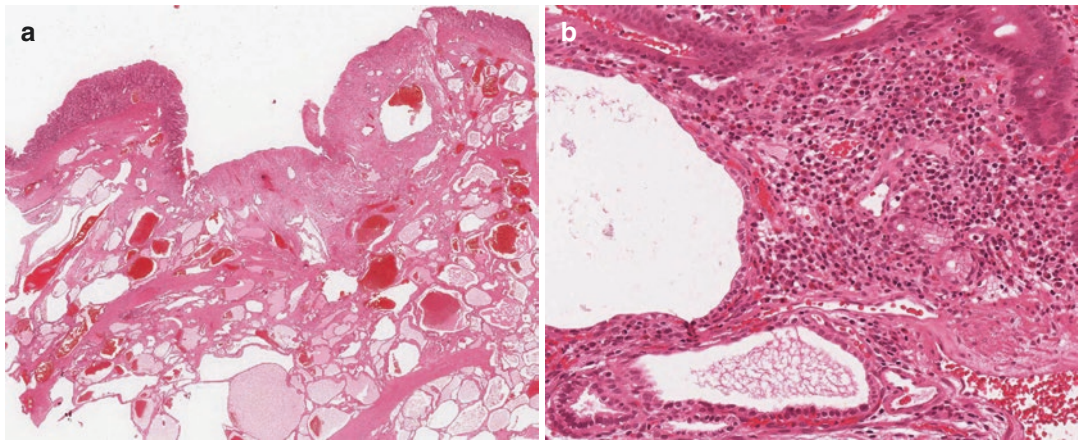

Fig. 15.4 Microcystic serous cystadenoma: this whole-mount cross-section shows extension of the neoplasm into the ulcerated duodenum with associated hemorrhage in the neoplasm (**a**). At higher power, the neoplastic cysts (*left*) are seen within the duodenal mucosa next to duodenal glands and Brunner's glands (**b**)

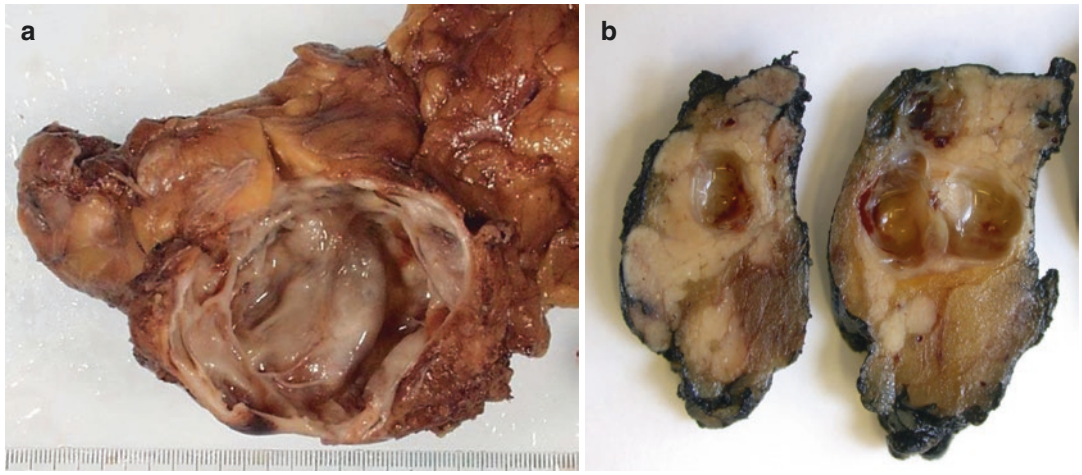

Fig. 15.5 Macrocystic serous cystadenoma: the wall is thin and there is a smooth lining (**a**). This smaller example contains watery fluid and is surrounded by normal pancreas (**b**)

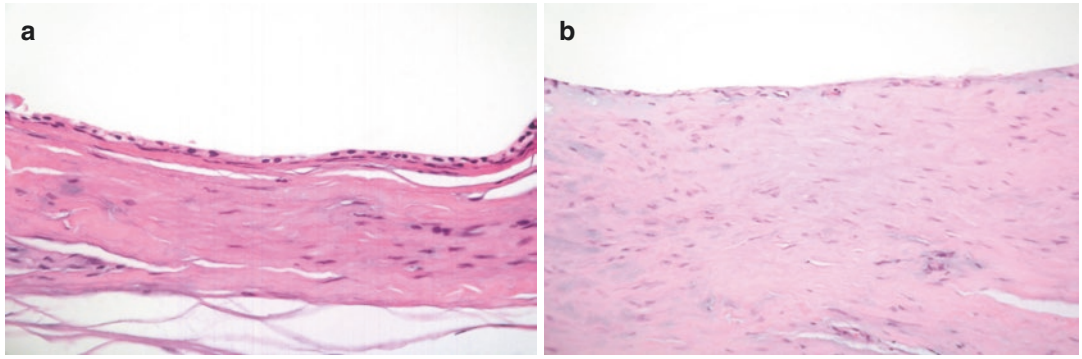

Fig. 15.6 Macrocystic serous cystadenoma: this unilocular cyst only showed focal epithelial lining (**a**). Most of the epithelium was denuded, mimicking a pseudocyst (**b**)

clear watery fluid (Fig. 15.5). Some examples may be unilocular. The inner lining of the cysts is smooth and there is no central stellate scar.

15.6.3 Sampling

Microcystic serous neoplasms do not need extensive sampling. However, much of the epithelium in macrocystic serous cystadenomas can be denuded (Fig. 15.6 and see Chap. 14, Sect. 14.2) and, therefore, these should be sampled extensively to confirm the diagnosis and/or distinguish them from other oligocystic pancreatic lesions.

15.7 Microscopy

The cysts in microcystic serous cystadenoma and macrocystic serous cystadenoma are lined by a single layer of uniform, cuboidal, epithelial cells with clear cytoplasm (due to abundant glycogen) and central round/oval hyperchromatic nuclei with inconspicuous nucleoli (Fig. 15.7a). Occasionally, the cytoplasm may be eosinophilic and granular. The neoplastic cells may be flattened and attenuated with little visible cytoplasm or may form intracystic microscopic papillae (Fig. 15.8a), occasionally with fibrovascular cores (Fig. 15.8b). These papillae are of no clinical significance. There may be occa-

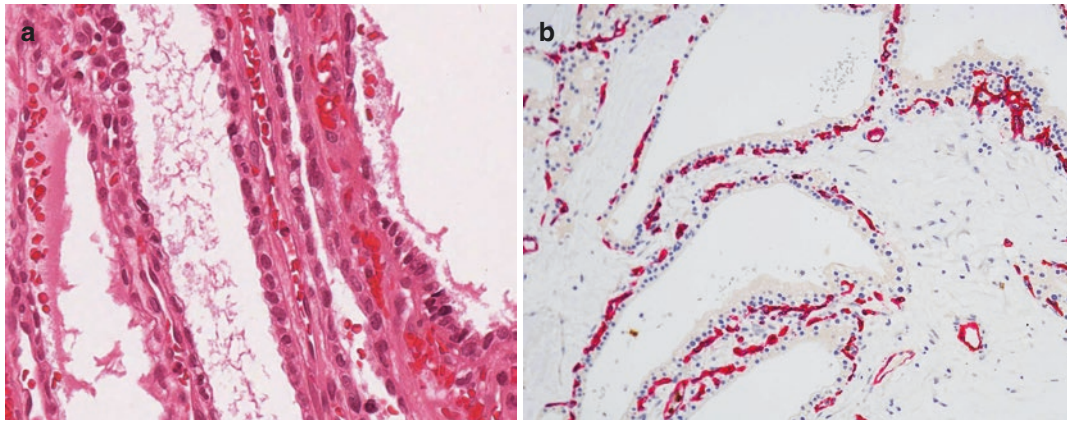

Fig. 15.7 Microcystic serous cystadenoma: the cysts are lined by cuboidal epithelial cells with clear cytoplasm and small, round, hyperchromatic nuclei (**a**). Prominent small capillary-sized vessels are present beneath the epithelium, which are highlighted on CD34 immunohistochemistry (**b**)

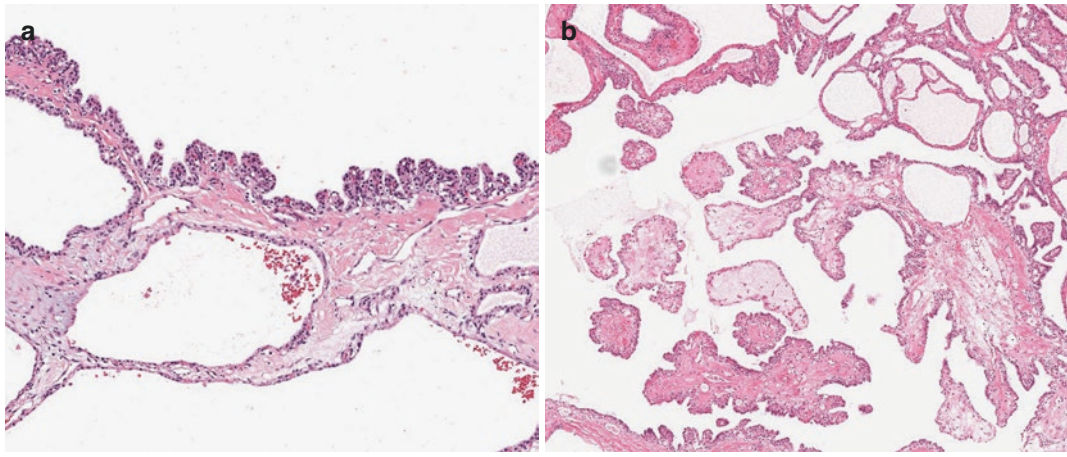

Fig. 15.8 Microcystic serous cystadenoma: there may be intracystic micropapillae (**a**) or larger papillae with fibrovascular cores (**b**). These are of no clinical significance

sional larger nuclei, but mitotic figures, nuclear pleomorphism, and necrosis are not found. There is a prominent network of small capillary-sized vessels immediately beneath the epithelium in microcystic serous cystadenoma (Fig. 15.7b) and macrocystic serous cystadenoma, which can be visualized in the latter, preoperatively, using endoscopic ultrasound-guided needle-based confocal laser endomicroscopy [4].

The central scar and radiating septa in microcystic serous cystadenoma are composed of hyalinized collagen, which can be calcified (Fig. 15.9), and may contain entrapped nerves, lymphocytic aggregates, acinar tissue, ducts, and islets (Fig. 15.10). Amyloid has also been described within the stroma [5]. There may be tiny cysts within the central scar and focal degenerative changes including cholesterol clefts, foreign-body-type giant cells, hemosiderin, inflammation, and calcification (Fig. 15.11).

Serous cystic neoplasms often show irregular extension into the adjacent pancreas, which may show atrophic changes.

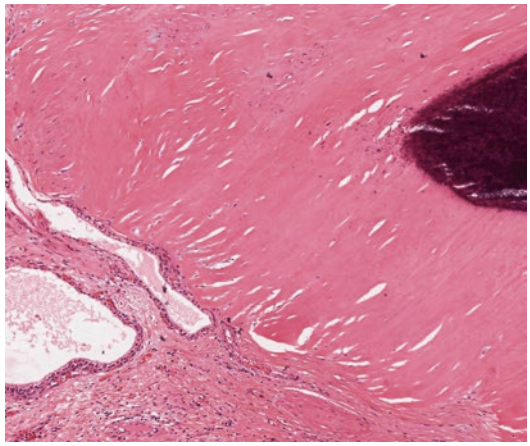

Fig. 15.9 Microcystic serous cystadenoma: the central scar is composed of sclerotic collagen which may be calcified, as seen here (*right* of picture)

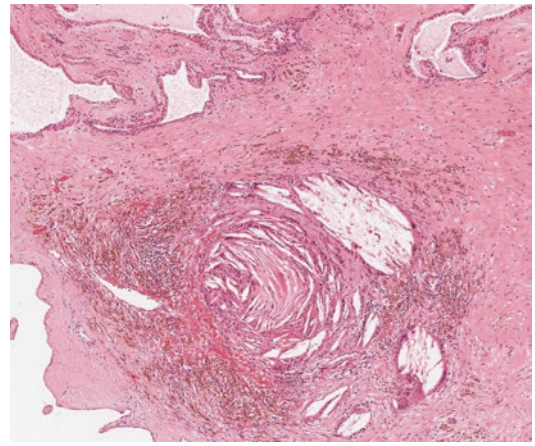

Fig. 15.11 Microcystic serous cystadenoma: there may be focal degeneration with hemosiderin-laden macrophages and foreign body-type giant cells surrounding cholesterol clefts

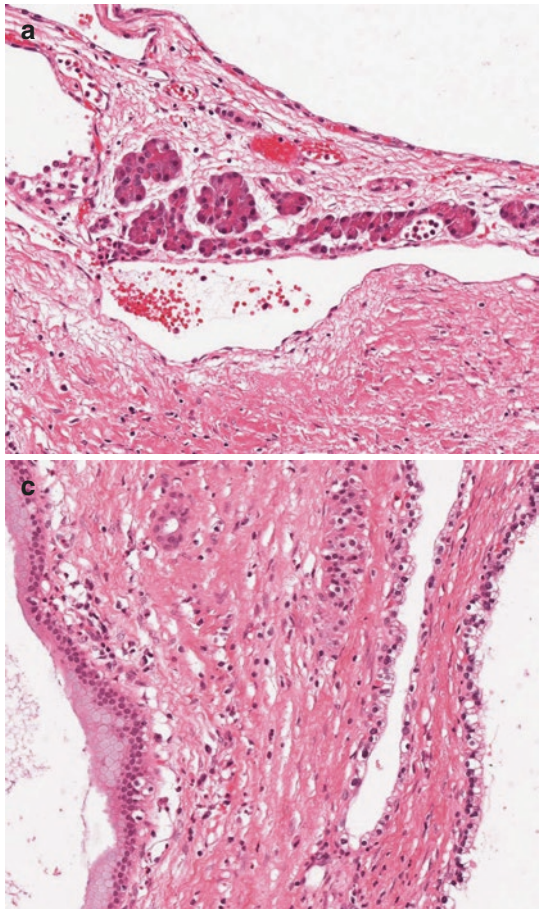

Fig. 15.10 Microcystic serous cystadenoma: there may be entrapped acini and islet cells (**a**) or ducts within the fibrous tissue. This entrapped duct shows low-grade PanIN (**b**). The tall mucinous epithelium of low-grade PanIN (*left* of picture) is readily distinguished from the clear cuboidal cells of the serous cystadenoma (**c**)

15.8 Histochemistry

Periodic acid Schiff (PAS) stains the abundant glycogen within the cytoplasm. Stains for mucin (PAS-diastase, mucicarmine, and alcian blue) are negative.

15.9 Immunohistochemistry

Serous cystic neoplasms express epithelial markers AE1-AE3, CAM5.2, EMA, CK7, CK8, CK18, and CK19. There may also be expression of MUC1, MUC6, alpha-inhibin, CAIX, and NSE. Beta-catenin immunohistochemistry shows normal membranous staining. Ki67 proliferative index is very low.

Serous cystic neoplasms are usually immunonegative for CEA, MUC2, MUC5AC, CK20, chromogranin A, synaptophysin, vimentin, and pancreatic hormones.

Immunohistochemistry is not usually needed to make the diagnosis of a serous cystic neoplasm, but may be helpful in diagnosing a macrocystic serous neoplasm when the epithelium is scanty and/or attenuated. Similarly, immunohistochemistry may be useful to confirm the diagnosis of a solid serous adenoma (see Sect. 15.11.1) and exclude other differential diagnoses, such as metastatic renal cell carcinoma (see Sect. 15.12).

15.10 Molecular Pathology

Loss of heterozygosity or (loss of function) mutations of the *VHL* tumor suppressor gene can be found in most sporadic serous neoplasms, and in all von Hippel-Lindau syndrome-associated serous neoplasms. These genomic alterations can be detected in pancreatic cyst fluid, which may aid preoperative diagnosis [6].

15.11 Rare Variants

15.11.1 Solid Serous Adenoma

This rare variant was first described in 1996 [7] and lacks the macroscopic cysts of the microcystic and macrocystic variants. The neoplasm is well-circumscribed, solid, pale, and typically small (2–4 cm in size). It may be admixed with a typical cystic serous neoplasm (Fig. 15.12). On microscopy, the neoplasm is composed of lobules of closely-packed clear epithelial cells, arranged in nests, sheets, and small acini with small central lumina, separated by collagenous stroma (Fig. 15.13). The cells are identical to those seen in serous cystadenomas. The delicate capillary network seen beneath the epithelium of the serous cystadenomas (see Sect. 15.7) is also present in solid serous adenoma (Figs. 15.13c, d). This combination of clear cells (arranged in nests or acini) and intervening vascular network can mimic a clear cell variant of pancreatic neuroendocrine tumor (see Sect. 15.12.3) or metastatic renal cell carcinoma (see Sect. 15.12.1).

15.11.2 von Hippel-Lindau Syndrome-Associated Serous Cystic Neoplasm

Serous cystic neoplasms are the most common pancreatic lesions found in patients with the rare autosomal dominant disorder von Hippel-Lindau (VHL) syndrome. These patients develop serous cystic neoplasms of the pancreas at a younger age (mean 32 years) than those patients with

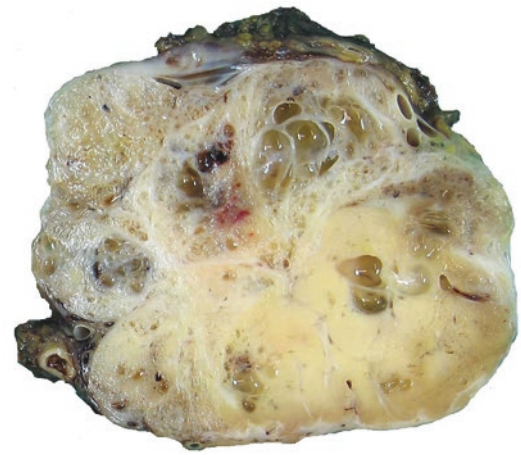

Fig. 15.12 Combined microcystic serous cystadenoma and solid serous adenoma: solid serous adenoma may be entirely solid, but in this example there was typical microcystic serous cystadenoma (*uppermost*) and solid serous adenoma in the same lesion

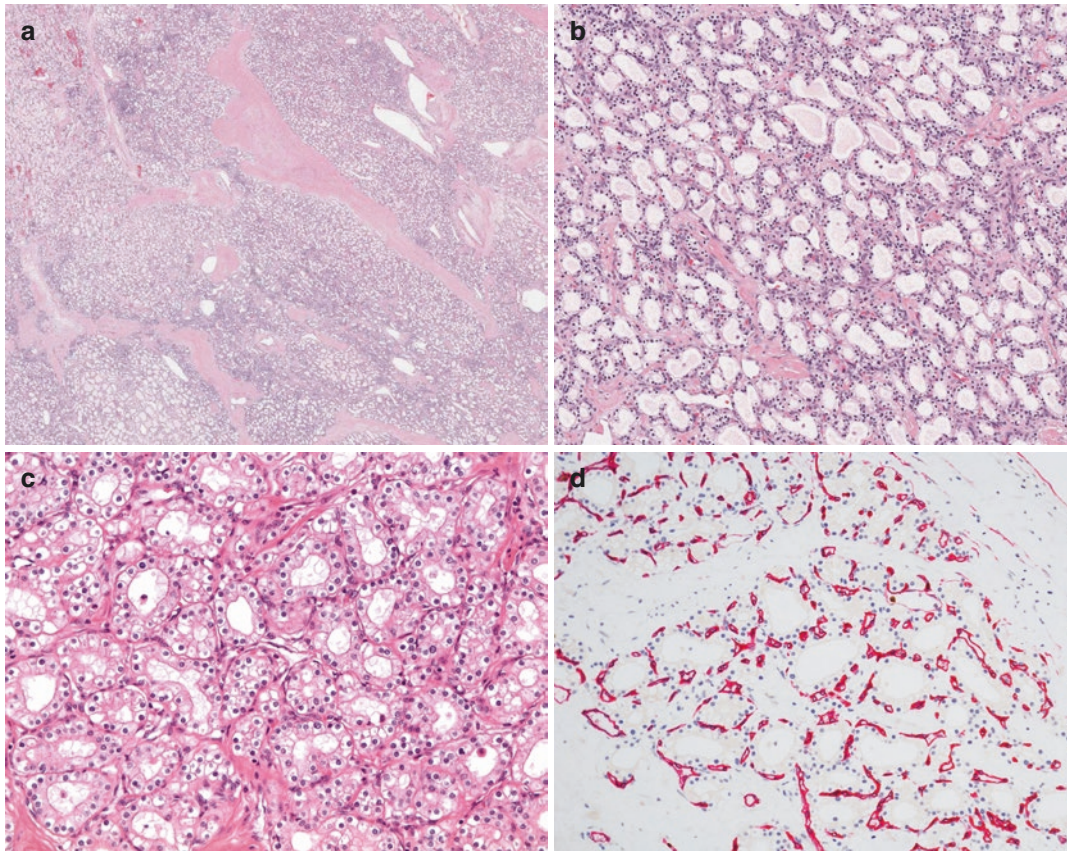

Fig. 15.13 Solid serous adenoma: there is a solid lobulated architecture with fibrous bands (**a**) between closely packed small acini of clear cuboidal cells, which are identical to those seen in serous cystadenomas (**b**). At higher power, small capillary-sized vessels can be seen between the acini of cuboidal cells (**c**), and are highlighted on CD34 immunohistochemistry (**d**)

nonsyndromic serous cystic neoplasms (mean age 50–60 years). The serous cystic neoplasms are usually multiple, macrocystic, and typically involve the whole pancreas diffusely (Fig. 15.14) or in a patchy fashion. VHL patients may also develop pancreatic endocrine neoplasms and mixed serous-neuroendocrine neoplasm of the pancreas, typically composed of a grade 1–3, clear cell, pancreatic neuroendocrine tumor (PanNET) with a serous cystadenoma (see Sect. 15.11.5).

Pancreatic cysts may be the first presentation of VHL syndrome and, therefore, when multiple pancreatic serous cystic neoplasms or a mixed serous-neuroendocrine neoplasm are diagnosed, the possibility of VHL syndrome should be raised.

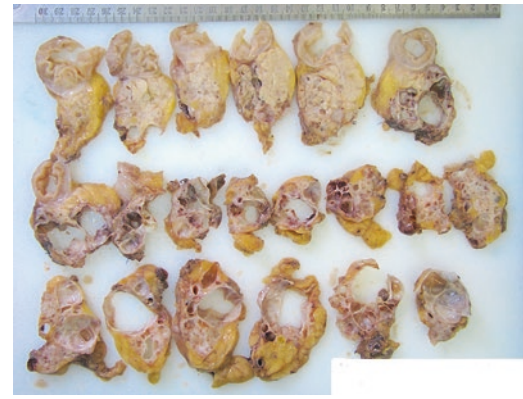

Fig. 15.14 von Hippel-Lindau syndrome: there is diffuse involvement of the pancreas by serous cystic neoplasia

15.11.3 Microcystic Serous Cystadenoma with Subtotal Cystic Degeneration

Microcystic serous cystadenoma with subtotal cystic degeneration has been described [8]. Extensive degeneration within a microcystic serous neoplasm may result in a unilocular or multilocular cystic lesion, which radiologically, macroscopically, and microscopically can mimic a pseudocyst. Multilocular cases retain focal macroscopic features of a microcystic serous cystadenoma, but these gross features are not present in the unilocular examples. The neoplasm has a well-defined border and the adjacent pancreas may be normal or show peritumoral fibrosis.

Microscopically, much of the epithelial lining is denuded and the cyst wall is fibrotic with associated chronic inflammation, foamy macrophages, cholesterol clefts, reactive myofibroblasts, hemorrhage, and hemosiderin, resembling the wall of a pseudocyst. Foci of residual epithelium are found embedded within the fibrotic wall, forming small solid nests or submillimeter-sized cysts, which are surrounded by a dense network of small capillary-sized vessels. The epithelium is identical to that seen in all serous cystic neoplasms, but may be attenuated with minimal cytoplasm.

This entity differs from a macrocystic serous cystadenoma, which is composed of thin-walled cysts lined by a continuous layer of epithelium. Although the epithelium may be denuded in a macrocystic serous cystadenoma, it is not accompanied by the pseudocyst-like degenerative changes in the wall. Macrocystic serous cystadenomas are inherently macrocystic and not the result of degenerative change.

15.11.4 Serous Cystic Neoplasm with Complex Florid Papillary Architecture

There is a recent single case report of a serous cystic neoplasm with a peripheral solid nodule, which was composed of a back-to-back arrangement of complex branching papillae (lined by bland, clear, cuboidal, inhibin-immunopositive epithelium) with prominent fibrovascular cores and intervening delicate sieve-like channels [9]. The solid component was mistaken for a neuroendocrine tumor on imaging, and the microscopic florid papillary growth pattern distinguished it from a solid serous adenoma.

15.11.5 Mixed Serous-Neuroendocrine Neoplasm

Very occasionally, serous cystic neoplasms may be associated with a grade 1–3 pancreatic neuroendocrine tumor (PanNET), which may occur either adjacent to the cystic neoplasm or admixed with it. This association is seen most commonly in von Hippel-Lindau syndrome, where the pancreatic endocrine neoplasm is often of clear cell type (see Chap. 20, Sect. 20.12). However, not all patients with a mixed serous-neuroendocrine neoplasm have a genetic syndrome [10].

15.11.6 Serous Cystadenocarcinoma

There are extremely rare reports (approximately 25 in total) of serous cystadenocarcinoma, which was diagnosed on the basis of synchronous or metachronous distant metastases to the liver, peritoneum or (non-peripancreatic) lymph nodes. The morphology of the pancreatic primary and the metastases was similar to that seen in benign serous cystic neoplasms. Hence, clinical behavior appears to be the only way to distinguish serous cystadenomas from serous cystadenocarcinoma. However, it should be noted that primary serous cystadenomas can occur in the liver, albeit rarely [11], and, therefore, liver involvement may represent multifocal disease rather than metastatic malignancy [12].

Locally aggressive growth (such as vascular invasion, perineural invasion, or direct invasion into lymph nodes, spleen, duodenum—Fig. 15.4—or stomach) in a serous cystadenoma does not warrant a diagnosis of malignancy.

15.12 Differential Diagnosis

15.12.1 Metastatic Renal Cell Carcinoma

Metastatic renal cell carcinoma (see Chap. 12, Sect. 12.5 and Table 12.1) may mimic a microcystic serous cystadenoma or a solid serous adenoma. Renal cell carcinoma usually shows nuclear pleomorphism, prominent nucleoli, and mitotic figures, none of which occur in serous neoplasms. Clinical history and immunohistochemistry for vimentin, CD10, renal cell carcinoma marker, and PAX-8 will confirm the diagnosis of renal cell carcinoma (Table 15.1).

15.12.2 Lymphangioma

Lymphangioma (see Chap. 11, Sect. 11.1.7) may be confused with a serous cystic neoplasm, particularly when the epithelial lining is attenuated or denuded in a macrocystic serous cystadenoma. Both entities may contain watery serous fluid. However, lymphangiomas typically have lymphoid aggregates in the cyst wall, do not have a cuboidal epithelial lining and, on immunohistochemistry, express CD31 and D2–40, but not epithelial markers.

Table 15.1 Differential diagnosis of pancreatic clear cell tumors

	PanNET	Metastatic RCC	SCN
Synaptophysin/ chromogranin	++	–	–
NSE/CD56	++	+	++
RCC	–	+/–	–
Vimentin	–	++	–
CAIX	–	++	+
CD10	+	+	–
PAX8	–	++	–

Abbreviations: *PanNET* pancreatic neuroendocrine tumor, *RCC* renal cell carcinoma, *SCN* serous cystic neoplasm
++ usually positive, + may be positive, – usually negative

15.12.3 Clear Cell Pancreatic Neuroendocrine Neoplasm

Clear cell variant of pancreatic neuroendocrine tumors (PanNETs) may mimic a solid serous adenoma macroscopically and microscopically. As discussed above (see Sects. 15.4.1 and 15.11.2), clear cell PanNETs may also coexist with a serous cystic neoplasm, particularly in von Hippel-Lindau syndrome. PanNETs can readily be distinguished from serous cystic neoplasms by immunohistochemistry for chromogranin A and synaptophysin (see Chap. 20, Sect. 20.9.1).

15.12.4 Pseudocyst

Macrocystic serous cystadenoma may be mistaken for a pseudocyst (see Chap. 7, Sect. 7.2.5), particularly when much of the epithelium is denuded. Extensive sampling should reveal residual, cuboidal, clear epithelial cells lining the cysts or entrapped within the wall of the macrocystic serous cystadenoma.

15.12.5 Mucinous Cystic Neoplasm

Mucinous cystic neoplasm (MCN) may mimic a macrocystic serous cystadenoma but MCN typically contains thick mucus, has a thick fibrous capsule, is lined by mucin-producing columnar cells, and has ovarian-type stroma (see Chap. 16). Mucin histochemistry will stain the epithelial lining of a MCN but not a serous cystadenoma. MCNs will also be immunopositive for CEA in contrast to serous cystadenomas, which are negative for CEA.

15.12.6 Intraductal Papillary Mucinous Neoplasm

Branch-duct-type intraductal papillary mucinous neoplasm (Fig. 15.15) may mimic a serous cystadenoma (see Chap. 17). However, intraductal

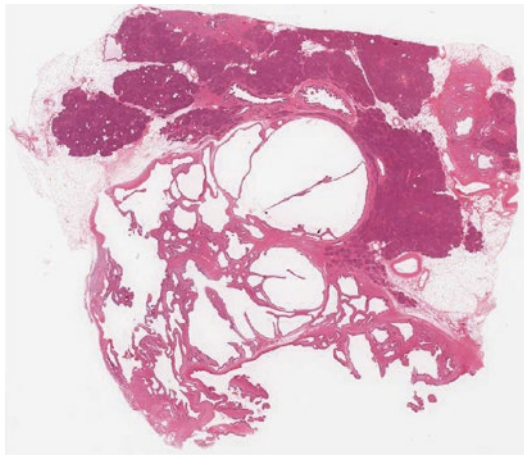

Fig. 15.15 Branch-duct intraductal papillary mucinous neoplasm (IPMN): this small peripheral multilocular cyst was thought to be a serous cystadenoma on macroscopic examination. Microscopy, however, revealed it to be a branch-duct-type IPMN

papillary mucinous neoplasm communicates with the duct system, is lined by papillary mucinous epithelium, and expresses CEA, unlike serous cystadenomas.

15.12.7 PEComa (see Chap. 11, Sect. 11.1.9)

PEComa (perivascular epithelioid cell neoplasm) can occur very rarely in the pancreas and may mimic solid serous adenoma. However, the clear cytoplasm in PEComas is negative for cytokeratins and positive for HMB45, Melan-A, CD31, and smooth muscle actin on immunohistochemistry.

15.13 Prognosis and Management

The prognosis for serous cystic neoplasms is excellent. Most appear to be slow growing and can be followed up clinically. Surgical resection is considered for symptomatic serous cystic neoplasms, for rapidly growing neoplasms, and when it is not possible to definitely exclude a premalignant or malignant cystic tumor such as a mucinous neoplasm [13]. Complete resection (including enucleation) is curative, with less than 2% recurring.

Table 15.2 Reporting checklist for serous cystic neoplasms

Macroscopic assessment
• Specimen type
• Additional resected structures, e.g., spleen
• Tumor location
• Solitary or multifocal (latter suggests von Hippel-Lindau syndrome)
• Tumor size (3-dimensions)
• Cut-surface
• Distance from resection margin(s)
Microscopic assessment
• Microcystic, macrocystic, or solid
• Presence of coexisting pancreatic endocrine neoplasm (suggests von Hippel-Lindau syndrome)
• Extension into adjacent organs or structures (does not equate with malignancy)
• Completeness of excision/resection margin status
• Immunohistochemical profile (if performed)
• Background changes

15.14 Reporting Checklist

A list of macroscopic and microscopic features to consider when reporting a serous cystic neoplasm is shown in Table 15.2.

References

1. Lokuhetty D, White VA, Watanabe R, Cree IA, editors. Digestive system tumours, WHO classification of tumours. 5th ed. Lyon: IARC Press; 2019. p. 296.
2. Khashab MA, Shin EJ, Amateau S, Canto MI, Hruban RH, Fishman EK, et al. Tumor size and location correlate with behavior of pancreatic serous cystic neoplasms. Am J Gastroenterol. 2011;106:1521–6.
3. Hashimoto M, Watanabe G, Miura Y, Matsuda M, Takeuchi K, Mori M. Macrocystic type of serous cystadenoma with a communication between the cyst and pancreatic duct. J Gastroenterol Hepatol. 2001;16:836–8.
4. Krishna SG, Brugge WR, Dewitt JM, Kongkam P, Napoleon B, Robles-Medranda C, et al. Needle-based confocal laser endomicroscopy for the diagnosis of pancreatic cystic lesions: an international external interobserver and intraobserver study (with videos). Gastrointest Endosc. 2017;86:644–54.
5. Tripodi SA, Civitelli S, Schurfeld K, Cintorino M. Microcystic adenoma of the pancreas (glycogen-

rich cystadenoma) with stromal amyloid deposits. Histopathology. 2000;37:147–9.
6. Singhi AD, McGrath K, Brand RE, Khalid A, Zeh HJ, Chennat JS, et al. Preoperative next-generation sequencing of pancreatic cyst fluid is highly accurate in cyst classification and detection of advanced neoplasia. Gut. 2018;67:2131–41.
7. Perez-Ordonez B, Naseem A, Lieberman PH, Klimstra DS. Solid serous adenoma of the pancreas. The solid variant of serous cystadenoma? Am J Surg Pathol. 1996;20:1401–5.
8. Panarelli NC, Park KJ, Hruban RH, Klimstra DS. Microcystic serous cystadenoma of the pancreas with subtotal cystic degeneration: another neoplastic mimic of pancreatic pseudocyst. Am J Surg Pathol. 2012;36:726–31.
9. Tracht J, Reid MD, Hissong E, Sekhar A, Sarmiento J, Krasinskas A, et al. Serous cystadenoma of the pancreas with florid papillary architecture: a case report and review of the literature. Int J Surg Pathol. 2019;27:907–11.
10. Blandamura S, Parenti A, Famengo B, Canesso A, Moschino P, Pasquali C, et al. Three cases of pancreatic serous cystadenoma and endocrine tumour. J Clin Pathol. 2007;60:278–82.
11. Devaney K, Goodman ZD, Ishak KG. Hepatobiliary cystadenoma and cystadenocarcinoma. A light microscopic and immunohistochemical study of 70 patients. Am J Surg Pathol. 1994;18:1078–91.
12. Reid MD, Choi HJ, Memis B, Krasinskas AM, Jang KT, Akkas G, et al. Serous neoplasms of the pancreas. A clinicopathological analysis of 193 cases and literature review with new insights on macrocystic and solid variants and critical reappraisal of so-called ‘serous cystadenocarcinoma’. Am J Surg Pathol. 2015;39:1597–610.
13. European Study Group on Cystic Tumours of the Pancreas. European evidence-based guidelines on pancreatic cystic neoplasms. Gut. 2018;67:789–804.

Further Reading

Singhi AD, Adsay NV, Hiraoka N, Terris B. Serous neoplasms of the pancreas. In: Lokuhetty D, White VA, Watanabe R, Cree IA, editors. Digestive system tumours, WHO classification of tumours. 5th ed. Lyon: IARC Press; 2019. p. 303–6.

Mucinous Cystic Neoplasia

16

Mucinous cystic neoplasm is a cystic, epithelial, mucin-producing neoplasm with associated ovarian-type stroma. In contrast to intraductal papillary neoplasms (see Chap. 17), mucinous cystic neoplasms do not communicate with the pancreatic ductal system. Mucinous cystic neoplasms (MCNs) are solitary and may be unilocular or multilocular. The epithelial lining is composed of tall, columnar, mucin-producing epithelium, which may be flat or papillary depending on the degree of dysplasia. MCNs are generally considered to progress from low-grade dysplasia through high-grade dysplasia to invasive carcinoma and are one of the three main precursors of pancreatic invasive carcinoma, the other two being PanIN (see Chap. 8) and intraductal papillary neoplasm (see Chap. 17).

16.1 WHO Classification

Mucinous cystic neoplasms are included in 'benign epithelial tumors and precursors' in the 2019 WHO classification of tumors of the pancreas, [1] and are classified into the following three categories:

1. Mucinous cystic neoplasm with low-grade dysplasia.
2. Mucinous cystic neoplasm with high-grade dysplasia.
3. Mucinous cystic neoplasm with associated invasive carcinoma.

16.2 Terminology

Mucinous cystic neoplasm is the currently recognized terminology for this tumor, which has been referred to previously as mucinous cystadenoma and mucinous cystadenocarcinoma (non-invasive or invasive).

16.3 Epidemiology

MCN is relatively uncommon and accounts for approximately 10% of resected pancreatic cystic lesions. They occur almost exclusively in women (female to male ratio of 20:1) with a mean age of diagnosis at 45–50 years (range 16–95 years). Patients with associated invasive carcinoma tend to be 5–10 years older than those with non-invasive MCNs. Men appear to have a higher rate of high-grade MCN and MCN with associated invasive adenocarcinoma [2].

16.4 Clinical Features

Small MCNs are usually asymptomatic and found incidentally on imaging during clinical evaluation for other conditions. Larger MCNs may

© Springer Nature Switzerland AG 2021
F. Campbell, C. S. Verbeke, *Pathology of the Pancreas*,
https://doi.org/10.1007/978-3-030-49848-1_16

produce symptoms including abdominal pain, nausea and vomiting, anorexia, and weight loss. Patients may present with a palpable abdominal mass. In contrast to intraductal papillary neoplasms (see Chap. 17), there is no related history of pancreatitis. There are case reports describing rapid growth of MCNs during pregnancy, which may be related to the hormone sensitivity of the MCN ovarian-type stroma.

16.4.1 Associations

There are no well-established environmental etiological factors, and no associations with any genetic syndromes.

16.4.2 Imaging

Computed tomography (CT), magnetic resonance imaging (MRI), or endoscopic ultrasound (EUS) will reveal a solitary, sharply demarcated, thick-walled cyst that may be unilocular or multilocular. Often there is one large cyst, within which thin-walled, daughter cysts can be seen. Calcification may be present in the wall as a rim of peripheral 'eggshell' calcification in 20% of cases. There is no communication with the duct system. Features suggestive of malignancy include large size, irregular thickening of the cyst wall, mural nodules, and/or papillary excrescences projecting into the cyst lumen.

16.5 Macroscopy

The vast majority of MCNs (>98%) occur in the body or tail of the pancreas. They form a solitary large cystic mass, mean size 6–10 cm (range 2–35 cm), with smooth outer surface (Fig. 16.1) and thick fibrous capsule (Fig. 16.2), which may be calcified (Fig. 16.3). Opening may reveal a single cyst cavity, a multilocular cyst (with cysts ranging from a few millimeters to several centimeters in diameter), or one large cyst cavity with smaller thin-walled daughter cysts arising from the inner wall (Fig. 16.4). The cysts contain thick

Fig. 16.1 Mucinous cystic neoplasm: this large tumor in the tail of the pancreas has a smooth outer surface and abuts the spleen

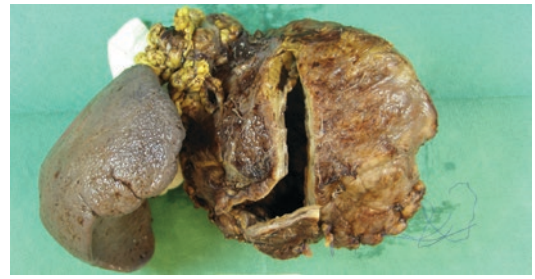

Fig. 16.2 Mucinous cystic neoplasm: the incised wall is thick and fibrotic

Fig. 16.3 Mucinous cystic neoplasm: this neoplasm has eggshell calcification throughout the wall

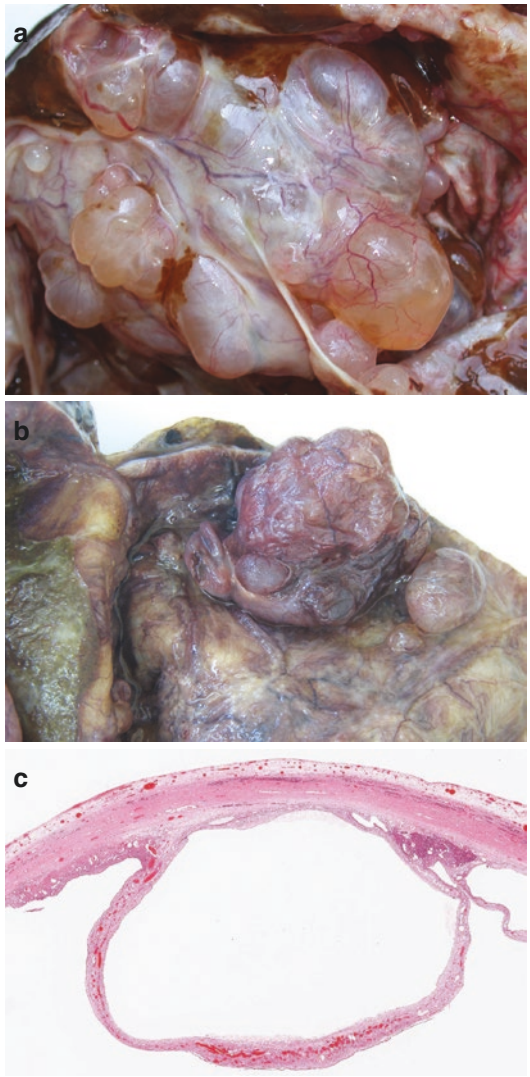

Fig. 16.4 Daughter cysts: there are smaller daughter cysts within this mucinous cystic neoplasm (**a**), which can be seen protruding from the smooth inner lining of the main cyst wall (**b**). These daughter cysts can be multilocular or unilocular (**c**)

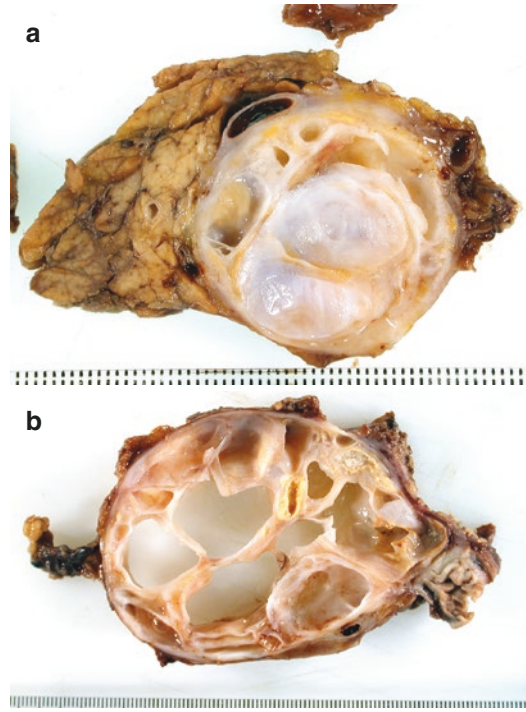

Fig. 16.5 Mucinous cystic neoplasm: cross-sections of these two tumors (**a**, **b**) show multilocular cysts with a glistening inner lining

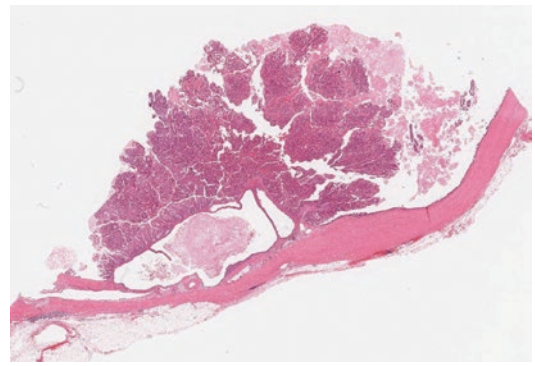

Fig. 16.6 Papillary projection: this single papillary projection, in an otherwise smooth-lined mucinous cystic neoplasm, showed low-grade and high-grade dysplasia

viscous mucin but may also contain hemorrhagic, watery fluid and necrotic debris. The inner surface of the cyst(s) is usually smooth and glistening (Fig. 16.5). When papillary projections are present, they should always be sampled because they usually represent high-grade foci (Fig. 16.6). MCNs do not communicate with the duct system, but, rarely, there may be erosion and fistula formation with the pancreatic ductal system.

MCNs with associated invasive carcinoma are usually large, multilocular cystic lesions with papillary projections, mural nodules (Fig. 16.7), or grossly visible invasion of the pancreas and adjacent structures. However, the invasive carcinoma may be very small and only detected microscopically. Lymph node metastases are rare.

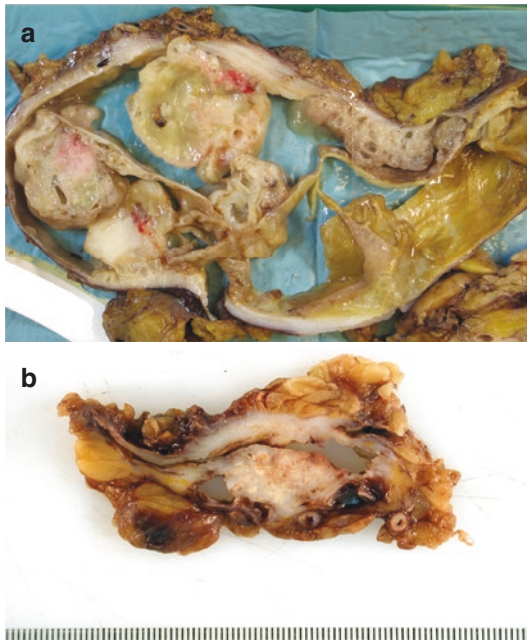

Fig. 16.7 Mural nodules: mural nodules in a mucinous cystic neoplasm should always be sampled. In both of these examples, a discrete focus of invasive carcinoma can be seen macroscopically, *lower left* (**a**) and *bottom center* (**b**)

16.5.1 Sampling

MCNs should always be sampled thoroughly to establish the diagnosis and the grade of dysplasia and to exclude invasive carcinoma. In larger lesions, much of the epithelium may be denuded (see Chap. 14, Sect. 14.2) and the capsule may be so sclerotic (Fig. 16.8) that it may be difficult to find the ovarian-type stroma to confirm the diagnosis. Papillary areas and solid areas (Figs. 16.6 and 16.7) must always be sampled because these are most likely to show high-grade dysplasia or invasive carcinoma. However, high-grade dysplasia and invasive carcinoma may be focal and not apparent macroscopically. In the absence of macroscopic invasive carcinoma, embedding the entire lesion may be considered, particularly if initial microscopic examination reveals high-grade dysplasia but no invasion.

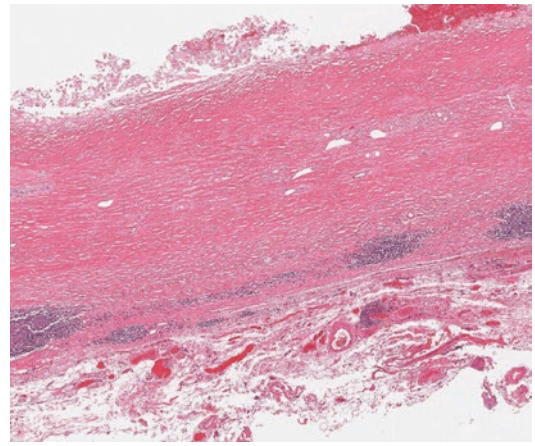

Fig. 16.8 Mucinous cystic neoplasm: the wall of this tumor is sclerotic with no evidence of epithelial lining (*uppermost*) or ovarian-type stroma

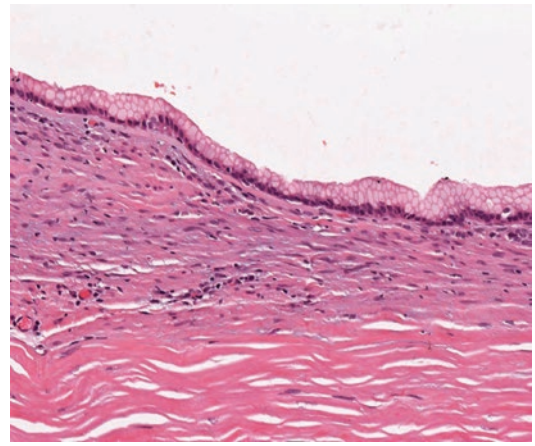

Fig. 16.9 Mucinous cystic neoplasm: this low-grade tumor is lined by tall, columnar, mucin-producing epithelial cells which resemble gastric-type epithelium

16.6 Microscopy

The cysts of MCN are lined by tall, columnar, mucin-producing epithelial cells (Fig. 16.9), which usually resemble gastric-type epithelium, but there may be intestinal differentiation with goblet cells and occasional paneth cells (Fig. 16.10). Nonmucinous, flat or cuboidal epithelium may also be present, as a minor or

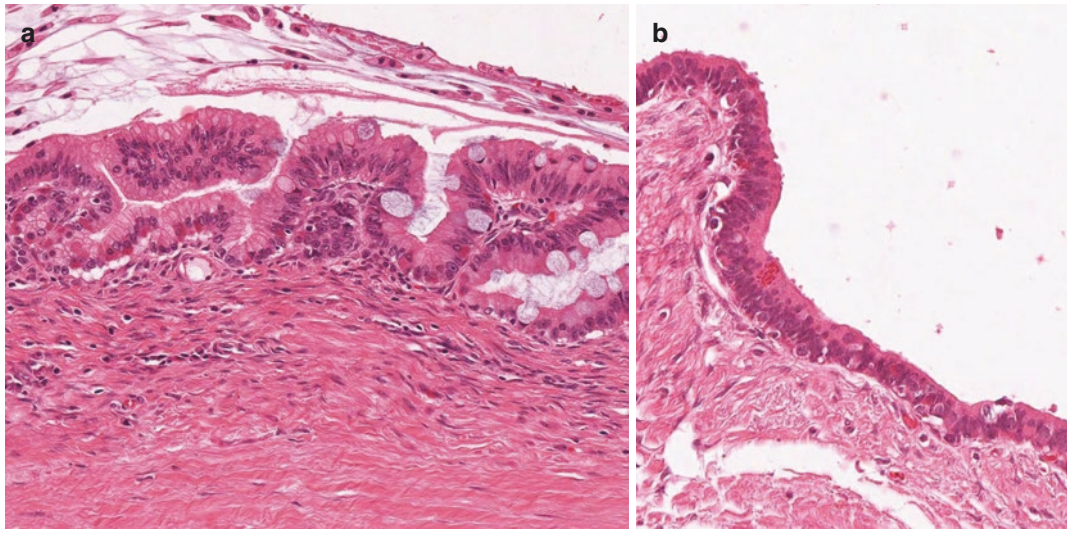

Fig. 16.10 Mucinous cystic neoplasm: there are goblet cells and prominent endocrine cells in this low-grade tumor (**a**). In another example of a low-grade tumor (**b**), there is a single paneth cell (*above center*) as well as endocrine cells

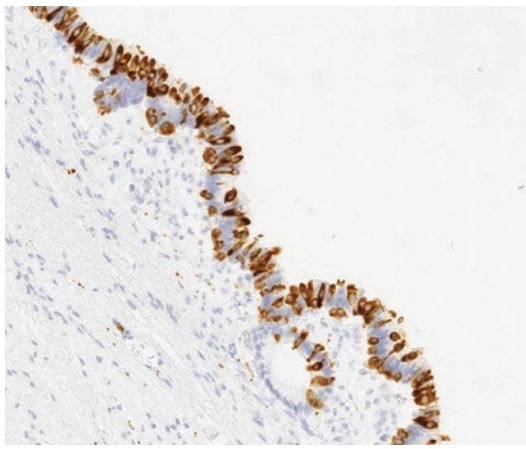

Fig. 16.11 Mucinous cystic neoplasm: synaptophysin immunohistochemistry shows abundant endocrine cells in the same tumor as shown in Fig. 16.10b

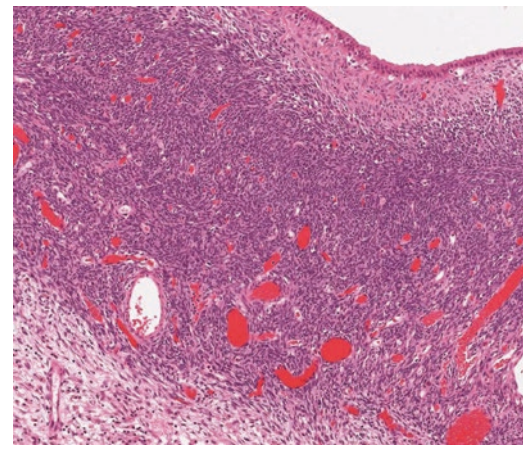

Fig. 16.12 Mucinous cystic neoplasm: typical ovarian-type stroma present as a thick subepithelial band in this tumor

major component [3], and particularly when there is marked hemorrhage and fibrosis. Very rarely, there may be squamous metaplasia [4]. Endocrine cells may be present within the epithelium and are reported to be more numerous in high-grade neoplasms (Figs. 16.10 and 16.11). In larger neoplasms, much of the lining epithelium may be denuded (Fig. 16.8) and thorough sampling is required to find it.

The ovarian-type stroma (Fig. 16.12) beneath the epithelium consists of closely packed spindle cells with round or elongated nuclei and sparse cytoplasm. There may be stromal luteinization (with epithelioid cells showing abundant clear or eosinophilic cytoplasm), but this is usually only seen in low-grade lesions. Mitotic figures are not present. There may be entrapped normal acini, islets, and ducts within the ovarian-type stroma.

The neoplastic epithelium may also invaginate into this ovarian-type stroma. In larger neoplasms, much of the stroma can become degenerate or sclerotic (Fig. 16.8) with only small foci of residual ovarian-type stroma (Fig. 16.13) or foci with the appearance of corpora albicantia.

There is usually a thick band of collagen, which may show focal calcification, between the cyst and the adjacent pancreas. The adjacent pancreas is usually fibrotic and atrophic.

The epithelium of MCNs can show different degrees of dysplasia within the same neoplasm, and there can be abrupt transition between low-grade and high-grade dysplasia. The grade of dysplasia is determined by the degree of architectural and cytological atypia, and until recently was classified as low grade, intermediate grade or high grade. Following a consensus meeting in Baltimore, it was recommended that this three-tiered grading system should be replaced by a two-tiered system [5], with the categories of low-grade dysplasia and intermediate-grade dysplasia being combined into low-grade MCN, and high-grade dysplasia remaining as high-grade MCN. This two-tiered system has been adopted into the 2019 WHO classification of tumors of the pancreas [1].

16.6.1 MCN with Low-Grade Dysplasia

MCN with low-grade dysplasia is characterized by tall columnar epithelium with small basally located nuclei (Fig. 16.14) or pseudostratified nuclei. The epithelium may be flat or have papillary projections and crypt-like invaginations (Fig. 16.15). There may be occasional mitotic figures.

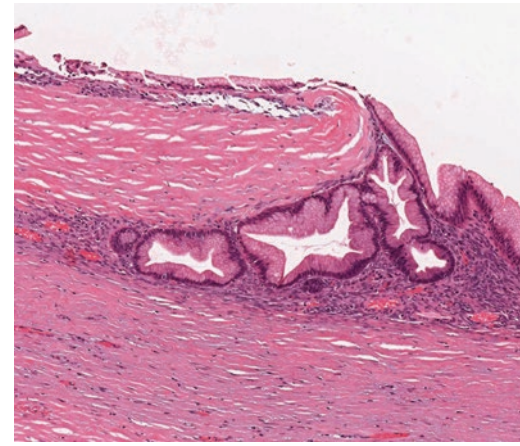

Fig. 16.14 Low-grade dysplasia: the epithelium is tall, columnar, and mucinous with basal nuclei and no atypia. Note the underlying ovarian-type stroma (*right*) and the sclerotic wall (*left*) where the epithelium is beginning to detach

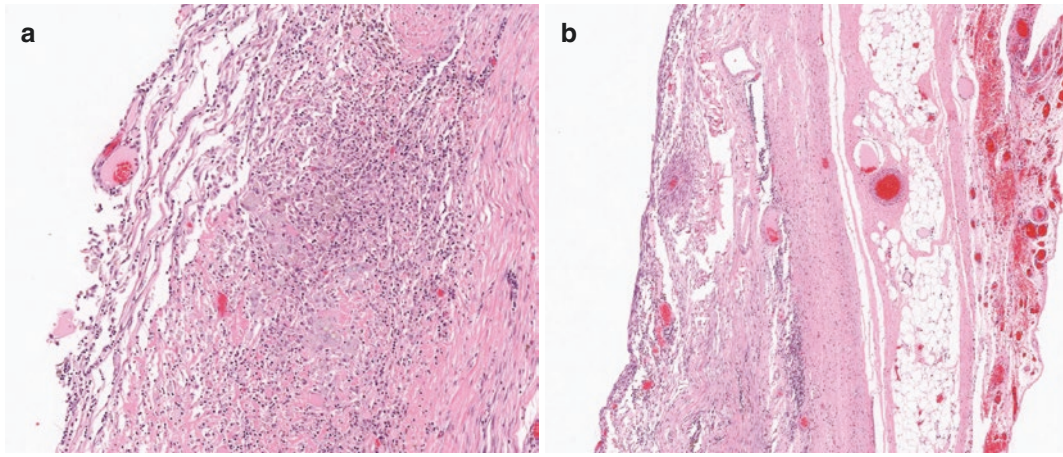

Fig. 16.13 Mucinous cystic neoplasm: there is loss of surface epithelium and a large focus of macrophages within the wall of this large degenerate tumor (**a**). There was only a single focus of residual ovarian-type stroma left in the wall (**b**), which is particularly cellular around the vessel (*center, left*)

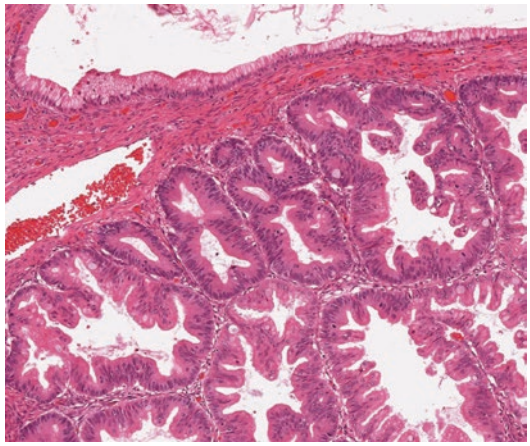

Fig. 16.15 Low-grade dysplasia: the low-grade epithelium in this case shows papillary architecture, pseudostratified elongated nuclei, and scattered mitotic figures, as well as flat columnar epithelium

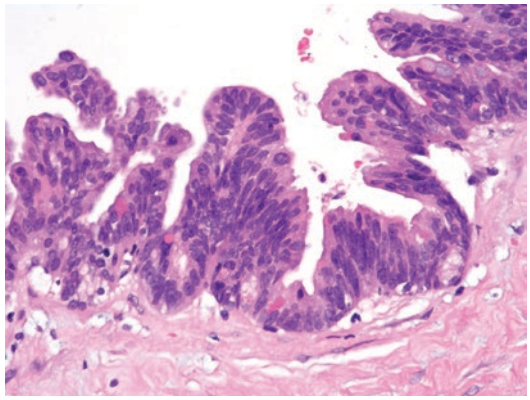

Fig. 16.16 High-grade dysplasia: there is micropapillary architecture with significant cytological atypia. There is nuclear stratification and pleomorphism, together with prominent nucleoli

16.6.2 MCN with High-Grade Dysplasia

MCN with high-grade dysplasia is characterized by significant architectural and cytological atypia with the formation of papillae with irregular branching and budding, nuclear stratification and pleomorphism, prominent nucleoli, and frequent mitotic figures, including atypical forms (Fig. 16.16).

16.6.3 MCN with Associated Invasive Carcinoma

Approximately 10–20% of MCNs have associated invasive carcinoma [6]. The carcinoma may be focal and small with limited invasion, or it may be more extensive and deeply invasive. The presence of desmoplastic stroma will distinguish invasive carcinoma from entrapped non neoplastic glands in the cyst wall. The invasive carcinoma may occur within intratumoral septa or intracystic nodules, as well as in the outermost wall of the MCN.

The invasive component usually resembles conventional pancreatic ductal adenocarcinoma (see Chap. 9, Sect. 9.6) but rare subtypes of pancreatic ductal adenocarcinoma have been described, including undifferentiated carcinoma (Fig. 16.17), undifferentiated carcinoma with

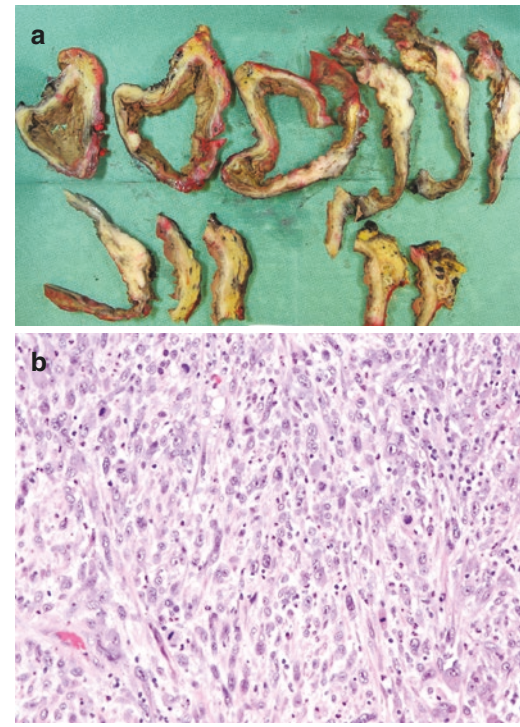

Fig. 16.17 Undifferentiated carcinoma arising in a mucinous cystic neoplasm: the solid white mural nodules in this tumor (**a**) are foci of undifferentiated carcinoma (**b**)

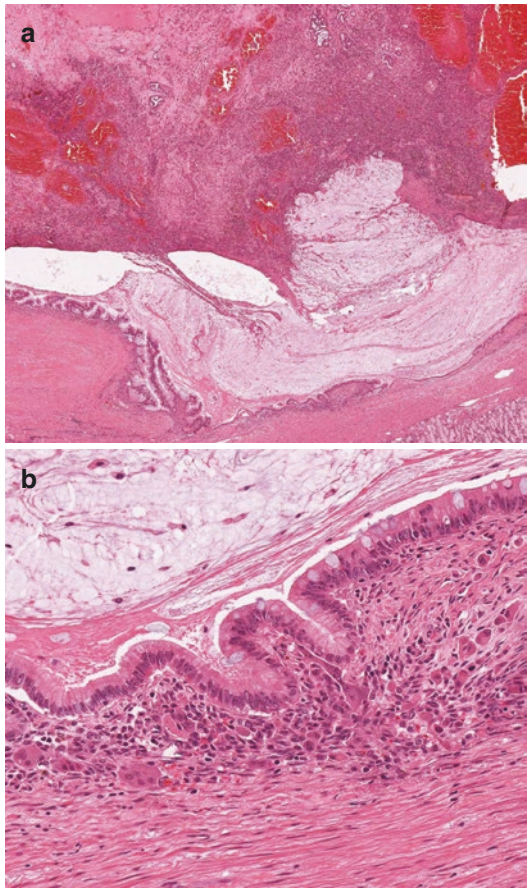

Fig. 16.18 Undifferentiated carcinoma with osteoclast-like giant cells arising in a mucinous cystic neoplasm: the low-power view shows typical mucinous cystic neoplasm *lowermost* with hemorrhagic carcinoma *uppermost* (**a**). At higher power, undifferentiated carcinoma and abundant osteoclast-like giant cells are present beneath mucinous epithelium, which contains scattered goblet cells (**b**)

osteoclast-like giant cells (Fig. 16.18), and adenosquamous carcinoma (see Chap. 9, Sect. 9.14). Invasive carcinomas arising in an MCN should be reported in the same way as a non-MCN-related invasive carcinoma (see Chap. 9, Sect. 9.11).

16.7 Immunohistochemistry

The epithelial cells express CK7, CK8, CK18, CK19, EMA, CEA, MUC5AC, and CA19-9. Scattered goblet cells express MUC2 and CDX2, while the intraepithelial endocrine cells express chromogranin A and synaptophysin (Fig. 16.11).

Ovarian-type stroma expresses vimentin, smooth muscle actin, progesterone receptor (60–90% cases) and, less frequently, ER (30%) (Fig. 16.19). It can also show immunopositivity for CD10, which is not expressed in normal ovarian stroma. Luteinized cells express alpha-inhibin and calretinin.

Immunohistochemistry is not usually needed to make the diagnosis of MCN, but progesterone receptor (PGR) may, on occasion, be helpful for confirming the presence of scanty ovarian-type stroma.

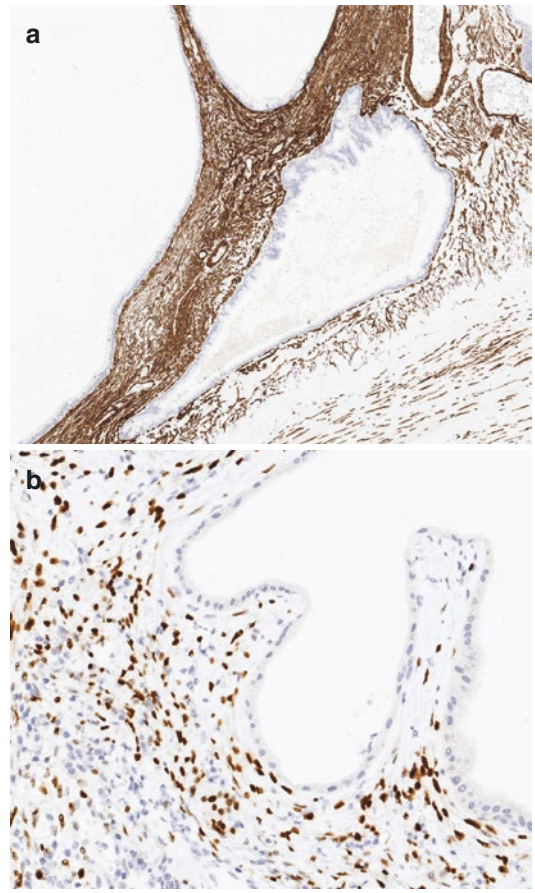

Fig. 16.19 Mucinous cystic neoplasm: the ovarian-type stroma is diffusely immunopositive with smooth muscle actin (**a**) and shows nuclear immunopositivity with progesterone receptor (**b**)

16.8 Molecular Pathology

Mutations in the *KRAS* gene can be detected in MCNs, in both the mucinous epithelium and the nonmucinous epithelium [7], and occur more frequently in high-grade tumors [8]. Mutations in the *PIK3CA* oncogene and the tumor suppressor genes *TP53*, *SMAD4*, *RNF43,* and *P16INK4A* appear to be associated with tumor progression.

16.9 Variants

16.9.1 MCN Involving the Main Pancreatic Duct

There is a single case report of MCN involving the entire main pancreatic duct [9]. This mucin-producing papillary neoplasm of the main pancreatic duct had clinical, radiological, and pathological features overlapping intraductal papillary mucinous neoplasm (see Chap. 17) and MCN. However, there was extensive ovarian-type stroma accompanying the neoplasm and, therefore, it was classed as an MCN of the main pancreatic duct.

16.9.2 MCN with Mesenchymal Overgrowth

In this rare benign tumor, the ovarian-type stroma predominates over the epithelial component, resulting in a solid tumor. There is abundant ovarian-type stroma, entrapped within which are small cysts lined by mucinous epithelium [10].

16.9.3 MCN with Sarcomatous Differentiation of the Stroma

There are case reports of sarcomatous differentiation of the stroma in MCNs characterized by hypercellular spindle cell sarcoma with numerous mitoses, including atypical forms, nuclear atypia, vascular invasion, and sarcomatous metastases [4, 11]. The accompanying epithelial component can be benign or malignant.

16.10 Differential Diagnosis

16.10.1 Intraductal Papillary Mucinous Neoplasm (IPMN) (see Chap. 17)

MCN may be confused with a branch-duct-type IPMN, but occurs almost exclusively in women, does not communicate with the duct system, is solitary, thick walled and, by definition, has ovarian-type stroma.

16.10.2 Simple Mucinous Cyst (Mucinous Nonneoplastic Cyst) (see Chap. 19, Sect. 19.2.1)

Simple mucinous cysts are benign, typically solitary, unilocular or multilocular cysts, lined by a single layer of bland, cuboidal to columnar mucinous epithelium. Beneath the epithelium, there is a thin band of paucicellular hyalinized stroma. They do not have nuclear atypia, papillae, or ovarian-type stroma.

16.10.3 Retention Cyst (see Chap. 19, Sect. 19.3.1)

Obstruction and fibrosis of a pancreatic duct may lead to cystic dilatation of the upstream ducts giving rise to so-called retention cysts. Retention cysts may be single or multiple, but are typically less than 1–2 cm in size, and are lined by pancreatobiliary-type epithelium. Occasionally, there may be low-grade PanIN within a retention cyst, with tall columnar mucinous epithelium. However, there is often a mixture of normal pancreatobiliary-type epithelium and PanIN within the same retention cyst, and ovarian-type stroma is lacking.

16.10.4 Retroperitoneal Mucinous Cystic Tumor

Primary retroperitoneal mucinous tumors are uncommon cystic neoplasms that occur almost exclusively in women, particularly those of reproductive age. They may be unilocular or multilocular, and the cysts are lined by mucin-producing epithelium and ovarian-type stroma similar to that seen in pancreatic MCNs. However, they do not involve the pancreas, which allows their distinction from pancreatic MCNs.

16.10.5 Pseudocyst or Macrocystic Serous Cystadenoma

Large MCNs may lose much of the epithelial lining and have abundant sclerotic stroma with only scanty foci of residual ovarian-type stroma. They may then be confused with a pseudocyst (see Chap. 7, Sect. 7.2.5), which lacks an epithelial lining, or a macrocystic serous cystadenoma (see Chap. 15, Sect. 15.6.2), which may also lose much of the epithelial lining.

Pseudocysts are associated with a history of pancreatitis. Macrocystic serous cystadenoma is usually a thin-walled cyst, and is lined by glycogen-rich, clear cuboidal cells. Thorough sampling of the cystic lesion may be needed to identify the defining ovarian-type stroma or the mucinous epithelium of MCN, neither of which are present in a pseudocyst or a macrocystic serous cystadenoma.

16.11 Staging

Invasive carcinoma arising with an MCN should be staged in the same way as conventional pancreatic ductal adenocarcinoma (see Chap. 9, Sect. 9.11).

16.12 Prognosis and Management

Given the risk of progression to invasive carcinoma, surgical resection is currently recommended for all surgically fit patients with an MCN [12, 13]. Surveillance, however, may be considered if the MCN is less than 4 cm in size and there are no risk factors such as a suspicious mural nodule or symptoms [13]. Complete resection of non-invasive MCNs is curative with a 5-year survival rate of 100%. Incomplete resection may lead to development of invasive carcinoma. The 5-year survival rate for resected MCN with associated invasive carcinoma is up to 60%, which is much better than for conventional, non-MCN-related pancreatic ductal adenocarcinoma. This probably reflects the earlier stage at diagnosis. Recently it has been suggested that T1a and T1b carcinomas may have a similar prognosis to non-invasive MCN [14].

Table 16.1 Reporting checklist for mucinous cystic neoplasm

Macroscopic assessment
• Specimen type
• Additional resected structures, e.g., spleen
• Tumor location
• Tumor size (3-dimensions)
• Involvement of adjacent organs
• Unilocular or multilocular tumor
• Invasive carcinoma identified or not
• Distance from resection margin(s)
Microscopic assessment
• Degree of dysplasia
• Invasive carcinoma present or not
• For invasive carcinoma:
Differentiation
Extent of invasion
Lymphatic, vascular or perineural invasion
Metastases
UICC TNM staging
• Completeness of excision/resection margin status
• Background changes

16.13 Reporting Checklist

A list of macroscopic and microscopic features to consider when reporting a mucinous cystic neoplasm is shown in Table 16.1.

References

1. Lokuhetty D, White VA, Watanabe R, Cree IA, editors. Digestive system tumours, WHO classification of tumours. 5th ed. Lyon: IARC Press; 2019. p. 296.
2. Ethun CG, Postlewait LM, McInnis MR, Merchant N, Parikh A, Idrees K, et al. The diagnosis of pancreatic

mucinous cystic neoplasm and associated adenocarcinoma in males: an 8-institution study of 349 patients over 15 years. J Surg Oncol. 2017;115:784–7.
3. Zhelnin K, Xue Y, Quigley B, Reid MD, Choi H, Memis B, et al. Nonmucinous biliary epithelium is a frequent finding and is often the predominant epithelial type in mucinous cystic neoplasms of the pancreas and liver. Am J Surg Pathol. 2017;41:116–20.
4. Thompson L, Becker R, Przygodzki R, Adair C, Heffess CS. Mucinous cystic neoplasm (mucinous cystadenocarcinoma of low-grade malignant potential) of the pancreas: a clinicopathologic study of 130 cases. Am J Surg Pathol. 1999;23:1–16.
5. Basturk O, Hong SM, Wood LD, Adsay NV, Albores-Saavedra J, Biankin AV, et al. A revised classification system and recommendations from the Baltimore consensus meeting for neoplastic precursor lesions in the pancreas. Am J Surg Pathol. 2015;39:1730–41.
6. Postlewait LM, Ethun CG, McInnis MR, Merchant N, Parikh A, Idrees K, et al. Association of preoperative risk factors with malignancy in pancreatic mucinous cystic neoplasms: a multicenter study. JAMA Surg. 2017;152:19–25.
7. An S, Kim MJ, Kim SJ, Sung YN, Kim YW, Song KB, et al. Multiple KRAS mutations in the non-mucinous epithelial lining in the majority of mucinous cystic neoplasms of the pancreas. Histopathology. 2019;75:559–67.
8. Connor JR, Marino-Enriquez A, Mino-Kenudson M, Garcia E, Pitman MB, Sholl LM, et al. Genomic characterization of low- and high-grade pancreatic mucinous cystic neoplasms reveals recurrent KRAS alterations in high-risk lesions. Pancreas. 2017;46:665–71.
9. Masia R, Mino-Kenudson M, Warshaw AL, Pitman MB, Misdraji J. Pancreatic mucinous cystic neoplasm of the main pancreatic duct. Arch Pathol Lab Med. 2011;135:264–7.
10. Handra-Luca A, Couvelard A, Sauvanet A, Flejou JF, Degott C. Mucinous cystadenoma with mesenchymal overgrowth: a new variant among pancreatic mucinous cystadenomas? Virchows Arch. 2004;445:203–5.
11. Wenig BM, Albores-Saavedra J, Buetow PC, Heffess CS. Pancreatic mucinous cystic neoplasm with sarcomatous stroma: a report of three cases. Am J Surg Pathol. 1997;21:70–80.
12. Tanaka M, Fernández-Del Castillo C, Adsay V, Chari S, Falconi M, Jang JY, et al. International consensus guidelines 2012 for the management of IPMN and MCN of the pancreas. Pancreatology. 2012;12:183–97.
13. The European Study Group on Cystic Tumors of the Pancreas. European evidence-based guidelines on pancreatic cystic neoplasms. Gut. 2018;67:789–804.
14. Hui L, Rashid A, Foo WC, Katz MH, Chatterjee D, Wang H, et al. Significance of T1a and T1b carcinoma arising in mucinous cystic neoplasm of pancreas. Am J Surg Pathol. 2018;42:578–86.

Further Reading

Basturk O, Esposito I, Fukushima N, Furukawa T, Hong SM, Klöppel G, et al. Pancreatic mucinous cystic neoplasm. In: Lokuhetty D, White VA, Watanabe R, Cree IA, editors. Digestive system tumours, WHO classification of tumours. 5th ed. Lyon: IARC Press; 2019. p. 319–21.

Check for updates

17 Intraductal Papillary Neoplasia

Intraductal papillary neoplasms include intraductal papillary mucinous neoplasm (IPMN), intraductal oncocytic papillary neoplasm (IOPN), and intraductal tubulopapillary neoplasm (ITPN). These are all characterized by intraductal proliferation of neoplastic ductal cells, dilatation of the pancreatic ducts, and clinically detectable, macroscopic (cystic or mass) lesions. All may give rise to invasive carcinoma. Other types of (non-ductal) neoplasm may occasionally grow into the ductal system, and these will also be briefly mentioned in this chapter.

17.1 WHO Classification

IPMNs, IOPNs, and ITPNs are included as 'precursor' epithelial tumors in the 2019 WHO classification of tumors of the pancreas [1], and are classified into the following categories:

- Intraductal papillary mucinous neoplasm (IPMN) with low-grade dysplasia.
- Intraductal papillary mucinous neoplasm (IPMN) with high-grade dysplasia.
- Intraductal papillary mucinous neoplasm (IPMN) with associated invasive carcinoma.
- Intraductal oncocytic papillary neoplasm (IOPN).
- Intraductal oncocytic papillary neoplasm (IOPN) with associated invasive carcinoma.
- Intraductal tubulopapillary neoplasm (ITPN).
- Intraductal tubulopapillary neoplasm (ITPN) with associated invasive carcinoma.

17.2 Intraductal Papillary Mucinous Neoplasm (IPMN)

Intraductal papillary mucinous neoplasm (IPMN) is defined as a grossly and radiologically visible, mucin-producing, predominantly papillary or rarely flat, epithelial neoplasm arising from the main pancreatic duct and/or branch ducts, and causing duct dilatation [2]. The degree of mucin production, papillary proliferation, and duct dilatation may vary considerably between tumors.

IPMN, together with IOPN and ITPN, pancreatic intraepithelial neoplasia (PanIN—see Chap. 8), and mucinous cystic neoplasm (see Chap. 16) are the main precursors of pancreatic invasive carcinoma.

17.2.1 Terminology

Intraductal papillary mucinous neoplasm is the currently recognized terminology for this tumor, which has been referred to previously as papillary adenoma, mucinous-producing tumor, mucinous duct ectasia, and duct-ectatic mucinous cystadenoma.

© Springer Nature Switzerland AG 2021
F. Campbell, C. S. Verbeke, *Pathology of the Pancreas*,
https://doi.org/10.1007/978-3-030-49848-1_17

17.2.2 Epidemiology

IPMN is the most common type of neoplastic cystic lesion of the pancreas, accounting for at least 20% of all resected cystic neoplasms of the pancreas. The incidence continues to rise, with increasing numbers of small IPMNs being detected on imaging. They are more common in the elderly, with a mean age of 65 years (range 25–94 years), and occur slightly more frequently in males. Patients with associated invasive carcinoma tend to be 3–5 years older than those with non-invasive IPMNs.

17.2.3 Clinical Features

Branch-duct IPMNs are usually asymptomatic and found incidentally on imaging during clinical evaluation for other conditions. Main-duct IPMNs are often symptomatic due to intermittent duct obstruction by the abundant mucin secreted by the neoplasm. The main clinical symptoms include abdominal and back pain, anorexia, weight loss, nausea, and vomiting. Jaundice appears to be more common in patients with associated invasive carcinoma.

IPMN is not uncommonly misdiagnosed as chronic pancreatitis because of its similar clinical presentation with recurrent pancreatitis, steatorrhea, and jaundice, as well as the radiological findings of cystic lesions that may be confused with pseudocysts.

17.2.3.1 Associations

There are no well-established environmental etiological factors. However, IPMNs have been reported in patients with Peutz-Jeghers syndrome, familial adenomatous polyposis and familial pancreatic cancer (see Chap. 6, Sects. 6.4 and 6.5). Three families with a familial form of IPMN have also been described [3]. An association between IPMN and pancreatic endocrine neoplasms has been suggested, but this is probably fortuitous.

Synchronous and metachronous extrapancreatic malignancies occur in 10–40% of patients with IPMN, but the incidence of extrapancreatic neoplasms in patients with IPMN does not appear to differ from that of the general population. These malignancies may be diagnosed before or after resection of an IPMN. The frequency and location of extrapancreatic malignancies differ from country to country. This is probably related to the incidences of the different cancers in the general populations in the different countries [4].

17.2.3.2 Imaging

IPMNs may be detected by computed tomography (CT), endoscopic retrograde cholangiopancreatography (ERCP), magnetic resonance imaging (MRI), magnetic resonance cholangiopancreatography (MRCP), or endoscopic ultrasound scan (EUS) as a cystic lesion communicating with the pancreatic duct system or dilated pancreatic ducts filled with mucus. These imaging modalities will reveal a segmentally or diffusely dilated main pancreatic duct or grape-like, cystically dilated branch duct(s), or a combination of the two, so-called mixed-type IPMNs. EUS may detect mucin oozing from the ampulla of Vater or occasionally the minor papilla (Fig. 17.1), and can be used to sample cyst fluid contents by FNA (see Chap. 24). Imaging may also detect irregular thickening of cystic septa or solid mural nodules that are recognized predictors of associated invasive carcinoma. The newly emerging technique endoscopic ultrasound-guided needle-based confocal laser endomicroscopy can also be used to identify intraductal

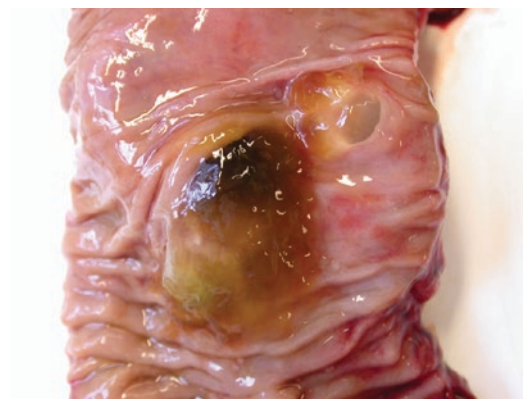

Fig. 17.1 Intraductal papillary mucinous neoplasm (IPMN): mucin oozes from both the major (*lower*) and minor (*upper*) papillae in this main-duct-type IPMN

papillary neoplasms on preoperative evaluation of pancreatic cystic lesions, by visualizing the intracystic papillae characteristic of IPMN [5].

17.2.4 Classification

IPMNs can be classified according to their site of duct involvement, their epithelial subtype, and their grade of dysplasia. All three methods of classification may be used to predict the risk of malignancy in an IPMN, but they are interrelated. IPMNs with associated invasive carcinoma can be classified on the basis of the type of invasive carcinoma (ductal/tubular or colloid).

17.2.4.1 Site of Duct Involvement

IPMNs may involve the main pancreatic duct of Wirsung or Santorini (referred to as main-duct type), branch ducts (branch-duct type), or a combination of the two (combined or mixed-type). Correlation between duct location on radiology and pathology is only about 70% [6]. On radiology, the vast majority of patients have either branch-duct or main-duct IPMNs; only a small proportion of patients have mixed-type IPMNs. In contrast, many IPMNs fall into the mixed-type category on histology [7, 8].

The risk of invasive carcinoma is higher in main-duct-type and mixed-type IPMNs than branch-duct-type IPMNs [4], unless there is only minimal microscopically detectable involvement of the main pancreatic duct, when the risk of invasive carcinoma is similar to that of a branch-duct-type IPMN (see Sect. 17.6).

17.2.4.2 Epithelial Subtype

IPMNs may show three epithelial subtypes, namely gastric, intestinal, and pancreatobiliary type (Fig. 17.2). Until recently, the oncocytic type of intraductal papillary neoplasm was included as a subtype of IPMN, but this is now recognized as a distinct entity in the 2019 WHO classification [1]. The three subtypes of IPMN are distinguished by their morphological appearances and by the immunohistochemical profiles of the mucin glycoproteins (Table 17.1).

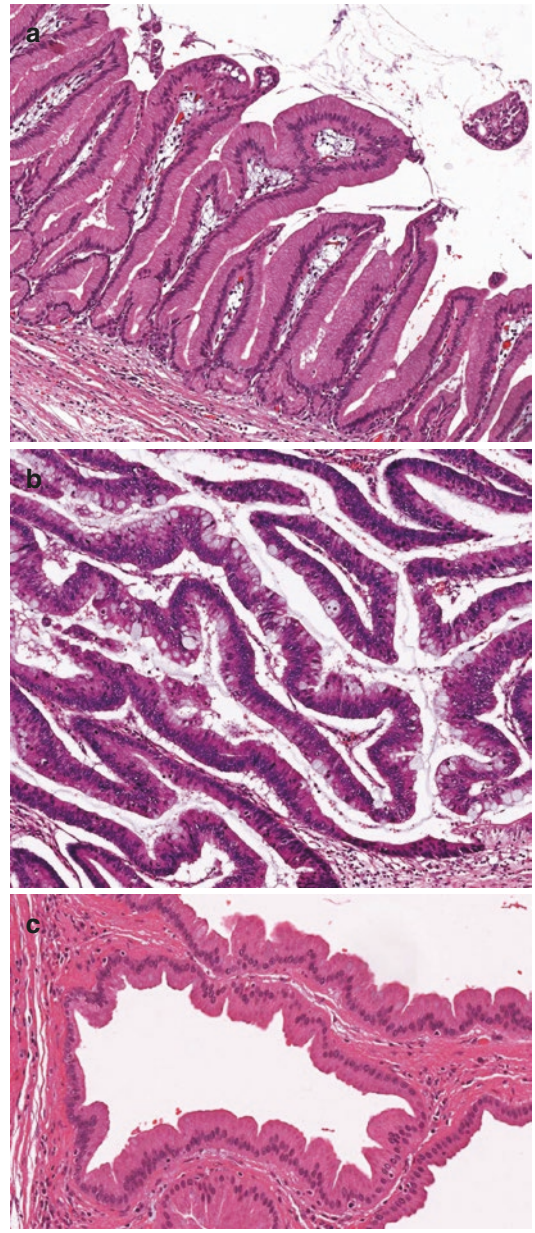

Fig. 17.2 Epithelial subtypes: intraductal papillary mucinous neoplasms may be lined by gastric-type (**a**), intestinal-type (**b**), or pancreatobiliary-type (**c**) epithelium

Gastric-type IPMN is the most common, intestinal-type IPMN the second most common, and pancreatobiliary-type the least common. There may be a mixture of epithelial subtypes within the same IPMN, in which case the predominant component is used for subtyping.

Table 17.1 Mucin profiles and expression of CDX2 and CK20 in the different epithelial subtypes of intraductal papillary mucinous neoplasia (IPMN), in intraductal oncocytic papillary neoplasm (IOPN), and in intraductal tubulopapillary neoplasm (ITPN)

	MUC1	MUC2[a]	MUC5AC	MUC6	CDX2/CK20[a]
Gastric IPMN	–	–	+	–/+	–
Intestinal IPMN	–	+	+	–	+
Pancreatobiliary IPMN	+	–	+	+	–
IOPN	+	–	+	+	–
ITPN	+	–	–	+	–

[a]Goblet cells, which may be scattered within non-intestinal epithelium, will be immunopositive for MUC2, CDX2, and CK20

Gastric-type IPMNs tend to be low-grade lesions, whereas intestinal-type IPMNs and pancreatobiliary-type IPMNs tend to be high-grade lesions.

17.2.4.3 Grade of Dysplasia

All IPMNs show dysplasia, which is now classified as either low-grade or high-grade dysplasia (Fig. 17.3), based on the degree of architectural and cytological atypia. This two-tiered grading system, initially proposed at the Baltimore consensus meeting [9] and included in the 2019 WHO classification of tumors of the pancreas [1], replaces the former three-tiered grading system of low-grade, intermediate-grade, and high-grade dysplasia. IPMNs showing low-grade dysplasia or intermediate-grade dysplasia are now categorized as low-grade IPMN, whilst IPMN with high-grade dysplasia remains as high-grade IPMN. Progression from low-grade dysplasia through high-grade dysplasia to invasive carcinoma appears to take several years. When an individual IPMN shows both grades of dysplasia, then it should be graded as high-grade dysplasia, regardless of whether the high-grade dysplasia is in the predominant epithelial subtype or not.

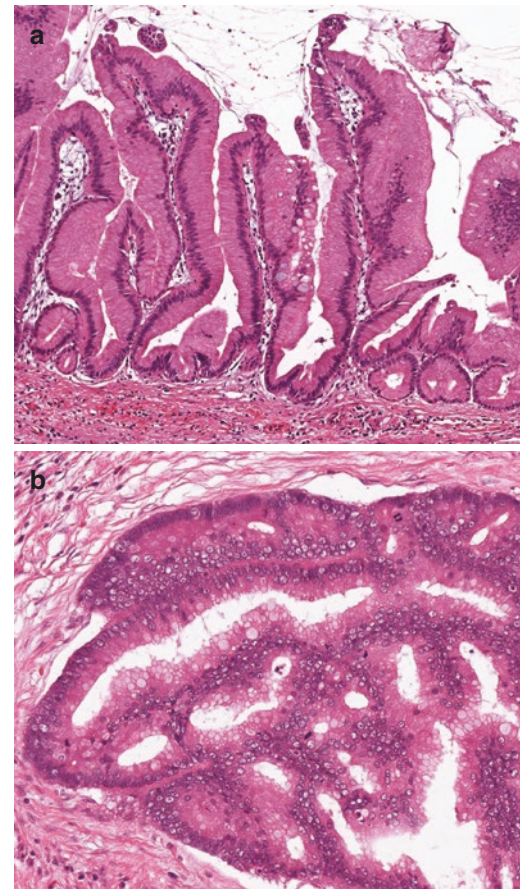

Fig. 17.3 Dysplasia in intraductal papillary mucinous neoplasm: this gastric-type epithelium shows low-grade dysplasia characterized by columnar cells with basal nuclei and minimal atypia. Note the occasional goblet cells (*center*) present in this case (**a**). This intestinal-type epithelium shows low-grade dysplasia characterized by nuclear crowding, some pleomorphism, and occasional mitotic figures (**b**). High-grade dysplasia is characterized by budding off of neoplastic cells into the duct lumen, loss of polarity, and marked nuclear pleomorphism (**c**)

17.2.4.4 Invasive Carcinoma

IPMNs with associated invasive carcinoma may have a small superficially invasive carcinoma that is only detected microscopically (Fig. 17.4) or may have a more deeply invasive, grossly visible, carcinoma (Fig. 17.5). The term 'minimally invasive carcinoma', often used for tumors with invasion ≤5 mm depth, should no longer be used,

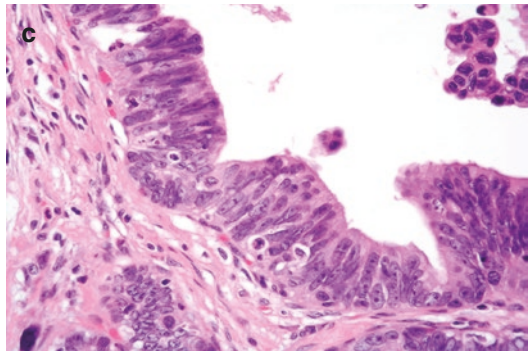

Fig. 17.3 (continued)

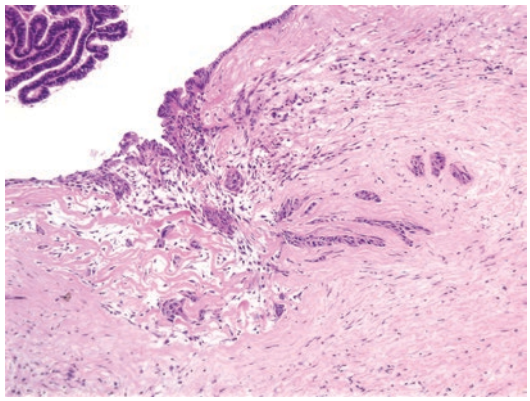

Fig. 17.4 Intraductal papillary mucinous neoplasm with associated invasive carcinoma: there is a small focus of invasive ductal (tubular) adenocarcinoma arising within this intraductal papillary mucinous neoplasm

since it has been variably defined by different authors.

Invasive carcinoma arising from an IPMN may be conventional ductal adenocarcinoma (tubular-type adenocarcinoma) or colloid type. All three epithelial subtypes (gastric, intestinal, and pancreatobiliary) may give rise to a conventional (tubular) carcinoma, but colloid carcinoma only arises from intestinal-type IPMN (Table 17.2) [10].

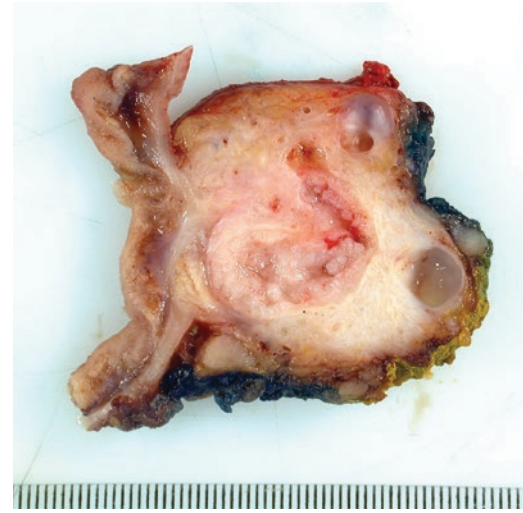

Fig. 17.5 Intraductal papillary mucinous neoplasm (IPMN) with associated invasive carcinoma: this main-duct-type IPMN shows papillae within the dilated main pancreatic duct. Invasive carcinoma partially surrounds a retention cyst. There are also enlarged lymph nodes in the peripancreatic fat

Table 17.2 Characteristics related to epithelial phenotype in intraductal papillary mucinous neoplasia (IPMN) and comparison with intraductal oncocytic papillary neoplasm (IOPN) and intraductal tubulopapillary neoplasm (ITPN)

	Gastric IPMN	Intestinal IPMN	Pancreatobiliary IPMN	IOPN	ITPN
Location	branch duct > main duct	main duct > branch duct	main duct > branch duct	main duct > branch duct	main duct > branch duct
Growth	flat or papillary	finger-like villi	complex papillae	solid growth	solid growth
Dysplasia	LGD	HGD	HGD	HGD	HGD
Present with invasive carcinoma	15%	30–60%	60–75%	40%	70%
Type of invasive carcinoma	conventional (tubular)	colloid or conventional (tubular)	conventional (tubular)	oncocytic	conventional (tubular)

Abbreviations: > more than, *LGD* low-grade dysplasia, *HGD* high-grade dysplasia

It is important to note that invasive carcinoma arising in IPMN may be focal or multifocal. Moreover, carcinoma arising within a pancreas containing IPMN may not have arisen from an IPMN (see Sect. 17.2.10.8 for discussion about concomitant pancreatic ductal adenocarcinoma).

17.2.5 Macroscopy

By definition, IPMNs involve the ducts of the pancreas and produce copious amounts of thick, viscous mucin, which fills the ducts and may be seen oozing from the ampulla/major papilla or, occasionally, the minor papilla (Fig. 17.1). Soft friable papillae (Fig. 17.5) may be seen in the lumina of the involved ducts. Many IPMNs are multifocal and may involve the entire pancreas. Occasionally, non-invasive IPMNs can form a fistula into the duodenum or stomach.

The site of involvement of the IPMN, in either the main pancreatic duct and/or branch duct(s), should be established macroscopically. Inserting a probe into the main pancreatic duct may be required to show the connection between a peripheral branch-duct cyst and the main duct. Microscopy, however, may be required to determine whether mucin-filled ducts are due to involvement by IPMN or due to mucin from an adjacent IPMN being extruded into the duct.

17.2.5.1 Main-Duct IPMN

In main-duct-type IPMN, the main pancreatic duct is dilated and filled with thick mucin, and papillae may be seen within the duct lumen (Fig. 17.5). Main-duct-type IPMN may extend into the ampulla and may involve the entire length of the main pancreatic duct. However, a main-duct-type IPMN within the head of the pancreas causing obstruction of the main pancreatic duct, by mucin, can result in secondary (nonneoplastic) dilatation of the main duct in the body and tail of the pancreas, mimicking diffuse IPMN. Similarly, a main-duct-type IPMN within the body or tail may give rise to dilatation of the main pancreatic duct downstream of the IPMN, due to drainage of large amounts of mucin, and mimic diffuse IPMN.

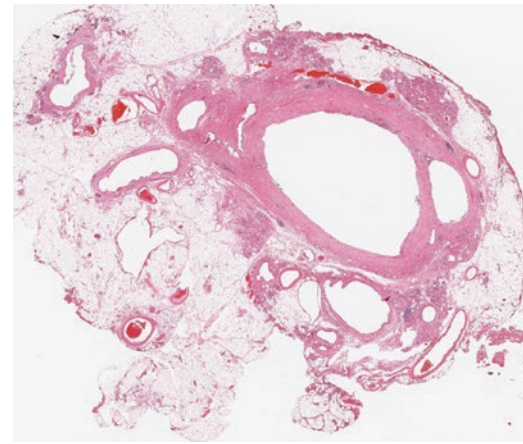

Fig. 17.6 Retention cysts in tail of pancreas: obstruction of the main pancreatic duct in the head of the pancreas by intraductal papillary mucinous neoplasm (not shown) resulted in secondary dilatation of the main duct and branch ducts in the body (not shown) and tail of the pancreas

The pancreatic parenchyma adjacent to a main-duct-type IPMN is usually atrophic, and pancreas upstream from an obstructing IPMN may show florid chronic obstructive pancreatitis (see Chap. 7, Sect. 7.2.6.4), including retention cysts (see Chap. 19, Sect. 19.3.1). These retention cysts may mimic branch-duct IPMN and mixed-type IPMN (Fig. 17.6). Calcification may be found in the adjacent pancreas, but does not appear to occur within the IPMN (i.e., there is no intratumoral calcification) [11].

17.2.5.2 Branch-Duct IPMN

Branch-duct IPMNs appear as grape-like dilatation of the branch ducts (Fig. 17.7). There may be a single cyst, a multilocular cyst, or a cluster of cysts. The dilated ducts are filled with mucus and may show papillae protruding into the lumen. Unlike main-duct-type IPMNs, the adjacent pancreas may be macroscopically normal.

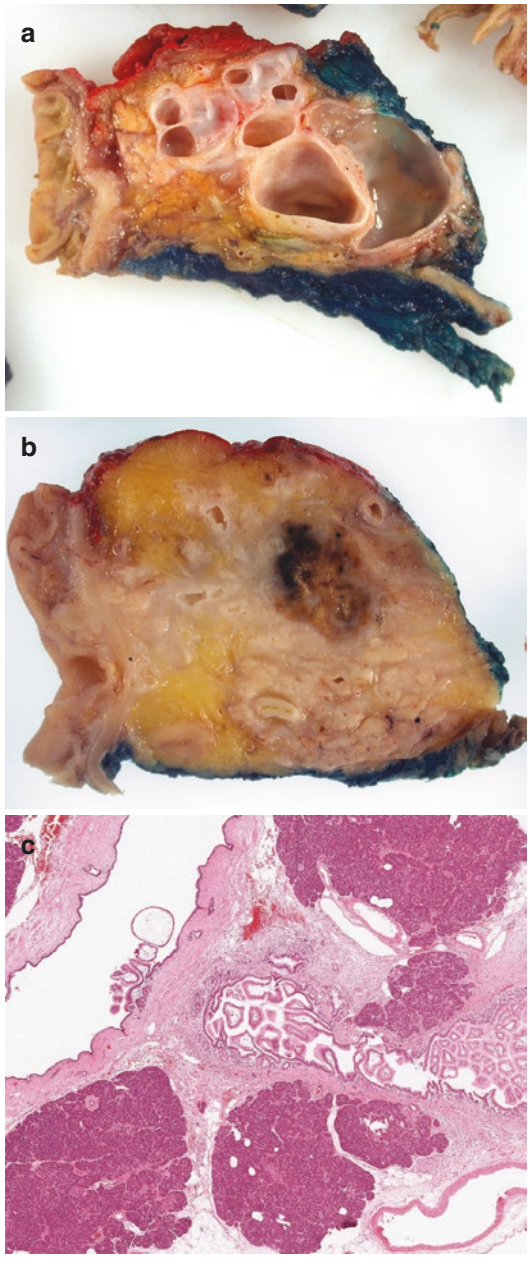

Fig. 17.7 Branch-duct-type intraductal papillary mucinous neoplasm (IPMN): this branch-duct-type IPMN shows marked grape-like dilatation of ducts (**a**). In contrast, the duct dilatation in this example is more subtle (**b**). Note the hemorrhagic area of mucus extravasation (*upper right*). This branch-duct IPMN (**c**) can be seen opening into the uninvolved main pancreatic duct (*left*)

17.2.5.3 Mixed-Duct IPMN

In mixed-duct-type IPMN, there is involvement of both the main pancreatic duct and the branch ducts. The main duct and branch ducts are dilated and may be filled with viscous mucin (Fig. 17.8).

Fig. 17.8 Mixed-duct-type intraductal papillary mucinous neoplasm: there is dilatation and thickening of the wall of the main pancreatic duct (*right*) with grossly visible intraductal papillae (**a**), together with dilatation of branch ducts (*left*). In this example, there is less marked dilatation of the main pancreatic duct (*center*) and branch ducts with adjacent macroscopically normal pancreatic parenchyma (**b**)

17.2.5.4 Invasive Carcinoma

When invasive carcinoma arises within an IPMN, it may be visible macroscopically (Fig. 17.5) as an irregular thickening of a cyst wall, as an irregular firm solid pale area in the adjacent pancreas, or as a soft mucoid mass (due to colloid carcinoma). Small and superficially invasive carcinomas may only be detected on microscopic examination.

17.2.6 Sampling

IPMNs should always be sampled thoroughly because high-grade dysplasia or invasive carcinoma may be focal or multifocal. Small invasive carcinomas are usually not identifiable macroscopically. Microscopic examination may also reveal that the IPMN is more extensive than appreciated by naked-eye inspection, involving both the main and branch ducts, or showing so-called (multifocal) 'skip lesions'. Extensive sampling is also required to accurately assess the extent of main duct involvement and the distance to the transection margin.

Solid areas and mucoid areas in the wall should always be sampled, as they likely represent invasive carcinoma. However, it may not be possible to distinguish invasive carcinoma from disrupted ducts, mucus extravasation (Fig. 17.7b), and associated fibrosis on macroscopic examination. All other areas require extensive sampling. In the absence of macroscopic invasive carcinoma, embedding the entire lesion may be considered, particularly if microscopic examination reveals high-grade dysplasia but no invasion [12]. Careful examination and sampling of the background pancreas is also important to identify skip lesions and/or concomitant invasive adenocarcinoma (see Sect. 17.2.10.8).

17.2.7 Microscopy

IPMNs typically show tall papillae with edematous fibrovascular cores within the dilated ducts, but the papillae may be small and lack fibrovascular cores, or the epithelial lining may be flat

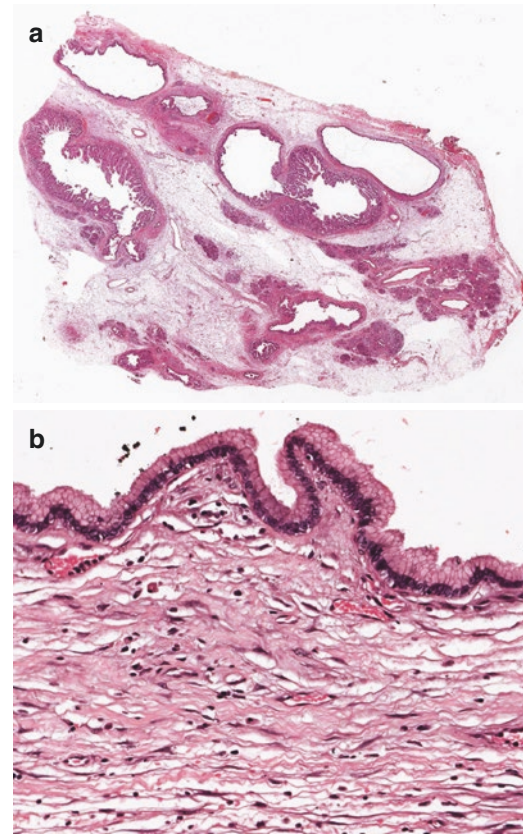

Fig. 17.9 Intraductal papillary mucinous neoplasm (IPMN): this branch-duct-type IPMN shows characteristic tall papillae within some ducts (**a**), but in other ducts (*top right*) the papillae are short or the epithelial lining is flat (**b**)

(Fig. 17.9). The papillae may be microscopic or macroscopically visible projections. IPMNs often extend beyond the macroscopically visible lesion and the neoplastic epithelium can extend into adjacent smaller ducts mimicking PanIN (Fig. 17.10). Ducts containing IPMN may rupture, resulting in mucus extravasation into the surrounding stroma, which may evoke an inflammatory response (Fig. 17.11). This extravasated mucus should not be confused with invasive colloid carcinoma (see differential diagnosis, Sect. 17.2.10.7).

IPMNs should always be classified according to the predominant epithelial subtype (Fig. 17.2). When an individual IPMN shows both grades of dysplasia, then it should be graded as high-grade dysplasia (Fig. 17.3).

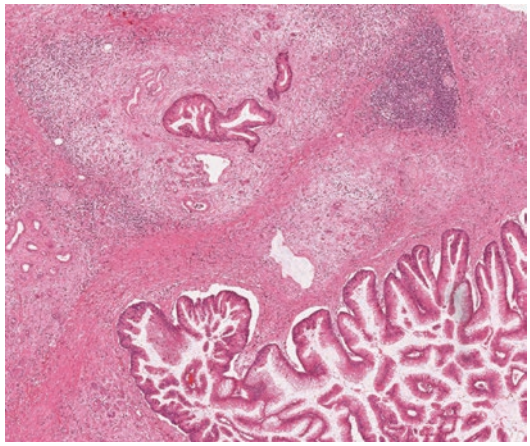

Fig. 17.10 Main-duct-type intraductal papillary mucinous neoplasm: neoplastic epithelium from the main duct (*below*) extends into adjacent smaller ducts and may mimic PanIN

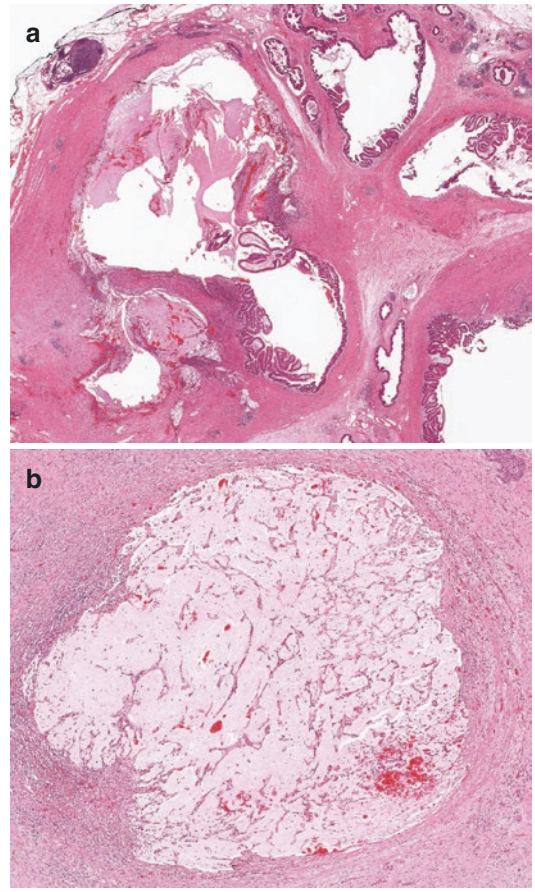

Fig. 17.11 Mucus extravasation: this non-invasive, mixed-type intraductal papillary mucinous neoplasm shows neoplastic epithelium within the main duct and branch ducts (**a**). There is also abundant extravasated mucus associated with a ruptured duct. In contrast to colloid carcinoma, there is no neoplastic epithelium within the extravasated mucus, which has evoked an inflammatory response (**b**)

17.2.7.1 Epithelial Subtype

Gastric-type IPMN is typically seen within branch-duct IPMNs, but can occur in main-duct IPMNs and is often multifocal. It is characterized by tall, columnar cells with abundant apical cytoplasmic mucin and basally located nuclei, resembling gastric foveolar-type epithelium (Fig. 17.2a). Scattered goblet cells may be seen within the epithelium (Fig. 17.3a). Gastric-type IPMNs may be flat or papillary with pyloric-like mucinous glands beneath the papillae (Fig. 17.12).

Intestinal-type IPMN is typically seen within the main pancreatic duct (main-duct type IPMN). It is characterized by tall, columnar, mucin-producing cells with basophilic cytoplasm and pseudostratified, cigar-shaped nuclei (Fig. 17.2b). There may be abundant goblet cells. Paneth cells and endocrine cells may also be present. The tall finger-like papillae resemble a colonic villous adenoma (Fig. 17.13).

Pancreatobiliary-type IPMN typically occurs within the main pancreatic duct but may involve the branch ducts. It is characterized by cuboidal cells with round nuclei, prominent nucleoli, and little mucin (Fig. 17.2c, which is a high power of Fig. 15.15). Pseudostratification of the nuclei is uncommon. They usually have a complex papillary architecture with bridging and cribriform formation (Fig. 17.14). Some regard pancreatobiliary-type IPMN as a high-grade transformation of gastric-type IPMN, but low-grade pancreatobiliary-type IPMNs do occur (Fig. 17.2c).

17.2.7.2 Grade of Dysplasia

IPMNs may show low-grade and/or high-grade dysplasia. When both grades of dysplasia are present, then the IPMN should be graded as high-grade dysplasia.

Low-grade dysplasia is characterized by either a single layer of uniform, columnar cells

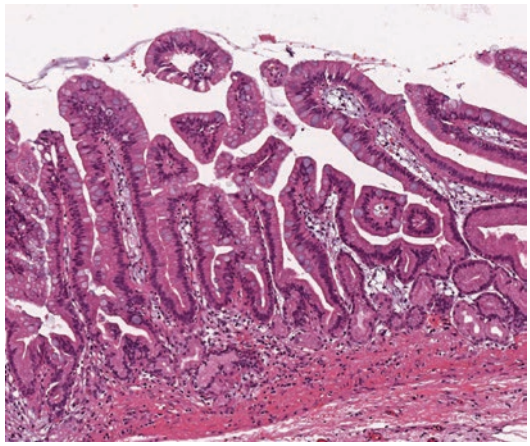

Fig. 17.12 Gastric-type intraductal papillary mucinous neoplasm (IPMN): this gastric-type IPMN shows abundant goblet cells and pyloric-like mucinous glands beneath the papillae

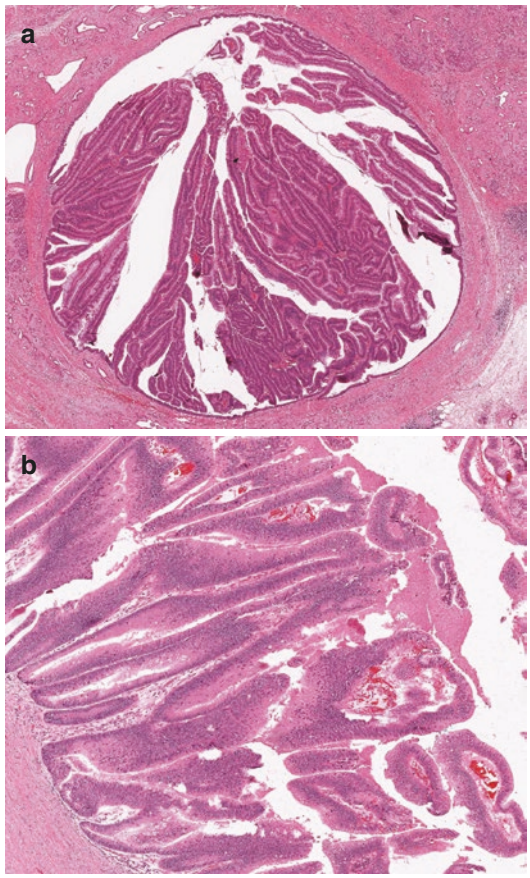

Fig. 17.13 Intestinal-type intraductal papillary mucinous neoplasm: the tall finger-like papillae within the main duct resemble a colonic villous adenoma (**a**). The epithelium is composed of tall, columnar, mucin-producing cells with pseudostratified, cigar-shaped nuclei (**b**)

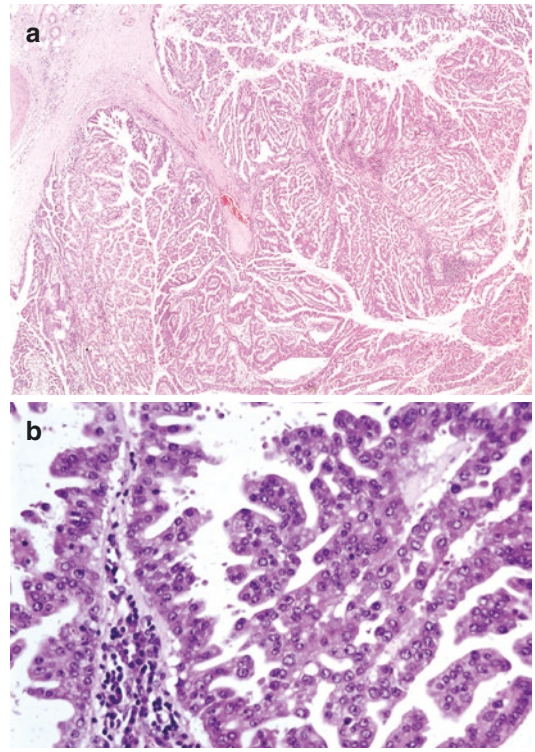

Fig. 17.14 Pancreatobiliary-type intraductal papillary mucinous neoplasm (IPMN): this pancreatobiliary-type IPMN has a complex papillary architecture (**a**). The epithelium is composed of cuboidal cells with round nuclei and prominent nucleoli (**b**)

with basal nuclei showing minimal atypia or by cells showing some nuclear crowding, loss of polarity, nuclear pleomorphism, and occasional mitotic figures (Figs. 17.3a, b). The epithelium may be flat or papillary with fibrovascular cores.

High-grade dysplasia is characterized by a complex papillary architecture, occasionally with a cribriform growth pattern, and budding off of neoplastic cells into the duct lumen, but high-grade dysplasia may also be flat. The epithelial cells show complete loss of polarity, marked nuclear pleomorphism, and prominent mitotic figures, including atypical forms (Fig. 17.3c).

17.2.7.3 Invasive Carcinoma

IPMNs may have an associated invasive carcinoma, which can be focal or multifocal. The carcinoma may show limited (Fig. 17.4) or more extensive invasion (Figs. 17.5 and 17.15).

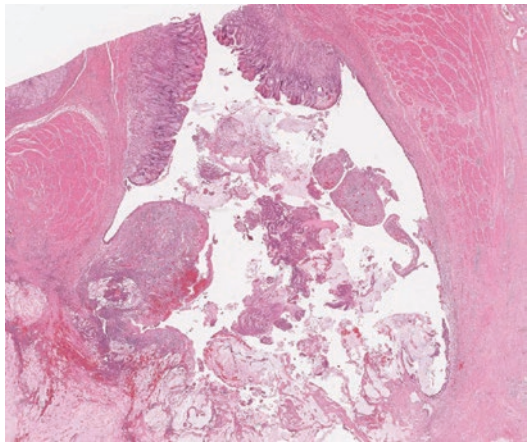

Fig. 17.15 Intraductal papillary mucinous neoplasm (IPMN) with associated invasive carcinoma: colloid carcinoma (*below*) arising from a main-duct (intestinal)-type IPMN (not shown) has invaded the wall of the stomach resulting in a fistula opening into the antrum. Residual gastric antral mucosa can be seen *center top*

Invasive carcinomas arising in IPMNs may be conventional ductal (tubular) type or colloid type (see Chap. 9, Sect. 9.14.2). The type of invasive carcinoma relates to the epithelial subtype and to the location of the IPMN (Table 17.2).

The majority of ductal (tubular) adenocarcinomas originate in gastric-type or pancreatobiliary-type IPMNs. Colloid carcinomas only arise in intestinal-type IPMNs (Table 17.2). The majority of invasive carcinomas arising in branch-duct-type IPMNs are of ductal (tubular) type, while the majority arising in main-duct-type IPMNs are colloid carcinomas (Table 17.2).

Invasive carcinomas arising in an IPMN should be reported in the same way as a non-IPMN related invasive carcinoma (see Chap. 9, Table 9.6).

17.2.8 Immunohistochemistry

IPMNs will express pancytokeratin markers (AE1/AE3 and CAM5.2), CK7, CK8, CK18, and CK19. Most IPMNs express CA19–9 and CEA.

Immunohistochemistry for the mucin glycoproteins (MUC1, MUC2, MUC5AC, and MUC6) and CDX2 can distinguish the different epithelial subtypes of IPMNs (Table 17.1). Gastric-type IPMNs express MUC5AC and MUC6, intestinal-type IPMNs express MUC2, MUC5AC, and CDX2, and pancreatobiliary-type IPMNs express MUC1, MUC5AC, and MUC6.

Immunohistochemistry is not usually needed to make the diagnosis of an IPMN, but may, on occasion, be helpful for confirming the epithelial subtype.

17.2.9 Molecular Pathology

Activating *KRAS* mutations are detected in the majority of IPMNs, as are activating *GNAS* mutations, which are more frequent in the intestinal type. Inactivating mutations in the *RNF43* gene are also frequently detected in IPMNs.

17.2.10 Differential Diagnosis

17.2.10.1 Macrocystic Serous Cystadenoma (see Chap. 15, Sect. 15.6.2)

Macrocystic serous cystadenoma may mimic a branch-duct-type IPMN. However, macrocystic serous cystadenoma will not contain mucin and the cysts are lined by bland, glycogen-containing, clear, cuboidal cells.

17.2.10.2 Mucinous Cystic Neoplasm (see Chap. 16)

Mucinous cystic neoplasms (MCNs) may mimic branch-duct-type IPMN. However, MCNs occur predominantly in females and at a younger age (mean of 45–50 years) than IPMNs. The vast majority (>98%) of MCNs occur in the body and tail of the pancreas. They are solitary, thick-walled cysts, which do not communicate with the pancreatic duct system, and have ovarian-type stroma in the wall.

17.2.10.3 Simple Mucinous Cysts (Mucinous Nonneoplastic Cysts)

Simple mucinous cysts are benign, typically solitary (unilocular or multilocular) cysts, lined by a single layer of bland, cuboidal to columnar, mucinous epithelium, with a thin band of paucicellular stroma beneath the epithelium (see Chap. 19,

Sect. 19.2.1). They are more common in women, do not communicate with the duct system, do not have papillae, and do not show epithelial atypia.

17.2.10.4 Retention Cysts (see Chap. 19, Sect. 19.3.1)

Retention cysts are localized dilatations of the pancreatic ducts caused by obstruction. IPMNs may cause obstruction of ducts, as may other neoplasms and nonneoplastic processes. Retention cysts are unilocular, typically less than 1–2 cm in size, and lined by a single layer of normal, often flattened, pancreatobiliary-type epithelium (Figs. 17.6 and 19.10a). Macroscopically and microscopically (when lined by low-grade PanIN), they can mimic branch-duct-type IPMN. However, IPMNs typically have abundant mucin within the dilated duct lumen, well-formed, tall, complex papillae with fibrovascular cores, and show cytological atypia within the epithelium.

17.2.10.5 Pancreatic Intraepithelial Neoplasia (PanIN) (see Chap. 8)

IPMNs are typically more than 5 mm in size, grossly or radiologically visible, and lined by papillary structures. In contrast, PanIN is not grossly visible, not associated with abundant mucin production, and is less than 5 mm in size (see Table 8.1). PanIN, however, may occur within grossly visible ducts or retention cysts, and IPMN may extend into small ducts (see Sect. 17.2.10.6), so the distinction between the two is not always straightforward [13].

When PanIN involves retention cysts, normal ductal epithelium is usually also present in the same cyst, but IPMNs can give rise to similar appearances, particularly when they are lined by flat (rather than papillary) mucinous epithelium. Step-sections may be used to show continuity of a small duct lesion with an IPMN, which will have a similar lining epithelium, and help to distinguish it from PanIN. The epithelium in IPMN can show gastric, intestinal, or pancreatobiliary differentiation, whereas the epithelium in PanIN almost always shows gastric foveolar differentiation.

The size definitions for PanIN and IPMN were originally <5 mm and > 10 mm respectively. This left a grey area for lesions measuring between 5 mm and 10 mm in diameter. The term ‘incipient IPMN’ was then introduced for morphologically typical IPMNs measuring 5 mm to 10 mm in diameter. The 2019 WHO classification now defines IPMNs as typically greater than 5 mm in size, and suggests that the terms ‘incipient IPMN’ and ‘incipient IOPN’ are only used for lesions that are 5–10 mm in diameter, have long finger-like papillae, intestinal or oncocytic differentiation, or a *GNAS* mutation.

It is recognized that there is considerable overlap between low-grade, gastric-type IPMN and low-grade PanIN, both of which can involve branch ducts, share similar morphological features, and have similar mucin profiles. Both lesions can also be frequently found together in pancreata from patients with a family history of pancreatic carcinoma (see Chap. 6, Sects. 6.4 and 6.5). It may be helpful to use the term ‘intraductal/intraepithelial neoplasm of low grade, either PanIN or IPMN’ in such circumstances (see Chap. 23, Sect. 23.3.2). Ultimately, it is the degree of dysplasia within these lesions that matters most. The distinction between PanIN and gastric-type IPMN does not appear to be prognostically significant if the lesion is low grade and has been completely excised.

17.2.10.6 Extension of IPMN into Smaller Ducts

IPMNs may grow into smaller ducts and mimic PanIN or be mistaken for invasive carcinoma (Figs. 17.10 and 17.11a). However, appreciation of this phenomenon, the lobular architecture of the pancreas, the smooth outline of the involved ducts, and the morphological similarity to the main lesion should help distinguish this from invasive carcinoma. When there is marked atrophy of the adjacent pancreas, these small secondarily-involved ducts may resemble well-differentiated invasive carcinoma, but, in general, these small ducts are widely spaced, lack the density of invasive carcinoma, and are surrounded by densely fibrotic (rather than desmoplastic)

stroma. The epithelium in the small ducts will still resemble that of the main lesion, and elastin stain can be used to outline these native ducts [14].

17.2.10.7 Mucus Extravasation

Ducts involved by IPMN may rupture with consequent mucus extravasation into the peri-ductal stroma (Figs. 17.7b and 17.11b). This extravasated mucus does not contain epithelial cells and generally evokes an inflammatory reaction. Mucus extravasation should not be misdiagnosed as colloid carcinoma, which can arise from intestinal-type IPMN. Colloid carcinoma (see Chap. 9, Sect. 9.14.2) is characterized by abundant mucin pools containing floating neoplastic cells (arranged in strips, clusters, and individually, sometimes with a signet ring appearance), with little or no associated inflammation (see Fig. 9.60). These malignant mucin pools are not related to disrupted ducts, i.e., are found away from the duct system.

17.2.10.8 Concomitant Pancreatic Ductal Adenocarcinoma

IPMN and pancreatic ductal adenocarcinoma may be present in the same pancreas, but the ductal adenocarcinoma may develop independently of IPMN (i.e., be a concomitant pancreatic ductal adenocarcinoma), rather than arise from an IPMN. The reported incidence of pancreatic ductal adenocarcinoma concomitant with IPMN is 5–10%.

On microscopy, adenocarcinoma derived from IPMN will show histological transition from IPMN to invasive adenocarcinoma, whereas ductal adenocarcinoma concomitant with IPMN does not show transition from an adjacent IPMN. However, with large pancreatic ductal adenocarcinomas and no evident histological transition from IPMN, it may not be possible to determine, on microscopy, whether the carcinoma has arisen in an IPMN or is concomitant with IPMN. Molecular analysis may then help in the distinction between IPMN-derived ductal adenocarcinoma and concomitant carcinoma [15].

Both carcinoma arising in IPMN and pancreatic ductal adenocarcinoma concomitant with IPMN can be detected at an earlier stage than ordinary pancreatic cancer and, consequently, may have a better prognosis [16].

17.2.10.9 Cystic Papillary Growth Pattern in Pancreatic Ductal Adenocarcinoma

This variant of pancreatic ductal adenocarcinoma may mimic IPMN [17]. It is characterized by large malignant glands containing abundant mucin and papillary projections (see Chap. 9, Sect. 9.8.4). However, it does not involve the duct system, which can be demonstrated by the random distribution of the malignant glands and the lack of elastic fibers around the glands.

17.2.10.10 Intraductal Papillary Neoplasm of the Bile Ducts

Intraductal papillary or tubular neoplasms may arise in bile ducts, including the intrapancreatic bile duct [18, 19]. Most are lined by pancreatobiliary-type epithelium, but they may also show gastric-, intestinal-, or oncocytic-type epithelium. Identifying their location within the common bile duct will distinguish them from IPMN, intraductal oncocytic papillary neoplasm (IOPN), or intraductal tubulopapillary neoplasm (ITPN) of the pancreas.

17.2.10.11 Intraductal Growth by Other Neoplasms

Other primary pancreatic neoplasms and, occasionally, secondary neoplasms to the pancreas (see Chap. 12, Sect. 12.3) can grow into and along large pancreatic ducts, thereby mimicking IPMN, IOPN, or ITPN (Table 17.3). Primary neoplasms showing such macroscopic intraductal growth include acinar cell carcinoma (see Figs. 10.3 and 10.15), undifferentiated carcinoma with osteoclast-like giant cells (see Fig. 9.67), and pancreatic endocrine neoplasm (see Chap. 20, Sect. 20.4).

Table 17.3 Neoplasms showing intraductal growth

Duct involved	Neoplasm
Pancreatic duct (main +/− branch)	Intraductal papillary mucinous neoplasm (IPMN)
	Intraductal oncocytic papillary neoplasm (IOPN)
	Intraductal tubulopapillary neoplasm (ITPN)
	Acinar cell carcinoma
	Undifferentiated carcinoma with osteoclast-like giant cells
	Pancreatic neuroendocrine tumor
	Metastases
Bile duct	Intraductal papillary neoplasm
	Intraductal tubulopapillary neoplasm
	Intraductal oncocytic papillary neoplasm

17.3 Intraductal Oncocytic Papillary Neoplasm (IOPN)

Intraductal oncocytic papillary neoplasm (IOPN) is grossly visible, typically forms a complex mass with both cystic and solid components, and produces minimal mucin [20].

17.3.1 Epidemiology and Clinical Features

IOPNs are rare intraductal neoplasms that typically occur in late adulthood and affect males and females equally. The mean age of presentation is 59 years (range 36–84 years). They present in the same way as IPMNs and, on imaging, are typically multilocular cystic, or cystic and solid, lesions [20–22].

17.3.2 Macroscopy

The majority of IOPNs occur in the head of the pancreas, within the main pancreatic duct, and range in size from 1 to 15 cm (median size 5.5 cm). The involved dilated ducts may be filled with abundant friable, solid and papillary growths such that it can be difficult to appreciate the intraductal nature of the neoplasm (Fig. 17.16).

Fig. 17.16 Intraductal oncocytic papillary neoplasm: the branch duct is partially filled with solid tumor

17.3.3 Microscopy

IOPNs are characterized by cuboidal or columnar cells with abundant granular eosinophilic cytoplasm and large round nuclei with a prominent single nucleolus (Fig. 17.17a). Scattered goblet cells may be present. They show a complex architecture with arborizing papillae, solid nests, and intraepithelial lumina (Fig. 17.17b). These intraepithelial lumina are round, punched-out spaces within the epithelium that give rise to a cribriform growth pattern. There may be areas of flat epithelium or less complex papillae (Fig. 17.17c). Up to 80% of IOPNs have high-grade dysplasia.

About 40% of IOPNs may have an invasive component at presentation, typically small pT1 carcinomas. The invasive component is typically characterized by small tubules lined by oncocytic cells, or by individual oncocytic cells infiltrating the stroma. However, the invasive component may have a nodular growth pattern with a pushing border or, rarely, may resemble colloid carcinoma with oncocytic cells floating in mucin

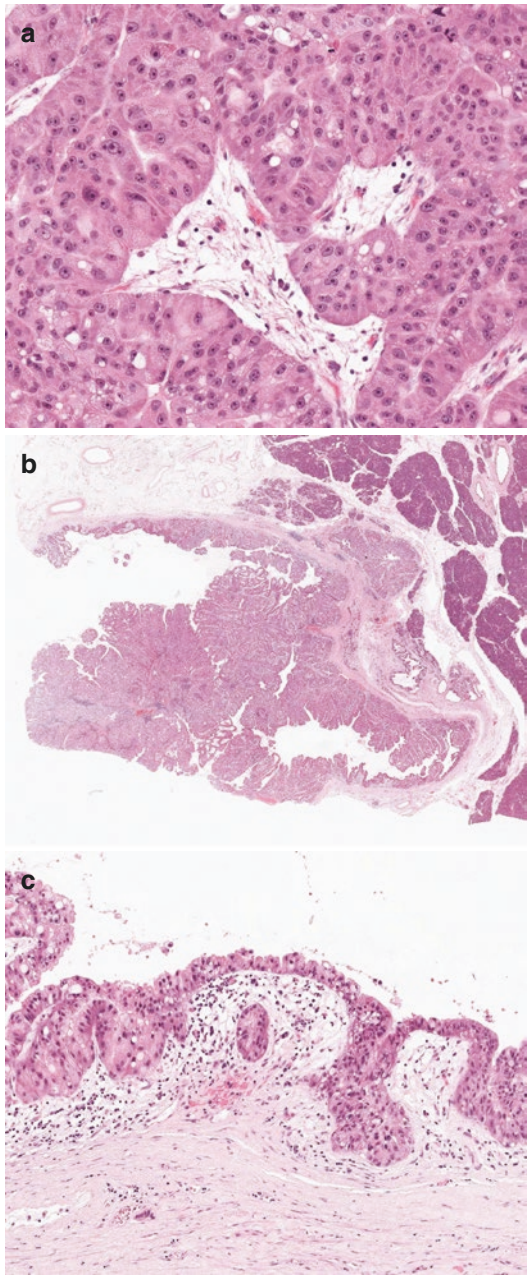

Fig. 17.17 Intraductal oncocytic papillary neoplasm: the cuboidal or columnar cells have abundant granular eosinophilic cytoplasm and large round nuclei with a prominent nucleolus (**a**). The architecture is complex with arborizing papillae, solid nests (**b**), and areas of flat epithelium (**c**)

pools. Conventional, non-oncocytic, ductal (tubular)-type adenocarcinoma is infrequent in IOPNs.

17.3.4 Immunohistochemistry

IOPNs express MUC1, MUC5AC, and MUC6, as well as HepPar-1. Scattered goblet cells may express MUC2 and CDX2 (Table 17.1).

17.3.5 Molecular Pathology

IOPNs are genetically distinct from IPMNs. They do not have mutations in *KRAS* or *GNAS*, and mutations in *RNF43* are extremely rare. Mutations in *ARHGAP26, ASXL1, EPHA8,* and *ERBB4* are found more commonly in IOPN than in IPMNs [23].

17.4 Intraductal Tubulopapillary Neoplasm (ITPN)

Intraductal tubulopapillary neoplasm (ITPN) is a grossly visible, tubule-forming, intraductal epithelial neoplasm without the excessive mucus production that is seen in IPMN [24, 25]. When invasive carcinoma occurs within an ITPN, it is classified as ITPN with associated invasive carcinoma.

17.4.1 Epidemiology and Clinical Features

ITPNs are rare, accounting for approximately 3% of pancreatic intraductal neoplasms. They appear to occur slightly more frequently in females, with a mean age at presentation of 55–60 years (range 25–84 years). They present in the same way as IPMNs, although jaundice is unusual, and, on imaging, are usually indistinguishable from IPMNs. There are rare case reports of co-existing IPMN and ITPN; in one case both tumors occurred in branch ducts [26].

17.4.2 Macroscopy

Macroscopically, they from solid nodular tumor masses within dilated pancreatic ducts (Fig. 17.18). There is no mucin secretion into the

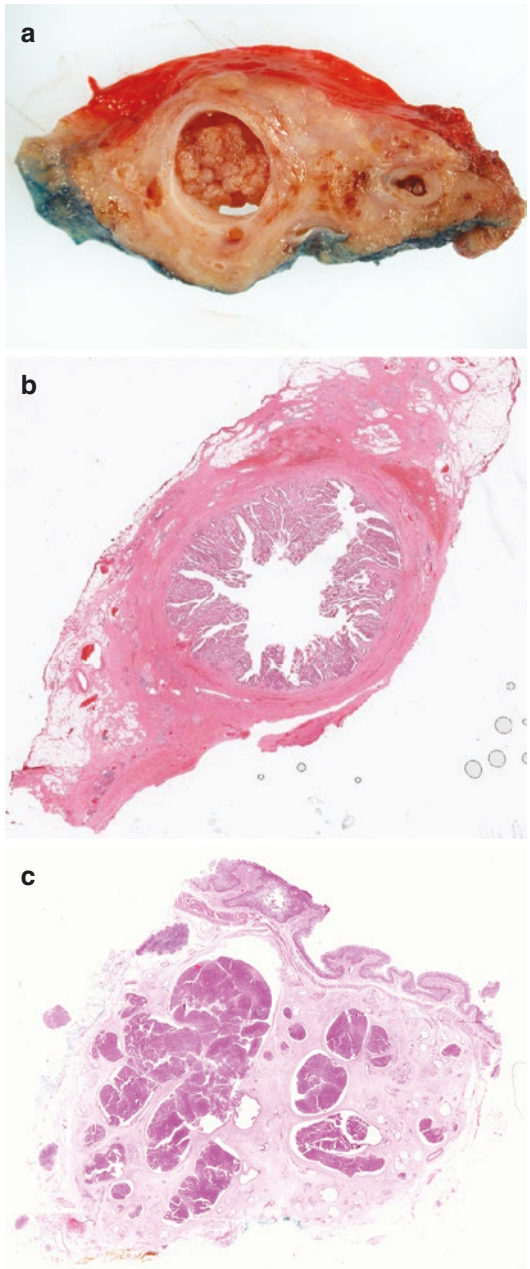

Fig. 17.18 Intraductal tubulopapillary neoplasm: solid nodular tumor can be seen within the main pancreatic duct (**a, b**) and dilated pancreatic ducts (**c**)

involved ducts. Most ITPNs arise in the main pancreatic duct with extension of the intraductal proliferation into branch ducts and smaller ducts giving rise to the multinodular appearance. Like IPMNs, they most commonly involve the head of

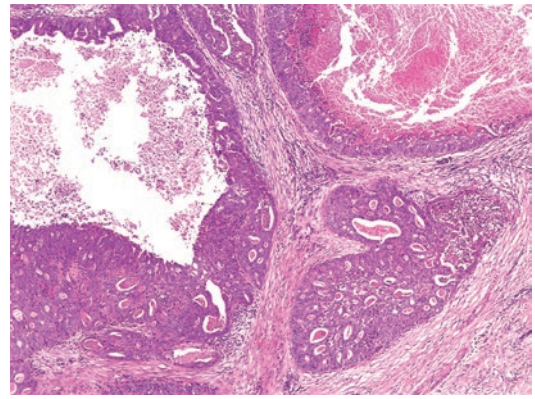

Fig. 17.19 Intraductal tubulopapillary neoplasm: this high-grade intraductal tumor is composed of nodules of cribriform, closely packed tubular glands with associated intraductal necrosis

the pancreas, but may also arise in the body/tail or involve the whole pancreas. The adjacent pancreas is atrophic and sclerotic.

17.4.3 Microscopy

On microscopy, there are multiple nodules composed of cribriform, closely packed tubular glands with only occasional papillary architecture or solid sheets (Fig. 17.19). There may be prominent lymphoid aggregates around the tumor [24]. The cells are cuboidal with eosinophilic cytoplasm and uniform round-to-oval nuclei. Most ITPNs show high-grade dysplasia with abundant mitotic figures. They may have foci of necrosis and desmoplastic stroma within the intraductal component, but this does not represent invasive carcinoma. Invasive carcinoma is usually focal, of ductal (tubular) type, and found in approximately 70% of cases [24]. It may be difficult to identify invasion, which is characterized by small cords of cells or individual cells invading into the stroma around the duct (Fig. 17.20).

17.4.4 Variants

ITPN with clear cell morphology has been described [24, 27]. Rare cases of ITPN with extensive calcification [28] or stromal osseous

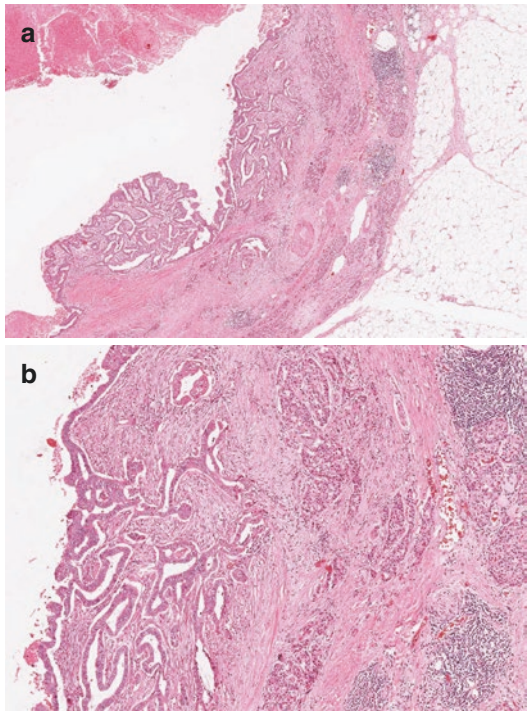

Fig. 17.20 Intraductal tubulopapillary neoplasm (ITPN) with associated invasive carcinoma: focal invasive carcinoma of ductal (tubular) type (**a**) with desmoplastic stroma (**b**) is seen arising from this ITPN

and cartilaginous metaplasia have also been described [29].

17.4.5 Immunohistochemistry

ITPN, like IPMN, shows ductal differentiation with immunopositivity for CK7, CK19, CA19–9, and monoclonal CEA. Occasional tumors may have scattered CK20- or CDX2-immunopositive tumor cells. ITPNs express MUC1 and MUC6, but not MUC2 (Table 17.1). Unlike IPMN, they typically do not express MUC5AC. However, there are extremely rare cases that have shown focal MUC5AC expression [24, 30].

17.4.6 Molecular Pathology

ITPN is genetically distinct from IPMN, showing wild type *KRAS* and *GNAS*. Mutations of *PIK3CA* and *BAP1* are found in approximately 30% of cases [31].

17.5 Staging

Invasive carcinoma arising within an IPMN, IOPN, or ITPN should be staged in the same way as conventional pancreatic ductal adenocarcinoma (see Chap. 9, Sect. 9.11). Determining the size of the carcinoma (needed for T-staging) may be difficult, since the extent of the invasive carcinoma can range from microscopic foci (that can be multicentric) to a macroscopically visible predominant component with only focal residual IPMN [14]. If multiple invasive foci are present, it is recommended that the size (measured microscopically) of the largest focus, as well as the overall estimated size of all foci in aggregate, are recorded. It is not yet clear which one of these measurements reflects the tumor burden and hence should be used for staging purposes [32].

17.6 Prognosis

The prognosis for IPMN is related to the location of the tumor (main duct or branch duct), the epithelial subtype (gastric, intestinal, or pancreatobiliary), and the stage and subtype (tubular or colloid) of the invasive carcinoma [10, 33].

The risk of invasive carcinoma is higher in main-duct-type (44%) and mixed-type (45%) than branch-duct-type IPMN (17%) [4]. Some mixed-type IPMNs, however, demonstrate only minimal involvement of the main pancreatic duct (Fig. 17.7c), defined as absence of gross abnormality (except for dilatation) of the main pancreatic duct, and noncircumferential microscopic involvement of the main pancreatic duct limited to very few histological sections. The risk of invasive carcinoma in this (minimal involvement) subgroup is comparable to that of a branch-duct-type IPMN [34].

Gastric-type IPMNs are more likely to be low grade, whilst the other epithelial subtypes of IPMN are more likely to have high-grade dysplasia (Table 17.2).

The 5-year survival rate (SR) for non-invasive IPMN is 90–100% after complete resection. Recurrence rates in non-invasive IPMNs are higher with main-duct involvement or intestinal-type epithelium.

Patients with resected invasive IPMNs have significantly better outcome than those with conventional pancreatic carcinoma. Some of this may be due to earlier detection of IPMN-associated invasive carcinoma. However, in subtype analysis of invasive carcinoma, this favorable outcome only remains for colloid carcinomas. The prognosis for IPMNs with associated colloid carcinoma is significantly better than for IPMNs with associated ductal (tubular) carcinoma (5-year SR 61–89% versus 37–55%). IPMN with associated invasive ductal (tubular) carcinoma has a prognosis equivalent to that of conventional pancreatic ductal adenocarcinoma (5-year SR 37% versus 16%) [10, 35, 36]. It has been suggested that invasive ductal (tubular) carcinoma arising in gastric-type IPMN is more likely to be poorly differentiated and have a significantly worse survival than invasive carcinoma arising in other types of IPMN [10].

The overall and disease-specific survival rates for IPMNs with invasive carcinoma ≤5 mm in greatest dimension (pT1a in TNM8) are both significantly better than that for IPMNs with more extensive invasive carcinoma. Moreover, there appears to be no difference in survival between patients with non-invasive IPMN and those who have an IPMN with pT1a invasive carcinoma [37].

The overall 10-year survival rate for IOPN, following resection, is 94% with no significant difference between invasive IOPN and non-invasive IOPN [20].

The prognosis for ITPN also appears to be favorable. The 5 year survival rate after surgery for non-invasive ITPN is 100% and for ITPN with an invasive component 71–82% [24, 25]

17.7 Management

In view of the high prevalence of malignancy in main-duct-type and mixed-type IPMNs, resection is recommended in all surgically fit patients with a main-duct or mixed-type IPMN.

Indications for resection of branch-duct IPMNs include when they are symptomatic, have mural nodules in the wall, are associated with dilatation of the main pancreatic duct, increase in size rapidly, have high-grade dysplasia on cytology, or are associated with elevated serum levels of CA19–9. Younger patients may also be considered for surgery without any of these risk factors, due to the cumulative risk of malignancy [4, 12].

Complete resection of IPMNs is essential and intraoperative frozen section of surgical margins is frequently needed to determine whether the IPMN (with or without invasive carcinoma) is completely excised, and to check if main pancreatic duct dilatation is due to tumor involvement, downstream drainage of large amounts of mucin, or (upstream) is secondary to obstruction (see Chap. 23, Sect. 23.3.2). Intraoperative pancreatoscopy (ductoscopy) of the dilated main pancreatic duct (Fig. 17.21),

Fig. 17.21 Intraductal papillary mucinous neoplasm (IPMN): intraoperative ductoscopy shows the papillae of IPMN within the main pancreatic duct (Kindly provided by Dr S. Yaqub, Oslo University Hospital, Norway)

with or without frozen section of intraductal biopsies, can also be used to establish the extent of an IPMN, and allow adaptation of the operative strategy [38].

Given the risk of recurrence following resection of non-invasive IPMNs and the fact that IPMNs can be multifocal (synchronously or metachronously), patients who have had a partial pancreatectomy should be followed up after surgery. Currently, it is suggested that surgically fit patients should have yearly follow-up with, preferably non-irradiating, imaging (i.e., MRI or EUS). Resected invasive carcinoma arising in IPMN is followed up as for conventional pancreatic carcinoma [4, 12].

17.8 Reporting Checklist

A list of macroscopic and microscopic features to consider when reporting an intraductal papillary neoplasm is shown in Table 17.4 [32, 39].

Table 17.4 Reporting checklist for intraductal papillary neoplasia (IPMN, IOPN or ITPN)

Macroscopic assessment
• Specimen type
• Additional resected structures, e.g., spleen
• Tumor location—head, body, tail
• Duct(s) involved—main pancreatic duct, branch duct, or mixed duct
• Tumor size (may require correction after microscopic assessment):
Size of the overall lesion
Maximum cyst diameter
Maximum diameter of the main pancreatic duct
Length of involvement of main pancreatic duct
• For multifocal disease:
Number of foci
Localization of foci
Size of largest focus
• Involvement of adjacent organs
• Invasive carcinoma identified or not
• Distance from resection margin(s)
Distance of main duct involvement to transection margin
Microscopic assessment
• Duct(s) involved—main duct, branch duct, mixed duct
• Focal or multifocal
• Type of epithelial lining—state which is predominant
• Degree of dysplasia:
Low grade
High grade—state which epithelial subtype is involved
• Invasive carcinoma present or not
• For invasive carcinoma:
Focal or multifocal invasion
Type of invasive carcinoma
Differentiation
Extent of invasion
Lymphatic, vascular, or perineural invasion
Lymph node metastases
UICC TNM staging
• Immunohistochemical profile (if performed)
• Involvement of other organs/structures (applies to non-invasive and invasive tumors)
• Completeness of excision/resection margin status (applies to non-invasive and invasive tumors)
Distance of main duct involvement to transection margin
• Background changes (e.g., obstructive pancreatitis, retention cysts)

References

1. Lokuhetty D, White VA, Watanabe R, Cree IA, editors. Digestive system tumours, WHO classification of tumours. 5th ed. Lyon: IARC Press; 2019. p. 296.
2. Hruban RH, Takaori K, Klimstra DS, Adsay NV, Albores-Saavedra J, Biankin AV, et al. An illustrated consensus on the classification of pancreatic intraepithelial neoplasia and intraductal papillary mucinous neoplasms. Am J Surg Pathol. 2004;28:977–87.
3. Rebours V, Couvelard A, Peyroux JL, Sauvanet A, Hammel P, Ruszniewski P, et al. Familial intraductal papillary mucinous neoplasms of the pancreas. Dig Liver Dis. 2012;44:442–6.
4. Tanaka M, Fernández-del Castillo C, Kamisawa T, Jang JY, Levy P, Ohtsuka T, et al. Revisions of international consensus Fukuoka guidelines for the management of IPMN of the pancreas. Pancreatology. 2017;17:738–53.
5. Krishna SG, Brugge WR, Dewitt JM, Kongkam P, Napoleon B, Robles-Medranda C, et al. Needle-based confocal laser endomicroscopy for the diagnosis of pancreatic cystic lesions: an international external interobserver and intraobserver study (with videos). Gastrointest Endosc. 2017;86:644–54.
6. Waters JA, Schmidt CM, Pinchot JW, White PB, Cummings OW, Pitt HA, Sandrasegaran K, Akisik F, Howard TJ, Nakeeb A, Zyromski NJ, Lillemoe KD. CT vs MRCP: optimal classification of IPMN type and extent. J Gastrointest Surg. 2008;12:101–9.
7. Correa-Gallego C, Ferrone CR, Thayer SP, Wargo JA, Warshaw AL, Fernández-Del Castillo C. Incidental pancreatic cysts: do we really know what we are watching? Pancreatology. 2010;10:144–50.
8. Tanaka M. Controversies in the management of pancreatic IPMN. Nat Rev Gastroenterol Hepatol. 2011;8:56–60.
9. Basturk O, Hong SM, Wood LD, Adsay NV, Albores-Saavedra J, Biankin AV, et al. A revised classification system and recommendations from the Baltimore consensus meeting for neoplastic precursor lesions in the pancreas. Am J Surg Pathol. 2015;39:1730–41.
10. Mino-Kenudson M, Fernández-del Castillo C, Baba Y, Valsangkar NP, Liss AS, Hsu M, et al. Prognosis of invasive intraductal papillary mucinous neoplasm depends on histological and precursor epithelial subtypes. Gut. 2011;60:1712–20.
11. Tsujimae M, Masuda A, Shiomi H, Toyama H, Sofue K, Ueshima E, et al. Significance of pancreatic calcification on preoperative computed tomography of intraductal papillary mucinous neoplasms. J Gastroenterol Hepatol. 2019;34:1648–55.
12. The European Study Group on Cystic Tumors of the Pancreas. European evidence-based guidelines on pancreatic cystic neoplasms. Gut. 2018;67:789–804.
13. Longnecker DS, Adsay NV, Fernandez-del Castillo C, Hruban RH, Kasugai T, Klimstra DS, et al. Histopathological diagnosis of pancreatic intraepithelial neoplasia and intraductal papillary-mucinous neoplasms: interobserver agreement. Pancreas. 2005;31:344–9.
14. Katabi N, Klimstra DS. Intraductal papillary mucinous neoplasms of the pancreas: clinical and pathological features and diagnostic approach. J Clin Pathol. 2008;61:1303–13.
15. Felsenstein M, Noe M, Masica DL, Hosoda W, Chianchiano P, Fischer CG, et al. IPMNs with co-occurring invasive cancers: neighbours but not always relatives. Gut. 2018;67:1652–62.
16. Yamaguchi K, Kanemitsu S, Hatori T, Maguchi H, Shimizu Y, Tada M, et al. Pancreatic ductal adenocarcinoma derived from IPMN and pancreatic ductal adenocarcinoma concomitant with IPMN. Pancreas. 2011;40:571–80.
17. Kelly PJ, Shinagare S, Sainani N, Hong X, Ferrone C, Yilmaz O, et al. Cystic papillary pattern in pancreatic ductal adenocarcinoma: a heretofore undescribed morphologic pattern that mimics intraductal papillary mucinous carcinoma. Am J Surg Pathol. 2012;36:696–701.
18. Nakanuma Y, Uesaka K, Miyayama S, Yamaguchi H, Ohtsuka M. Intraductal neoplasms of the bile duct. A new challenge to biliary tract tumor pathology. Histol Histopathol. 2017;32:1001–15.
19. Schlitter AM, Jang KT, Kloppel G, Saka B, Hong SM, Choi H, et al. Intraductal tubulopapillary neoplasms of the bile ducts: clinicopathologic, immunohistochemical, and molecular analysis of 20 cases. Mod Pathol. 2015;28:1249–64.
20. Wang T, Askan G, Adsay V, Allen P, Jarnagin WR, Memis B, et al. Intraductal papillary neoplasms: clinical-pathological characterization of 24 cases, with an emphasis on associated invasive carcinomas. Am J Surg Pathol. 2019;43:656–61.
21. Marchegiani G, Mino-Kenudson M, Ferrone CR, Warshaw AL, Lilleme KD, Fernandez-del Castillo C. Oncocytic-type intraductal papillary mucinous neoplasms: a unique malignant pancreatic tumor with good long-term prognosis. J Am Coll Surg. 2015;220:839–44.
22. Wang YZ, Lu J, Jiang BL, Guo JC. Intraductal oncocytic papillary neoplasm of the pancreas: a systematic review. Pancreatology. 2019;19:858–65.
23. Basturk O, Tan M, Bhanot U, Allen P, Adsay V, Scott SN, et al. The oncocytic subtype is genetically distinct from other pancreatic intraductal papillary mucinous neoplasm subtypes. Mod Pathol. 2016;29:1058–69.
24. Basturk O, Adsay V, Askan G, Dhall D, Zamboni G, Shimizu M, et al. Intraductal tubulopapillary neoplasm of the pancreas: a clinicopathologic and immunohistochemical analysis of 33 cases. Am J Surg Pathol. 2017;41:313–25.
25. Date K, Okabayashi T, Shima Y, Iwata J, Sumiyoshi T, Kozuki A, et al. Clinicopathological features and surgical outcomes of intraductal tubulopapillary neoplasm of the pancreas: a systematic review. Langenbeck's Arch Surg. 2016;401:439–47.
26. Inomata K, Kitago M, Obara H, Fujii-Nishimura Y, Shinoda M, Yagi H, et al. Concurrent presentation of

an intraductal tubulopapillary neoplasm and intraductal papillary mucinous neoplasm in the branch duct of the pancreas, with a superior mesenteric artery aneurysm: a case report. World J Surg Oncol. 2018;16:83.
27. Ahls MG, Niedergethmann M, Dinter D, Sauer C, Luttges J, Post S, et al. Case report: intraductal tubulopapillary neoplasm of the pancreas with unique clear cell phenotype. Diagn Pathol. 2014;9:11.
28. Takayama S, Maeda T, Nishihara M, Kanazawa A, Chong HS, Oka H, et al. A case of intraductal tubulopapillary neoplasm of pancreas with severe calcification, a potential pitfall in diagnostic imaging. Pathol Int. 2015;65:501–6.
29. Jokoji R, Tsuji H, Tsujimoto M, Shinno N, Torri M. Intraductal tubulopapillary neoplasm of pancreas with stromal osseous and cartilaginous metaplasia; a case report. Pathol Int. 2012;62:339–43.
30. Muraki T, Uehara T, Sano K, Oota H, Yoshizawa A, Asaka S, et al. A case of MUC5AC-positive intraductal neoplasm of the pancreas classified as an intraductal tubulopapillary neoplasm. Pathol Res Pract. 2015;211:1034–9.
31. Basturk O, Berger MF, Yamaguchi H, Adsay V, Askan G, Bhanot UK, et al. Pancreatic intraductal tubulopapillary neoplasm is genetically distinct from intraductal papillary mucinous neoplasm and ductal adenocarcinoma. Mod Pathol. 2017;30:1760–72.
32. Adsay V, Mino-Kenudson M, Furukasa T, Basturk O, Zamboni G, Marchegiani G, et al. Pathologic evaluation and reporting of intraductal papillary mucinous neoplasms of the pancreas and other tumoral intraepithelial neoplasms of pancreatobiliary tract. Recommendations of Verona consensus meeting. Ann Surg. 2016;263:162–77.
33. Furukawa T, Hatori T, Fujita I, Yamamoto M, Kobayashi M, Ohike N, et al. Prognostic relevance of morphological types of intraductal papillary mucinous neoplasms of the pancreas. Gut. 2011;60:509–16.
34. Sahora K, Fernández-del Castillo C, Dong F, Marchegiani G, Thayer SP, Ferrone CR, et al. Not all mixed-type intraductal papillary mucinous neoplasms behave like main-duct lesions: implications of minimal involvement of the main pancreatic duct. Surgery. 2014;156:611–21.
35. Nakata K, Ohuchida K, Aishima S, Sadakari Y, Kayashima T, Miyasaka Y, et al. Invasive carcinoma derived from intestinal-type intraductal papillary mucinous neoplasm is associated with minimal invasion, colloid carcinoma, and less invasive behavior, leading to a better prognosis. Pancreas. 2011;40:581–7.
36. Yopp AC, Katabi N, Janakos M, Klimstra DS, D'Angelica MI, DeMatteo RP, et al. Invasive carcinoma arising in intraductal papillary mucinous neoplasms of the pancreas: a matched control study with conventional pancreatic ductal adenocarcinoma. Ann Surg. 2011;253:968–74.
37. Nara S, Shimada K, Kosuge T, Kanai Y, Hiraoka N. Minimally invasive intraductal papillary-mucinous carcinoma of the pancreas: clinicopathologic study of 104 intraductal papillary-mucinous neoplasms. Am J Surg Pathol. 2008;32:243–55.
38. Navez J, Hubert C, Gigot JF, Borbath I, Annet L, Sempoux C, et al. Impact of intraoperative pancreatoscopy with intraductal biopsies on surgical management of intraductal papillary mucinous neoplasm of the pancreas. J Am Coll Surg. 2015;221:982–7.
39. Del Chiaro M, Verbeke C. Intraductal papillary mucinous neoplasms of the pancreas: reporting clinically relevant features. Histopathology. 2017;70:850–60.

Further Reading

Basturk O, Esposito I, Fukushima N, Furukawa T, Hong SM, Klöppel G, et al. Pancreatic intraductal papillary mucinous neoplasm. In: Lokuhetty D, White VA, Watanabe R, Cree IA, editors. Digestive system tumours, WHO classification of tumours. 5th ed. Lyon: IARC Press; 2019. p. 310–4.

Basturk O, Esposito I, Fukushima N, Furukawa T, Hong SM, Klöppel G, et al. Pancreatic intraductal oncocytic papillary neoplasm. In: Lokuhetty D, White VA, Watanabe R, Cree IA, editors. Digestive system tumours, WHO classification of tumours. 5th ed. Lyon: IARC Press; 2019. p. 315–6.

Basturk O, Esposito I, Fukushima N, Furukawa T, Hong SM, Klöppel G, et al. Pancreatic intraductal tubulopapillary neoplasm. In: Lokuhetty D, White VA, Watanabe R, Cree IA, editors. Digestive system tumours, WHO classification of tumours. 5th ed. Lyon: IARC Press; 2019. p. 317–8.

Solid Pseudopapillary Neoplasia 18

Solid pseudopapillary neoplasm (SPN) is a low-grade malignant epithelial neoplasm of uncertain cellular origin. It is characteristically composed of a mixture of solid areas, blood-lakes, cysts, and pseudopapillae within a fibrous capsule. Very rare examples have been described outwith the pancreas, for example, in the retroperitoneum, omentum, mesocolon, and ovary. The possibility that involvement of these extrapancreatic sites may represent metastatic disease from a pancreatic primary should always be considered.

18.1 WHO Classification

Solid pseudopapillary neoplasm is classified as a malignant epithelial tumor in the 2019 WHO classification of tumors of the pancreas [1].

18.2 Terminology

Solid pseudopapillary neoplasm is the currently recognized terminology for this tumor, which has been referred to previously as Frantz tumor, Hamoudi's tumor, solid and papillary epithelial neoplasm, solid and cystic tumor, and papillary cystic tumor.

18.3 Epidemiology

Solid pseudopapillary neoplasm (SPN) is a rare neoplasm accounting for approximately 5% of cystic neoplasms of the pancreas. There has been an increase in the incidence of SPNs in the last two decades, probably due to the more frequent use of modern imaging techniques. It occurs predominantly in adolescent girls and young women (80–90% of cases), but has been reported in childhood, and can occur in men. The mean age of presentation in females is 30 years, while men have a mean age of 40 years. The age range is 2–85 years. The etiology is unknown.

18.4 Clinical Features

SPN can be asymptomatic and found incidentally on imaging during clinical evaluation for other conditions. Patients may present with abdominal pain, back pain, early satiety, nausea and vomiting, a palpable mass, or an acute abdomen (following rupture and hemoperitoneum). Jaundice is exceedingly rare.

18.4.1 Associations

SPN is not associated with any clinical syndromes. Tumor growth may be accelerated dur-

© Springer Nature Switzerland AG 2021
F. Campbell, C. S. Verbeke, *Pathology of the Pancreas*,
https://doi.org/10.1007/978-3-030-49848-1_18

ing pregnancy, secondary to the influence of progesterone.

18.4.2 Imaging

Imaging usually shows a large, well-circumscribed, solid and cystic neoplasm. There is commonly a large central cystic area, but the size and location of the cystic change is variable. There may be calcification within the tumor or at the periphery.

18.5 Macroscopy

SPNs are large, round, well circumscribed, soft, and usually solitary, although there are case reports of multicentric tumors. They can occur anywhere within the pancreas. They may appear to be encapsulated and have a pushing border, but they can show irregular extension into the adjacent pancreas, and occasionally may extend into adjacent organs such as the colon, duodenum, kidney, or spleen. They can vary in size from 1 to 25 cm (mean size 10 cm). Cut-section reveals lobulated, brown, soft, friable, solid areas, together with areas of hemorrhage, and cysts filled with degenerate tumor debris (Fig. 18.1).

Small tumors (Fig. 18.2) may be entirely solid (the cystic change is a degenerative feature), while large tumors may be entirely cystic (Fig. 18.3), mimicking other cystic lesions, with residual tumor only present at the periphery.

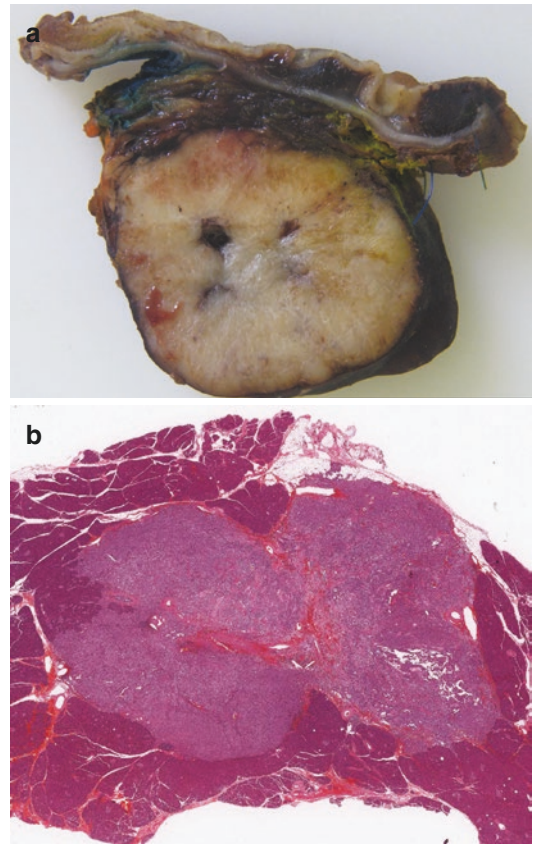

Fig. 18.2 Solid pseudopapillary neoplasm (SPN): cross-section of this small SPN shows a solid, yellow-white cut-surface with only very focal hemorrhage (**a**). Microscopy of this small mainly solid SPN shows central hemorrhage and cholesterol clefts with (*lower right*) early cystic degeneration and pseudopapillae formation (**b**)

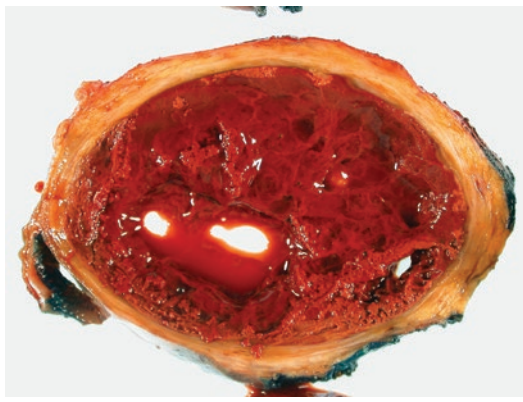

Fig. 18.1 Solid pseudopapillary neoplasm: cross-section showing fibrous capsule and hemorrhagic, degenerate, soft, brown tumor with cystic spaces

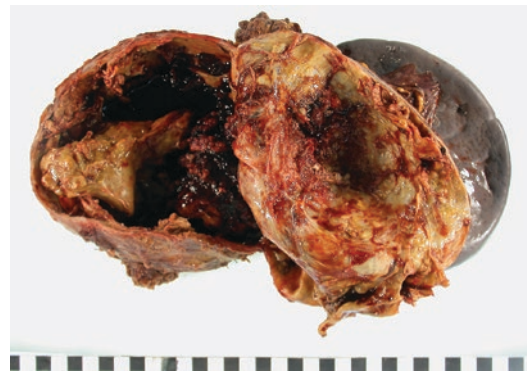

Fig. 18.3 Solid pseudopapillary neoplasm: this large solid pseudopapillary neoplasm is entirely cystic with shaggy degenerate residual tumor adherent to the fibrous capsule

18.5.1 Sampling

Cystic and degenerative areas should be sampled, as well as the solid tumor, since the pseudopapillae will be found in the cystic areas. In grossly cystic tumors, the wall should be sampled thoroughly to identify the residual tumor, and allow distinction from other cystic lesions (see Sect. 18.10).

18.6 Microscopy

SPNs are composed of poorly-cohesive, monomorphic, uniform epithelial cells forming solid nests and sheets, together with pseudopapillae (Fig. 18.4). There are bands of hyalinized and myxoid stroma (Fig. 18.5) containing small thin-walled blood vessels, which form the stalks of the pseudopapillae (Fig. 18.6). Degenerative changes include hemorrhage, cystic spaces (Fig. 18.7), cholesterol clefts with associated foreign-body-type giant cells, foamy macrophages (Fig. 18.8), and foci of calcification and, rarely, ossification. Infarction may also occur, but true tumor necrosis is not seen. Although the tumor is usually macroscopically well-demarcated from the normal pancreas, often by a fibrous capsule that may be incomplete (Figs. 18.1 and 18.7), microscopically, the neoplastic cells can infiltrate the capsule (Fig. 18.9a) and into the adjacent pancreas (Figs. 18.9b and c) or duodenum. This infiltration of the capsule or of adjacent structures has no prognostic significance.

The uniform neoplastic cells have a moderate amount of eosinophilic (Fig. 18.10a), foamy, or vacuolated cytoplasm (Fig. 18.10b), and centrally-located, round-to-oval, uniform nuclei with finely dispersed chromatin. The nuclei may be indented or have longitudinal grooves (Fig. 18.11). Eosinophilic hyaline globules of varying sizes may be seen within the cytoplasm of the neoplastic cells or extracellularly (Fig. 18.12). These globules are D-PAS positive and stain for alpha-1-an-

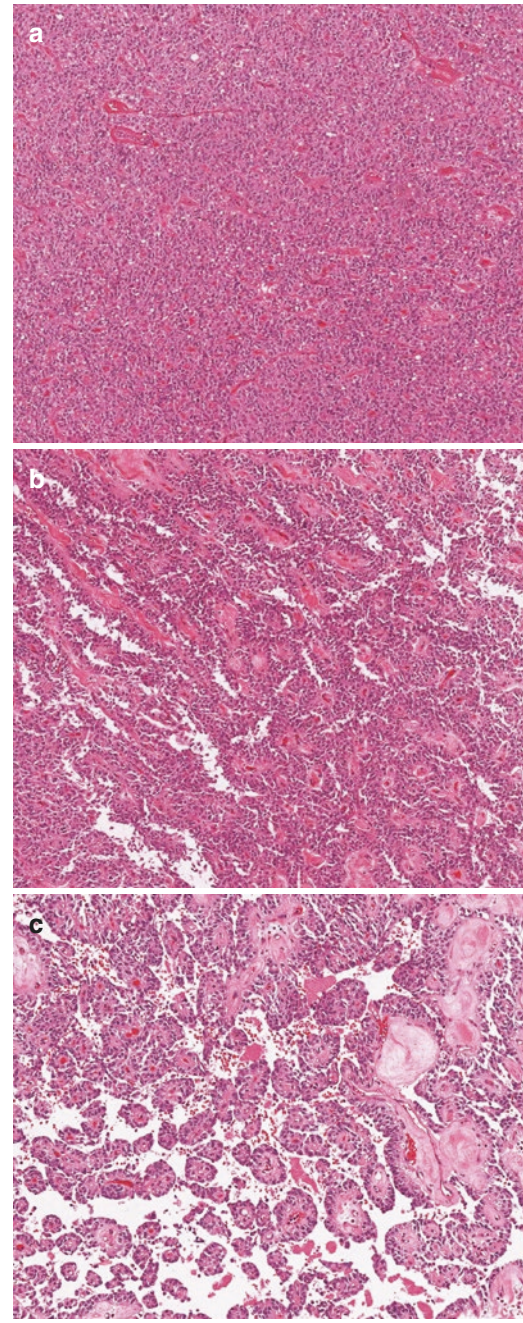

Fig. 18.4 Solid pseudopapillary neoplasm: solid sheets of uniform epithelial cells with delicate bands of fibrous stroma (**a**). As solid pseudopapillary neoplasms undergo degeneration, there is loss of adhesion between tumor cells, and small slit-like spaces develop between groups of tumor cells (**b**). These spaces enlarge to form macroscopically visible cystic areas, within which pseudopapillae can be found (**c**)

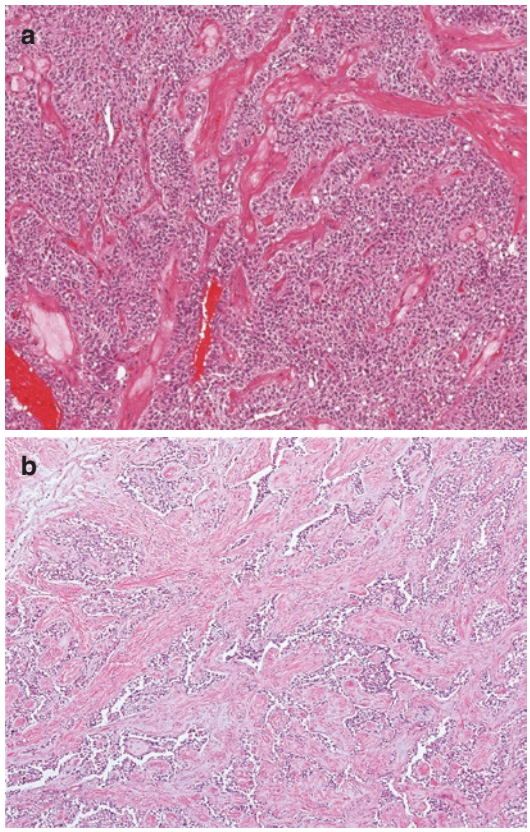

Fig. 18.5 Solid pseudopapillary neoplasm: the stroma is present as variably-sized bands of sclerotic and myxoid collagen (**a**). In this example, there is abundant myxohyaline stroma with only scanty groups of epithelial cells (**b**)

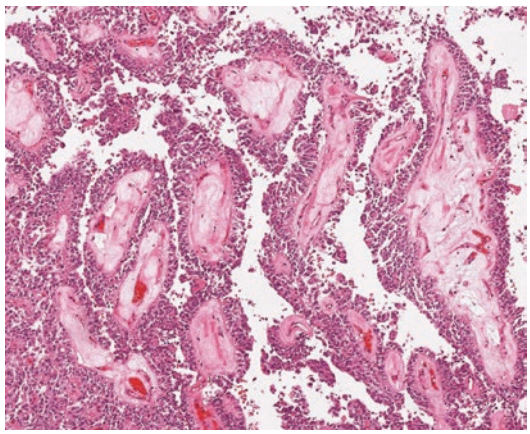

Fig. 18.6 Solid pseudopapillary neoplasm: the pseudopapillae have cores of myxoid stroma containing small capillary-sized blood vessels

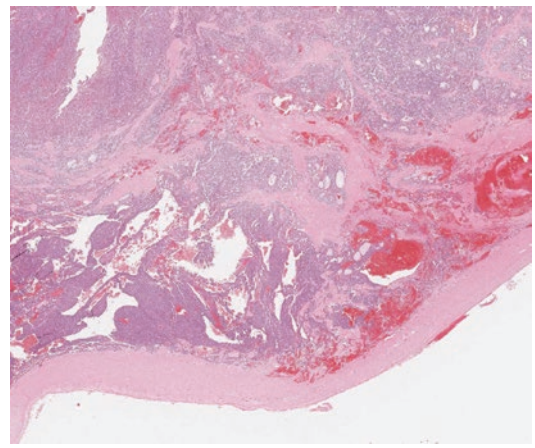

Fig. 18.7 Solid pseudopapillary neoplasm: there is a characteristic mixture of solid areas, blood-lakes, cysts, and pseudopapillae, together with a distinct fibrous capsule

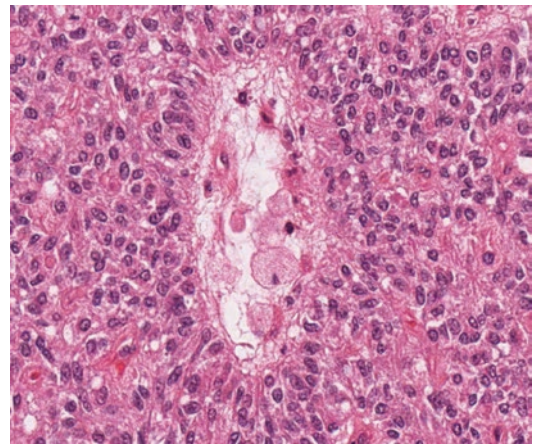

Fig. 18.8 Solid pseudopapillary neoplasm: foamy macrophages (*center*) may be present within the tumor

titrypsin (A1AT) or alpha-1-antichymotrypsin (A1ACT) on immunohistochemistry. They may only be present in focal areas of the neoplasm. There is no mucin, and mitotic figures are rare. Vascular and perineural invasion (Fig. 18.13) may occasionally be found, but do not indicate aggressive behavior.

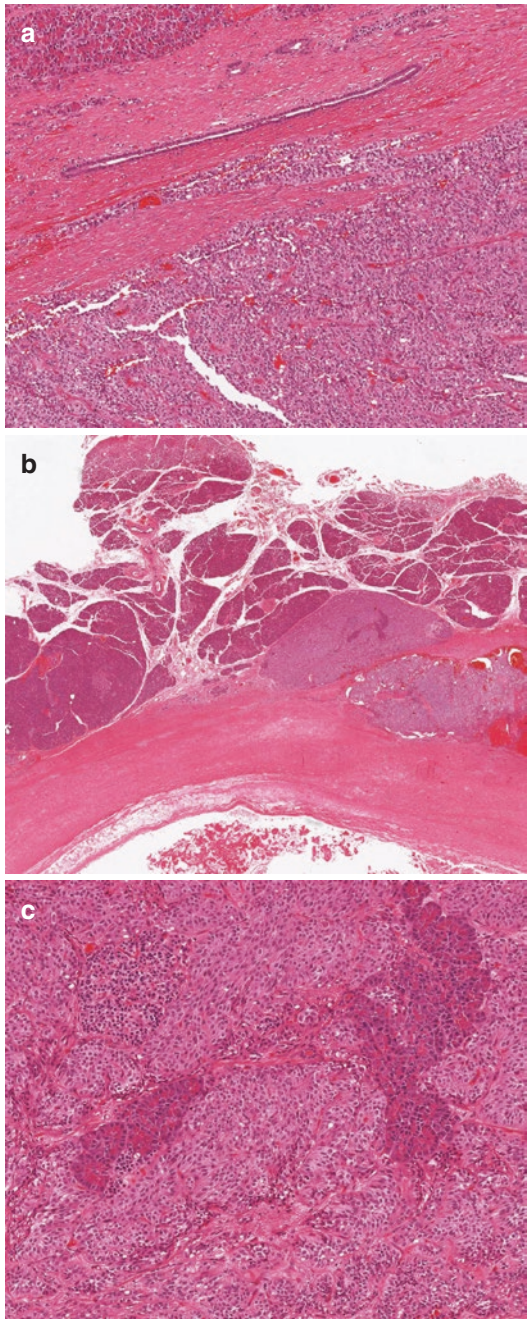

Fig. 18.9 Solid pseudopapillary neoplasm: tongues of neoplastic cells may infiltrate the capsule (**a**) or the adjacent pancreas (**b**). Here, the neoplastic cells infiltrate between and around normal pancreatic acinar cells and a single islet of Langerhans (*top left*) (**c**)

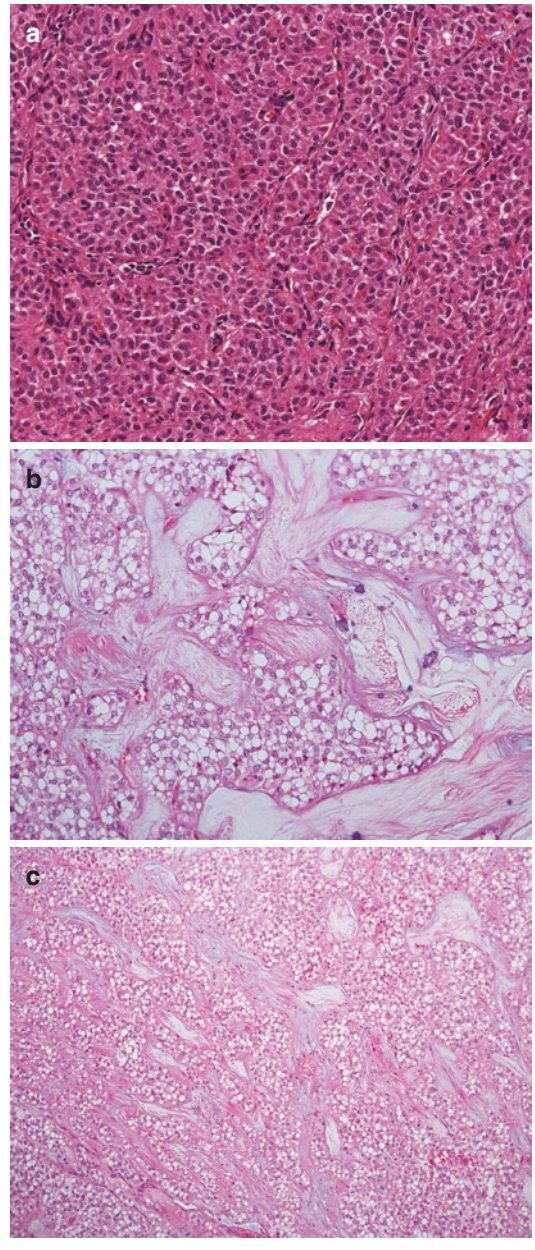

Fig. 18.10 Solid pseudopapillary neoplasm (SPN): the neoplastic cells may have eosinophilic cytoplasm (**a**) or vacuolated cytoplasm (**b**). In this example, the SPN is composed entirely of vacuolated tumor cells (**c**)

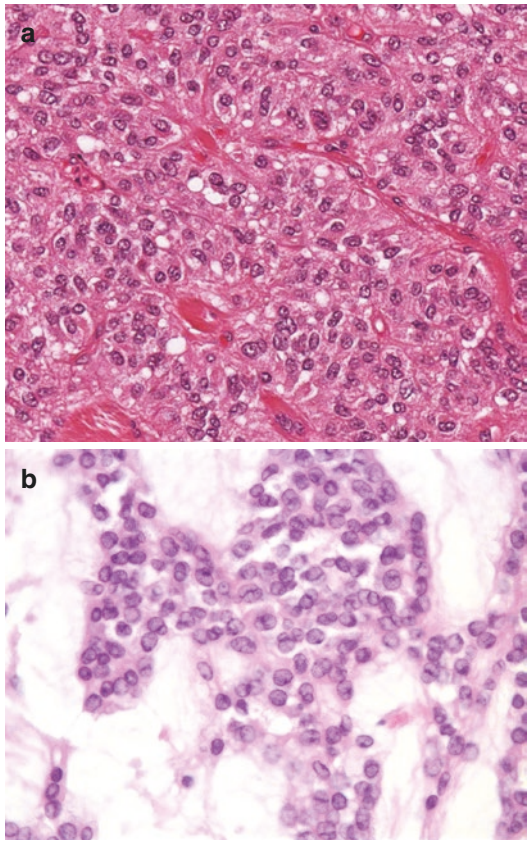

Fig. 18.11 Solid pseudopapillary neoplasm: the nuclei are uniform with irregular (indented) outlines, stippled chromatin (**a**) and occasional longitudinal grooves (**b**)

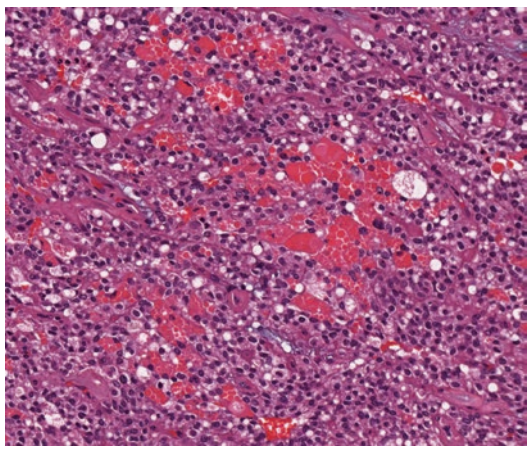

Fig. 18.12 Solid pseudopapillary neoplasm: abundant eosinophilic hyaline globules are present within and between tumor cells

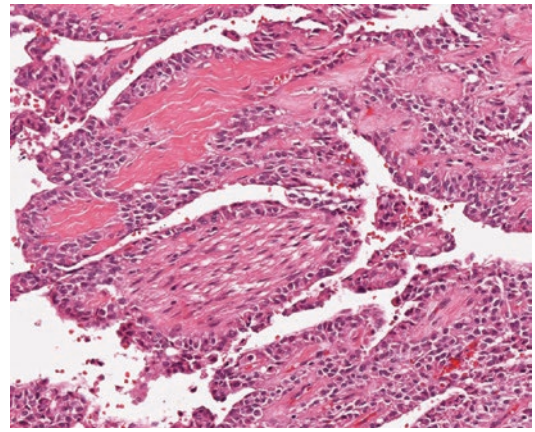

Fig. 18.13 Solid pseudopapillary neoplasm: tumor cells are seen around a single nerve (*center*). This does not indicate aggressive behavior

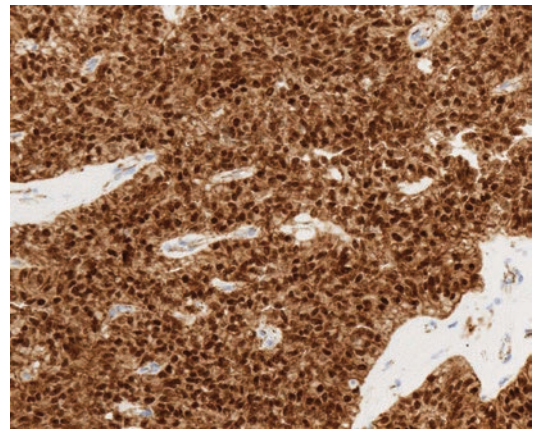

Fig. 18.14 Solid pseudopapillary neoplasm: abnormal nuclear and cytoplasmic immunopositivity with beta-catenin

18.7 Immunohistochemistry

Most SPNs will express vimentin, neuron-specific enolase, CD10, CD56, cyclin D1, beta-catenin—abnormal nuclear and cytoplasmic staining, rather than membranous staining—(Fig. 18.14), progesterone receptor, estrogen receptor beta, and CD99 (perinuclear dot-like staining). A1AT or A1ACT can be used to highlight the eosinophilic globules.

There may be some immunopositivity for synaptophysin and epithelial markers AE1-AE3 and CAM5.2, but there is usually no expression of cytokeratins 7 and 19. Ki67 proliferation index is low (typically <1%).

There is loss of membranous E-cadherin, and antibodies to chromogranin A, trypsin, pancreatic hormones, estrogen receptor-alpha, calretinin, and alpha-inhibin typically do not label the neoplastic cells.

A core panel of immunohistochemistry should include vimentin, beta-catenin, and progesterone receptor protein.

18.8 Molecular Pathology

Activation of the WNT signalling pathway through the oncogenic mutation of *CTNNB1* (the beta-catenin gene) is the major driver of SPN tumorigenesis. A somatic point mutation in exon 3 of *CTNNB1* is detected in almost all SPNs. Activating (gain-of-function) mutations of *CTNNB1* prevent degradation of the encoded protein beta-catenin, which accumulates in the nucleus. In the nucleus, beta-catenin activates transcription of the oncogene *CCND1* that is overexpressed in about 70% of SPNs [2]. SPNs are not associated with abnormalities in the *KRAS, p16* or *DPC4* genes. Recently it has been shown that inactivating mutations of the epigenetic regulators *BAP1* and *KDM6A* may be potential drivers of metastasis in SPNs [3].

18.9 Variants

Pigmented variants of SPN, due to the presence of either lipofuscin [4] or melanin [5], have been described, as has a *clear cell variant* [6]. SPN with *prominent microcystic pattern* has recently been described [7]. The microcystic pattern is characterized by a pseudocystic and/or microcystic arrangement of uniform tumor cells within myxoid stroma. The material within the microcysts is positive for Alcian blue, which is diminished after hyaluronidase digestion, leading the authors to suggest that stromal change caused by an accumulation of hyaluronan may contribute to the formation of the microcystic pattern.

A *pleomorphic variant* of SPN has been described in which 20–80% of the total tumor area had tumor cells with marked variation in nuclear size and shape, nuclear hyperchromasia, and occasional multinucleation, accompanied by abundant cytoplasm [8]. This nuclear pleomorphism was interpreted as a degenerative change, and was not associated with aggressive clinical behavior.

There are, however, very rare reported cases of SPN with *high-grade malignant transformation* (Fig. 18.15); such cases are now considered to be a histological subtype and are termed 'solid pseudopapillary neoplasm with high-grade carcinoma' in the 2019 WHO classification [1]. These neoplasms have areas of conventional

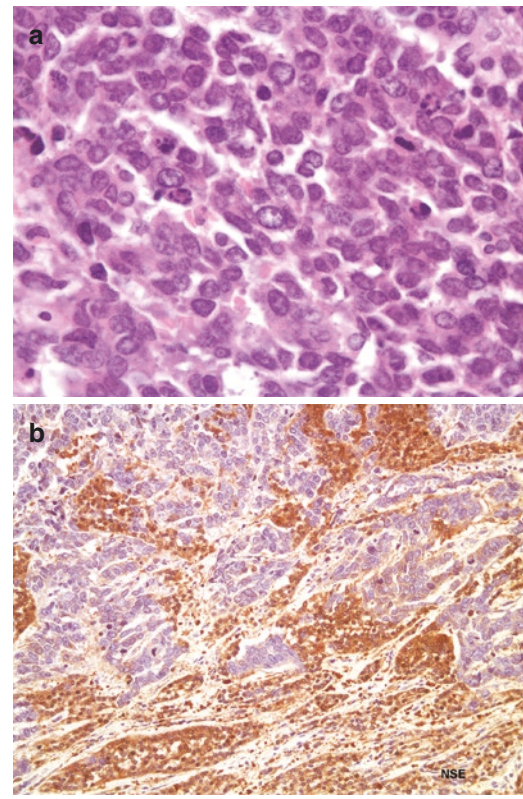

Fig. 18.15 Solid pseudopapillary neoplasm: within a conventional solid pseudopapillary neoplasm, there was this focus of high-grade malignant transformation with pleomorphic tumor cells (**a**) that had lost expression of neuron-specific enolase (NSE) (**b**)

SPN together with cellular sheets of tumor cells showing significant nuclear atypia, high mitotic count, and extensive tumor necrosis. There may also be undifferentiated or sarcomatoid components. They are clinically extremely aggressive, and in the two cases reported by Tang et al. [9] both patients died within 18 months of presentation.

18.10 Differential Diagnosis

18.10.1 Pseudocyst

Large entirely cystic SPNs (Fig. 18.3) may radiologically and macroscopically mimic a pseudocyst. However, pseudocysts are associated with a history of pancreatitis (unlike SPNs), have high levels of amylase in the cyst fluid (whereas SPNs have low levels), and, on microscopy, lack an epithelial lining (see Chap. 7, Sect. 7.2.5).

18.10.2 Pancreatic Endocrine Neoplasm

Small solid SPNs (Fig. 18.2a) and large cystic SPNs with only a small rim of residual tumor (Fig. 18.3) may mimic a typical, or a cystic, pancreatic neuroendocrine tumor, respectively (see Fig. 20.4). SPNs may also show a packeted growth pattern (Fig. 18.16) resembling a grade 1–3 pancreatic neuroendocrine tumor (PanNET). Both SPNs and PanNETs can affect younger patients. Grade 1–3 PanNETs do not show the degenerative changes found in SPNs such as pseudopapillae with fibrovascular stalks, foamy macrophages, and cholesterol clefts. Grade 1–3 PanNETs are characterized by cells with relatively uniform round/oval nuclei showing stippled chromatin, so-called 'salt and pepper' nuclei (see Chap. 20, Sects. 20.5.1 and 20.9.1). In contrast, the nuclei in SPNs are often grooved or indented (Fig. 18.11). The intracytoplasmic and extracellular eosinophilic hyaline globules that are typically seen in SPNs can also be found in up to 5% of PanNETs [10] (see Fig. 20.13). Both types of neoplasm can be immunopositive for synaptophysin and CD56, but chromogranin A is typically immunonegative in SPNs. Diffuse immunopositivity for vimentin, nuclear immunopositivity for beta-catenin, and loss of (membranous) E-cadherin will help distinguish SPNs from PanNETs (see Table 20.5), but it should be noted that a small proportion of PanNETs can be immunopositive for vimentin and nuclear beta-catenin. A clinical background of MEN1 or von Hippel-Lindau can also be useful in recognising PanNETs.

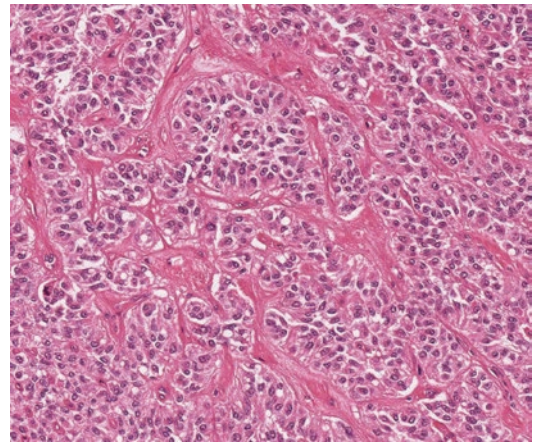

Fig. 18.16 Solid pseudopapillary neoplasm: the tumor cells in this solid pseudopapillary neoplasm are arranged in nests mimicking a pancreatic neuroendocrine tumor (PanNET)

18.10.3 Acinar Cell Carcinoma

Solid SPNs may mimic acinar cell carcinoma (see Chap. 10). Acinar cell carcinoma, however, occurs more frequently in men and typically in an older age group (mean age of 60 years). Acinar cell carcinomas are solid neoplasms characterized by cells with granular cytoplasm, round to oval nuclei with a single prominent nucleolus, and frequent mitoses. Mitoses are rarely seen in SPNs. Immunopositivity for trypsin, chymotrypsin, or lipase will be seen in acinar cell carcinoma, but not in SPN (see Table 20.5).

18.11 Staging

SPNs may be staged using the UICC TNM system for carcinoma of the exocrine pancreas, but most behave in an indolent fashion.

18.12 Prognosis and Management

The prognosis for SPN is generally excellent, even with locally advanced or metastatic disease. It has low malignant potential and, following complete resection, the 5-year survival rate is 95%. Incomplete resection may lead to recurrence in 5–15% of patients. Large tumor size, young patient age, tumor rupture, male gender, and Ki67 index ≥4% [11] have been reported to be potential risk factors for recurrent disease, but have not been confirmed in other studies [12]. Metastases occur in 5–15% of patients, usually to the liver and peritoneum, but occasionally to lymph nodes (Fig. 18.17), and are usually present at the time of presentation. However, metastases may occur many years after complete resection of the primary SPN. Patients with recurrence or metastases rarely die of their disease. There are no recognized pathological factors that can predict prognosis other than high-grade transformation (see Sect. 18.9) which is associated with aggressive behavior.

All SPNs should be surgically resected, provided the patient is fit for surgery [13].

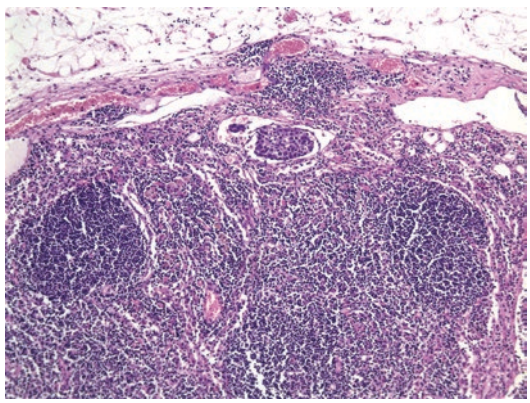

Fig. 18.17 Solid pseudopapillary neoplasm: lymph node metastasis in solid pseudopapillary neoplasm

Table 18.1 Reporting checklist for solid pseudopapillary neoplasm

Macroscopic assessment
• Specimen type
• Additional resected structures, e.g., spleen
• Tumor location
• Tumor size (3-dimensions)
• Cut-surface
• Involvement of adjacent organs
• Distance from resection margin(s)
Microscopic assessment
• Architecture (solid, cystic, pseudopapillae)
• Extension into adjacent organs
• Presence of (rare) high-grade transformation within the tumor
• Metastases
• Completeness of excision/ resection margin status
• Immunohistochemical profile
• UICC TNM staging
• Background changes

Recurrences and metastases can also be resected. There is very limited data on the role of neoadjuvant and adjuvant chemotherapy or radiotherapy. Given the indolent behavior of SPNs and the occurrence of metastases years after complete resection of the primary tumor, life-long follow-up is recommended [13].

18.13 Reporting Checklist

A list of macroscopic and microscopic features to consider when reporting a solid pseudopapillary neoplasm is shown in Table 18.1.

References

1. Lokuhetty D, White VA, Watanabe R, Cree IA. Digestive system tumours. WHO classification of tumours. 5th ed. Lyon: IARC Press; 2019. p. 296.
2. Tiemann K, Heitling U, Kosmahl M, Klöppel G. Solid pseudopapillary neoplasms of the pancreas show an interruption of the Wnt-signaling pathway and express gene products of 11q. Mod Pathol. 2007;20:955–60.
3. Amato E, Mafficini A, Hirabayashi K, Lawlor RT, Fassan M, Vicentini C, et al. Molecular alterations associated with metastases of solid pseudopapillary neoplasms of the pancreas. J Pathol. 2019;247:123–34.

4. Daum O, Sima R, Mukensnabl P, Vanecek T, Brouckova M, Benes Z, et al. Pigmented solid-pseudopapillary neoplasm of the pancreas. Pathol Int. 2005;55:280–4.
5. Chen C, Jing W, Gulati P, Vargas H, French SW. Melanocytic differentiation in a solid pseudopapillary tumor of the pancreas. J Gastroenterol. 2004;39:579–83.
6. Albores-Saavedra J, Simpson KW, Bilello SJ. The clear cell variant of solid pseudopapillary tumor of the pancreas: a previously unrecognized pancreatic neoplasm. Am J Surg Pathol. 2006;30:1237–42.
7. Abe A, Ohishi Y, Miyazaki T, Ozono K, Mochidome N, Saeki K, et al. 'Microcystic pattern' should be recognised as part of the morphological spectrum of solid-pseudopapillary neoplasm of the pancreas. Histopathology. 2018;72:216–26.
8. Kim SA, Kim MS, Kim MS, Kim SC, Choi J, Yu E, et al. Pleomorphic solid pseudopapillary neoplasm of the pancreas: degenerative change rather than high-grade malignant potential. Hum Pathol. 2014;45:166–74.
9. Tang LH, Aydin H, Brennan MF, Klimstra DS. Clinically aggressive solid pseudopapillary tumors of the pancreas: a report of two cases with components of undifferentiated carcinoma and a comparative clinicopathologic analysis of 34 conventional cases. Am J Surg Pathol. 2005;29:512–9.
10. Meriden Z, Shi C, Edil BH, Ellison T, Wolfgang CL, Cornish TC, et al. Hyaline globules in neuroendocrine and solid-pseudopapillary neoplasms of the pancreas: a clue to the diagnosis. Am J Surg Pathol. 2011;35:981–8.
11. Yang F, Yu X, Bao Y, Du Z, Jin C, Fu D. Prognostic value of Ki-67 in solid pseudopapillary tumor of the pancreas: Huashan experience and systematic review of the literature. Surgery. 2016;159:1023–31.
12. Gao H, Gao Y, Yin L, Wang G, Wei J, Jiang K, et al. Risk factors of the recurrences of pancreatic solid pseudopapillary tumours: a systematic review and meta-analysis. J Cancer. 2018;9:1905–14.
13. The European Study Group on Cystic Tumors of the Pancreas. European evidence-based guidelines on pancreatic cystic neoplasms. Gut. 2018;67:789–804.

Further Reading

Klöppel G, Basturk O, Klimstra DS, Lam AK, Notohara K. Solid pseudopapillary neoplasm of the pancreas. In: Lokuhetty D, White VA, Watanabe R, Cree IA, editors. Digestive system tumours. WHO classification of tumours. 5th ed. Lyon: IARC Press; 2019. p. 340–2.

Check for updates

19 Other Cystic Lesions

There are many different cystic lesions that occur in the pancreas, not all of which are neoplastic (see Table 14.2). Those with an epithelial lining can be classified according to the type of epithelium present (see Table 14.3) namely acinar, mucinous, pancreatobiliary, serous, or squamous.

Acinar cell-lined cystic lesions include acinar cystic transformation (see Sect. 19.1), cystic change in acinar cell carcinoma, and acinar cell cystadenocarcinoma (see Chap. 10).

Mucinous epithelium-lined cysts include mucinous cystic neoplasm (see Chap. 16), intraductal papillary mucinous neoplasm (see Chap. 17), and simple mucinous cyst (see Sect. 19.2.1).

Pancreatobiliary epithelium-lined cysts include choledochal cyst (of the common bile duct) and retention cysts. Both of these entities are discussed in this chapter.

All of the *serous* cystic lesions are discussed in Chap. 15.

Squamous epithelium-lined cysts include squamous-lined foregut (duplication) cysts (Fig. 19.1 and see Chap. 13), lymphoepithelial cyst, mature cystic teratoma (dermoid cyst), epidermoid cyst in intrapancreatic heterotopic spleen, squamoid cyst of pancreatic ducts, and squamous metaplasia in cystic lesions, including mucinous cystic neoplasm (see Chap. 16). These squamous epithelium-lined cysts are discussed in this chapter.

Pancreatic cystic lesions lacking an epithelial lining include pseudocysts (see Chap. 7, Sect. 7.2.5), lymphangioma, hemangioma, and mesenchymal tumors with cystic degeneration (see Chap. 11).

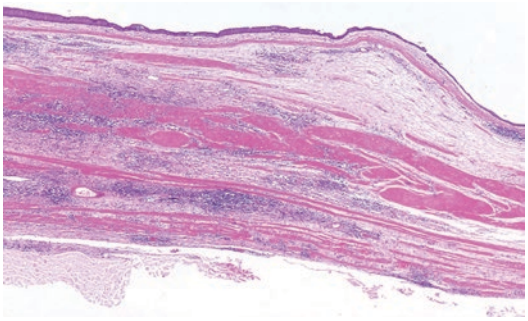

Fig. 19.1 Foregut cyst: squamous epithelium lines this foregut (duplication) cyst. Note the bundles of smooth muscle in the wall

Other cystic lesions which will be briefly discussed in this chapter include cystic hamartoma, duodenal diverticular disease, endometriotic cyst, and hydatid cyst.

19.1 Acinar Cystic Transformation (Acinar Cell Cystadenoma)

Acinar cystic transformation or acinar cell cystadenoma is a rare benign cystic epithelial lesion lined by cells with morphological and immunohistochemical resemblance to acinar cells. The entity was initially called 'cystic acinar transfor-

© Springer Nature Switzerland AG 2021
F. Campbell, C. S. Verbeke, *Pathology of the Pancreas*,
https://doi.org/10.1007/978-3-030-49848-1_19

mation' (of single acini or clusters of acini) [1], but subsequently the term 'acinar cell cystadenoma' was proposed [2, 3]. There has been uncertainty over whether it is a neoplastic or nonneoplastic lesion, but it is now considered to be nonneoplastic and, therefore, is no longer included in the 2019 WHO classification of pancreatic tumors [4]. In the 2019 WHO classification, 'acinar cystic transformation of the pancreas' is the preferred terminology for this entity, but 'acinar cell cystadenoma' can still be used.

Acinar cystic transformation of the pancreas occurs more frequently in women (female to male ratio 7:3) with a mean age at presentation of 50 years. However, it has been described in childhood [5], and the age range is 9–77 years. It is most frequently found in the head and body of the pancreas [6], usually as a solitary lesion, but it may be multifocal or involve the pancreas diffusely. It may also be an incidental microscopic finding in pancreata resected for other lesions (Fig. 19.2). Patients may present with abdominal pain or the lesion may be found incidentally on imaging.

19.1.1 Macroscopy

Acinar cystic transformation is a unilocular or multilocular, well-circumscribed, cystic lesion containing watery fluid. The mean size is 6 cm in diameter (range 1.5–15 cm). There may be a fibrous capsule. The multilocular variant has thin internal septa and is composed of multiple cysts varying in size from 1 mm to several centimeters (Fig. 19.3). The inner lining of the cysts is smooth.

19.1.2 Microscopy

The cysts contain eosinophilic and lamellated secretions and are lined by one or more layers of bland acinar cells (Fig. 19.4). The acinar cells contain eosinophilic granules in the apical cytoplasm and have basophilic staining at the base of the cell. There may be apical snouting of the cytoplasm (Fig. 19.4). The nuclei are uniform, basally located, and may have small nucleoli.

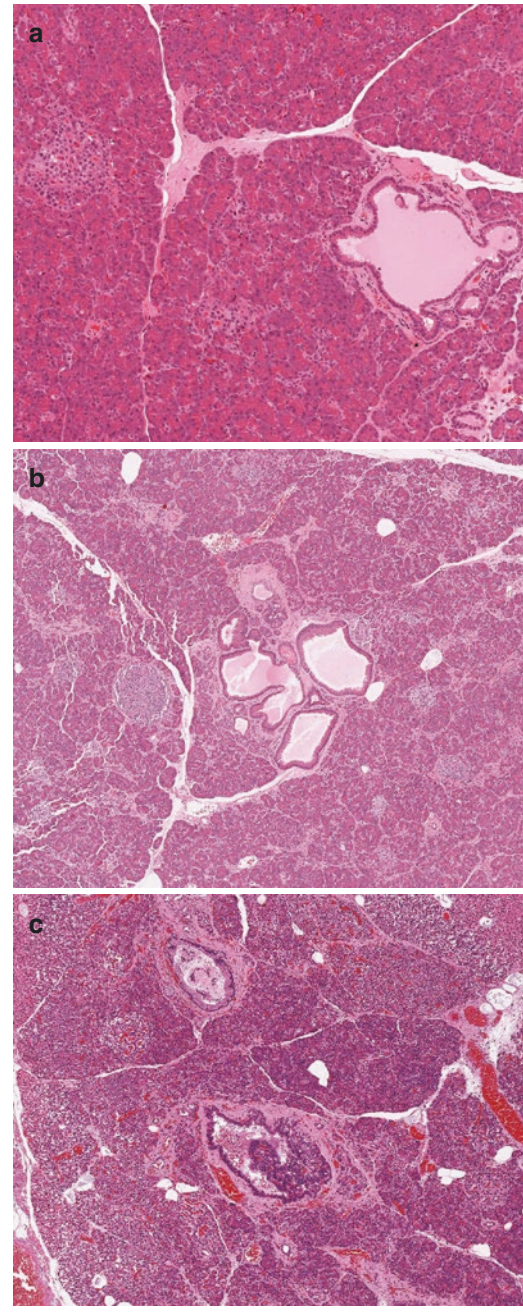

Fig. 19.2 Acinar cystic transformation: incidental microscopic acinar cell cystadenoma. These two examples (**a** & **b**) are not much bigger than the background islets of Langerhans. This larger example (**c**) is seen below a focus of low-grade PanIN

There may be invagination of the acinar cells into the underlying stroma and a rete-like appearance. Scanty pseudopapillae with fibro-

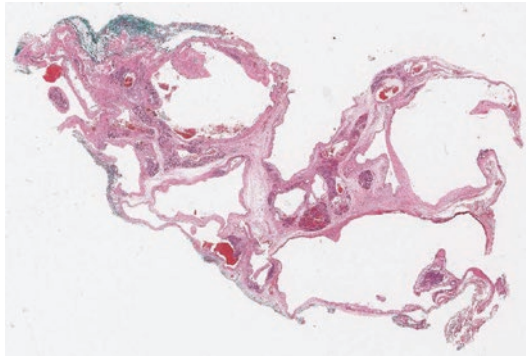

Fig. 19.3 Acinar cystic transformation: wholemount of multilocular acinar cystic transformation showing the smooth cystic outlines

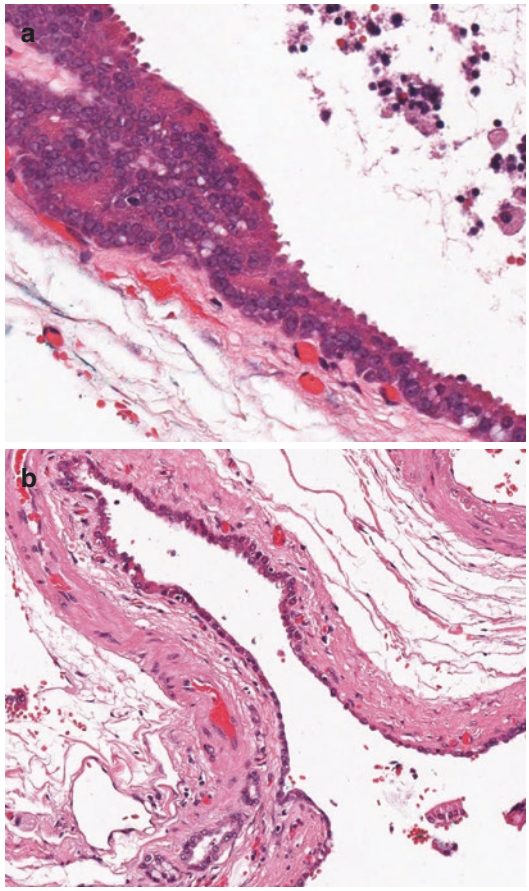

Fig. 19.4 Acinar cystic transformation: the cysts are lined by bland acinar cells with granular cytoplasm and basal nuclei with a single central nucleolus (**a**). There is snouting of the apical cytoplasm, which is also present in this attenuated lining where there is only a single layer of acinar cells (**b**)

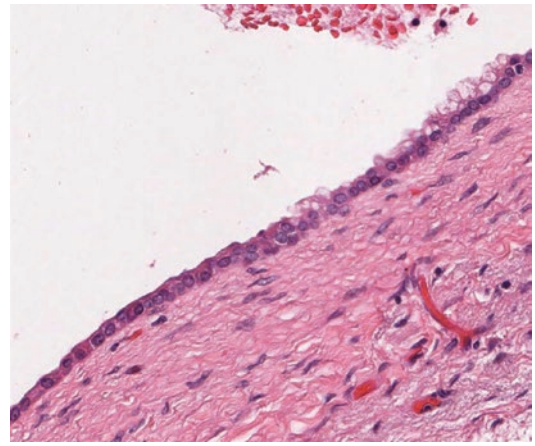

Fig. 19.5 Acinar cystic transformation: the lining may be heterogeneous. Attenuated acinar cells (*bottom half*) merge with a focus of bland mucinous cells (*top half*) lining the cyst

vascular cores have been described in multilocular cysts, as have nodules of acinar cells between the cysts [6].

There may be epithelial heterogeneity within the cysts [6]. As well as acinar cells, there may be foci of cuboidal ductal epithelium and bland mucinous epithelium (Fig. 19.5) lining the cyst. There may also be focal squamous metaplasia. Endocrine cells are not present. There is no epithelial atypia, mitoses are extremely rare, and there is no necrosis.

The cyst wall is usually fibrous and hyalinized (Figs. 19.4b and 19.5). Multilocular cysts may have focal calcification and osseous metaplasia in the wall. If the epithelium becomes denuded, there may be a histiocytic reaction in the wall.

19.1.3 Histochemistry and Immunohistochemistry

The cytoplasmic (zymogen) granules will stain with periodic acid-Schiff (PAS) and PAS-diastase. The acinar cells are immunopositive for trypsin (Fig. 19.6), chymotrypsin, BCL10, and lipase as well as CAM5.2, AE1-AE3, and the cytokeratins CK7, CK8, CK18, and CK19. The Ki67 proliferation index is less than 1%.

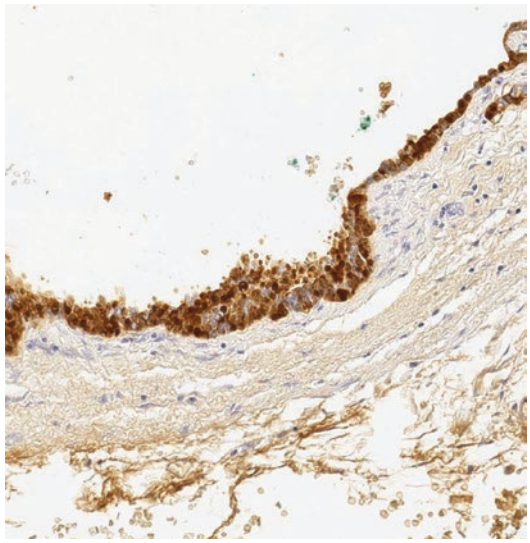

Fig. 19.6 Acinar cystic transformation: trypsin immunohistochemistry confirms the acinar cell lining of the cyst

19.1.4 Differential Diagnosis

Macroscopically, acinar cystic transformation may resemble a macrocystic serous cystadenoma (see Chap. 15) or a mucinous cystic neoplasm (see Chap. 16). Microscopy will reveal the clear, cuboidal, glycogen-rich epithelium of a macrocystic serous cystadenoma or the extensive mucinous epithelium and ovarian-type stroma of a mucinous cystic neoplasm.

Acinar cystic transformation may be distinguished from acinar cystadenocarcinoma by the absence of nuclear atypia, mitoses, necrosis, hemorrhage, solid or complex acinar cell growth pattern, and invasive growth.

Extrapancreatic acinar cell cystadenoma has been reported in the retroperitoneum [7]. The lesion showed the morphological and immunohistochemical features of acinar cell differentiation, but there was no connection with the pancreas. One reported case was located predominantly within the mesentery anterior to the pancreas [6]. However, on microscopy, an intrapancreatic component was identified.

19.1.5 Prognosis and Management

Acinar cystic transformation is entirely benign. Recurrence has not been reported following resection.

19.2 Mucinous Epithelium-Lined Cysts

19.2.1 Simple Mucinous Cyst (Mucinous Nonneoplastic Cyst)

In addition to intraductal papillary mucinous neoplasm and mucinous cystic neoplasm, there are macroscopically detectable pancreatic mucinous cysts greater than 1 cm in size that are lined by flat gastric-type epithelium with minimal cytological atypia, do not communicate with the pancreatic duct, and lack ovarian-type stroma. These mucinous cysts were originally described by Kosmahl et al. in 2002 [8], who reported no evidence of recurrence or malignant transformation in follow-up after resection, and proposed the term 'mucinous nonneoplastic cyst' for these cysts. In 2014, the Baltimore Consensus Meeting [9] recommended that the term 'mucinous nonneoplastic cyst' be changed to 'simple mucinous cyst'. Their pathogenesis is unclear.

Simple mucinous cysts are more common in women, and their frequency increases with age (mean age 65 years, range 20–90 years). They occur more commonly in the body and tail of the pancreas [10], and do not communicate with the duct system. Patients may be asymptomatic (cyst detected on imaging) or present with nonspecific symptoms or obstructive jaundice caused by compression of the common bile duct by the cyst.

The cysts are typically solitary, well circumscribed, round, unilocular or occasionally multilocular, average 2.5 cm in size (range 1.1–12 cm), and are filled with serous or thick viscous fluid. The multilocular cysts are characterized by 2–4 cysts separated by thin septa. The cysts are lined by a single layer of bland cuboidal to columnar mucinous epithelium with basal nuclei, no

atypia, and no mitotic figures. Beneath the epithelium, there is a thin band of paucicellular stroma, which may be hyalinized and, occasionally, show calcification and osseous metaplasia. On immunohistochemistry, they express CK7, CK8, CK18, and CK19. The majority show strong diffuse immunopositivity with MUC5AC and/or MUC6, there may be expression of MUC1, and there may also be focal immunopositivity for CDX2 and/or MUC2 despite the lack of obvious goblet cells.

Cyst fluid carcinoembryonic antigen (CEA) is elevated in most samples, and up to 55% of these cysts harbor *KRAS* mutations [10, 11]. The latter indicates that some of these cysts should be considered to be neoplastic.

Simple mucinous cysts are benign and should be distinguished from mucinous cystic neoplasm (see Chap. 16) and intraductal papillary mucinous neoplasm (see Chap. 17), both of which have malignant potential. Mucinous cystic neoplasms (MCNs) show atypia within the mucinous epithelium and the characteristic ovarian-type stroma. However, the epithelium within low-grade MCNs may be bland, and the ovarian-type stroma may be replaced by hyalinized collagen. Therefore, extensive sampling of the cyst wall may be needed to identify residual ovarian-type stroma. Intraductal papillary mucinous neoplasms, in contrast to simple mucinous cysts, communicate with the duct system, typically have well-formed papillae with fibrovascular cores (but may have an attenuated/flat lining), and show epithelial atypia. Some small mucinous epithelium-lined cysts may represent retention cysts lined by low-grade PanIN. Simple mucinous cysts, however, are not associated with obstruction and do not communicate with the duct system.

19.3 Pancreatobiliary Epithelium-Lined Cysts

19.3.1 Retention Cyst

Retention cysts (simple cysts) are unilocular cysts formed by the dilatation of an obstructed pancreatic duct (Fig. 19.7). They may be single

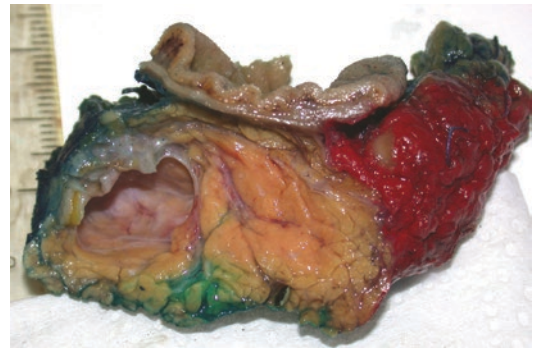

Fig. 19.7 Retention cyst: single cyst with smooth lining

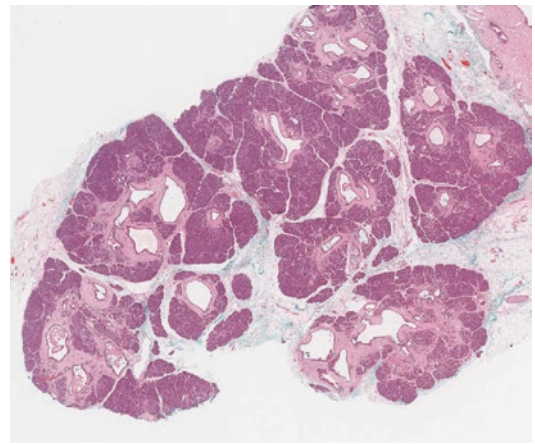

Fig. 19.8 Retention cyst: multiple small cysts which are clearly dilated ducts

or multiple (Fig. 19.8), and are typically less than 1–2 cm in size. The obstruction can be extrinsic to the pancreatic ducts (e.g., fibrosis in chronic pancreatitis or adenocarcinoma) or luminal (e.g., viscid mucin of cystic fibrosis, calculi in chronic pancreatitis, or intraductal neoplasm).

Retention cysts are lined by a single layer of normal, often attenuated, pancreatobiliary-type epithelium, which can become denuded. Eosinophilic secretions are often present within the lumen (Fig. 19.9), and, if large, may be macroscopically visible as white, soft, or rubbery material (see Fig. 7.45). There may be squamous metaplasia or focal low-grade PanIN (Fig. 19.10). Involvement of a retention cyst by low-grade PanIN may mimic a branch-duct-type intraductal papillary mucinous neoplasm

(IPMN). However, IPMNs typically have abundant mucin within the dilated duct lumen and well-formed, tall complex papillae with fibrovascular cores.

19.3.2 Choledochal Cyst

Choledochal cysts (also known as bile duct cysts) are congenital cystic dilatations of the bile ducts, which occur most often in the common bile duct and, radiologically, may mimic a pancreatic cyst. The segmental cystic dilatation of the common bile duct may be spherical or fusiform. Bile is present in the lumen and the cyst wall is lined by normal pancreatobiliary-type epithelium with underlying fibrous stroma. The epithelium may be attenuated or denuded and replaced by granulation tissue. It may also show pyloric, intestinal, or squamous metaplasia. In cystic dilatation of the common bile duct at the ampulla, so called choledochocele, the lining may include duodenal mucosa. Recognising that the 'cyst' involves the common bile duct will enable distinction from pancreatic cysts such as retention cysts.

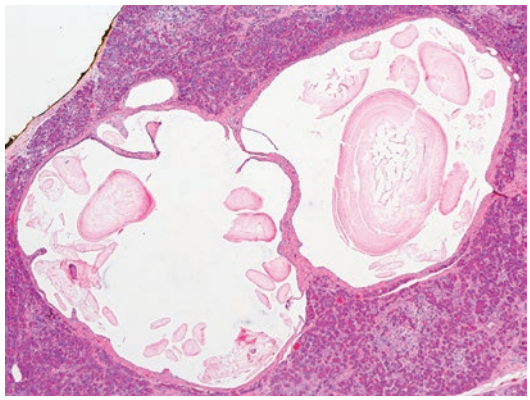

Fig. 19.9 Retention cyst: eosinophilic inspissated secretions within the cysts

19.4 Squamous Epithelium-Lined Cysts

19.4.1 Lymphoepithelial Cyst

Lymphoepithelial cysts are the most common, squamous epithelial-lined pancreatic cyst and occur anywhere in the pancreas. They are benign cysts and occur more frequently in men (male to female ratio 4:1) with a mean age at presentation of 56 years. Patients present with nonspecific symptoms (including pain, nausea, and anorexia) or are asymptomatic with the cyst detected incidentally on imaging.

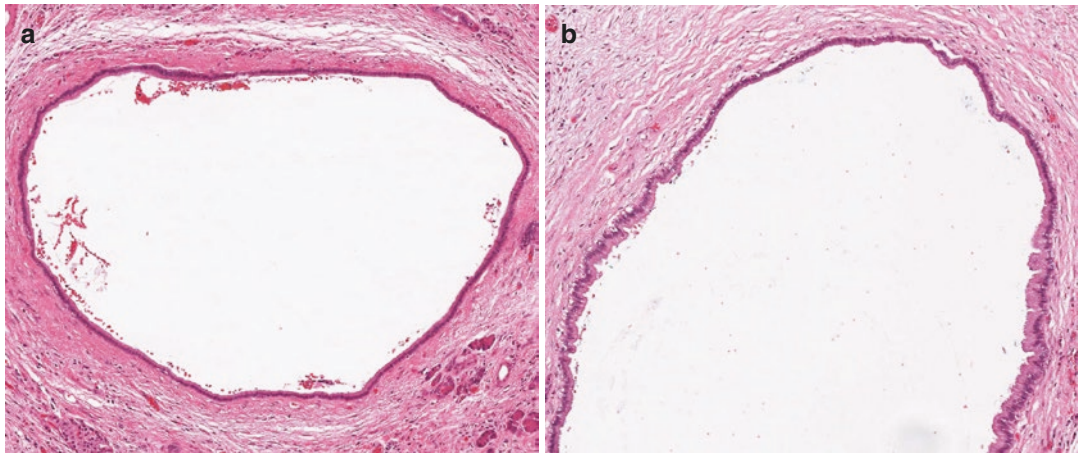

Fig. 19.10 Retention cyst: the lining is composed of normal pancreatobiliary epithelium (**a**). In this adjacent retention cyst (**b**), however, the pancreatobiliary-type epithelium (*top*) has been partially replaced (*both sides*) by bland, columnar, mucinous epithelium (low-grade PanIN)

The cysts range from 1 to 17 cm in size and may be unilocular or multilocular with thin septa between the locules. They are well circumscribed and often peripancreatic (Fig. 19.11). The wall is usually only 1–3 mm thick and there is abundant keratin debris within the lumen.

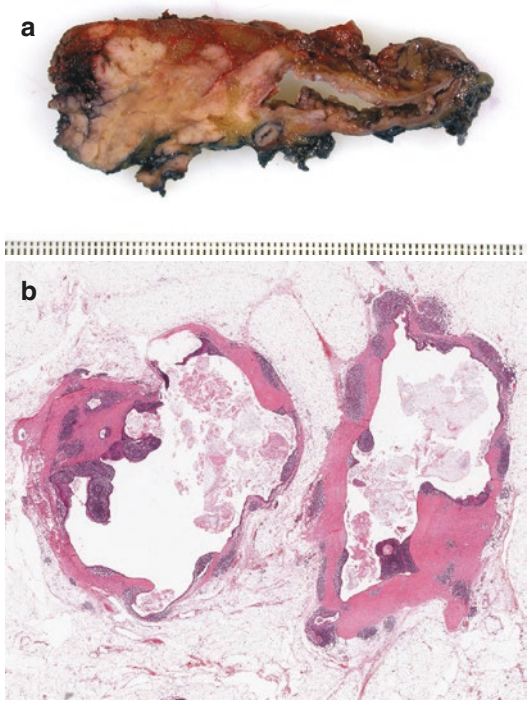

Fig. 19.11 Lymphoepithelial cyst: the cyst is present (**a**) in the peripancreatic fat (*right*). This wholemount shows the peripancreatic location of the cyst and the irregular fibrous wall containing patchy lymphoid tissue (**b**)

The cysts are lined by mature stratified squamous epithelium and surrounded by a dense rim of nonneoplastic lymphoid tissue with scattered lymphoid follicles (Fig. 19.12). The lymphoid tissue may form a band around the entire cyst or may be patchy (Fig. 19.11b).

The squamous epithelium is usually keratinizing with a prominent granular layer (Fig. 19.12b). However, it may be non-keratinizing and, in areas, flat and cuboidal. There may be occasional sebaceous cells and mucinous cells scattered within the epithelium, but skin adnexal structures are not present. The squamous epithelium can invaginate into the lymphoid tissue or be denuded and associated with cholesterol clefts, macrophages, and foreign-body-type giant cells in the cyst wall. The adjacent pancreas is usually entirely normal.

19.4.1.1 Differential Diagnosis

The differential diagnosis for a lymphoepithelial cyst includes mature cystic teratoma (dermoid cyst) and squamous epithelial cyst (epidermoid cyst) arising in intrapancreatic heterotopic spleen (see Sect. 19.4.3). Although lymphoepithelial cysts may have small foci of mucinous cells or sebaceous cells in the epithelium, they do not have associated skin adnexal structures. If adnexal structures (e.g., sebaceous glands or hair

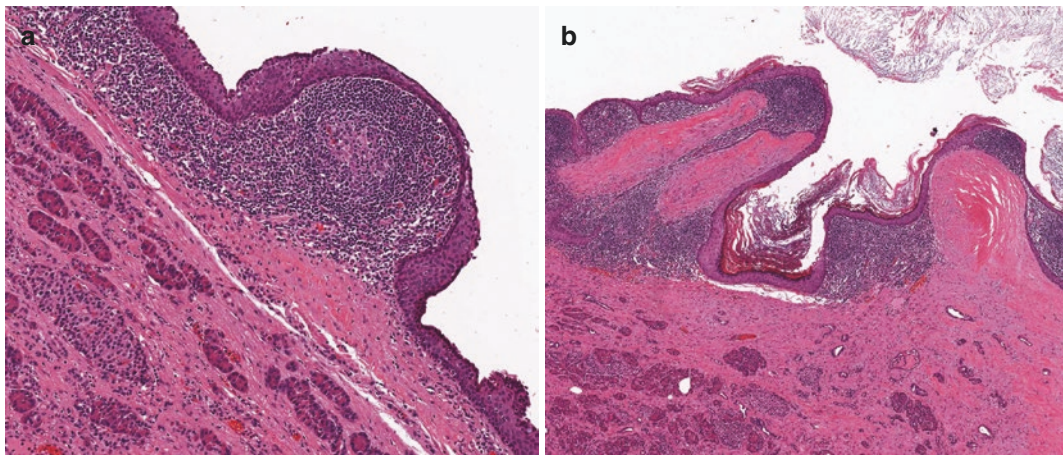

Fig. 19.12 Lymphoepithelial cyst: the cyst is lined by mature squamous epithelium and lymphoid tissue forming occasional lymphoid follicles (**a**). The squamous epithelium is often keratinizing (**b**)

follicles) or other types of epithelium (intestinal or respiratory) are present, then the lesion is a teratoma.

19.4.2 Mature Cystic Teratoma (Dermoid Cyst)

Mature cystic teratomas are very rare in the pancreas. They are usually monodermal and composed only of ectodermal tissue (dermoid cysts). The morphological appearances are identical to those seen elsewhere in the body. The cysts are normally lined by squamous epithelium, but intestinal or respiratory epithelium can occasionally be found (Fig. 19.13).

The main differential diagnosis is a lymphoepithelial cyst (see Sect. 19.4.1), but this lacks adnexal structures and does not have intestinal or respiratory epithelial lining.

Although mature cystic teratomas are benign, they should be examined thoroughly to exclude malignant transformation. It should also be noted that malignant teratomas can metastasize to the pancreas.

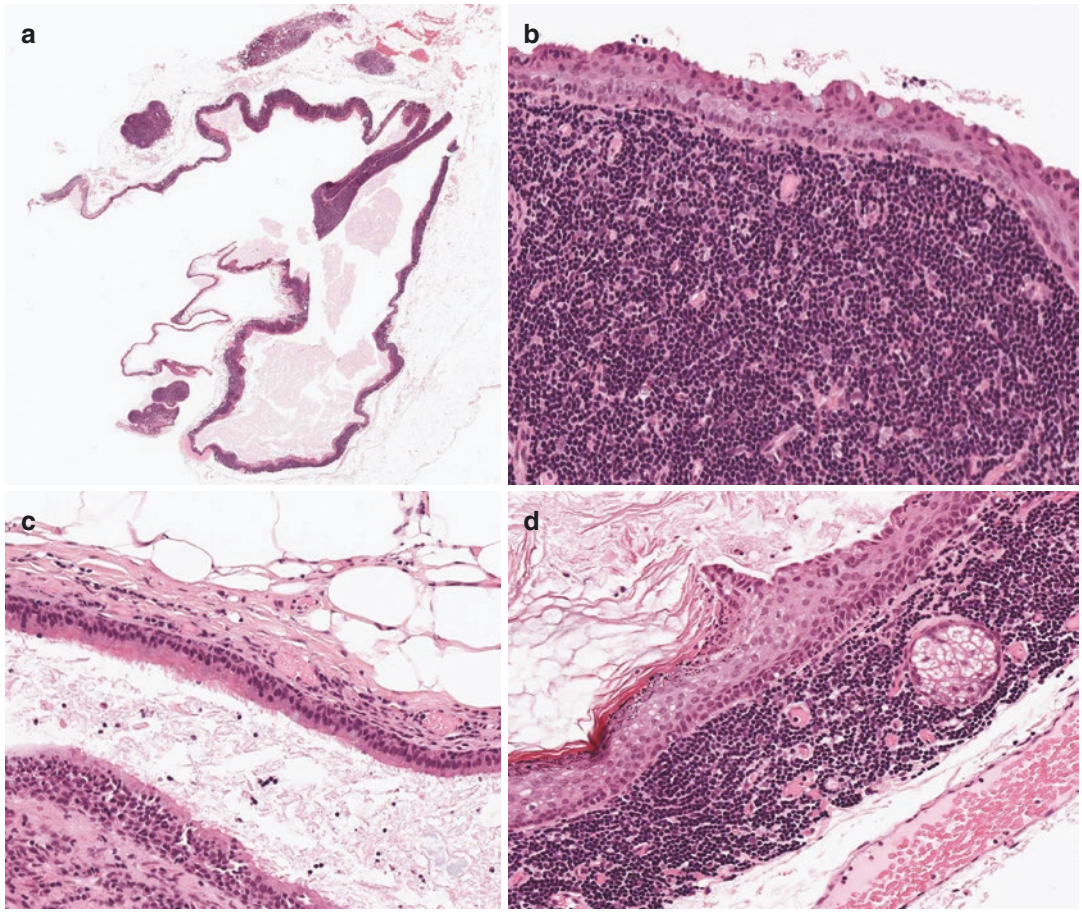

Fig. 19.13 Mature cystic teratoma: this unilocular cystic teratoma, with abundant lymphoid tissue in the wall, was initially misdiagnosed as a lymphoepithelial cyst (**a**). The cyst lining is predominantly squamous with occasional mucin cells in the epithelium (**b**). However, this cyst (**c**) is also lined by ciliated respiratory type epithelium (*top*), and there is a sebaceous unit within the wall (**d**)

19.4.3 Squamous Epithelial (Epidermoid) Cyst in Intrapancreatic Heterotopic Spleen

Heterotopic spleen may occasionally be found in the pancreas (see Chap. 13, Sect. 13.5). Very rarely, squamous epithelium-lined cysts (also known as epidermoid cysts) can occur within this intrapancreatic heterotopic spleen (Fig. 19.14a). All the reported cases have been found in the tail of the pancreas and, on imaging, are characteristically hypervascular, well-demarcated, solid and cystic lesions with an average size of 4.5 cm.

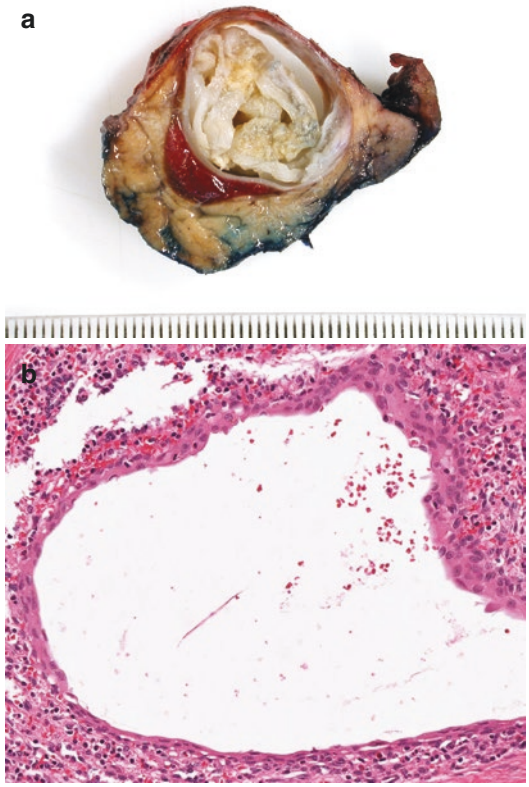

Fig. 19.14 Squamous epithelium-lined cyst in intrapancreatic heterotopic spleen: within this (dark red-brown) intrapancreatic spleen (**a**), there is a cyst lined by squamous epithelium (**b**). (Picture 19.14a kindly provided by Dr. Judy Wyatt, St James's University Hospital, Leeds, UK)

The cysts may be unilocular or multilocular, contain serous fluid or keratin debris, and are lined by mature stratified squamous epithelium, which may or may not be keratinizing (Fig. 19.14b). The surrounding splenic tissue is composed of normal red and white pulp, although the latter may be scanty.

The differential diagnosis includes lymphoepithelial cyst (see Sect. 19.4.1) and mature cystic teratoma (see Sect. 19.4.2). It is worth noting that not all epithelium-lined cysts arising within intrapancreatic heterotopic spleen are squamous in nature. There is a single case report of a serous cystic neoplasm occurring within intrapancreatic heterotopic spleen in a patient with von Hippel-Lindau syndrome [12].

19.4.4 Squamoid Cyst of Pancreatic Ducts

Squamoid cyst of pancreatic ducts [13] is characterized by a unilocular cyst (median size 1.5 cm, range 0.8–9 cm) with a thin fibrotic wall (Fig. 19.15a), and lined by nonkeratinizing squamous epithelium. The cyst contains clear serous fluid and has a smooth glistening inner surface. The squamous epithelium may be attenuated, transitional, or stratified, but does not have a granular layer (Fig. 19.15b). The epithelium expresses duct epithelium markers CK7 (Fig. 19.15c) and CK19, as well as MUC1 and MUC6 (markers of intercalated duct cells). The basal epithelial cells express p63 (a marker of squamous/transitional epithelium), p40 (a squamous-specific isoform of p63), and CK5/6 (Fig. 19.15d and e).

These cysts occur predominantly within the head of the pancreas and appear to be metaplastic cystic transformation of small pancreatic ducts. Although they could represent squamous metaplasia within retention cysts, there has been no evidence of an obstructive process in the reported cases, and retention cysts are generally much smaller.

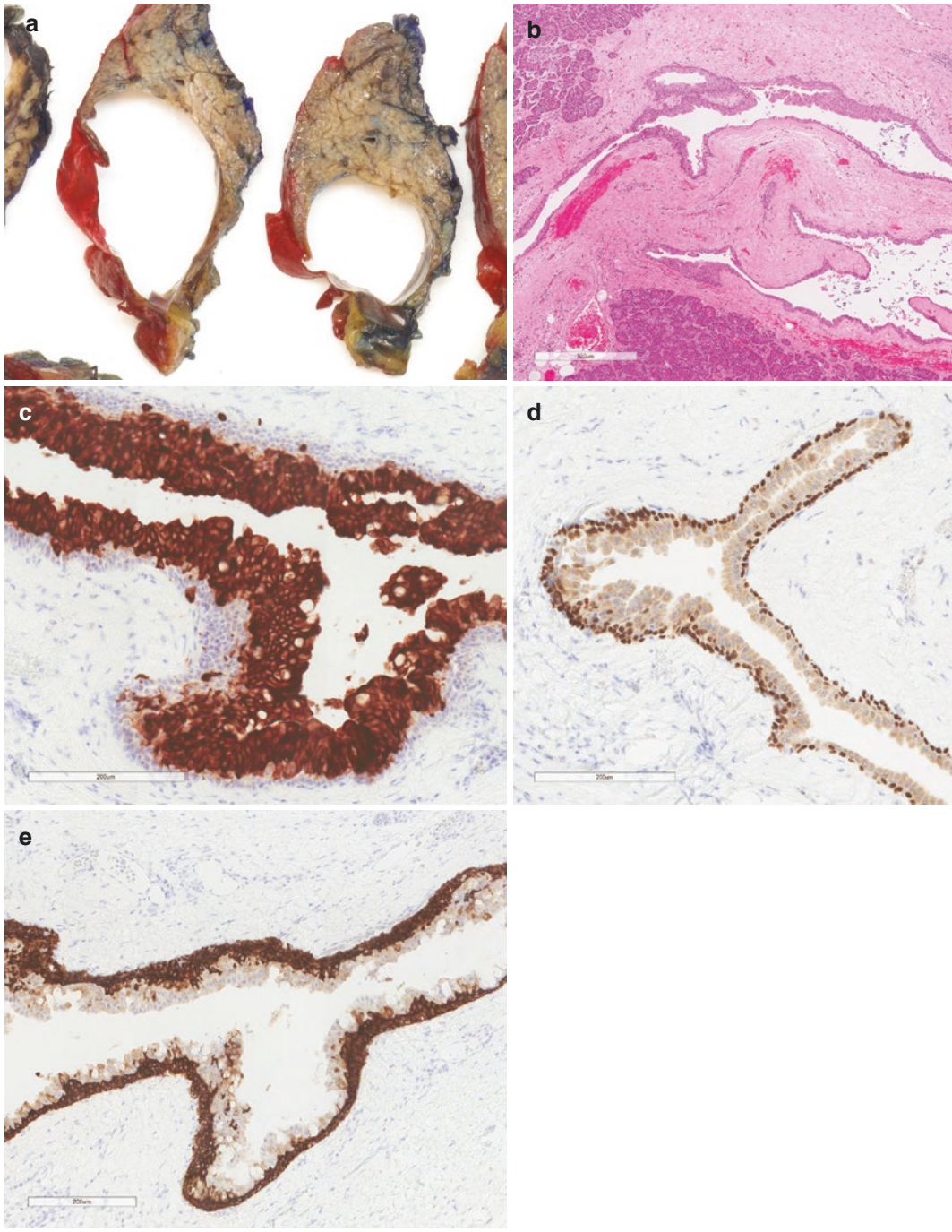

Fig. 19.15 Squamoid cyst of pancreatic ducts: the unilocular cyst has a thin wall (**a**), and is lined by transitional squamous epithelium (**b**) that expresses duct epithelium marker CK7 (**c**) and, in the basal epithelial cells, squamous markers p40 (**d**) and CK5/6 (**e**)

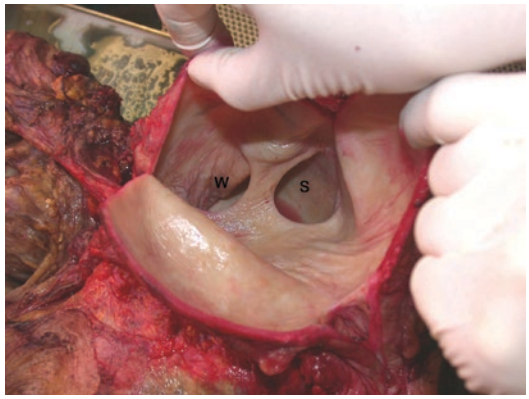

Fig. 19.16 Squamous metaplasia of pancreatic duct: the main pancreatic duct of Wirsung (W) and the accessory duct of Santorini (S) are both grossly distended, following pancreatic duct obstruction by a slow-growing duodenal neuroendocrine tumor. Note the 'skin-like' appearance of the pancreatic duct surface, which is due to complete squamous metaplasia of the duct lining epithelium

19.4.5 Squamous Metaplasia in a Cystic Lesion

Squamous metaplasia may occur within dilated pancreatic ducts (Fig. 19.16), in nonneoplastic cysts (choledochal cysts and retention cysts), and in neoplastic cysts (mucinous cystic neoplasm—see Chap. 16).

19.5 Other Cystic Lesions

19.5.1 Cystic Hamartoma

There are very rare case reports of hamartomata occurring in the head, body, or tail of the pancreas [14]. Hamartomata are composed of haphazardly arranged exocrine and endocrine pancreatic tissue in either fibroblast-rich or paucicellular stroma. Adipose tissue may be present. They form well-demarcated nodules and may be entirely solid, or have solid and cystic features. The cysts are dilated ducts, lined by cuboidal or flattened ductal epithelium, and may or may not be a prominent component of the hamartoma.

19.5.2 Duodenal Diverticulum

Diverticula may occur within the duodenum and the majority are found close to the ampulla. There are several classifications of periampullary diverticula, but the one most commonly used distinguishes intraluminal and extraluminal diverticula. Intraluminal diverticula are rare, result from a defect in embryological development (see Table 13.1), and usually cause mechanical duodenal obstruction.

Extraluminal diverticula are much more common than the intraluminal variety and are usually solitary. They may be intrapancreatic (extending into the head of the pancreas) or peripancreatic (Fig. 19.17), and often mimic a primary pancreatic cystic lesion or cystic neoplasm. They are usually acquired in middle age (median age range 56–76 years) and are rarely seen in patients less than 40 years of age. The majority are asymptomatic and do not require treatment. Complications include bleeding, inflammation, obstruction (jaundice), and perforation.

Duodenal diverticula are out-pouchings of the duodenum and, therefore, are lined by duodenal mucosa. They differ from foregut cysts, which do not communicate with the duodenal lumen.

19.5.3 Endometriotic Cyst

Endometriotic cysts are extremely rare in the pancreas [15] and occur in reproductive-aged women. They are lined by endometrial epithelium and endometrial-type stroma. They may be distinguished from a mucinous cystic neoplasm by the presence of a rich capillary network, hemorrhage and hemosiderin-laden macrophages (evidence of chronic hemorrhage) within the stroma, as well as by the lack of mucinous epithelial lining and typical ovarian-type stroma of a mucinous cystic neoplasm.

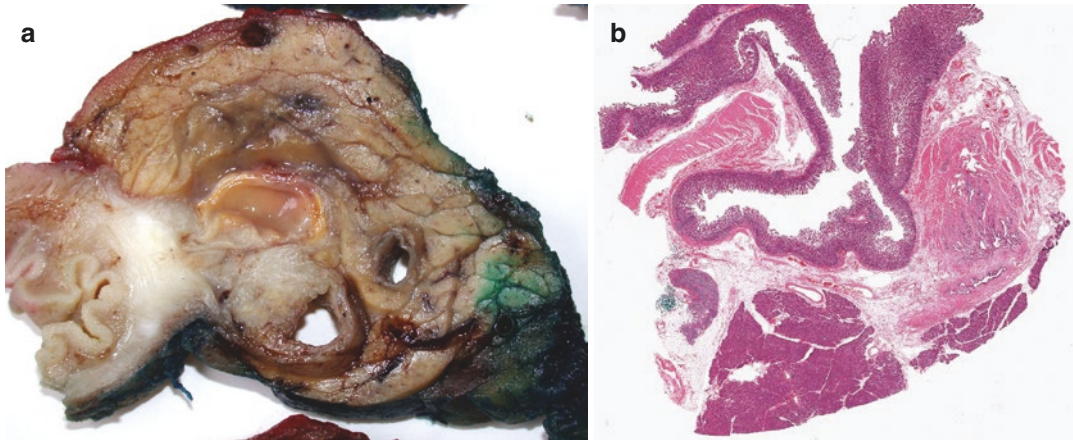

Fig. 19.17 Periampullary diverticulum: this (**a**) intrapancreatic diverticulum (*top*) displaces the ampulla (*below*). This wholemount of a peripancreatic diverticulum shows the periampullary location (**b**) with ampulla (*right*), normal pancreas (*below*), and posterior pancreatoduodenal lymph node (*left*)

19.5.4 Foregut (Duplication) Cyst

Foregut or duplication cysts are rare congenital cysts (see Table 13.1) that originate from the wall of the stomach or duodenum. They are usually found adjacent to the pancreas rather than within it. Most occur immediately adjacent to the head of the pancreas, and they may communicate with the pancreatic ducts. Foregut cysts may be lined by a mixture of squamous epithelium (Fig. 19.1), gastric epithelium (see Fig. 13.1), small intestinal epithelium, and ciliated columnar epithelium. The wall contains relatively well-orientated bundles of smooth muscle which, together with the lack of skin adnexal structures, allows distinction from a mature cystic teratoma (see Sect. 19.4.2).

19.5.5 Parasitic Cyst

Hydatid (Echinococcal) cysts occur very rarely in the pancreas and can mimic a choledochal cyst or pancreatic cystic neoplasm on imaging [16]. The embryo of a hydatid cyst probably reaches the pancreas by hematogenous spread. The diagnosis should be considered in the differential diagnosis of pancreatic cysts in the appropriate epidemiological setting.

References

1. Klöppel G. Pseudocysts and other non-neoplastic cysts of the pancreas. Semin Diagn Pathol. 2000;17:7–15.
2. Albores-Saavedra J. Acinar cystadenoma of the pancreas: a previously undescribed tumor. Ann Diagn Pathol. 2002;6:113–5.
3. Zamboni G, Terris B, Scarpa A, Kosmahl M, Capelli P, Klimstra DS, et al. Acinar cell cystadenoma of the pancreas: a new entity? Am J Surg Pathol. 2002;26:698–704.
4. Lokuhetty D, White VA, Watanabe R, Cree IA, editors. Digestive system tumours. WHO classification of tumours. 5th ed. Lyon: IARC Press; 2019. p. 296.
5. McEvoy MP, Rich B, Klimstra D, Vakiani E, La Quaglia MP. Acinar cell cystadenoma of the pancreas in a 9-year-old boy. J Ped Surg. 2010;45:E7–9.
6. Khor TS, Badizadegan K, Ferrone C, Fernández-Del Castillo C, Desai GS, Saenz A, et al. Acinar cystadenoma of the pancreas: a clinicopathologic study of 10 cases including multilocular lesions with mural nodules. Am J Surg Pathol. 2012;36:1579–91.
7. Pesci A, Castelli P, Facci E, Romano L, Zamboni G. Primary retroperitoneal acinar cell cystadenoma. Hum Pathol. 2012;43:446–50.
8. Kosmahl M, Egawa N, Schröder S, Carneiro F, Lüttges J, Klöppel G. Mucinous nonneoplastic cyst of the pancreas: a novel nonneoplastic cystic change? Mod Pathol. 2002;15:154–8.
9. Basturk O, Hong SM, Wood LD, Adsay NV, Albores-Saavedra J, Biankin AV, et al. A revised classification system and recommendations from the Baltimore

consensus meeting for neoplastic precursor lesions in the pancreas. Am J Surg Pathol. 2015;39:1730–41.
10. Krasinskas AM, Oakley GJ, Bagci P, Jang KT, Kuan SF, Reid MD, et al. 'Simple mucinous cyst' of the pancreas. A clinicopathologic analysis of 39 examples of a diagnostically challenging entity distinct from intraductal papillary mucinous neoplasms and mucinous cystic neoplasms. Am J Surg Pathol. 2017;41:121–7.
11. Zhu B, Finkelstein SD, Feng G, Keswani RN, Lin X. Molecular analysis of mucinous nonneoplastic cyst of the pancreas. Hum Pathol. 2016;55:159–63.
12. Hori S, Nara S, Shimada K, Ojima H, Kanai Y, Hiraoka N. Serous cystic neoplasm in an intrapancreatic accessory spleen. Pathol Int. 2010;60:681–4.
13. Othman M, Basturk O, Groisman G, Krasinskas A, Adsay NV. Squamoid cyst of pancreatic ducts: a distinct type of cystic lesion in the pancreas. Am J Surg Pathol. 2007;31:291–7.
14. Matsushita D, Kurahara H, Mataki Y, Maemura K, Higashi M, Iino S, et al. Pancreatic hamartoma: a case report and literature review. BMC Gastroenterol. 2016;16:3.
15. Yamamoto R, Konagaya K, Iijima H, Kashiwagi H, Hashimoto M, Shindo A, et al. A rare case of pancreatic endometrial cyst and review of the literature. Intern Med. 2019;58:1097–101.
16. Dziri C, Dougaz W, Bouasker I. Surgery of the pancreatic cystic echinococcosis: systematic review. Transl Gastroenterol Hepatol. 2017;2:105.

Part IV

Endocrine Pancreas

Endocrine Neoplasia

20

20.1 Terminology and Classification

This group of pancreatic neoplasms is characterized by a predominant neuroendocrine differentiation. Over the years, the terminology and classification of endocrine neoplasia arising in the pancreas has undergone multiple changes. The most recent alterations were introduced in 2019 by the 5th edition of the WHO classification of tumors of the digestive system [1], ten years after the 4th edition [2] and 15 years after the WHO classification of tumors of endocrine organs [3] had been published.

The term 'carcinoid' is outdated and confusing, because it is often used in a more general sense than its original meaning of a serotonin-producing well-differentiated endocrine tumor. The term "islet cell tumor" has also been used previously. 'Neuroendocrine tumor' or 'neuroendocrine neoplasm' seem to be more appropriate terms, as they refer to the histogenesis of these tumors only, without connotations regarding the grade of tumor differentiation or hormonal production. 'Endocrine tumor' is preferred by some, because the prefix 'neuro-'refers back to the time when endocrine cells in the digestive system were believed to be derived from the neuroectodermal crest. However, sufficient features are shared between the endocrine and neural system to justify this prefix, and both 'endocrine' and 'neuroendocrine' are currently used interchangeably.

According to the WHO classification 2010 [2], pancreatic neuroendocrine neoplasms were divided into the two main categories of neuroendocrine tumors (PanNETs) and neuroendocrine carcinomas (PanNECs), whereby PanNETs could be further distinguished as grade 1 and grade 2 tumors. PanNETs differ from PanNECs morphologically, genetically, clinically, and epidemiologically. Overall, PanNETs are by far the most common entity within the group of pancreatic neuroendocrine neoplasms. They are characterized by an indolent clinical course and a typical organoid microscopic growth pattern. Their proliferative activity covers a range from <1% to up to 20%, and the tumors frequently harbor mutations in the *MEN1*, *DAXX*, and *ATRX* genes. In contrast, PanNECs are rare, highly aggressive tumors that despite a good response to platinum-based chemotherapy are associated with poor survival. They do not exhibit an organoid growth pattern on microscopic examination and show a high proliferative activity (>20%) that often lies in the range of 70–90%. They are associated with mutation of *TP53* and inactivation of the RB1/p16 pathway, and lack the mutations that are found frequently in PanNETs. Taken together, PanNECs share with PanNETs the expression of neuroendocrine markers, but they are not closely related neoplasms. PanNECs do not usually arise in association with PanNETs.

In 2019, the new WHO classification [1] introduced a new entity, PanNET grade 3, based on

© Springer Nature Switzerland AG 2021
F. Campbell, C. S. Verbeke, *Pathology of the Pancreas*,
https://doi.org/10.1007/978-3-030-49848-1_20

the concept that well-differentiated neuroendocrine neoplasms can be high-grade. Indeed, growing evidence shows that neuroendocrine tumors with morphological features similar to those of grade 1 and grade 2 PanNETs but with a higher proliferative activity that falls into the range of PanNECs (Ki67 index >20%) show clinical and genetic features that are more akin PanNETs than PanNECs. To avoid confusion with the newly introduced entity of PanNET grade 3, PanNECs are no longer assigned a grade, since all PanNECs are high-grade.

The term mixed adenoneuroendocrine carcinoma (MANEC) has been substituted by the category of mixed neuroendocrine—non-neuroendocrine neoplasms (MiNENs), which now encompasses a broader range of mixed neoplasms, including also tumors with squamous carcinoma or PanNET as a component of the neoplasm. The term MiNEN refers to an overarching diagnostic category that for the diagnosis of an individual tumor needs to be supplemented with the description of the exact nature of both tumor components.

The rationale for the change in classification and the defining criteria of the various categories are discussed in detail in this chapter. Table 20.1 provides a comparison between the WHO classification systems of 2010 and 2019.

Table 20.1 Comparison of terminology for pancreatic neuroendocrine neoplasia used by the WHO classifications 2010 and 2019

WHO 2010	WHO 2019
1. PanNET *grade 1*	1. PanNET *low-grade (grade 1)*
2. PanNET *grade 2*	2. PanNET *intermediate-grade (grade 2)*
	3. PanNET *high-grade (grade 3)*
3. PanNEC grade 3 (large or small cell type)	4. PanNEC (large or small cell type) *high-grade*
Mixed adenoneuroendocrine carcinoma (MANEC)	Mixed neuroendocrine—non-neuroendocrine neoplasm (MINEN) *variable grade*

Adapted from [1, 2]
Abbreviations: *PanNEC* pancreatic neuroendocrine carcinoma, *PanNET* pancreatic neuroendocrine tumor

20.2 Epidemiology

Pancreatic neuroendocrine neoplasms are rare, and they represent only 2–5% of all pancreatic tumors. Within the group of pancreatic endocrine tumors, PanNETs grade 1–3 are by far the most common, whereas PanNECs are rare and constitute <1% of all pancreatic tumors and 2–3% of all pancreatic endocrine neoplasms. The incidence of PanNETs in the general population is less than 1/100,000. Post mortem studies report a higher incidence (up to 1.5% of unselected autopsies), which results from the fact that PanNETs may remain occult during life, especially if they are small (<1 cm diameter) and hormonally inactive. A mild increase in incidence over recent years may be due to increased awareness and an improved detection rate both by imaging and laboratory testing. Within the group of sporadic functioning PanNETs, insulinoma is the most frequent (approximately 70% of all pancreatic neuroendocrine neoplasms). While there is no sex predilection for PanNETs, PanNECs are diagnosed slightly more frequently in males than in females. The age range is wide for PanNETs, with most patients being between 30 and 60 years old. Patients with PanNEC are usually 50–60 years of age, but younger individuals may also be affected.

While very little is known about risk factors for sporadic pancreatic endocrine neoplasia, the genetics of syndromic PanNETs in multiple endocrine neoplasia (MEN) type 1 and type 4, von Hippel-Lindau syndrome (VHL), neurofibromatosis type 1 (NF1), and tuberous sclerosis complex (TSC) are well established. Recently, a few kindreds with insulinomatosis have been reported (see Sect. 20.14).

20.3 Clinical Features

Clinically, the distinction between functioning and nonfunctioning PanNETs is important. *Functioning PanNETs* are associated with a clinical syndrome related to the inappropriate hormone release by the tumor. Table 20.2 summarizes the key features of the most common functioning

Table 20.2 Functioning pancreatic neuroendocrine tumors, in descending order of relative incidence

	Incidence (%)	Localization	Clinical presentation	Morphological features	Genetics	Prognosis
Insulinoma	• 27% of all PanNETs • Most frequent among functioning PanNETs (42%) • 0.4 cases/100,000 person-years	• <2% in duodenum • Extremely rare in small bowel, splenic hilum, stomach, lung, cervix, ovary	Whipple triad: 1. Symptoms of hypoglycemia: • Neurological: diplopia, blurred vision, confusion, abnormal behavior, amnesia, coma, focal seizures • Autonomic nervous response: sweating, weakness, hunger, tremor, nausea, anxiety, palpitation 2. Plasma glucose <2.2 mmol/l 3. Symptom relief upon intake of glucose	• Macroscopy: Size: 0.5–11 cm, 75% 0.5–2 cm; 10% are multiple, syn-/metachronous • Microscopy: amyloid uncommon but relatively characteristic; may contain psammoma bodies	• 4–7% associated with MEN 1 • Rare reports of association with insulinomatosis	2–18% malignant
Gastrinoma	• Up to 30% of functioning PanNETs • 4–8% of all PanNETs	• 25% pancreatic • 70% duodenal (mainly in 1st and 2nd part) • Rare in stomach, small bowel, bile duct, liver, kidney, mesentery, heart • Primary existence in peripancreatic/ periduodenal lymph nodes questioned	Zollinger-Ellison syndrome: • Duodenal ulcer • Gastro-esophageal reflux disease • Abdominal pain • Diarrhea • ECL-like cell hyperplasia/ neoplasia in gastric fundus	• Macroscopy: – Pancreatic: most >2 cm – duodenal: most <1 cm, confined to (sub-)mucosa – Lymph node metastasis may be larger than primary tumor • Microscopy: As in other PanNETs	• 25% associated with MEN 1 (predominantly duodenal SSToma) • Rare reports on association with NF1, NF2 and TSC	• Usually malignant • Liver metastasis in 22–35% of pancreatic gastrinomas • Liver metastasis in 0–10% of duodenal gastrinomas
VIPoma	3–8% of all PanNETs	• 80% pancreatic • Rarely in extrapancreatic location: small bowel, esophagus, kidney • Neurogenic VIP-secreting tumors in sympathetic ganglia and adrenal glands	WDHA syndrome (Verner-Morrison syndrome): • Watery diarrhea (large volume) • Hypokalemia • Achlorhydria/hypochlorhydria • Acidosis	• Macroscopy: – Size: 2–20 cm (mean: 4.5 cm) • Microscopy: As in other PanNETs	10% associated with MEN 1	Approximately 50–80% present with distant metastasis (mainly liver)

(continued)

Table 20.2 (continued)

	Incidence (%)	Localization	Clinical presentation	Morphological features	Genetics	Prognosis
Glucagonoma	• 1–2% of all PanNETs • 8–13% of functioning PanNETs	• Extremely rare outside pancreas • Predilection for pancreatic tail	Glucagonoma syndrome (% of patients): • Necrolytic migratory erythema (70%), stomatitis, cheilitis, alopecia, vulvovaginitis, urethritis • Mild glucose intolerance (50%) • Normochromic/normocytic anemia (33%) • Weight loss (65%) • Depression (20%) • Diarrhea (20%) • Deep venous thrombosis (10–15%)	• Macroscopy: Usually large (mean diameter: 7 cm) • Microscopy: As in other PanNETs	• <5% associated with MEN 1 (but nonfunctioning PanNETs with immunoreactivity for glucagon common in MEN 1) • Rare reports on association with glucagon cell hyperplasia and neoplasia	Mostly malignant, 60–70% present with metastasis
Somatostatinoma (SSToma)	2% of all PanNETs	• Pancreatic head more commonly involved than body or tail • Also in duodenum and ampulla	SSToma syndrome: • Diabetes mellitus/glucose intolerance • Hypochlorhydria • Gallbladder disease (stones, reduced motility) • Diarrhea, steatorrhea • Anemia • Weight loss Duodenal SSTomas are rarely associated with SSToma syndrome	• Macroscopy: Usually large (mean diameter: 5.5 cm) • Microscopy: Prominent glandular growth pattern and psammoma bodies mainly in duodenal SSToma	• Occasional association with MEN 1 and VHL • Ampullary/duodenal SSToma often associated with NF1	Mostly malignant, 66% present with metastasis

Adapted from [1, 3]

Abbreviations: *ECL* enterochromaffin-like, *MEN 1* multiple endocrine neoplasia type 1, *NF1* neurofibromatosis type 1, *PanNET* grade 1–3 pancreatic neuroendocrine tumor, *SSToma* somatostatinoma, *VHL* von Hippel-Lindau syndrome, *VIP* vasoactive intestinal polypeptide

PanNETs, including incidence, clinical symptoms and outcome, localization, association with inherited syndromes, and specific morphological features.

Nonfunctioning PanNETs are not associated with a distinct clinical syndrome (if sporadic). However, they may still secrete hormones, which can be detected as abnormally increased serum levels or by immunhistochemical staining of the tumor tissue. The absence of clinical symptoms can be due to hormonal release at a level that is too low to have any clinically apparent effect. Alternatively, nonfunctioning PanNETs may release hormones, such as pancreatic polypeptide (PP) or neurotensin, which do not cause symptoms. Most commonly, nonfunctioning PanNETs become clinically apparent by symptoms that are related to a large tumor size, tumor infiltration of neighboring organs, or the development of metastasis. Overall, nonfunctioning PanNETs are more common than functioning tumors and represent over 60% of all PanNETs.

The distinction between functioning and nonfunctioning PanNETs is made solely on the basis of the clinical picture. Hence, the positive result of immunhistochemical staining of the tumor tissue for a particular hormone, for example insulin, does not allow the diagnosis of an insulinoma, unless the patient presents with the corresponding clinical symptomatology. However, somatostatinomas can occasionally be an exception to this principle. The symptoms related to increased somatostatin levels are subtle and nonspecific (e.g., gallstones, diabetes, anemia, weight loss), and their connection to the PanNET may not always be appreciated clincally. In this situation, the pathologist's report on the positive immunostaining for somatostatin may sometimes prompt a reconsideration of the patient's symptomatology with subsequent correct diagnosis of a somatostinoma syndrome.

Pancreatic neuroendocrine neoplasms only rarely secrete ectopic hormones. Adrenocorticotrope hormone (ACTH)-producing pancreatic tumors account for 10% of ectopic Cushing's syndrome. Further ectopic hormones that can be secreted are growth hormone-releasing hormone and growth hormone (causing acromegaly), corticotropin-releasing hormone (Cushing's syndrome), parathyroid hormone (PTH) and PTH-related peptide (hypercalcemia), calcitonin (diarrhea), prolactin (galactorrhea, amenorrhea), and cholecystokinin (CCK).

Serotonin-producing endocrine tumors are extremely rare in the pancreas. The characteristic symptoms of the carcinoid syndrome, that is, flushing, diarrhea, and bronchoconstriction, develop only when the tumor has metastasized to the liver or retroperitoneum. Serotonin is not regarded as an 'ectopic' hormone, because low numbers of serotonin-producing extrainsular endocrine cells are present in the pancreas (see Chap. 1, Sect. 1.4.4).

Occasionally, a tumor can secrete different hormones, or the type of hormone that is expressed can change over time. The latter is usually a poor prognostic sign.

The small group of patients who develop a PanNET as part of a hereditary syndrome (MEN, VHL, NF1, TSC), may present with a complex clinical picture that is determined by the presence of other tumors and lesions associated with the genetic defect (see Sect. 20.12).

Multiple PanNETs, developing synchronously and/or metachronously raise the suspicion of a genetic syndrome but can occasionally also be seen in the absence of clinical or genetical evidence of MEN, VHL, NF1, or TSC. Recently, insulinomatosis has been described as the synchronous and metachronous occurrence of insulinomas, multiple insulinoma precursor lesions, and rare development of metastases but common recurrent hypoglycemia. This disease differs from solitary sporadic and MEN1-associated insulinomas [4].

PanNECs usually present with signs and symptoms that are similar to those of ductal adenocarcinoma of the pancreas. Most patients have metastatic disease at the time of diagnosis. Serum analysis does not usually show an elevated level of chromogranin A nor any evidence of hormonal secretion, with the occasional exception of elevated calcitonin. Unlike in PanNETs, somatostatin receptor (SSTR) scintigraphy is usually negative. PanNECs are not part of the above-mentioned genetic syndromes that may include PanNETs.

20.4 Macroscopy

PanNETs are usually well-circumscribed tumors with smooth, pushing-type contours. Some tumors may appear surrounded by a fibrous pseudocapsule (Fig. 20.1), whereas others show gross invasion into neighboring tissues and organs (Fig. 20.2). Scalloped tumor outlines raise the suspicion of gross vascular invasion (Fig. 20.3). The vast majority of PanNETs are solid tumors. While some tumors may contain cystic areas of varying size, entirely cystic PanNETs are not common and mainly present as a unilocular cavity surrounded by a rim of tumor tissue (Fig. 20.4). The tumor tissue is often a pale, red-tan, or fawn color. Black or deep yellow discoloration is rare and indicates the accumulation of lipofuscin or lipids within the tumor cells (Fig. 20.3). The tumor tissue is usually relatively soft but, depending on the extent of fibrosis or hyalinosis, PanNETs may be of a firmer consistency. Focal calcification is not uncommon.

PanNETs can vary in size from less than 1 cm to well over 5 cm (Fig. 20.5). Insulinomas are usually small (< 2 cm), probably because the associated symptomatology leads to earlier detection. Most other functioning PanNETs are of a similar size as nonfunctioning tumors, and there are no distinctive macroscopic features associated with the hormonal activity of the tumor.

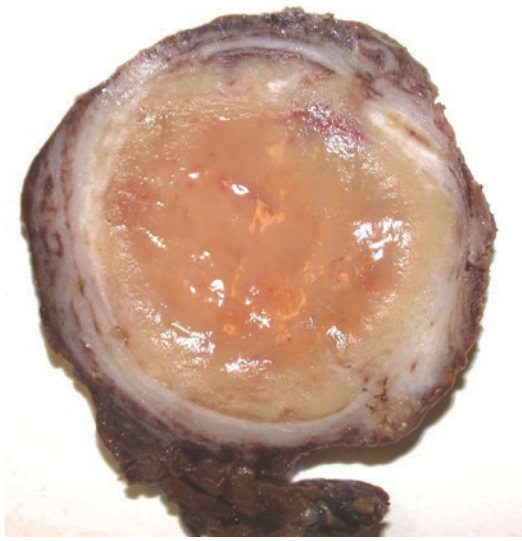

Fig. 20.1 Macroscopy of a PanNET: the tumor consists of tan-colored solid tissue with well-circumscribed pushing borders and a pseudocapsule of varying thickness

Fig. 20.2 Locally advanced PanNET: this large tumor originating from the pancreatic tail has invaded the spleen. Note the subcapsular splenic infarction

PanNETs can occur anywhere in the pancreas. A predominantly intraductal tumor location has been reported but is rare. Most sporadic tumors are single. Multiple PanNETs raise the suspicion of an underlying genetic syndrome.

In many cases, pancreatic parenchyma surrounding the PanNET shows a degree of fibrosis and atrophy. However, these changes are usually limited in extent, and pancreatic tissue further away from the tumor is often remarkably well preserved, irrespective of the tumor size. PanNETs located in the pancreatic head compress rather than infiltrate the main pancreatic duct or common bile duct. Due to the slow growth of PanNETs, adaptive dilatation of these ducts ensures proper drainage of bile and pancreatic juice (see Fig. 19.16).

PanNECs are usually large at the time of diagnosis. They consist of fleshy, grey-white tissue that may be better delineated than ductal adenocarcinoma (Fig. 20.6). Necrosis and hemorrhage of varying extent may be visible.

Fig. 20.3 Gross vascular invasion in a PanNET: the tumor has a multinodular appearance with scalloped outlines. One of the tumor nodules represents gross invasion of the splenic vein (*arrow*). Note the bright *yellow* color of part of the tumor as a result of the accumulation of lipids within the tumor cells (same tumor as in Fig. 20.8)

20.5 Microscopy

Neuroendocrine tumors of the pancreas can exhibit a wide variety of microscopic appearances but, with few exceptions, these are of no known clinical or prognostic relevance. The main significance of the morphological variation in growth pattern and cytomorphology lies in the awareness of its existence and the distinction from other tumor entities.

In this section, the microscopic features of PanNETs grade 1–3 and PanNECs will be described, while a more detailed discussion of the WHO classification 2019 follows separately (see Sect. 20.6).

20.5.1 Pancreatic Neuroendocrine Tumors (Grade 1–3)

PanNETs grade 1–3, as defined by the WHO classification 2019, constitute a group of well-differentiated endocrine tumors (see Table 20.1). They represent the vast majority of all endocrine neoplasms in the pancreas. Their diagnostic hallmarks are cytological uniformity and a so-called organoid growth pattern. A wide range of such growth patterns exists (Fig. 20.7): trabecular, ribbon-like, acinar, glandular, cribriform, pseudorosette-like, gyriform, insular, nested, and

Fig. 20.4 Cystic PanNET: the tumor consists of a single cystic cavity surrounded by a rim of tumor tissue (**a**). The latter shows microscopic features characteristic of a PanNET (**b**). In this case, the focal presence of more extensive tumor tissue within the cystic PanNET was misinterpreted on preoperative imaging as a mural nodule in a mucinous cystic neoplasm

occasionally solid. In PanNETs with an angiomatoid pattern, small lakes of erythrocytes are present within dilated glandular tumor cell structures and occasionally also in the intervening stroma. It is not uncommon to find several different growth patterns within a single tumor.

Fig. 20.5 Incidental PanNET: this 0.9 cm large tumor (*arrows*) was found incidentally in a distal pancreatectomy specimen resected for intraductal papillary mucinous neoplasia (not shown)

Fig. 20.6 Macroscopy of a PanNEC: the tumor consists of fleshy, grey-white tissue with well-circumscribed, scalloped outlines

Cytologically, PanNETs usually exhibit only a mild degree of pleomorphism, although exceptions are well recognized (see below). The tumor cells usually contain a round to ovoid nucleus, which is located in the center of the tumor cell, but may be polarized in tumors with a trabecular growth pattern. Chromatin is predominantly coarsely stippled, resulting in a 'salt and pepper' appearance. Nucleoli are usually absent or small and present in only a proportion of the tumor cell population. Mitotic figures are rare and atypical mitotic figures exceptional. The tumor cells usually have a cuboidal or polygonal shape and contain a copious amount of finely granular, amphophilic, or eosinophilic cytoplasm. While these features characterize the majority of PanNETs, there are multiple distinct, but usually rare, variants. Not uncommonly, only a proportion of the tumor cells show features of a particular variant. There is currently no agreed cut-off value, but in general it is suggested that a 'significant' proportion of the tumor cell population—set by some arbitrarily at 25% or more—should exhibit the specific morphology for it to be reported. As most of these variants have no known correlation with clinical features, it suffices to report on the presence of the variant morphology together with an estimate of its extent.

The *clear cell variant* of PanNETs is characterized by the presence of abundant cytoplasm with countless clear vesicles, which impart a foamy appearance, similar to that of sebaceous cells (Fig. 20.8), and may scallop the nuclei. As the cytoplasmic vacuoles contain lipid, the term *lipid-rich variant* is also used. This variant is more common in patients with von Hippel-Lindau syndrome, who are at risk of developing—amongst various other lesions—renal cell carcinoma, which has a known propensity to metastasize to the pancreas. The differential diagnosis of clear cell variant PanNET and metastatic renal cell carcinoma of clear cell type is discussed in Chap. 12, Sect. 12.5.

In the *oncocytic variant*, the tumor cells also contain abundant cytoplasm, but this is granular and eosinophilic in appearance due to the accumulation of mitochondria. Tumor cells of this variant often show moderate nuclear atypia with more than usual nucleolar prominence (Fig. 20.9). Oncocytic nonfunctioning PanNETs seem to be more aggressive.

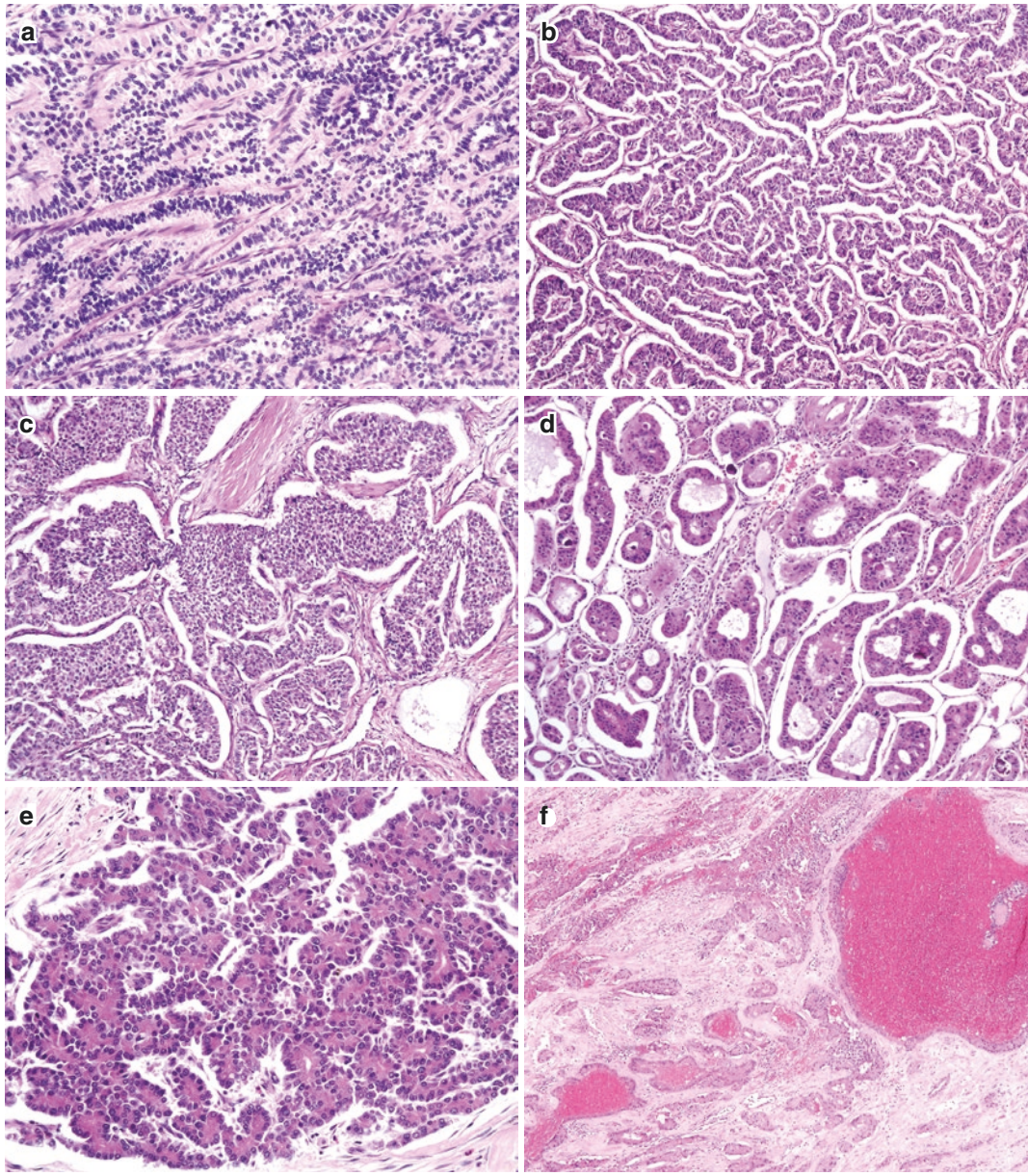

Fig. 20.7 Growth patterns of PanNETs: grade 1–3 pancreatic neuroendocrine tumors can show a range of organoid growth patterns: ribbon-like (**a**), gyriform (**b**), insular (**c**), glandular (**d**), acinar (**e**), and angiomatoid (**f**)

In the *pleomorphic variant*, the tumor cells display moderate to marked nuclear atypia (Fig. 20.10). However, this is not associated with increased proliferative activity or necrosis, and the tumor cells with large nuclei usually also have copious cytoplasm ('cytomegaly'), that is, the nucleus:cytoplasm ratio remains unaltered. These features are helpful in distinguishing the pleomorphic PanNET variant from other high-grade malignant neoplasms, such as adenocarcinoma or PanNEC. There is no convincing evidence that pleomorphic PanNETs are more aggressive in their behavior than conventional PanNETs.

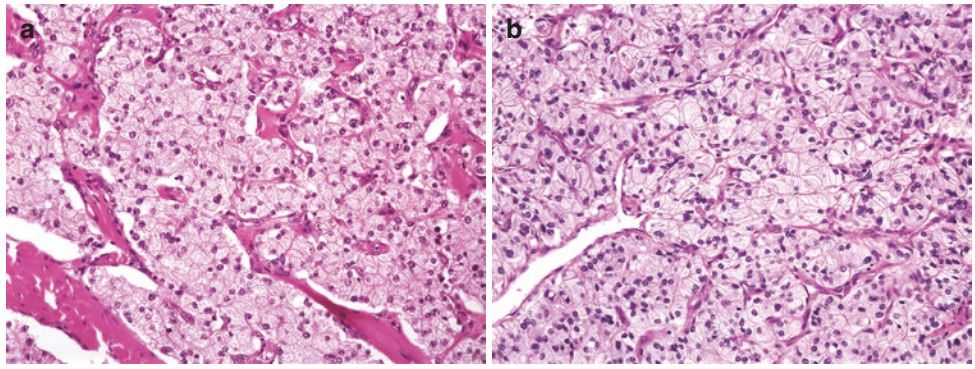

Fig. 20.8 Clear cell or lipid-rich PanNET: the tumor cells have a clear cytoplasm, which contains more (**a**) or less (**b**) conspicuous microvesicles. The tumor in (**b**) is the same as in Fig. 20.3 and stems from a patient with von Hippel-Lindau syndrome

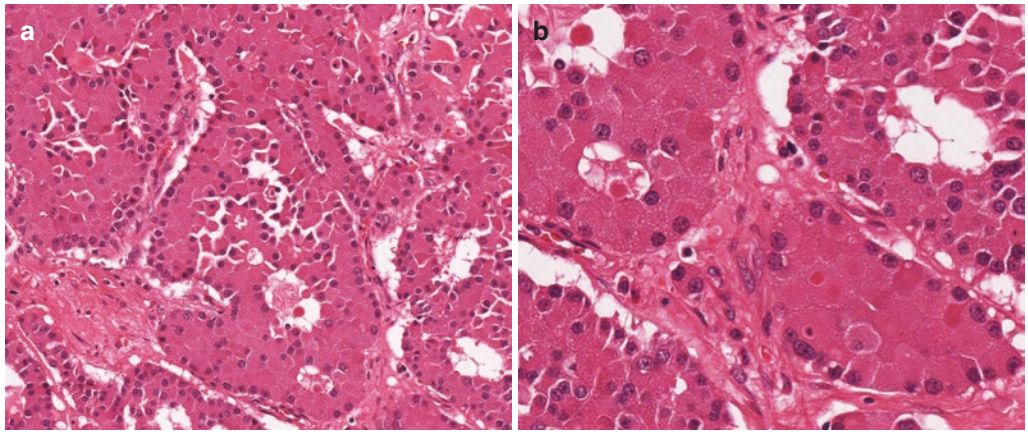

Fig. 20.9 Oncocytic PanNET: tumor cells have copious, deeply eosinophilic, and granular cytoplasm (**a**). There is mild nuclear pleomorphism, and multiple tumor cells have one or two nucleoli (**b**)

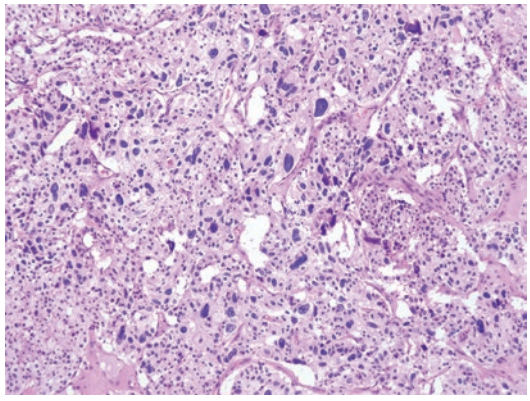

Fig. 20.10 Pleomorphic PanNET: there is marked nuclear pleomorphism. Note the absence of mitotic figures and the abundance of cytoplasm in cells with large hyperchromatic nuclei ('cytomegaly')

The so-called *rhabdoid variant* is characterized by prominent, hyaline, pale, or eosinophilic intracytoplasmic inclusions. The term 'rhabdoid' is in fact a misnomer, because the cellular inclusions are composed of keratin whorls.

In the *hepatoid variant*, the tumor cells resemble hepatocytes because of the glycogen-containing cytoplasm, the vesicular nucleus with a prominent nucleolus, and the positive immunolabeling for hepatocellular markers (at least HepPar1). These tumors show a perisinusoidal growth pattern, can contain bile canaliculi, and may occasionally contain bile droplets (Fig. 20.11). This rare variant is of clinical relevance, because it is associated with prominent

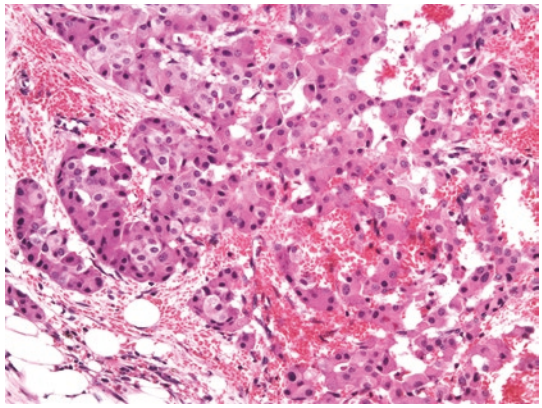

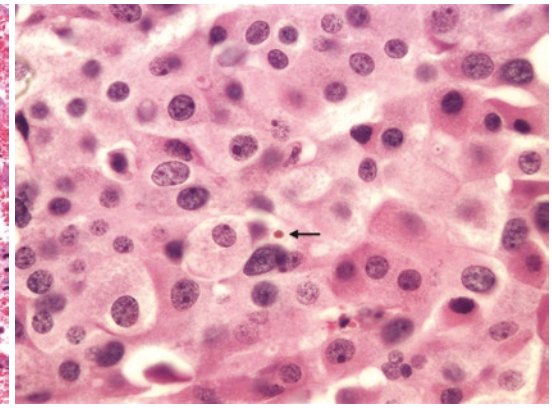

Fig. 20.11 Hepatoid PanNET: tumor cells with ample eosinophilic cytoplasm and a central round nucleus resemble hepatocytes. Note the liver-like trabecular arrangement and sinusoidal vascular network (**a**) as well as the presence of a bile droplet (**b**; *arrow*) (Reproduced with permission from Verbeke [5]. Blackwell Publishing Ltd)

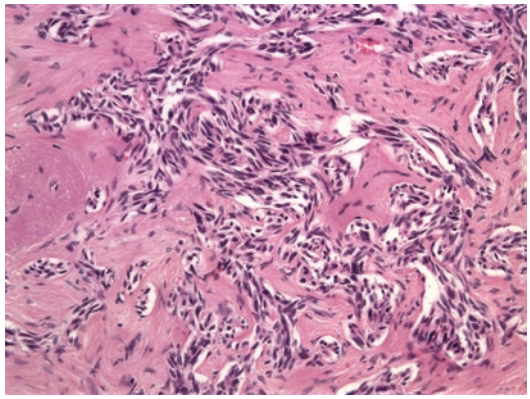

Fig. 20.12 Spindle cell variant of PanNET: endocrine tumor cells are spindle shaped and arranged in short irregularly intersecting bundles. Note the cytological uniformity of the tumor cells (Reproduced with permission from Verbeke [5], Blackwell Publishing Ltd)

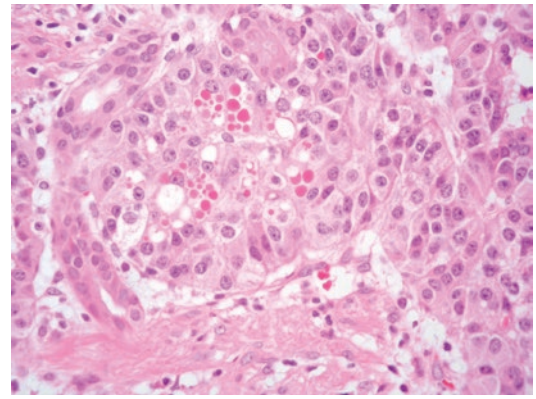

Fig. 20.13 PanNET with globules: eosinophilic round globules of varying size are present within the cytoplasm of tumor cells and occasionally also in the extracellular space

vascular invasion, early liver metastasis, and a shorter survival. As similar hepatoid features may be seen in ductal adenocarcinoma of the pancreas (see Chap. 9, Sect. 9.14.5), this should always be considered as a differential diagnosis.

Spindle cell morphology is a rare and often focal feature (Fig. 20.12).

Tumor cells may contain PAS-positive *globules*, which can also be present extracellularly (Fig. 20.13). Psammoma bodies are most frequently seen in somatostatinomas (Fig. 20.14) and can also be found in insulinoma. Rare cases of a *pigmented variant* have been reported, in

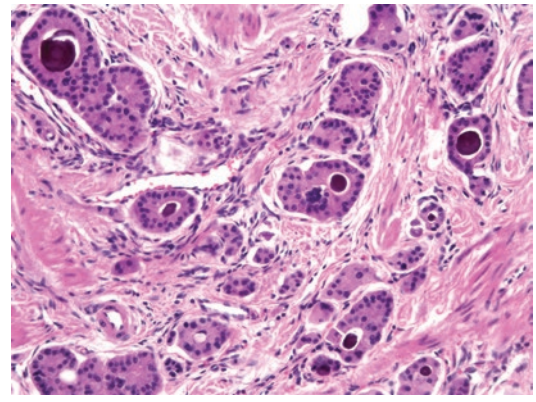

Fig. 20.14 PanNET with psammoma bodies: round and deeply basophilic psammoma bodies are present within the glandular lumina of a somatostatinoma

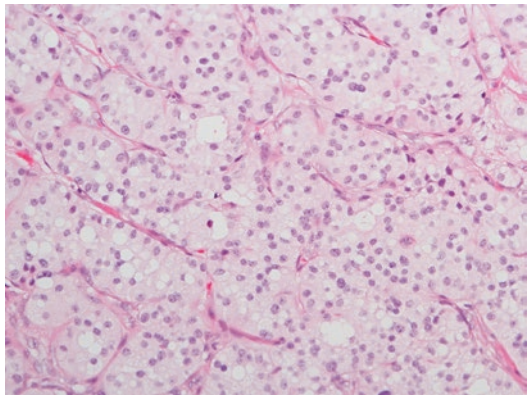

Fig. 20.15 Stroma in PanNET: a delicate fibrovascular network supports the tumor cell nests

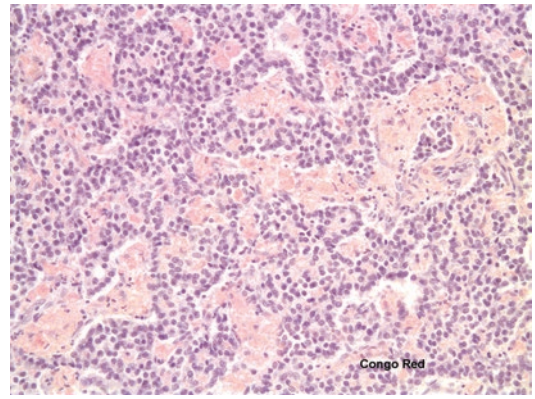

Fig. 20.17 Insulinoma with amyloid: Congo red staining highlights the amorphous intercellular deposits of amyloid in an insulinoma

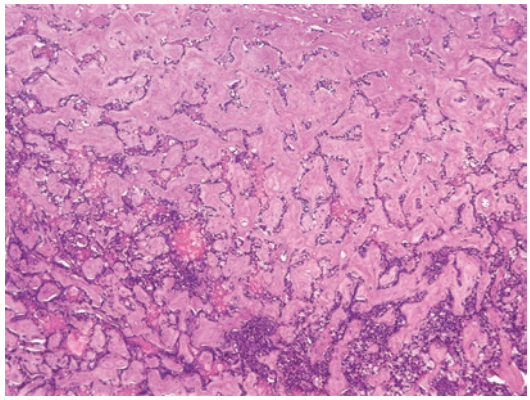

Fig. 20.16 PanNET with hyaline stroma: tumor cell trabeculae are small and widely spread in this prominent hyaline stroma

which the dark brown-black color, visible both macroscopically and microscopically, is due to the accumulation of lipofuscin.

The stroma in PanNETs characteristically consists of a delicate fibrovascular network (Fig. 20.15). However, a hyaline stroma is not uncommon and is seen more frequently in insulinoma than in other PanNETs. On occasion, the hyaline stroma may be prominent and nearly eclipse the tumor cell population (Fig. 20.16). Calcification can vary in extent and is usually irregular in shape. It does not have the stellate or egg shell configuration as seen in other pancreatic tumors (see Chaps. 15 and 16). Amyloid deposition is suggestive of an insulinoma (Fig. 20.17).

Occasionally, residual small nonneoplastic ducts and islets may be entrapped in the neoplastic proliferation, a finding that should not be misinterpreted as evidence of a nonendocrine tumor component.

20.5.2 Pancreatic Neuroendocrine Carcinomas

PanNECs are very rare in the pancreas and must be distinguished from NECs that develop somewhat more frequently in the ampulla (see Sect. 20.9.3). PanNECs are characterized by brisk mitotic activity, and they often contain areas of necrosis. Two types of PanNECs are distinguished, a small cell and a large cell type. *Small cell-type* PanNEC resembles small cell carcinoma in other sites. It is characterized by diffuse sheets of small to medium-sized cells with minimal ill-defined cytoplasm. The tumor cell nuclei have a finely granular chromatin, do not usually contain nucleoli, and may show nuclear molding (Fig. 20.18). Within the group of PanNECs, the small cell type is less common compared with the large cell type. Small cell-type PanNECs tend to be larger in size and have a higher proliferative index than the PanNECs of large cell type [6].

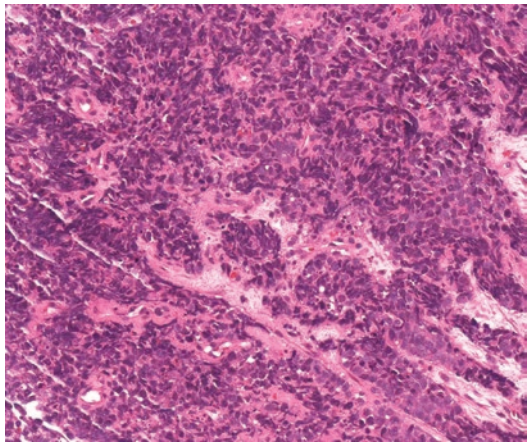

Fig. 20.18 PanNEC of small cell type: small to medium-sized tumor cells with minimal ill-defined cytoplasm grow in indistinct solid sheets. The tumor nuclei show a diffuse chromatin pattern without nucleoli

Large cell-type PanNEC is composed of large round to polygonal cells with a moderate amount of cytoplasm. The nuclei are large and show coarsely clumped chromatin and often a prominent nucleolus (Fig. 20.19). In most cases, mitotic activity is not as high as in the small cell type but remains usually well above 20 mitotic figures/10 high power fields, as defined by the WHO classification 2019 (see Sect. 20.6). Some of the tumors may show a more or less organoid rather than an indistinct solid growth pattern. Large cell-type PanNECs are more common and account for approximately 60% of the PanNECs.

The distinction between small and large cell type is important first and foremost for diagnostic purposes. Awareness of both cell types will avoid misdiagnosis of other poorly differentiated tumors, in particular poorly differentiated adenocarcinoma in the case of large cell-type PanNEC, and neoplasms from the group of 'small blue round cell tumors' in the case of small cell-type PanNEC (see Sect. 20.9.2). Whether the different cell types are associated with differences in tumor behavior, response to chemotherapeutic treatment, and patient outcome has not yet been well established. However, recent data indicate that both types are at least genetically similar and clearly distinct from grade 1–3 PanNETs [6].

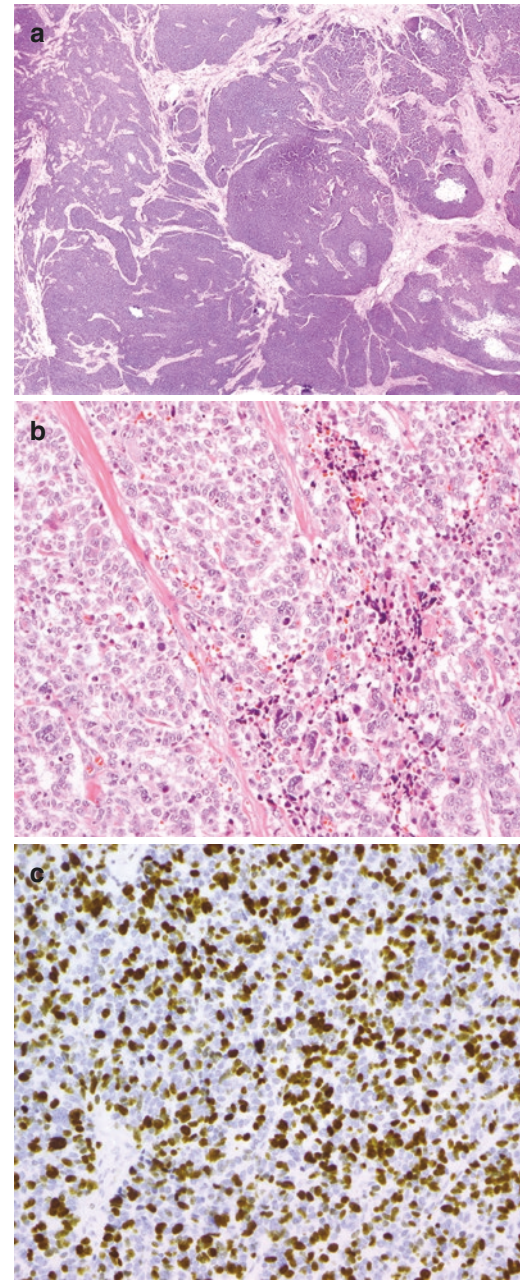

Fig. 20.19 PanNEC of large cell type: solid tumor sheets and clusters of varying size (**a**) are composed of large tumor cells with pleomorphic vesicular nuclei. Note the presence of foci of tumor cell necrosis (**b**). Immunostaining for Ki67 shows high proliferative activity (Ki67 index: 62%) (**c**)

As PanNECs lack the distinctive morphological features of their grade 1–3 counterparts, immunohistochemistry for neuroendocrine markers is usually required to reach a definitive diagnosis (see Sect. 20.7.1).

20.6 Classification

The WHO classification 2019 introduced the entity PanNET grade 3 in recognition of the existence of neuroendocrine tumors that morphologically, clinically, and genetically are similar to PanNET grade 1–2 but show a proliferative activity that exceeds 20% (Ki67 proliferative index) or >20 mitotic figures/10 high-power fields (HPF) (Fig. 20.20).

The classification of pancreatic neuroendocrine neoplasms is based on *morphology* and proliferative activity. As described above, PanNETs (grade 1–3) show a relatively monotonous microscopic morphology with mild nuclear atypia and a variety of organoid growth patterns that are characteristic of these tumors. Tumor necrosis is not usually seen. In contrast, PanNECs usually lack a convincing organoid tumor growth pattern, often contain multifocal necrosis, and may show marked cytological atypia.

The *proliferative activity* in PanNETs grade 1–3 and PanNECs is summarized in Table 20.3. Either the Ki67 index or the mitotic count, or both, can be used to assess the proliferative activity. In PanNECs, the Ki67 index usually well exceeds the threshold of 20%: in the vast majority of cases it is >50%, and it commonly ranges between 60 and 80%. However, lower proliferative activity, between 20 and 50%, may be seen, especially following chemotherapy. Conversely, PanNETs grade 3 usually show a lower Ki67 index than that seen in PanNECs, but values as high as 70–80% have been reported. Consequently, proliferative activity cannot be used as the sole criterion to distinguish between PanNET grade 3 and PanNEC.

In general, the Ki67 index is preferable to the mitotic rate, in particular when reporting on a small tumor sample, for example, a biopsy of the primary pancreatic tumor or a liver metastasis, because Ki67-positive cells are usually more numerous than mitotic figures. Practical issues regarding the evaluation of the Ki67 index are discussed below. Screening for mitoses should be performed on at

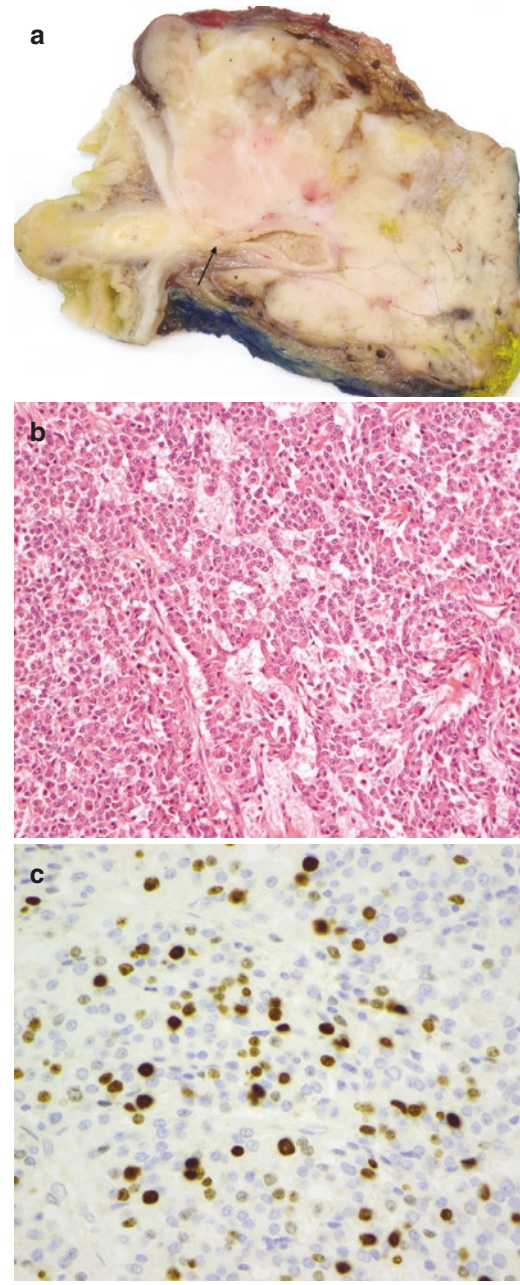

Fig. 20.20 PanNET grade 3: a fairly poorly demarcated tumor consisting of pale, soft tissue compresses the junction of the main pancreatic duct with the ampulla of Vater (*arrow*), resulting in dilatation of the former (**a**). Histologically, the tumor shows features of a well-differentiated neuroendocrine tumor (**b**), but the Ki67 index is 40% (**c**: immunostaining for Ki67)

Table 20.3 Grading of pancreatic neuroendocrine neoplasms according to the WHO classification 2019 [1]

Terminology	Differentiation	Grade	Mitotic count	Ki67 index
PanNET, G1	Well differentiated	Low	<2/10 HPF	<3%
PanNET, G2		Intermediate	2–20/10 HPF	3–20%
PanNET, G3		High	>20/10 HPF	>20%
PanNEC, small-cell type PanNEC, large-cell type	Poorly differentiated	High	>20/10 HPF	>20%
MiNEN	Well or poorly differentiated	Variable	Variable	Variable

Abbreviations: *G* grade, *HPF* high power fields, *MiNEN* mixed neuroendocrine—non-neuroendocrine neoplasm, *PanNEC* pancreatic neuroendocrine carcinoma, *PanNET* pancreatic neuroendocrine tumor

least 50 fields of 0.2 mm^2, an area that equals 10 HPF at 400x magnification (and an ocular field diameter of 0.5 mm). In case of discrepant findings between Ki67 index and mitotic count, the tumor should be graded according to the higher proliferation rate. In most such cases, the Ki67 index is found to be higher than the mitotic count.

As future changes to the cut-off values of either the mitotic count or the Ki67 index may occur, it is important to record the exact value for either parameters, to allow regrading of tumors following future amendments to the grading system [7, 8].

Because PanNETs and PanNECs differ genetically [6], immunohistochemistry may help, in particular with distinguishing PanNEC from PanNET grade 3. As PanNECs usually harbor mutant *TP53* and inactivation of the RB1/p16 pathway, they are characterized by immunopositivity for TP53 and loss of staining for RB1 or p16.

20.7 Immunohistochemistry

Immunohistochemistry is an integral part of the diagnostic work-up of pancreatic neuroendocrine neoplasms. The indications for immunostaining and the use of various markers are discussed below.

20.7.1 Confirmation of Neuroendocrine Differentiation

All suspected pancreatic endocrine neoplasms should be immunostained with the generic neuroendocrine markers synaptophysin and chromogranin A. While immunopositivity for the former is usually strong and diffuse, chromogranin immunopositivity can be more focal or even negative in poorly granulated, that is, less well differentiated tumors. Therefore, the rare PanNECs arising in the pancreas are often only faintly and focally immunopositive for chromogranin, especially the small cell type, in which tumor cells have only scant cytoplasm with few neurosecretory granules. Although immunohistochemistry for neuroendocrine markers is particularly important to establish the diagnosis of a PanNEC and exclude other differential diagnoses, there are currently no recommendations as to the intensity and extent of labeling that is required to confirm the diagnosis. It should be borne in mind that expression of neuroendocrine markers—usually only focally—may also be found in non-endocrine neoplasia, in particular acinar cell carcinoma (see Sect. 20.9.1). If the amount of tissue is limited (e.g., in biopsy material), synaptophysin is the best single neuroendocrine marker to use. Neuron-specific enolase (NSE), PGP9, CD56, and CD57 are not recommended, as these markers are of limited specificity. Similarly, histochemical stains such as the Grimelius silver stain are nonspecific, and their use is therefore no longer recommended. Other immunohistochemical markers that may be helpful in the distinction of pancreatic neuroendocrine neoplasia from other pancreatic tumors are discussed in the section on differential diagnosis. On rare occasion, a diagnosis of small-cell PanNEC may be reached in the absence of positive immunostaining for synaptophysin and chromogranin A, based on morphology, Ki67 index/mitotic count, and careful exclusion of other differential diagnoses [9].

20.7.2 Evaluation of Hormonal Production

Immunohistochemical evaluation of hormonal production is generally not required for the diagnosis of every pancreatic neuroendocrine neoplasm, as the diagnosis of a functioning neuroendocrine tumor is determined by the presence of a clinical syndrome due to hormonal oversecretion, irrespective of immunohistochemical findings. However, as an exception to the rule, a PanNET that is immunopositive for pancreatic polypeptide (PP) can be diagnosed as a 'PPoma', since overproduction of this hormone remains clinically silent. For all other hormones, positive immunolabeling in the absence of the corresponding clinical symptoms does not justify the diagnosis of a functioning tumor. Instead, the tumor may be reported as, for example, a grade 1 PanNET with immunohistochemical evidence of glucagon production.

While immunohistochemistry for hormones is generally not needed, there are three scenarios in which it is required. First, in patients with a clinical syndrome due to hormonal oversecretion, immunohistochemical confirmation that the surgically resected tumor is indeed the source of hormone overproduction is considered good practice. However, it should be borne in mind that the immunohistochemical findings in the tumor tissue may not always correlate with the biochemical or clinical evidence of hormone production. Immunolabeling may be absent in functioning tumors if the hormone is quickly released from the tumor cells and intracytoplasmic hormone levels remain undetectably low. Conversely, immunostaining may be positive for a particular hormone without corresponding clinical syndrome or even serum levels, as the tumor may produce but not release the hormone, or the hormone may be secreted at levels too low to cause clinical symptoms.

Second, positive immunostaining for somatostatin in a resected PanNET may sometimes prompt the (retrospective) clinical identification of a somatostatinoma syndrome, whose symptoms can be subtle and nonspecific (see Sect. 20.3). Morphological findings that may raise the suspicion of somatostatinoma are psammoma bodies and a glandular growth pattern, especially if the patient has neurofibromatosis 1 and the tumor is located in the ampulla or duodenum.

A third indication for immunohistochemical hormone detection is the confirmation of the neoplastic nature of a small endocrine cell lesion. Occasionally, it may be difficult to confidently distinguish small PanNETs or endocrine microadenomas (see Sect. 20.15) from enlarged islets of Langerhans, for example, in the context of chronic pancreatitis. Immunohistochemical demonstration of the preservation or loss of the numerical and specific spatial distribution of the various hormone-producing cells (positive for insulin, glucagon, somatostatin, and PP) will indicate the correct diagnosis (see Fig. 20.35). While endocrine microadenomas usually immunostain diffusely for a single hormone (most commonly glucagon, followed by PP), up to 40% of nonfunctioning PanNETs may show positive immunostaining for multiple hormones, most frequently glucagon, followed by PP and somatostatin.

20.7.3 Ki67 Immunostaining

Immunostaining for Ki67 should be performed on every pancreatic neuroendocrine neoplasm, because the proliferative activity is a defining criterion of tumor grade. As proliferative activity may vary within the same tumor, the proliferation index, that is, the percentage of tumor cells showing nuclear Ki67 immunolabeling, should be assessed in the areas of highest labeling, the so-called hot spots. Recommendations vary regarding the number of tumor cells that are to be counted. The WHO classification 2019 suggests that 500 tumor cells should be counted [1], whereas the European Neuroendocrine Tumor Society (ENETS) proposes assessment of 500–2000 tumor cells in hot spots [10]. Eye-piece grids may be helpful when counting. An alternative, relatively simple, and reliable approach is to take one or several high-power microphotographs from the hot spots and to count the positive and negative tumor cells, either on a paper print of the

microphotograph or directly on screen using image processing software. It is currently not known if the proliferation index should be assessed in multiple disease sites, that is, the primary tumor and lymph node or liver metastasis.

Assessment of the proliferative activity by counting mitoses is usually a less desirable option, because identification of the hot spots is more difficult for mitotic figures than for Ki67-positive cells.

20.7.4 Other Prognostic Factors

Several factors, including expression of CK19 and CD117, or loss of expression of CD99, progesterone receptor, or PTEN have been reported to allow prognostic substratification of PanNETs. However, validation of these factors is still awaited and therefore their use is currently not recommended.

20.7.5 Biopsy Diagnosis of Liver Metastasis

Because over 50% of patients with pancreatic endocrine neoplasia present with liver metastasis at the time of diagnosis, liver biopsy specimens from such metastatic tumor deposits are not uncommon. Reporting on these samples requires first and foremost the immunohistochemical confirmation of the neuroendocrine nature of the tumor. The grade of tumor differentiation should be determined as discussed above, that is, a formal assessment of the Ki67 index should be performed, as this has important management implications. Evaluation of the proliferative activity in biopsies is obviously limited by the small sample size.

Immunostaining for ISL1 (insulin gene enhancer protein) provides the best support for confirming the pancreatic origin of a metastatic neuroendocrine tumor deposit, but it should be kept in mind that up to 20% of liver metastases of PanNETs may be negative [11]. Of some, but less reliable, help are PDX1 (which is also positive in duodenal NETs), CDX2 (which is mainly, but not exclusively a marker of midgut NETs), and PAX8 (which is positive in approximately 50% of metastatic PanNETs) [12, 13]. TTF1 is present in over 60% of well-differentiated neuroendocrine tumors of pulmonary origin, but cannot be used for NECs, because the latter may also be positive even if of extrapulmonary origin. Cytokeratin staining (CK7, 19, 20) is unhelpful, because—unlike adenocarcinomas—the cytokeratin expression profile in neuroendocrine tumors does not directly relate to the tissue of origin. A proportion of PanNETs may stain positively for CK7, as do the majority of bronchopulmonary and a small number of gastrointestinal neuroendocrine tumors. Absence of immunolabeling for serotonin may be a further useful test, as serotonin-producing tumors are mainly of intestinal origin and exceedingly rare in the pancreas [11]. Conversely, positive immunostaining for insulin or glucagon is indicative of, but not specific for, a pancreatic origin. It should be borne in mind that metastases may occasionally produce hormones that differ from those found in the primary tumor.

20.8 Staging

20.8.1 Primary Tumor

Staging of PanNETs is done according to the UICC TNM (eighth edition) for these tumors [14] (Table 20.4). The staging criteria are tumor size, with 2 cm and 4 cm as thresholds, and the extent of the tumor, separating PanNETs that are limited to the pancreas (including the peripancreatic adipose tissue) from those that invade the duodenum, bile duct, or other adjacent organs, or breach the visceral peritoneum that overlies the anterior pancreatic surface. The staging system proposed by the European Neuroendocrine Tumor Society (ENETS) is highly similar (Table 20.4) [15].

Because PanNETs are usually well demarcated, macroscopic measurement of the tumor dimensions is straightforward. However, microscopic confirmation is advisable, especially when the maximum tumor size lies at either of the cut-

Table 20.4 Staging of pancreatic neuroendocrine tumors grade 1–3 (PanNETs) according to ENETS and TNM UICC 8th edition

Stage	ENETS	TNM UICC 8th edition
T1	Tumor confined to pancreas and size <20 mm	Tumor confined to pancreas[a] and size ≤20 mm
T2	Tumor confined to pancreas and size 20–40 mm	Tumor confined to pancreas[a] and size >20 mm and <40 mm
T3	Tumor confined to pancreas and size >40 mm or Invading duodenum or bile duct	Tumor confined to pancreas[a] and size >40 mm or Invading duodenum or bile duct
T4	Tumor invading adjacent organs or wall of large vessels (celiac axis or superior mesenteric artery)	Tumor perforates visceral peritoneum (serosa) or invades other organs or adjacent structures
N0	No regional lymph node metastasis	No regional lymph node metastasis
N1	Regional lymph node metastasis	Regional lymph node metastasis

Adapted from [14, 15]

[a]Invasion of adjacent peripancreatic adipose tissue is accepted but invasion of adjacent organs is excluded

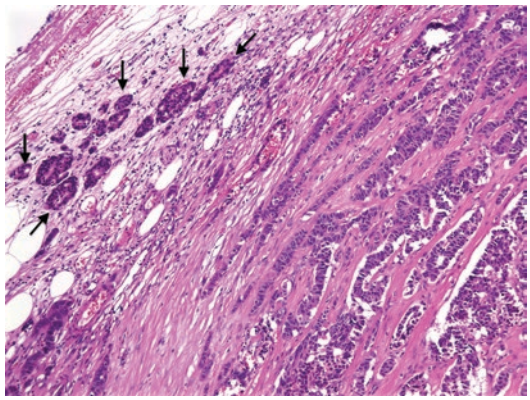

Fig. 20.21 T-staging of PanNETs: the cluster of atrophic islets (*arrows*) on the outside of the neuroendocrine tumor should not be included when measuring the tumor size

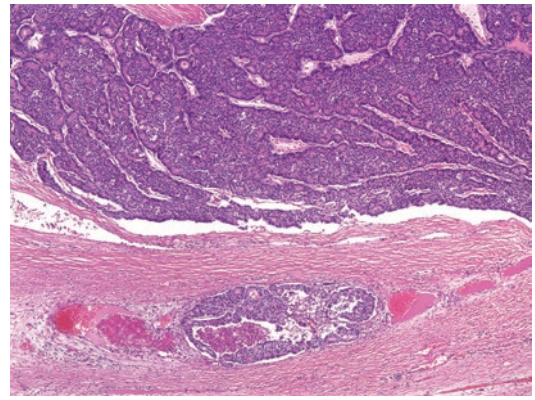

Fig. 20.22 Vascular invasion: a venous channel within the tumor pseudocapsule contains tumor cells. Note the thrombotic reaction

off points, that is, 2 cm or 4 cm. In such cases, it may be necessary to reliably distinguish between tumor cells and nonneoplastic islets at the tumor edge (Fig. 20.21). If needed, immunohistochemical staining for insulin, glucagon, somatostatin, and PP can help distinguish residual islets from tumor cell clusters.

Staging of PanNECs follows the UICC TNM system for ductal adenocarcinoma of the pancreas (see Chap. 9, Sect. 9.11) [14].

20.8.2 Tumor Propagation and Metastasis

The other staging descriptors—L, V, Pn, N, M—can be used to denote lymphovascular, perineural, or lymph node involvement and distant metastasis. Vascular invasion may be difficult to detect in PanNETs due to the intimate association of tumor cells with small blood vessels. Care should be taken not to misinterpret retraction artefact around tumor cell clusters as invasion of small vascular spaces. Vascular propagation is often more easily detected at the tumor periphery, where vessels may be of a larger caliber and association with the tumor may not be so close (Fig. 20.22).

20.8.3 Resection Margins

There is currently no clear definition of microscopic margin involvement (pR1), as the minimum clearance for pancreatic neuroendocrine neoplasms has not been established. However, because the majority of PanNETs are relatively well-circumscribed and

grow in a compact fashion with expansile, pushing-type margins, it has been suggested that resection can be regarded as complete, even if the margin is very close (i.e., less than 1 mm). In the absence of an evidence-based prognostically relevant definition of microscopic margin involvement, reporting of the exact distance between the tumor and the closest margin provides more robust information than a rather arbitrary attribution to R0 or R1.

Opinions differ regarding the prognostic relevance of incomplete surgical resection of a PanNET. While a positive margin does not seem to be critical for long-term overall survival, microscopic margin involvement may shorten disease-free survival in nonmetastatic PanNETs [16]. Evaluation of resection margins by intraoperative frozen section examination is usually not performed for PanNETs (see Chap. 23).

The resection margin status for PanNECs is of limited clinical significance, as these are highly aggressive malignancies, which are often diagnosed at an advanced stage and require systemic treatment.

20.9 Differential Diagnosis

In view of the enormous diversity in histological appearance of pancreatic neuroendocrine neoplasms, the list of differential diagnoses is long, and in many instances, immunohistochemistry may be required to reach a confident diagnosis. Because of the divergent morphological appearance of PanNETs and PanNECs, the differential diagnoses for both tumor groups are discussed separately. A summary of the main differential diagnostic features is shown in Table 20.5.

Table 20.5 Differential diagnosis of pancreatic neuroendocrine tumors

	Pancreatic neuroendocrine tumor	Ductal adenocarcinoma	Acinar cell carcinoma	Pancreatoblastoma	Solid pseudopapillary neoplasm
Morphology					
Compact, cellular tumor	++	–	++	++	++
Lobulated architecture	+	–	++	++	+
Pseudopapillae	+	–	–	–	++
Dense tumor stroma	+	++	–	++ (often hypercellular)	–
Salt and pepper chromatin	++	–	–	–	–
Nuclear grooves	–	–	–	–	++
Nucleoli	+	++	++	++	–
Intracytoplasmic mucin	–	++	–	–	–
PAS-positive hyaline globules	+	–	–	–	++
Squamoid nests	–	–	–	++	–
Immunohistochemistry					
CK19	+	++	+	+	–
CAM5.2	++	++	++	++	Focal
Vimentin	–/+	–	+	–	++
Chromogranin/ synaptophysin	++	Focal	Focal	+	Focal (synaptophysin only)
NSE/CD56	++	–	+	+	++
Trypsin, chymotrypsin, BCL10	–	–	++	++	–
Apha-1-antitrypsin	+	–	++	++	++
CD10	+	+	–	–	++
Beta-catenin (nuclear)	–/+	–	+	+	++
PR	+	–	–	ID	+

Abbreviations: ++ usually positive, + may be positive, – usually negative, *ID* insufficient data

20.9.1 Neuroendocrine Tumors of the Pancreas (Grade 1–3)

The single most important differential diagnosis of PanNETs is *ductal adenocarcinoma* of the pancreas. This holds true both clinically—given the different prognosis and treatment of either tumors—and from a pathology point of view. PanNETs with a glandular growth pattern, as commonly seen in somatostatinomas (see Table 20.2), may be misdiagnosed as well-differentiated adenocarcinoma. Marked nuclear atypia in pleomorphic PanNETs may cause confusion with adenocarcinoma. The low proliferative activity and nuclear-to-cytoplasmic ratio as well as the lack of mucin production exclude ductal adenocarcinoma. Immunostaining for neuroendocrine markers allows unequivocal confirmation of the neuroendocrine nature of the neoplasm. Absence of immunolabeling for MUC1 also supports the diagnosis of PanNET. However, care should be taken when using PAS-staining as a means of discrimination, because PAS-positive secretions can occasionally be found in the glandular lumina of pure PanNETs (Fig. 20.23). Similarly, there can be focal immunohistochemical staining for CA19-9 or CEA, especially in tumors with a glandular or tubular growth pattern. Cytokeratin 7 expression may be present in a small proportion of PanNETs. While the presence of psammoma bodies favors a PanNET, in particular an insulinoma or somatostatinoma, the occurrence of psammoma body-like structures has also been reported in rare cases of ductal adenocarcinoma [17, 18].

Solid pseudopapillary neoplasms of the pancreas share several features with PanNETs, which may make the distinction difficult. Both tumors can affect younger patients and present macroscopically as well-circumscribed expansile solid tumors with possible cystic areas. Microscopically, the characteristic pseudopapillary growth pattern of solid pseudopapillary neoplasms may be present only focally, while the solid areas of these tumors can mimic PanNETs in terms of growth pattern, cytological uniformity, low mitotic activity, and stromal reaction (Fig. 20.24). The presence of nuclear grooves supports the diagnosis of a solid pseudopapillary neoplasm, whereas PAS-positive globules may occasionally be seen also in PanNETs. Care should be taken not to limit immunohistochemical investigation to staining for neuroendocrine markers, because solid pseudopapillary neoplasms are diffusely positive for NSE and can show patchy labeling for CD56 and synaptophysin. Positive immunolabeling for vimentin is usually helpful in excluding PanNET, as is nuclear immunoreactivity for β-catenin, although a small proportion of PanNETs (< 5%) may show a similar staining pattern. Caution should also be taken when interpreting staining for CD10 and α1-antitrypsin, since both are positive in solid pseudopapillary neoplasms as well as in a proportion of PanNETs.

Acinar cell carcinoma can mimic PanNET by its lobulated appearance, acinar growth pattern, and low stromal content within the tumor lobules (Fig. 20.25). Immunohistochemistry is usually helpful, because acinar cell carcinomas

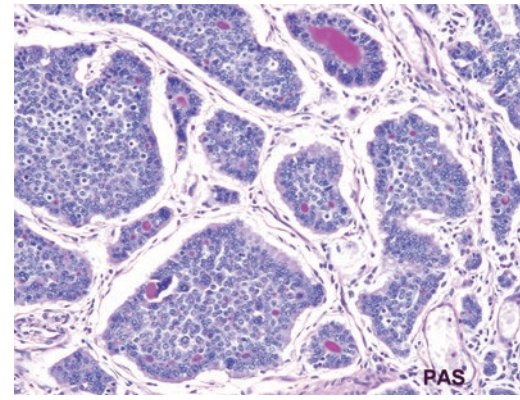

Fig. 20.23 PAS-positivity in pure PanNETs: PAS-positive secretions can occasionally be found in pure PanNETs with a glandular growth pattern. This should not be misinterpreted as evidence of exocrine differentiation

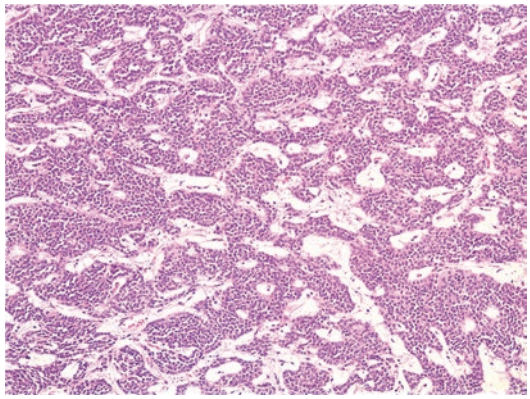

Fig. 20.24 Solid pseudopapillary neoplasm mimicking a PanNET: the organoid growth pattern, delicate stroma, and cytological uniformity in the solid area of this solid pseudopapillary neoplasm show marked resemblance to a PanNET

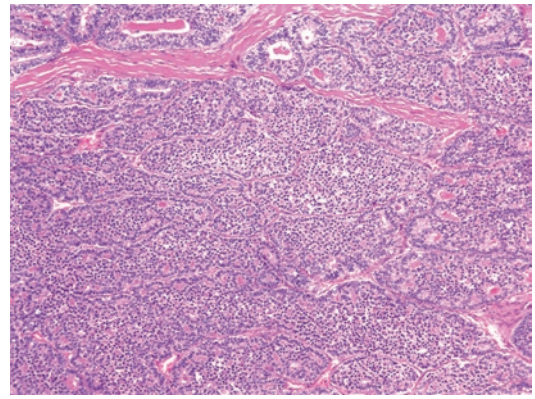

Fig. 20.25 Acinar cell carcinoma mimicking a PanNET: the acinar and insular growth pattern and low stromal component in this acinar cell carcinoma resemble a PanNET

label for (chymo-)trypsin, amylase, lipase, or BCL10. It should be borne in mind that immunostaining for chromogranin and synaptophysin can be focally positive in acinar cell carcinoma. If this is found in more than 30% of the tumor, a diagnosis of MiNEN (see Sect. 20.10) should be considered. PAS-positive granules in the apical cytoplasm also support the diagnosis of acinar cell carcinoma, but this feature is usually only present in well-differentiated tumors. Extensive necrosis is usually not a feature of PanNETs, but may occur in acinar cell carcinoma. The differential diagnosis is often more difficult if the acinar cell carcinoma is less well differentiated and characteristic features such as an acinar growth pattern or apical PAS-positivity are lacking. In that case, the nuclear morphology of the tumor cells may give a useful clue. The nuclei in acinar cell carcinoma are characterized by a vesicular chromatin pattern and a prominent central nucleolus. Moreover, the nuclei remain remarkably uniform, even if the acinar cell carcinoma has a high proliferative activity (see Chap. 10, Fig. 10.7).

Pancreatoblastoma, though rare, may also be considered. In addition to multiple histological and immunohistochemical features shared with acinar cell carcinoma, pancreatoblastoma includes squamoid nests and hypercellular stroma bands (see Chap. 10, Sect. 10.11.3).

Paraganglioma or gangliocytic paraganglioma must be excluded if a PanNET has a nested or zellballen-like growth pattern. Diffuse labeling for vimentin, absence of staining for cytokeratins, and demonstration of sustentacular cells, which stain positively for S100 and glial fibrillary acidic protein (GFAP), confirm the diagnosis of paraganglioma (Fig. 20.26). Immunohistochemical confirmation of the presence of Schwann cells and ganglion-like cells (positive for S100, GFAP, NSE and neurofilament) allows distinction of a gangliocytic paraganglioma from a PanNET (Fig. 20.27).

Metastatic renal cell carcinoma requires distinction from the clear cell variant of PanNET, especially in patients with von Hippel-Lindau syndrome, who may suffer from either or both. As renal cell carcinoma can be positive for NSE, CD56, and, on rare occasion, also for synaptophysin, vimentin is a useful marker to resolve the differential (positive in renal cell carcinoma, negative in PanNET). Further differential diagnostic criteria are discussed in Chap. 12, Sect. 12.5 and

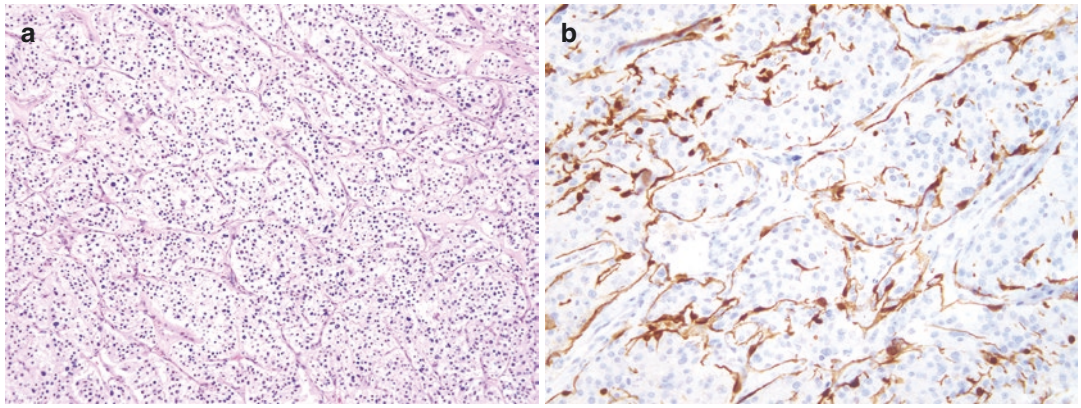

Fig. 20.26 Paraganglioma: the tumor has a 'neuroendocrine' appearance, but the zellballen arrangement (**a**) and immunohistochemical identification of S100-positive sustentacular cells (**b**) indicate that this is a paraganglioma

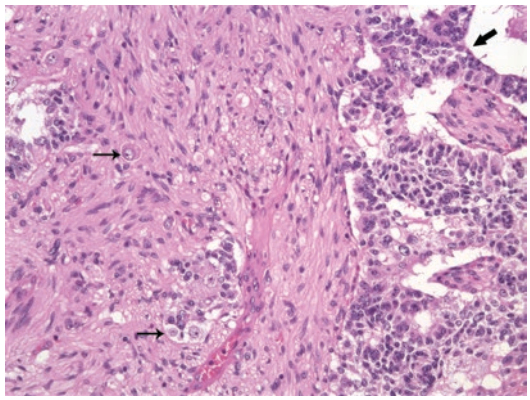

Fig. 20.27 Gangliocytic paraganglioma: this tumor is characteristically composed of three different cell populations: neuroendocrine cells (*block arrow*), ganglion-like cells (*arrows*), and spindle-shaped Schwann-like cells

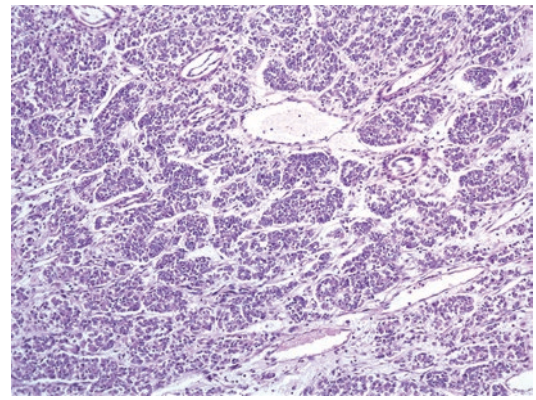

Fig. 20.28 PEComa: the nested growth pattern, cytological uniformity, and delicate fibrovascular stroma in PEComa can mimic a PanNET

summarized in Table 12.1. Oncocytic PanNET should be distinguished from *metastatic hepatocellular carcinoma* (HepPar1, arginase 1, glypican 3 positive) and *adrenal cortical carcinoma* (vimentin, melanin-A, inhibin positive; chromogranin A negative).

PEComa (perivascular epithelioid cell tumor) is a further tumor entity that can be confused with PanNET showing clear cell and spindle cell morphology (Fig. 20.28). Histological features that can be shared by both tumors are a nested growth pattern, an intimate association of tumor cells with blood vessels, a low degree of cytological pleomorphism, inconspicuous nucleoli, a possible combination of epithelioid and spindle cell morphology, and a sharp macroscopic delineation. Absence of immunostaining for generic neuroendocrine markers and positive labeling for Melan-A, HMB45, and actin and/or desmin usually allow unequivocal diagnosis of a PEComa, which very rarely can develop in the pancreas (see Chap. 11, Sect. 11.1.9).

A further differential diagnosis of clear cell variant PanNETs is the rare *solid serous adenoma* (see Chap. 15, Sect. 15.11.1).

Finally, an *ectopic adrenal cortical nodule* (see Chap. 13, Sect. 13.5, Fig. 13.8), which on rare occasion may occur in the pancreas, should not be misinterpreted as a PanNET. Immunohistochemistry may be helpful in

reaching the correct diagnosis (positive for synaptophysin; variable staining for cytokeratins; vimentin positive in some cells; absence of staining for EMA, chromogranin, S100).

20.9.2 Neuroendocrine Carcinoma of the Pancreas

The differential diagnosis of PanNECs is often challenging, as it encompasses a group of uncommon tumors, which may show only few morphological characteristics and often require specialist immunohistochemical staining and molecular testing to reach a definitive diagnosis. Because PanNECs usually have a very high proliferative activity, other tumor entities should be carefully considered if the Ki67 index is below 40%. Immunopositivity for desmin and WT1 is helpful in distinguishing PanNEC from a desmoplastic small round cell tumor (Fig. 20.29). Labeling for CD99 and Fli-1 is suggestive of a primitive neuroectodermal tumor, which can also show positive immunolabeling for neuroendocrine markers and cytokeratins (see Chap. 11, Sect. 11.1.10). High-grade malignant lymphoma may need consideration and require the use of generic leucocytic or specific lymphoma markers. Malignant melanoma may also need to be included in the differential diagnosis. Criteria to distinguish PanNEC from acinar cell carcinoma are described above. As large cell-type PanNEC may retain a certain degree of glandular or trabecular growth pattern, poorly differentiated ductal adenocarcinoma is always to be considered as a differential diagnosis. Metastatic carcinoma needs consideration and may require clinical input, as the transcription factors TTF1, ISL1, PDX1, and CDX2 may be positive in small cell carcinoma from any location.

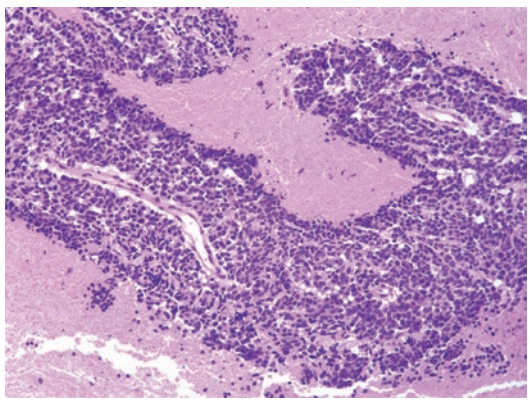

Fig. 20.29 Desmoplastic small round cell tumor: the small tumor cells with scanty cytoplasm and pleomorphic nuclei, the indistinct solid growth pattern, and the presence of necrosis resemble PanNEC

20.9.3 Neuroendocrine Neoplasms of the Ampulla, Common Bile Duct, and Duodenum

Neuroendocrine neoplasia arising from the ampulla, distal common bile duct, or duodenum is morphologically not different from primary pancreatic neuroendocrine neoplasms. As there are no known precursor lesions of these neoplasms that may aid in identifying the site of origin, the distinction is based almost exclusively on the localization of the tumor and its spatial relationship with the ampulla, distal common bile duct, or duodenal wall. However, certain neuroendocrine tumor types are more common in the ampulla and duodenum compared to the pancreas, which may help in establishing the correct diagnosis.

In the ampullary region, somatostatinoma (especially in patients with neurofibromatosis type 1), gangliocytic paraganglioma, neuroendocrine carcinoma, and mixed neuroendocrine—non-neuroendocrine neoplasm (MiNEN) are the most frequent neuroendocrine neoplasms. Gangliocytic paraganglioma and neuroendocrine carcinoma occur almost exclusively in the ampulla. Neuroendocrine neoplasms are more frequent in the major ampulla than in the minor ampulla.

The duodenum may harbor somatostatinomas, especially in patients suffering from neurofibromatosis type 1, and gastrinomas. Duodenal somatostatinomas are usually small (mean size 0.9 cm, 77% < 1 cm) compared to the larger pancreatic counterparts (mean size 3.8 cm, 6% < 1 cm). They often show a prominent glandular growth pattern and contain psammoma

bodies. Both of these features are usually absent or less prominent in pancreatic somatostatinomas. Liver metastasis at the time of presentation is rare in duodenal somatostatinoma (< 10%) but affects over half of the patients with a pancreatic primary (see Table 20.2). However, despite the small tumor size, 40–60% of the duodenal tumors have already spread to regional lymph nodes. The majority of duodenal gastrinomas occur in the clinical context of Zollinger-Ellison syndrome, either sporadically or in association with MEN1.

20.10 Mixed Neuroendocrine—Non-Neuroendocrine Neoplasm (MiNEN)

Mixed neuroendocrine—non-neuroendocrine neoplasms (MiNEN) contains two morphologically recognizable components: a neuroendocrine and a non-neuroendocrine neoplasm. Both components of a MiNEN should be characterized: ductal adenocarcinoma or acinar cell carcinoma as the non-neuroendocrine part, and PanNET or PanNEC as the neuroendocrine component (Table 20.6). MiNEN is to be distinguished from a pure pancreatic neuroendocrine neoplasm with entrapped nonneoplastic ductules. Conversely, adenocarcinoma containing scattered endocrine cells or enlarged residual nonneoplastic islets should not be mistaken for MiNEN.

MiNEN is extremely rare in the pancreas, where it represents only 0.5–2% of all ductal adenocarcinomas and 15–20% of all acinar cell carcinomas. Eighteen percent of all PanNECs are associated with an adenocarcinomatous component. Interestingly, MiNENs are less uncommon in the ampullary region, and in most of these tumors the neuroendocrine component is poorly differentiated. MiNENs are usually solid tumors that may be fairly large and show macroscopically visible areas of necrosis and cystic degeneration (Fig. 20.30).

Table 20.6 Subtypes of pancreatic mixed neuroendocrine—non-neuroendocrine neoplasms (MiNENs)

- Mixed ductal adenocarcinoma—neuroendocrine carcinoma (small-cell or large-cell)
- Mixed ductal adenocarcinoma—neuroendocrine tumor
- Mixed acinar cell carcinoma—neuroendocrine carcinoma (distinct components)
- Mixed acinar cell carcinoma—ductal adenocarcinoma-neuroendocrine carcinoma (distinct components)

Adapted from [1]

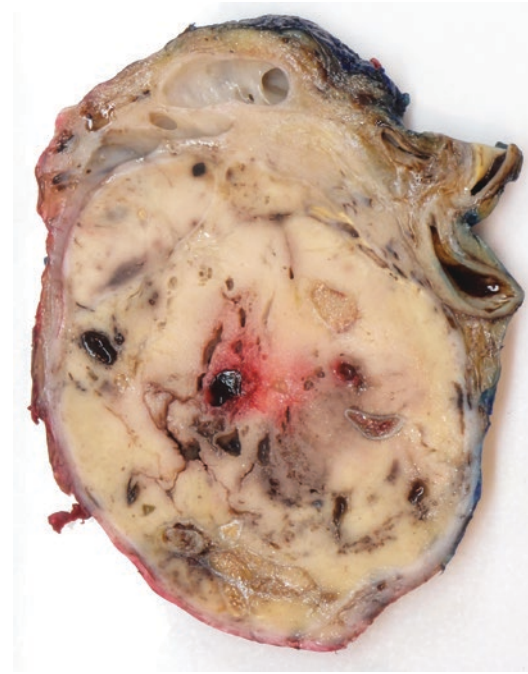

Fig. 20.30 Macroscopy of a MiNEN: this large well-circumscribed tumor in the pancreatic body consists of soft, fleshy, greyish tissue with foci of necrosis and hemorrhage. Histologically, the tumor was a MiNEN composed of NEC and acinar cell carcinoma

In pancreatic MiNENs, the neuroendocrine component is usually a NEC and only very rarely a NET (Fig. 20.31). While the outcome of a mixed ductal adenocarcinoma—PanNET is currently not known, the prognosis of a mixed ductal adenocarcinoma—PanNEC is possibly slightly better than that of a pure PanNEC. The NEC-component of a MiNEN should be characterized as small- or large-cell, and the extent of the NEC should be reported. While tumors with focal (< 30%) presence of a NEC component do not qualify as a MiNEN, the presence and extent of the NEC should be mentioned in the report.

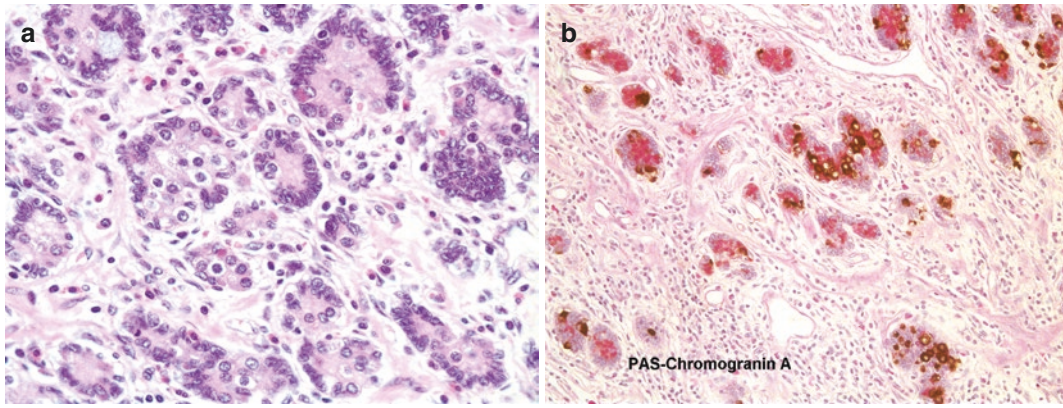

Fig. 20.31 MiNEN with a PanNET-component: the organoid growth pattern and cytological uniformity of this tumor are suggestive of a PanNET. However, scattered tumor cells have a foamy cytoplasm (**a**). PAS-staining (*pink*) combined with immunohistochemistry for chromogranin A (*brown*) reveals the intimate admixture of mucin-producing and endocrine tumor cells. Both cell populations represent >30% of the tumor (**b**)

The diagnosis of MiNENs usually requires immunohistochemical examination. Immunohistochemistry for neuroendocrine markers and Ki67 is valuable in confirming the presence of the neuroendocrine component and assessing its proliferative activity. Immunostaining for CK19 and MUC1/MUC2 can be used for confirmation of the ductal adenocarcinoma component, if the latter is poorly differentiated and cannot be unequivocally diagnosed morphologically. Interpretation of the results of PAS-staining and immunohistochemistry for CEA and CA19-9 should be circumspect, as these may also be positive in pure pancreatic neuroendocrine neoplasia, in particular in areas with a glandular growth pattern (see Sect. 20.9.1).

The definitive diagnosis of MiNENs containing acinar cell carcinoma as the non-neuroendocrine component usually requires immunohistochemical confirmation of the presence of acinar (trypsin, chymotrypsin, BCL10 positive) and neuroendocrine differentiation (synaptophysin, chromogranin positive). Both components should be present as distinct albeit closely connected compartments within the tumor. Acinar cell carcinomas in which neuroendocrine differentiation is detected only immunohistochemically do not qualify as a MiNEN (see Chap. 10, Sect. 10.8).

Mixed acinar cell carcinoma-ductal adenocarcinoma-neuroendocrine carcinoma is considered a MiNEN (Table 20.6) but it is extremely rare.

20.11 Prognosis

The prognosis for patients with PanNETs is significantly better than for those suffering from ductal adenocarcinoma. Following surgical resection, the 5-year survival rate for PanNETs (excluding insulinomas) is 65–86%, the 10-year rate 45–68%. Overall, PanNETs are more aggressive than their counterparts in the tubular digestive tract. The functional status does not convincingly influence outcome, with the exception of insulinomas, of which approximately 80–90% are benign. Patients suffering from a PanNET with ectopic hormonal production have a poorer outcome, as these tumors are usually large and have metastasized at the time of presentation.

The difference in survival between patients with local and regional disease is not significant. However, the presence of distant metastasis—usually to the liver—confers a prominent reduction in survival, the 5-year survival rate being 59% and the 10-year rate 36%. Nevertheless, many patients survive for several years following development of

liver metastasis due to the slow progression of the disease. The most important histological predictor of outcome is the proliferative activity, based on the Ki67 index or mitotic count. The newly introduced category of PanNET grade 3 progresses more rapidly than PanNET grade 2 (5-year survival rate: 29% versus 62%), but is less aggressive than PanNEC (5-year survival rate: 16%). The next most potent predictor is tumor size. Low-grade PanNETs smaller than 2 cm have a very indolent behavior, which is the rationale to suggest a watch-and-wait approach for patients with these tumors. Tumor extent, vascular invasion, necrosis, and lymph node metastasis all confer an increased risk for distant metastasis. Cystic PanNETs seem to have a better prognosis, because they often lack adverse prognostic factors and present at a lower stage. In recent years, the advancement in multimodality treatment of metastatic disease has contributed significantly to the improvement in survival. Surgery is generally the procedure of choice in patients with resectable tumors. Over 30% of patients with a PanNET have distant metastasis at the time of diagnosis, which is not necessarily a contraindication for surgical resection of the primary tumor.

PanNECs are aggressive malignancies, which often have reached an advanced and unresectable stage at the time of diagnosis. Accordingly, the prognosis is only 6–12 months. Less than 25% of patients survive longer than 2 years. PanNECs of large cell type are only marginally less aggressive than those of small cell type.

20.12 Inherited Syndromes

PanNETs can occur in the context of four inherited syndromes: multiple endocrine neoplasia type 1 and type 4 (MEN1, MEN4), von Hippel-Lindau syndrome (VHL), neurofibromatosis type 1 (NF1), and the tuberous sclerosis complex (TSC) (Table 20.7). All are autosomal dominant tumor syndromes. PanNETs are most frequent in patients with MEN1, significantly less common in VHL, and rare in NF1 and TSC. The most common PanNETs occurring in MEN1 are nonfunctioning. Gastrinomas, though frequent in MEN1 (54% of neuroendocrine tumors), are usually duodenal, not pancreatic, in origin. Many PanNETs are multihormonal but with one dominant hormone, most commonly glucagon, followed in decreasing frequency by pancreatic polypeptide, insulin, somatostatin, and rarely other hormones. PanNETs account for a significant proportion of MEN1-related deaths, and therefore they require careful management. In contrast, PanNETs are an uncommon cause of mortality in patients with VHL. Only 11–17% of these patients develop PanNETs, which are

Table 20.7 Pancreatic neuroendocrine tumors in inherited syndromes

Inherited syndrome	Gene (encoded protein)	Frequency of PanNETs	Type of PanNETs (in decreasing order of relative frequency)
MEN 1	*MEN1* (Menin)	30–75%	Nonfunctioning (including microadenomas) Gastrinoma (duodenal) Insulinoma Glucagonoma Other
MEN 4	*CDKN1B* (p27)	Unknown	Nonfunctioning
VHL	*VHL* (VHL)	11–17%	Nonfunctioning (>98%)
NF1	*NF1* (Neurofibromin)	0–10%	Somatostatinoma (mainly duodenal, rarely pancreatic)
TSC	*TSC2* (Hamartin) *TSC1* (Tuberin)	Uncommon	Nonfunctioning Functioning

Abbreviations: *MEN 1* multiple endocrine neoplasia type 1, *MEN 4* multiple endocrine neoplasia type 4, *NF1* neurofibromatosis type 1, *PanNET* grade 1–3 pancreatic neuroendocrine tumor, *TSC* tuberous sclerosis complex, *VHL* von Hippel-Lindau syndrome

almost invariably nonfunctioning and asymptomatic. Up to 60% of PanNETs in VHL contain clear cells or multivacuolated lipid-rich cells, focally or diffusely, which are immunopositive for CAIX. Neuroendocrine tumors in NF1 are almost exclusively somatostatinomas of the periampullary region. PanNETs, both functioning and nonfunctioning, have been reported in a small proportion of individuals with TSC. The main clinical features of the four inherited syndromes associated with PanNETs are summarized in Table 20.8.

MEN4 is a very rare tumor syndrome with a phenotype that is similar to MEN1. Hence, patients presenting with features suggestive of MEN1 but without *MEN1* mutations should be tested for *CDKN1B* mutations, which are the underlying gene defect in MEN4 [19].

Table 20.8 Extrapancreatic lesions in multiple endocrine neoplasia type 1, von Hippel-Lindau syndrome, neurofibromatosis type 1, and tuberous sclerosis complex

Inherited syndrome	Prevalence	Lesions
MEN 1	1:40,000–1:20,000	• Parathyroid hyperplasia/adenoma • Duodenal endocrine tumors • Cutaneous lesions (lipoma, angiofibroma) • Anterior pituitary adenoma (functioning/nonfunctioning) • Adrenocortical tumors (functioning/nonfunctioning) • Thymic and bronchial neuroendocrine tumors • Gastric ECL-cell hyperplasia/tumors • Central nervous system tumors • Soft tissue tumors
MEN 4	Very rare	MEN1-like phenotype: NETs in parathyroid glands, pituitary, pancreas, and rarely other sites (cervix, bronchus, stomach)
VHL	1:36,000	• Pheochromocytoma, paraganglioma • Renal cell carcinoma • Hemangioblastoma (central nervous system, peripheral/spinal nerves, retina) • NETs in ampulla, duodenum, gallbladder, common bile duct • Papillary cystadenoma of epididymis/broad ligament, mesosalpinx • Endolymphatic sac tumor • Cysts of adrenal gland, kidney, testis, ovary
NF1	1:2500–1:3000	• Cafe au lait spots • Neurofibroma • Malignant peripheral nerve sheath tumor • Axillary or inguinal freckling • Duodenal NET, gangliocytic paraganglioma • Pheochromocytoma • CNS tumors (pilocytic astrocytoma of optic nerve, brain stem glioma, cerebellar astrocytoma) • Bone lesions • Lisch nodules
TSC	7–12:100,000	• Facial angiofibromas • Periungual fibroma • Hypomelanotic macules • Connective tissue nevus • Subependymal astrocytoma • Retinal nodular hamartomas • Lymphangioleiomyomatosis • Renal angiomyolipoma • Bone cysts • Hamartomatous rectal polyps • Gingival fibromas

Abbreviations: *ECL* enterochromaffin like, MEN1 multiple endocrine neoplasia type 1, *MEN4* multiple endocrine neoplasia type 4, *NET* neuroendocrine tumor, *NF1* neurofibromatosis type 1, *TSC* tuberous sclerosis complex, *VHL* von Hippel-Lindau syndrome

20.13 Glucagon Cell Hyperplasia and Neoplasia

Glucagon cell hyperplasia and neoplasia (GCHN), also known as Mahvash syndrome, is an autosomal recessive inherited disorder caused by germline mutation of the *GCGR* (glucagon receptor) gene [20]. It is characterized by the presence of glucagon cell hyperplasia, glucagon cell microadenomas, and glucagon-producing macroscopically visible PanNETs [21, 22]. It is believed that germline mutation of *GCGR* results in the absence of glucagon signaling in the liver, which in its turn induces glucagon cell hyperplasia and subsequent glucagon cell neoplasia. The pancreas may be diffusely enlarged or of normal size and contains numerous enlarged, hyperplastic islets with increased numbers of α-cells. In addition, there are endocrine microadenomas and PanNETs which immunohistochemically consist almost exclusively of glucagon-producing cells (Fig. 20.32). The Ki67 index in these tumors is usually very low (<1%).

GCHN is an extremely rare disease, and only a few cases have been reported to date. While glucagon serum levels are usually elevated, not all patients with GCHN have glucagonoma syndrome. The disease is usually benign, although metastasis has been reported. Not all patients with GCHN have a *GCGR* mutation, and in those with wild-type *CGCR*, the pathomechanism of the disease remains unknown.

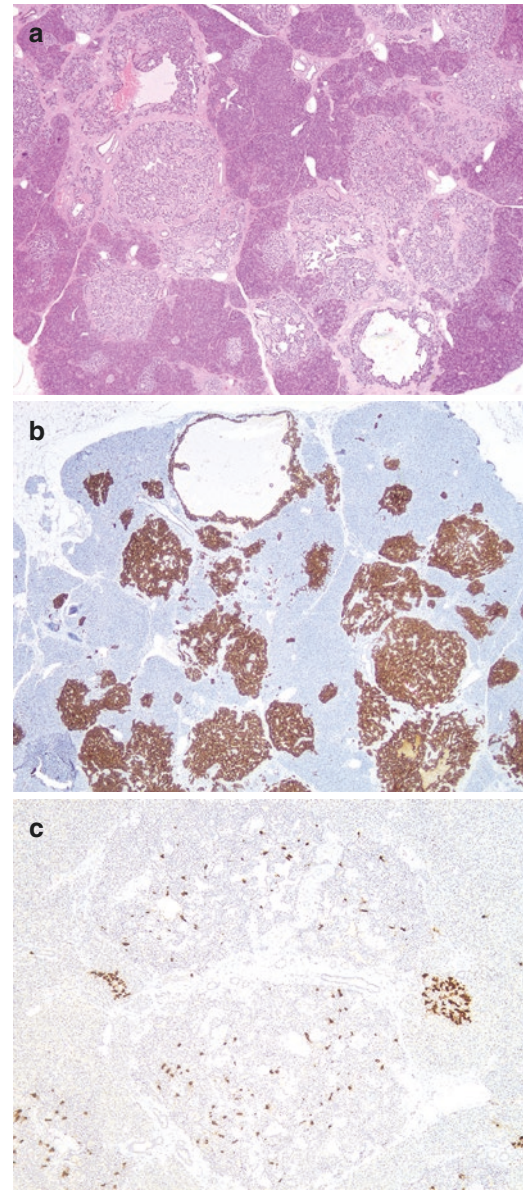

Fig. 20.32 Alpha-cell hyperplasia: islets appear more numerous than normal. They are enlarged and show some architectural irregularity. There is mild fibrosis in and around some of the abnormal islets. Note the presence of scattered normal-appearing islets (**a**). Immunostaining for glucagon demonstrates the predominance of α-cells in the enlarged islets. Note the normal number of α-cells in the unremarkable islets (**b**). Immunohistochemistry for insulin highlights the presence of very few β-cells within the hyperplastic islets, whereas a normal high number is present in unremarkable islets (**c**)

20.14 Insulinomatosis

Insulinomatosis is a condition characterized by the synchronous or metachronous occurrence of multicentric insulinomas causing hyperinsulinemic hypoglycemia [4]. Insulinomatosis usually occurs sporadically but has also been reported in a few kindreds and was recently linked to missense mutation of the gene encoding V-Maf avian musculoaponeurotic fibrosarcoma oncogene homolog A (*MAFA*) [23]. The insulinomas can be macrotumors or microscopically small tumors, but all express insulin exclusively (Fig. 20.33). In addition, small,

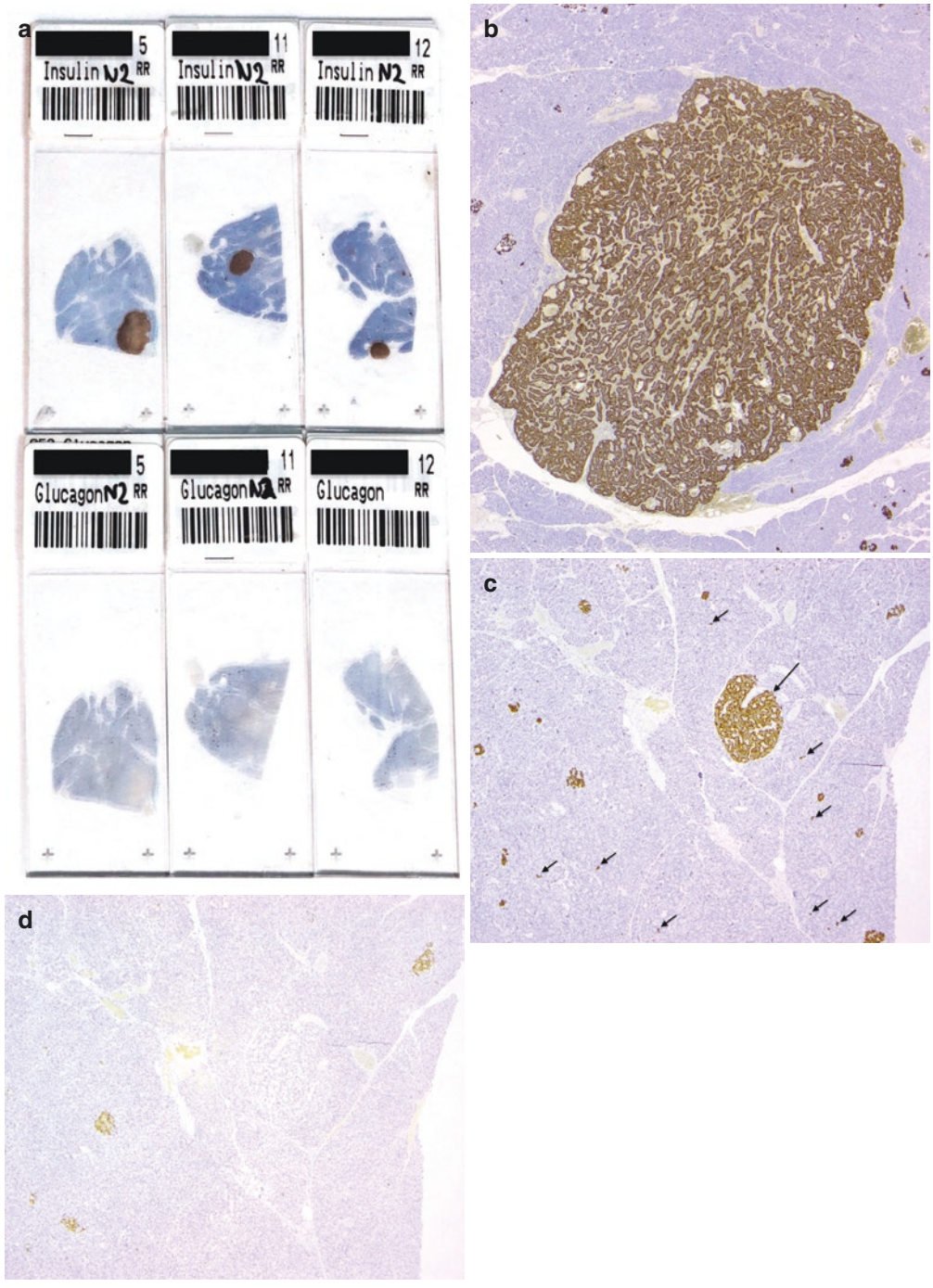

Fig. 20.33 Insulinomatosis: a distal pancreatectomy specimen contains three macroscopically visible PanNETs. On immunostaining, all three are positive for insulin and negative for glucagon (**a**: immunostaining for insulin [upper row] and glucagon [lower row]). All tumor cells show strong immunostaining for insulin (**b**). In addition to the three gross tumors, there are endocrine microadenomas that consist exclusively of β-cells (*long arrow*). Note the presence of scattered, small clusters of insulin-producing cells (*short arrows*) in addition to β-cells in normal islets (**c**). Immunostaining for glucagon is positive only in the islets of Langerhans, while the endocrine microadenoma and the small, scattered endocrine cell foci seen in (**c**) are negative (**d**)

proliferative, insulin-expressing monohormonal endocrine cell clusters have been described as the putative precursor lesions of the multifocal insulinomas. The tumors are usually benign, and metastatic spread is rare. The disease differs from solitary sporadic and MEN1-associated insulinomas.

20.15 Endocrine Microadenoma and Endocrine Microadenomatosis

An endocrine microadenoma of the pancreas is defined as a neuroendocrine neoplasm measuring less than 5 mm in size (Fig. 20.34). The features that distinguish an endocrine microadenoma from an enlarged nonneoplastic islet are the altered, usually trabecular, cell arrangement, the presence of a more prominent hyaline stroma, and the absence of the normal distribution of α-, β-, δ- and PP-cells in terms of cell numbers and localization within the islets of Langerhans (Fig. 20.35) (see Chap. 1, Sect. 1.4.4). In endocrine microadenomas, immunostaining for hormones is either absent or dominated by one islet hormone, with loss of the usual topographical distribution. Enlarged or aggregated islets in the context of chronic pancreatitis may exhibit an increased number of glucagon- and PP-producing cells, but the β- and δ-cells are always preserved, albeit in slightly reduced numbers (see Chap. 21, Fig. 21.1). Endocrine microadenomas are considered benign, but it is currently not known whether all or only some progress to clinically relevant PanNETs.

Endocrine microadenomatosis is defined as the presence of multiple, usually innumerable, microadenomas (Fig. 20.36). It is considered the hallmark of MEN1 but may also occur in patients with VHL, and, occasionally, in individuals without an apparent genetic syndrome. Multiple endocrine microadenomas that are exclusively composed of β-cells are seen in patients with insulinomatosis, who also develop multiple synchronous and metachronous macroscopic insulinomas. Endocrine microadenomatosis is to be distinguished from reactive islet clustering and enlargement (see above), from the diffuse type of islets normally present in the inferior part of the pancreatic head (see Chap. 1, Sect. 1.4.4) and from endocrine cell hyperplasia (see Chap. 21, Sect. 21.1).

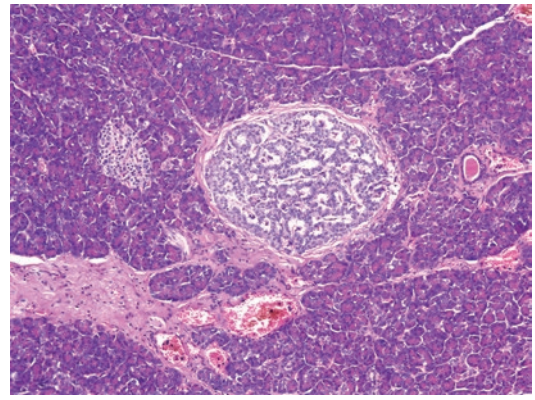

Fig. 20.34 Endocrine microadenoma: the increased size, trabecular cell arrangement, and surrounding thin sheath of fibrous stroma distinguish this endocrine microadenoma from an adjacent normal islet

20.16 Reporting Checklist

A reporting checklist of the data items to consider when reporting on pancreatic neuroendocrine neoplasia is provided in Table 20.9.

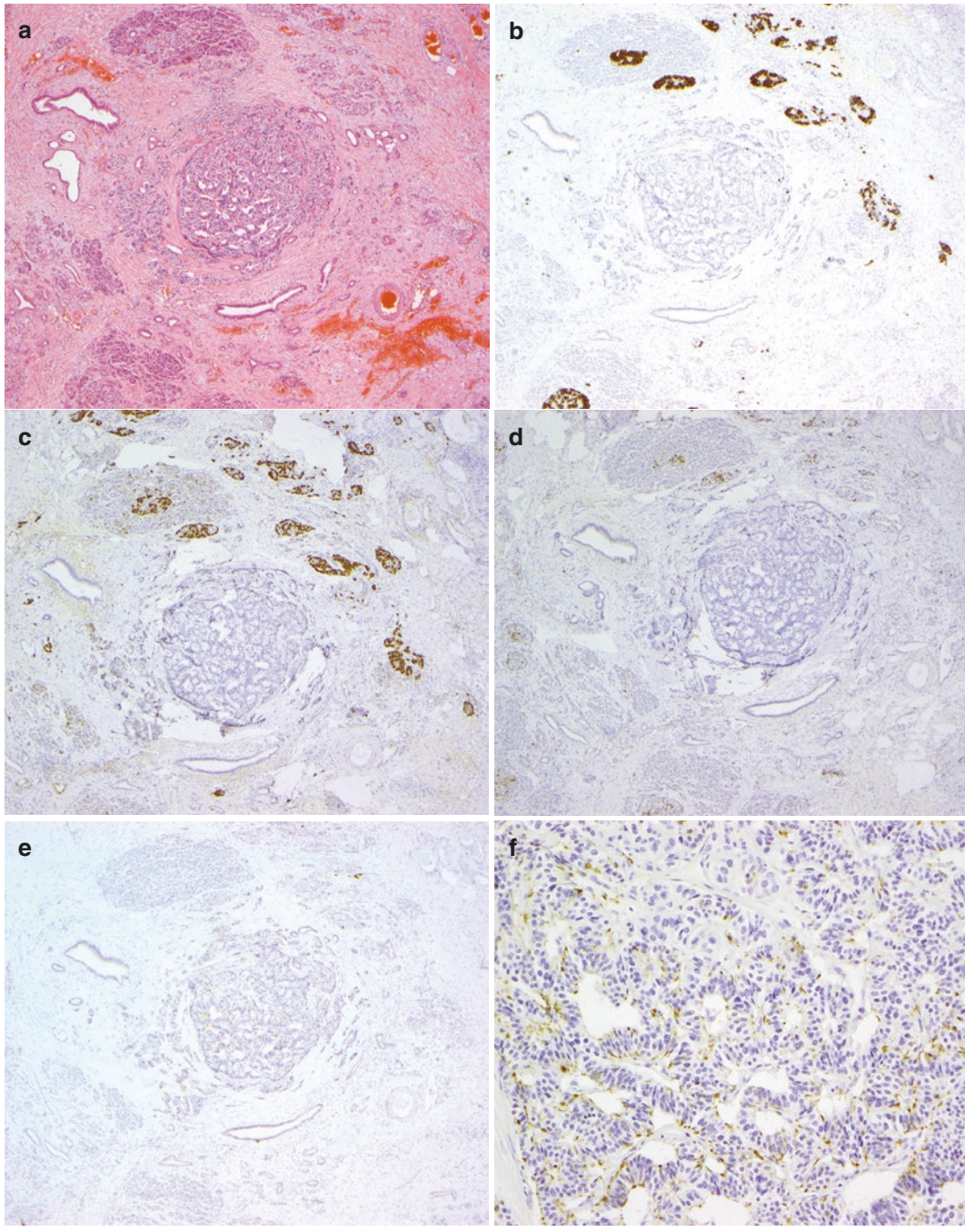

Fig. 20.35 Endocrine microadenoma: this incidentally identified endocrine microadenoma measures 0.8 mm in diameter and consists of monomorphous lesional cells that are arranged in a trabecular pattern. Note the increased fibrous stroma, especially in the periphery of the lesion (**a**). Immunostaining for insulin (**b**), glucagon (**c**), and somatostatin (**d**) is negative in the lesion but preserved in the surrounding islets of Langerhans. In contrast, all cells of the endocrine microadenoma show labeling for pancreatic polypeptide (**e** and **f**)

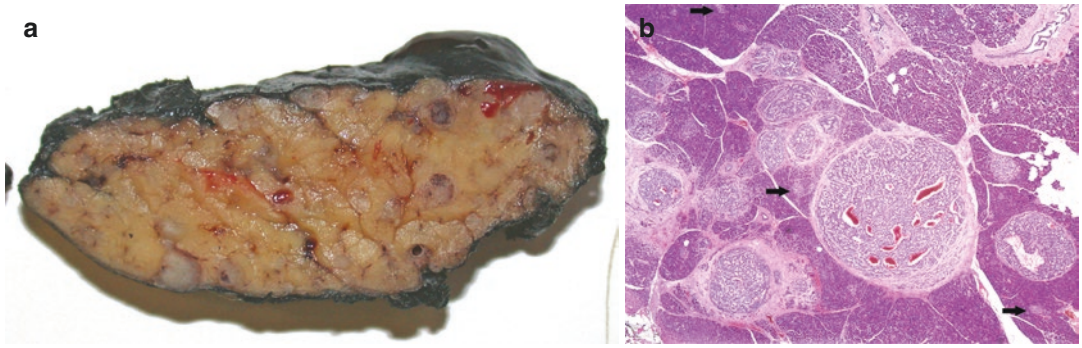

Fig. 20.36 Endocrine microadenomatosis: pancreatic parenchyma in this patient with MEN1 is studded with numerous well-circumscribed tumors, the vast majority of which measure less than 5 mm in size (**a**). Histologically, there are countless endocrine microadenomas. Note the presence of scattered normal-appearing islets (*arrows*) (**b**)

Table 20.9 Reporting checklist for pancreatic endocrine neoplasia

Microscopic assessment
• Specimen type (e.g., pancreatoduodenectomy, distal/total pancreatectomy, enucleation)
• Additional resected structures/organs (e.g., spleen, SMV)
• Tumor: – Unifocal/multifocal – Site – Size (3 dimensions) – Solid/cystic, color
Microscopic assessment
• Classification: – Pure neuroendocrine neoplasm Neuroendocrine tumor Neuroendocrine carcinoma – Mixed tumor (MiNEN): Mixed with ductal adenocarcinoma Mixed with acinar cell carcinoma Proportion of each component (in %)
• Differentiation: – Well-differentiated – Poorly differentiated
• Grade (based on WHO classification 2019): – Low – Intermediate – High
• Morphological variant
• Local tumor extent (e.g., limited to pancreas, or invasion of duodenum/ampulla, common bile duct, peripancreatic soft tissue, spleen, SMV, splenic vein)
• Tumor propagation: lymphatic, vascular, perineural
• Tumor metastasis: – Regional lymph nodes (location, number involved, total number) – Extraregional lymph nodes (location, number involved, total number) – Other

Table 20.9 (continued)

Microscopic assessment
• Completeness of resection (nearest margin(s), minimum clearance)
• Staging: – pTNM (according to UICC 8th edition and/or ENETS) – Further descriptors (pLVPnR)
• Ancillary tests/Immunohistochemistry: – Neuroendocrine markers: confirmation of neuroendocrine differentiation – Ki67: proliferation index (or mitotic count, if higher than Ki67 index) – p53, RB1, p16 – Hormones: Stained for/positive Clinically functioning tumor? – Markers of non-endocrine differentiation (in MiNEN): Adenocarcinoma (e.g., mucin stains, MUC1/2, CK19) Acinar cell carcinoma (e.g., trypsin, chymotrypsin, BCL10)
• Background changes (e.g., multiple endocrine neoplasia type 1, von Hippel-Lindau syndrome, neurofibromatosis 1)

Abbreviations: *ENETS* European Neuroendocrine Tumour Society, *G* grade, *MiNEN* mixed neuroendocrine—non-neuroendocrine neoplasm, *SMV* superior mesenteric vein, *UICC* International Union Against Cancer

References

1. Lokuhetty D, White V, Watanabe R, Cree IA, editors. Digestive system of malignant tumours. WHO classification of tumours. 5th ed. Lyon, France: IARC Press. 2019. Chap. 10, p. 343–72.
2. Bosman FT, Carneiro F, Hurban RH, Theise ND, editors. WHO classification of tumours of the digestive system. WHO classification of tumours. 4th ed. Lyon, France: IARC Press. 2010. Chap. 12, 322–6.
3. Heitz PhU, Komminoth P, Perren A, Klimstra DS, Dayal Y, Bordi C, Lechago J, Centeno BA, Klöppel G. Tumours of the endocrine pancreas. In: DeLellis RA, Lloyd RV, Heitz PU, Eng C, editors. Pathology & genetics. Tumours of endocrine organs. WHO classification of tumours. Lyon: International Agency for Research on Cancer (IARC); 2004. Chap. 4. p. 176–208.
4. Anlauf M, Bauersfeld J, Raffel A, Koch CA, Henopp T, Alkatout I, et al. Insulinomatosis. A multicentric insulinoma disease that frequently causes early recurrent hyperinsulinemic hypoglycaemia. Am J Surg Pathol. 2009;33:339–46.
5. Verbeke CS. Endocrine tumours of the pancreas. Histopathology. 2010;56:669-82.
6. Yachida S, Vakiani E, White CM, Zhong Y, Saunders T, Morgan R, et al. Small and large cell neuroendocrine carcinomas of the pancreas are genetically similar and distinct from well-differentiated pancreatic neuroendocrine tumors. Am J Surg Pathol. 2012;36:173–84.
7. Klöppel G, Rindi G, Perren A, Komminoth P, Klimstra DS. The ENETS and AJCC/UICC TNM classifications of the neuroendocrine tumors of the gastrointestinal tract and the pancreas: a statement. Virchows Arch. 2010;456:595–7.
8. Couvelard A. Neuroendocrine tumours of the pancreas: recent developments in staging and grading. Diagnostic Pathol. 2012;18:1–7.
9. Basturk O, Tang L, Hruban RH, Adsay NV, Yang Z, Krasinskas AM, et al. Poorly differentiated neuroendocrine carcinomas of the pancreas: a clinicopathologic analysis of 44 cases. Am J Surg Pathol. 2014;38:437–47.
10. Perren A, Couvelard A, Scoazec J-Y, Costa F, Borbath I, Delle Fave G, et al. ENETS consensus guidelines for the standards of care in neuroendocrine tumors: Pathology: diagnosis and prognostic stratification. Neuroendocrinology. 2017;105:196–200.
11. Selberherr A, Koperek O, Riss P, Scheuba C, Kaderli R, Perren A, Niederle B. Neuroendocrine liver metastasis—a specific set of markers to detect primary tumor sites. Endocr Pathol. 2019;30:31–4.
12. Yang MX, Coates RF, Ambaye A, Cortright V, Mitchell JM, Buskey AM, et al. NKX2.2, PDX-1 and CDX-2 as potential biomarkers to differentiate well-differentiated neuroendocrine tumors. Biomark Res. 2018;6:15.
13. Lai JP, Mertens RB, Mirocha J, Koo J, Venturina M, Chung F, Mendez AB, Kahn M, Dhall D. Comparison of PAX6 and PAX8 as immunohistochemical markers for pancreatic neuroendocrine tumors. Endocr Pathol. 2015;26:54–62.

14. Brierly JD, Gospodarowicz MK, Wittekind C, editors. UICC: TNM classification of malignant tumours. 8th ed. Oxford: Wiley-Blackwell; 2017.
15. Rindi G, Falconi M, Klersy L, Albarello L, Boninsegna M, Büchler MW, et al. TNM staging of neoplasms of the endocrine pancreas: results from a large international cohort study. J Natl Cancer Inst. 2012;104:764–77.
16. Zhang XF, Cloyd J, Lopez-Aguiar AG, Poultsides G, Makris E, Rocha F, et al. Margin status and long-term prognosis of primary pancreatic neuroendocrine tumor after curative resection: results from the US Neuroendocrine Tumor Study Group. Surgery. 2019;165:548–56.
17. Takahashi T, Hatakeyama S, Machida T. Ductal adenocarcinoma of the pancreas with psammomatous calcification: report of a case with immunohistochemical study for bone morphogenetic protein. Pathol Int. 2011;61:603–7.
18. Schneider NI, Bauernhofer T, Schöllnast H, Ott A, Langner C. Pancreatic adenocarcinoma with multiple eosinophilic extracellular deposits consistent with noncalcified psammoma bodies. Virchows Arch. 2011;459:623–5.
19. Alrezk R, Hannah-Shmouni F, Stratakis CA. MEN4 and CDKN1B mutations: the latest of the MEN syndromes. Endocr Relat Cancer. 2017;24:T195–208.
20. Miller HC, Kidd M, Modlin IM, Cohen P, Dina R, Drymousis P, et al. Glucagon receptor gene mutations with hyperglucagonemia but without the glucagonoma syndrome. World J Gastrointest Surg. 2015;7:60–6.
21. Sipos B, Sperveslage J, Anlauf M, Hoffmeister M, Henopp T, Buch S, et al. Glucagon cell hyperplasia and neoplasia with and without glucagon receptor mutations. J Clin Endocrinol Metab. 2015;100:E783–8.
22. Henopp T, Anlauf M, Schmitt A, Schlenger R, Zalatnai A, Couvelard A et al. Glucagon cell adenomatosis: a newly recognised disease of the endocrine pancreas. J Clin Endocrinol Metab. 2009;94:213–7.
23. Iacovazzo D, Flanagan SE, Walker E, Quezado R, de Sousa Barros FA, Caswell R, et al. MAFA missense mutation causes familial insulinomatosis and diabetes mellitus. PNAS. 2018;11:1027–32.

Further Reading

Falconi M, Eriksson B, Kaltsas G, Bartsch DK, Capdevila J, Caplin M, et al. ENETS consensus guidelines update for the management of patients with functional pancreatic neuroendocrine tumors and non-functional pancreatic neuroendocrine tumors. Neuroendocrinology. 2016;103:153–71.

Check for updates

Endocrine Cell Hyperplasia

21

21.1 Definition

The term 'endocrine cell hyperplasia' refers in fact to two separate groups of nonneoplastic disorders. The larger group encompasses several conditions in which the hyperplastic process affects the *entire endocrine cell compartment*, that is, the α-, β-, δ- and PP-cell populations. The second and much smaller group is characterized by hyperplasia of *only one specific endocrine cell type*. Thus far, endocrine cell hyperplasia of only a single cell type has been reported for the α-, β-, and PP-cell types. The group of hyperplastic disorders affecting all endocrine cell types usually represents an adaptive or secondary process, for instance in infants of diabetic mothers, or in erythoblastosis fetalis (see Chap. 13, Table 13.1). In contrast, for some of the endocrine cell hyperplasias affecting a single specific cell type, the underlying cause has been identified as a single-gene defect.

Histologically, both groups of hyperplastic processes show a similar picture that is characterized by a *diffuse* expansion of the endocrine cell compartment. The criteria for the histological diagnosis of endocrine cell hyperplasia are not well defined. An expansion of the endocrine cell mass by more than 2% in adults or 10% in infants has been proposed [1]. However, this definition is impractical in diagnostic practice. Currently, an islet size larger than 250 μm together with an increase in islet numbers is regarded by most as an acceptable definition of endocrine cell hyperplasia, provided the change is present diffusely throughout the pancreas. In addition, immunohistochemistry is required to identify the specific endocrine cell type(s) that are involved in the hyperplastic process.

Similar but *focal* hyperplastic changes affecting all endocrine cell populations are not uncommon incidental findings. In autopsy series they have been described in up to 10% of individuals, occasionally in association with endocrine microadenomas. Also to be distinguished from endocrine cell hyperplasia is the patchy, reactive enlargement and clustering of islets that is commonly seen in chronic pancreatitis. All four islet cells types are expanded, although sometimes there seems to be a preponderance of α- and PP-cells (Fig. 21.1) (see Chap. 7, Sect. 7.2.4).

A further differential diagnosis for endocrine cell hyperplasia is the endocrine microadenomatosis that occurs in patients with multiple endocrine neoplasia type 1 (MEN1) or von Hippel-Lindau syndrome. While in endocrine microadenomatosis each individual endocrine microadenoma usually has a dominant particular cell type (e.g., β-cells), the numerous tumors that are present throughout the pancreas are of varying cell types (e.g., α-, β-, δ-, PP-cells). Similarly, the diffuse hyperplasia of pancreatic endocrine cells that often accompanies endocrine microadenomatosis, also affects all endocrine cell types.

© Springer Nature Switzerland AG 2021
F. Campbell, C. S. Verbeke, *Pathology of the Pancreas*,
https://doi.org/10.1007/978-3-030-49848-1_21

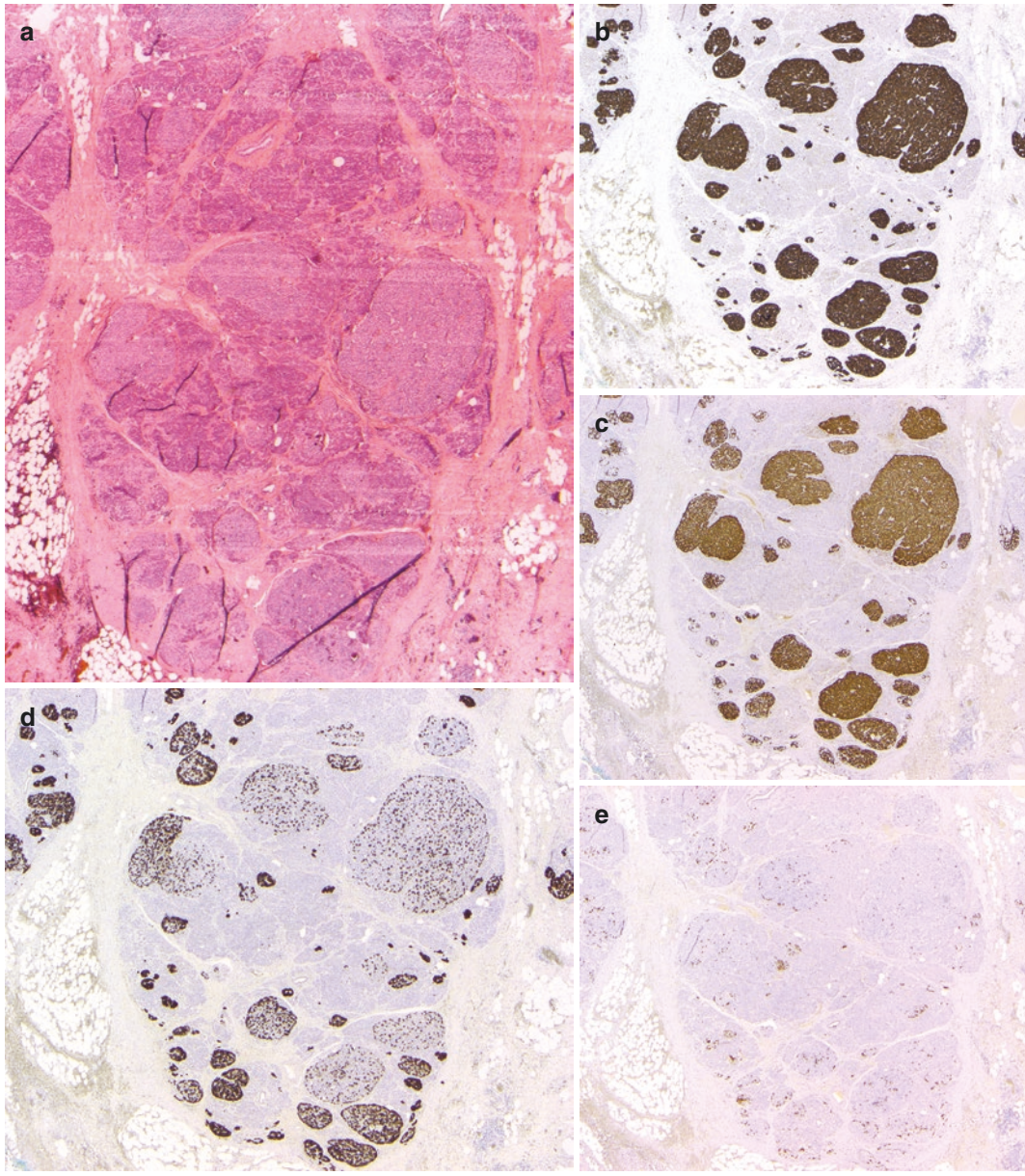

Fig. 21.1 Reactive islet enlargement with expansion of α-cells: enlarged islets, usually in the context of acinar atrophy, may be seen in various settings, including chronic pancreatitis (**a**: HE-staining, **b**: immunostaining for synaptophysin). Immunostaining shows a dominance of glucagon-producing α-cells (**c**) over insulin-producing β-cells (**d**) and somatostatin-producing δ-cells (**e**). Compare with the dominance of β-cells over α-cells in normal islets as shown in Fig. 1.19

Described below in more detail are three forms of endocrine cell hyperplasia of the pancreas in the strict sense, that is, the nonneoplastic processes characterized by hyperplasia of a single specific endocrine cell type. While these conditions are rare, the incidence differs depending on which specific endocrine cell type is affected: β-cell hyperplasia is significantly more frequent than hyperplasia of the α- or PP-cell population, of which only a few cases have been reported so

far. Equally different are the clinical signs and symptoms, the morphological features, and possible genetic aberrations of these three disorders. In none of the conditions is there evidence for an association with MEN1, MEN4, von Hippel-Lindau syndrome, neurofibromatosis type 1, or the tuberous sclerosis complex [2].

21.2 Beta-Cell Hyperplasia

Beta-cell hyperplasia is the morphological change seen in infants and neonates with persistent hyperinsulinemic hypoglycemia (PHIH) and in the rare condition found in adults with non-insulinoma-pancreatogeneous hypoglycemia (NIPH). The majority of PHIH patients show diffuse changes in size and shape of the islets, which still contain all endocrine cell types in a preserved spatial distribution but with an overall increase in the number of β-cells. In approximately a third of patients with PHIH, β-cell hyperplasia is focal and characterized by huge islet-like structures, which contain all types of endocrine cells, but lead to an overall increase in the proportion of β-cells (raised from the normal 50% to 70–90%). Distinction of both forms of PHIH is clinically important, because partial pancreatectomy is sufficient for patients with the focal form, whereas (sub-)total pancreatectomy is required for those with the diffuse form. Recent advances in genetics have linked congenital PHIH to mutations in 14 different genes that play a key role in regulating insulin secretion [3].

In adults, NIPH is characterized mainly by postprandial hypoglycemia (rather than the fasting hypoglycemia of patients with insulinoma). Islets have a preserved structure with normal distribution of all endocrine cell types, but the β-cells are more numerous, and the islets are increased in size and number. Unlike the β-cell hyperplasia found in infants and neonates, NIPH in adults is not associated with mutations of the ATP-sensitive potassium channel. Nesidioblastosis, which in the current strict morphological sense describes budding of endocrine cells (of any type, not only β-cells) from duct epithelium, is seen in both PHIH and NIPH. Neither NIPH nor PHIH has ever been observed in association with the development of pancreatic endocrine tumors, nor have these conditions been described in patients with MEN1 or von Hippel-Lindau syndrome.

Beta-cell hyperplasia must be distinguished from insulinomatosis, a disease characterized by the synchronous and metachronous occurrence of insulinomas, β-cell endocrine microadenomas, and small β-cell clusters in patients with insulinomatosis (see Chap. 20, Sect. 20.14).

21.3 Alpha-Cell Hyperplasia

Alpha-cell hyperplasia is part of the inherited autosomal recessive disorder glucagon cell hyperplasia and neoplasia, which is described in Chap. 20, Sect. 20.13 (see Fig. 20.32).

21.4 PP-Cell Hyperplasia

The morphological findings in PP-cell hyperplasia are similar to those described for α-cell hyperplasia, except that the hyperplastic cell population is of a PP-cell type (Fig. 21.2) [4, 5]. PP-cell hyperplasia is a diffuse process that affects the entire pancreas, and is therefore readily distinguished from the diffuse islets, which also contain an increased number of PP-cells but are confined to the posteroinferior part of the pancreatic head (see Chap. 1, Sect. 1.4.4). In most patients, PP-cell hyperplasia is an incidental finding in pancreatic specimens resected for other reasons. As serum PP levels have not been measured in most reported cases, it is currently not clear if PP-cell hyperplasia causes elevated PP levels. Some of the reported patients presented with diarrhea, but it is uncertain whether this is related to PP-cell hyperplasia. The etiology of this condition remains elusive so far.

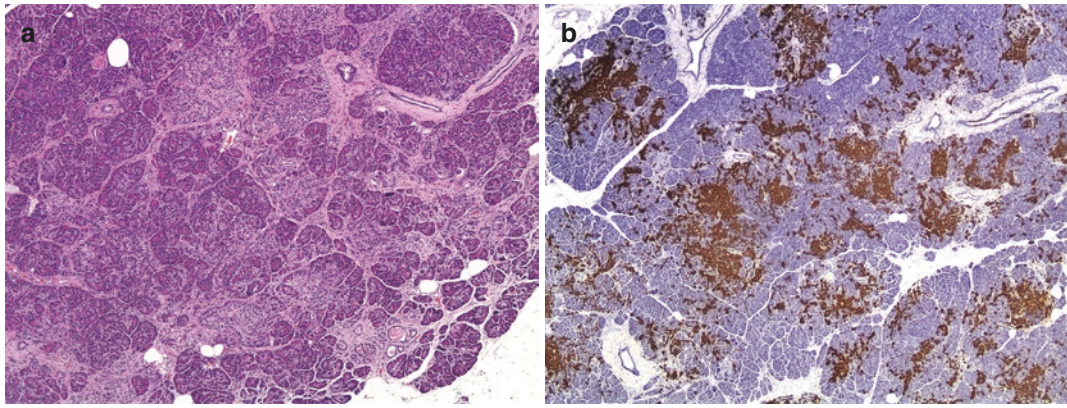

Fig. 21.2 PP-cell hyperplasia: numerous ill-defined and enlarged islets are present throughout the pancreatic tissue (**a**). Immunostaining illustrates the dominance of PP-cells within the expanded endocrine compartment (**b**)

References

1. Rindi G, Solcia E. Endocrine hyperplasia and dysplasia in the pathogensis of gastrointestinal and pancreatic endocrine tumors. Gastroenterol Clin North Am. 2007;36:851–65.
2. Ouyang D, Dhall D, Yu R. Pathologic pancreatic endocrine cell hyperplasia. World J Gastroenterol. 2011;17(2):137–43.
3. Galcheva S, Al-Khawaga S, Hussain K. Diagnosis and management of hyperinsulinaemic hypoglycaemia. Best Pract Res Clin Endocrinol Metab. 2018;32:551–73.
4. Albazaz R, Da Costa PE, Verbeke CS. Pancreatic polypeptide cell hyperplasia of the pancreas. J Clin Pathol. 2006;59:1087–90.
5. Talmon GA, Wren JD, Nguyen CL, Pour PM. Pancreatic polypeptide cell proliferation in the pancreas and duodenum coexisting in a patient with pancreatic adenocarcinoma treated with a GLP-1 analog. Pancreas. 2017;46:820–4.

Part V

Transplant Pathology

Pathology of Pancreas Transplantation

22

René P. Michel

22.1 Introduction

Diabetes mellitus (either overt or undiagnosed) is the principal indication for pancreas transplantation. In the USA in 2015, an estimated 30.3 million people, equivalent to 9.4% of the population, had diabetes mellitus (DM) with 5–10% having type 1 diabetes mellitus (T1DM) [1]. Diabetes is also the most common cause of end-stage renal failure, blindness, and a major contributing factor for peripheral vascular and coronary artery disease [2, 3]. Administration of exogenous insulin is an effective treatment for T1DM and selected patients with type 2 diabetes, and tight control of blood glucose levels reduces or slows down complications [4]. However, large fluctuations in levels of glucose (including hypoglycemia) remain serious concerns particularly in T1DM, and annual mortality rates of up to 3–6% have been attributed to insulin-related hypoglycemic crises [5].

Pancreatic transplantation improves quality of life and is potentially curative for patients who are insulin-dependent, because of type 1 or type 2 DM, or following total pancreatectomy. In the long term, it prevents, arrests, or reverses the onset or progression of DM complications and restores hypoglycemic counter-regulation [6]. At the molecular level, circulating microRNAs associated with diabetic nephropathy and systemic microvascular damage are normalized after simultaneous pancreas-kidney transplantation [7].

22.1.1 History and Outcomes of Pancreas Transplantation

The history of pancreas transplantation, reviewed elsewhere in detail [8, 9], is inextricably intertwined with the history of DM. The first human pancreas transplant (combined with a renal transplant) was performed in 1966 by Kelly and colleagues [10]. Between the first pancreas transplant in 1966 and the end of 2011, the International Pancreatic Transplant Registry (IPTR) recorded over 27,000 pancreas transplants in the USA, and more than 15,000 elsewhere in the world [5, 11]. The annual number of transplants in the USA peaked between 2002 and 2005 at over 1400, and then decreased by 20% between 2005 and 2014. In 2017, adult transplant recipients numbered 971, including

R. P. Michel (✉)
Department of Pathology, McGill Univeristy Health Center, McGill University, Montreal, QC, Canada
e-mail: rene.michel@mcgill.ca

© Springer Nature Switzerland AG 2021
F. Campbell, C. S. Verbeke, *Pathology of the Pancreas*,
https://doi.org/10.1007/978-3-030-49848-1_22

retransplants, of which over 80% were simultaneous pancreas-kidney (SPK) transplants, 8% pancreas after kidney (PAK), and 10% pancreas transplants alone (PTA) [3, 12].

In the USA at present, five-year patient survival rates are 93% for SPK, 91% for PAK, and 78% for PTA recipients, respectively, whereas five-year graft survival rates are 73% for SPK, 65% for PAK, and 53% for PTA [3].

22.1.2 Indications for Pancreas Transplantation

According to the OPTN/SRTR 2017 Annual Data Report, approximately 80% of transplants are performed for T1DM, 14% for T2DM, and 6% for "other" indications (e.g., chronic pancreatitis, benign neoplasms) [12, 13]. The type of pancreas transplant procedure depends on several clinical factors [3, 5]. Patients with dialysis-dependent advanced renal disease and insulin dependence undergo SPK, freeing them from both dialysis and insulin therapies. However, if the patient receives a kidney from a living donor, this may be followed by a PTA. Patients who have previously undergone renal transplantation and have brittle DM and secondary complications, including in the renal allograft, are candidates for PAK. Pancreatic transplant alone (PTA) is reserved for patients suffering from brittle DM with preserved renal function.

22.1.3 Alternatives to Whole Pancreas Transplantation

The principal alternatives to whole pancreas transplantation are islet cell transplantation and living donor pancreas transplants, omitting the more exotic xenotransplants and bionic pancreata [14].

22.1.3.1 Islet Cell Transplantation

A total of 1086 allogeneic islet cell transplants were performed between 2002 and 2015 [15]. Islet cell transplantation in patients with TIDM has been successful recently in achieving insulin independence in over 50% of well-selected patients at 5 years and can be considered in patients at high cardiovascular risk, those reluctant to undergo abdominal surgery, or in selected non-uremic patients with a low body mass and low insulin requirements [16]. Drawbacks include a reduced chance of achieving insulin independence (50% vs. 70% in SPK at 5 years), a continued need for immunosuppression (albeit at reduced dosages), and the need for 2–4 donors per transplant [14]. **Autologous islet cell transplants**, extracted predominantly from pancreata of patients with chronic pancreatitis, cumulatively numbered 819 between 1999 and 2015 [17]. Insulin independence rates following autologous islet cell transplantation show considerable variability, related to age and other factors [17].

22.1.3.2 Living Donor Transplantation

Since 1979, the year of the first living donor segmental pancreas transplant, over 160 have been performed globally [18]. Advantages include shorter waiting times and improved outcomes, particularly if the recipient is highly sensitized. Furthermore, it provides an opportunity for a simultaneous pancreas-kidney transplant from the same donor. Drawbacks include hyperglycemia (or overt diabetes) in the donor (mandating careful selection) and surgical complications in both donor and recipient [18–20].

22.2 Role of the Pathologist in Pancreas Transplantation

Pancreas transplants are broadly separated into whole/segmental organ transplant and islet transplant. Pathologists are principally involved in the assessment of the former. That said, pancreas allografts in the setting of simultaneous pancreas-kidney (SPK) transplant are infrequently biopsied in most centers. The pathologist has several important responsibilities in the management of **whole pancreas transplantation**. These include the interpretation of **post-transplant core biopsies**, obtained by CT or ultrasound. The primary indications for biopsy are concerns over rejection, heralded by an elevated serum amylase and/or lipase, or falling urinary amylase in bladder-drained allografts. However, as in liver and kidney transplantation, the biochemical alterations are

relatively non-specific, and biopsy is very useful to distinguish acute rejection from other processes. Another critical role of the pathologist is **assessment of the failed allograft** at the time of re-transplantation or post mortem examination. In most centers, biopsies are not obtained to evaluate the donor organ at the time of transplantation (although this may be performed for the kidney in SPK procedures). Another important responsibility of the pathologist is the detailed examination of the **native pancreas explant**, which can follow available protocols [21–23] (see also Chaps. 2 and 3).

The role of pathologists in **islet cell transplantation** is limited. There may be occasions to examine the allograft such as post mortem or to assess the liver or other organs for concomitant abnormalities [24, 25].

22.3 Pathologic Alterations Related to Operative Complications, and Examination and Findings in Failed Allografts

22.3.1 Surgical Procedure of Pancreas Transplantation

A brief review of the surgical procedure of whole organ pancreatic transplantation is relevant to understanding the complications, and for optimal handling and examination of the failed allograft. The entire graft consists of the pancreas per se, the attached segment of donor duodenum, the venous and arterial anastomoses, and a route for drainage of exocrine secretions [20, 26].

The venous anastomosis is established with the recipient's systemic or portal venous system. At present, 80–90% of transplants are performed with the **systemic venous drainage** from the pancreatic portal vein connected to the right common or external iliac vein or the inferior vena cava. The advantage of this approach is its relative simplicity. The principal disadvantage is peripheral hyperinsulinemia that may promote insulin resistance and increased atherosclerosis.

The arterial anastomosis is more complex and involves the preparation of a Y-graft from the donor common, external, and internal iliac arteries, followed by anastomosis of its two peripheral branches to the donor superior mesenteric and splenic arteries. The final step is the surgical connection of the main segment of the Y-graft to the recipient common iliac artery or aorta.

Drainage of the exocrine secretions occurs via the urinary bladder or small bowel. Although the former was previously preferred, at present over 80–90% of pancreatic transplants utilize enteric drainage. The donor "C" loop of duodenum attached to the pancreas is anastomosed to the recipient small bowel, most often without a Roux-en-Y. This shift in drainage to the enteric route was driven by the side effects of urinary bladder drainage, which include reflux pancreatitis, metabolic acidosis, dehydration, and hematuria. These disadvantages outweigh the potential benefit of monitoring for allograft rejection by reductions of urinary amylase in pancreas transplant alone (PTA) and pancreas after kidney (PAK) transplant recipients.

22.3.2 Surgical Complications of Pancreas Transplantation

The principal surgical complications are vascular thrombosis of the graft, bleeding, anastomotic leaks, fluid collections in the abdomen, and infections, including pancreatitis. These remain significant issues compared to transplantation of other solid organs. In the 1980s, graft failure rates caused by technical issues hovered around 25%, but currently are below 10% [27, 28].

22.3.3 Vascular Thrombosis

Large venous or arterial thrombosis remains the chief cause of non-immunological allograft loss, with enteric-drained pancreas after kidney (PAK) and pancreas transplant alone (PTA) patients at greatest risk [29]. Pathogenetic factors include an intrinsically lower blood flow compared with other solid organs (e.g., liver, heart, and kidney), operative trauma, donor pancreas-related preservation injury, and a hypercoagulable state [20, 27, 30, 31]. Vascular thrombosis usually occurs early, within the first 2 weeks post-transplant.

Late onset thrombosis should prompt investigation for other etiologies such as rejection or atherosclerotic vascular disease.

Thrombosis may cause stenosis or complete obstruction of the affected vessel. Occlusion of the splenic or superior mesenteric artery may produce partial infarction of the allograft, the extent of injury depending on collateral circulation. The corresponding clinical picture ranges from minimal effect to complete loss of the graft. Elevation of blood glucose levels should raise clinical suspicion, and Doppler ultrasound can assess flow in the arterial Y-graft, venous outflow, and flow to the pancreatic parenchyma [29, 32]. Without early diagnosis and intervention (anticoagulants, thrombectomy), arterial or venous thrombosis results in irreversible infarction necessitating removal of the entire transplanted pancreas and duodenal cuff [33].

22.3.4 Examination of the Failed Allograft

Examination of the failed allograft by the pathologist requires knowledge of (1) the precise surgical procedure utilized, (2) the interval from transplant, (3) clinical findings, laboratory data, and imaging studies focused on peri- and post-operative events, and (4) any prior episodes of acute cellular rejection (ACR) or antibody-mediated rejection (AMR).

22.3.4.1 Macroscopic Examination

Macroscopic examination of the failed allograft entails weighing, measuring, and describing the specimen including (1) the segments of recipient small bowel (generally jejunum) and donor duodenum, (2) the pancreas, and (3) the arterial and venous segments, carefully sectioning the latter to look for thrombosis or other causes of obstruction (e.g., atherosclerosis, stenosis). The pancreas is serially sectioned, and generous sampling is taken from multiple sites for microscopic examination.

22.3.4.2 Macroscopic Pathologic Findings in Vascular Thrombosis

The macroscopic pathologic findings in vascular thrombosis (Fig. 22.1) include the presence of (1) an intact segment of recipient small bowel since its vascularization is independent of the donor, (2) thrombus within the lumen of a vessel, (3) pancreas and donor duodenal segment displaying hemorrhagic necrosis (depending on whether the thrombosis is arterial or venous in origin) with dark red parenchyma and duodenal mucosa, and possibly pancreatitis (see Sect. 22.3.5).

22.3.4.3 Histopathologic Findings in Vascular Thrombosis

The histopathologic findings in vascular thrombosis include classic ischemic and/or hemorrhagic necrosis of the duodenal segment and pancreatic parenchyma and vessels, with variable acute inflammation. Secondary abscess formation and opportunistic infections, including fungal (particularly candidiasis), can develop [34]. Histopathologic examination may elucidate the underlying etiology. "Idiopathic" causes may be related to surgical or technical complications and reveal organizing thrombotic occlusion of large arteries and/or veins and ischemic necrosis. Antibody-mediated rejection (AMR) including "hyperacute rejection", is characterized by fibrinoid necrosis or necrotizing vasculitis in arteries and/or veins of any size [30]. In some cases, primary vascular injury can be difficult to distinguish from necrotic vessels embedded within infarcted pancreatic parenchyma. To circumvent this problem, the pathologist should search for evidence of vasculitis in the least necrotic or damaged areas or ideally in viable areas. In addition, immunohistochemistry for C4d and correlation with donor-specific antibodies (DSA) may be of value. A comment should be included in the pathology consultation report that in view of the extensive infarction, the possibility of AMR cannot be entirely excluded. Graft vascular thrombosis related to acute cellular rejection (ACR) is discussed below (see Sect. 22.5.2).

22.3.5 Post-Transplant Ischemic and Infectious Pancreatitis

Graft pancreatitis is often caused by several interacting factors including ischemia/reperfusion injury and technical/surgical complications. It may lead to anastomotic leaks, intra-abdominal

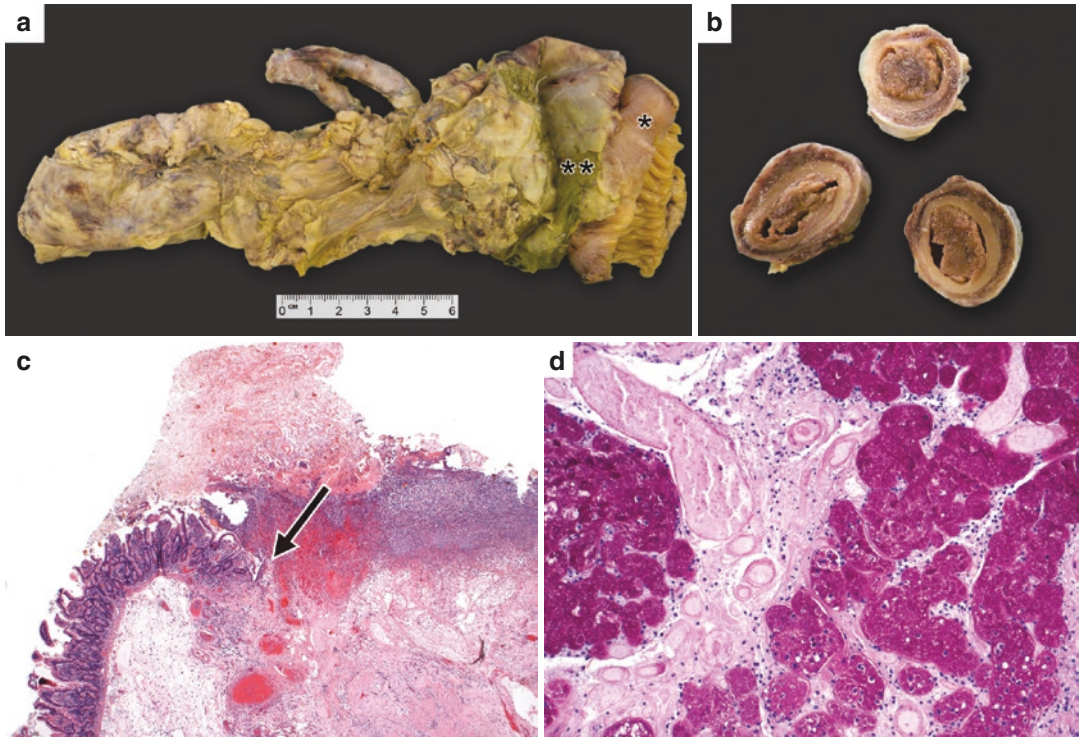

Fig. 22.1 Pancreas allograft removed following arterial thrombosis: the viable recipient small bowel (*) is anastomosed to the necrotic donor duodenum (**) and necrotic pancreatic allograft (**a**). The arterial segment enters the pancreas at the top. The sectioned arterial segment shows total thrombotic occlusion (**b**). Low power shows the junction (*arrow*, **c**) between the intact recipient small bowel and the necrotic, inflamed donor duodenum. PAS stain shows the necrotic pancreatic tissue (**d**)

fluid accumulations and superimposed infections. If extensive, this complication frequently requires removal of the graft. The pathologic features of graft pancreatitis mimic those of necrotizing pancreatitis in the non-transplant setting with macroscopic fat necrosis, parenchymal necrosis, and/or hemorrhage (Fig. 22.2) (see also Chap. 7). Microscopic examination reveals acinar (and variable islet cell) necrosis, infiltration of neutrophils and macrophages, edema, and hemorrhage. Secondary infectious pancreatitis can be caused by a variety of microbial agents, notably bacterial and fungal [30, 35].

22.3.6 Post-Transplant Ischemia/Reperfusion Injury

Ischemic/reperfusion injury resembles that in other transplants. Its pathogenesis centers on microvascular injury due to donor- and recipient-related factors. Microscopic alterations (generally in core biopsies) (Fig. 22.3) include interstitial and intracellular edema, focal acinar cell or adipocyte necrosis, and a variable neutrophilic infiltrate [35, 36]. Both ischemic/reperfusion injury and post-transplant pancreatitis are in the differential diagnosis of acute rejection in core biopsies, and indeed may co-exist with rejection.

22.4 Core Biopsy Specimens in Pancreas Transplantation: Procedures and Technical Aspects

The role of the pathologist in pancreatic transplantation is more restricted than in most other solid organ transplants, and largely limited to the assessment of core biopsies. These are generally

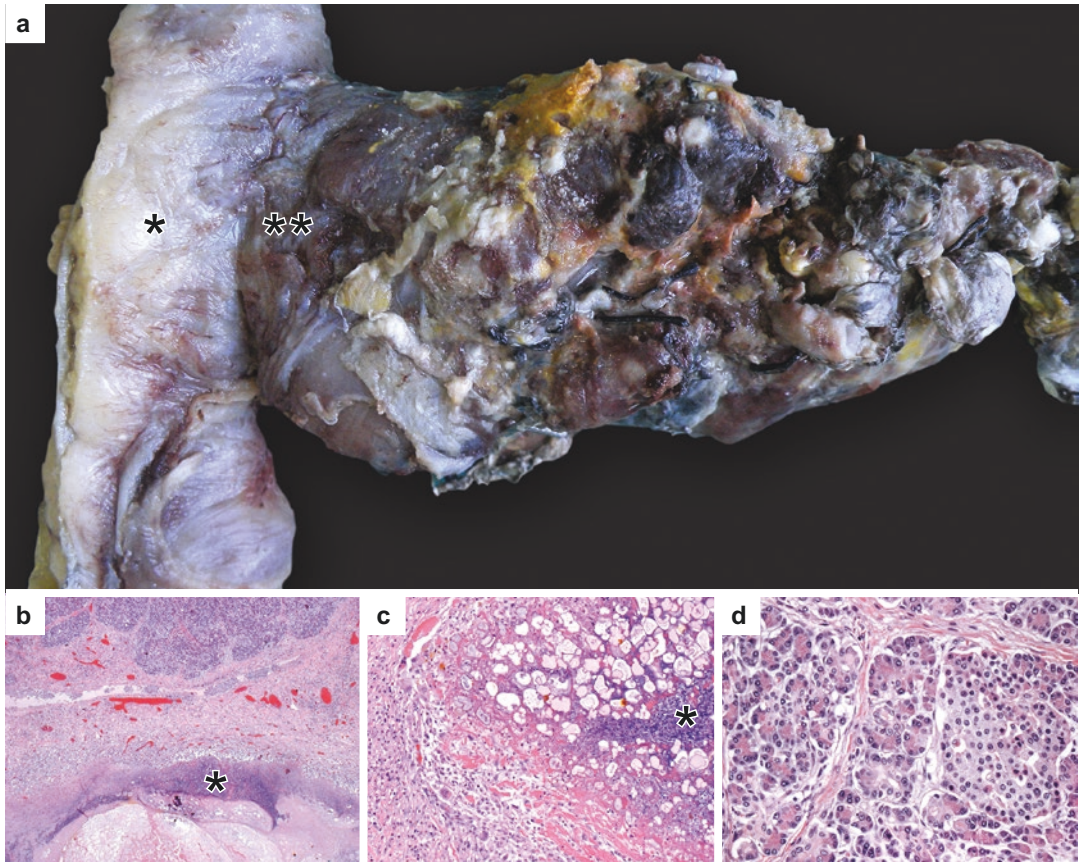

Fig. 22.2 Peripancreatitis and pancreatitis secondary to partial vascular thrombosis in a resected transplant: the pancreas (*right*) with recipient small bowel (*) and donor duodenum (**) shows prominent surface fibrinous exudate (**a**). Low power shows fat necrosis (*bottom*), adjacent abscess (*), a layer of active chronic inflammation and early granulation tissue and intact parenchyma (*top*) without overt necrosis (**b**). Medium power shows fat necrosis (*right*) admixed with acute inflammation (*), and a layer (*left*) of active chronic inflammation (**c**). The adjacent parenchyma is intact (**d**)

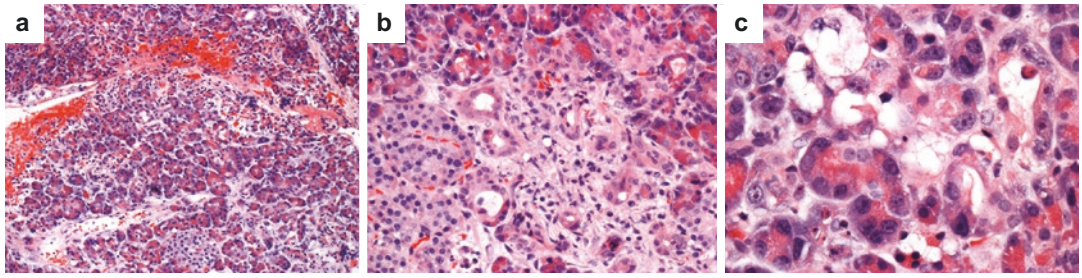

Fig. 22.3 Mild ischemia-reperfusion injury in a core biopsy 9 days post-transplant: there is septal hemorrhage, damage to acini at the periphery of the lobule, and mild acute inflammation (**a**). Note the small area with damage and dropout of acini, and mild neutrophilic infiltrate (**b**). High power shows swelling, hypereosinophilia, and dropout of acinar cells (**c**)

performed for elevated serum amylase, lipase, and/or glucose, or to assess reduced urinary amylase in patients with bladder drainage of pancreatic exocrine secretions. The principal goal is to identify acute cellular rejection (ACR), chronic rejection (CR), and less commonly antibody-mediated rejection (AMR), and their morphologic mimics. Ultrasound- or CT-guided percutaneous core needle biopsies, with an 18 g or 20 g needle, are currently the gold standard to evaluate pancreas allografts, yielding adequate tissue in 88% to 96% of cases with minimal complications [37–39].

22.4.1 Surrogate Biopsy Options to Assess Rejection in the Pancreas Allograft

The first option is the **kidney** in the setting of simultaneous pancreas-kidney (SPK) or pancreas after kidney (PAK) transplants. Although experimental animal models previously suggested that both kidney and pancreas are rejected simultaneously, this has not been borne out in human transplant recipients. Indeed, the conclusion to draw from several studies is that between a quarter and a third of rejection episodes in SPK and PAK transplant biopsies can be discordant, the pancreas being more sensitive to rejection than the kidney [35, 40–43]. Furthermore, even in the cases concordant for rejection, over one third can have different types of rejection (i.e., acute cellular vs. antibody-mediated vs. mixed) [43]. Therefore, until proven otherwise, it is recommended to biopsy both organs at the same time, or at least, if the kidney allograft biopsy shows no rejection, to then biopsy the pancreas allograft [42].

The second surrogate biopsy site potentially applicable to all three types of pancreas transplants is the **donor duodenal cuff** that forms part of the allograft, sampled either endoscopically near the enteric anastomosis or cystoscopically for bladder-drained pancreata. A few studies using this method have shown that a diagnosis of rejection is possible, albeit with significant disagreements with concurrent pancreas allograft biopsies [44, 45]. However, the discrepancies, including potentially missing cases of vascular or chronic rejection, and the lack of criteria to precisely grade ACR or interpret C4d staining, have impeded this approach [44–47].

In summary, at present, neither renal nor duodenal cuff biopsy sampling, at least alone, is clearly recommended to accurately assess rejection in the pancreas allograft.

22.4.2 Protocol or Surveillance, and Post-Therapy Core Biopsies

Protocol or surveillance biopsies are not widely accepted in pancreas transplantation. Nevertheless, a few studies have recommended surveillance biopsies, particularly when initiated early after transplant and in pancreas transplant alone (PTA) or PAK recipients, as they can detect clinically significant rejection in about 20–50% of patients before demonstrable clinical or biochemical alterations. However, surveillance biopsies showing minimal or mild rejection rarely progress, and indeed, rejection may persist in a significant number of patients with biopsy-proven rejection after therapy. Therefore, although early detection of rejection may improve survival of the allograft, additional longitudinal studies are needed [41, 46, 48, 49].

22.4.3 Pancreas Allograft Core Biopsy: Handling and Processing

The pancreas allograft core biopsy obtained under CT or ultrasound guidance using 18 or 20 g needles should be fixed immediately in 10% neutral buffered formalin or a comparable fixative. Depending on clinical circumstances, it can be processed for emergent same day interpretation or overnight for the next day. The Banff

multidisciplinary international consensus panel [39] recommends that at least 10 sequential slides be cut and prepared as follows: 3 H&E-stained slides (e.g., cuts 1, 5, 9), 1 slide for C4d immunohistochemistry (e.g., cut 4), and 1 slide for Masson trichrome or other collagen stain to assess fibrosis or to highlight fibrinoid necrosis in arteritis associated with high-grade rejection. Immunohistochemistry for CMV and in situ hybridization for EBV are optional. If the indication for the biopsy is hyperglycemia and/or a strong clinical suspicion for recurrent type 1 diabetic autoimmune isletitis (or insulitis), immunohistochemistry for insulin and glucagon can be performed (discussed in Sect. 22.7).

22.4.3.1 Adequacy of the Pancreas Allograft Core Biopsy

For adequacy of the pancreas allograft core biopsy, the 2008 Banff panel's guidelines [39] propose the presence of **at least three lobular areas** and their associated inter-lobular septa. Although arteries are desirable in the biopsy, their presence is variable. In view of the diagnostic importance of arterial lesions (particularly for the higher grades of ACR), their presence or absence should be mentioned in the pathology report. Islets of Langerhans may or may not be seen but are not strictly necessary to assess adequacy or rejection, because the inflammation affects predominantly the exocrine component. Of note, the Banff panel emphasizes that the final determination of biopsy adequacy rests with the individual pathologist. Certainly, even in the face of a suboptimal biopsy, any diagnostic findings should be clearly indicated, thereby averting the need for re-biopsy.

22.5 Pancreas Allograft Rejection

Rejection represents the recipient's immune response to antigens in a non-syngeneic graft. Its pathogenesis implicates the innate and adaptive immune systems, the latter mediated by combinations of antibodies and mononuclear and polymorphonuclear cells (lymphocytes, monocytes, plasma cells, eosinophils) [50, 51]. Allograft rejection of the pancreas is classified into antibody-mediated (AMR), acute cellular rejection (ACR), and chronic rejection (CR). The loss of pancreas allografts from chronic allograft rejection at 2 years post-transplant is 1.5% for simultaneous pancreas-kidney (SPK), 5.7% for pancreas after kidney (PAK), and 10.3% for pancreas transplant alone (PTA) transplants [52].

22.5.1 Antibody-Mediated Rejection (AMR)

The spectrum of the clinicopathological manifestations of AMR is broad, ranging from fulminant graft failure ("hyperacute rejection") to its incidental identification in otherwise stable grafts. **The clinicopathological findings and criteria for AMR** are as follows [53]:

- Circulating donor-specific antibodies (DSA)
- Morphologically discernible tissue injury
  - Capillaritis
  - Interacinar inflammation
  - Acinar cell damage (swelling, necrosis, or apoptosis)
  - Vasculitis or thrombosis
- Immunopositivity for C4d of interacinar capillaries in ≥5% of the acinar lobular surface area

Of note, the requirement of "graft dysfunction" (a component of the 2008 Banff Schema) is no longer a requirement for AMR [39].

22.5.1.1 Hyperacute Rejection

Now very rare, hyperacute rejection (HAR) typically occurs in the setting of circulating preformed anti-donor antibodies [27, 53]. The pathologic findings in hyperacute rejection in its earliest stages are rarely encountered in patients, but have been described in experimental animals. They include margination of neutrophils in capillaries and venules, congestion, interstitial edema, and focal acinar cellular damage (vacuolization, degranulation, and necrosis) [54]. Later alterations observed in biopsy specimens or explanted failed allografts comprise extensive

vascular deposition of immune complexes and complement (typically IgG and C4d), resulting in endotheliitis or intimitis, arterial and venous fibrinoid necrosis and thrombosis, a prominent neutrophilic infiltrate, culminating in widespread hemorrhagic necrosis of the parenchyma. The differential diagnosis of hyperacute rejection includes other causes of vascular thrombosis [53]. As previously indicated, distinguishing AMR from other causes includes the presence of the aforementioned alterations in viable tissue sections (particularly bona fide vasculitis), positive donor-specific antibodies (DSA) and C4d deposition in the vasculature [39].

Of note, the term "accelerated AMR" or "delayed hyperacute rejection" is not included in the latest Banff schema for AMR, but is defined as delayed onset (hours to days) of hyperacute AMR, with similar histopathologic and serologic findings [27].

22.5.1.2 Acute Antibody-Mediated Rejection AMR

About 75% of patients who develop acute AMR present in the first 6 months, although a minority present much later [53]. **Clinically**, most patients with acute AMR exhibit graft dysfunction with one or more of the following: elevation of serum amylase and/or lipase, reduction in urinary amylase, and less commonly, hyperglycemia. There is an overlap of clinical findings in AMR and ACR so that a biopsy is required to establish the diagnosis.

Pathologic Features of Acute AMR

The pathologic features of acute AMR include some or all the following (Fig. 22.4) [53]:

- **Acinar and interacinar inflammation** with infiltration of neutrophils, monocytes, and macrophages. In those instances where the neutrophils are inconspicuous, the monocytes can be highlighted by immunohistochemistry for CD68.
- **An interacinar capillaritis** with variably prominent and distributed intraluminal neutrophils and monocytes. Microvascular damage can result in prominent interstitial edema and hemorrhage in the severe forms.

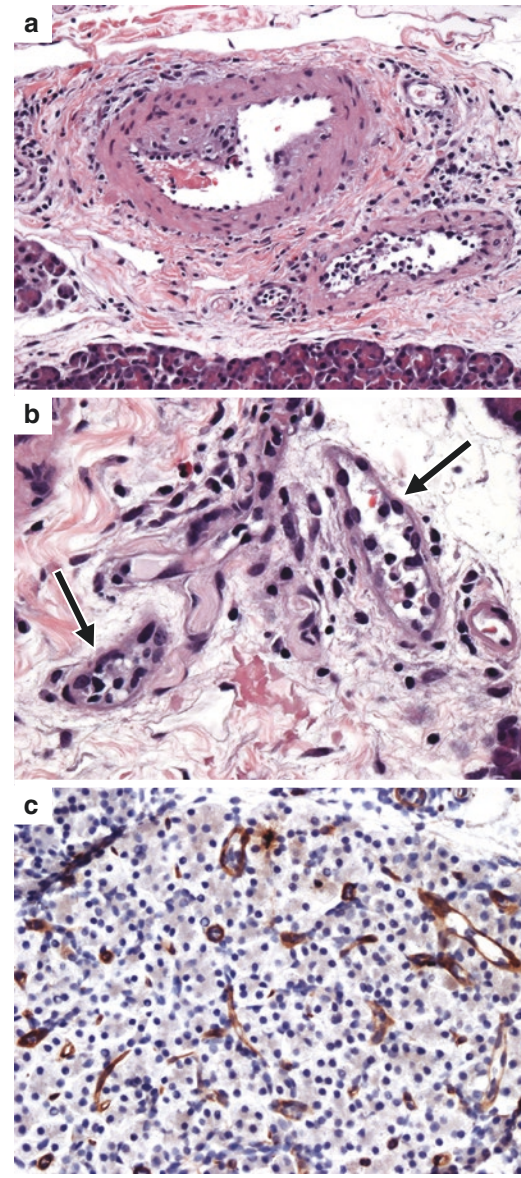

Fig. 22.4 Antibody-mediated rejection in a pancreas core biopsy from a patient post kidney-pancreas transplant: there is focal arteritis and intravascular inflammatory cells in a small artery, as well as capillaritis (**a**). Arteritis may be a sign of both acute cellular and antibody-mediated rejection. Capillaries with increased intraluminal inflammatory cells are indicative of capillaritis (*arrows*, **b**). There is positive staining of interacinar capillaries for C4d (**c**)

- **Damage to acinar cells** and pancreatic parenchyma, with variable cellular swelling, vacuolization, apoptosis, and necrosis. In severe

AMR, these findings can overlap with those encountered in hyperacute rejection [30, 53].

Histopathologic Grading of Acute AMR

The histopathologic grading of acute AMR according to the 2011 Banff schema is:

- **Grade I or mild acute AMR:** preserved architecture with mild monocytic or mixed monocytic and neutrophilic inflammatory infiltrates and sparse acinar cellular damage.
- **Grade II or moderate acute AMR:** largely preserved architecture with interacinar monocytic or mixed monocytic and neutrophilic infiltrates, dilated capillaries with capillaritis, congestion and extravasation of erythrocytes, and multifocal acinar cellular dropout or necrosis.
- **Grade III or severe acute AMR:** variably disordered architecture, preponderance of interstitial hemorrhage, multifocal or confluent parenchymal necrosis, thrombosis and necrosis of arteries and veins, and sparse monocytic and/or neutrophilic inflammatory infiltrates.

Immunohistochemistry for C4d in Pancreas Allografts

Immunohistochemistry for C4d in pancreas allografts is key for the diagnosis of AMR and should be performed in all cases of suspected AMR [53, 55–57]. In the **assessment of staining for C4d**, only linear or granular staining pattern of interacinar capillaries in exocrine lobular parenchyma is considered positive, as it correlates with serum donor-specific antibodies (DSA) and with clinical outcomes. The presence of C4d staining of arteries or veins, of the interstitial connective tissue, or extra pancreatic tissues is nonspecific, although helpful as an internal quality control for the staining technique. The threshold for positive staining remains at ≥ 5% as established by the 2008 Banff grading schema [39, 58, 59].

The recommended grading scheme for C4d staining is [53]:

- **Negative**: absence or <5% interacinar capillary staining in exocrine lobules
- **Focal positive**: 5–50% staining of capillaries
- **Diffuse positive**: >50% of capillaries staining

Reporting Nomenclature for AMR

The final clinical diagnosis of acute AMR requires the combination of (1) histopathologic features, (2) positive immunohistochemistry for C4d, and (3) serological evidence of DSA. The recommended reporting nomenclature is the following [53]:

- **Acute AMR** (i.e., definite) when all 3 above diagnostic criteria are present.
- **"Consistent with acute AMR"** when 2 of 3 criteria are present.
- **"Requires exclusion of AMR"** when only 1 of 3 criteria is present.

Of note, the concept of AMR in the absence of immunopositivity for C4d, i.e., "C4d-negative AMR", mirrors that observed in heart and kidney allografts [55–57].

22.5.1.3 Chronic Active Antibody-Mediated Rejection

"Humoral" mechanisms in general, and particularly circulating DSA, have been implicated in the pathogenesis of the graft fibrosis and failure characteristic of chronic rejection. Thus, the diagnosis of chronic active AMR is established in allograft biopsies exhibiting the following [53]:

- Histopathologic and immunopathologic features of acute AMR (including C4d positivity)
- Features of chronic rejection/graft sclerosis in absence of other etiologies of fibrosis (see below)
- Absence of acute cellular rejection (ACR)

Other findings supporting a component of AMR include vascular mural fibrinoid necrosis and the presence of organizing luminal thrombi. To make a definitive diagnosis of chronic active AMR, all three components of AMR are required as detailed above, in addition to the sclerotic changes of CR. If only 2 of the 3 are present, then the term "suspicious for chronic active AMR" should be reported.

22.5.1.4 Mixed AMR and ACR

Perhaps unsurprising in view of the nature of immune mechanisms in transplantation, both AMR and ACR can be observed in the same biopsy. Histopathologic features include the interstitial mononuclear infiltrate of ACR (detailed in the next section) along with the classic triad of findings in AMR [53]. Each component should be evaluated, graded, and reported separately using the Banff schema.

22.5.2 Acute Cellular Rejection (ACR)

22.5.2.1 Clinical and Laboratory Features of ACR

Cellular rejection rarely produces overt clinical symptoms or signs, so suspicion is driven by altered biochemical parameters. In about 80% of cases of ACR, exocrine dysfunction is characterized by a rise in serum amylase and/or lipase, reflecting acinar cell injury. In patients with bladder-drained grafts a fall in urinary amylase is seen in over 50% of cases of ACR. In contrast, endocrine dysfunction i.e., hyperglycemia (or a reduction in urinary insulin or peptide C) is usually indicative of severe ACR or another severe insult to the allograft, such as a surgical complication (e.g., vascular thrombosis), chronic rejection, or recurrent autoimmune isletitis [27, 39].

22.5.2.2 Histopathologic Findings of ACR in the Pancreas Allograft

The 2008 Banff schema provides clear definitions and descriptions of the histopathologic findings in ACR (as well as in AMR) [39]. The histopathologic features are summarized below (Figs. 22.5, 22.6, 22.7, 22.8, 22.9, 22.10, 22.11):

- **Septal inflammatory infiltrates** composed of activated lymphocytes and monocytes with a variable number of eosinophils (Fig. 22.5).
- **Acinar inflammatory infiltrates** composed of mononuclear cells permeating the acini (Fig. 22.8a). These may take the form of (1) an acinar inflammatory focus with ≥10 inflammatory cells, (2) "focal acinar inflammation" with 2 or more inflammatory foci per acinar lobule, but without acinar cell injury, (3) "multifocal acinar inflammation" with 3 or more foci of inflammation per acinar lobule and with single or focal isolated acinar cell damage or necrosis in the midst of uninvolved acini, or (4) "severe or extensive acinar inflammation" with marked diffuse acinar inflammation with extensive acinar cell damage or necrosis and few, if any, spared acinar areas. These inflammatory infiltrates damage the exocrine acini.
- **Inflammation of veins and venules (venulitis)** characterized by perivascular and mural

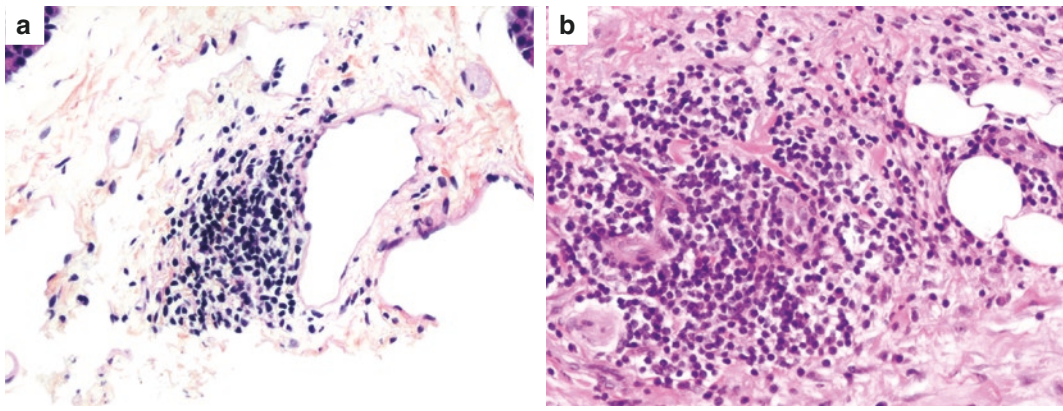

Fig. 22.5 "Indeterminate" grade of acute cellular rejection: septal lymphocytic infiltrates can be either focal (**a**) or more extensive (**b**). Findings of grade I or higher were absent. Note the absence of venulitis in (**a**)

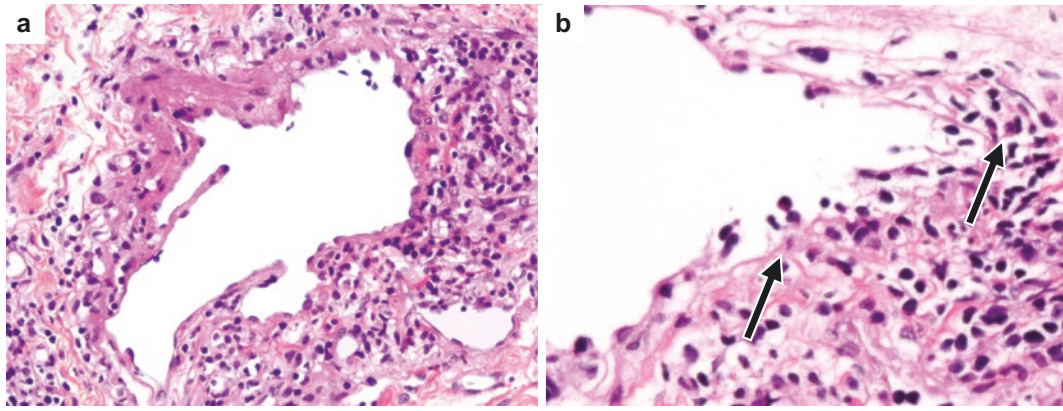

Fig. 22.6 Acute cellular rejection grade I: venulitis is characterized by activated lymphocytes cuffing and infiltrating the venular subendothelial space (**a**), lifting and damaging the endothelium (*arrows*), and spilling into the lumen (**b**)

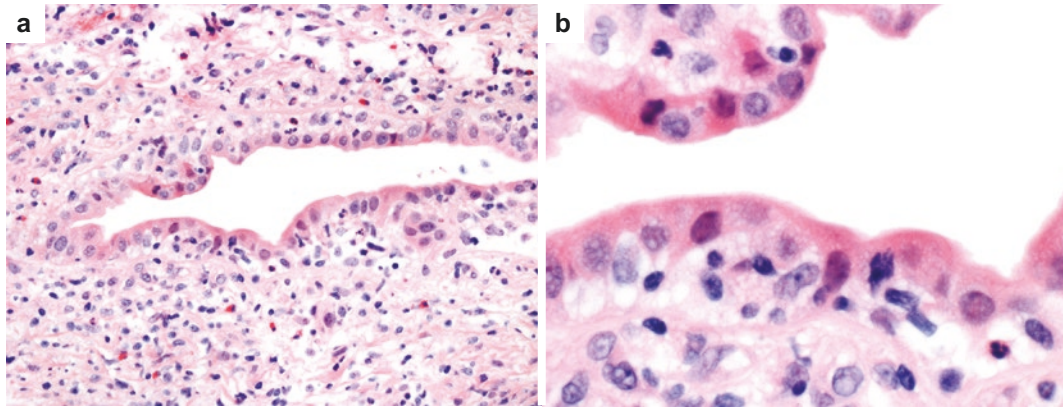

Fig. 22.7 Acute cellular rejection at least grade I: in ductitis, the duct is surrounded (**a**) and infiltrated by lymphocytes admixed with a few eosinophils (**b**)

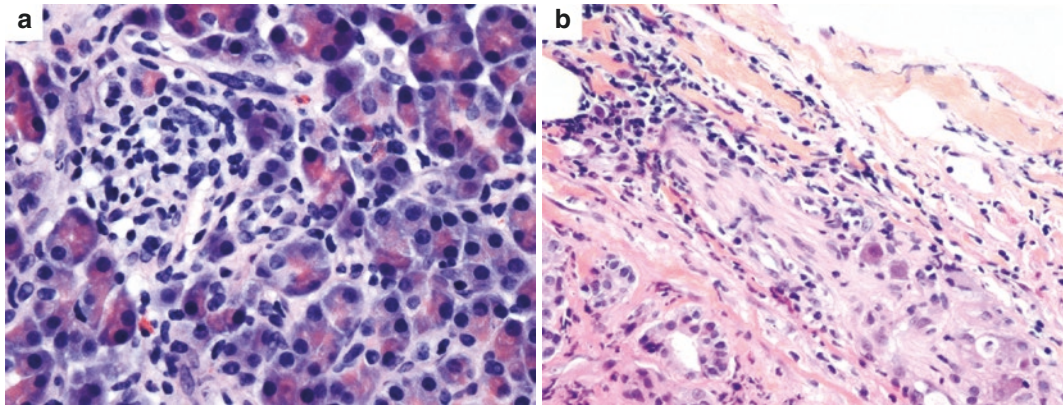

Fig. 22.8 Acute cellular rejection (ACR) at least grade I: there is a focus of acinar inflammation with ≥10 inflammatory cells and no definite acinar cell damage (**a**). With ≥ 2 of these foci per acinar lobule, the descriptor is "focal acinar inflammation". This core biopsy shows a nerve surrounded and infiltrated by lymphocytes, a feature also found in higher grades of ACR (**b**)

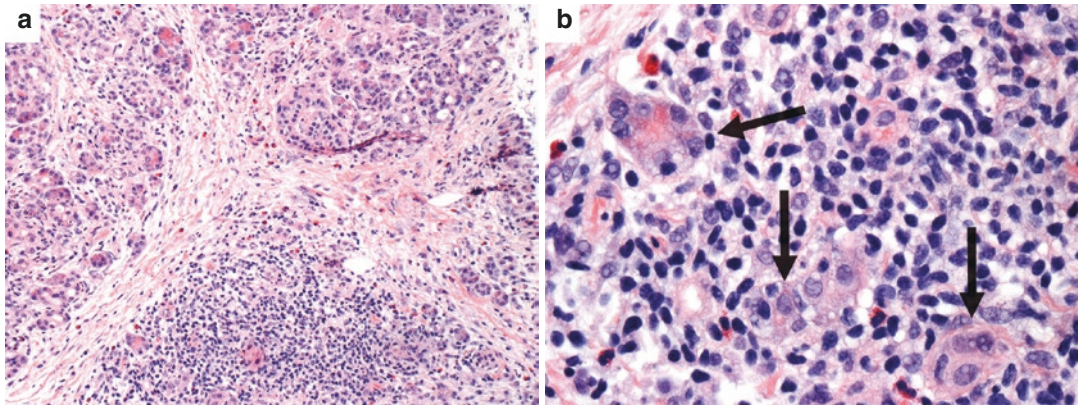

Fig. 22.9 Acute cellular rejection grade III: low power shows lobules of acini with variable inflammation separated by mildly to moderately thickened fibrous septa (**a**). The lobule at the top is least affected, the one on the left shows "multifocal acinar inflammation" with focal acinar cell damage or necrosis, and the one at the bottom shows extensive activated lymphocytic and eosinophilic infiltrate and loss of many acini. High power shows extensive lymphocytic infiltrate with eosinophils, together with degranulating and damaged acini (*arrows*, **b**)

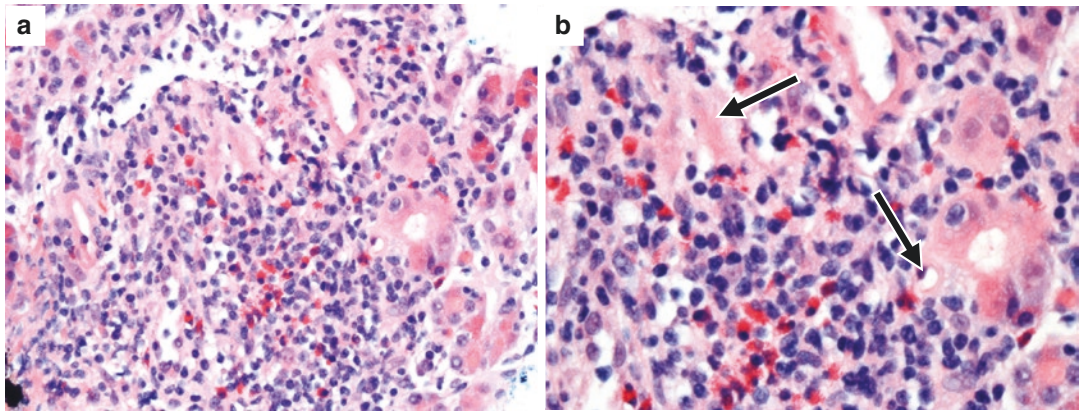

Fig. 22.10 Acute cellular rejection grade III with severe or extensive acinar inflammation: there is a prominent activated lymphocytic and eosinophilic infiltrate with loss of many acini (**a**). There is acinar epithelial cell damage with hypereosinophilia (*arrows*, **b**)

infiltrates of mononuclear inflammatory cells and/or eosinophils with lifting of the endothelium (Fig. 22.6).

- **Inflammation of interlobular ducts (ductitis)** with infiltration of ductal epithelium (i.e., localized to the mucosal epithelium inside the basement membrane) by mononuclear cells and/or eosinophils, plus ductal epithelial damage and/or denudation (Fig. 22.7).
- **Inflammation in and around the nerves** in interlobular septa (Fig. 22.8b).
- **Acinar cell injury or necrosis**, characterized by swelling or vacuolization of the cytoplasm, nuclear pyknosis, as well as apoptosis or necrosis leaving an empty space, i.e., dropout (Figs. 22.9 and 22.10). This may take the form of (1) "single cell/spotty acinar cell injury/necrosis" with preservation of the majority of acinar cells, or (2) "multicellular/confluent acinar cell injury/necrosis" with involvement of groupings of acinar cells of variable size.
- **Inflammation of arteries (arteritis)** that can take the form of (1) a "minimal intimal arteritis" with occasional very focal intimal inflammatory infiltrates of mononuclear cells without activation or damage of the endothe-

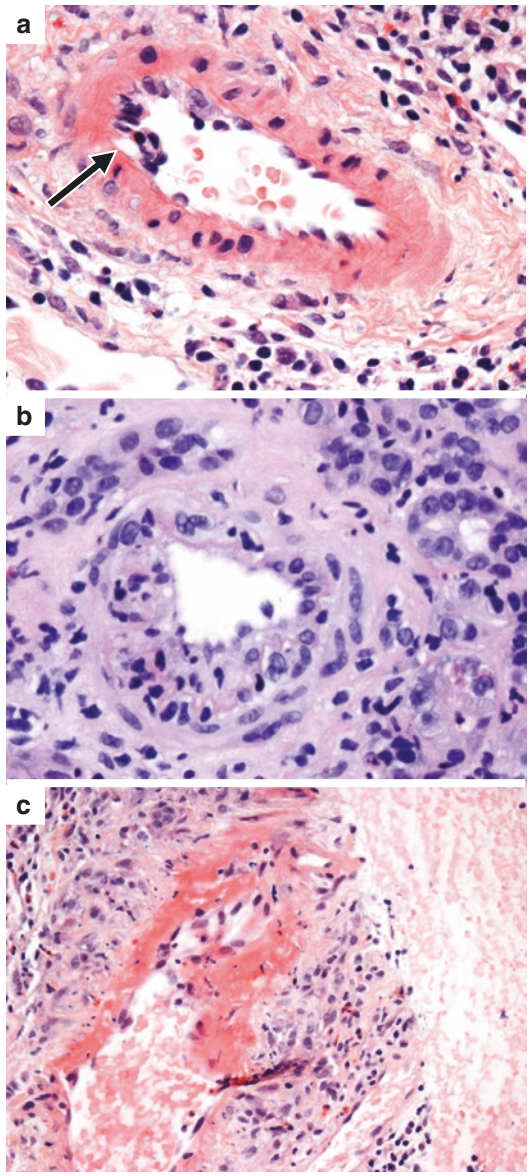

Fig. 22.11 Arteritis in acute cellular rejection (ACR): minimal intimal arteritis with focal infiltration of intima by inflammatory cells (*arrow*) is indicative of moderate ACR (**a**). Note also the lymphocytes and eosinophils around the artery. Moderate arteritis with infiltration of the intima and media by lymphocytes, and with endothelial damage, is a criterion of severe ACR (**b**). This medium-sized artery shows severe transmural arteritis with fibrinoid necrosis and endothelial damage (**c**). Note that vasculitis is also a feature of antibody-mediated rejection and an indication for C4d immunohistochemistry

lial cellular layer (Fig. 22.11a), (2) "moderate to severe intimal arteritis" with a clearly evident intimal mononuclear inflammatory infiltrate, plus damage to the intima, i.e., endothelial hypertrophy or sloughing, presence of fibrin, margination of neutrophils, or activation or proliferation of myofibroblasts (Fig. 22.11b), and (3) a "necrotizing arteritis" i.e., the presence of localized or circumferential mural fibrinoid necrosis and/or a transmural inflammatory infiltrate (Fig. 22.11c).

Note that these features do not include a description of inflammation or damage to the islets of Langerhans. Indeed, the prime target of the cell-mediated immune reaction is the acinar compartment. As in chronic pancreatitis, the islets are spared significant damage unless the process is severe or longstanding, or if the microvasculature supplying the islets is compromised.

22.5.2.3 Grading of ACR in the Pancreas Allograft

The diagnostic features and criteria are incorporated into the rejection **categories of the 2008 and 2011 Banff schemes for grading ACR** [39, 53]. They reflect the components that should be included in the pathology consultation report.

- **Normal:** characterized by absence of, or very minimal, inflammation composed of only small lymphocytes and/or rare plasma cells in septa only. Nerves, acini, ducts, and vessels are normal.
- **Indeterminate for rejection:** shows only focal septal or rarely acinar infiltrates of activated lymphocytes and/or eosinophils but without any of the definite criteria of ACR (Fig. 22.5). This category may be seen in protocol biopsies or with graft dysfunction and is either of unclear significance or may represent early or treated ACR. Management of these patients varies depending on clinical findings.

- **Mild or grade I ACR:** defined as septal inflammatory infiltrates (activated lymphocytes ± eosinophils) with either (1) venulitis and/or (2) ductitis, and/or less commonly (3) inflammation of nerves. Instead of the septal inflammatory component, there may be occasional focal acinar inflammation or spotty acinar cell injury or necrosis (Figs. 22.6, 22.7, 22.8). Grade I ACR usually manifests with graft dysfunction but is reversible with immunosuppressive therapy in about 90% of patients.
- **Moderate or grade II ACR:** defined as one or both of the following histopathologic features: (1) three or more foci of inflammation per acinar lobule, i.e., multifocal, with isolated or spotty acinar cell damage and dropout, and/or (2) a "minimal intimal arteritis", defined as very focal intimal inflammatory infiltrates of mononuclear cells and without endothelial activation or damage. Patients with grade II ACR usually have graft dysfunction and respond to immunosuppressive medications in 70–85% of cases [39].
- **Severe or grade III ACR:** defined as one or more of the following 3 histopathologic features: (1) **severe acinar inflammation and damage** plus focal or "multicellular/confluent acinar cell injury/necrosis" (Fig. 22.9, 22.10). Biopsies may show (a) polymorphous infiltrates of neutrophils, mononuclear cells and eosinophils, and (b) interstitial edema and hemorrhage. There should be minimal, if any, spared exocrine parenchyma; (2) **moderate to severe intimal arteritis** (Fig. 22.11b), and/or (3) a necrotizing arteritis (Fig. 22.11c). The prognosis of Grade III ACR is poor on account of inflammatory injury progressing to exocrine parenchymal loss, compromise of the microvasculature, and consequent loss of islets. The advanced vascular lesions increase the risk of thrombosis or may initiate or promote transplant arteriopathy. These biopsies are encountered in patients with prominent graft dysfunction including hyperglycemia. Response to augmented immunosuppression is generally poor [39].

22.5.2.4 Chronic Active Cell-Mediated Rejection

This subtype of ACR was included in the 2008 Banff schema and refers to the presence of an "active transplant arteriopathy" within the spectrum of chronic ACR. It is indicative of a pattern intermediate between the intimal arteritis of moderate or severe ACR and established "chronic transplant arteriopathy" [39]. These lesions, readily found in excised failed pancreatic allografts, are seldom encountered in core biopsies because they are generally not sampled. They arise in the setting of suboptimal immunosuppression, and if detected and promptly treated, potential arrest or partial reversal of the rejection may be achieved [30, 39].

22.5.3 Chronic Rejection or graft sclerosis in the pancreas allograft

Chronic rejection (CR) is the principal cause of late pancreas allograft loss. Indeed, whereas allograft loss due to acute rejection peaks between 3 and 12 months post-transplant, loss from chronic rejection continually rises after transplant and is one of the principal causes of long-term allograft loss after one year, the other being death from other causes [5].

Unlike acute cellular rejection that is "graded", chronic rejection is "staged", and the stage of CR is a good predictor of remaining graft function [60]. Moreover, the good correlations between ACR and CR, and between AMR and CR highlight the shared pathogenetic mechanisms [53].

22.5.3.1 Clinical and Laboratory Features of Cellular Rejection (CR)

The clinical and laboratory features of CR are nonspecific, and the diagnosis rests principally on manifestations related to loss of β-cell mass and function, i.e., blood glucose levels and/or measurements of C-peptide. Other causes of islet cell injury include calcineurin inhibitor toxicity or recurrence of autoimmune isletitis. It is noteworthy that the pancreas requires a substantial portion of islet cell mass loss before glucose or C-peptide abnormalities appear and therefore, by the time hyperglycemia occurs, the changes are largely irreversible. Furthermore, measurements of lipase and amylase, which herald ACR, lack sensitivity and specificity in the context of CR, due to the destruction of acini [60]. Therefore, the diagnosis of CR rests with the pathologist, and percutaneous core biopsies remain the gold standard.

22.5.3.2 Histopathologic Features of CR

The morphologic hallmark of CR in core biopsies is **graft sclerosis or fibrosis**, with concomitant atrophy and loss of acinar lobules (Figs. 22.12, 22.13) [39, 53]. Chronic vascular lesions may be present, but are rarely encountered in core biopsies and thus are not criteria in the staging scheme. The fibrosis, with admixed mononuclear infiltrates, starts in the interstitial perivascular areas of septa and gradually encroaches upon and obliterates the acinar lobules. The process culminates in subtotal replacement of the pancreas by dense collagenous tissue interspersed with residual atrophic acini, rare ducts, and a few islets. In addition, there is periductal fibrosis, and the ductal epithelial changes may show dysmorphic alterations (Fig. 22.14). The islets disappear relatively late in this fibrosing process and loss of α- and β-cells can be assessed with immunohistochemistry (Fig. 22.15). Masson's trichrome stain can be very useful in delineating the extent of fibrosis in CR.

22.5.3.3 Staging of CR in the Pancreas Allograft

The 4-point scheme for CR (stages 0-III) is primarily based on the percent surface area of the biopsy occupied by fibrous tissue [39, 53, 60]. The extent of acinar atrophy accompanying the fibrosis is not directly taken into account. The scheme is elucidated below and illustrated in Figs. 22.12 and 22.13.

- **Stage 0, normal pancreas:** the fibrous septa are of normal width and do not extend beyond the confines of the adjacent ducts and vessels; the acinar parenchyma is normal.

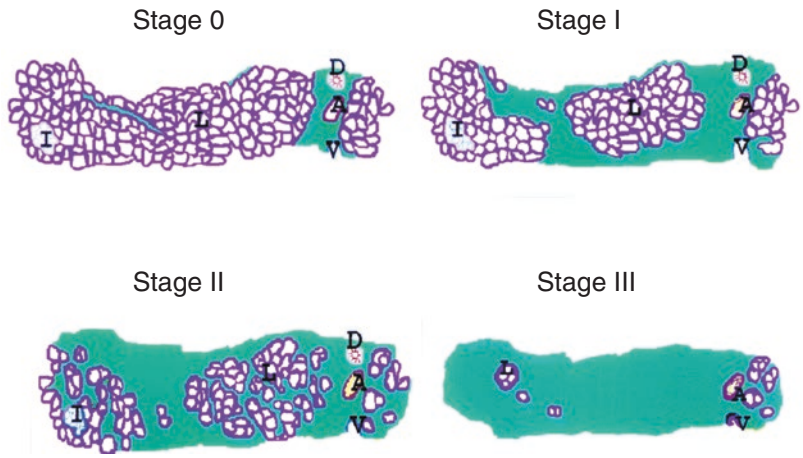

Fig. 22.12 Diagrammatic representation of the stages of chronic rejection according to the Banff scheme. Stage 0 is normal, with normal narrow interlobular septa; stage I has <30% of the biopsy area replaced by fibrous tissue, stage II, 30–60%, and stage III, >60% occupied by fibrous tissue. A, artery, D; duct, I, islet; L; lobule; V, vein (Reproduced with permission from Papadimitriou et al. [60], John Wiley and Sons)

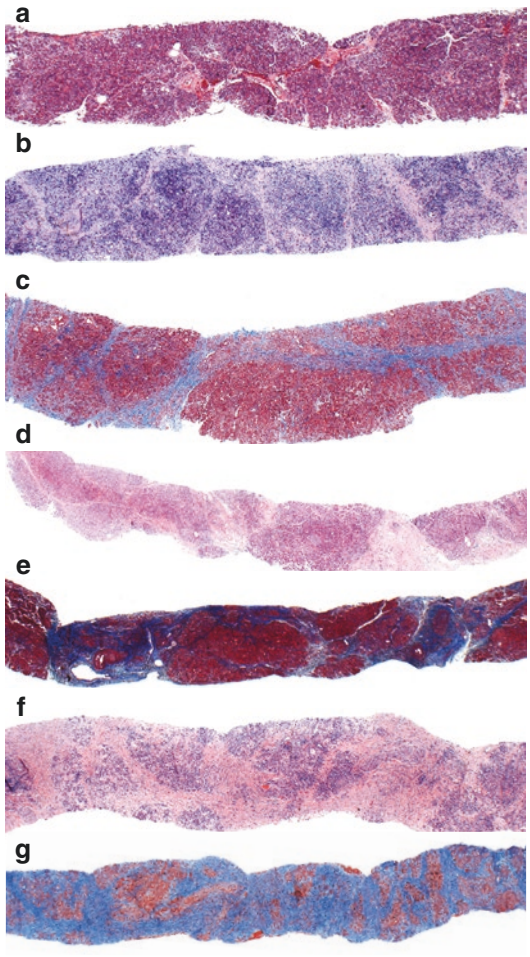

Fig. 22.13 Chronic rejection: normal parenchyma with thin interlobular septa corresponds to "stage 0" in the chronic rejection scheme (**a**). Stage I, mild chronic rejection shows large areas of preserved lobular tissue, and fibrous septa occupying <30% of the area of the biopsy (**b**, **c**). In chronic rejection stage II (**d**, **e**), and stage III (**f**, **g**), there is gradual atrophy of lobules and an increase in the proportion of septa giving the appearance of "cirrhosis". Masson trichrome (**c**, **e**, **g**)

- **Stage I, mild CR:** the fibrous septa are expanded, but the fibrosis comprises under 30% of the surface area of the biopsy. The centers of most acinar lobules are preserved, but the periphery can be irregular and focally eroded.
- **Stage II, moderate CR:** the fibrosis occupies 30 to 60% of the area of the biopsy and all lobules show some fragmentation and atrophy with focal drop-out of acini; the peripheral contours of most lobules are irregular with some atrophy in central areas. New fibrous septa traverse the lobules between acini.
- **Stage III, severe CR:** the fibrosis occupies over 60% of the surface area of the biopsy, with few remaining acini and islets.

22.5.3.4 Chronic Allograft Arteriopathy in the Pancreas Allograft

Chronic allograft arteriopathy is a distinctive intimal fibroproliferative and inevitable obliterative vascular lesion associated with chronic rejection that is similar in all solid organ transplants. Its **histopathologic features** include proliferation of intimal myofibroblasts, fibroblasts, and smooth muscle cells to form a concentrically thickened intimal layer, often accompanied by a variable mononuclear inflammatory cell infiltrate including foamy histiocytes (i.e., an endarteritis) (Fig. 22.16). These lesions produce ischemic damage to the graft and may predispose to thrombotic events.

The 2008 Banff schema distinguishes between **"transplant arteriopathy"** and **"active transplant arteriopathy"**. The former is characterized by predominantly fibrous thickening of the arterial intima, leading to narrowing of the lumen. It is graded based on the most advanced lesions into mild (< 25% of luminal area), moderate (25–50% of luminal area), or severe (>50% of luminal area). **Active transplant arteriopathy**, in addition to the above findings, also shows infiltration by mononuclear inflammatory cells (Fig. 22.16). This must be distinguished from the classic intimal arteritis found in severe ACR (Fig. 22.11) and in the vasculitis of AMR, in which necrosis and inflammation (acute and chronic) occur without substantial intimal myofibroblastic or smooth muscle proliferation.

In summary, paraphrasing the 2011 Banff conceptual approach to chronic allograft arteriopathy (or vasculopathy) [53], it is a relatively nonspecific entity that combines cellular and antibody-mediated immune mechanisms, and

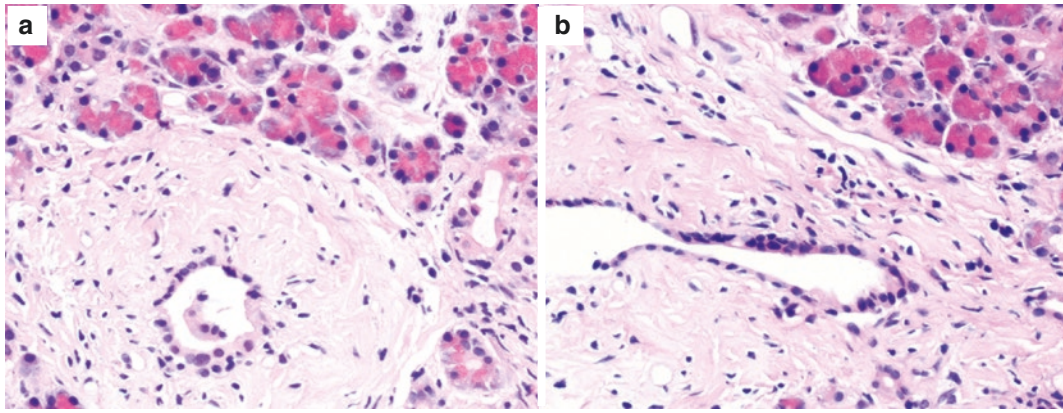

Fig. 22.14 Chronic rejection: the interlobular ducts in chronic rejection are surrounded by dense fibrosis and show irregularities and pleomorphism of the ductal cells (**a**, **b**)

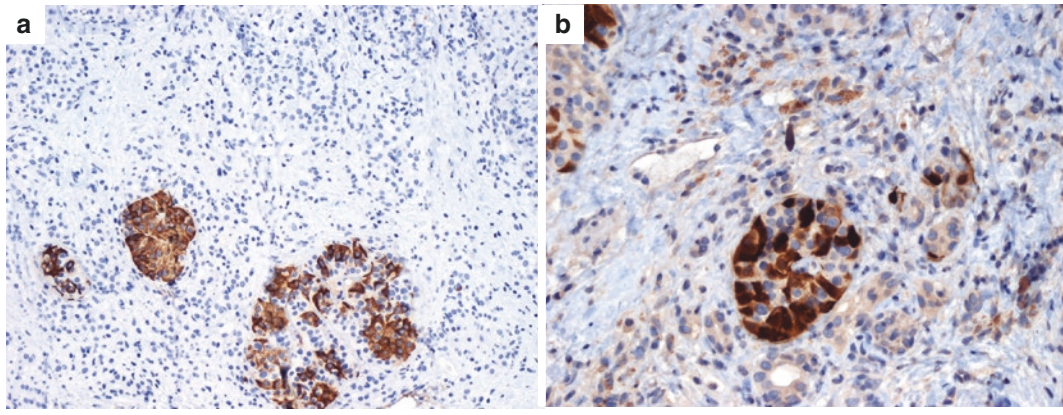

Fig. 22.15 Chronic rejection: there is variable atrophy and loss of cells in the islets, although this is much less marked than the loss of acinar parenchyma. Immunohistochemistry for insulin (**a**) and for glucagon (**b**)

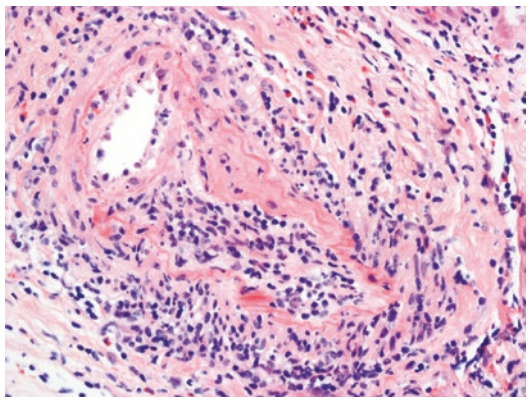

Fig. 22.16 Active transplant arteriopathy: there is a combination of mononuclear cells in the intima and media, and some fibrous thickening with luminal stenosis

is seen at the more severe end of the spectrum of ACR and AMR, as well as in CR. In other words, it fits into a continuum that starts with moderate or severe ACR and AMR, traverses through chronic active cell-mediated rejection and chronic active antibody-mediated rejection, and with time or perhaps if suboptimally treated, terminates in chronic rejection. In practice, it is recommended that finding either intimal arteritis or chronic allograft arteriopathy should prompt the search for other pathological features of both ACR and AMR, including immunopositivity for C4d, as well as an assessment of the fibrosis to accurately stage the CR.

22.5.4 Differential Diagnosis of Forms of Rejection, and Distinction from Other Entities Encountered in Core Biopsies

Acute cellular rejection (ACR) must be differentiated from antibody-mediated rejection (AMR) because the clinical management differs. That said, both ACR and AMR can co-exist. Helpful morphologic clues that aid in their distinction include the following [53]:

- **Features predominating in AMR** are (1) an inflammatory infiltrate composed of neutrophils and monocytes/macrophages; (2) acinar cell injury; (3) interacinar capillaritis; (4) necrotizing arteritis ± thrombosis; (5) hemorrhagic necrosis if severe; and importantly (6) focal or diffuse immunopositivity for C4d in interacinar capillaries.
- **Features predominating in ACR** are (1) septal infiltrates composed predominantly of mononuclear cells, i.e., T-cells ± eosinophils (neutrophils can be found in severe ACR); (2) acinitis with infiltration of mononuclear cells inside the acinar basement membrane; (3) venulitis and/or ductitis and/or peripheral nerve inflammation.
- **Features shared by AMR and ACR** are (1) to some extent acinar cellular injury and (2) active transplant arteriopathy in severe or advanced lesions.

The other differential diagnostic considerations of acute allograft rejection, and to a lesser extent chronic rejection (CR), are summarized in Table 22.1. Parenthetically, these other disorders are now infrequently observed in core biopsies [44].

Table 22.1 Pathologic alterations in the differential diagnosis of rejection

Diagnostic entity	Histopathologic and related features	Type of rejection with key differentiating features
Ischemia-reperfusion injury and ischemic pancreatitis	Ischemic damage or necrosis of acini (vacuolization, apoptosis, necrosis, drop-out). Principally interlobular septal acute inflammation with neutrophils, foamy macrophages, fat necrosis, interstitial edema ± hemorrhage. Fibrosis typically absent.	Principally AMR: necrotizing vasculitis ± fibrinoid necrosis; positive staining for C4d.
Infectious pancreatitis, peripancreatitis and peripancreatic fluid collection	Mixed septal and peripheral lobular acute and chronic inflammation with neutrophils, some lymphocytes, plasma cells, and eosinophils. May be granulomas, abscesses, and bacterial or fungal organisms (special stains useful). May be bundles of active fibroblastic proliferation in interlobular septa at periphery of acinar lobules.	AMR: vasculitis, interacinar capillaritis; positive staining for C4d. ACR: predominantly septal and acinar activated lymphocytes ± eosinophils, venulitis, ductitis. When severe, neutrophils and arteritis. CR: occurs later, dense septal fibrosis, acinar ± islet atrophy, vasculopathy.
Pancreatitis due to CMV	Predominantly mononuclear inflammation, focal in septa and acini, with viral cytopathic changes in endothelium, acinar or stromal cells. Positive immunohistochemistry for CMV. Correlate with serum PCR studies.	Mostly mild ACR: venulitis, ductitis. Absent viral cytopathic changes, negative immunohistochemistry and PCR for CMV.

(continued)

Table 22.1 (continued)

Diagnostic entity	Histopathologic and related features	Type of rejection with key differentiating features
Recurrent autoimmune isletitis, diabetes mellitus	Lymphocytic infiltration of specifically islets (isletitis). Absence of inflammation in late stages after disappearance of β-cells. Immunohistochemical stains for insulin and glucagon show preferential loss of β-cells. Correlate with autoantibodies to islet cells, insulin, GAD.	ACR: lymphocytic infiltration predominantly in acini, not in islets. CR: fibrosis, acinar atrophy; loss of both insulin- and glucagon-producing cells.
Acute islet cell toxicity from calcineurin inhibitors (cyclosporine, tacrolimus)	**Islet cell damage**: vacuolization or swelling of cytoplasm, loss of islet cells replaced by lacunae, focal necrosis or apoptosis. Absence of isletitis. **Immunohistochemistry**: markedly decreased staining for insulin compared with glucagon. **Electron microscopy**: vacuolization of β-cells with specific loss of insulin dense core granules. Observed more with tacrolimus (dose-dependent and reversible).	Recurrent autoimmune diabetes: associated with isletitis, autoantibodies.
Post-transplant lymphoproliferative disorder (PTLD)	Polymorphic type: infiltrate of variably atypical lymphocytes, polyclonal or monoclonal plasma cells, few eosinophils. Monomorphic type: infiltrate of large atypical B-cells (diffuse large B-cell lymphoma or other). Frequent positivity for EBV (in situ hybridization for EBER). May form a mass (correlate with clinical findings and imaging studies).	ACR: infiltrating lymphocytes small or activated, not frankly atypical; venulitis, ductitis; no mass; EBV absent.

Abbreviatons: *ACR* acute cellular rejection, *AMR* antibody-mediated rejection, *CR* chronic rejection, *EBV* Epstein-Barr virus, *EBER* EBV-encoded small RNA, *GAD* glutamic acid decarboxylase, *PCR* polymerase chain reaction
See also references [27, 35, 39]

22.6 Infections in Pancreas Allografts

Bacterial and fungal infections may occur because of surgical complications, and the findings resemble those of acute pancreatitis in the non-transplant setting (Figs. 22.17 and 22.18). Of the fungal infections, *Candida* species are the most common [34, 61].

Infections due to cytomegalovirus (CMV) remain a lingering concern despite prophylaxis. Up to 44% of CMV-negative recipients of a pancreas from a CMV-positive donor developed CMV infection/disease, despite CMV prophylaxis. **Pathologic findings** are detailed in Table 22.1. Immunohistochemistry and PCR studies of the blood are helpful if histopathologic findings are equivocal.

Other viral infections can occur in pancreatic transplant recipients, particularly those in the *Herpes* family. Two studies report the incidence of Herpes simplex infection of about 10% and Varicella zoster virus around 11%, primarily involving the gastrointestinal tract and skin, but not the allograft [62, 63].

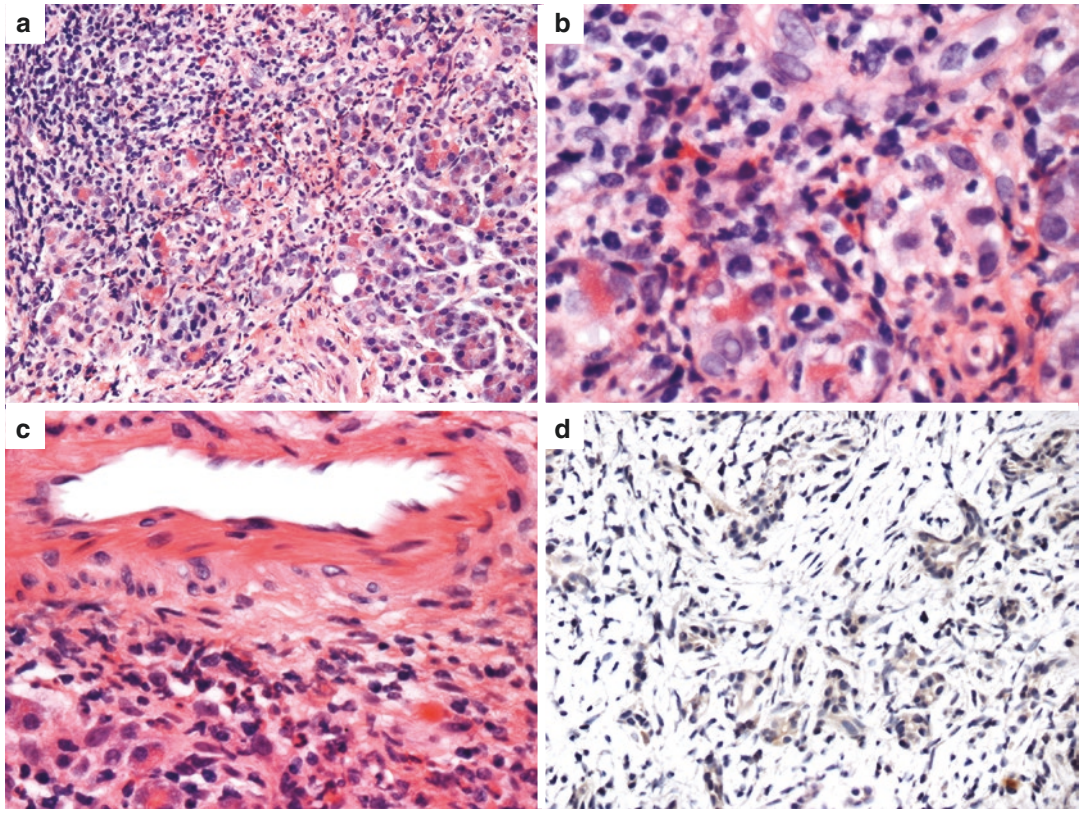

Fig. 22.17 Post-transplant patient with acute pancreatitis: the core biopsy shows a predominantly neutrophilic infiltrate in the septum and amongst acini (**a**, **b**). The differential diagnoses include acute cellular rejection (ACR) and particularly antibody-mediated rejection (AMR). However, note the absence of arteritis (**c**), and the negative C4d immunohistochemistry (**d**)

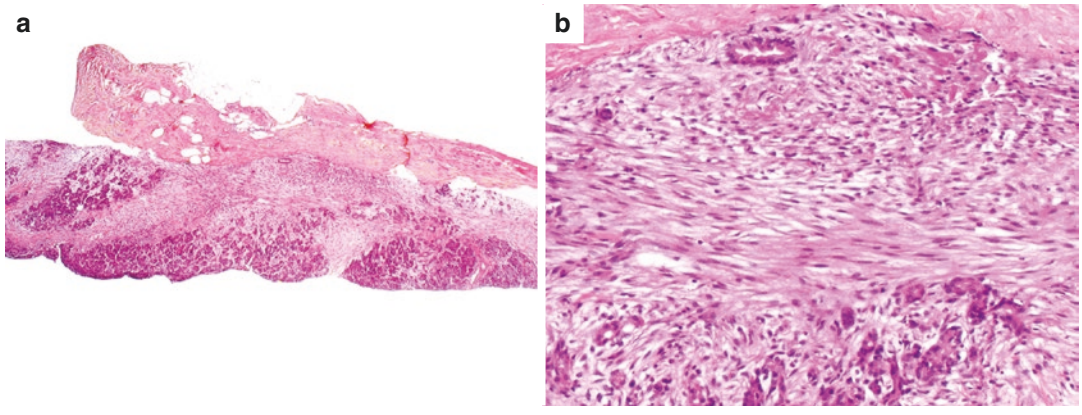

Fig. 22.18 Post-transplant patient with peripancreatitis: there is active granulation tissue at the surface (**a**) and dissecting between lobules (**b**)

22.7 Recurrent Autoimmune Isletitis (Insulitis) and Diabetes Mellitus

The incidence of recurrent TIDM, initially reported in sets of identical twins, approaches 17% for T1DM after a median follow-up of 39 months [27, 64–68]. However, recurrent autoimmune DM is not the only cause of hyperglycemia. In one long-term study, 15% of recipients presented with significant hyperglycemia associated with different etiologies, including chronic rejection (5–6%), post-transplant DM with insulin resistance secondary to weight gain and/or medications (6–7%), recurrent T1DM in 5–6%, and rarely, vascular thrombosis [65].

The pathogenesis of recurrent autoimmune isletitis recapitulates that of the original disease. The β-cells are targeted specifically by immune mechanisms involving B- and T-cells, and antibodies, leaving α- and δ-cells unharmed [64, 65, 69].

Clinically, there is gradual or rapid loss of glycemic control and the variable appearance of serum autoantibodies. Although these autoantibodies are good predictors of autoimmune DM, biopsy is frequently required to confirm the diagnosis [27, 69].

22.7.1 Pathologic Findings in Recurrent Autoimmune Isletitis

Pathologic findings in recurrent autoimmune isletitis include early infiltration of the islets (not acini as in rejection) by predominantly T-cells, followed by gradual disappearance of β-cells, and of the lymphocytes [66, 67]. Immunohistochemistry using antibodies against insulin and glucagon is useful to demonstrate the selective loss of β-cells (Fig. 22.19).

22.8 Acute Islet Cell Toxicity from Calcineurin Inhibitors

Another cause of post-transplant hyperglycemia is targeted damage to β-cells by calcineurin inhibitors, particularly tacrolimus, a dose-related, reversible effect [27, 39]. Light microscopy shows cytoplasmic swelling and vacuolization of β-cells, with apoptosis. Immunohistochemistry shows decreased staining for insulin compared with glucagon. The inflammation seen in recurrent autoimmune isletitis is lacking in calcineurin inhibitor toxicity. The findings can be correlated with the serum tacrolimus and/or with serum autoantibodies.

22.9 Reporting Checklists

A list of macroscopic and microscopic features to consider when reporting failed allografts is shown in Table 22.2. A list of microscopic features to consider when reporting an allograft core biopsy for the principal forms of rejection and other findings is shown in Table 22.3. These checklists are meant only as guidelines and should be adapted to local reporting practices.

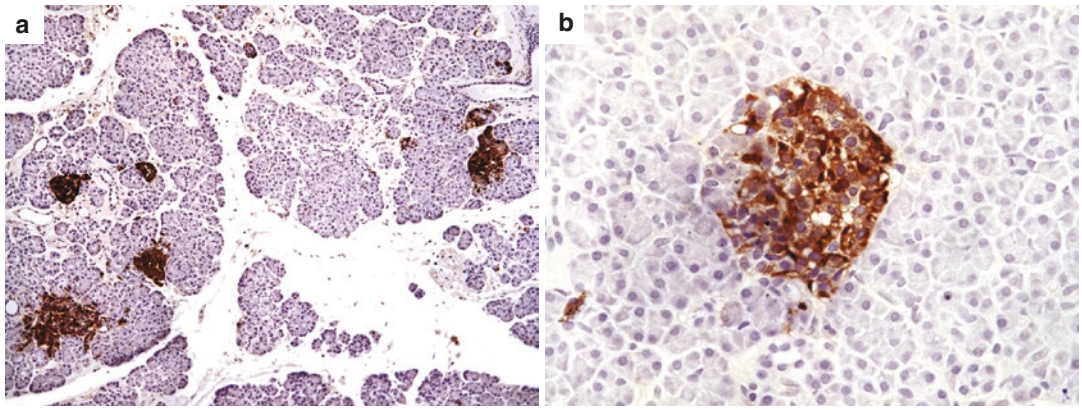

Fig. 22.19 Recurrent isletitis of type I diabetes: immunohistochemistry for glucagon (**a**, **b**) and for insulin (**c**, **d**) shows the selective loss of insulin-producing β-cells

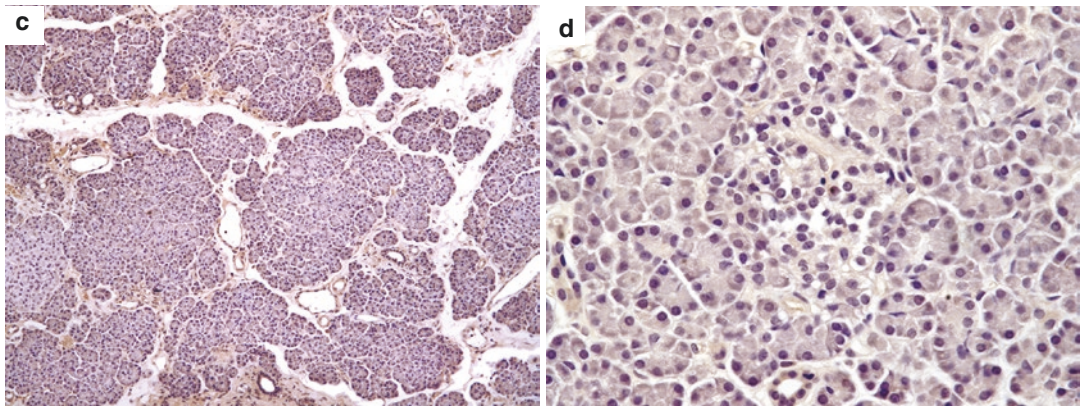

Fig. 22.19 (continued)

Table 22.2 Reporting of failed pancreas allograft

Macroscopic assessment
Specimen type (e.g., pancreas allograft, with or without donor duodenum, recipient small bowel)
Pancreas, donor duodenum, recipient small bowel, artery, vein
Weight of specimen
Dimensions of each part
Other features
Appearance of
Pancreas (necrotic, viable, hemorrhagic, inflamed, other)
Donor and recipient small bowel (necrotic, viable, hemorrhagic, inflamed, other)
Arteries, veins (patent, thrombosed, other)
Microscopic assessment
Pancreatic parenchyma
Total, subtotal, partial necrosis with edema, hemorrhage, abscess formation, organisms, other
Donor duodenum
Total, subtotal, partial necrosis, ulceration, edema, hemorrhage
Recipient small bowel
No necrosis, focal, partial necrosis, inflammation, other
Artery
Patent, partial or complete thrombosis
Vein
Patent, partial or complete thrombosis
Other findings

Table 22.3 Reporting of pancreas allograft core biopsies (template) [53]

Antibody-mediated rejection
Adequate biopsy showing capillaritis, interacinar inflammation, acinar cell damage, vasculitis or thrombosis, most consistent with antibody-mediated rejection, grade I (mild), grade II (moderate), grade III (severe)
C4d stain negative/faintly/moderately/strongly positive in about % of interstitial capillaries
Conclusion (with or without presence of DSA): definite acute antibody-mediated rejection (AMR) / consistent with acute AMR/requires exclusion of AMR.
Acute cellular rejection, grade I out of III
Adequate biopsy showing active septal inflammation, and venulitis with lymphocytes, and few eosinophils most consistent with acute cell-mediated rejection, mild, grade I out of III
Two to three small arteries and few arterioles present on biopsy with no diagnostic abnormality.
Masson trichrome stains shows minimal if any septal and acinar fibrosis.
C4d stain negative/faintly/moderately/strongly positive in about % of interstitial capillaries
Acute cellular rejection, grade II or III out of III
Adequate biopsy showing inflammation with mostly lymphocytes and few eosinophils, multifocal acinar inflammation, with acinar cell injury, ductitis, venulitis and minimal arterial arteritis /necrotizing arteritis, consistent with acute cell-mediated rejection, moderate, grade II or III out of III

(continued)

Table 22.3 (continued)

Masson trichrome stains shows minimal if any septal and acinar fibrosis.
C4d stain negative/faintly/moderately/strongly positive in about % of interstitial capillaries
Chronic rejection, grade I, II, or III out of III
Adequate biopsy showing mild/moderate/severe septal fibrosis and acinar atrophy, with or without arterial changes/foam cell arteriopathy, consistent with chronic allograft rejection/graft sclerosis, mild/moderate/severe, grade I or II or III out of III
Masson trichrome stains shows mild/moderate/severe septal fibrosis.
C4d stain negative/faintly/moderately/strongly positive in about % of interstitial capillaries
Other findings
Infections (CMV, other…)
Inflammation, pancreatitis
Ischemia/reperfusion injury
Changes of calcineurin inhibitor toxicity
Recurrent isletitis

Abbreviations: *CMV* Cytomegalovirus, *DSA* Donor-specific antibodies

References

1. National Diabetes Statistics Report, 2017. Estimates of diabetes and its burden in the United States Atlanta, Georgia: Center for Disease Control and Prevention; 2017 [updated 06/2019; cited 2019 December 11, 2019]. https://dev.diabetes.org/sites/default/files/2019-06/cdc-statistics-report-2017.pdf.
2. American Diabetes Association. Statistics about diabetes data from the national diabetes statistics report, 2015 2015 [cited 2019 December 11]. https://www.diabetes.org/resources/statistics/statistics-about-diabetes.
3. Dean PG, Kukla A, Stegall MD, Kudva YC. Pancreas transplantation. BMJ. 2017;357:j1321.
4. Nathan DM. The diabetes control and complications trial/epidemiology of diabetes interventions and complications study at 30 years: overview. Diabetes Care. 2014;37(1):9–16.
5. Gruessner RW, Gruessner AC. The current state of pancreas transplantation. Nat Rev Endocrinol. 2013;9(9):555–62.
6. White SA, Shaw JA, Sutherland DE. Pancreas transplantation. Lancet. 2009;373(9677):1808–17.
7. Bijkerk R, Duijs JM, Khairoun M, Ter Horst CJ, van der Pol P, Mallat MJ, et al. Circulating microRNAs associate with diabetic nephropathy and systemic microvascular damage and normalize after simultaneous pancreas-kidney transplantation. Am J Transplant. 2015;15(4):1081–90.
8. Sutherland DER, Gruessner RWG. History of pancreas transplantation. In: Gruessner RWG, Sutherland DER, editors. Transplantation of the pancreas. New York, NY: Springer-Verlag; 2004. p. 39–68.
9. Squifflet JP, Gruessner RW, Sutherland DE. The history of pancreas transplantation: past, present and future. Acta Chir Belg. 2008;108(3):367–78.
10. Kelly WD, Lillehei RC, Merkel FK, Idezuki Y, Goetz FC. Allotransplantation of the pancreas and duodenum along with the kidney in diabetic nephropathy. Surgery. 1967;61(6):827–37.
11. Gruessner AC, Gruessner RW. Pancreas transplant outcomes for United States and non United States cases as reported to the United Network for Organ Sharing and the International Pancreas Transplant Registry as of December 2011. Clin Transpl. 2012:23–40.
12. Kandaswamy R, Stock PG, Gustafson SK, Skeans MA, Urban R, Fox A, et al. OPTN/SRTR 2017 annual data report: pancreas. Am J Transplant. 2019;19(Suppl 2):124–83.
13. Mehrabi A, Golriz M, Adili-Aghdam F, Hafezi M, Ashrafi M, Morath C, et al. Expanding the indications of pancreas transplantation alone. Pancreas. 2014;43(8):1190–3.
14. Bux Rodeman K, Hatipoglu B. Beta-cell therapies for type 1 diabetes: Transplants and bionics. Cleve Clin J Med. 2018;85(12):931–7.
15. CITR Tenth Annual Report (2016) Rockville, MD: Collaborative Islet Transplant Registry; 2017. https://citregistry.org/system/files/10th_AR.pdf. Accessed 14 Dec 2019.
16. Wisel SA, Braun HJ, Stock PG. Current outcomes in islet versus solid organ pancreas transplant for beta-cell replacement in type 1 diabetes. Curr Opin Organ Transplant. 2016;21(4):399–404.
17. Inaugural Report on Autologous Islet Transplantation Rockville, MD: CITR Coordinating Center; 2017. https://citregistry.org/system/files/10th_AR.pd. Accessed 14 Dec 2019.
18. Han DJ, Sutherland DER. Living donor pancreas transplantation. In: Oniscu GC, Forsythe JLR, Pomfret EA, editors. Transplantation surgery. Springer surgery atlas series, vol. 1. Berlin, Germany: Springer-Verlag; 2019. p. 485–500.
19. Choi JY, Jung JH, Kwon H, Shin S, Kim YH, Han DJ. Pancreas transplantation from living donors: a single center experience of 20 cases. Am J Transplant. 2016;16(8):2413–20.
20. Samoylova ML, Borle D, Ravindra KV. Pancreas transplantation: indications, techniques, and outcomes. Surg Clin North Am. 2019;99(1):87–101.
21. Kakar S, Shi C, Adsay NV, Fitzgibbons P, Frankel WL, Klimstra DS, et al. Protocol for the examination of specimens from patients with carcinoma of the exocrine pancreas. College of American Pathologists (CAP), 2017. www.cap.org. Accessed 8 Jan 2020.
22. Campbell F, Cairns A, Duthie F, Feakins R. Dataset for the histopathological reporting of carcinomas of the pancreas, ampulla of Vater and common bile duct. London: The Royal College of Pathologists; 2017.

23. The Royal College of Pathologists of Australasia. Cancer of the exocrine pancreas, ampulla of Vader and distal common bile duct. Structured reporting protocol, 2014. www.rcpa.edu.au/Library/Practising-Pathology/Structured-Pathology-Reporting-of-Cancer/Cancer-Protocols. Accessed 8 Jan 2020.
24. Westermark GT, Davalli AM, Secchi A, Folli F, Kin T, Toso C, et al. Further evidence for amyloid deposition in clinical pancreatic islet grafts. Transplantation. 2012;93(2):219–23.
25. Desai CS, Khan KM, Megawa FB, Rilo H, Jie T, Gruessner A, et al. Influence of liver histopathology on transaminitis following total pancreatectomy and autologous islet transplantation. Dig Dis Sci. 2013;58(5):1349–54.
26. Laftavi MR, Gruessner A, Gruessner R. Surgery of pancreas transplantation. Curr Opin Organ Transplant. 2017;22(4):389–97.
27. Patil DT, Yerian LM. Pancreas transplant: recent advances and spectrum of features in pancreas allograft pathology. Adv Anat Pathol. 2010;17(3):202–8.
28. Troppmann C. Complications after pancreas transplantation. Curr Opin Organ Transplant. 2010;15(1):112–8.
29. Farney AC, Rogers J, Stratta RJ. Pancreas graft thrombosis: causes, prevention, diagnosis, and intervention. Curr Opin Organ Transplant. 2012;17(1):87–92.
30. Drachenberg CB, Papadimitriou JC, Farney A, Wiland A, Blahut S, Fink JC, et al. Pancreas transplantation: the histologic morphology of graft loss and clinical correlations. Transplantation. 2001;71(12):1784–91.
31. Drachenberg CB, Papadimitriou JC. The inflamed pancreas transplant: histological differential diagnosis. Semin Diagn Pathol. 2004;21(4):255–9.
32. Khaja MS, Matsumoto AH, Saad WE. Vascular complications of transplantation: part 2: pancreatic transplants. Cardiovasc Intervent Radiol. 2014;37(6):1415–9.
33. Delis S, Dervenis C, Bramis J, Burke GW, Miller J, Ciancio G. Vascular complications of pancreas transplantation. Pancreas. 2004;28(4):413–20.
34. Bono B. Managment of infections in pancreatic transplant recipients. In: Kumar D, Humar A, editors. AST handbook of transplant infections, vol. 2. Hoboken, NJ, USA: Wiley-Blackwell; 2011. p. 22.
35. Drachenberg CB, Papadimitriou JC. Pancreas transplantation pathology. In: Ruiz P, editor. Transplantation pathology. Cambridge: Cambridge University Press; 2009. p. 249–89.
36. Maglione M, Ploeg RJ, Friend PJ. Donor risk factors, retrieval technique, preservation and ischemia/reperfusion injury in pancreas transplantation. Curr Opin Organ Transplant. 2013;18(1):83–8.
37. Klassen DK, Weir MR, Cangro CB, Bartlett ST, Papadimitriou JC, Drachenberg CB. Pancreas allograft biopsy: safety of percutaneous biopsy-results of a large experience. Transplantation. 2002;73(4):553–5.
38. Atwell TD, Gorman B, Larson TS, Charboneau JW, Ingalls Hanson BM, Stegall MD. Pancreas transplants: experience with 232 percutaneous US-guided biopsy procedures in 88 patients. Radiology. 2004;231(3):845–9.
39. Drachenberg CB, Odorico J, Demetris AJ, Arend L, Bajema IM, Bruijn JA, et al. Banff schema for grading pancreas allograft rejection: working proposal by a multi-disciplinary international consensus panel. Am J Transplant. 2008;8(6):1237–49.
40. Gruessner RW, Nakhleh R, Tzardis P, Schechner R, Platt JL, Gruessner A, et al. Differences in rejection grading after simultaneous pancreas and kidney transplantation in pigs. Transplantation. 1994;57(7):1021–8.
41. Troxell ML, Koslin DB, Norman D, Rayhill S, Mittalhenkle A. Pancreas allograft rejection: analysis of concurrent renal allograft biopsies and posttherapy follow-up biopsies. Transplantation. 2010;90(1):75–84.
42. Assalino M, Hadaya K, Andres A, Berney T. Discordant rejection in simultaneous pancreas and kidney transplantation: true discordance or analysis artefact? Transpl Int. 2018;31(1):17–9.
43. Parajuli S, Arpali E, Astor BC, Djamali A, Aziz F, Redfield RR, et al. Concurrent biopsies of both grafts in recipients of simultaneous pancreas and kidney demonstrate high rates of discordance for rejection as well as discordance in type of rejection – a retrospective study. Transpl Int. 2018;31(1):32–7.
44. Redfield RR, Kaufman DB, Odorico JS. Diagnosis and treatment of pancreas rejection. Curr Transplant Rep. 2015;2(2):169–75.
45. Gunther Brockmann J, Butt A, AlHussaini HF, AlMana H, AlSaad K, Al-Awwami M, et al. Protocol duodenal graft biopsies aid pancreas graft surveillance. Transplantation. 2019;103(3):622–9.
46. de Kort H, Roufosse C, Bajema IM, Drachenberg CB. Pancreas transplantation, antibodies and rejection: where do we stand? Curr Opin Organ Transplant. 2013;18(3):337–44.
47. Drachenberg CB. Is the duodenum trustworthy? Transplantation. 2019;103(3):463–4.
48. Casey ET, Smyrk TC, Burgart LJ, Stegall MD, Larson TS. Outcome of untreated grade II rejection on solitary pancreas allograft biopsy specimens. Transplantation. 2005;79(12):1717–22.
49. Drachenberg CB, Papadimitriou JC, Schweitzer E, Philosophe B, Foster C, Bartlett ST. Histological findings in "incidental" intraoperative pancreas allograft biopsies. Transplant Proc. 2004;36(3):780–1.
50. Chinen J, Buckley RH. Transplantation immunology: solid organ and bone marrow. J Allergy Clin Immunol. 2010;125(2). Suppl 2:S324–35.
51. Farrar CA, Kupiec-Weglinski JW, Sacks SH. The innate immune system and transplantation. Cold Spring Harb Perspect Med. 2013;3(10)
52. Singh R, Sutherland DER, Kandaswamy R. Pancreas transplantation. In: Mamode N, Kandaswamy R, editors. Abdominal organ transplantation. Oxford, UK: John Wiley & Sons, Ltd; 2013. p. 80–106.
53. Drachenberg CB, Torrealba JR, Nankivell BJ, Rangel EB, Bajema IM, Kim DU, et al. Guidelines for the

diagnosis of antibody-mediated rejection in pancreas allografts-updated Banff grading schema. Am J Transplant. 2011;11(9):1792–802.
54. Hawthorne WJ, Griffin AD, Lau H, Hibbins M, Grierson JM, Ekberg H, et al. Experimental hyperacute rejection in pancreas allotransplants. Transplantation. 1996;62(3):324–9.
55. Haas M. An updated Banff schema for diagnosis of antibody-mediated rejection in renal allografts. Curr Opin Organ Transplant. 2014;19(3):315–22.
56. Haas M, Sis B, Racusen LC, Solez K, Glotz D, Colvin RB, et al. Banff 2013 meeting report: inclusion of C4d-negative antibody-mediated rejection and antibody-associated arterial lesions. Am J Transplant. 2014;14(2):272–83.
57. Berry GJ, Burke MM, Andersen C, Bruneval P, Fedrigo M, Fishbein MC, et al. The 2013 International Society for Heart and Lung Transplantation Working Formulation for the standardization of nomenclature in the pathologic diagnosis of antibody-mediated rejection in heart transplantation. J Heart Lung Transplant. 2013;32(12):1147–62.
58. Torrealba JR, Samaniego M, Pascual J, Becker Y, Pirsch J, Sollinger H, et al. C4d-positive interacinar capillaries correlates with donor-specific antibody-mediated rejection in pancreas allografts. Transplantation. 2008;86(12):1849–56.
59. De Kort H, Munivenkatappa RB, Berger SP, Eikmans M, Van Der Wal A, De Koning EJ, et al. Pancreas allograft biopsies with positive C4d staining and anti-donor antibodies related to worse outcome for patients. Am J Transplant. 2010;10(7):1660–7.
60. Papadimitriou JC, Drachenberg CB, Klassen DK, Gaber L, Racusen LC, Voska L, et al. Histological grading of chronic pancreas allograft rejection/graft sclerosis. Am J Transplant. 2003;3(5):599–605.
61. Fallatah SM, Marquez MA, Bazerbachi F, Schiff JR, Cattral MS, McGilvray ID, et al. Cytomegalovirus infection post-pancreas-kidney transplantation – results of antiviral prophylaxis in high-risk patients. Clin Transplant. 2013;27(4):503–9.
62. Netchiporouk E, Tchervenkov J, Paraskevas S, Sasseville D, Billick R. Evaluation of herpes simplex virus infection morbidity and mortality in pancreas and kidney-pancreas transplant recipients. Transplant Proc. 2013;45(9):3343–7.
63. Netchiporouk E, Tchervenkov J, Paraskevas S, Sasseville D, Billick R. Evaluation of varicella zoster virus infection morbidity and mortality in pancreas and kidney-pancreas transplant recipients. Transplant Proc. 2013;45(2):701–4.
64. Tyden G, Reinholt FP, Sundkvist G, Bolinder J. Recurrence of autoimmune diabetes mellitus in recipients of cadaveric pancreatic grafts. N Engl J Med. 1996;335(12):860–3.
65. Burke GW 3rd, Vendrame F, Pileggi A, Ciancio G, Reijonen H, Pugliese A. Recurrence of autoimmunity following pancreas transplantation. Curr Diab Rep. 2011;11(5):413–9.
66. Sibley RK, Sutherland DE. Pancreas transplantation. An immunohistologic and histopathologic examination of 100 grafts. Am J Pathol. 1987;128(1):151–70.
67. Sibley RK, Sutherland DE, Goetz F, Michael AF. Recurrent diabetes mellitus in the pancreas iso- and allograft. A light and electron microscopic and immunohistochemical analysis of four cases. Lab Invest. 1985;53(2):132–44.
68. Dean PG, Kudva YC, Larson TS, Kremers WK, Stegall MD. Posttransplant diabetes mellitus after pancreas transplantation. Am J Transplant. 2008;8(1):175–82.
69. Martins LS, Henriques AC, Fonseca IM, Rodrigues AS, Oliverira JC, Dores JM, et al. Pancreatic autoantibodies after pancreas-kidney transplantation – do they matter? Clin Transplant. 2014;28(4):462–9.

Part VI

Frozen Section

The Role of Frozen Section

23

Frozen section may be used at the time of a surgical resection to exclude a metastasis (within the liver, lymph nodes, peritoneum), to assess unexpected other pathology (e.g., incidental gastrointestinal stromal tumor or small bowel neuroendocrine tumor), to assess a surgical resection margin, or to establish or confirm the diagnosis. During pancreatic surgery, distinguishing metastatic pancreatic ductal adenocarcinoma from a primary biliary lesion in a frozen section liver biopsy can be problematic, as can distinction of ductal adenocarcinoma from chronic pancreatitis in a pancreatic biopsy. This chapter will concentrate on these two areas of difficulty and will also briefly discuss the role of frozen section in assessing resection margin status in pancreatic resections. Frozen section should not be used to establish the nature of a pancreatic cystic lesion, since loss of the cyst epithelial lining occurs frequently (see Chap. 14, Sect. 14.2) and may result in a misdiagnosis of a pseudocyst on a small frozen section biopsy. The value of good communication between pathologist and surgeon at the time of frozen section cannot be over-emphasized.

23.1 Excluding a Metastasis

Locoregional lymph node metastases are not a contraindication for pancreatic surgery. Preoperative diagnosis of distant metastatic pancreatic adenocarcinoma on imaging, however, will generally mean that a patient will not proceed to surgery. Unfortunately, small metastases may be missed on imaging and only be detected at the time of surgery. The diagnosis of distant metastasis from a pancreatic adenocarcinoma on frozen section, performed at the time of pancreatic resection, will then mean that surgery can no longer be curative. Surgery may, therefore, be stopped or converted to a palliative procedure. In contrast, diagnosis of a distant metastasis from a pancreatic neuroendocrine tumor is not a contraindication to resection of the primary tumor.

It is always worth considering the possibility that a metastasis, detected at frozen section, may have arisen from an unsuspected second primary tumor (e.g., small bowel neuroendocrine tumor, renal cell carcinoma), and unsuspected lymphoma may be detected in a lymph node (see Fig. 12.1) sent for frozen section (Fig. 23.1).

Recognizing metastatic pancreatic adenocarcinoma in a lymph node or peritoneal biopsy is usually straightforward, although the possibility of cellular fat necrosis or mesothelial inclusion cysts should always be considered in a peritoneal biopsy. In the liver, however, distinguishing metastatic pancreatic ductal adenocarcinoma (or indeed bile duct carcinoma) from benign biliary entities can be difficult. On occasion, it may be possible to determine that a proliferation of ducts is not malignant, but the true nature of the benign lesion may be uncertain. In these circumstances,

© Springer Nature Switzerland AG 2021
F. Campbell, C. S. Verbeke, *Pathology of the Pancreas*,
https://doi.org/10.1007/978-3-030-49848-1_23

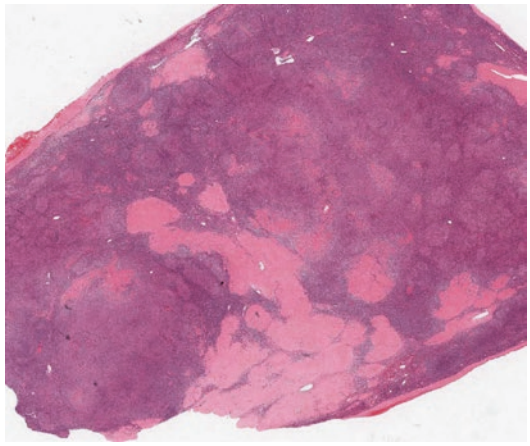

Fig. 23.1 Non-Hodgkin lymphoma: this large peripancreatic lymph node was thought to be a pancreatic neoplasm on preoperative imaging. Frozen section was reported as lymphoma. Paraffin sections and immunohistochemistry confirmed a follicular lymphoma

it is appropriate to report to the surgeon that this is a benign ductular proliferation and that there is no evidence of metastatic disease.

23.1.1 Liver Lesions

23.1.1.1 Bile Duct Hamartoma

Bile duct hamartomata (von Meyenburg complexes) may mimic a metastasis macroscopically. They are pale white, well-circumscribed lesions, usually less than 5 mm in size, and may be solitary or scattered throughout the liver. Although they are composed of irregularly-shaped, dilated bile ductules, these ductules are regularly spaced within abundant hyalinized fibrous stroma and have smooth lumina (Fig. 23.2). The most helpful diagnostic feature is the presence of bile within the ductular lumina. The ductular cells are cuboidal or flat with small uniform nuclei and do not contain mucin.

Luminal bile is not seen in the irregular neoplastic glands of pancreatic ductal adenocarcinoma. The stroma in pancreatic ductal adenocarcinoma is desmoplastic, and the neoplastic glands are not evenly distributed within the desmoplastic stroma. The neoplastic glands have irregular lumina and are lined by cells showing variation in nuclear size, cytoplasmic mucin, and mitotic figures.

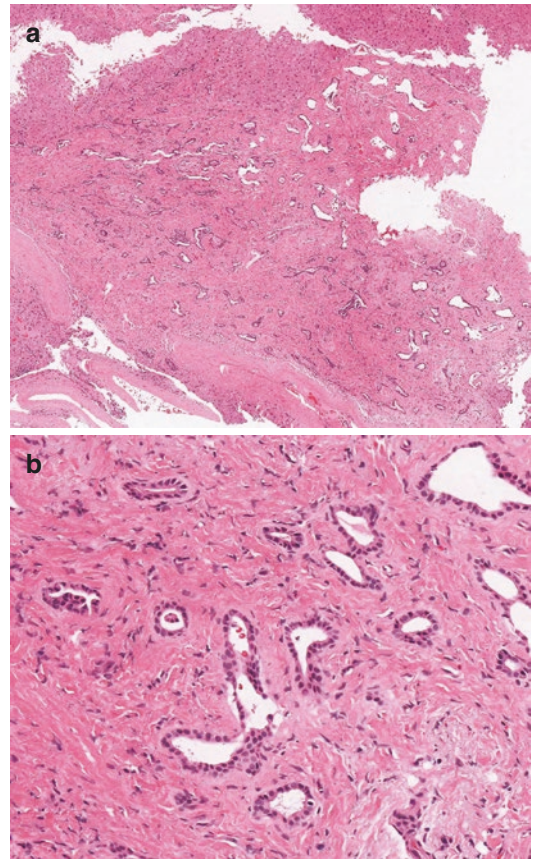

Fig. 23.2 Liver biopsy—bile duct hamartoma (von Meyenburg complex): this well-demarcated lesion is composed of irregularly-shaped bile ductules within abundant hyalinized fibrous stroma (**a**). The ductules have smooth lumina and are lined by bland cuboidal cells (**b**)

23.1.1.2 Bile Duct Adenoma (Peribiliary Gland Hamartoma)

Bile duct adenomata are usually small, solitary, subcapsular, well-circumscribed, pale white lesions less than 1–2 cm in size, which may be wedge-shaped. On microscopy, the lesion may be seen surrounding a central large bile duct. They are composed of closely-packed acini and small ductules with smooth contours and little or no lumen (Fig. 23.3). There is no luminal bile. The epithelium is cuboidal with no, or minimal, nuclear atypia and there are no mitotic figures. Cytoplasmic mucin is usually present in some cells. The stroma between the ductules is fibrous and may be scanty or dense and hyalinized.

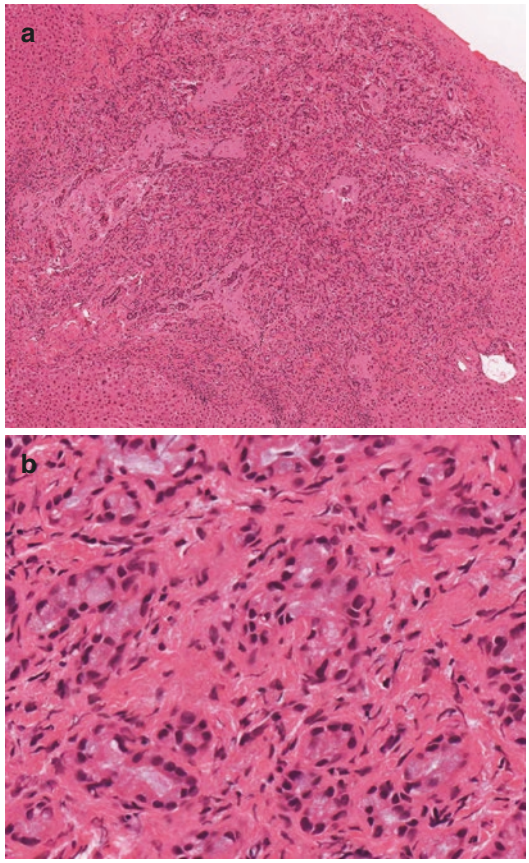

Fig. 23.3 Liver biopsy—bile duct adenoma (peribiliary gland hamartoma): this ductular proliferation can be seen between hyalinised portal areas (**a**). Higher power shows the closely-packed small ductules lined by bland cuboidal cells containing cytoplasmic mucin (**b**). There is collagenous stroma between the ductules

The neoplastic glands of pancreatic ductal adenocarcinoma are irregularly shaped and haphazardly arranged within desmoplastic stroma. The neoplastic epithelium shows more marked atypia and mitotic figures.

23.1.1.3 Focal Nodular Hyperplasia

Occasionally, a small example of focal nodular hyperplasia (FNH) may be mistaken macroscopically for a metastasis. However, FNH is characterized microscopically by abnormal lobular architecture with fibrous septa containing abundant bland bile ducts (resembling the normal hepatic bile ducts), chronic inflammation, and the pathognomonic abnormal arteries (Fig. 23.4), so that distinction from metastatic pancreatic ductal adenocarcinoma should be straightforward.

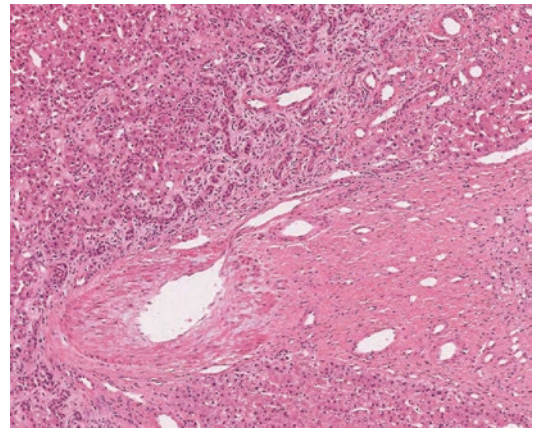

Fig. 23.4 Liver biopsy—focal nodular hyperplasia: this bland ductular proliferation accompanies an aberrant blood vessel characteristic of focal nodular hyperplasia

23.1.1.4 Reactive Ductular Proliferation

In biliary obstruction, such as that occurring with pancreatic ductal adenocarcinoma, there may be ductular proliferation within portal tracts. This proliferation can be quite florid and accompanied by acute inflammation and fibrocellular stroma. The ductules may be angulated and show reactive cellular atypia, but there is no cytoplasmic mucin (Fig. 23.5). Often the ductules lie close to the limiting plate.

It may be very difficult to distinguish reactive ductular proliferation from metastatic well-differentiated pancreatic ductal adenocarcinoma. Some of the features used to distinguish chronic pancreatitis from pancreatic ductal adenocarcinoma (see Sect. 23.2) are equally applicable to reactive ductular proliferations within the liver. However, there will be occasions when it is not possible to establish the true nature of the ductular proliferation, and this should be communicated to the surgeon. Further levels on the submitted tissue may be helpful. There may be other potentially metastatic nodules within the abdomen that could be biopsied for frozen section, deferring to paraffin sections may be an option, or the surgeon may be prepared to continue with surgery to give the patient the benefit of the doubt.

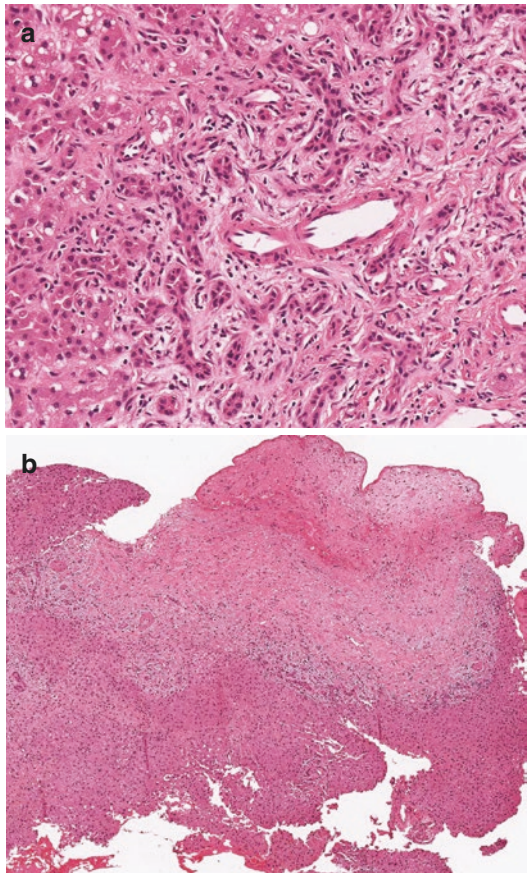

Fig. 23.5 Liver biopsy—benign ductular reaction: these reactive ductules next to the limiting plate have smooth outlines, small lumina, and uniform nuclei (**a**). They are separated by loose stroma. In this large scar (**b**), the ductular proliferation can be seen adjacent to the limiting plate

23.1.1.5 Metastatic Pancreatic Adenocarcinoma

Metastatic pancreatic ductal adenocarcinoma is composed of irregular glands or, in the case of poorly differentiated tumors, small groups of cells and single cells, within desmoplastic stroma (Fig. 23.6). The glands are haphazardly arranged, do not have luminal bile, and show cytological atypia with large pleomorphic nuclei (Fig. 23.7). There are usually mitotic figures, which may be atypical. The glands may infiltrate into the sinusoids between hepatocytes (Fig. 23.8). Cytoplasmic mucin may be readily visible (Fig. 23.9) and there may be tumor apoptosis and/or necrosis (Fig. 23.10).

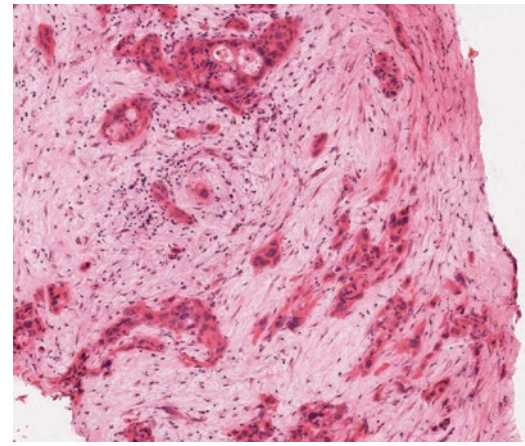

Fig. 23.6 Metastatic pancreatic carcinoma: single pleomorphic cells together with cords and irregular glands of carcinoma cells within desmoplastic stroma

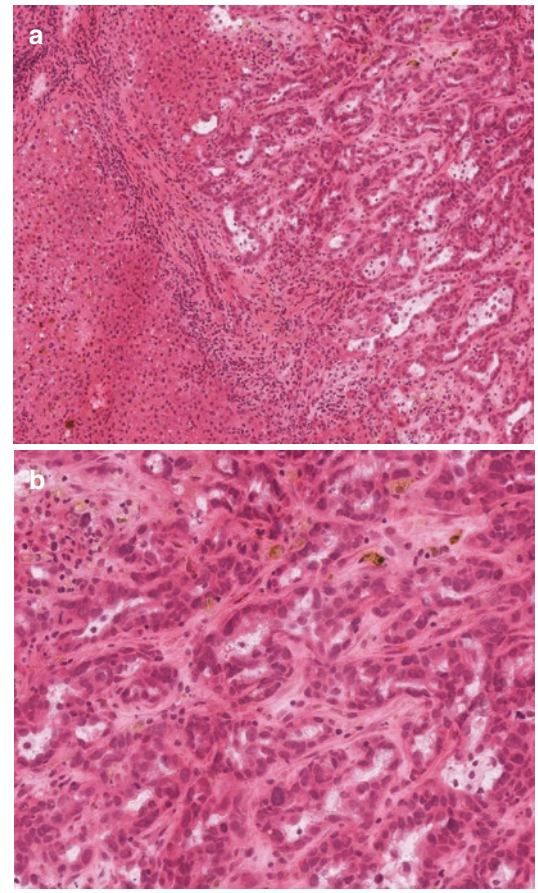

Fig. 23.7 Metastatic pancreatic carcinoma: the carcinoma is composed of haphazardly arranged glands showing irregular budding (**a**). Liver parenchyma can be seen on the left. At higher power (**b**), there are degenerate cells within the gland lumina, marked nuclear pleomorphism, and mitotic figures (*lower left*)

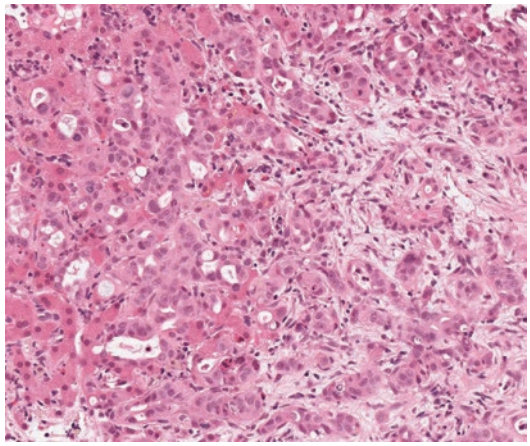

Fig. 23.8 Metastatic pancreatic carcinoma: carcinoma infiltrates the hepatic sinusoids

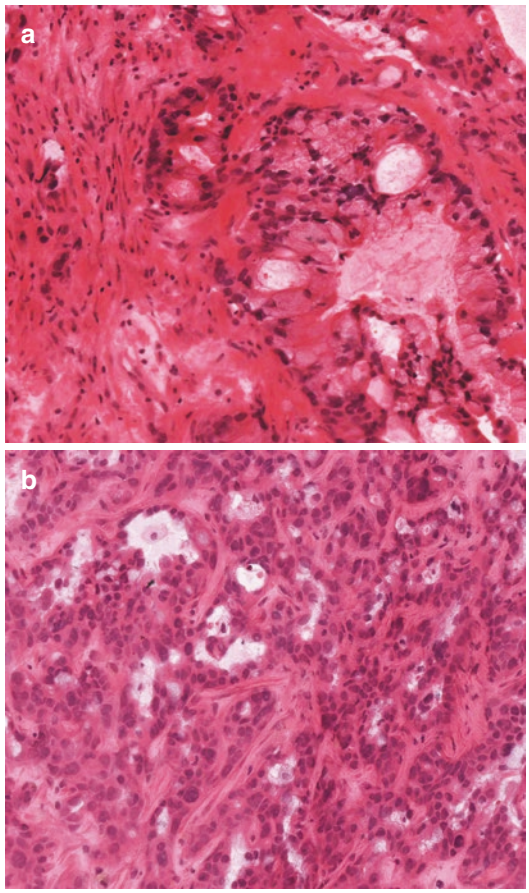

Fig. 23.9 Metastatic pancreatic carcinoma: this carcinoma shows abundant cytoplasmic mucin and complex cribriform architecture (**a**). The intracytoplasmic mucin in this metastasis (same case as Fig. 23.7) is less prominent (**b**)

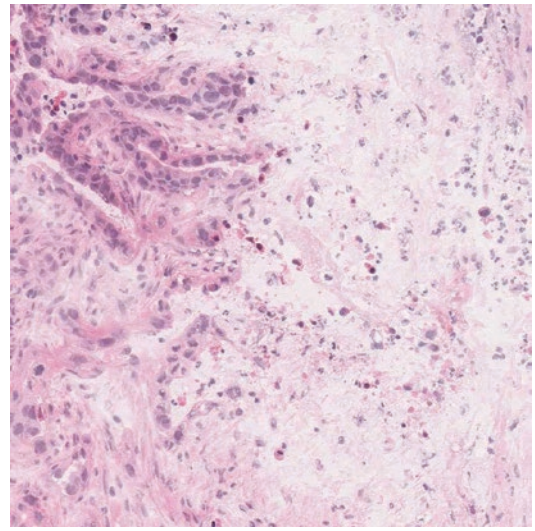

Fig. 23.10 Metastatic pancreatic carcinoma: there is abundant tumor necrosis (*right*) in this metastasis

Necrosis, desmoplastic stroma, apoptosis, mitotic figures, and cellular atypia are the most helpful features for identifying metastatic pancreatic ductal adenocarcinoma.

23.2 Pancreatic Ductal Adenocarcinoma Versus Chronic Pancreatitis

Frozen section of the pancreas may be performed to confirm complete resection or to confirm the diagnosis of adenocarcinoma, for example, during bypass surgery, so that the patient may be entered into a clinical trial and/or receive chemo/radiotherapy. In either situation, distinguishing adenocarcinoma from chronic pancreatitis is required. Pancreatic ductal adenocarcinoma will have associated features of chronic pancreatitis, so there may well be the features of both in the same biopsy. Diathermy or crush-artefact can also hinder interpretation. Recognizing poorly differentiated adenocarcinoma in a frozen section is usually straightforward (Fig. 23.11). However, when adenocarcinoma is well differentiated with minimal cytological atypia, distinction from chronic pancreatitis (with atypical ductules and abundant stroma) can be difficult. Occasionally,

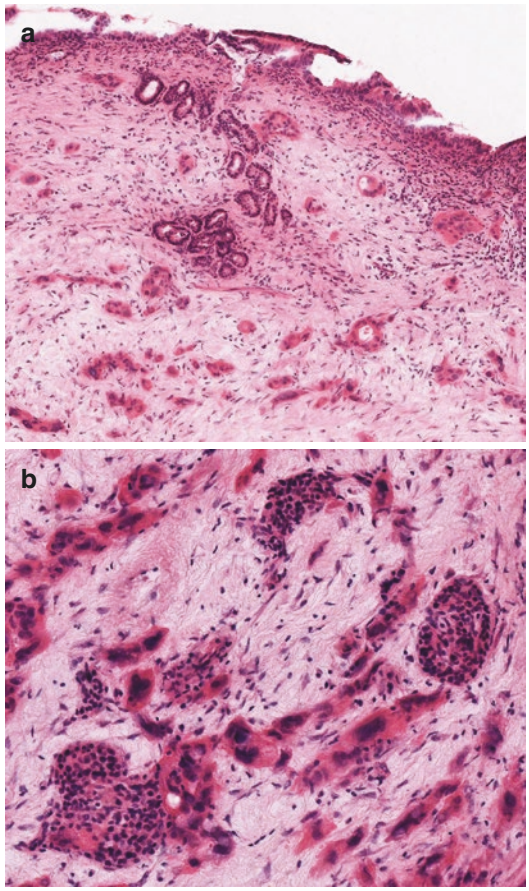

Fig. 23.11 Pancreatic biopsy: poorly differentiated pancreatic ductal adenocarcinoma infiltrates beneath the common bile duct epithelium (**a**) and between islets (**b**)

unexpected autoimmune pancreatitis may be detected at frozen section (Fig. 23.12), but this is readily distinguished from chronic pancreatitis by the presence of dense periductal, plasma cell-rich, chronic inflammation, with or without lobular chronic inflammation and storiform fibrosis (see Chap. 7, Sect. 7.2.7.4).

The two key features for distinguishing pancreatic ductal adenocarcinoma from chronic pancreatitis are the lobular architecture and the proximity of ducts to muscular blood vessels (see Chap. 9, Sect. 9.12.1). The lobular architecture is preserved in chronic pancreatitis, whereas in pancreatic ductal adenocarcinoma the neoplastic glands are haphazardly arranged (Fig. 23.13) and can be seen between lobules. Recognizing the lobular architecture is readily done at low power and on large sections of tissue (Fig. 23.14), but it is not always possible on a needle biopsy. However, even in chronic pancreatitis, the intralobular stroma is looser and paler than the dense collagen that surrounds lobules (Fig. 23.15). It also lacks the cellularity of typical desmoplastic stroma. In the normal pancreas, ducts do not run alongside muscular blood vessels. Although in advanced chronic pancreatitis, with marked acinar atrophy, residual ducts may come to lie close to muscular vessels (see Chap. 9, Fig. 9.51), the presence of an atypical duct adjacent to a muscular blood vessel should be considered suspicious for adenocarcinoma.

Pancreatic ductal adenocarcinoma may have necrosis and/or lymphatic, vascular or perineural invasion, none of which will be found in chronic pancreatitis. Another helpful diagnostic feature for pancreatic ductal adenocarcinoma is the presence of 'naked tumor glands' (see Fig. 9.15) within fat. In fatty atrophy, the ducts of chronic pancreatitis are still surrounded by a small amount of connective tissue.

The distinction between pancreatic ductal adenocarcinoma and chronic pancreatitis on the basis of ductular architecture and cytological atypia can be difficult. In 1981, Hyland et al. [1] established three major and five minor criteria for distinguishing neoplastic from nonneoplastic ducts on frozen section (Table 23.1), which are discussed further here. These criteria are equally applicable to paraffin-embedded tissue. The major criteria are seen in all pancreatic adenocarcinomas. The minor criteria occur with variable frequency in adenocarcinoma.

23.2.1 Major Criteria

23.2.1.1 Nuclear Size Variation Equal to, or Greater than, 4:1

In pancreatic ductal adenocarcinoma, there can be varying degrees of nuclear pleomorphism. Within the same neoplastic gland, there may be little difference in the sizes of the nuclei or there may be marked variation (Fig. 23.16a). Hyland et al. [1] found that the largest nucleus in pancreatic ductal adenocarcinoma was at least 4 times the size of the smallest, whereas in chronic

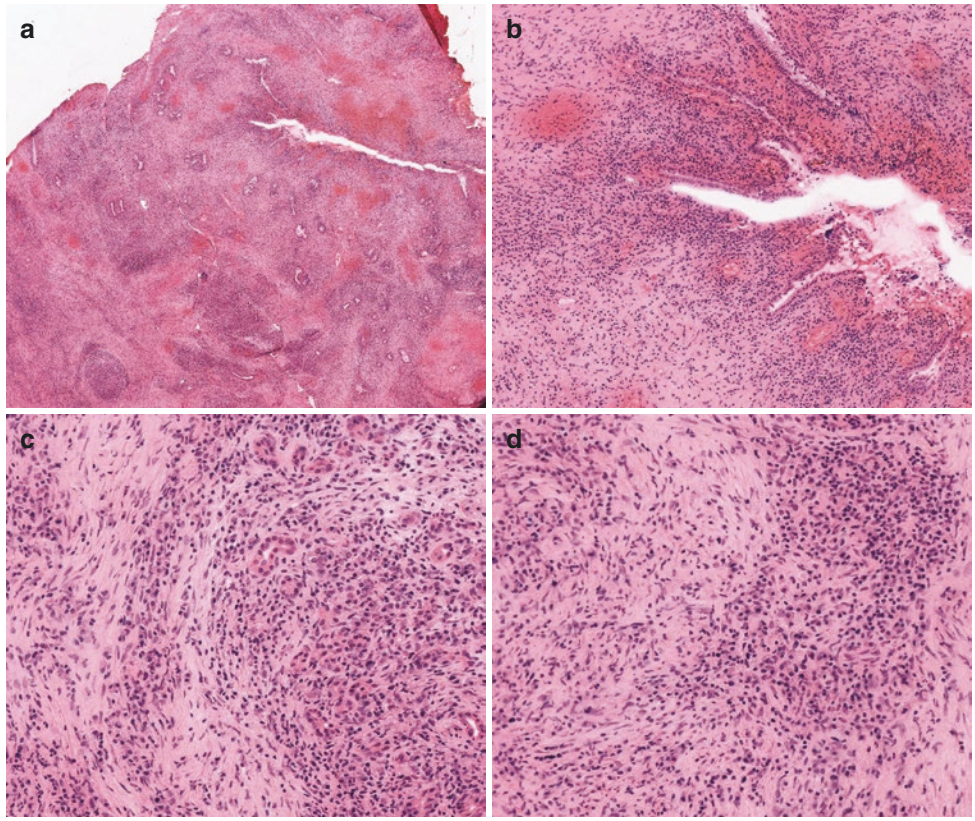

Fig. 23.12 Autoimmune pancreatitis: at low power inflammatory cells can be seen around ducts and within lobules (**a**). At higher power, (**b**) there is a periductal plasma cell-rich infiltrate, which is also present within (**c**) and between (**d**) the lobules

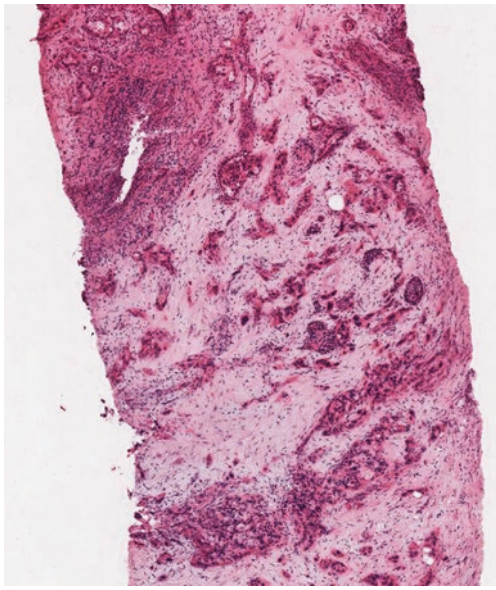

Fig. 23.13 Pancreatic biopsy: there is widespread pancreatic ductal adenocarcinoma, which invades in a haphazard manner

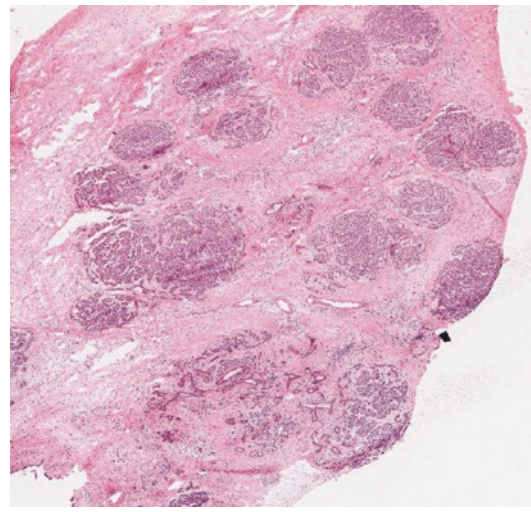

Fig. 23.14 Chronic pancreatitis: at low power, the lobular architecture is still evident and the ductules at the bottom are still confined within a fibrotic lobule

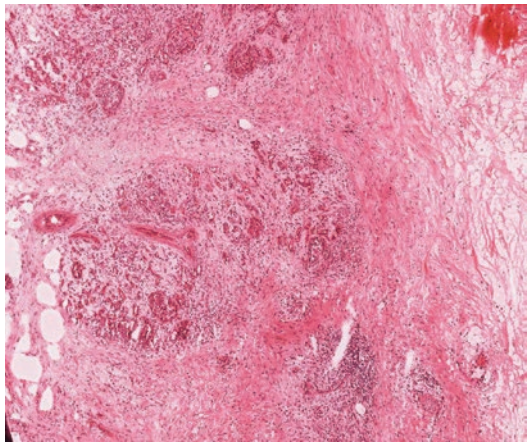

Fig. 23.15 Chronic pancreatitis: the intralobular stroma is paler and less dense than the perilobular collagen

Table 23.1 The major and minor criteria of Hyland et al. [1] for distinguishing pancreatic ductal adenocarcinoma from nonneoplastic ducts

Major criteria
• Nuclear size variation equal to, or greater than, 4:1
• Incomplete glandular lumina
• Disorganized duct distribution
Minor criteria
• Huge, irregular epithelial nucleoli
• Necrotic glandular debris
• Glandular mitoses
• Glands unaccompanied by stroma in smooth muscle fascicles
• Perineural invasion

pancreatitis the maximum nuclear size variation observed within ducts was 3:1 (Fig. 23.16b). It is worth noting that normal islets can also show variation in nuclear size up to 4:1.

23.2.1.2 Incomplete Glandular Lumina

Hyland et al. [1] found that in every biopsy of adenocarcinoma, neoplastic glands exhibited incomplete lumina. These consist of cords of cells, small groups of cells without lumina, ducts with gaps or defects in the epithelial lining such that the lumen opens on to the stroma, and cribriform glands (Fig. 23.17). None of these features are found in chronic pancreatitis.

23.2.1.3 Disorganized Duct Distribution

As discussed above (see Sect. 23.2), in pancreatic ductal adenocarcinoma the neoplastic glands are haphazardly arranged (Fig. 23.13) and can be seen between lobules, in lobules admixed with benign ducts (see Fig. 9.10), adjacent to muscular blood vessels (see Figs. 9.50 and 9.51), and infiltrating peripancreatic fat (see Fig. 9.15). In contrast, in chronic pancreatitis, the duct distribution is fairly regular, despite the fibrosis, with ductules still retained in a lobular arrangement surrounded by loose stroma (Fig. 23.18).

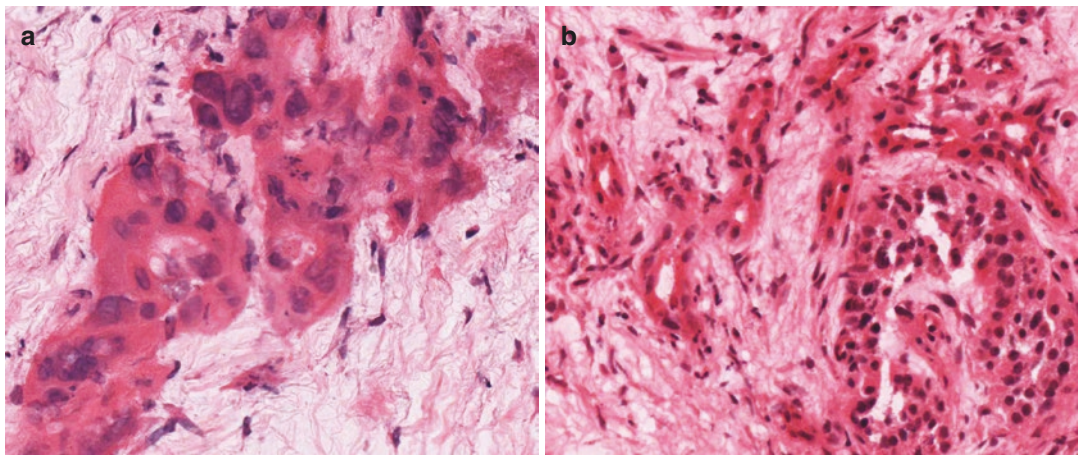

Fig. 23.16 Pancreatic biopsy: this pancreatic ductal adenocarcinoma shows marked variation in the sizes of the malignant nuclei, with the largest nucleus more than four times the size of the smallest (i.e. ratio greater than 4:1) (**a**). In contrast, in chronic pancreatitis, the variation in nuclear size is less than 3:1. Note the variation in nuclear size in the islet (*bottom right*) (**b**)

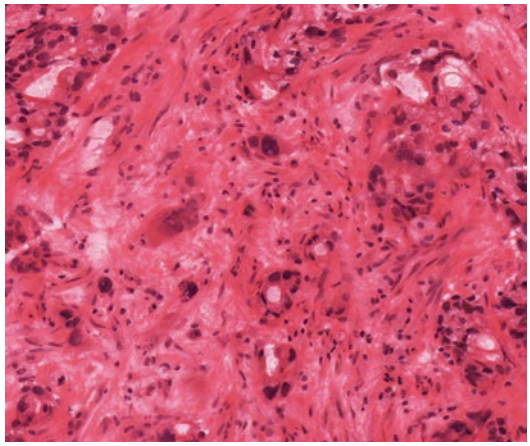

Fig. 23.17 Incomplete lumina in pancreatic carcinoma: there are cords of tumor cells and (*bottom center*) malignant glands with defects in the epithelial lining resulting in the lumina opening on to the stroma

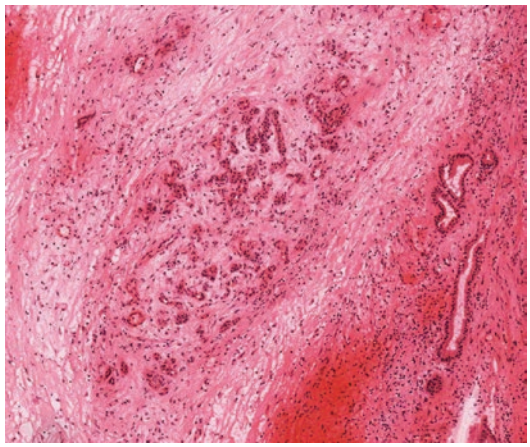

Fig. 23.18 Chronic pancreatitis: the ductules are still retained in a lobular arrangement surrounded by loose stroma

23.2.2 Minor Criteria

23.2.2.1 Huge Irregular Epithelial Nucleoli

In pancreatic ductal adenocarcinoma, the neoplastic cells can have large nucleoli, which can have an irregular contour and be eosinophilic. In contrast, the nucleoli in chronic pancreatitis are small, round, and regular.

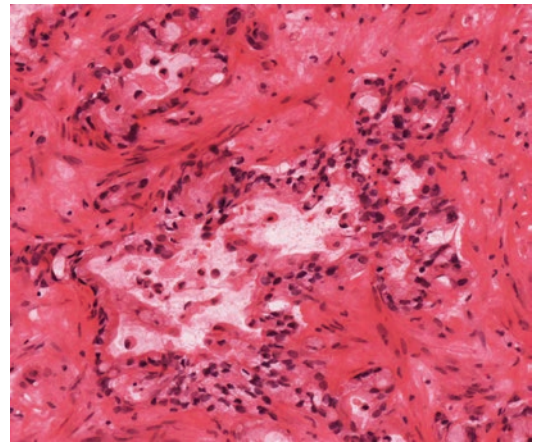

Fig. 23.19 Pancreatic carcinoma: there are degenerating epithelial cells within the lumina of these malignant glands

23.2.2.2 Necrotic Glandular Debris

Necrotic material consisting of amorphous debris and degenerating epithelial cells may be found within the lumina of neoplastic glands in pancreatic ductal adenocarcinoma (Fig. 23.19). Such necrotic debris is not found in the small ducts of chronic pancreatitis.

23.2.2.3 Glandular Mitoses

Mitotic figures, including atypical forms, can be found in the neoplastic glands of pancreatic ductal adenocarcinoma. Mitoses are not found in the ducts of chronic pancreatitis.

23.2.2.4 Glands Unaccompanied by Stroma in Smooth Muscle Fascicles

In pancreatic ductal adenocarcinoma, there may be infiltration of the duodenal muscularis propria by neoplastic glands (see Figs. 9.18 and 9.19). These invasive glands do not have accompanying connective tissue. There is no such infiltration of smooth muscle by ducts in chronic pancreatitis. However, a transduodenal biopsy for frozen section may sample ampulla or accessory duct. In both of these structures, the ducts are arranged in lobules with associated stroma and do not infiltrate as single glands in the muscle.

23.2.2.5 Perineural Invasion

Perineural invasion can occur in pancreatic ductal adenocarcinoma (see Fig. 9.30) and may be found within the pancreas and/or the peripancreatic tissue. Perineural invasion should always be looked for in the adipose tissue around a pancreatic neck margin and/or around the extrapancreatic bile duct. It should be noted that perineural (nonneoplastic) islet cells may be found in chronic pancreatitis (see Chap. 7, Sect. 7.2.4).

23.3 Assessing Margin Status

The transection margin of the pancreatic neck and (for distal bile duct carcinoma) the bile duct margin may be sampled for frozen section, during pancreatoduodenectomy (see Chap. 2, Sect. 2.1), to determine whether further resection is needed to achieve clear margins. The transection margin should be embedded as a 'shave section' so that the whole margin can be assessed. Similarly, the bile duct margin should be embedded 'en face' so that the whole duct cross-section can be assessed. It is helpful if the surgeon marks (for example, with a suture) which side of the specimen is the true resection margin.

In distal pancreatectomy specimens and central (medial) pancreatectomy specimens (see Chap. 2, Sects. 2.1 and 2.6), the transection margins may again be submitted (as shave sections) for frozen section. In enucleation specimens (see Chap. 2, Sect. 2.7) for branch-duct intraductal papillary neoplasm, the surgeon may mark the communicating duct margin with a stitch or submit it separately. The communicating duct should be orientated by the surgeon and again be embedded 'en face'.

Electrocautery can cause a lot of tissue artefact and, therefore, it is suggested that transections for frozen section should be performed with a scalpel rather than electrocautery, when possible.

23.3.1 Transection Margin for Pancreatic Ductal Adenocarcinoma

The transection margin of the pancreatic neck may be sampled for frozen section to confirm that a pancreatic ductal adenocarcinoma is completely resected. Distinguishing pancreatic ductal adenocarcinoma from chronic pancreatitis at frozen section is discussed above (see Sect. 23.2). If invasive adenocarcinoma is present at the margin, then further resection should be considered by the surgeon. In the absence of invasive adenocarcinoma at the margin, it is generally agreed that further resection is not required if low-grade pancreatic intraepithelial neoplasia (formerly PanIN-1 & -2) is present at this margin. It has also been shown that high-grade PanIN (formerly PanIN-3) at the transection margin does not influence outcome in patients with pancreatic ductal adenocarcinoma [2]. This reflects the fact that survival after resection for pancreatic adenocarcinoma is generally too short for PanIN to become prognostically relevant. However, in patients with a small invasive carcinoma without evidence of lymph node metastases, or in those undergoing surgery for benign disease, the presence of high-grade PanIN at the transection margin may justify consideration of further resection. It should be noted that pancreatic ductal adenocarcinoma can be associated with duct cancerization (see Chap. 8, Sects. 8.4 and 8.6.2), which can mimic high-grade PanIN, and morphological distinction between these two entities may not be possible on frozen section. Therefore, if the invasive adenocarcinoma is located close to the transection margin, then it may be prudent to state that duct cancerization cannot be excluded.

PanIN lesions can be multifocal and, hence, the histological findings at the transection margin do not allow conclusions to be made about the presence or absence of PanIN in the pancreatic remnant.

23.3.2 Margin Status for Intraductal Papillary Mucinous Neoplasia (see Chap. 17)

Frozen section may be used to determine whether an intraductal papillary mucinous neoplasm (with or without associated invasive carcinoma) is completely excised and to check if duct dilatation is due to tumor involvement or is secondary to obstruction [3]. When there are numerous dilated ducts at the transection margin, the surgeon should identify the main pancreatic duct (for example, with a suture) so that the pathologist can then paint a small amount of ink on it to allow recognition on microscopy. If intraductal papillary mucinous neoplasm (IPMN) is present at the margin, then the ink will allow the pathologist to determine whether the IPMN involves the main duct, branch ducts, or both the main duct and branch ducts (i.e., is mixed-type IPMN).

Frozen section in IPMN does have its limitations. IPMNs can be multifocal with so-called 'skip lesions' and, therefore, the absence of IPMN at the transection margin does not exclude a skip lesion in the pancreatic remnant. The grade of dysplasia within a single IPMN can also be variable, so the identification of low-grade dysplasia at the margin does not rule out high-grade dysplasia in the adjacent pancreas. Low-grade PanIN at the margin may be indistinguishable from low-grade IPMN of gastric type, and in such circumstances it may be preferable to report that 'intraductal/intraepithelial neoplasm of low grade, either PanIN or IPMN, is present' [4].

Frozen section analysis of ducts can also be difficult because there may be erosion of the duct epithelium, duct inflammation, and reactive epithelial atypia. The duct epithelium may be denuded (Fig. 23.20), in which case, deeper levels should be cut from the tissue block and/or further tissue samples should be requested from the surgeon. In the absence of any duct epithelium for assessment, the pathologist cannot state whether (non-invasive) neoplasm is present at the margin or not.

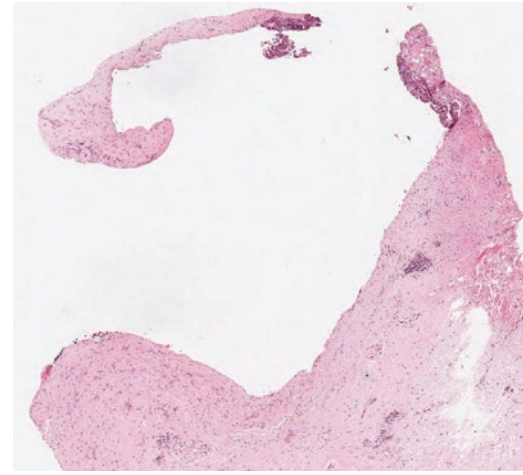

Fig. 23.20 Main pancreatic duct: most of the epithelium has been denuded from the pancreatic duct. Residual diathermied and disrupted epithelium is present top right. The frozen section was sent for assessment of margin status at the time of resection of an intraductal papillary mucinous neoplasm

Current guidelines recommend that when intraductal papillary mucinous neoplasm (IPMN) with high-grade dysplasia or invasive adenocarcinoma is present at the transection margin, further resection is warranted [4, 5]. It is now generally accepted that IPMN with low-grade dysplasia at the margin does not require additional therapy.

23.3.3 Margin Status for Other Pancreatic Neoplasms

Frozen section analysis of margins is generally not required for other cystic neoplasms of the pancreas or for pancreatic neuroendocrine tumors (see Chap. 20, Sect. 20.8.3), because they are so well circumscribed, and because an R1-resection does not seem to have a major impact on long-term overall survival.

References

1. Hyland C, Kheir SM, Kashlan MB. Frozen section diagnosis of pancreatic carcinoma. A prospective study of 64 cases. Am J Surg Pathol. 1981;5:179–91.
2. Matthaei H, Hong SM, Mayo SC, dal Molin M, Olino K, Venkat R, et al. Presence of pancreatic intraepithelial neoplasia in the pancreatic transection margin does not influence outcome in patients with R0 resected pancreatic cancer. Ann Surg Oncol. 2011;18:3493–9.
3. Sauvanet A, Couvelard A, Belghiti J. Role of frozen section assessment for intraductal papillary and mucinous tumor of the pancreas. World J Gastrointest Surg. 2010;2:352–8.
4. Tanaka M, Castillo F-d, Kamisawa T, Jang JY, Levy P, Ohtsuka T, et al. Revisions of international consensus Fukuoka guidelines for the management of IPMN of the pancreas. Pancreatology. 2017;17:738–53.
5. The European Study Group on Cystic Tumors of the Pancreas. European evidence-based guidelines on pancreatic cystic neoplasms. Gut. 2018;67:789–804.

Part VII

Cytology

The Role of Cytology

24

M. Priyanthi Kumarasinghe and Ian Yusoff

Cytological assessment forms an integral part of the multidisciplinary and multimodality approach required for the diagnosis of pancreatic lesions. The cytopathologist has a central role in making or confirming the diagnosis, guiding preoperative therapy, and providing prognostic information. The advent of endoscopic ultrasound-guided fine needle aspiration (EUS-FNA) has allowed safe, targeted, cytological sampling via the transduodenal route for lesions in the pancreatic head and neck, or via the transgastric route for lesions in the pancreatic body and tail. Lesions arising from or invading into the main pancreatic duct and common bile duct can now be sampled directly (brush cytology) or indirectly (exfoliated cells from aspirated bile or pancreatic juice) via endoscopic retrograde cholangiopancreatoscopy (ERCP). More recent advances in endoscopic technology have allowed histological specimens to be obtained, using microbiopsy forceps (of bile duct, pancreatic duct, and pancreatic cyst wall) or microcore fine needle biopsy (FNB) needles, complementing traditional cytology,

Pancreatic masses are usually subdivided into solid and cystic (mucinous and nonmucinous) lesions (Fig. 24.1). With modern imaging modalities, many of these lesions have a typical and often diagnostic appearance. The majority of solid masses are pancreatic adenocarcinoma (see Chap. 9) or neuroendocrine tumors (see Chap. 20), and the majority of cystic lesions are intraductal papillary mucinous neoplasms (see Chap. 17). The diagnostic approach may vary, but the clinical scenario from a cytological (and diagnostic) perspective is usually either that a specific diagnosis is suspected on imaging or the diagnosis is uncertain. For solid lesions where the diagnosis is suspected, the role of cytology is usually confirmatory before definitive management (e.g., surgery, chemotherapy, observation, or palliation). In this setting, EUS-FNA has repeatedly been shown to perform very well with a high sensitivity and very low false-positive rate [1, 2]. More recently, a role for cytology in risk stratification and prognostication has emerged. For instance, small asymptomatic pancreatic neuroendocrine tumors (<10 mm) are often observed if they have a low proliferation index and no high-risk cytological features [3]. With the evolution of

M. P. Kumarasinghe (✉)
Department of Anatomical Pathology,
QEII Medical Centre, Nedlands, Western Australia
e-mail: priyanthi.kumarasinghe@health.wa.gov.au

I.Yusoff (✉)
QEII Medical Centre, Perth, WA, Australia
e-mail: ian.yusoff@health.wa.gov.au

© Springer Nature Switzerland AG 2021
F. Campbell, C. S. Verbeke, *Pathology of the Pancreas*,
https://doi.org/10.1007/978-3-030-49848-1_24

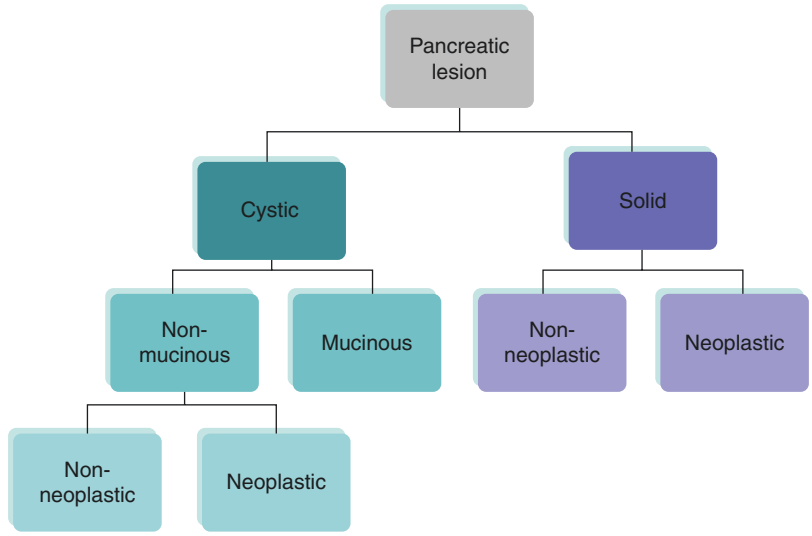

Fig. 24.1 Algorithmic approach to interpretation of pancreatic cytology samples

targeted cancer therapies, tissue sampling now has the additional role of treatment direction. For example, recent guidelines for managing metastatic pancreatic adenocarcinoma now recommend routine testing for d-MMR/MSI-H using immunohistochemistry, polymerase chain reaction, or next generation sequencing [4]. For solid lesions where the diagnosis is uncertain, the need for cytology is usually to distinguish malignancy from an inflammatory condition. Historically, cytology has performed less well in this situation but close cooperation between clinician and cytopathologist, together with rapid on-site evaluation, and the development of new needles, has improved performance, and a positive diagnosis can now be made in many inflammatory conditions such as IgG4-related disease and chronic pancreatitis [1, 5].

Guidelines for the management of pancreatic cystic lesions are well established [6, 7]. The commonest cystic lesions are branch-duct-type intraductal papillary mucinous neoplasms. However, imaging is not always definitive (especially for smaller cysts) and the diagnosis is often presumptive. Historically, routine FNA was undertaken with the aim of distinguishing mucinous from nonmucinous lesions [6]. This approach has lost favor, and EUS-FNA is now mainly reserved for cysts with so-called high-risk features, to risk stratify these patients and guide management [6, 7].

24.1 Tissue Acquisition

24.1.1 EUS-Guided Tissue Acquisition

A number of factors influence the outcome of EUS-FNA, including lesion location and type, the experience of the endoscopist and cytopathologist, needle choice, sampling technique (suction, use of a stylet and fanning), and availability of rapid on-site evaluation (ROSE). Currently, three sizes of EUS-FNA needles are available: 19G, 22G, and 25G. The 19G needle is usually reserved for cyst aspiration. Solid lesions are usually sampled with a 22G or 25G needle, with two meta-analyses concluding that the 25G needle is more sensitive [8, 9]. In the past, EUS-guided fine needle biopsy (FNB) needles were unwieldy and the yield was not superior to EUS-FNA. However, over the past three years, there has been a significant improvement in needle design. Two FNB needles [SharkCore® with a forktip design (Medtronic, Minneapolis,Minn.), and Acquire® with a Franceen tip (Boston Scientific, Natick, Mass)] have been introduced. The early literature suggests that these needles provide more tissue compared to FNA and may save costs associated with ROSE, but the issue remains unresolved, and multicenter studies are currently underway to assess the potential value of these needles in the diagnosis of solid pancreatic lesions [1, 10]. Needle pinch biopsy microforceps have

now also been developed (Moray® microforceps biopsy US Endoscopy, Mentor, Ohio) for sampling of pancreatic cyst walls and septa. This technique is associated with a greater complication rate, but it may allow more accurate cyst characterization in selected cases where fluid analysis is inconclusive [11].

24.1.2 ERCP-Guided Tissue Acquisition

Bile or, less frequently, pancreatic juice can be aspirated at the time of endoscopic retrograde cholangiopancreatoscopy (ERCP) to obtain exfoliated cells. Similarly, strictures of the common bile duct (CBD) and main pancreatic duct (MPD) can be sampled with brush cytology. As an extension of this technique, both the CBD and MPD can now be directly inspected with a cholangioscope (passed through the duodenoscope), and microbiopsies can be taken using the SpyGlass® direct visualization system (Boston Scientific, Natick, Mass). This technique is usually reserved for biliary strictures and main-duct-type intraductal papillary mucinous neoplasm (see Fig. 17.21), while EUS-FNA is the preferred technique for pancreatic masses. Imprint cytology may prove to be useful [12].

24.1.3 The Non-Diagnostic FNA

The yield of FNA or brushings appears to be dependent upon the operator, technique employed, and equipment used. When FNA is not diagnostic, further clinical management decisions may still be taken on the basis of the clinical scenario and imaging. For example, if the suspected diagnosis is likely autoimmune pancreatitis, an empiric trial of steroids may be appropriate [13]. If a tissue diagnosis is indispensable for the management of a solid pancreatic mass, an alternative technique and/or a different operator could be employed. Repeat EUS and sampling at a tertiary center with rapid on-site evaluation (ROSE) may be a cost-effective approach [14, 15]. If an FNA needle was used for the index procedure, then it may be appropriate to consider using an FNB for the repeat examination [16, 17].

24.1.4 Rapid On-Site Evaluation (ROSE)

The EUS-FNA procedure is costly. Rapid on-site evaluation (ROSE), used to assess sample adequacy, and provide on-site triage of the sample for ancillary testing, can be performed by an experienced cytologist or a cytopathologist. ROSE has proven to be effective in reducing the number of inadequate samples, thereby minimizing the need for a repeat procedure. The inadequacy rate, with and without ROSE by a cytopathologist, was shown to be 1.0% vs 12.6% and 2.3% vs 29.3%, respectively, in two independent studies [18, 19]. Remote gross evaluation by telecytology has been proposed as an alternative to ROSE [20, 21]. Monaco et al. have shown that it is highly cost-effective, reducing the cytopathologist's time spent on ROSE by 89% [22].

24.2 Sample Preparation

The approach to sample preparation of pancreatic cytology specimens is essentially determined by the cystic or solid nature of the lesion (Fig. 24.1 and Table 24.1). Gross evaluation is a useful tool in the setting of a cystic lesion. Viscosity, clarity, color, and volume of the fluid can give important clues. These qualities also may dictate triaging for ancillary testing. Solid neoplasms generally produce granular smears. Conversely, solid

Table 24.1 A protocol for handling cyst fluids (adopted from Chai SM et al.) [23]

Cyst fluid volume ≤ 1 ml	Cyst fluid volume > 1 ml
Centrifuge the specimen	Neat fluid (~0.5 ml) sent for biochemical analysis
Generates a deposit and supernatant fluid	Centrifuge the rest for a deposit and supernatant fluid
Deposit processed as a cell block for microscopic assessment and molecular testing	Deposit processed as a cell block and smears for microscopic assessment
Supernatant fluid sent for biochemical analysis	Supernatant and any excess fluid may be frozen and stored for future use/ molecular testing
Remaining supernatant is frozen and stored for future use	Molecular testing on cell block

nonneoplastic lesions, such as localised chronic pancreatitis and autoimmune pancreatitis, may produce scant smears, and EUS-guided biopsies may be necessary to obtain adequate material.

24.2.1 Cyst Fluids

A standard approach to handling cyst fluids is desirable for diagnosis, and on-site evaluation is not required. Table 24.1 shows a potential protocol for handling cyst fluids [23]. Combination of the cytological features and the results of biochemical and molecular studies gives the highest diagnostic accuracy (Table 24.2) [7, 23–25]. Neat cyst fluid as well as supernatant can be used for CEA and *KRAS* testing. Cytological assessment can be done on smears, cytospin preparations, and cell blocks. Samples from a mural nodule or a solid area are prepared as for solid lesions (see Sect. 24.2.2), preferably with rapid on-site evaluation.

24.2.2 Solid Lesions

Direct smears are prepared from EUS-FNA samples of solid lesions. Both air-dried and alcohol-fixed direct-spread slides may be made. Needle rinses using air and/or saline to expel material into preservative fluid for liquid-based cytology and/or cell blocks may be prepared according to personal and institutional preferences. A dedicated pass may be obtained, depending on the impressions at rapid on-site evaluation, for specific ancillary tests such as flow cytometry and microbiological studies. In many institutions, cell blocks are routinely prepared for all EUS-FNA cases. In addition to performing ancillary tests such as histochemistry and immunohistochemistry, cell block material may also be required for ancillary testing for prognostication and optimizing targeted therapy.

24.2.3 Brush Cytology Specimens

Brush cytology specimens can be made into direct smears, cytospins, liquid-based cytology (LBC) preparations, or a combination of methods. LBC has the advantages of allowing quick fixation of the cellular sample, thereby preserving cellular detail, and collection of all of the cellular material sampled. Following completion of the procedure, the cytobrush can be cut out and rinsed in saline or appropriate preservative fluid to collect the maximum amount of material sampled.

Table 24.2 Cyst fluid analysis

	Mucinous cysts		Nonmucinous cysts			
	IPMN	MCN	SCA	Pseudocyst	Acinar cystic transformation	Solid neoplasms with cystic change
Epithelial cellularity	high/low	low	very low	none[a]	low	variable
Proteinaceous material	mucin	mucin	non-mucin	non-mucin	non-mucin	variable
Viscosity	high	high /low	low	low	low	variable
CEA	high	high /low	low	low	low	variable
Amylase	high	high/low	low	very high	high	variable
Lipase	variable	variable	variable	high	not known	variable
KRAS	++	++	–	–	–	variable
GNAS	++	–/+	–	–	–	variable
Beta-catenin	–	–	–	–	–	variable
VHL	–	–	+	–	–	variable

Abbreviations: *IPMN* intraductal papillary mucinous neoplasm, *MCN* mucinous cystic neoplasm, *SCA* serous cystadenoma, *VHL* von Hippel-Lindau gene

[a]Except for contaminants

24.3 Microscopic Evaluation

24.3.1 Terminology

The Papanicolaou Society of Cytopathology Guidelines for Reporting Pancreatobiliary Cytology (PSGPBC) is a system of classification of pancreatobiliary cytology [26]. These guidelines were introduced as part of a worldwide attempt to standardize terminology, and a summary of the nomenclature and salient features for the six diagnostic categories is shown in Table 24.3.

24.3.2 Contaminants

A very important aspect in evaluation of samples, from both solid and cystic lesions of the pancreas, is to distinguish contaminants from lesional material. These include gastric and duodenal mucosal cells and normal pancreatic tissue, depending on the EUS route used to obtain the sample. Cytological features of common contaminants and their mimics are shown in Table 24.4 and Fig. 24.2. The EUS needle may have to pass through a large volume of pancreatic parenchyma to reach deep-seated lesions, resulting in abundant normal pancreatic tissue with only small numbers of lesional cells in the smears. Duodenal contaminants are easier to identify with their classic cytomorphology, while gastric contaminants may mimic low-grade neoplastic epithelium of gastric type (see Sect. 24.3.4.1.1). Brush cytology specimens will contain native biliary or pancreatic ductal epithelium.

24.3.3 Solid Lesions

The most common solid pancreatic neoplasms are pancreatic ductal adenocarcinoma and neuroendocrine tumor, while the most common non-neoplastic lesions are autoimmune pancreatitis and localized chronic pancreatitis. Other solid pancreatic lesions include the subtypes of ductal adenocarcinoma, acinar cell carcinoma, solid

Table 24.3 The Papanicolaou Society of Cytopathology categories for reporting pancreatobiliary cytology [26]

	General cytological criteria and specific or probable diagnoses
I. Nondiagnostic	No lesional cells seen • Preparation artefact precludes cytological evaluation • Cystic lesions without any clues on cyst fluid analysis
II. Negative for malignancy	Benign pancreatic parenchyma in the appropriate clinical setting Cytological features of a specific benign entity: • Pancreatitis (acute/chronic/autoimmune) • Pseudocyst • Lymphoepithelial cyst • Accessory spleen
III. Atypical	Cytological or architectural atypia that is beyond what can be classified as reactive or contaminants but insufficient for a diagnosis of neoplasia or "suspicious for malignancy". Essentially it is an 'indeterminate' result
IV. Neoplastic (benign) and Neoplastic (other)	Benign neoplasms • Serous cystadenoma • Lymphangioma Other neoplasms: • Pancreatic neuroendocrine tumor (PanNET) • Neoplastic mucinous cysts (NMCs): IPMN, MCN • Solid pseudopapillary neoplasm (SPN): categorised as 'malignant' by WHO 2019
V. Suspicious for malignancy	Significant cytoarchitectural and morphological atypia, but qualitatively or quantitatively not fulfilling the threshold for a definitive diagnosis of malignancy
VI. Malignant	• Pancreatic ductal adenocarcinoma, NOS and its subtypes • Acinar cell carcinoma • Poorly differentiated (small cell and large cell) neuroendocrine carcinoma • Metastases • Lymphoma

Table 24.4 Common cytological contaminants and their mimics

	Cytoarchitecture and morphology	Mimics	Comments
Gastric foveolar epithelial cells	Flat honeycomb sheets of cells with well-defined cell borders (can be appreciated better by focusing up and down) May occur as very large tissue fragments, very well organized ('regimented') Columnar nature of the cells may be appreciated at the edges of the sheets	Well-differentiated pancreatic ductal adenocarcinoma, including foamy gland pattern Gastric-type neoplastic mucinous cysts, low-grade	Clinical and EUS findings are helpful Repeat EUS may be needed to sample areas that may show classic cytomorphology Low-grade neoplastic mucinous cysts in the tail and body, accessed through the stomach, can be extremely challenging
Gastric specialized epithelium (parietal cells and chief cells)	In small clusters and singly admixed with chief cells	Pancreatic neuroendocrine tumors	Consider the specific EUS approach (via gastric body)
Duodenal mucosa	Background of a honeycomb sheet of epithelial cells Presence of scattered "holes" which represent mucin goblets in goblet cells Well organized (regimented)	Very rarely well-differentiated adenocarcinoma	Usually easy to identify as contaminants; only present in head of pancreas aspirations via transduodenal route
Pancreatic acinar cells	Large intact lobules with stroma (bunch of grapes) Individual acinar arrangements Dispersed cells with comparatively smaller nuclei than mimics	Pancreatic neuroendocrine tumours (PanNETs)	The cells of PanNETs are significantly larger than benign acinar cells, and usually exhibit stippled chromatin (see Table 24.7)
		Acinar cell carcinoma	Numerous single nuclei with prominent central nucleolus (see Table 24.8)
		Renal cell carcinoma	Clinical history and immunoprofile
Pancreatic ductal epithelial cells	Small numbers, regular architecture, and regular nuclear cytology	Well-differentiated adenocarcinoma	Benign epithelium is generally present in small numbers, admixed with stroma and acini

pseudopapillary neoplasm, intrapancreatic common bile duct carcinoma, and metastases to the pancreas. Cytoarchitecture and cellular (nuclear and cytoplasmic) features may give individual and collective clues to the diagnosis, but cell block immunohistochemistry (see Tables 12.1 and 20.5) is often required. With the increased use of neoadjuvant and induction chemotherapy for pancreatic malignancy, accurate and conclusive preoperative cytological diagnosis is essential.

24.3.3.1 Pancreatic Ductal Adenocarcinoma (see Chap. 9)

The heterogeneous cytoarchitecture and morphology of conventional pancreatic ductal adenocarcinoma (PDAC) is a very useful diagnostic feature (Fig. 24.3), with many cases showing the full spectrum of well-differentiated malignant glands to poorly differentiated tumor in representative samples. The classical cytoarchitectural and cytomorphological features of PDAC

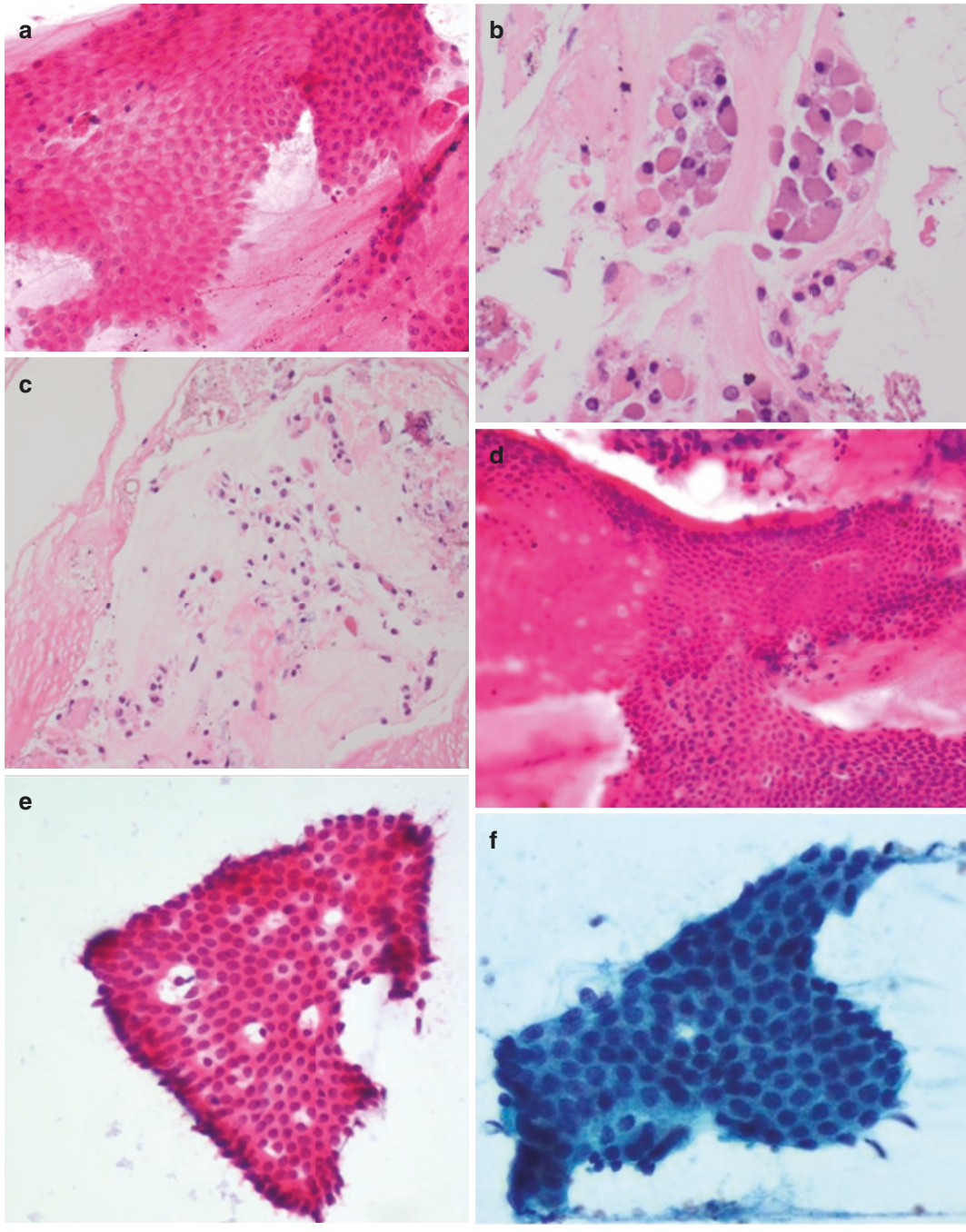

Fig. 24.2 Contaminants found in EUS-guided aspirates of the pancreas: gastric foveolar cells (**a**), gastric parietal and chief cells (**b**, **c**), duodenal mucosa (**d**, **e**), benign pancreatic ductal cells (**f**), pancreatic acinar cells (**g**, **h**), and bile duct epithelium (**i**)

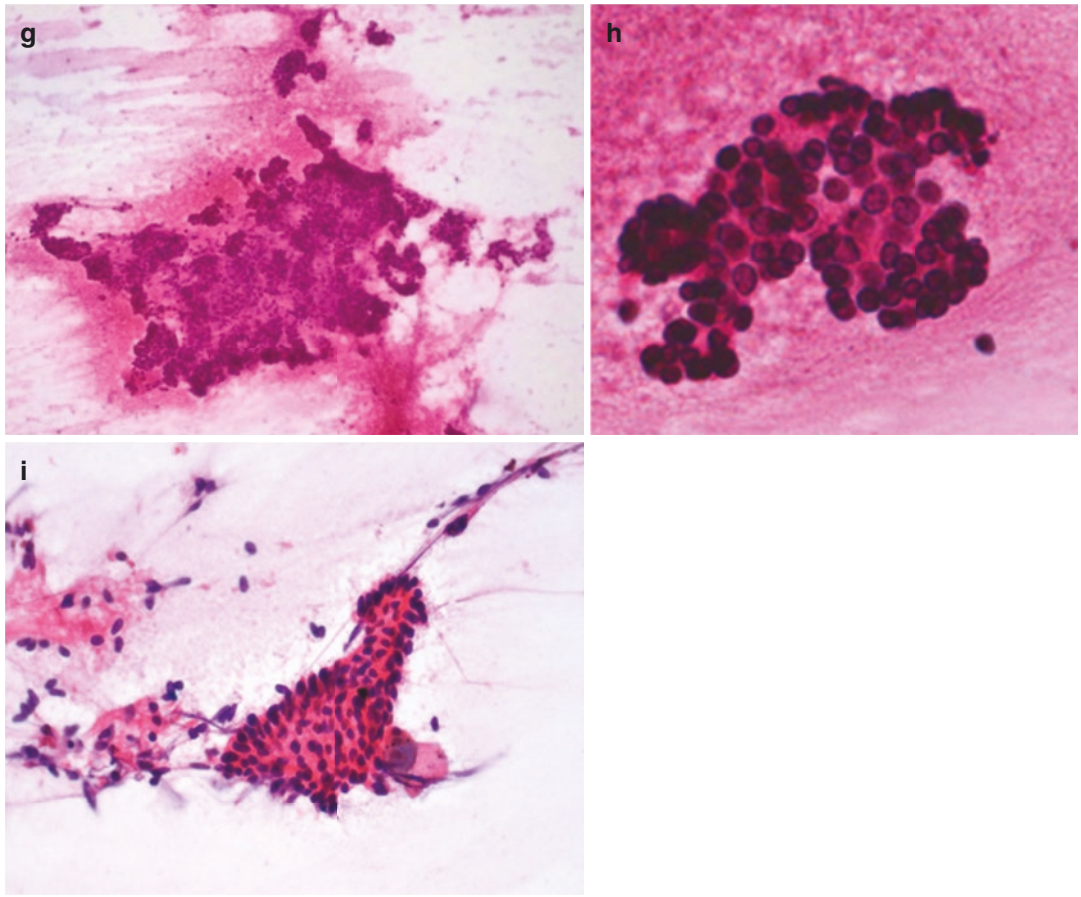

Fig. 24.2 (continued)

are summarized in Table 24.5. Moderately and poorly differentiated PDACs are usually relatively easy to recognize, whereas well-differentiated adenocarcinomas may be mistaken for benign reactive ductal epithelium and gastric contaminants. Disorganised sheets and clusters of PDAC cells are often referred to as a 'drunken honeycomb' pattern and may show distorted architecture resembling 'distorted animal-like configurations' (Fig. 24.3d). The presence of background necrosis is usually associated with more poorly differentiated carcinomas (Figs. 24.3b and e).

The foamy gland pattern of PDAC (see Chap. 9, Sect. 9.8.1), or PDAC subtypes such as undifferentiated carcinoma and colloid carcinoma (see Chap.9, Sect. 9.14), may occasionally be seen in cytology preparations and mimic other entities (Table 24.6 and Fig. 24.4) [27].

Some cases may show significantly abnormal cytological features without fulfilling the cytoarchitectural and cytomorphological features that are diagnostic of malignancy. These cases can be designated "suspicious of malignancy". In such cases a combination of S100P, monoclonal CEA, and MUC1 immunopositivity in cell block material may help to clinch the diagnosis (Fig. 24.5) [28]. Although patients with tumors that are resectable may proceed to surgery on the basis of 'suspicious for malig-

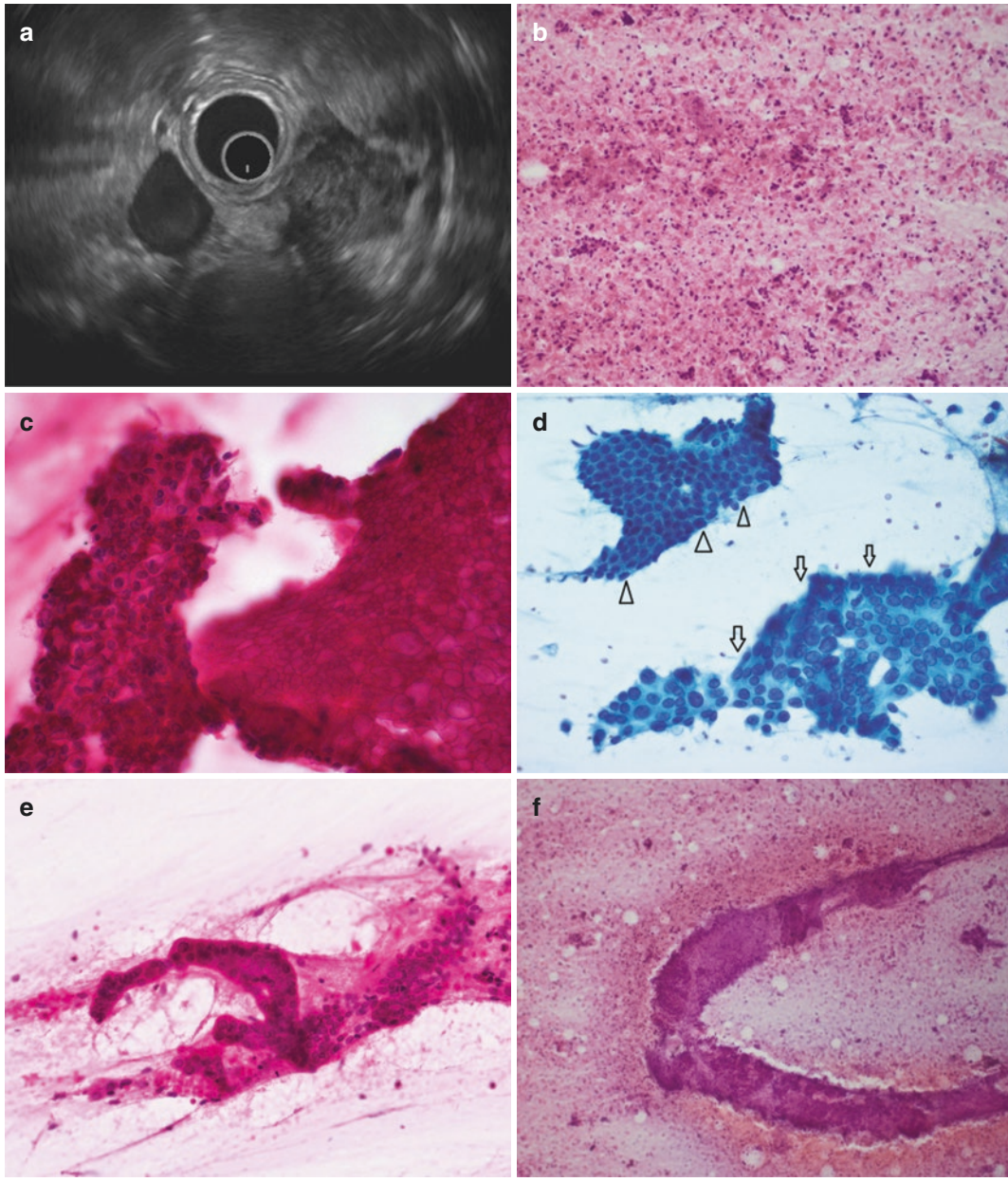

Fig. 24.3 EUS and cytological features of PDAC: hypoechoic lesion in the pancreatic head with an irregular border that appears to invade the duodenal muscularis propria, highly suggestive of a malignant nature (**a**). Cellular smears with abnormal cells in loose aggregates and as single cells, and background necrosis (**b**). Three-dimensional fragments with 'drunken honeycomb' and 'stacked potatoes' appearance (**c**). Abnormal architectural forms ('deformed-animal figures', *arrows*) compared to the adjacent benign ductal cells (*arrow head*) (**d**). Abnormal architectural forms with necrosis (**e**) and accompanying fibrous stroma with abnormal cells in the background (**f**)

nancy', those that are to be treated with neoadjuvant chemoradiation are generally subject to repeat FNA for a definitive diagnosis of malignancy.

24.3.3.2 Pancreatic Neuroendocrine Tumor (see Chap. 20)

The classical features of pancreatic neuroendocrine tumor (PanNET) are summarized in Table 24.7 and illustrated in Fig. 24.6. Ancillary studies are routinely performed to confirm the neuroendocrine nature of the tumor, to distinguish PanNET from acinar cell carcinoma and solid pseudopapillary neoplasm, which may show some overlapping cytological features, and to grade the PanNET. The proliferation index assessed in cell block preparations is reported to show high concordance with histology, in particular for grade 1 PanNETs [29]. The basic principles of Ki-67 assessment in histology samples are also applied to cytology. If clinically indicated, immunohistochemistry for specific hormones, such as glucagon, insulin, or somatostatin may be performed. PanNETs may need to be distinguished from metastases to the pancreas, in particular renal cell carcinoma. Variants of PanNETs (Fig. 24.7), such as oncocytic and foamy types, may also pose specific diagnostic

Table 24.5 Cytological features of pancreatic ductal adenocarcinoma

Cytoarchitecture	Cytomorphology	Other features	Comments
Classic architectural heterogeneity Three-dimensional fragments with: Drunken honeycomb and stacked potatoes appearance Crowded sheets Papillary structures Abnormal 'animal-like' sheets Single 'abnormal' cells with stripped off cytoplasm (bare nuclei) Single 'tombstone' cells (large, tall, atypical, columnar cells)	Classic cellular heterogeneity Nuclei: membrane irregularity, hyperchromasia, or parachromatin clearing with variably prominent nucleoli Nuclear heterogeneity: a range of nuclear atypia from mildly atypical to extremely pleomorphic within the smear and within a single sheet cluster Cytoplasm: variable, vacuolated to dense and scant to ample	Necrosis	Be aware of the clinical, radiological, and EUS findings, and the EUS route of the FNA

Table 24.6 Cytological features of PDAC subtypes and the foamy gland pattern of PDAC

Tumor type	Architecture	Cellular features	Other features	Mimics
Undifferentiated carcinoma	Poorly cohesive	Pleomorphic, epithelioid, spindle, bizarre or multinucleated cells	Necrosis	Metastatic malignancies
Adenosquamous carcinoma	Generally similar to PDAC	Squamous differentiation		Metastatic malignancies
Colloid carcinoma	3-dimensional clumps and ball-like aggregates	Nuclei are not pleomorphic	Background of abundant mucin Intestinal differentiation in neoplastic cells	Intestinal IPMN and metastatic mucinous carcinomas
Foamy gland pattern	Mostly fairly well organized flat sheets	Low grade nuclei (basal, slightly irregular and hyperchromatic) Abundant finely vacuolated cytoplasm	Apical brush border condensation of cytoplasm (in cell blocks only)	Chronic pancreatitis Metastatic low nuclear grade carcinomas. e.g., RCC

Abbreviations: *PDAC* pancreatic ductal adenocarcinoma, *IPMN* intraductal papillary mucinous neoplasm, *RCC* renal cell carcinoma

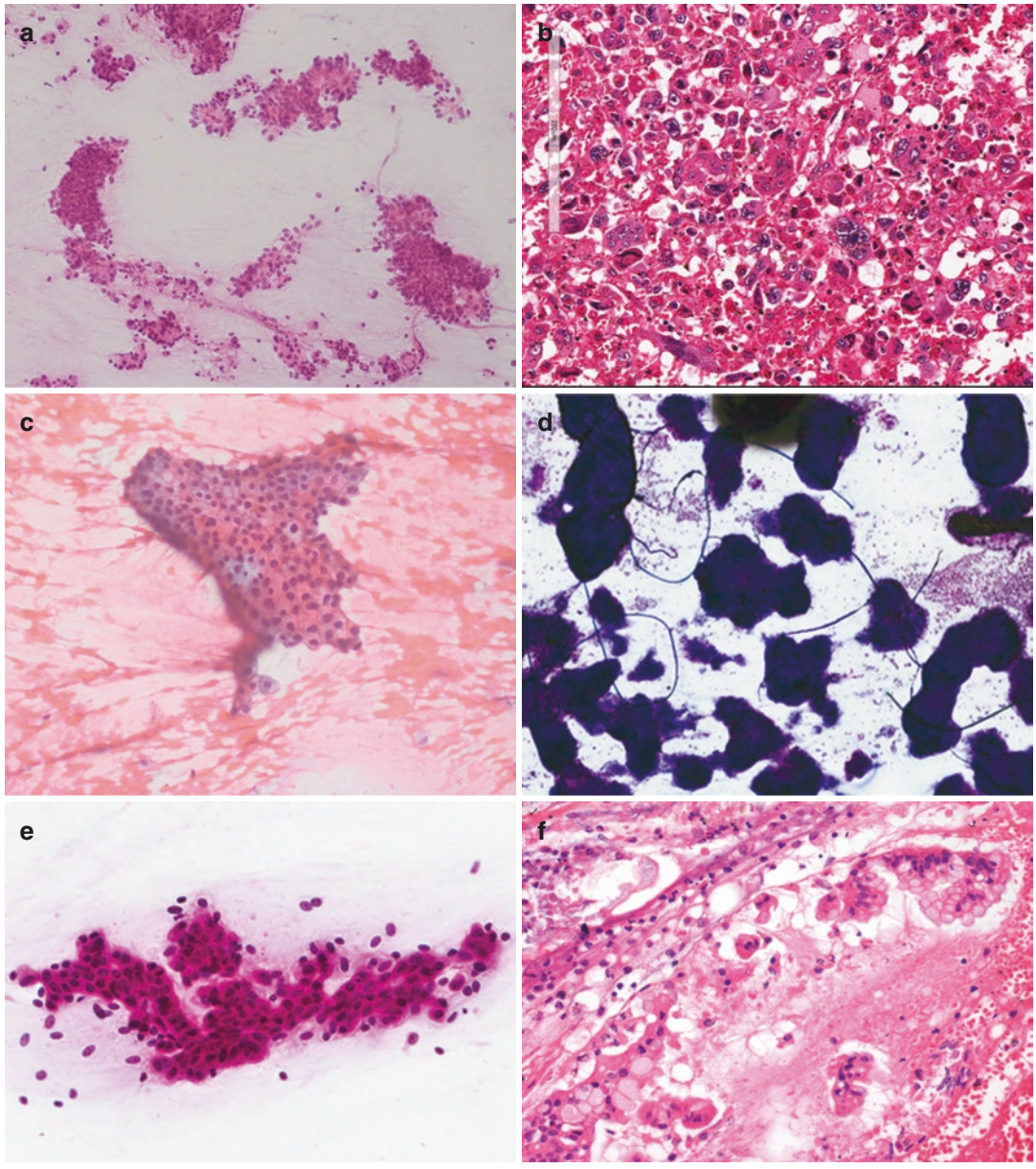

Fig. 24.4 Cytological features of subtypes of PDAC: very well-differentiated tubular type PDAC (**a**), undifferentiated carcinoma (**b**), foamy gland pattern of PDAC (**c**), thick mucin background in colloid carcinoma (**d**), and mucinous epithelium of intestinal type associated with colloid carcinoma in a smear (**e**) and a cell block (**f**)

challenges, and cystic PanNETs may be mistaken for other cystic lesions (Fig. 24.7d–f). Distinction between pancreatic neuroendocrine carcinoma (PanNEC) and a PanNET are based on cytomorphology. A neuroendocrine carcinoma may be mistaken for other high-grade malignancies.

24.3.3.3 Acinar Cell Carcinoma (see Chap. 10)

The classical features of acinar cell carcinoma are summarized in Table 24.8 and illustrated in Fig. 24.8. Acinar formations in acinar cell carcinoma (ACC) may be mistaken for pseudorosettes in PanNET (Fig. 24.6c). The individual tumor cells

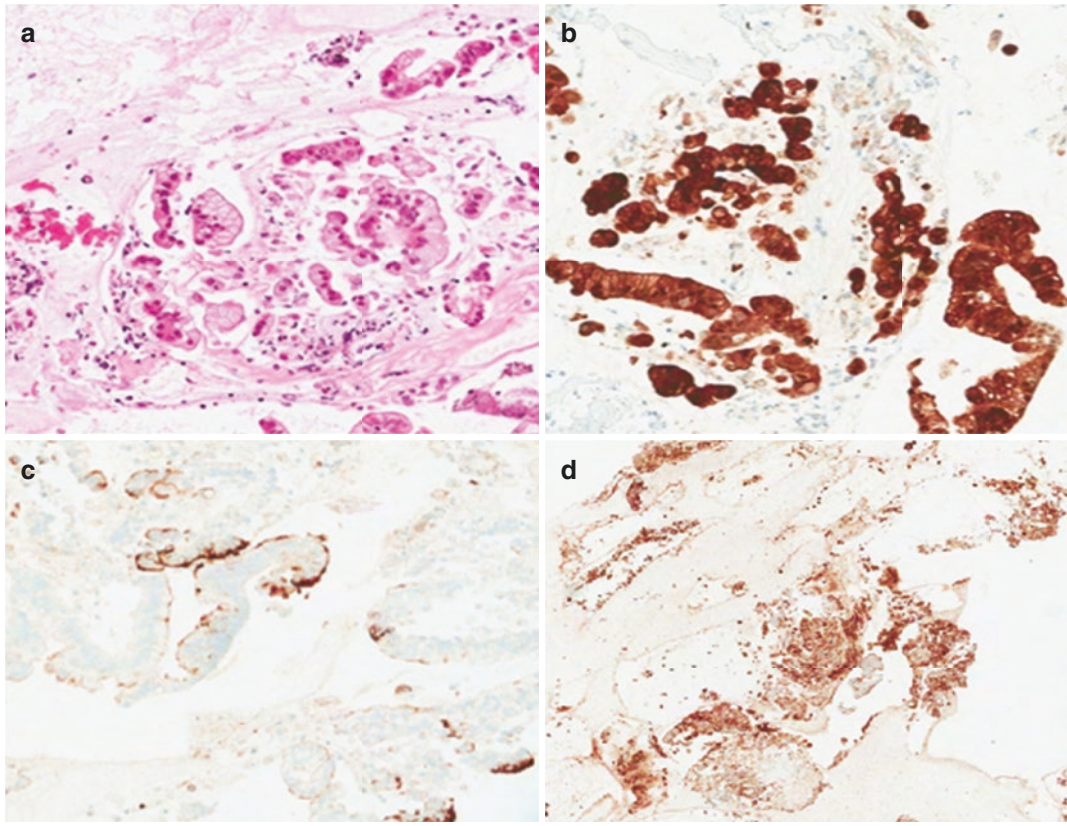

Fig. 24.5 Cell block of PDAC with complimentary immunohistochemistry: fairly bland cells with abundant mucin and moderately atypical nuclei, prepared from a EUS FNA of a solid mass, highly suspicious for malignancy (**a**). Immunohistochemistry is positive for S100P (nuclear + cytoplasmic) (**b**), MUC1 (membranous) (**c**), and monoclonal CEA (cytoplasmic and often in the background) (**d**)

Table 24.7 Cytological features of pancreatic neuroendocrine tumor (PanNET)

Cellularity	Cytoarchitecture	Cytomorphology	Other features	Comments
Highly cellular except in cystic and sclerotic PanNETs	Mostly loose cells Monotonous appearance Vascular network/ stroma	Small to medium-sized cells with random nuclear pleomorphism (endocrine atypia) Generally bland nuclei with salt and pepper chromatin Inconspicuous nucleoli Clear, vacuolated, and oncocytic cytoplasm in variants Very rare mitosis (except in high-grade tumors)	Blood-stained background No necrosis Rarely, psammoma bodies, amyloid	Consider SPN, ACC, and well-differentiated PDAC in the differential diagnosis Always obtain material for a cell block for immunohistochemistry and Ki67-proliferation index The cytomorphology of PanNECs resembles high-grade carcinoma, unlike PanNETs

Abbreviations: *SPN* solid pseudopapillary neoplasm, *ACC* acinar cell carcinoma, *PDAC* pancreatic ductal adenocarcinoma, *PanNEC* pancreatic neuroendocrine carcinoma

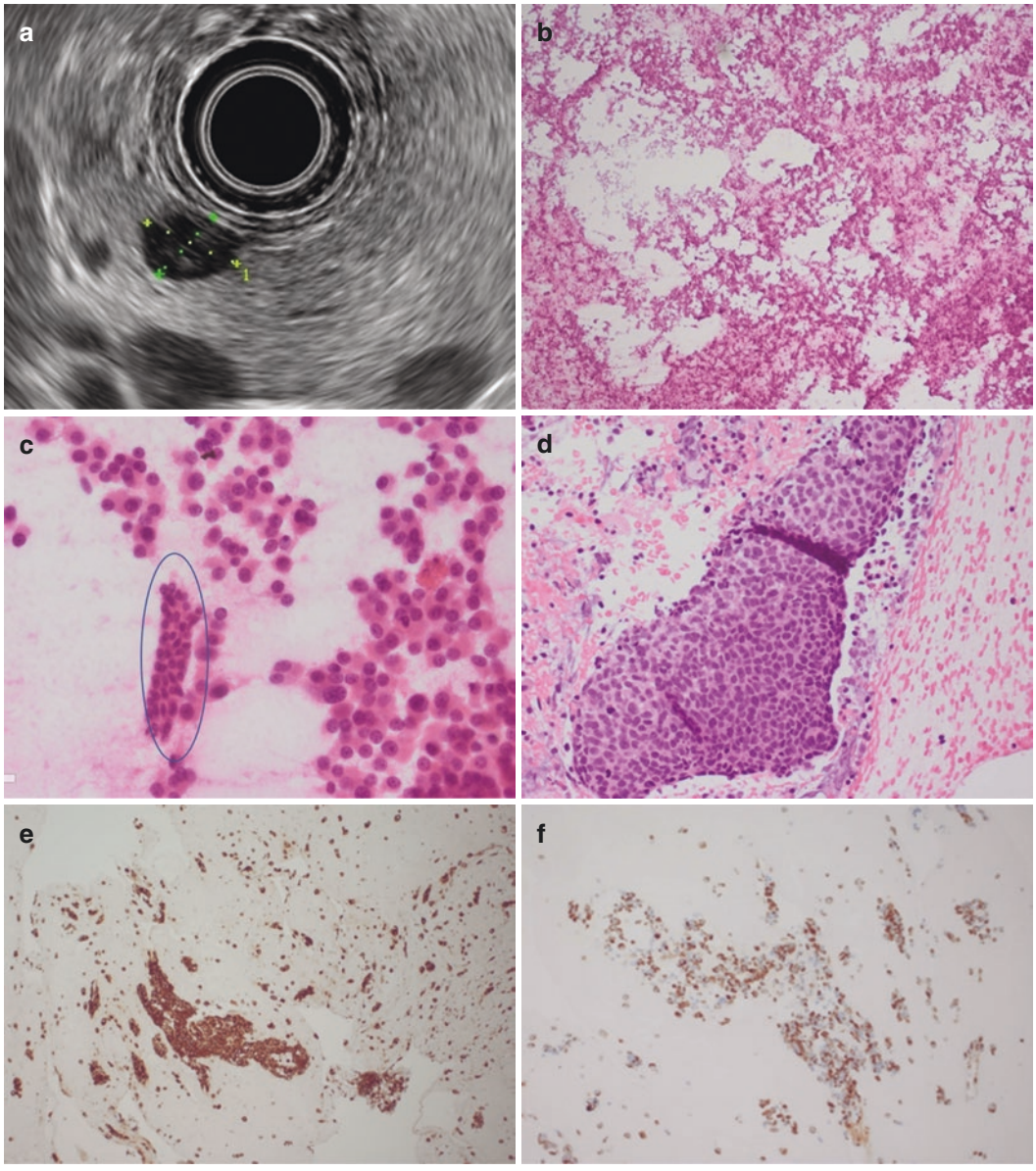

Fig. 24.6 EUS and cytological features of pancreatic neuroendocrine tumors: a well-defined 10 mm, hypoechoic lesion is seen in the pancreatic head (**a**). Highly cellular smears with loose monotonous cells (**b**). Small to medium-sized cells with round nuclei and salt and pepper chromatin with inconspicuous nucleoli, in contrast to cells of benign ductal epithelium (*circled*) (**c**). Cell block preparation (**d**). Synaptophysin (**e**) and chromogranin (**f**) immunohistochemistry

in ACC have central to eccentric round nuclei, which often contain a single prominent nucleolus, and the chromatin tends to be coarse in contrast to PanNETs. Ancillary testing on cell block material (Fig. 24.8d) is required for the distinction between ACC and PanNET. Neoplastic acinar cells may show PAS-diastase resistant granular staining, which is not seen in PanNET. Trypsin and BCL10 immunohistochemistry is useful for differentiating ACC from other tumors (Figs. 24.8e and f). However, immunopositivity for these markers does not differentiate normal pancreatic acini from ACC. Nonneoplastic acinar groups should not be mistaken for ACC (Fig. 24.2h).

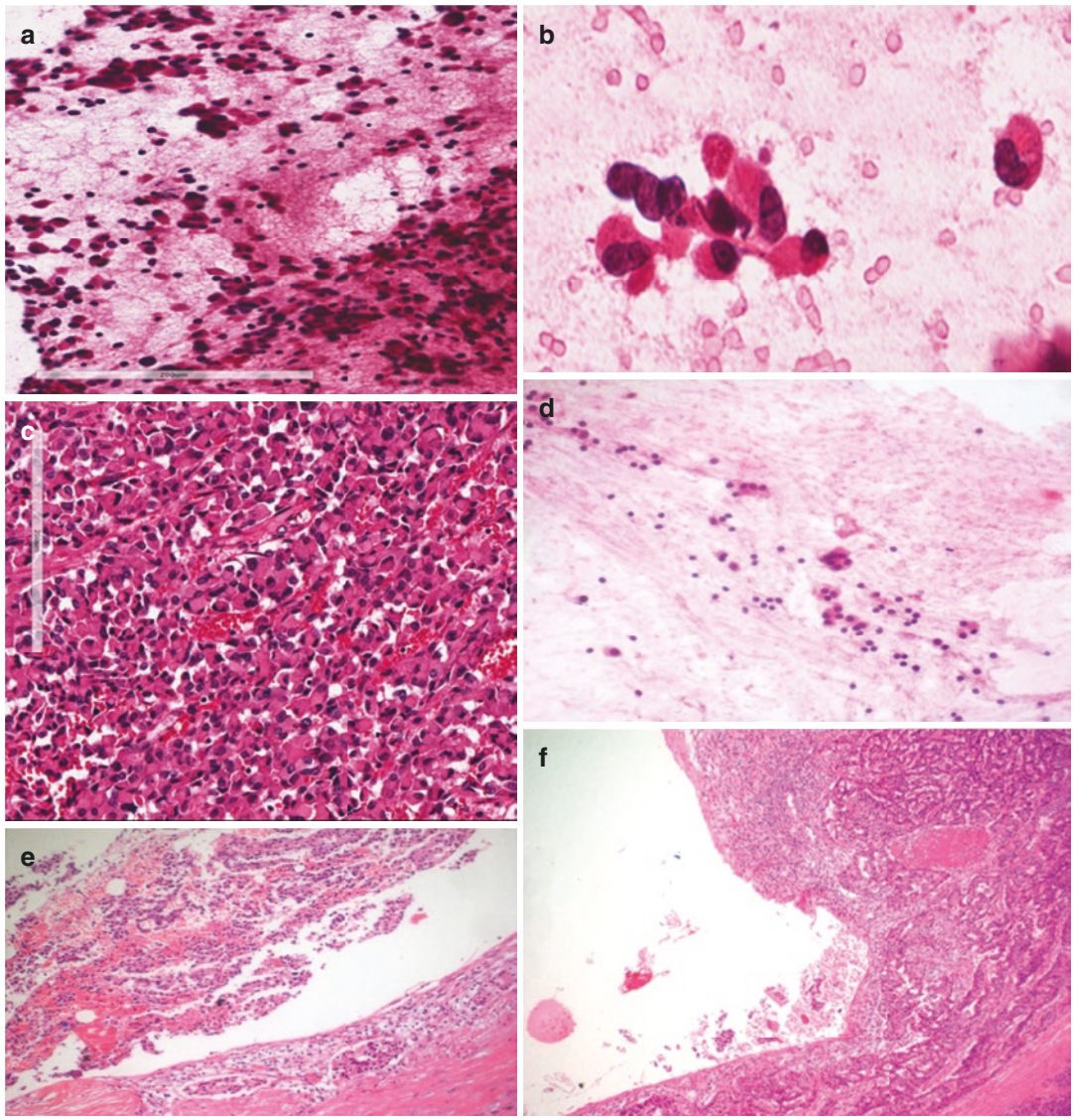

Fig. 24.7 Cytological features of variants of pancreatic neuroendocrine tumor (PanNET): oncocytic PanNET on cytology (**a**, **b**) and histology (**c**), cystic PanNET on cytology (**d**, **e**), and histology (**f**), clear cell PanNET (**g**, **h**) and PanNET grade 3 (**i**)

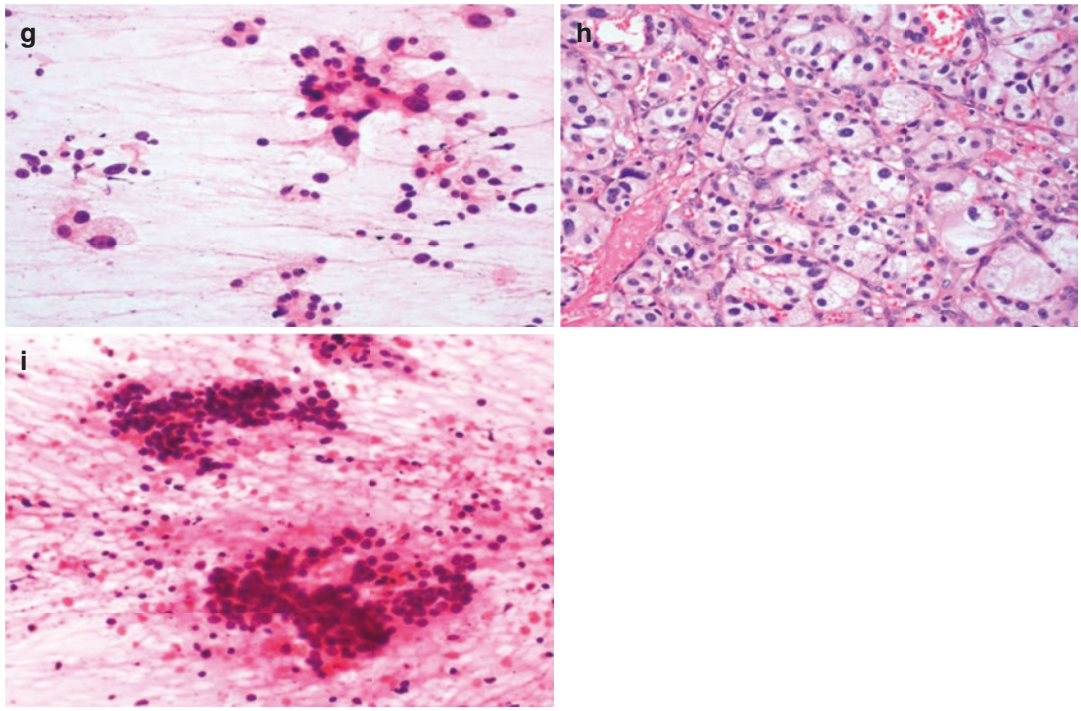

Fig. 24.7 (continued)

Table 24.8 Cytological features of acinar cell carcinoma

Cellularity	Cytoarchitecture	Cytomorphology	Other features	Comments
Highly cellular	Small/medium-sized clusters and fragments together with single cells and bare nuclei in the background Acinar and pseudorosette arrangement Very rare syncytial sheets	Small to medium-sized cells with minimal pleomorphism and only mild increase in nuclear to cytoplasmic ratio Round to oval, central to eccentric nuclei with coarse chromatin, single conspicuous or prominent nucleolus, focal anisocytosis Finely granular or dense basophilic cytoplasm Very rare mitosis	Rare or no necrosis No desmoplastic response	Benign and reactive acinar structures have more cohesive cell groups, well-defined acini, and may be associated with ductal epithelium Neuroendocrine tumor can be a challenge with many overlapping cytological features, but the chromatin pattern is different and immunohistochemistry is helpful

24.3.3.4 Solid Pseudopapillary Neoplasm (see Chap. 18)

Similar to pancreatic neuroendocrine tumor (PanNET) and acinar cell carcinoma (ACC), solid pseudopapillary neoplasm yields cellular aspirates. However, the cytoarchitectural and morphological features are quite characteristic (Table 24.9 and Fig. 24.9), featuring branching sheets and papillary formations described as "Chinese characters', often with delicate fibrovascular cores and myxoid stroma. The tumor cells tend to be monomorphic with minimal variability, and moderate or scant, granular cytoplasm. Nuclei are round to oval with slight

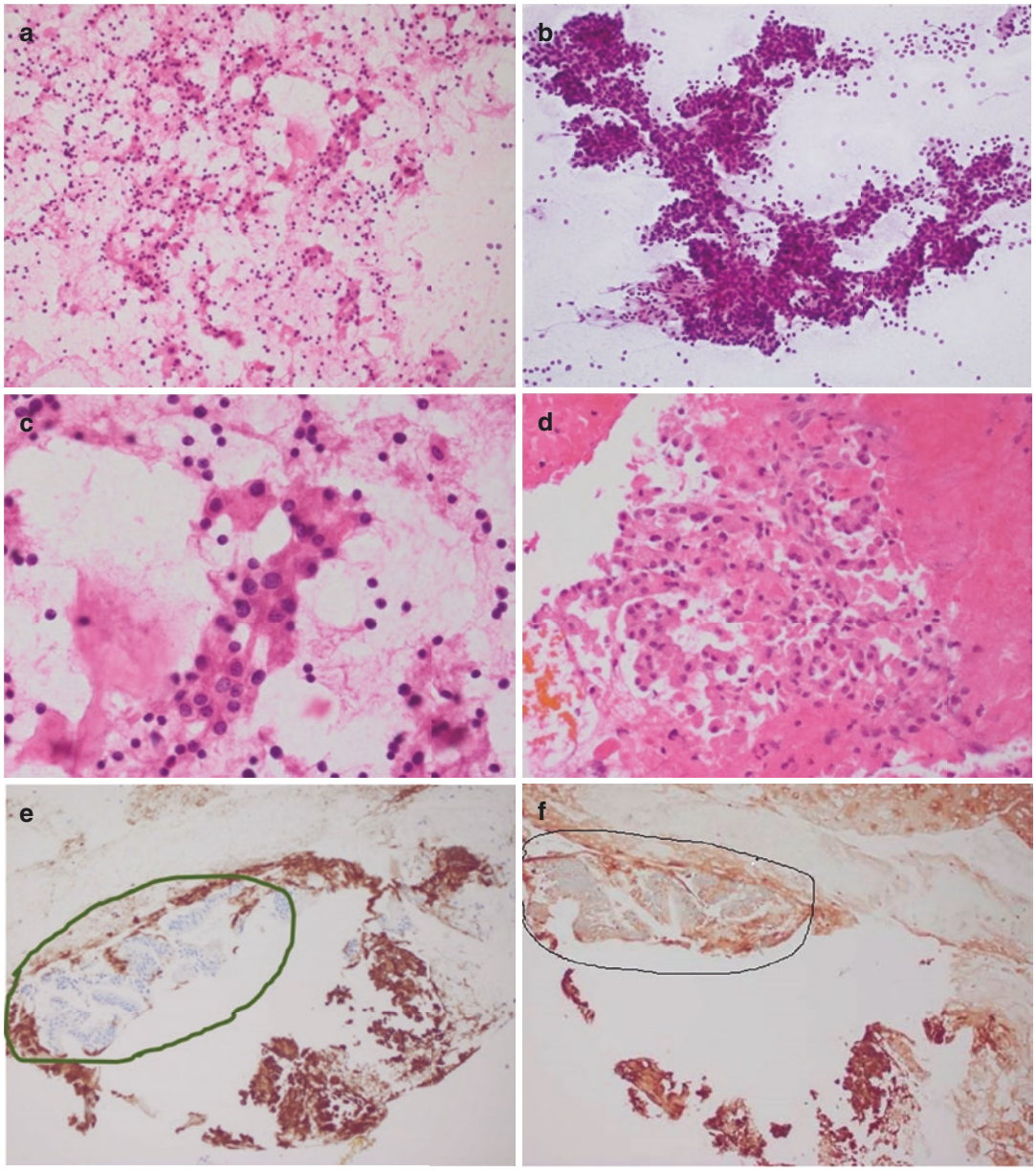

Fig. 24.8 Cytological features of acinar cell carcinoma: smears featuring a dispersed population of cells with small to medium-sized nuclei that may resemble a PanNET on low power (**a**). Aggregates and rare syncytial sheets (**b**). High-power picture featuring loose cells with round to oval nuclei with granular cytoplasm (**c**). A satisfactory cell block with loose neoplastic acinar cells (**d**), positive trypsin immunohistochemistry with immunonegative (*circled*) contaminant gastric mucosa (**e**), and positive BCL10 immunohistochemistry with immunonegative (*circled*) contaminant gastric mucosa (**f**)

Table 24.9 Cytological features of solid pseudopapillary neoplasm

Cellularity	Cytoarchitecture	Cytomorphology	Other features	Comments
Generally cellular smears	Cohesive Branching with delicate fibrovascular cores and myxoid stroma Often papillary formations (Chinese characters) Small clusters and single neoplastic cells	Monomorphic cells with minimal variability Round to oval nuclei with shallow grooves ('coffee bean') Inconspicuous nucleoli Moderate or scant cytoplasm; sometimes granular and with vacuoles or hyaline globules Very rare mitosis	May show hemorrhagic debris, foamy histiocytes, and multinucleated cells associated with cystic degeneration	May show overlapping features with neuroendocrine tumors

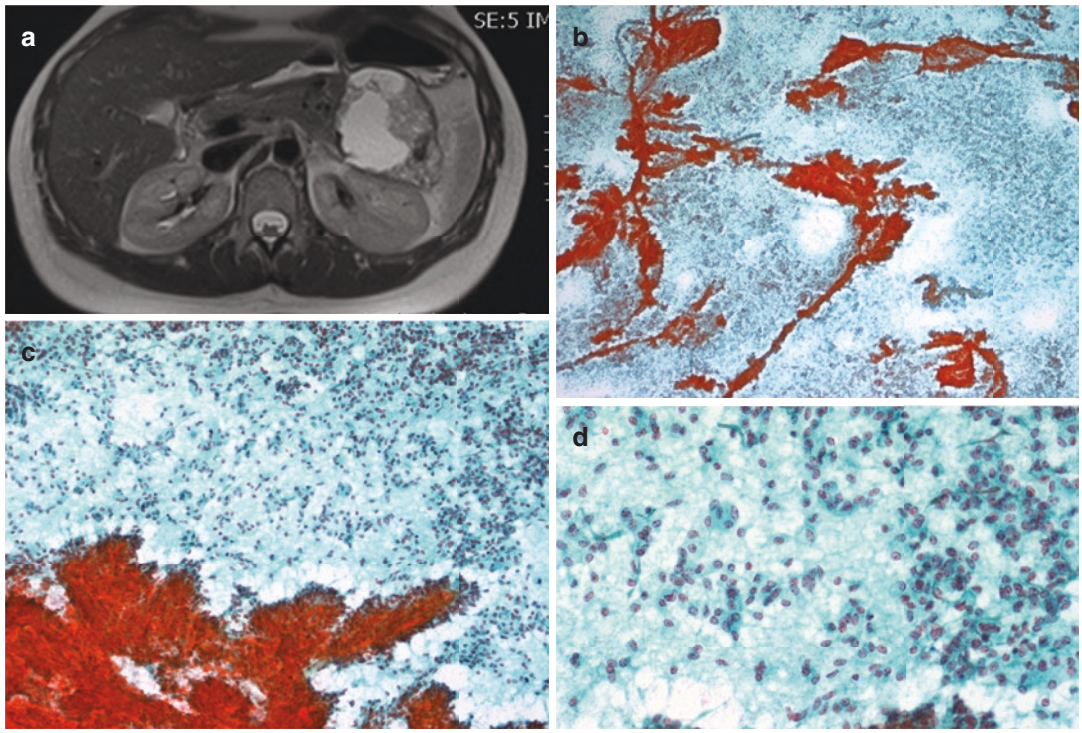

Fig. 24.9 MRI and cytological features of a solid pseudopapillary neoplasm: well-circumscribed pancreatic tail lesion on MRI that is partially cystic (white areas) and partially solid, with no invasion of surrounding structures (**a**). Branching sheets with delicate fibrovascular cores, so-called "Chinese characters" pattern (**b**, **c**). Monomorphic cells with minimal variability and round to oval nuclei with slight grooves, so-called 'coffee bean' nuclei (**d**)

grooves ('coffee bean' like), a feature not found in PanNETs. However, similar to PanNETs, nucleoli are inconspicuous and mitoses are very rare. Hyaline globules may be observed in the cytoplasm occasionally, and immunohistochemistry is essential to make the diagnosis (see Table 20.5).

24.3.3.5 Autoimmune Pancreatitis (see Chap. 7)

CT imaging and positron emission tomography (PET) can be helpful in diagnosing autoimmune pancreatitis (Fig. 24.10a–b). Cytoarchitecture and cytomorphology are often not diagnostic (Table 24.10 and Fig. 24.10). However, in

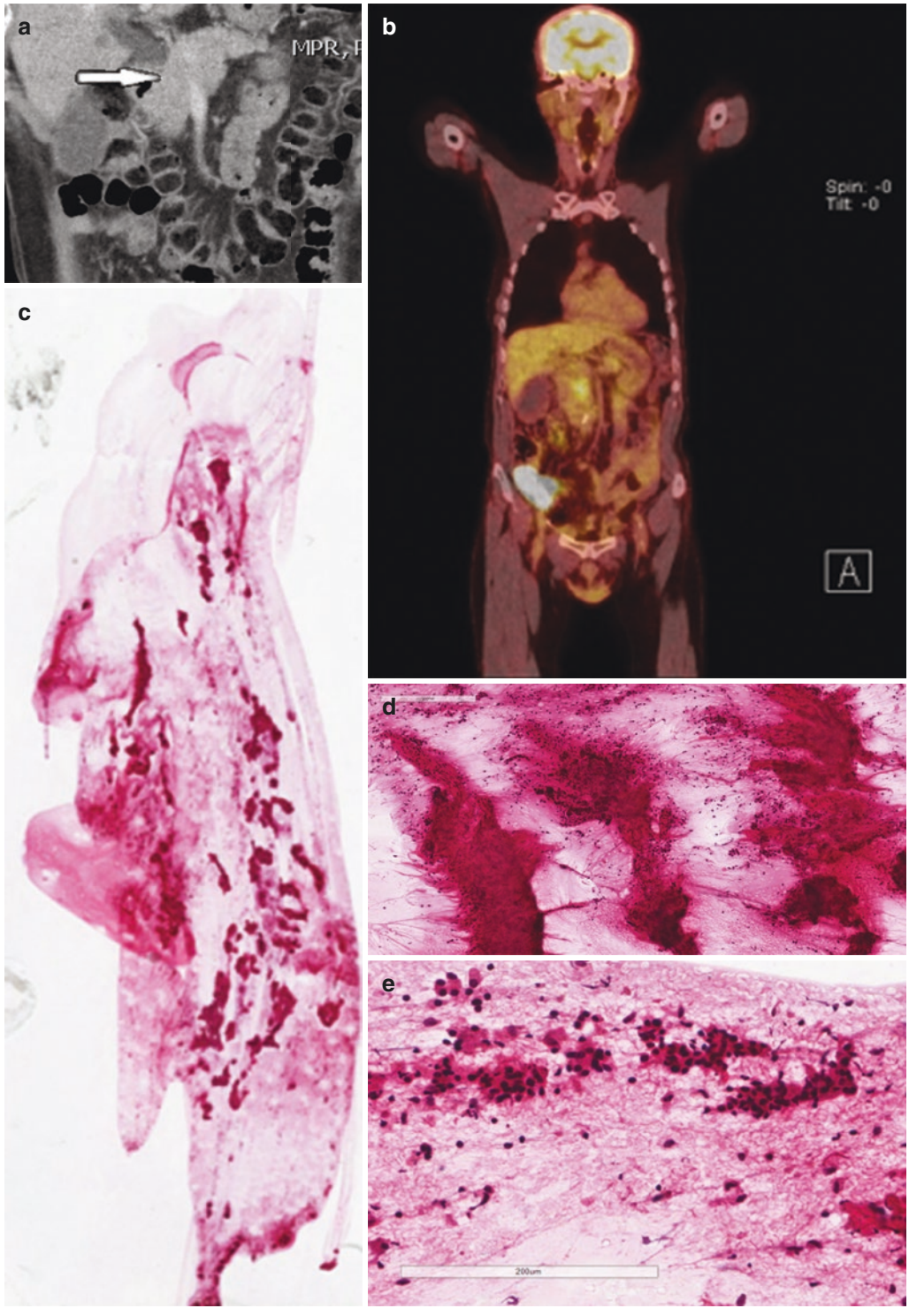

Fig. 24.10 Imaging and cytological features of autoimmune pancreatitis: CT scan shows a diffusely expanded pancreas (*white arrow*) with bile duct obstruction but no pancreatic duct obstruction (**a**). FGT PET demonstrates moderate avidity in the pancreatic head (**b**). This is seen in most pancreatic malignancies but also in IgG4-related disease and acute pancreatitis. Abundant stromal material mixed with inflammatory cells (**c**, **d**). Ductal epithelial cells with reactive atypia (**e**)

Table 24.10 Cytological features of autoimmune pancreatitis (AIP)

Cellularity	Cytoarchitecture	Cytomorphology	Other features	Comments
May be very low	Reactive ductal epithelial cells with atypia Stromal material mixed with inflammatory cells	Nuclear enlargement and 'atypia' but generally variable Above changes may be seen in ductal and acinar epithelium or even in stromal cells	Background lymphocytes and plasma cells (may not be present in some cases)	Similar stroma may occur in ductal adenocarcinoma Double pathology: AIP and primary pancreatic neoplasm

the correct clinical setting, cellular stroma (Figs. 24.10c–d) infiltrated by chronic inflammatory cells is a useful feature to suggest this diagnosis, in the absence of any evidence of a neoplasm. Immunohistochemistry on cell block material to identify $IgG4^+$ plasma cells can be performed, but interpretation may be difficult. It is not unusual for these lesions to be sampled more than once. Larger needles and core biopsies may give superior material and more conclusive results. Autoimmune pancreatitis and neoplasms may coexist, confounding diagnostic challenges [30].

24.3.3.6 Chronic Pancreatitis (see Chap. 7)

Aspirates from areas of localized chronic pancreatitis, which may appear as a mass lesion radiologically, are variably cellular and characterized by fragments of fibrous tissue, amorphous and calcific debris, lymphocytes, and histiocytes. The cellularity of chronic pancreatitis is generally low. Sheets of reactive ductal epithelial cells are more prevalent than atrophic acinar epithelial cells. Reactive ductal cells may mimic a well-differentiated pancreatic ductal adenocarcinoma. As chronic obstructive pancreatitis is often present adjacent to a carcinoma, and malignant cells may be scant, cytological distinction between the two entities can be challenging.

24.3.3.7 Paraduodenal (Groove) Pancreatitis (see Chap. 7, Sect. 7.2.8)

Paraduodenal (groove) pancreatitis can mimic both solid and cystic pancreatic lesions with variable cytological features, depending on the area sampled. Inflammation and Brunner's gland hyperplasia (often associated with paraduodenal pancreatitis) present as foamy cells with abundant vacuolated cytoplasm and eccentric bland nuclei, as well as naked nuclei mimicking PDAC.

24.3.3.8 Intrapancreatic Common Bile Duct Carcinoma

Brush cytology smears of bile duct carcinoma show similar features to pancreatic ductal adenocarcinoma (Fig. 24.11), and it is not possible to distinguish between distal common bile duct carcinoma and pancreatic ductal adenocarcinoma on cytology alone. The distinction of benign from malignant bile duct strictures is also challenging from an endoscopic, radiological, and cytological perspective.

The sensitivity of biliary brushing cytology is variable and linked to challenges with sampling, technique, and interpretation. The main diagnostic dilemma in bile duct brushing cytology is the distinction of reactive atypia from malignancy in the setting of previous procedures and the presence of stents. The presence of stones, stent, or primary sclerosing cholangitis, all of which may cause reactive changes in ductal epithelial cells, are recognized pitfalls, which may result in a false-positive diagnosis.

A confirmative diagnosis of pancreatic malignancy should be rendered only when both cytoarchitectural and morphological criteria are fulfilled. Any one feature in isolation or a few features are rarely diagnostic. A panel of immunohistochemistry on a cell block may be helpful (Fig. 24.5), but results should never be considered in isolation (see Chap. 9, Sect. 9.9.3). In cases where cytological, clinical, and radiological criteria are significantly discrepant, a repeat examination should be considered.

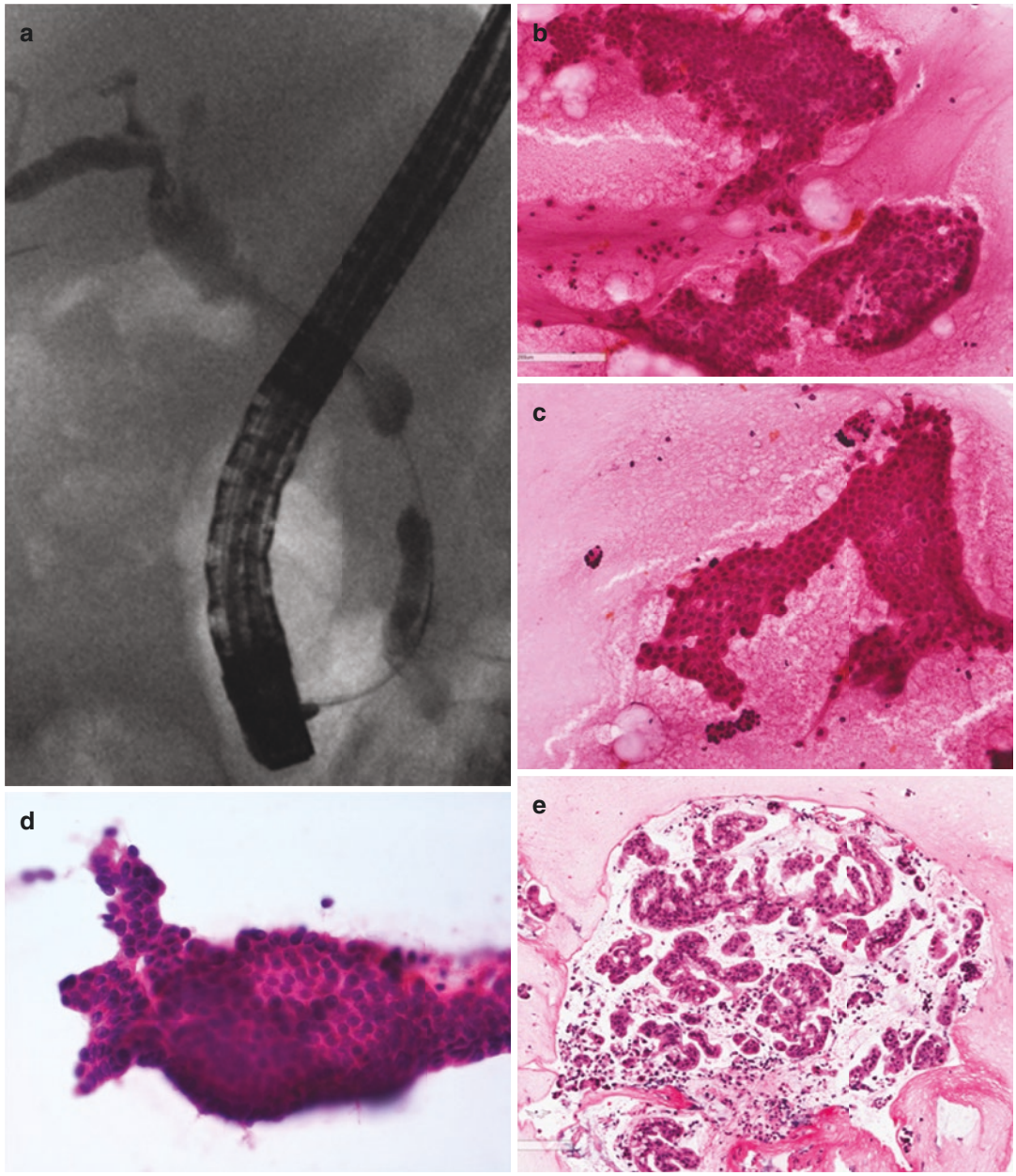

Fig. 24.11 ERCP and cytological features of carcinoma of the common bile duct: a shouldered, high-grade, distal biliary stricture on ERCP suggestive of malignancy (**a**). Crowded sheets with drunken honeycomb and abnormal 'animal-like' configuration (**b**, **c**) in contrast to nonneoplastic reactive bile duct epithelium (**d**). Cell block preparation with similar material diagnostic of pancreatobiliary-type carcinoma (**e**)

24.3.4 Cystic Lesions (see Chaps. 14 and 19)

Cystic lesions of the pancreas can be mucinous or nonmucinous. Contaminant mucin from gastric or duodenal mucosa may be difficult to distinguish from neoplastic mucin. The gross appearance and some microscopic features may help in the distinction (Table 24.11 and Fig. 24.12), but it can be extremely challenging particularly in cases with a low yield and low cellularity. A high CEA level in cyst fluid is considered to be the most reliable fea-

ture to determine the mucinous nature of a cyst [31, 32]. The subdivision of mucinous and nonneoplastic cysts is best determined considering a combination of cytological, biochemical, molecular, EUS, and radiological findings. Before embarking on assessment of cytological features, it is essential to be aware of the EUS and radiological findings.

Table 24.11 Distinguishing neoplastic mucin from contaminant mucin

	Neoplastic mucin	Contaminant mucin
Gross features	Viscid and stranding	Thin and watery
Microscopic features:		
Mucin quality	Thick and colloid-like	Clear and thin
Degenerate cells and debris	Present and may be abundant	Absent
Calcification	May be present	Absent
Accompanying cells	Abnormal cells and epithelium randomly distributed	Accompanied by gastric or duodenal epithelium, often closely associated

24.3.4.1 Mucinous Cystic Lesions

"Mucinous cystic lesion" is a diagnostic umbrella term that encompasses intraductal papillary mucinous neoplasm (IPMN) and mucinous cystic neoplasm (MCN) (see Chaps. 16 and 17), because these entities generally cannot be distinguished from each other based on cytology only. However, because the diagnostic features and differential diagnostic considerations are different for neoplastic mucinous cystic lesions with low-grade versus high-grade dysplasia, they are discussed separately.

Low-Grade Neoplastic Mucinous Cysts

The cytological features of low-grade neoplastic mucinous cysts (NMCs) are summarized in Table 24.12 and illustrated in Fig. 24.13. While the neoplastic epithelium of NMCs can be of gastric, intestinal, or pancreatobiliary type (or a combination of these), most low-grade NMCs have a gastric-type epithelial lining (Figs. 24.13 and 24.14). Hence, for cysts accessed with the transgastric approach, it is often difficult to distinguish between gastric contaminants and the low-grade dysplastic, gastric-type epithelium of an NMC. In contrast, for cysts sampled via the

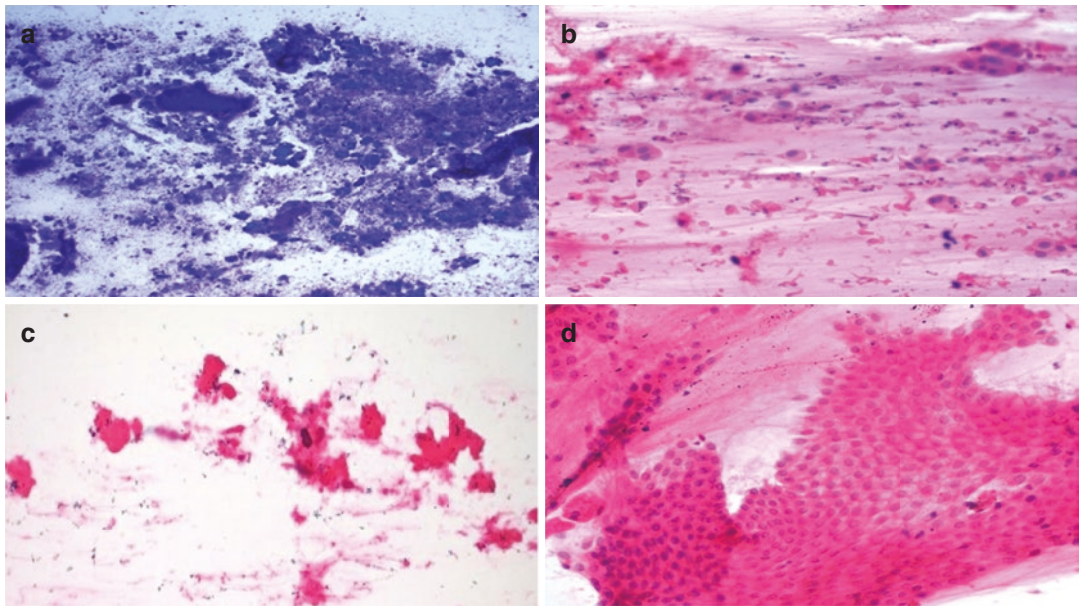

Fig. 24.12 Distinguishing neoplastic mucin from contaminant mucin: neoplastic mucin is thick and colloid-like (**a**), with abundant degenerate cells and debris (**b**) and calcification (**c**). Contaminant mucin is associated with contaminant gastric epithelium (**d**)

Table 24.12 Cytological features of low-grade neoplastic mucinous cysts

Cellularity	Cytoarchitecture	Cytomorphology	Other features	Comments
Scant to moderate cellularity	Small flat sheets, a few clusters and single cells	Bland nuclei Conspicuous but infrequent prominent nucleoli	Background mucin Foamy histiocytes Occasional calcifications	Epithelium is mostly of gastric phenotype Always consider EUS access and be aware of possibility of gastric contaminants (body and tail lesions are accessed via the stomach) Results of cyst fluid analysis can be very helpful

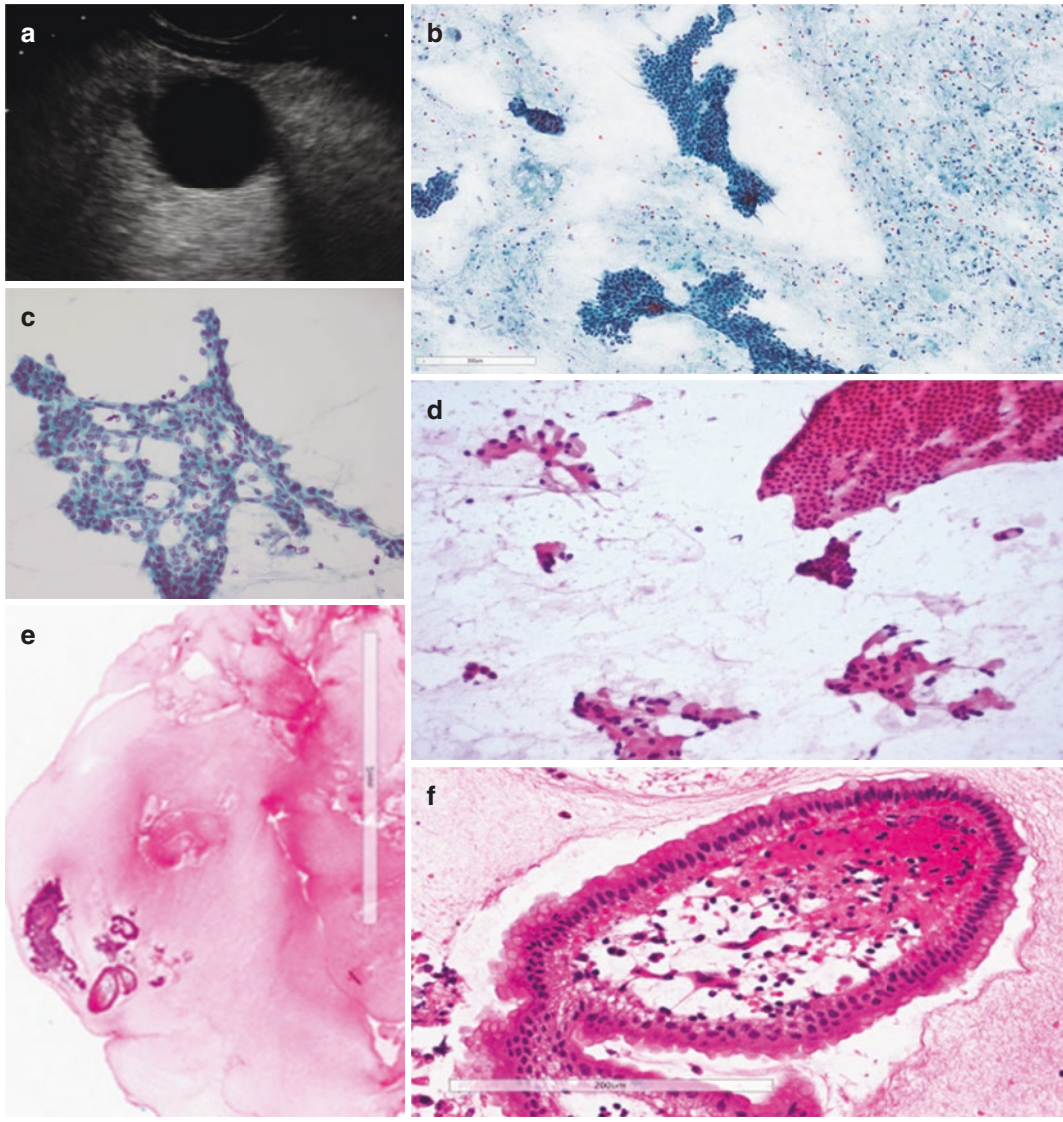

Fig. 24.13 EUS and cytological features of low-grade neoplastic mucinous cysts: an anechoic pancreatic body cyst (**a**). High-risk features are not present. Moderately cellular smear with flat sheets, a few clusters of cells, and single cells in a mucinous background (**b**), and bland nuclei with infrequent nucleoli (**c**, **d**). Cell block with similar epithelium (**e**). High power of gastric phenotype epithelium in cell block (**f**)

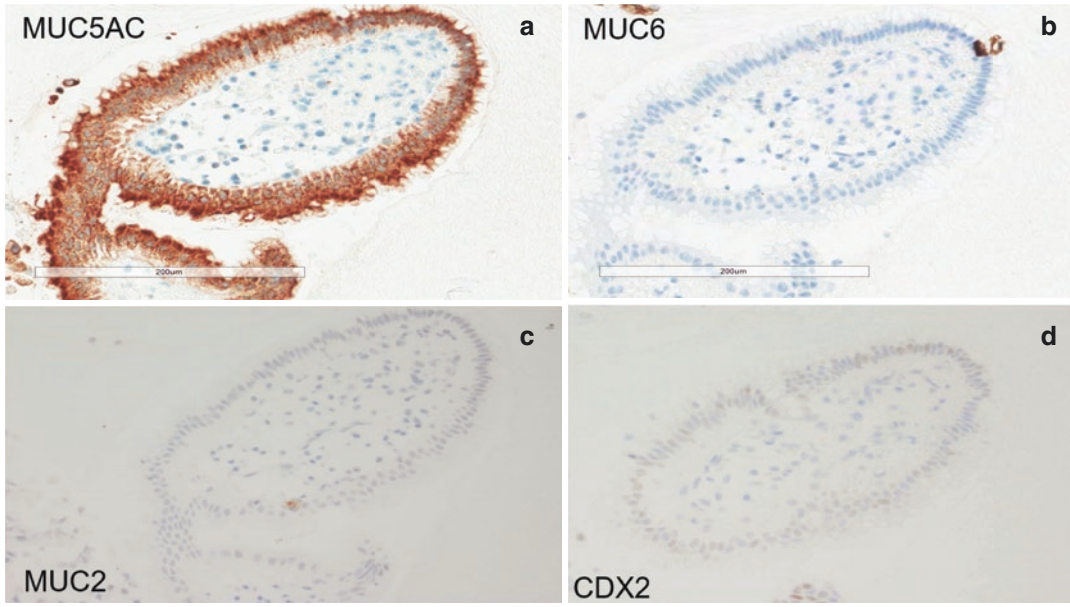

Fig. 24.14 Immunohistochemical profile of a low-grade gastric-type IPMN: immunohistochemistry performed on the epithelium seen in Fig. 24.13 is positive for MUC5AC (**a**), and negative for MUC6 (**b**), MUC2 (**c**), and CDX2 (**d**)

duodenum, the diagnosis of a low-grade NMC is easier when gastric-type epithelial cells are seen against a mucinous background.

Guidelines for the diagnosis of cystic lesions of the pancreas are well established [6, 7] and recommend the triple approach, that is, the correlation of cytological features, fluid biochemistry, and molecular findings to confirm the radiological diagnosis of a NMC. As it is rare to find ovarian-type stroma in cytology preparations, the cytological features of IPMN and MCN are highly similar. Of all the biochemical markers, cyst fluid CEA is the most accurate test available for the diagnosis of a neoplastic mucinous cyst (Tables 24.1 and 24.2). A high concentration of CEA reflects the presence of neoplastic mucinous epithelium and is mainly useful to distinguish neoplastic mucinous cysts from nonmucinous cysts [31, 32]. A CEA cut-off level of >192 ng/mL has a sensitivity of 73%, a specificity of 84%, and an accuracy of 79% for distinguishing mucinous from nonmucinous cysts [23–25, 31]. However, cyst fluid CEA does not differentiate IPMNs from MCNs or non-invasive tumors from those with invasion.

IPMNs frequently harbor somatic *KRAS* mutations (60–80%) and activating *GNAS* mutations (50–70%), the latter being particularly frequent in IPMNs of intestinal type. A specific diagnosis of MCN may be achieved only after careful correlation of cytological features with cyst fluid biochemistry and mutational analysis, and the clinical and radiological features. While the detection of *KRAS* and/or *GNAS* mutations supports the diagnosis of NMC, it does not provide a risk categorization, that is, grading of dysplasia and identification of invasive carcinoma, as this is based exclusively on morphological features [25].

It should be noted that dilated pancreatic ducts with low-grade PanIN (see Chap. 8) and so-called simple mucinous cysts (see Chap. 19, Sect. 19.2.1) may mimic the cytological features of NMC and may even harbor *KRAS* mutations [33].

High-Grade Neoplastic Mucinous Cysts

Table 24.13 summarizes the cytological features of high-grade NMCs, which are often lined by pancreatobiliary- or intestinal-type epithelium, or both. Material is more cellular than that of low-grade NMCs (Fig. 24.15), and the diagnosis of epithelial dysplasia is more straightforward.

Table 24.13 Cytological features of high-grade neoplastic mucinous cysts

Cellularity	Cytoarchitecture	Cytomorphology	Other features	Comments
Generally cellular, but could be scant	Sheets, small clusters, 3-dimensional groups and papillary arrangements +/−loose single cells	Obvious nuclear abnormality Nuclear crowding and variability High nuclear:cytoplasmic ratio, nuclear membrane irregularity, abnormal chromatin patterns (hyper- or hypochromasia) Often prominent or distinct nucleoli	Mucin Degenerate cyst contents and cells: may mimic necrosis, often impossible to differentiate	Papillary arrangements are very supportive of intraductal papillary mucinous neoplasm

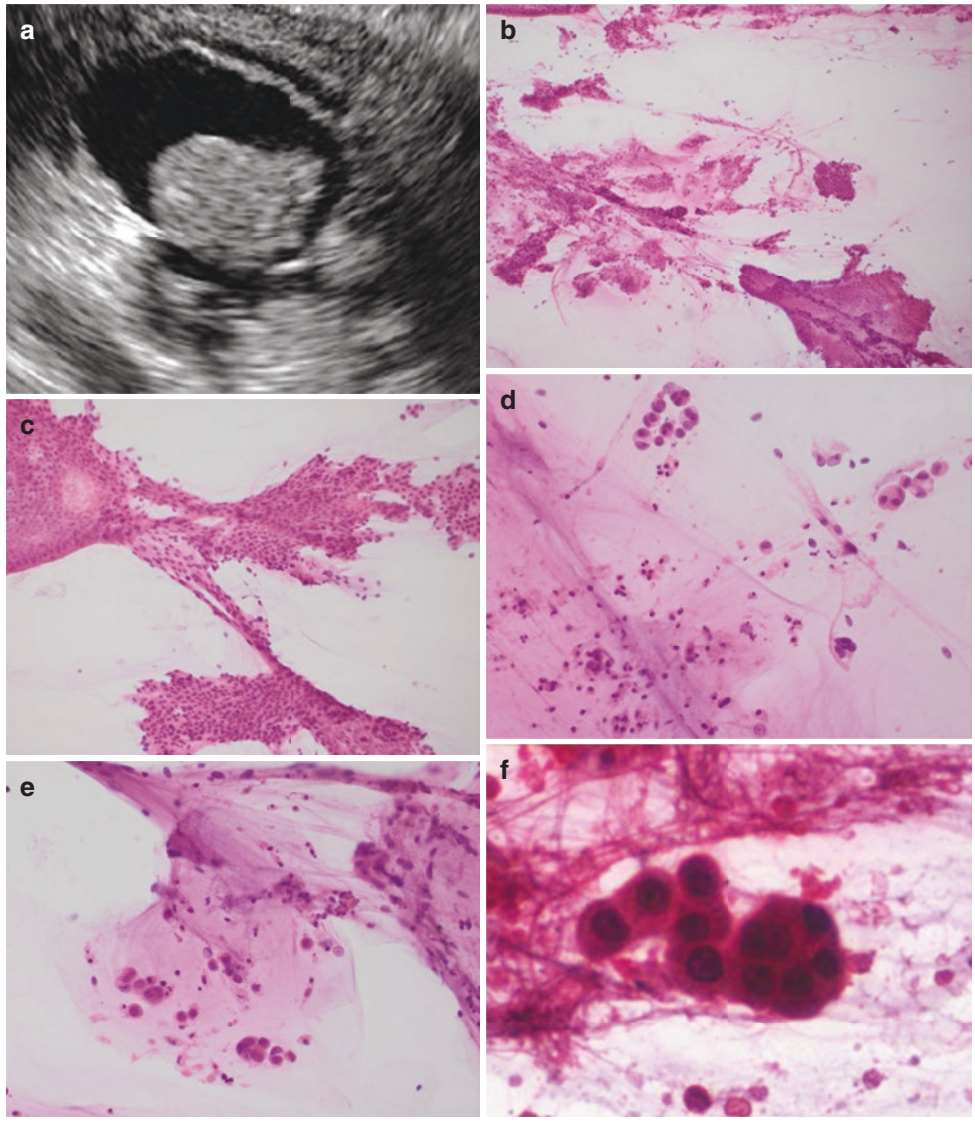

Fig. 24.15 EUS and cytological features of high-grade neoplastic mucinous cysts: pancreatic cyst with a 10 mm solid nodule arising from the cyst wall (**a**). Cellular smear with background mucin (**b**) and large sheets of abnormal cells (**c**). Background contains mucin, degenerate material, and a number of highly atypical cells in small clusters and as single cells (**d**, **e**). High-grade atypia at high power (**f**)

The presence of necrosis raises the suspicion of an invasive component ("transformed neoplastic cyst"). However, one should be aware of the fact that degenerate cyst content, and cells that may be present in non-invasive high-grade NMCs can be mistaken for genuine necrosis (Fig. 24.15d–e). Large papillary projections or papillary-like sheets are suggestive of an IPMN, in which case EUS findings and high CEA cyst fluid levels may corroborate that diagnosis. If high-grade epithelial dysplasia can be confirmed on cytological examination, biochemical and mutational analysis of the cyst fluid is not essential for the diagnosis, but may allow subtyping of the NMC.

High-Grade Neoplastic Mucinous Cysts with Invasive Carcinoma

It is exceptionally difficult, and often impossible, to identify invasive carcinoma in cytology samples from high-grade NMCs. Firstly, the degree of architectural and cytological abnormality may be the same in high-grade NMCs with or without invasive carcinoma (Fig. 24.3). Secondly, the presence of necrotic cellular debris or so-called tumor diathesis is often considered diagnostic of invasive carcinoma, but may be exceedingly difficult to differentiate from degeneration of background mucinous material in a neoplastic cyst. Moreover, an invasive cystic mucinous neoplasm may not always be accompanied by necrosis. In other words, for FNA samples from high-grade NMCs showing high cellularity and widespread high-grade epithelial atypia/dysplasia, it may be extremely difficult or impossible to either exclude or confirm the presence of invasive carcinoma (Fig. 24.16 and Table 24.13).

In terms of clinical management, the identification or exclusion of invasion is not critical, because clear-cut high-grade epithelial dysplasia in a neoplastic cyst is an indication for surgical resection of the neoplastic cysts [6, 7]. Indeed, the presence of high-grade epithelial atypia/dysplasia in a neoplastic mucinous cyst predicts malignancy with high specificity and sensitivity, over 85% and 72% respectively [34, 35]. Because high-grade dysplasia and/or invasive carcinoma may be only a focal finding, it is important that FNA-sampling is targeted at so-called mural nodules, that is, solid areas in the cyst wall.

The presence of large branching papillary sheets of high-grade neoplastic epithelium in a targeted sample from a cystic lesion is a useful clue to an IPMN (Fig. 24.16e). However, one should be aware that similar cytoarchitectural features may be seen in invasive ductal adenocarcinoma of large duct pattern and cystic papillary pattern (see Chap. 9, Sects. 9.8.3 and 9.8.4). Correlation with clinical and EUS findings is imperative.

24.3.4.2 Nonmucinous Cysts (Fig. 24.17)

These include serous cystadenoma, pseudocysts, lymphoepithelial cysts, lymphangioma, and squamous cysts. In the WHO classification 2019, intraductal oncocytic papillary neoplasm (IOPN) is now a separate entity, distinct from IPMN on a morphological and molecular basis. IOPNs are rare lesions, and almost all show high-grade features as well as marked degenerative changes of the oncocytic epithelium in the cyst fluid (Fig. 24.17a–b).

Serous Cystic Neoplasms (see Chap. 15)

The fluid of serous cystic neoplasms is characteristically paucicellular or acellular (Fig. 24.18). The background is clear and occasional uniform nonmucinous cuboidal cells with centrally placed, small round nuclei are noted (Table 24.14). A multimodal approach with cyst fluid analysis usually showing low levels of CEA, amylase, and lipase is very useful (Table 24.2). While demonstration of *VHL* gene mutation may be diagnostic, it may not be required; for example, the radiologically more challenging serous cystic neoplasms with a solid component (see Chap. 15, Sect. 15.15.11.1) tend to yield more cellular material, which can be used for cell block cytology, with immunohistochemistry, and will usually allow a definitive diagnosis to be made (Fig. 24.18f).

Other Types of Cysts (see Chap. 19)

The accurate diagnosis of other nonneoplastic cysts requires a multidisciplinary approach and multimodal cyst fluid analysis (Table 24.2).

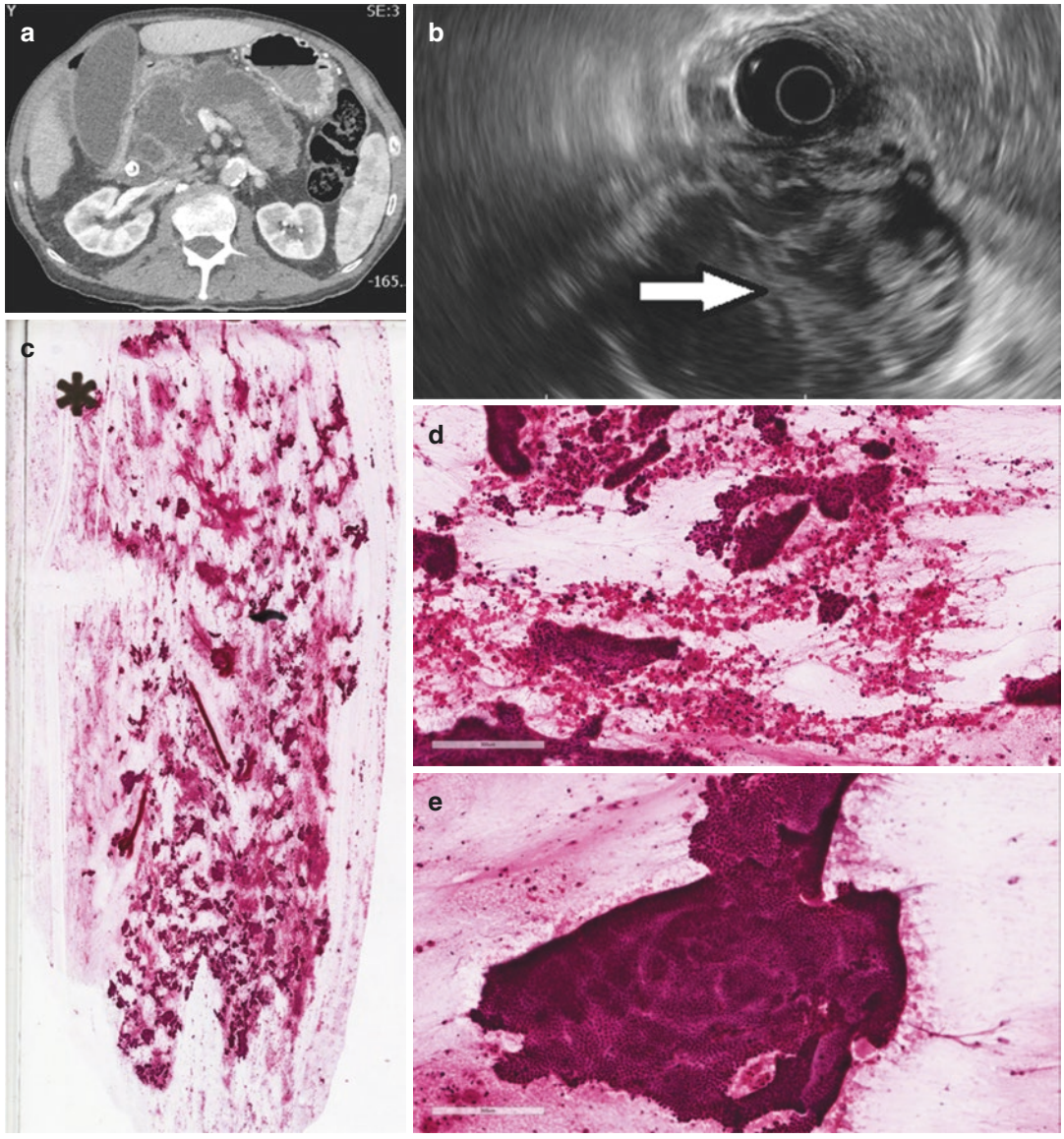

Fig. 24.16 Imaging and cytological features of a transformed IPMN: on CT scan, the main pancreatic duct is grossly dilated (**a**). On EUS, solid mural nodules project into the duct lumen (*white arrow*) (**b**). Highly cellular smear (**c**) with sheets and small clusters of abnormal cells in a background of degenerate material and necrosis (**d**). Large sheets of abnormal epithelium characteristic of IPMN (**e**)

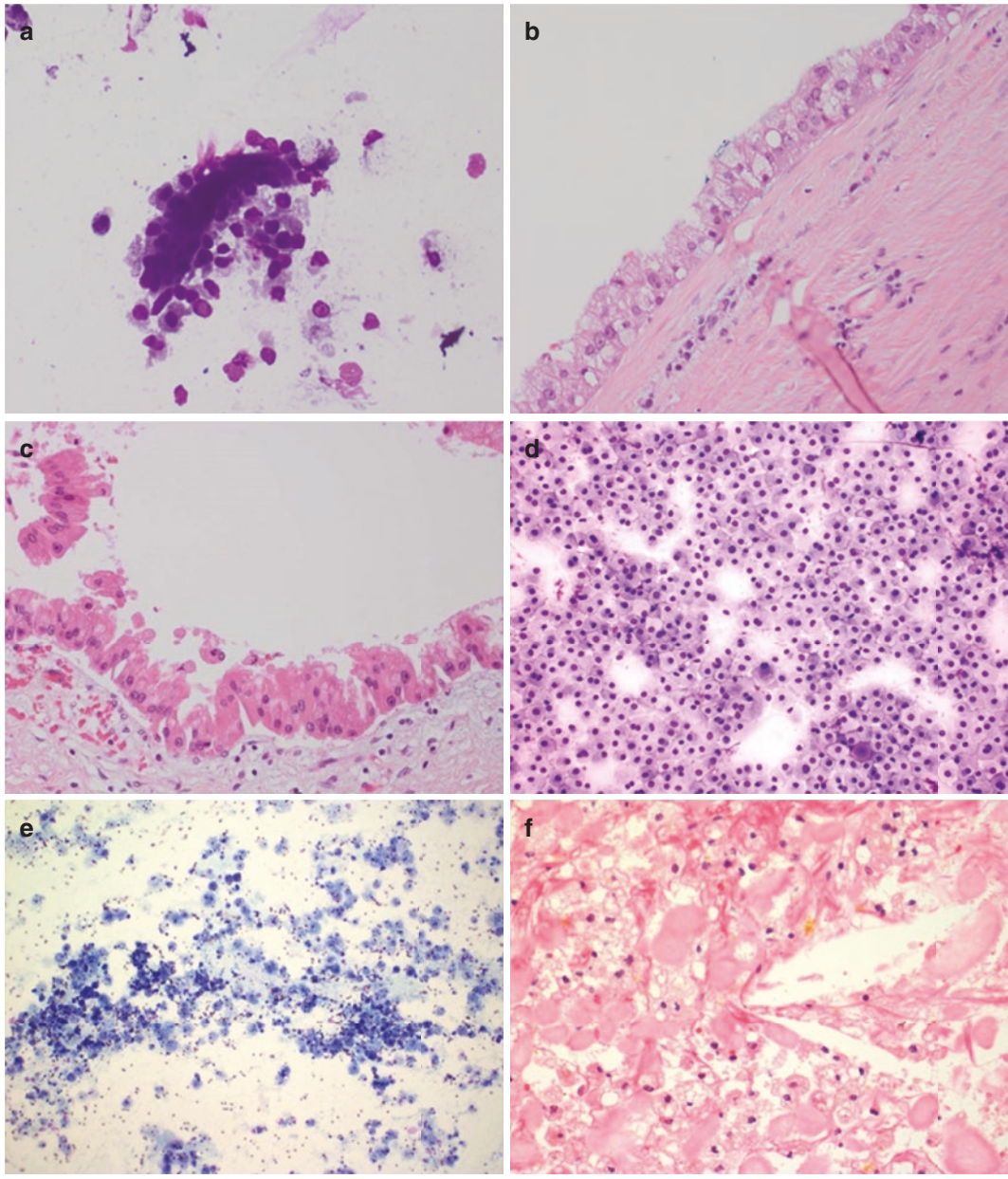

Fig. 24.17 Nonmucinous cysts: intraductal oncocytic papillary neoplasm (IOPN) on cytology (**a**) with degenerate oncocytic cells that could mimic histiocytes in cyst fluid (compare with **d**–**f**). Degenerate oncocytic epithelium (**b**) and fairly intact oncocytic cells (**c**) in IOPN on histology sections. Pseudocyst contains cellular debris and histiocytes, with and without hemosiderin (**d**). Granular debris and histiocytes in a benign nonmucinous cyst (**e**). Histiocytes, yellow pigment, and cholesterol clefts in a pseudocyst (**f**)

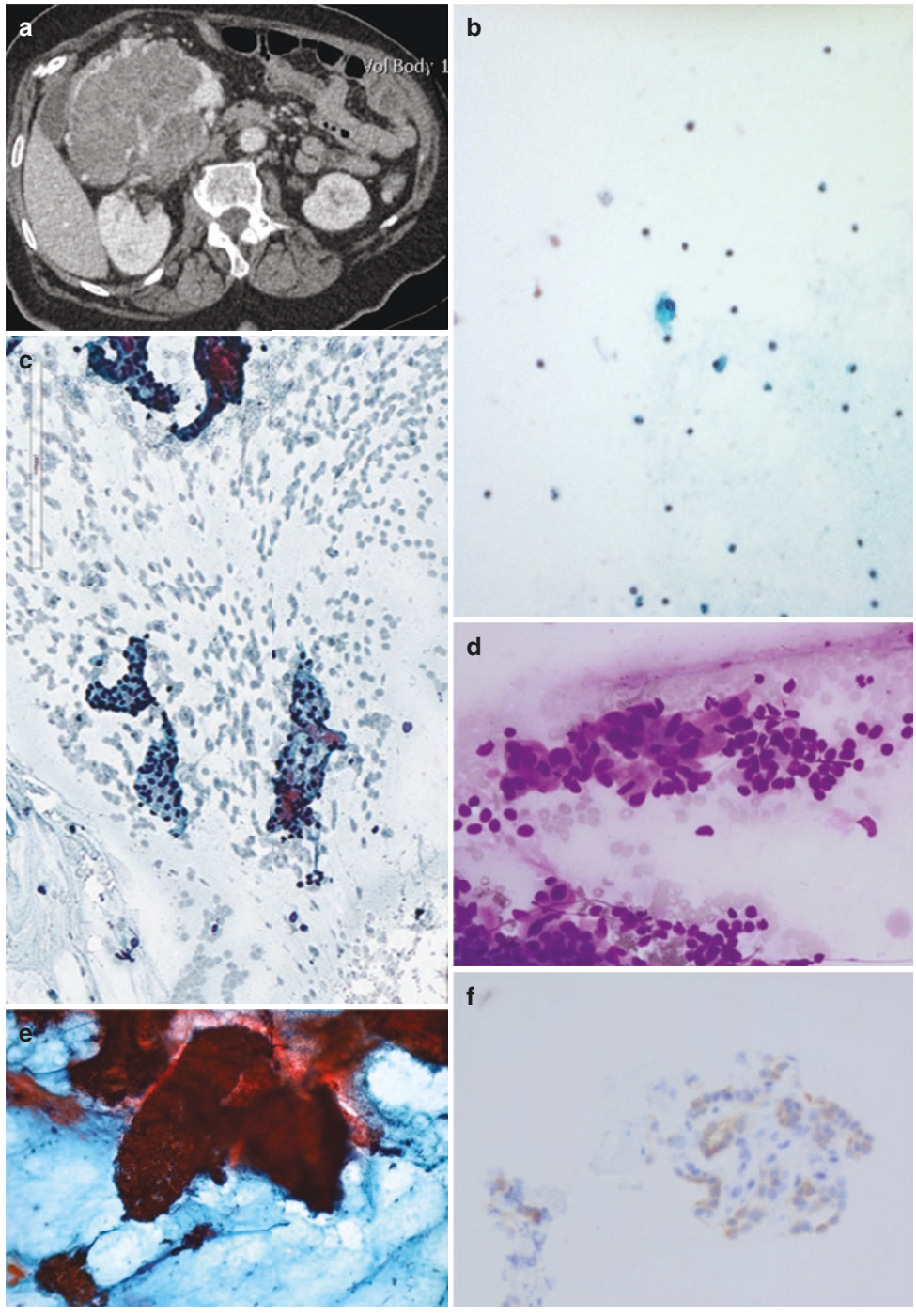

Fig. 24.18 CT and cytological features of serous cystadenoma: on CT scan, there is a large lesion in the pancreatic head and body composed of microcysts with a central scar (**a**). The absence of macrocysts often means that no fluid can be aspirated for analysis. A typical paucicellular smear with a few single cells stripped of cytoplasm (**b**). Flat sheets and small groups (**c**) of uniform cuboidal cells with round, central, or slightly eccentric nuclei, and regular even chromatin (**d**). Tissue fragments with fibrous septa are usually only seen in solid components (**e**). Cell block preparation showing immunopositivity for inhibin (**f**)

Table 24.14 Cytological features of serous cystic neoplasms

Cellularity	Cytoarchitecture	Cytomorphology	Other features
Paucicellular or acellular smears	Small clusters, flat sheets, small groups, and single cells stripped of cytoplasm Fibrous stroma in solid types/ solid components	Uniform cuboidal cells with a round, central, or slightly eccentric nucleus Regular nuclear contours with normal chromatin No mitosis	Clear background without necrosis or mucin Glycogen (PAS-positive and DPAS-negative) in epithelial cells Inhibin-immunopositive cells

24.4 Metastases

The most common primary malignancies that metastasize to the pancreas include melanoma and renal, colorectal, breast, and lung carcinoma. When the cytological features indicate poor differentiation, the use of a cell block for immunohistochemistry should always be considered in order to exclude metastasis from an extrapancreatic malignancy (see Table 12.1).

24.5 Molecular Testing in Pancreatobiliary Cytology

The value of *KRAS* and *GNAS* mutation testing in cyst fluid is well established. Integration of next-generation sequencing into the assessment of specimens obtained from pancreatic cysts and biliary lesions has been shown to improve the diagnostic yield in recent studies [36–38]. Currently, such testing is not part of routine clinical practice and has cost and technical implications.

References

1. Kandel P, Wallace MB. Recent advancement in EUS-guided fine needle sampling. J Gastroenterol. 2019;54:377–87.
2. Puli SR, Bechtold ML, Buxbaum JL, Eloubeidi MA. How good is endoscopic ultrasound-guided fine-needle aspiration in diagnosing the correct etiology for a solid pancreatic mass?: a meta-analysis and systematic review. Pancreas. 2013;42:20–6.
3. Partelli S, Bartsch DK, Capdevila J, Chen J, Knigge U, Niederle B, et al. ENETS consensus guidelines for standard of care in neuroendocrine tumours: surgery for small intestinal and pancreatic neuroendocrine tumours. Neuroendocrinology. 2017;105:255–65.
4. Sohal DPS, Kennedy EB, Khorana A, Copur MS, Crane CH, Garrido-Laguna I, et al. Metastatic pancreatic cancer: ASCO clinical practice guideline update. J Clin Oncol. 2018;36:2545–56.
5. Cheng B, Zhang Y, Chen Q, Sun B, Deng Z, Shan H, et al. Analysis of fine-needle biopsy vs fine-needle aspiration in diagnosis of pancreatic and abdominal masses: a prospective, multicenter, randomized controlled trial. Clin Gastroenterol Hepatol. 2018;16:1314–21.
6. Lennon AM, Ahuja N, Wolfgang CL. AGA guidelines for the management of pancreatic cysts. Gastroenterology. 2015;149:825.
7. European Study Group on Cystic Tumours of the Pancreas. European evidence-based guidelines on pancreatic cystic neoplasms. Gut. 2018;67:789–804.
8. Hewitt MJ, McPhail MJ, Possamai L, Dhar A, Vlavianos P, Monahan KJ. EUS-guided FNA for diagnosis of solid pancreatic neoplasms: a meta-analysis. Gastrointest Endosc. 2012;75:319–31.
9. Thornton GD, McPhail MJ, Nayagam S, Hewitt MJ, Vlavianos P, Monahan KJ. Endoscopic ultrasound guided fine needle aspiration for the diagnosis of pancreatic cystic neoplasms: a meta-analysis. Pancreatology. 2013;13:48–57.
10. Crinò SF, Manfrin E, Scarpa A, Baldaque-Silva F, Carrara S, De Nucci G, et al. EUS-FNB with or without on-site evaluation for the diagnosis of solid pancreatic lesions (FROSENOR): Protocol for a multicenter randomized non-inferiority trial. Dig Liver Dis. 2019;51:901–6.
11. Zhang ML, Arpin RN, Brugge WR, Forcione DG, Basar O, Pitman MB. Moray microforceps biopsy improves the diagnosis of specific pancreatic cysts. Cancer Cytopathol. 2018;126:414–20.
12. Novikov A, Kowalski TE, Loren DE. Practical management of indeterminate biliary strictures. Gastrointest Endosc Clin N Am. 2019;29:205–14.
13. Moon SH, Kim MH, Park DH, Hwang CY, Park SJ, Lee SS, et al. Is a 2-week steroid trial after initial negative investigation for malignancy useful in differentiating autoimmune pancreatitis from pancreatic cancer? A prospective outcome study. Gut. 2008;57:1704–12.
14. Mitchell RA, Stanger D, Shuster C, Telford J, Lam E, Enns R. Repeat endoscopic ultrasound-guided fine-needle aspiration in patients with suspected pancreatic cancer: diagnostic yield and associated change

in access to appropriate care. Can J Gastroenterol Hepatol. 2016;2016:7678403.
15. Conti CB, Cereatti F, Grassia R. Endoscopic ultrasound-guided sampling of solid pancreatic masses: the fine needle aspiration or fine needle biopsy dilemma. Is the best needle yet to come? World J Gastrointest Endosc. 2019;11:454–71.
16. Bang JY, Kirtane S, Krall K, Navaneethan U, Hasan M, Hawes R, Varadarajulu S. In memoriam: Fine-needle aspiration, birth: Fine-needle biopsy: The changing trend in endoscopic ultrasound-guided tissue acquisition. Dig Endosc. 2019;31:197–202.
17. Facciorusso A, Wani S, Triantafyllou K, Tziatzios G, Cannizzaro R, Muscatiello N, et al. Comparative accuracy of needle sizes and designs for EUS tissue sampling of solid pancreatic masses: a network meta-analysis. Gastrointest Endosc. 2019;90:893–903.
18. Iglesias-Garcia J, Dominguez-Munoz JE, Abdulkader I, Larino-Noia J, Eugenyeva E, Lozano-Leon A, et al. Influence of on-site cytopathology evaluation on the diagnostic accuracy of endoscopic ultrasound-guided fine needle aspiration (EUS-FNA) of solid pancreatic masses. Am J Gastroenterol. 2011;106:1705–10.
19. Ecka RS, Sharma M. Rapid on-site evaluation of EUS-FNA by cytopathologist: an experience of a tertiary hospital. Diagn Cytopathol. 2013;41:1075–80.
20. Buxbaum JL, Eloubeidi MA, Lane CJ, Varadarajulu S, Linder A, Crowe AE, et al. Dynamic telecytology compares favorably to rapid onsite evaluation of endoscopic ultrasound fine needle aspirates. Dig Dis Sci. 2012;57:3092–7.
21. Lin O, Rudomina D, Feratovic R, Sirintrapun SJ. Rapid on-site evaluation using telecytology: a major cancer center experience. Diagn Cytopathol. 2019;47:15–9.
22. Monaco SE, Koah AE, Xing J, Ahmed I, Cuda J, Cunningham J, et al. Telecytology implementation: deployment of telecytology for rapid on-site evaluations at an academic medical center. Diagn Cytopathol. 2019;47:206–13.
23. Chai SM, Herba K, Kumarasinghe MP, de Boer WB, Amanuel B, Grieu-Iacopetta F, et al. Optimizing the multimodal approach to pancreatic cyst fluid diagnosis: developing a volume-based triage protocol. Cancer Cytopathol. 2013;121:86–100.
24. Pitman MB. Pancreatic cyst fluid triage: a critical component of the preoperative evaluation of pancreatic cysts. Cancer Cytopathol. 2013;121:57–60.
25. Springer S, Wang Y, Dal Molin M, Masica DL, Jiao Y, Kinde I, et al. A combination of molecular markers and clinical features improve the classification of pancreatic cysts. Gastroenterology. 2015;149:1501–10.
26. Pitman MB, Centeno BA, Ali SZ, Genevay M, Stelow E, Mino-Kenudson M, et al. Standardized terminology and nomenclature for pancreatobiliary cytology: the Papanicolaou Society of Cytopathology guidelines. Diagn Cytopathol. 2014;42:338–50.
27. Stelow EB, Pambuccian SE, Bardales RH, Debol SM, Mallery S, Lai R, et al. The cytology of pancreatic foamy gland adenocarcinoma. Am J Clin Pathol. 2004;121:893–7.
28. Deng H, Shi J, Wilkerson M, Meschter S, Dupree W, Lin F. Usefulness of S100P in diagnosis of adenocarcinoma of pancreas on fine-needle aspiration biopsy specimens. Am J Clin Pathol. 2008;129:81–8.
29. Díaz DA, Díaz Pérez JÁ, Ortega ML, Sastre Valera J, Fernández Aceñero MJ. Reliability of Ki-67 determination in FNA samples for grading pancreatic neuroendocrine tumors. Endocr Pathol. 2016;27:276–83.
30. Tabata T, Kamisawa T, Hara S, Kuruma S, Kuwata G, Fujiwara T, et al. Intraductal papillary mucinous neoplasm of the pancreas and IgG4-related disease: a coincidental association. Pancreatology. 2013;13:379–83.
31. Brugge WR, Lewandrowski K, Lee-Lewandrowski E, et al. Diagnosis of pancreatic cystic neoplasms: a report of the cooperative pancreatic cyst study. Gastroenterology. 2004;126:1330–6.
32. Cizginer S, Turner B, Bilge AR, et al. Cyst fluid carcinoembryonic antigen is an accurate diagnostic marker of pancreatic mucinous cysts. Pancreas. 2011;40:1024–8.
33. Krasinskas A, Oakley GJ, Bagci P, Jan KT, Kuan SF, Reid MD, et al. "Simple mucinous cyst" of the pancreas. A clinicopathologic analysis of 39 examples of a diagnostically challenging entity distinct from intraductal papillary mucinous neoplasms and mucinous cystic neoplasms. Am J Surg Pathol. 2017;41:121–7.
34. Pitman MB, Yaeger KA, Brugge WR, Mino-Kenudson M. Prospective analysis of atypical epithelial cells as a high-risk cytologic feature for malignancy in pancreatic cysts. Cancer Cytopathol. 2013;121:29–36.
35. Pitman MB, Genevay M, Yaeger K, Chebib I, Turner BG, Mino-Kenudson M, et al. High-grade atypical epithelial cells in pancreatic mucinous cysts are a more accurate predictor of malignancy than "positive" cytology. Cancer Cytopathol. 2010;118:434–40.
36. Singhi AD, Nikiforova MN, Chennat J, Papachristou GI, Khalid A, Rabinovitz M, et al. Integrating next-generation sequencing to endoscopic retrograde cholangiopancreatography (ERCP)-obtained biliary specimens improves the detection and management of patients with malignant bile duct strictures. Gut. 2020;69:52–61.
37. Matthew W, Rosenbaum MW, Jones M, Dudley JC, Le PL, Iafrate J, et al. Next-generation sequencing adds value to the preoperative diagnosis of pancreatic cysts. Cancer Cytopathol. 2017;125:41–7.
38. Singhi AD, McGrath K, Brand RE, Khalid A, Zeh HJ, Chennat JS, et al. Preoperative next-generation sequencing of pancreatic cyst fluid is highly accurate in cyst classification and detection of advanced neoplasia. Gut. 2018;67:2131–41.

Appendix: WHO Classification of Tumors of the Pancreas 2019

(Modified from Lokuhetty D, White VA, Watanabe R, Cree IA (eds). Digestive system tumors. WHO classification of tumors 5th edition. Lyon: IARC Press; 2019, p. 296)

Benign Epithelial Tumors and Precursors

- Serous cystadenoma NOS
  - Macrocystic (oligocystic) serous cystadenoma
  - Solid serous adenoma
  - Von Hippel-Lindau syndrome-associated serous cystic neoplasm
  - Mixed serous-neuroendocrine neoplasm
- Serous cystadenocarcinoma NOS
- Glandular intraepithelial neoplasia, low grade
- Glandular intraepithelial neoplasia, high grade
- Intraductal papillary mucinous neoplasm with low-grade dysplasia
- Intraductal papillary mucinous neoplasm with high-grade dysplasia
- Intraductal papillary mucinous neoplasm with associated invasive carcinoma
- Intraductal oncocytic papillary neoplasm NOS
- Intraductal oncocytic papillary neoplasm with associated invasive carcinoma
- Intraductal tubulopapillary neoplasm
- Intraductal tubulopapillary neoplasm with associated invasive carcinoma
- Mucinous cystic neoplasm with low-grade dysplasia
- Mucinous cystic neoplasm with high-grade dysplasia
- Mucinous cystic neoplasm with associated invasive carcinoma

Malignant Epithelial Tumors

- Ductal adenocarcinoma NOS
  - Colloid carcinoma
  - Signet-ring cell (poorly cohesive cell) carcinoma
  - Medullary carcinoma
  - Adenosquamous carcinoma
  - Hepatoid carcinoma
  - Invasive micropapillary carcinoma
  - Carcinoma, undifferentiated, NOS
  - Undifferentiated carcinoma with osteoclast-like giant cells
- Acinar cell carcinoma
  - Acinar cell cystadenocarcinoma
  - Mixed acinar cell carcinoma-neuroendocrine carcinoma
  - Mixed acinar cell carcinoma-ductal adenocarcinoma-neuroendocrine carcinoma
  - Mixed acinar-ductal carcinoma
- Pancreatoblastoma
- Solid pseudopapillary neoplasm of the pancreas
  - Solid pseudopapillary neoplasm with high-grade carcinoma

© Springer Nature Switzerland AG 2021
F. Campbell, C. S. Verbeke, *Pathology of the Pancreas*,
https://doi.org/10.1007/978-3-030-49848-1

Pancreatic Neuroendocrine Neoplasms

- Pancreatic neuroendocrine microadenoma
- Neuroendocrine tumor NOS
  - Neuroendocrine tumor, grade 1
  - Neuroendocrine tumor, grade 2
  - Neuroendocrine tumor, grade 3
- Pancreatic neuroendocrine tumor, nonfunctioning
  - Oncocytic neuroendocrine tumor, nonfunctioning pancreatic
  - Pleomorphic neuroendocrine tumor, nonfunctioning pancreatic
  - Clear cell neuroendocrine tumor, nonfunctioning pancreatic
  - Cystic neuroendocrine tumor, nonfunctioning pancreatic
- Functioning pancreatic neuroendocrine tumors
  - Insulinoma
  - Gastrinoma
  - VIPoma
  - Glucagonoma
  - Somatostatinoma
  - ACTH-producing tumor
  - Enterochromaffin-cell carcinoid
  - Serotonin-producing tumor
- Neuroendocrine carcinoma NOS
  - Large cell neuroendocrine carcinoma
  - Small cell neuroendocrine carcinoma
- Mixed neuroendocrine—non-neuroendocrine neoplasm (MiNEN)
  - Mixed ductal adenocarcinoma-neuroendocrine carcinoma
  - Mixed ductal adenocarcinoma-neuroendocrine tumor
  - Mixed acinar cell carcinoma-neuroendocrine carcinoma
  - Mixed acinar cell carcinoma-ductal adenocarcinoma-neuroendocrine carcinoma

Index

© Springer Nature Switzerland AG 2021
F. Campbell, C. S. Verbeke, *Pathology of the Pancreas*,
https://doi.org/10.1007/978-3-030-49848-1